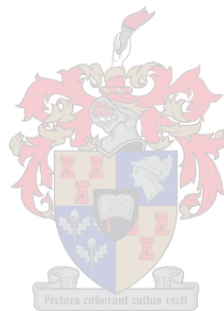# TRANSIENT MODELLING OF INDUCTION MOTORS IN A PETROCHEMICAL PLANT USING MATLAB

ANDRIES JOHANNES CLAASSENS

Thesis presented in partial fulfillment of the degree of Master of Science in Engineering at the University of Stellenbosch

Supervisor: Prof. H.J. Vermeulen

March 2008

DECLARATION

I, the undersigned, hereby declare that the work contained in this thesis is my own original work and that I have not previously in its entirety or in part submitted it at any university for a degree.

A. J. Claassens

10 Feruary 2008

SYNOPSIS

The behaviour of induction motors at a petrochemical plant under transient conditions was investigated with the view to improve plant immunity to voltage fluctuations. The benefits of using a phase-variable induction motor model rather than the simpler *d-q* models usually employed are investigated.

A simplified model of the plant electrical distribution system was derived. Phase variable and *d-q* induction motor models were implemented as well as a synchronous generator model. Practical considerations precluded the use of commercial software for the simulation of transient conditions and a basic simulation program was developed using Matlab to evaluate the behaviour of the dynamic machine models and distribution system.

It was established that the configuration of the installed re-acceleration system can be optimised to reduce the possibility of plant outages as a result of voltage fluctuations. It was found that the use of more detailed induction machine models provide valuable insight into system behaviour and is justified if accurate motor parameters are available or can be estimated. The simplified plant model yielded useful results and enabled the identification of incorrect system data. The investigation showed that Matlab is suitable for the rapid development of a basic transient simulation program that can be used to study the behaviour of different interconnected dynamic machine models.

Die gedrag van induksiemotors in 'n petrochemiese aanleg onder oorgangstoestande is ondersoek ten einde die immuniteit van die aanleg vir spanningsfluktuasies te verbeter. Die voordele van die gebruik van 'n fase-veranderlike induksiemotor model eerder as die eenvoudiger d-q modelle wat normaalweg gebruik word is ondersoek.

'n Vereenvoudigde model van die aanleg se elektriese distribusiestelsel is afgelei. Fase-veranderlike en d-q induksiemotor modelle is geimplementeer sowel as 'n sinkroongenerator model. Praktiese oorwegings het die gebruik van kommersiële programmatuur vir die simulasie van oorgangstoestande verhoed en 'n basiese program is in Matlab ontwikkel om die gedrag dinamiese masjienmodelle en die distribusiestelsel te evalueer.

Daar is vasgestel dat die konfigurasie van die geinstalleerde herversnellerstelsel geoptimeer kan word om die moontlikheid van aanleg onderbrekings as gevolg van spanningsfluktuasies te verminder. Daar is gevind dat die gebruik van meer gedetaileerde induksiemasjien modelle waardevolle insig in die gedrag van die stelsel lewer en geregverdig is indien akkurate motorparameters beskikbaar is of afgeskat kan word. Die vereenvoudigde model van die aanleg het bruikbare resultate gelewer en die het die identifikasie van foutiewe stelseldata moontlik gemaak. Die ondersoek het getoon dat Matlab geskik is vir die snelle ontwikkeling van 'n basiese oorgangsimulasie program wat gebruik kan word om die gedrag van verskillende gekoppelde dinamiese masjienemodelle te bestudeer.

CONTENTS

LIST OF SYMBOLS

$A \Rightarrow B$	A is defined as B
f	Frequency in Hertz (Hz)
H	Inertia constant, defined as the stored energy per VA rating (J/VA) [16]
J	Moment of inertia of a rotating mass(kg m^2)
P	Power (W)
p.u.	Per unit
Q	Reactive power (VA)
V	Voltage [V]
$\underline{x}, \underline{y}$	Vector quantities

GLOSSARY

AVR: *Automatic Voltage Regulator.*

Distribution System: Refer to *"Power System"*.

Disturbance: A *'disturbance'* in a power system is a sudden change or sequence of changes in one or more of the parameters of the system, or in one or more of the physical quantities. Two types of disturbances are defined, small and large [23].

CT: Current Transformer.

HV: High Voltage (132kV).

Large Disturbance: A *"large disturbance"* is a disturbance for which the set of equations which describe the power system cannot be linearised for the purposes of analysis [23].

LV: Low voltage (550V and below).

MV: Medium Voltage (11kV and 6.6kV).

MCC: Motor Control Centre

ODE: Ordinary Differential Equation.

Operating Condition: An "*operating condition*" or "*operating point*" of a power system is a set of physical quantities or physical variables that can be measured or calculated and which can meaningfully describe the *state* of the system completely [23].

Pre-Fault System: A power system immediately preceding the initiation of a large disturbance is termed a *"pre-fault (pre-disturbance) system"* . The system is considered to be in the steady-state in this phase [23].

Power dip: A power dip is defined as a momentary reduction in line voltage, typically of the order of 100-200ms duration with a voltage reduction of > 20% of the nominal line voltage.

Power System: A "*power system*" is a collection of generating units, transformers, transmission lines, loads, capacitors[1], reactors, associated auxiliaries and switchgear to connect the various components [23]. Note the terms *"Distribution System"* and *"Power System"* are used interchangeably in this report.

Small Disturbance: A *"small disturbance'* is a disturbance for which the set of equations which describe the power system can be linearised for the purposes of analysis [23].

Steady-state operating Condition: *"Steady State operating condition"* of a power system is an operating condition in which all the physical quantities that characterize the system can be considered to be constant for the purposes of analysis [23].

Transient Period: The *"Transient period"* is the time duration between the initiation of a large disturbance (or sequence of disturbances) and restoration of operation to an acceptable steady state after the fast electrical transients have died out [23].

Voltage Instability: Apart from insufficient synchronizing and damping torques causing instability, insufficient reactive power to support the system can result in voltage collapse which can also lead to instability. The term "voltage instability" is used to describe this phenomenon [23].

---

[1] Capacitors and reactors may be shunt or series connected

LIST OF FIGURES

LIST OF TABLES

1   INTRODUCTION

1.1   Research Objective

The transient behaviour of the electrical distribution system at PetroSA[1] is to be investigated.

Due to the nature of operations at PetroSA, it is imperative that the manufacturing plant operates in a stable manner, without any unnecessary interruptions or disturbances at all times. In common with any large electrical consumer, the electrical supply to PetroSA is subject to regular disturbances of varying magnitudes. In an attempt to minimise the effect of such disturbances on the steady operation of the plant, many induction motors are equipped with re-acceleration circuits. The purpose of these re-acceleration circuits are to de-energise and re-start motors in a controlled sequence after voltage dips have occurred on the electrical supply. This system is thus intended to allow the plant to continue operating without interruption after a brief disturbance on the electrical supply. A review of the stability studies carried out during the design of the PetroSA plant confirmed that the behaviour of the re-acceleration system has never been investigated. The re-acceleration system clearly plays a major role in determining the behaviour of the PetroSA distribution system following a disturbance. It is therefore reasonable to expect that an investigation into the transient behaviour of the PetroSA distribution system will reveal if the performance of the re-acceleration system, and hence, possibly the stability of the PetroSA distribution system can be improved.

The obvious course of action would be to carry out these simulations on commercial transient stability analysis software. There are several considerations, which preclude this initial approach:

- PetroSA does not currently possess a suitable commercial software package. With prices for this type of software being in the R300 000 – R500 000 range, a sound business case for the purchase of such software is required. In addition, the execution of this work will not be a trivial task and will require a significant allocation of resources. Diverting already limited resources from existing plant performance and cost improvement initiatives requires justification.

- A second alternative would be to make use of external consultants to carry out the necessary studies. Again, a sound business case is required to justify the expenses which are anticipated to easily exceed the software purchase costs mentioned above.

- PetroSA is not currently experiencing any major system stability problems directly attributable to the re-acceleration systems. This makes it difficult to justify a financial commitment to investigating system performance.

Based on the foregoing discussion, it could be argued that further investigation is not really justified. There has however been a considerable, ongoing expansion in the Mossel Bay area which is placing increasing demands on the electrical distribution system supplying PetroSA and the surrounding towns. This has already resulted in Eskom having to increase the bus voltage at the substation feeding PetroSA during high demand periods. As the number of consumers on the system increases, it is likely that quality of supply will deteriorate resulting in more frequent and possibly more severe voltage dips. It is also possible that the current sequence in which motors are re-started can be optimised to reduce the impact on the distribution system and avoid excessively low voltages and in severe cases, motors stalling.

It is important to gain insight into the behaviour of the re-acceleration system to determine what potential scope for improvement exists. Optimising the operation of the re-acceleration

---

[1] PetroSA was formerly known as Mossgas

system is financially attractive since it will only entail re-adjustment of undervoltage relay and delay timer settings and does not require the installation of additional equipment or physical modifications.

It will be necessary to carry out an initial investigation into the transient behaviour of the PetroSA distribution system on a limited scale. A representative portion of the entire system will have to be selected and modelled. This investigation should provide insight into the behaviour of the PetroSA distribution system during motor re-acceleration. In addition, the behaviour of motors during the re-acceleration phase needs to be investigated to determine if the assumptions upon which the design of the system is based are valid. The initial investigation should provide an indication of the steps to be taken to optimise the performance of the re-acceleration system as well as the justification (or otherwise) for carrying out more extensive studies as mentioned above.

The PetroSA manufacturing facility is capacity constrained and not market constrained, therefore any process interruption will result in a financial loss, which cannot be recovered.[2] It is therefore important to identify potential problem areas and implement corrective actions before actual production losses occur.

Consideration of the above clearly indicates the need for examining the transient behaviour of the PetroSA distribution system, taking the effect of the re-acceleration system into account.

1.2   Overview Of The Re-Acceleration System

The re-acceleration systems described above are designed to prevent unnecessary plant outages due to minor disturbances on the electrical power supply. Short duration (100-300ms) voltage dips are typically caused by line flashovers due to veldt fires and system faults on the Eskom Transmission network. Faults closer to the PetroSA plant will usually result in more severe voltages dips or even supply interruptions.

A large number of the induction motors on site are equipped with undervoltage relays, which detect power dips and de-energise the motor for power dips longer than approximately 100ms exceeding a 20% volt drop. The time constants relating to the petrochemical processes are generally long when compared to the duration of such electrical disturbances. It is thus possible to re-start all motors that were running before the disturbance occurred without unduly affecting the production process. Simply permitting all motors to re-start in an uncontrolled fashion following a disturbance may result in excessive voltage drops on the PetroSA electrical distribution system. Since most of the motors drive fans and pumps, these motors would not stall, but simply continue running at reduced speed with high slip [29]. This could result in a total plant outage since motors will then trip on over-current and/or locked rotor protection.

The re-acceleration systems prevent all motors being re-started simultaneously following a disturbance on the Eskom supply. This is accomplished by equipping motor control circuits with delay timers. All critical motors that need to re-start following an electrical disturbance are divided into groups which are re-started at preset time intervals. These intervals are typically 3, 6, 9 and 12 seconds. The timers in the various motor starters are set to the appropriate time delay. When the power supply returns to normal following a power dip, the re-acceleration timer will prevent the motor contactor from closing until the preset time has elapsed. This ensures that all the motors that were running before the electrical disturbance occurred are started in a controlled sequence

---

[2] A market-constrained facility can manufacture final product at a rate exceeding market demand. This implies that a certain degree of process interruption can be tolerated, since production throughput can be increased to compensate for process downtime.

1.3　Key Aspects Addressed In This Investigation

1.3.1　Re-acceleration system optimisation

The existing re-acceleration system is intended to re-start motors in a controlled manner following a power disturbance. The intent is to minimise the impact upon the electrical distribution system of a large number of induction motors starting simultaneously. The assumption is that the motor (and load) will still be running at reduced speed when re-energised and the starting currents will be lower than normally required to start from standstill. The effect of the re-acceleration system upon the electrical distribution system was never simulated or investigated. It is likely that the overall performance of this system can be improved simply by adjusting the re-acceleration time delays, the undervoltage relay settings and possibly the sequence of starting up motors.

1.3.2　Faults due to veldt fires.

The re-acceleration system has been designed to respond to a single voltage dip. At times PetroSA experiences voltage dips caused by veldt fires near power lines. A number of short duration dips separated by a couple of seconds are usually observed, due to the operation of auto-reclosers on the Eskom supply lines. The original transient stability studies used for designing the plant were reviewed and it was found that this type of situation was never modelled or analysed.

After a voltage dip, motors will be decelerating, and then re-started by the re-acceleration system. When voltage dips take place due to veldt fires, several dips are usually observed, with subsequent dips occurring while motors are being re-started by the re-acceleration systems. Provided that dips subsequent to the initial power dip are short, the re-acceleration timer circuits will be reset. This re-starts the re-acceleration sequence after each dip. System response under these conditions should also be examined.

1.3.3　Software development

It will be necessary to develop software to carry out the proposed analysis of the transient behaviour of the re-acceleration system. A software development platform will have to be selected and the suitability of that platform when applied to the transient stability problem assessed. As discussed in paragraph 1.1, the use of specialised commercially available software packages are not justified under present circumstances. One alternative is to conduct preliminary investigations using more commonly available general purpose software tools. The advantages and disadvantages of using this approach as well as an evaluation of the applicability of the selected software to the problem at hand will provide guidelines for carrying out similar types of investigations in future.

2 LITERATURE STUDY

2.1 Review Of Existing Transient Stability Studies

Transient stability studies were carried out during the design of the PetroSA (then Mossgas) onshore facility. These studies are discussed in detail in Appendix E.

The scope of the study by Powerplan Systems Analysis [28] was to undertake a series of supplementary power system analyses in conjunction with Merz & McLellan [27] in order to validate key results of the Merz & McLellan studies and identify any potential problem areas in the proposed design of the PetroSA electrical power system. It was necessary to assume typical data for most equipment parameters [28] since vendor data was not yet available. The performance of the re-acceleration system was not evaluated.

2.2 Powerplan Study [28]

A greatly simplified representation of the PetroSA system as shown in Figure 2-1 was utilised. The majority of the system was modelled using lumped equivalent models or omitted entirely.

Figure 2-1 Approximate PetroSA system representation.

Note: The original drawing is illegible in some places, this diagram is only included to illustrate the degree of complexity of the system model that was used.

Lumped LV and HV motors were assumed to run at 85% of full load torque, based on the rating of the motor. Typical HV[1] and LV motor characteristics were used to represent numerous equivalent or lumped motors. Due to the approximate nature of the modelling data, a simple equivalent circuit model was used for modelling of induction machines. Synchronous machines were also modelled using typical data. These models were detailed and included a full d-q axis representation taking transient, sub-transient and saturation effects into account. Variable speed drives were modelled simply as constant power loads.

It was incorrectly assumed that three 10MVAr filters installed at each of the three Synthol variable speed drives will provide reactive power compensation[2].

Stability studies were carried out assuming a solid 3-phase fault of 100ms duration at different locations on the PetroSA distribution system. It was assumed that all load contactors, i.e. for motors, static loads and drives, remain held in during low control voltage conditions and ride through the fault even if the busbar voltage falls to zero. This represents the most severe recovery condition, which is prevented in practice by the re-acceleration system. It was also assumed that no busbars are isolated by disconnecting network branches after the fault.

2.2.1 Summary of main conclusions and recommendations

The Powerplan study gave rise to the following conclusions and recommendations:

- For all 100ms fault and system conditions specified, recovery of all induction motors is possible.
- The local generators are stable for the specified fault conditions.
- The 26MW synchronous motors are stable for the specified fault conditions, but become unstable when subjected to a 400kV fault longer than 200ms.
- Stability for all machines for the 100ms fault condition is achieved by a wide margin.

2.3 Merz and McLellan Study [27]

The purpose of the Merz and McLellan studies were to determine whether the plant with the then proposed distribution system would recover satisfactorily after a 100ms supply interruption, or any short circuit in the distribution system that is cleared within 100ms.

2.3.1 PetroSA plant data

When these studies were carried out, vendor data on drives was minimal. Typical data was therefore assumed throughout with regard to motor load characteristics and drive inertias. The Total Feed Compressor variable speed drives were represented as a constant power (PQ) type load which was correctly assumed to be switched out during the period the fault persisted and switched in after fault clearance. In general, summated equivalent loads based on available load lists were used. The rotating machine models differ from those used by Powerplan Systems [27]. Induction machine modelling was based on a simple equivalent linear impedance model. Saturation was not taken into account and only rotor resistance was changed as a function of slip.

---

[1] Note that the definition of HV (high voltage) used in [27] and [28] differs from that used in this document and refers to 11kV and 6.6kV motors. In this section the terms HV and MV will be used interchangeably and both refer to 11kV - 6.6kV motors.

[2] It is not clear from Figure 2-1 how these drives and filters were represented. These drives are supplied from busses 3, 4 and 10 as shown in Figure 3-4

2.3.2 *Summary of main conclusions and recommendations*

The studies showed [27]:

- The PetroSA system would recover satisfactorily after a 100ms supply interruption, or any short circuit in the distribution system that is cleared within 100ms.

- Sufficient reactive power was available to limit the demand from Eskom.

2.4 Comments On Study Results

In practice, the 26MW air-compressors, 03KC101 & 03KC201 (Figure 3-5) usually trip during electrical disturbances, and the critical power generator, 48GT102 (Figure 3-4,) is automatically disconnected from the Eskom system when any disturbance is detected. The available reactive power is therefore approximately 27MVAr less than assumed. The two 10MW oxygen compressor motors, 03KC102 and 03KC202 (Figure 3-5), will also trip 10 to 15 seconds after the main air compressors trip due to process reasons. This large load reduction on the system will reduce the demand for reactive power to some extent. It will be necessary to determine the response of the system without the 26MW air compressors (03KC101/201) and the critical generator 48GT102 (Figure 3-4). The main generator has also been found to trip under certain conditions[3] during power dips. In these cases, all reactive power has to be supplied by Eskom during system recovery and therefore a study with 48GT101 offline will also be required when a transient stability study encompassing the entire PetroSA system is carried out. Past experience has shown that the PetroSA system is able to recover following a voltage dip without the main generator being online, but it is important to investigate the system behaviour under these conditions.

None of these studies evaluated the impact of the re-acceleration system at PetroSA. A pessimistic approach was taken where it was assumed that all induction motors remain online irrespective of bus voltage levels. Motors were represented by lumped equivalents and generic data used since vendor data was unavailable. Motors were assumed to be operating at 85% full load torque. Surveys have shown that motors purchased individually (not part of an appliance) are usually oversized [10]. Since this practice improves system dynamic performance, it is important to determine the actual motor loadings when carrying out system analysis.

It has also been shown that the practice of assuming what is believed to be a pessimistic system representation can be a dangerous approach [11]. It is not always possible to select representations that would be pessimistic for all parts of the system or all test conditions. Static load models such as the linear impedance model used in the Merz & McLellan studies have also proven to be inaccurate in cases involving large voltage and/or frequency deviations. In such cases, dynamic load models should be used [30, 11].

2.5 Transient Stability Analysis

Transient analysis of electrical distribution systems is mainly carried out by electricity suppliers and distributors such as Eskom. There is also a need to limit the complexity of the mathematical models used due to time, cost, manpower and computer hardware constraints when carrying out system studies [23]. It appears as if the majority of large power consumers would typically restrict electrical distribution system analysis to short circuit and load flow studies. Stability studies may only be carried out during the initial design of large industrial

---

[3] These trips are due to limitations in the design of the protection system, which will result in erroneous tripping of the main generator breaker under certain conditions. Detailed studies were carried out to investigate this problem and the protection settings optimised to some extent. Further improvement will require significant capital investment and is not justifiable at this stage.

plants. This is evidenced by the fact that most research effort remains directed at solving the problems encountered by electricity suppliers and distributors. In the case of PetroSA, such studies were carried out, but were limited in scope and accuracy due to the use of generic data parameters, load models used and the limitations of computer hardware available at the time. These studies did not evaluate the behaviour of the re-acceleration system. There have been significant changes to the loading of the Eskom network supplying the PetroSA plant and the PetroSA distribution system transient response could well be significantly different from that originally calculated. The ever-increasing capabilities of personal computers have also provided the means to carry out analysis with model complexity that was not practical several years ago [21, 23].

In order to analyse the dynamic performance of an electrical system, suitable mathematical models have to be developed which represent the system components to the desired degree of accuracy. Solutions to these models that lead to an understanding of the system behaviour during various types of disturbances have to be obtained. Two types of stability studies are carried out. The analysis of system behaviour following a large disturbance is generally referred to as a *transient stability study*. The time frame for this type of simulation is between a fraction of a second to tens of seconds. The term *dynamic stability* is used to describe the long-time response of a system to small disturbances or badly set controls and solutions can be obtained in the time or frequency domain. This type of problem will not be considered here.

Most of the available literature dealing with transient analysis of electrical distribution systems consider the problem from the perspective of the electricity supplier and not the electricity consumer [21, 23]. Emphasis is placed on detailed modelling of generators, prime-movers and transmission systems. Various approximations are used to model loads, since it is assumed that the exact composition and behaviour of the loads on the system is unknown [10, 11, 29, 30]. Lesieutre *et al* [34] comment that although detailed induction motor models are included in some transient stability programs, they capture induction motor dynamic characteristics which lack meaning at the power systems level. Emphasis is therefore placed on developing dynamic models in terms of meaningful bus variables, *P, Q, V, θ* and *ω*.[4] The purpose of this research is to investigate the behaviour of the system loads (induction motors) under transient conditions as well as the response of the associated distribution system. Load composition is known and can be modelled in greater detail. It is therefore obvious that the general assumptions used to model loads will not apply and a more detailed load representation can be applied.

The multi-machine analysis techniques developed by Smith and Chen [22] are primarily directed at the modelling of small capacity, geographically limited systems. Detailed models are used for all system components. Whilst these techniques could theoretically be extended to the PetroSA distribution system, the additional computational effort involved would be prohibitive.

In transient stability studies, generators with their controls and dynamic loads are usually described by a set of differential equations, whilst the transmission system with static loads is represented by a set of algebraic equations [21, 23]. Two general approaches, namely numerical methods and non-conventional methods are currently used to analyse the transient performance of electrical systems [23]. Numerical methods are able to handle mathematical models of various components of a power system to any desired degree of sophistication. One disadvantage is that, depending on the size, complexity and modelling refinement, a huge computational effort may be required. In addition, the time domain solutions obtained do not provide insight into the response of the system to parameter changes. Such investigations can only be carried out by means of repetitive numerical analysis.

---

[4] Where: P = Bus Power, Q = bus reactive power, V = bus voltage, θ = Bus voltage angle and ω = bus frequency

Non-conventional methods of analysis such as Lyapunov-like direct methods, and extended equal area criterion have been developed to address these shortcomings. Pavella and Murthy [23] comment that although a great deal of research effort has been devoted to developing Lyapunov-like direct methods, the expectations initially put on direct methods have not been fully realized. They are of the opinion that continuing development of these methods should preserve the features for which they have initially been designed, namely features complementary to, rather than competitive with time-domain methods. Various other methods such as Extended Equal-Area Criterion, Decision Tree Transient Stability Method and the Composite Electromechanical Distance Method can be used to investigate system transient stability. These methods were excluded based on the following considerations:

- A time domain solution as provided by conventional numerical analysis will provide a clear insight into the behaviour of the PetroSA system after the occurrence of single and multiple voltage dips. The impact of the re-acceleration system on induction motor behaviour can also be easily assessed.

- Conventional numerical analysis is able to handle system component models of any degree of complexity. It will thus be easy to use load models of differing complexity to determine the degree of modelling sophistication required to adequately determine the behaviour of the PetroSA distribution system.

- A brief review of non-conventional methods indicates that the electrical system representation generally has to be simplified. One of the aims of the current work is to determine the merits of a more detailed representation of induction motor loads when compared to the simplified models generally used.

- It is necessary to restrict the scope of work for the current research to manageable limits.

2.5.1 System representation

The mathematical model of an electrical power system usually consists of a set of differential and a set of algebraic equations. These equations need to be solved in transient stability calculations. A step by step procedure normally followed is that during each time interval the differential equations are solved by numerical integration. The values of the variables obtained are then used at the end of the time step in the solution of the algebraic equations. [21, 23] This is usually referred to as the *alternating solution* method. An alternative approach entails the application of implicit integration techniques which allow the differential equations to be converted to algebraic equations. These equations can then be incorporated with the network's algebraic equations and solved simultaneously. The use of implicit trapezoidal integration has proved very stable, permitting step lengths greater than the smallest time constant of the system [21]. This is termed the *combined solution* method.

It was necessary to decide upon a solution method, and the *alternating solution* method was chosen based on the following considerations:

- Existing Matlab routines and functions could be readily applied – for example, Ordinary Differential Equation (ODE) solvers and matrix calculation routines.

- The resulting software is modular and separate modules can be independently tested, e.g. loadflow (algebraic) and motor dynamic models (differential equations)

- The literature survey carried out yielded more information on the alternating-solution approach. The combined-solution approach appears to be less well documented.

The emphasis is generally on achieving as much reduction in computer time as possible, whilst keeping storage requirements to a minimum. The number of variables that the program has to handle increases dramatically with increasing system size and computer programs must be able to handle large dimensions. Due to the vastly differing time constants associated with different system components, the associated differential equations are usually stiff. Sparsity

programming, optimal ordering, triangular factorization and other techniques have been developed by various researchers to address these problems.

Computer programs for transient stability generally employ some form of step-by-step calculation procedure where the values of the system variables are calculated at regular time intervals, providing a time-domain solution.

The requirements for the present work are as follows:

- Load behaviour following transients needs to be carefully assessed. Exact load composition and behaviour is known. Accurate induction motor models can be employed to simulate the dynamic behaviour of the PetroSA system during the re-acceleration phase following single or multiple voltage dips.

- It would be advantageous if the software developed for transient analysis is modular. This will simplify testing and verification of results with other available software packages. This will also allow evaluation of different induction motor models.

- The Eskom supply network and generators can be represented as a swing bus connected to the PetroSA system via a suitable impedance. The type of disturbance to be considered typically arises due to a line to ground fault on the transmission lines relatively close to PetroSA resulting in voltage dips. Only the stability of the local PetroSA system is to be investigated.

- The single generator embedded in the PetroSA network must be modelled. For the purposes of this work, only a relatively small portion of the PetroSA electrical system will be represented in detail. Clearly, if the entire system is modelled, the behaviour of this generator can be expected to have a significant influence on system behaviour. The importance of modelling the generator, and its potential impact, when a small portion of the system is modelled needs to be determined.

- The size of system to be simulated is reduced quite significantly, thus the system dimensions are kept relatively small[5]. The specialized techniques developed for handling systems with large dimensions are unlikely to be required.

- Reduction in computer time, although desirable, is not an essential requirement, since determining the behaviour of the distribution system and performance of the induction motor models are of primary concern. The merits of using more complex models will be assessed taking computing time into consideration.

It is thus obvious that the requirements for the present work differs from that of typical transient stability analysis. Detailed models of the induction motors selected for study will be required. The disturbances to be investigated do not affect the stability of the Eskom system, but only have a localized effect on the PetroSA distribution system. It is necessary to model the system loads to a greater level of detail than is normally required and the generation to a lesser degree.

2.6   Modelling Of Loads

The following brief review of load modelling was carried out in order to obtain an overview of the typical load models used in power system analysis. In contrast with the present work, load composition and behaviour is generally assumed to be unknown [10, 11, 12, 26]. Various models have been proposed to provide an approximate load representation. In this context, a load model can be defined as a mathematical relationship between a bus voltage (magnitude and frequency) and the power (active and reactive) or current flowing into the bus load [11]. A significant research effort has been directed at improving load modelling with most researchers being of the opinion that more accurate load models are required. The load

---

[5] The system is small when compared to systems with hundreds, if not thousands of busses and thousands of branches.

models are generally derived from measurements of small step disturbances on feeders or from large step tests of actual loads [26] or laboratory tests. These composite models and measured parameters are not valid for modelling industrial loads consisting mainly of induction motors, with tests having been conducted on equipment such as domestic appliances, air conditioners, power electronic equipment (< 10kVA) and fluorescent lighting. The models are also only valid for dynamic studies where voltages are above the minimum voltages used during laboratory tests [12], typically 0,5 to 0,87 pu. These models are not suitable for modelling the behaviour of the PetroSA system. In fact, there is little justification for using static models to represent induction motor loads, especially when modern computer capabilities and numerical techniques are considered [10].

Since the exact load composition and behaviour is known for the PetroSA system, more detailed models can be derived for all induction motors as required. For power systems analysis, the dynamics of induction motors are not considered important since the aim is to analyse the behaviour of the power system. Load models for these purposes are usually defined in terms of bus quantities, rather than motor internal flux, torques and currents [34]. In order to investigate the re-acceleration system performance, attention needs to be given not only to the response of the electrical system, but also to the possible effects on the mechanical equipment being driven by the various motors as well as the motors themselves.

The remainder of this section gives a brief summary of typical models in use [11].

2.6.1 Constant impedance load model

The Constant Impedance load model is a static load model where the power varies directly with the square of the voltage magnitude. This is also called a constant admittance load model.

2.6.2 Constant current load model

The Constant Current load model is a static load model where the power varies directly with the voltage magnitude.

2.6.3 Constant power load model

The Constant Power load model is a static load model where the power does not vary with changes in voltage magnitude. It may also be called a constant MVA model. This model is sometimes considered a conservative representation for induction motor loads, but should be used with caution [11]. The constant MVA characteristic is only true for the active part of the load and only above a certain voltage (80-90%). The reactive part of an induction motor load can be expected to increase as the voltage decreases beyond a certain value. In an attempt to overcome these shortcomings many load models provide for changing constant MVA to constant impedance or tripping the load below a specified voltage [21].

2.6.4 Polynomial load model (ZIP model)

The Polynomial load model is a static model representing the power relationship to voltage magnitude as a polynomial equation, usually as follows [11]:

$$P = P_0 \left[a_1 \left(\frac{V}{V_0} \right)^2 + a_2 \left(\frac{V}{V_0} \right) + a_3 \right]$$

$$Q = Q_0 \left[a_4 \left(\frac{V}{V_0} \right)^2 + a_5 \left(\frac{V}{V_0} \right) + a_6 \right]$$

(2-1)

where P, Q and V = input power, reactive power and bus voltage, respectively, P_0, Q_0 and V_0 = power, reactive power and bus voltage at the initial system operating condition for the study and a_1 to a_6 are model coefficients dependant upon the type of load being represented.

This model is also sometimes referred to as the "ZIP" model, since it consists of the sum of constant impedance (Z), constant current (I) and constant power (P) terms. An alternative form employed in several widely used transient stability programs is given by the relationship [10]:

$$\frac{P}{P_0} = \left[P_1 \left(\frac{V}{V_0} \right)^2 + P_2 \left(\frac{V}{V_0} \right) + P_3 \right] \left(1 + L_{DP} \Delta f \right)$$

(2-2)

where P and V = input power and bus voltage, respectively, P_0 and V_0 = power and bus voltage at the initial system operating condition for the study, L_{DP} = the frequency sensitivity parameter, Δf = the difference between bus frequency and nominal system frequency and P_1 to P_3 are model coefficients dependant upon the type of load being represented. This is the "ZIP" model multiplied by a linearized frequency dependent term.

2.6.5 Exponential load model

The Exponential load model is a static load model representing the power to voltage relationship as an exponential equation, usually in the following form [11]:

$$P = P_0 \left(\frac{V}{V_0} \right)^{np}$$

$$Q = Q_0 \left(\frac{V}{V_0} \right)^{nq}$$

(2-3)

where P,Q and V = input power, reactive power and bus voltage, respectively, P_0, Q_0 and V_0 = power, reactive power and bus voltage at the initial system operating condition for the study and exponents np and nq are model parameters dependant upon the type of load being represented. Two or more terms with different exponents are sometimes included in each equation. By setting the exponents to 0,1 or 2 , the load can be represented by constant power, constant current or constant impedance models, respectively. Other exponents are used to represent the aggregate effects of different load combinations or load components. Each equation can be multiplied by a frequency dependent term as in (2-3) above.

The frequency of the bus voltage is not an inherent variable in fundamental-frequency network analysis and is not used in many dynamic performance analysis programs. Bus frequency can be computed by taking the numerical derivative of the bus voltage angle.

2.6.6 Static load model for dynamic simulation

The following model is recommended by the IEEE [10] and used by Pereira *et al* [30]:

$$\frac{P}{P_{frac} P_0} = K_{pz} \left(\frac{V}{V_0} \right)^2 + K_{pi} \frac{V}{V_0} + K_{pc} + K_{p1} \left(\frac{V}{V_0} \right)^{n_{pv1}} \left(1 + n_{pf1} \Delta f \right) + K_{p2} \left(\frac{V}{V_0} \right)^{n_{pv2}} \left(1 + n_{pf2} \Delta f \right)$$

(2-4)

with

$$K_{pz} = 1 - \left(K_{pi} + K_{pc} + K_{p1} + K_{p2} \right)$$

(2-5)

where P and V = input power and bus voltage, respectively, P_{frac} = the fractional part of the bus load represented by the model, P_0 and V_0 = power and bus voltage at the initial system operating condition for the study, n_{pf1} and n_{pf2} are the frequency sensitivity parameters, Δf = the difference between bus frequency and nominal system frequency and K_{pi}, K_{pc}, K_{p1}, K_{p2}, n_{pv1} and n_{pv2} are model coefficients dependant upon the type of load being represented. Similarly, for reactive power:

$$\frac{Q}{Q_{frac}Q_0} = K_{qz}\left(\frac{V}{V_0}\right)^2 + K_{qi}\frac{V}{V_0} + K_{qc} + K_{q1}\left(\frac{V}{V_0}\right)^{n_{qv1}}\left(1+n_{qf1}\Delta f\right) +$$

$$K_{q2}\left(\frac{V}{V_0}\right)^{n_{qv2}}\left(1+n_{qf2}\Delta f\right)$$

(2-6)

with

$$K_{qz} = 1 - \left(K_{qi} + K_{qc} + K_{q1} + K_{q2}\right)$$

(2-7)

where *Q and V* = input reactive power and bus voltage, respectively, Q_{frac} = the fractional part of the bus load represented by the model, Q_0 *and* V_0 = reactive power and bus voltage at the initial system operating condition for the study, n_{qf1} and n_{qf2} are the frequency sensitivity parameters, Δf = the difference between bus frequency and nominal system frequency and $K_{qi}, K_{qc}, K_{q1}, K_{q2}, n_{qv1}$ and n_{qv2} are model coefficients dependant upon the type of load being represented. The above model consists of ZIP plus two voltage/frequency dependent terms. Provision should also be made to convert all static load to constant impedance at very low voltages (0.3p.u -0.7p.u.). This helps the solution to converge and is consistent with the physical fact that near nominal load cannot be consumed at abnormally low voltages [10].

2.7   System Equations

Two sets of equations need to be solved in transient stability calculations using a step-by-step approach [23]:

$$\dot{\underline{y}} = f\left(\underline{x},\underline{y}\right)$$

(2-8)

$$0 = g\left(\underline{x},\underline{y}\right)$$

(2-9)

Equation (2-8) consists of the differential equations for all machines and controls, whilst equation (2-9) comprises the network and non-dynamic load equations. $\underline{y}$ is a vector of state variables associated with the set of differential equations and $\underline{x}$ is a vector associated with the algebraic equations consisting of network bus voltages, voltage angles, bus power and bus reactive power.

The interaction of the models typically required to perform transient system analysis is shown in Figure 2-2, below [23].
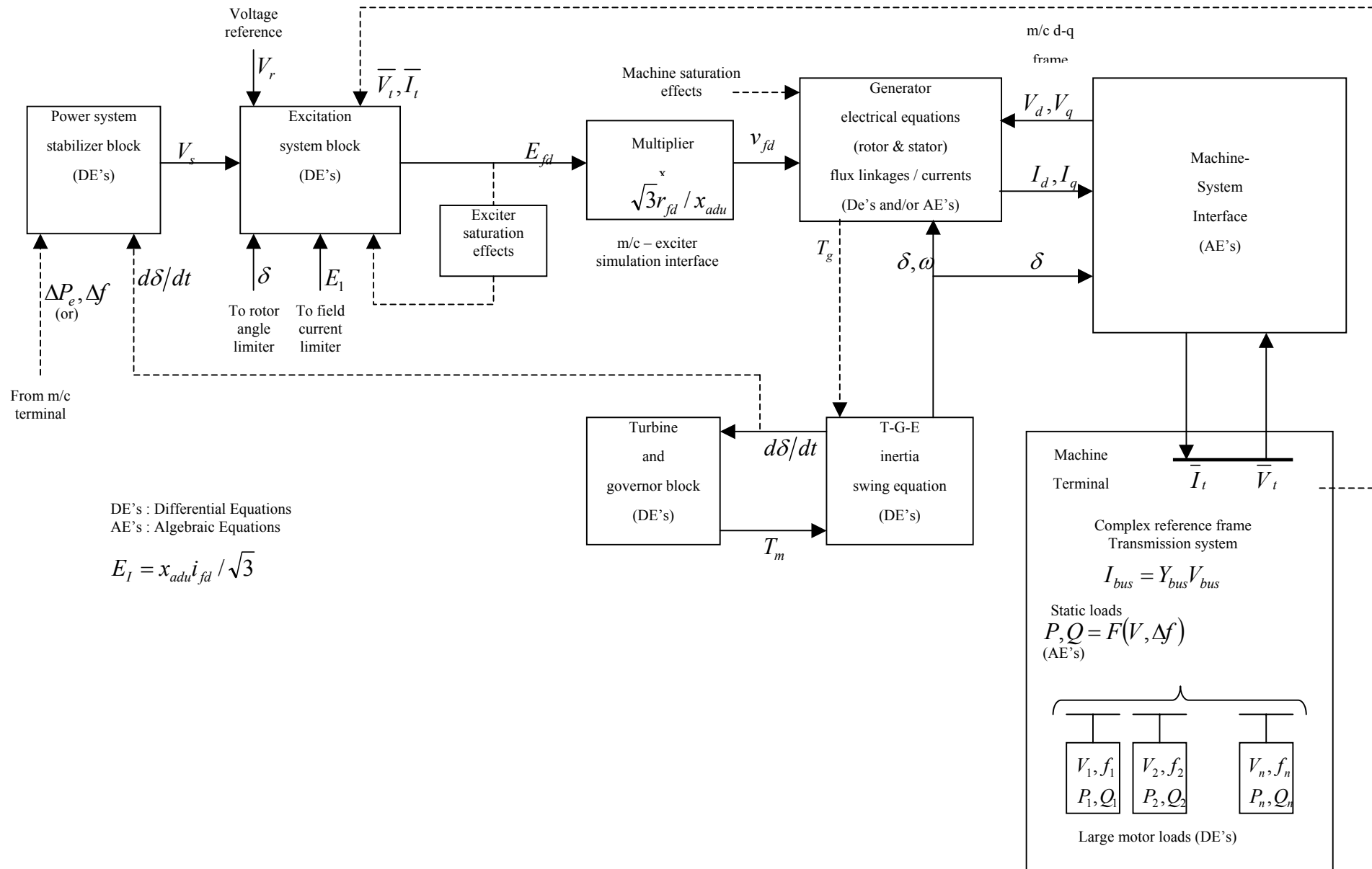
Figure 2-2 Block diagram showing interaction of models for transient stability studies [23].

2.8   Solution Of System Equations

There are two main approaches to the solution of the electrical system equations:

- The commonly used alternating-solution or partitioned approach
- The combined-solution or simultaneous approach.

It was necessary to choose between one of the above methods for the current work. The alternating-solution approach was chosen and the combined-solution method is therefore not discussed further.

2.8.1 The alternating solution approach

The usual method is to solve equation set (2-8) for y using numerical integration. Equation set (2-9) is then solved algebraically for x alternately at each time step. This does not reflect the true simultaneous nature of the solution resulting in accumulated errors. An overview of the scheme is given below [23]:

i)   Obtain the results of initial load-flow and establish the initial conditions at time $t = 0$.

ii)   Solve the differential equation set (2-8) for $y(t)$ by numerical integration techniques, using the value of x obtained from the loadflow solution.

iii)   Using the value of $y(t)$ from ii, solve the algebraic equations (2-9) for $x(t)$ using the Newton-Raphson technique.

iv)   Advance the time by one time step and go to step (ii)

A more accurate method is the following [23]:

i)   Obtain the results of initial load-flow and establish the initial conditions at time t = 0.

ii)   Predict how x behaves over the next interval of time by extrapolation techniques

iii)   Solve the differential equation set (2-8) for $y(t)$ by numerical integration techniques, using the interpolation formula obtained above to determine the behaviour of x.

iv)   Using the value of $y(t)$ from step(iii), solve the algebraic equations (2-9) for $x(t)$ using the Newton-Raphson technique.

v)   Correct the prediction for $x(t)$ over the interval *(t-h)* to t using the value of $x(t)$ from step(iv).

vi)   Solve the differential equation set (2-8) for $y(t)$ by numerical integration techniques, using the interpolation formula obtained above.

vii)   If the difference between the two successive solutions of $y(t)$ are negligible, proceed to step viii, otherwise go back to step (iv).

The first scheme was implemented, mainly to reduce software complexity.

2.9   Induction Motor Models

In order to investigate the effects of the re-acceleration system, a reasonably detailed induction motor model will be required. The models discussed in section 2.6 are not suitable. A model based on the direct solution of the machine equations using phase quantities was selected. An equivalent circuit-based model commonly used in stability programs was used as a reference model. The results obtained from the more complex model were compared to those obtained from the reference model to determine if the additional model complexity is justified.

Motor bus frequency should be used when computing slip and reactance parameters in induction motor models. Bus frequency can be computed by taking the time derivative of the bus voltage angle calculated at each simulation step during the loadflow solution. The proposed transient studies will investigate the behaviour of a total induction motor load of 2MVA. When compared to the rest of the PetroSA distribution system load of approximately 205MVA, any disturbances caused by a load of 2MVA should be negligible. It has been assumed that motor bus frequency is equal to system frequency. Motor models therefore use the system frequency and not the motor bus frequency.

2.9.1 Equivalent circuit models

Most stability programs include a dynamic induction motor model based on one or both of the following equivalent circuits [21, 23]:
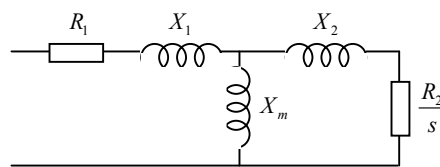
Figure 2-3 Single cage induction motor equivalent circuit [21].
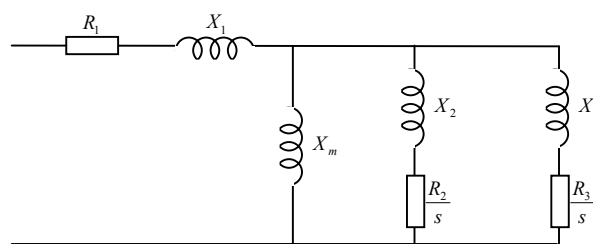
Figure 2-4 Double cage induction motor steady-state equivalent circuit [21].

The parameters for these models are defined as follows:

R_1 = Stator resistance

X_1 = Stator leakage reactance

X_2, X_3 = Rotor leakage reactance/s

R_2, R_3 = Rotor resistances

X_m = Magnetising reactance

Single cage induction motors have low starting torques. As a result of this, the single cage model is often not accurate enough. These problems can be overcome by the use of a double cage or deep bar rotor model. The use of double cage and deep bar models is often restricted by a lack of data [21]. A simple solution in such cases is to modify the torque-slip characteristic of the single-cage model. The rotor resistance is usually varied with slip and is easily done at each integration step of the simulation. A dynamic model based on the equivalent circuit shown in Figure 2-3 is commonly used for transient stability studies [21][23].

2.9.2 The d-q induction motor model

The induction motor model is based on the steady state equivalent circuit shown in Figure 2-5. The simplified model shown in Figure 2-6 is used for transient stability analysis. This model, referred to as the d-q model in this work, was considered accurate enough to serve as a reference model and used to evaluate the suitability of other models when applied to voltage stability studies [29].
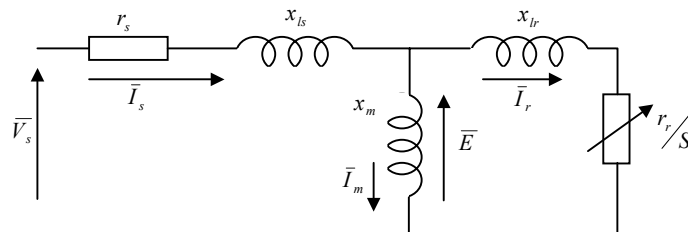
Figure 2-5 Steady-state equivalent circuit of an induction motor [23]
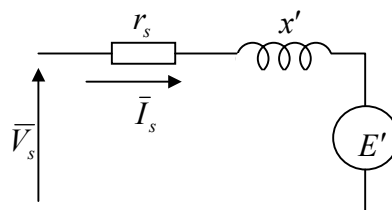
Figure 2-6 Simplified representation of induction motor for transient analysis [23,15]

The parameters for the models shown in Figure 2-5 and Figure 2-6 are defined as follows: [23]

r_s stator resistance

r_r rotor resistance (referred to stator)

x_{ls} stator leakage reactance

x_{lr} rotor leakage reactance at standstill (referred to stator)

x_m magnetising reactance

I_s stator current

I_r rotor current (referred to stator)

I_m magnetising current

V_s stator terminal voltage

E emf induced in the stator by the airgap flux = emf induced in rotor at standstill by airgap flux (referred to stator)

S Slip

E' transient voltage behind stator resistance and an equivalent reactance x'

x' transient reactance

The above definitions apply to equations (2-10) through (2-16)

For the d-q model the induction motor is modelled by the equivalent circuit shown in Figure 2-6 with a voltage E' (representing the instantaneous emf induced in the stator) behind the stator resistance and a transient reactance x'. This transient reactance is the apparent reactance when the rotor is locked stationary and is given by [21][23]:

$$x' = x_{ls} + \left(\frac{x_{lr} x_m}{x_{lr} + x_m} \right) \tag{2-10}$$

The rotor open circuit time constant is defined by [21][23]:

$$T_0' = \frac{(x_{lr} + x_m)}{2\pi f_0 r_r} \tag{2-11}$$

where f_0 = bus frequency (assumed equal to nominal system frequency). The open circuit reactance is given by [21][23]:

$$x_0 = x_{ls} + x_m \tag{2-12}$$

The reactances are unaffected by rotor position and the model is described in the synchronously rotating reference frame used for the network. The model is defined by the following equations [21][23]:

$$V_{\text{Re}} - E_{\text{Re}}' = r_s I_{\text{Re}} - x' I_{\text{Im}} \, , \tag{2-13}$$

$$V_{\text{Im}} - E_{\text{Im}}' = r_s I_{\text{Im}} + x' I_{\text{Re}} \, , \tag{2-14}$$

$$\frac{dE_{\text{Re}}'}{dt} = 2\pi f_0 S E_{\text{Im}}' - \left(E_{\text{Re}}' + (x_0 - x') I_{\text{Im}} \right) / T_0' \, , \tag{2-15}$$

and

$$\frac{dE_{\text{Im}}'}{dt} = -2\pi f_0 S E_{\text{Re}}' - \left(E_{\text{Im}}' - (x_0 - x') I_{\text{Re}} \right) / T_0' \tag{2-16}$$

where *Re* and *Im* denote *real* and *imaginary* axis quantities, S = slip and the remaining variables are defined above.

2.9.3 Mechanical equations

Unlike a synchronous machine, the equation of motion of an induction machine is expressed in terms of torque and not power. The angular position of the rotor is unimportant due to symmetry and slip is used in the model rather than angular velocity [21, 23], such that:

$$S = \frac{(\omega_0 - \omega)}{\omega_0} \qquad\qquad (2\text{-}17)$$

where ω_0 = system synchronous angular velocity and ω = instantaneous rotor angular velocity. If friction and windage losses are neglected and smooth shaft power assumed, the equation of motion is [21, 23]:

$$\frac{dS}{dt} = \frac{T_m - T_e}{2H_m} \qquad\qquad (2\text{-}18)$$

where T_m = mechanical torque, T_e = electrical torque and H_m is the inertia constant measured in kWs/kVA at synchronous speed. Mechanical torque is assumed to vary with speed according to the following characteristic:

$$T_m \propto (speed)^k \qquad\qquad (2\text{-}19)$$

with $k = 1$ for fan-type loads and $k = 2$ for centrifugal pumps.

2.9.4 The abc – induction motor model

The *abc* motor model is described in several textbooks [22, 23]. The various motor parameters are expressed in terms of phase quantities. The *abc* model involves time-varying inductance parameters, and is generally considered too difficult, or too time consuming to solve [23, 19, 14, 16], particularly in literature that is more than about five years old. The *dqo* model utilising Park's transform was developed to eliminate the time-varying induction parameters, and thus simplify the differential equations to be solved when modelling motor transient behaviour. With a modern computer[1], the solution of the state variable model no longer presents a formidable problem, and the simulation of a motor start-up generally takes less than one to two minutes to calculate. The use of the *abc* model eliminates the need for mathematical transformations between the *dqo* and *abc* reference frames. In addition, the physical significance of the various model parameters and quantities is more readily apparent in the *abc* model.

Implementation of this model using the built-in functionality of Matlab is relatively straightforward. It was decided to investigate the applicability of the *abc* model for simulation purposes and compare the results obtained to those of the *d-q* model described above to determine if the additional complexity is justified. A further aspect which can be directly investigated with this model is the validity of assuming that voltage dips occur on all three phases during simulations. Most voltage dips observed at PetroSA only occur on one phase, and this modelling approximation needs to be evaluated.

The following simplifying assumptions have been made:

- Both the rotor and stator can be described by balanced, three phase windings.
- The air-gap of the machine is uniform
- The stator and rotor windings are sinusoidally distributed and the established airgap MMF's are sinusoidal.
- The effects of saturation, eddy currents and hysteresis are neglected.
- The rotor magnetic paths are assumed to be symmetrical about the pole axes

---

[1] Pentium IV processor, 2.8GHz

2.9.5 Voltage equations

The voltage equations for a three-phase induction machine are given by [22]:

$$
\begin{bmatrix} V_{as} \\ V_{bs} \\ V_{cs} \\ V_{ar} \\ V_{br} \\ V_{cr} \end{bmatrix} =
\begin{bmatrix}
R_{as} & & & & & \\
& R_{bs} & & & & \\
& & R_{cs} & & & \\
& & & R_{ar} & & \\
& & & & R_{br} & \\
& & & & & R_{cr}
\end{bmatrix}
\begin{bmatrix} I_{as} \\ I_{bs} \\ I_{cs} \\ I_{ar} \\ I_{br} \\ I_{cr} \end{bmatrix} + p
\begin{bmatrix} \lambda_{as} \\ \lambda_{bs} \\ \lambda_{cs} \\ \lambda_{ar} \\ \lambda_{br} \\ \lambda_{cr} \end{bmatrix}
\tag{2-20}
$$

where p is the differential operator, R_{xx} are stator and rotor winding resistances, V_{xx} are stator and rotor winding voltages and I_{xx} are stator and rotor currents. The matrix equation for the flux linkages is given by [22]:

$$
\begin{bmatrix} \lambda_{as} \\ \lambda_{bs} \\ \lambda_{cs} \\ \lambda_{ar} \\ \lambda_{br} \\ \lambda_{cr} \end{bmatrix} =
\begin{bmatrix}
L_{asas} & L_{asbs} & L_{ascs} & L_{asar} & L_{asbr} & L_{ascr} \\
L_{bsas} & L_{bsbs} & L_{bscs} & L_{bsar} & L_{bsbr} & L_{bscr} \\
L_{csas} & L_{csbs} & L_{cscs} & L_{csar} & L_{csbr} & L_{cscr} \\
L_{aras} & L_{arbs} & L_{arcs} & L_{arar} & L_{arbr} & L_{arcr} \\
L_{bras} & L_{brbs} & L_{brcs} & L_{brar} & L_{brbr} & L_{brcr} \\
L_{cras} & L_{crbs} & L_{crcs} & L_{crar} & L_{crbr} & L_{crcr}
\end{bmatrix}
\begin{bmatrix} I_{as} \\ I_{bs} \\ I_{cs} \\ I_{ar} \\ I_{br} \\ I_{cr} \end{bmatrix}
\tag{2-21}
$$

where I_{as}, I_{bs}, I_{cs} are stator currents, I_{ar}, I_{br}, I_{cr} are rotor currents and the inductances are defined below.

2.9.6 Stator inductances

All stator inductances are equal as given by the relationships [22]

$$
L_{asas} = L_{bsbs} = L_{cscs} = L_{ls} + L_{ms}
\tag{2-22}
$$

where L_{ls} denotes the stator leakage inductance and is identical for all phases and L_{ms} is the stator magnetising inductance. The mutual inductance between any two stator windings is the same due to symmetry [22]:

$$
\begin{aligned}
L_{asbs} &= L_{bsas} = -0.5 L_{ms} \\
L_{bscs} &= L_{csbs} = -0.5 L_{ms} \\
L_{csas} &= L_{ascs} = -0.5 L_{ms}
\end{aligned}
\tag{2-23}
$$

where L_{ms} is the stator magnetising inductance and the subscripts denote between which stator windings the mutual inductance is defined..

2.9.7 Rotor inductances

Similar to the stator, the rotor self-inductances are given by the relationships [22]

$$
L_{arar} = L_{brbr} = L_{crcr} = L_{lr} + L_{mr}
\tag{2-24}
$$

where L_{lr} denotes the rotor leakage inductance and is identical for all phases and L_{mr} is the rotor magnetising inductance. The mutual inductances are given by [22]:

$$
\begin{aligned}
L_{arbr} &= L_{brar} = -0.5 L_{mr} \\
L_{brcr} &= L_{crbr} = -0.5 L_{mr} \\
L_{crar} &= L_{arcr} = -0.5 L_{mr}
\end{aligned}
\tag{2-25}
$$

where L_{mr} is the stator magnetising inductance and the subscripts denote between which rotor windings the mutual inductance is defined.

2.9.8 Mutual inductances between stator and rotor windings

The mutual inductance between a stator winding and any rotor winding varies sinusoidally with the rotor position [22]:

$$
\begin{aligned}
L_{asar} &= L_{bsbr} = L_{csc\,r} = L_{msr}\cos(\theta_r) \\
L_{ascr} &= L_{bsar} = L_{csbr} = L_{msr}\cos\left(\theta_r - \tfrac{2\pi}{3}\right) \\
L_{asbr} &= L_{bscr} = L_{csar} = L_{msr}\cos\left(\theta_r + \tfrac{2\pi}{3}\right)
\end{aligned}
\tag{2-26}
$$

where θ_r = rotor angle, L_{msr} denotes the mutual inductance between a rotor and stator winding when the rotor angle is such that the magnetic axes of the rotor and stator are aligned and the subscripts denote between which rotor and stator windings the mutual inductance is defined. By implication, the derivatives of these inductances with respect to time are present in the machine equations. Substitution of eq. (2-21) into eq. (2-20) gives the following[2] [22]:

$$
\begin{aligned}
[V] &= [R][I] + p[L][I] \\
&= [R][I] + \omega_r \tfrac{d[L]}{d\theta} + [L]\tfrac{d[I]}{dt}
\end{aligned}
\tag{2-27}
$$

The matrix $\frac{d[L]}{d\theta}$ is denoted by [G] and is called the rotational inductance matrix. The voltage equations for the motor can thus be expressed in terms of electrical circuit quantities, rotor position and rotational speed as [22]:

$$
[V_s] = [R_s][I_s] + [L_{ss}]p[I_s] + [L_{sr}]p[I_r] + \omega_r[G_{ss}][I_s] + \omega_r[G_{sr}][I_r]
\tag{2-28}
$$

$$
[V_r] = [R_r][I_r] + [L_{rs}]p[I_s] + [L_{rr}]p[I_r] + \omega_r[G_{rs}][I_s] + \omega_r[G_{rr}][I_r]
\tag{2-29}
$$

where subscript s relates to stator and r to rotor, $[I_s]$ = stator current vector, $[I_r]$ = rotor current vector, $[R_s]$ = stator resistance matrix, $[R_r]$ = rotor resistance matrix, ω_r = rotor angular velocity and the various inductance matrices are defined below.

Substitution of rotor and stator inductances into the inductance matrix in eq. (2-21) gives the following [22]:

$$
L = \begin{bmatrix}
L_{ls}+L_{ms} & -\tfrac{1}{2}L_{ms} & -\tfrac{1}{2}L_{ms} & L_{msr}\cos\theta_r & L_{msr}\cos\left(\theta_r+\tfrac{2\pi}{3}\right) & L_{msr}\cos\left(\theta_r-\tfrac{2\pi}{3}\right) \\
-\tfrac{1}{2}L_{ms} & L_{ls}+L_{ms} & -\tfrac{1}{2}L_{ms} & L_{msr}\cos\left(\theta_r-\tfrac{2\pi}{3}\right) & L_{msr}\cos\theta_r & L_{msr}\cos\left(\theta_r+\tfrac{2\pi}{3}\right) \\
-\tfrac{1}{2}L_{ms} & -\tfrac{1}{2}L_{ms} & L_{ls}+L_{ms} & L_{msr}\cos\left(\theta_r+\tfrac{2\pi}{3}\right) & L_{msr}\cos\left(\theta_r-\tfrac{2\pi}{3}\right) & L_{msr}\cos\theta_r \\
L_{msr}\cos\theta_r & L_{msr}\cos\left(\theta_r-\tfrac{2\pi}{3}\right) & L_{msr}\cos\left(\theta_r+\tfrac{2\pi}{3}\right) & L_{lr}+L_{mr} & -\tfrac{1}{2}L_{mr} & -\tfrac{1}{2}L_{mr} \\
L_{msr}\cos\left(\theta_r+\tfrac{2\pi}{3}\right) & L_{msr}\cos\theta_r & L_{msr}\cos\left(\theta_r-\tfrac{2\pi}{3}\right) & -\tfrac{1}{2}L_{mr} & L_{lr}+L_{mr} & -\tfrac{1}{2}L_{mr} \\
L_{msr}\cos\left(\theta_r-\tfrac{2\pi}{3}\right) & L_{msr}\cos\left(\theta_r+\tfrac{2\pi}{3}\right) & L_{msr}\cos\theta_r & -\tfrac{1}{2}L_{mr} & -\tfrac{1}{2}L_{mr} & L_{lr}+L_{mr}
\end{bmatrix}
$$

or

$$
L = \begin{bmatrix} L_{ss} & L_{sr} \\ L_{rs} & Lrr \end{bmatrix}.
$$

where the self and mutual inductance sub-matrices are given by:

---

[2] For Detailed derivation refer to Appendix D, 10.1

$$L_{ss} = \begin{bmatrix} L_{ls} + L_{ms} & -\frac{1}{2}L_{ms} & -\frac{1}{2}L_{ms} \\ -\frac{1}{2}L_{ms} & L_{ls} + L_{ms} & -\frac{1}{2}L_{ms} \\ -\frac{1}{2}L_{ms} & -\frac{1}{2}L_{ms} & L_{ls} + L_{ms} \end{bmatrix}$$ (2-30)

$$L_{rr} = \begin{bmatrix} L_{lr} + L_{mr} & -\frac{1}{2}L_{mr} & -\frac{1}{2}L_{mr} \\ -\frac{1}{2}L_{mr} & L_{lr} + L_{mr} & -\frac{1}{2}L_{mr} \\ -\frac{1}{2}L_{mr} & -\frac{1}{2}L_{mr} & L_{lr} + L_{mr} \end{bmatrix}$$ (2-31)

$$L_{srm} = L_{msr} \begin{bmatrix} \cos\theta_r & \cos(\theta_r + 2\pi/3) & \cos(\theta_r - 2\pi/3) \\ \cos(\theta_r - 2\pi/3) & \cos\theta_r & \cos(\theta_r + 2\pi/3) \\ \cos(\theta_r + 2\pi/3) & \cos(\theta_r - 2\pi/3) & \cos\theta_r \end{bmatrix}$$ (2-32)

$$L_{rs} = L_{sr}^T$$ (2-33)

The rotational inductance matrix, G is given by the following [22]:

$$G = -L_{srm} \begin{bmatrix} 0 & 0 & 0 & \sin\theta_r & \sin(\theta_r + \frac{2\pi}{3}) & \sin(\theta_r - \frac{2\pi}{3}) \\ 0 & 0 & 0 & \sin(\theta_r - \frac{2\pi}{3}) & \sin\theta_r & \sin(\theta_r + \frac{2\pi}{3}) \\ 0 & 0 & 0 & \sin(\theta_r + \frac{2\pi}{3}) & \sin(\theta_r - \frac{2\pi}{3}) & \sin\theta_r \\ \sin\theta_r & \sin(\theta_r - \frac{2\pi}{3}) & \sin(\theta_r + \frac{2\pi}{3}) & 0 & 0 & 0 \\ \sin(\theta_r + \frac{2\pi}{3}) & \sin\theta_r & \sin(\theta_r - \frac{2\pi}{3}) & 0 & 0 & 0 \\ \sin(\theta_r - \frac{2\pi}{3}) & \sin(\theta_r + \frac{2\pi}{3}) & \sin\theta_r & 0 & 0 & 0 \end{bmatrix}$$ (2-34)

or

$$G = \begin{bmatrix} 0 & G_{sr} \\ \hline G_{rs} & 0 \end{bmatrix}.$$ (2-35)

where

$$G_{sr} = -L_{srm} \begin{bmatrix} \sin\theta_r & \sin(\theta_r + 2\pi/3) & \sin(\theta_r - \frac{2\pi}{3}) \\ \sin(\theta_r - \frac{2\pi}{3}) & \sin\theta_r & \sin(\theta_r + 2\pi/3) \\ \sin(\theta_r + 2\pi/3) & \sin(\theta_r - \frac{2\pi}{3}) & \sin\theta_r \end{bmatrix}$$ (2-36)

and

$$G_{rs} = G_{st}^T.$$ (2-37)

This allows equations (2-28) and (2-29) to be rewritten as follows [22]:

$$[V_s] = [R_s][I_s] + [L_{ss}]p[I_s] + [L_{sr}]p[I_r] + \omega_r[G_{sr}][I_r]$$ (2-38)

and

$$[V_r] = [R_r][I_r] + [L_{rs}]p[I_s] + [L_{rr}]p[I_r] + \omega_r[G_{rs}][I_s].$$ (2-39)

2.9.9 Torque and power

The air-gap torque T_e produced by an electrical machine is given by [22]:

$$T_e = [I]^T [G][I].$$ (2-40)

where $[I]$ denotes the stator and rotor current vector and $[G]$ denotes the rotational inductance matrix defined in eq. (2-34)

The instantaneous power P_e received by the motor is given by [22]:

$$P_e = V_{as}I_{as} + V_{bs}I_{bs} + V_{cs}I_{cs}$$ (2-41)

where V and I denote stator voltages and currents as identified by the subscripts.

The instantaneous reactive power Q_e is given by [22]:

$$Q_e = \tfrac{1}{\sqrt{3}}\left(V_{as}(I_{bs} - I_{cs}) + V_{bs}(I_{cs} - I_{as}) + V_{cs}(I_{as} - I_{bs})\right)$$ (2-42)

where V and I denote stator voltages and currents as identified by the subscripts.

2.9.10 Inertia constant and mechanical equations

The mechanical equation of motion is expressed as [22]:

$$\tfrac{d}{dt}\omega_r = \frac{1}{2H}\left(T_e - T_o\right)$$ (2-43)

where T_e is the electromagnetic torque which is produced to overcome the load torque T_o. The inertia constant H is defined as [22]:

$$H = \frac{J\omega_{base(m)}^2}{2P_{base}} = (n)^2 \cdot \frac{J\omega_{base(e)}^2}{2P_{base}}$$ (2-44)

where n is the number of pole pairs, $\omega_{base(m)}$ = synchronous speed in mechanical rad/s, $\omega_{base(e)}$ = synchronous speed in electrical rad/s, P_{base} = base power for p.u. system and J = the moment of inertia of the rotating mass(kg m^2).

2.10 Parameter Estimation

The major difficulty encountered when attempting to construct a mathematical model of a motor is the unavailability of accurate performance data, especially for motors with lower power ratings. This data is needed to determine the values of the various parameters used in the mathematical model.

At PetroSA there are limited adequate datasheets available for the larger motors, with minimal data on smaller motors. A summary of typical motor data available is given in Appendix C.

Unfortunately, there is no data available for the smaller motors, apart from nameplate data. Manufacturer's representatives have also been unable to supply any data. It is therefore necessary to resort to estimation of parameters and comparison of results predicted by the motor model with field measurements.

2.10.1 Field measurements

Due to the operational nature of the plant, access to equipment for test purposes is severely restricted. Virtually all motors are installed in classified areas, which precludes using any test equipment in the field, or any field connections for measurement purposes. All measurements have to be carried out from within the substations. Most of the motors on the PetroSA plant have an installed spare with at least two (or more) motors being available. These motors are designated 'A', 'B', 'C', etc. One of these motors is normally idle, whilst the other is running.

The only test which can be carried out while the plant is operational, is to start a motor and measure motor currents and busbar voltages. This test can easily be carried out when routine changeovers between 'A' and 'B' motors are made[3]. The loading on the motor will also differ from that encountered following a voltage dip in most cases, but actual loading cannot be simulated. Simulation of a power dip is also clearly out of the question (even on 1 motor), due to the possibility of causing a process upset, and incurring the associated financial losses.

For safety reasons, it is not possible to carry out measurements on the 525V motors. Such measurements require opening the MCC door to install current probes. The drive then has to be started with the MCC door open, and the current probes removed while the circuit is energised. In the majority of cases, production personnel are not able to start and then immediately stop a motor without risking a process upset. The safety risks associated with taking this type of measurement are unacceptable and it will be necessary to estimate parameters for these motors.

Tests can be carried out on medium voltage motors, because the CT secondary circuits are accessible in the protection panels.

---

[3] Changeovers are required between running motors and idle motors to prevent damage to the idle motor and associated equipment. Typical problems encountered if this is not done are brinelling of bearings, failure of pump seals and corrosion.

2.10.2 Equivalent circuit and torque/slip relation

The parameters of the per phase equivalent circuit shown in Figure 2-7 are the following: R_s = stator resistance, X_s = stator reactance, L_0 = magnetising reactance, R_0 = resistance representing core losses, X'_s = rotor reactance referred to the stator and R'_r = rotor resistance referred to the stator.
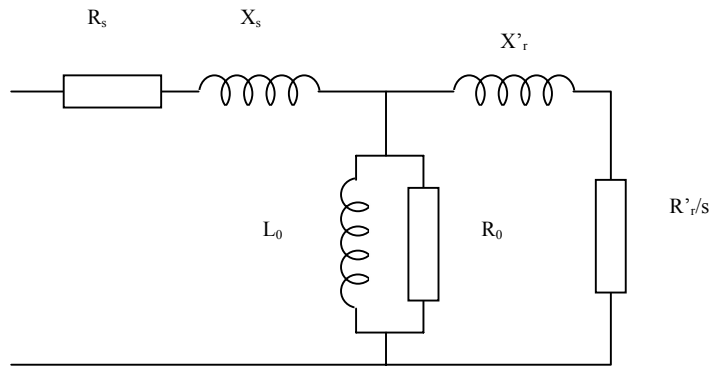
Figure 2-7 Induction motor equivalent circuit [16].

Note that in the equations derived below, the apostrophe, which is used to designate a rotor quantity which has been referred to the stator are omitted. All rotor quantities are assumed to have been referred to the stator, unless stated otherwise. The mechanical output per phase, P_M is represented by a rotor resistance whose value varies with slip:

$$P_M = I_r^2 \left(\tfrac{1-s}{s} \right) R_r \tag{2-45}$$

where I_r denotes rotor current, R_r denotes rotor resistance and s denotes slip. The core losses can be grouped with the friction and windage losses and R_0 removed, giving the equivalent circuit shown in Figure 2-8:
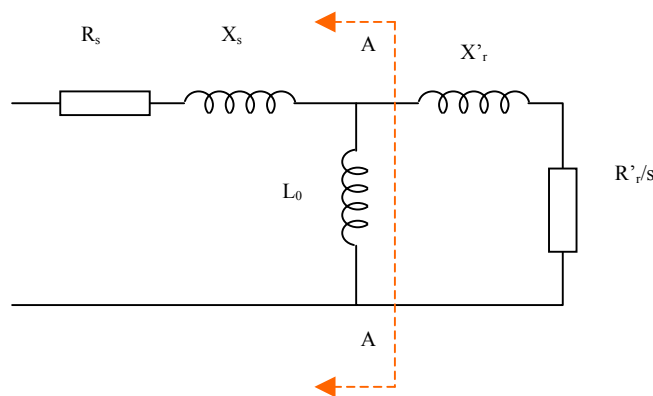
Figure 2-8 Simplified induction motor equivalent circuit [16].

The Thevenin equivalent circuit is determined for the portion of the circuit to the left of A-A in Figure 2-8, and the following expression for gross torque can be derived[4] [16]:

---

[4] Refer to Appendix D, 10.2 for detailed derivation

$$\tau = \frac{m E_{TH}^2 R_r'}{s \omega_s \left[\left(R_{TH} + \frac{R_r'}{s} \right)^2 + (X_{TH} + X_r')^2 \right]} \, Nm \qquad \textbf{(2-46)}$$

where m denotes the number of phases, ω_s denotes synchronous speed and E_{TH}, R_{TH} and X_{TH} are the thevenin equivalent voltage, resistance and reactance respectively.

2.10.3 Torque/slip relation

When the slip $= 0$

$$\frac{R_r'}{s} \rightarrow \infty$$

and equation (2-46) gives [16]:

$$\tau \approx \frac{m E_{TH}^2 R_r'}{s \omega_s \left(\frac{R_r'}{s} \right)^2}$$

$$\approx \frac{m E_{TH}^2}{\omega_s R_r'} s \qquad \textbf{(2-47)}$$

i.e. torque is proportional to slip.

When the slip $= 1$: $R_{TH} + \frac{R_r'}{s} \ll (X_{TH} + X_r')^2$ and equation (2-46) gives [16]:

$$\tau \approx \frac{m E_{TH}^2 R_r'}{s \omega_s (X_{TH} + X_r')^2}$$

ie

$$\tau \propto \frac{1}{s} \qquad \textbf{(2-48)}$$

i.e. torque is inversely proportional to slip. The maximum torque is given when $\frac{d\tau}{ds} = 0$. Taking the derivative of equation. (2-46) allows the following to be derived[5] [16]:

$$\tau_{MAX} = \frac{K R_r'}{s_m} \cdot \frac{1}{\left(R_{TH} + \frac{R_r'}{s} \right)^2 + X^2}$$

$$= \frac{K}{2 \left[\left(R_{TH}^2 + X^2 \right)^{\frac{1}{2}} + R_{TH} \right]} \qquad \textbf{(2-49)}$$

where

$$X = X_{TH} + X_r'$$

and

$$K = \frac{m E_{TH}^2}{\omega_s} .$$

Starting torque is obtained when s = 1, hence [16]

---

[5] Refer to Appendix D, 10.3 for detailed derivation

$$\tau_{start} = \frac{KR_r'}{\left(R_{TH} + R_r'\right)^2 + \left(X_{TH} + X_r'\right)^2} \qquad \text{(2-50)}$$

The above relations can be used to deduce the form of the torque-speed curve as follows. From standstill, the torque will increase from the starting torque value in inverse proportion to slip. As the maximum torque is approached, torque will increase less rapidly until the maximum torque is reached. As the speed continues to increase, torque will start decreasing in proportion to the slip.
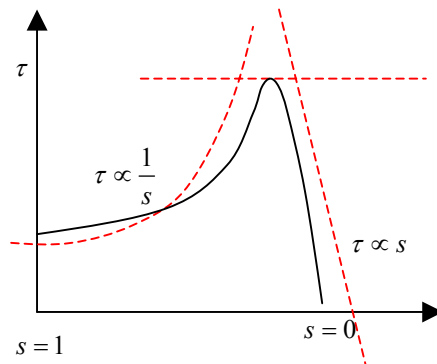
Figure 2-9 Torque/slip relation [16].

The above relations may be used to check if estimates of motor equivalent circuit parameters are reasonable.

2.10.4 Approximate parameter estimation.

Derivation of equivalent circuit parameters is discussed in textbooks dealing with induction machine theory [16, 14, 15, 24]. The following method based on these discussions is used to derive the equivalent circuit parameters for motors where only nameplate data is available. The motor model will obviously only be able to provide an approximate performance prediction when using these parameters.

Given the output power P_{out} and the rated speed ω_r of the motor, the output torque τ is calculated [16]:

$$\tau = \frac{P_{out}}{\omega_r} \qquad \text{(2-51)}$$

The airgap flux is rotating at synchronous speed, and exerts torque on the rotor. The airgap power is thus [16]:

$$P_{ag} = \omega_s \tau \qquad \text{(2-52)}$$

where ω_s = synchronous speed and τ = output torque as calculated above.

This is an approximation of the airgap power, since output (or shaft) torque is used and not mechanical torque. The friction and windage losses are therefore not accounted for. If desired, friction and windage can be estimated based on the size of the motor and added to the output torque to provide an estimate of the mechanical torque. This estimated torque is then used in the above equation rather than the output torque.

The rotor copper loss P_r can then be determined by subtracting the output power P_{out} from the airgap power P_{ag}:

$$P_r = P_{ag} - P_{out} \qquad \text{(2-53)}$$

The approximate stator power loss (copper and iron losses) is estimated by subtracting the airgap power from the input power P_{in}:

$$P_{stator} = P_{in} - P_{ag}$$
$$= \sqrt{3} V_s I_s - P_{ag} \tag{2-54}$$

It is further assumed that all stator losses are due to the stator winding resistance. Iron losses are thus included with the stator copper losses. The stator resistance can be calculated as follows:

$$R_s = \frac{P_{stator}}{3 I_{fl}^2} \tag{2-55}$$

where I_{fl} denotes motor full load current. At full load, the equivalent circuit input impedance is given by [16]:

$$Z_{in} = \frac{V_{phase}}{I_{fl}^2 \cos(\varphi)} \tag{2-56}$$
$$= R + jX$$

where, from Figure 2-8. the following equations are derived if it is assumed that the impedance of L_0 is high enough to be considered an open circuit.

$$R = R_s + \frac{R_r'}{s} \tag{2-57}$$

and

$$X = X_s + X_r'. \tag{2-58}$$

The slip can be calculated at rated speed allowing the rotor resistance to be calculated. For Nema type motors, the relationship between stator and rotor reactances can be estimated from the following table:

Table 2-1 Rotor/stator reactances for nema motors [24].

Nema Type	Stator Reactance	Rotor Reactance
Class A, D & wound rotor	0.5X	0.5X
Class B	0.4X	0.6X
Class C	0.3X	0.7X

The no-load current is usually specified, or can be easily determined allowing L_0 and R_0 to be estimated. The rotor current is assumed to be negligible allowing the following simplified equivalent circuit to be derived from Figure 2-8[6] where V_l = nominal line voltage and R_s, X_s are stator parameters as derived above:

---

[6] Note, that the core losses were grouped with the stator copper losses and R_0 omitted in Figure 2-8. Here core losses are represented by R_0 in parallel with L_0 giving the impedance $Z_0 = \frac{R_0 j X_0}{R_0 + j X_0}$.
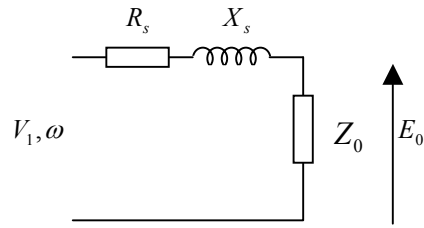
Figure 2-10 Equivalent circuit for no-load.

Since V_1, Rs, Xs and the no-load current are known, Z_0 can be calculated.

2.10.5 Relationship between equivalent circuit and model parameters

The parameters used in the *abc* model are related to the equivalent circuit parameters as follows [22]:

L_{sl} = *stator leakage inductance*
L_m = *stator magnetising inductance*

L'_{rl} = *referred rotor leakage inductance*

R_s = *stator resistance*

R'_r = *rotor resistance*

The model parameters are given by the relationships [22]

$$L_{ss} = L_{sl} + L_m$$
$$L_{rr} = L'_{rl} + L_m$$
$$M_s = M_r = -\tfrac{1}{2} L_m$$
$$M_{sr} = L_m$$

(2-59)

where L_{ss} = stator self inductance, L_{rr} = rotor self inductance, M_s = stator mutual inductance, M_r = rotor mutual inductance and M_{sr} = stator/rotor mutual inductance.

2.11 Synchronous Generator Models

The general mathematical description of the synchronous machine is presented in the *abc*-frame. The model is then presented in the *dqo*-frame using Park's transform. The 'standard' two axis models typically used for stability studies are then derived.

2.11.1 Inductances in the abc-frame [23]

A three phase synchronous machine consists of three windings on the stator and one field winding on the rotor. There are also several damper bars embedded in the rotor connected together at the ends by means of continuous rings or segments. Since all synchronous machines in use at PetroSA utilise cylindrical rotors, salient pole machines will not be considered. As discussed in chapter 4, only the main generator installed at PetroSA will be modelled, thus all equations will be written as for generators.

The magnetic axis of the field winding is defined as the *direct axis* or *d*-axis. Since the field winding is excited by direct current, the main field winding flux is established along the *d*-axis. The axis of symmetry midway between the poles is called the interpole or quadrature axis, abbreviated to *q*-axis, located 90 electrical degrees from the *d*-axis. The rotor flux induces an electromotive force in the stator windings. Since this emf leads the flux by 90 degrees, the machine voltage will appear primarily along the *q*-axis. Figure 2-1 describes such a machine from the circuit theory point of view.

The field winding is shown placed on the d-axis in Figure 2-11. A number of equivalent rotor windings are placed along the d and q-axes to represent the effects of induced currents in damper bars as well as in the solid rotor body. The various winding resistances, self and mutual inductances are represented. The coupling between phase windings and the rotor circuits as well as some of the mutual inductances are not shown for the sake of clarity. The positive direction of rotation is counter-clockwise and positive angle θ is measured from the axis of phase a to the d-axis in the direction of rotation. The d-axis leads the q-axis. Current directions in Figure 2-11 are shown for generator action.

The flux linkages for the various windings are given by [22, 23]:

$$
\begin{bmatrix} \psi_a \\ \psi_b \\ \psi_c \\ \psi_{fd} \\ \psi_{1d} \\ \vdots \\ \psi_{nd} \\ \psi_{1q} \\ \vdots \\ \psi_{nq} \end{bmatrix} = \begin{bmatrix} L_{aa} & L_{ab} & L_{ac} & L_{afd} & L_{a1d} & \cdots & L_{and} & L_{a1q} & \cdots & L_{anq} \\ L_{ba} & L_{bb} & L_{bc} & L_{bfd} & L_{b1d} & \cdots & L_{bnd} & L_{b1q} & \cdots & L_{bnq} \\ L_{ca} & L_{cb} & L_{cc} & L_{cfd} & L_{c1d} & \cdots & L_{cnd} & L_{c1q} & \cdots & L_{cnq} \\ L_{fda} & L_{fdb} & L_{fdc} & L_{ffd} & L_{f1d} & \cdots & L_{fnd} & L_{fd1q} & \cdots & L_{fdnq} \\ L_{1da} & L_{1db} & L_{1dc} & L_{1fd} & L_{11d} & \cdots & L_{1nd} & L_{1d1q} & \cdots & L_{1dnq} \\ \vdots & \vdots & \vdots & \vdots & \vdots & \vdots & \vdots & \vdots & \vdots & \vdots \\ L_{nda} & L_{ndb} & L_{ndc} & L_{nfd} & L_{n1d} & \cdots & L_{nnd} & L_{nd1q} & \cdots & L_{ndnq} \\ L_{1qa} & L_{1qb} & L_{1qc} & L_{1qfd} & L_{1q1d} & \cdots & L_{1qnd} & L_{11q} & \cdots & L_{1nq} \\ \vdots & \vdots & \vdots & \vdots & \vdots & \vdots & \vdots & \vdots & \vdots & \vdots \\ L_{nqa} & L_{nqb} & L_{nqc} & L_{nqfd} & L_{nqnd} & \cdots & L_{nqnd} & L_{n1q} & \cdots & L_{nnq} \end{bmatrix} \begin{bmatrix} i_a \\ i_b \\ i_c \\ i_{fd} \\ i_{1d} \\ \vdots \\ i_{nd} \\ i_{1q} \\ \vdots \\ i_{nq} \end{bmatrix}
\tag{2-60}
$$

or in matrix format

$$[\psi] = [\mathbf{L}][\mathbf{i}] \tag{2-61}$$

where the inductances are identified by combining the following subscripts:

- *a,b,c* denote stator windings
- *fd* denotes the field winding

- *1d, 2d, .. ,nd* denote direct axis damper windings

- *1q, 2q,..,nq* denotes quadrature axis damper windings

For example: L_{aa} denotes stator phase *a* self inductance, $L_{afd} = L_{fda}$ denotes the mutual inductance between stator phase a and the field winding. Self inductances are written L_{ffd} and L_{11d} and not L_{fdfd} or L_{1d1d}.

In eq.(2-60) all diagonal elements are self-inductances of windings and off diagonal elements are mutual inductances between windings. All voltages, currents and flux linkages are assumed to be instantaneous values. Since the *d* and *q* axes are orthogonal there will be no mutual inductance between the respective windings on these axes, allowing eq. (2-60) to be re-written as follows [23, 22]:

$$
\begin{bmatrix} \mathbf{\psi_S} \\ \mathbf{\psi_{Rd}} \\ \mathbf{\psi_{Rq}} \end{bmatrix} = \mathbf{L} \begin{bmatrix} \mathbf{i_S} \\ \mathbf{i_{Rd}} \\ \mathbf{i_{Rq}} \end{bmatrix} = \begin{bmatrix} \mathbf{L_S} & \mathbf{L_{SRd}} & \mathbf{L_{SRq}} \\ \mathbf{L_{SRd}^T} & \mathbf{L_{Rd}} & \mathbf{O_{(n+1)xn}} \\ \mathbf{L_{SRq}^T} & \mathbf{O_{nx(n+1)}} & \mathbf{L_{Rq}} \end{bmatrix} \begin{bmatrix} \mathbf{i_S} \\ \mathbf{I_{Rd}} \\ \mathbf{i_{Rq}} \end{bmatrix}
\tag{2-62}
$$

where

$\mathbf{\psi_s}$ denotes the vector of stator flux linkages

$\mathbf{\psi_{Rd}}$ denotes the vector of rotor flux linkages in the *d*-axis

$\mathbf{\psi_{Rq}}$ denotes the vector of rotor flux linkages in the *q*-axis

$\mathbf{i_s}$ denotes the vector of stator (or phase) currents

$\mathbf{i_{Rd}}$ denotes the vector of rotor currents in the *d*-axis circuits

$\mathbf{i_{Rq}}$ denotes the vector of rotor currents in the *q*-axis circuits

$\mathbf{L_S}$ denotes the matrix of self and mutual inductances of the three phase windings in the stator

$\mathbf{L_{SRd}}$ denotes the matrix of mutual inductances between the stator windings and rotor windings in the *d*-axis

$\mathbf{L_{SRq}}$ denotes the matrix of mutual inductances between the stator windings and rotor windings in the *q*-axis

$\mathbf{L_{Rd}}$ denotes the matrix of self and mutual inductances of all the rotor windings on the *d*-axis

$\mathbf{L_{Rq}}$ denotes the matrix of self and mutual inductances of all the rotor windings on the *q*-axis

On the assumption that the effects of stator slots and saturation can be neglected, the following sub matrices in eq. (2-62) are considered constant [22, 23]:

- $\mathbf{L_{Rd}}$ = all self and mutual inductances of rotor windings on the *d-axis*

- $\mathbf{L_{Rq}}$ = all self and mutual inductances of rotor windings on the *q-axis*

- $\mathbf{L_S}$ = all self and mutual stator winding inductances. Note that this is only true if the machine is assumed to have a smooth round rotor.

These sub-matrices with constant elements are given by:

$$
\mathbf{L_S} = \begin{bmatrix} L_s & -M_s & -M_s \\ -M_s & L_s & -M_s \\ -M_s & -M_s & L_s \end{bmatrix}
\tag{2-63}
$$

$$\mathbf{L_{Rd}} = \begin{bmatrix} L_f & M_{f1d} & M_{f2d} & \cdots & M_{fnd} \\ M_{1df} & L_{1d} & M_{1d2d} & \cdots & M_{1dnd} \\ M_{2df} & M_{2d1d} & L_{2d} & \cdots & M_{2dnd} \\ \vdots & \vdots & \vdots & \vdots & \vdots \\ M_{ndf} & M_{nd1d} & M_{nd2d} & \cdots & L_{nd} \end{bmatrix} \qquad \textbf{(2-64)}$$

$$\mathbf{L_{Rq}} = \begin{bmatrix} L_{1q} & M_{1q2q} & \cdots & M_{1qnq} \\ M_{2q1q} & L_{2q} & \cdots & M_{2qnq} \\ \vdots & \vdots & \vdots & \vdots \\ M_{nq1q} & M_{nq2q} & \cdots & L_{nq} \end{bmatrix} \qquad \textbf{(2-65)}$$

where L_s denotes the stator self inductance and M_s denotes the mutual inductance between stator windings in matrix $\mathbf{L_s}$. The elements of matrices $\mathbf{L_{Rd}}$ and $\mathbf{L_{Rq}}$ are the same inductances as shown in equations (2-60) and (2-62) but with self inductances designated by L_{xx} and mutual inductances by M_{xx}.

The remaining inductance values are periodic functions of the rotor position θ, given by the following [22, 23]:

$$\mathbf{L_{SRd}} = \mathbf{L_{RSd}^T} = \begin{bmatrix} M_{afd}\cos\theta & M_{a1d}\cos(\theta) & \cdots & M_{and}\cos\theta \\ M_{afd}\cos(\theta - \frac{2\pi}{3}) & M_{a1d}\cos(\theta - \frac{2\pi}{3}) & \cdots & M_{and}\cos(\theta - \frac{2\pi}{3}) \\ M_{afd}\cos(\theta + \frac{2\pi}{3}) & M_{a1d}\cos(\theta + \frac{2\pi}{3}) & \cdots & M_{and}\cos(\theta + \frac{2\pi}{3}) \end{bmatrix} \qquad \textbf{(2-66)}$$

$$\mathbf{L_{SRq}} = \mathbf{L_{RSq}^T} = \begin{bmatrix} M_{a1q}\sin\theta & \cdots & M_{anq}\sin\theta \\ M_{a1q}\sin(\theta - \frac{2\pi}{3}) & \cdots & M_{anq}\sin(\theta - \frac{2\pi}{3}) \\ M_{a1q}\sin(\theta + \frac{2\pi}{3}) & \cdots & M_{anq}\sin(\theta + \frac{2\pi}{3}) \end{bmatrix} \qquad \textbf{(2-67)}$$

where M_{xx} denotes mutual inductances identified by combining the following subscripts:

- *a,b,c* denote stator windings
- *fd* denotes the field winding
- *1d, 2d, .. ,nd* denote direct axis damper windings
- *1q, 2q,..,nq* denotes quadrature axis damper windings

for example: M_{afd} = the mutual inductance between the stator winding *a* and the field winding.

Figure 2-11 describes the synchronous machine from the circuit theory point of view and illustrates the interrelationships between the various windings used to model the machine.
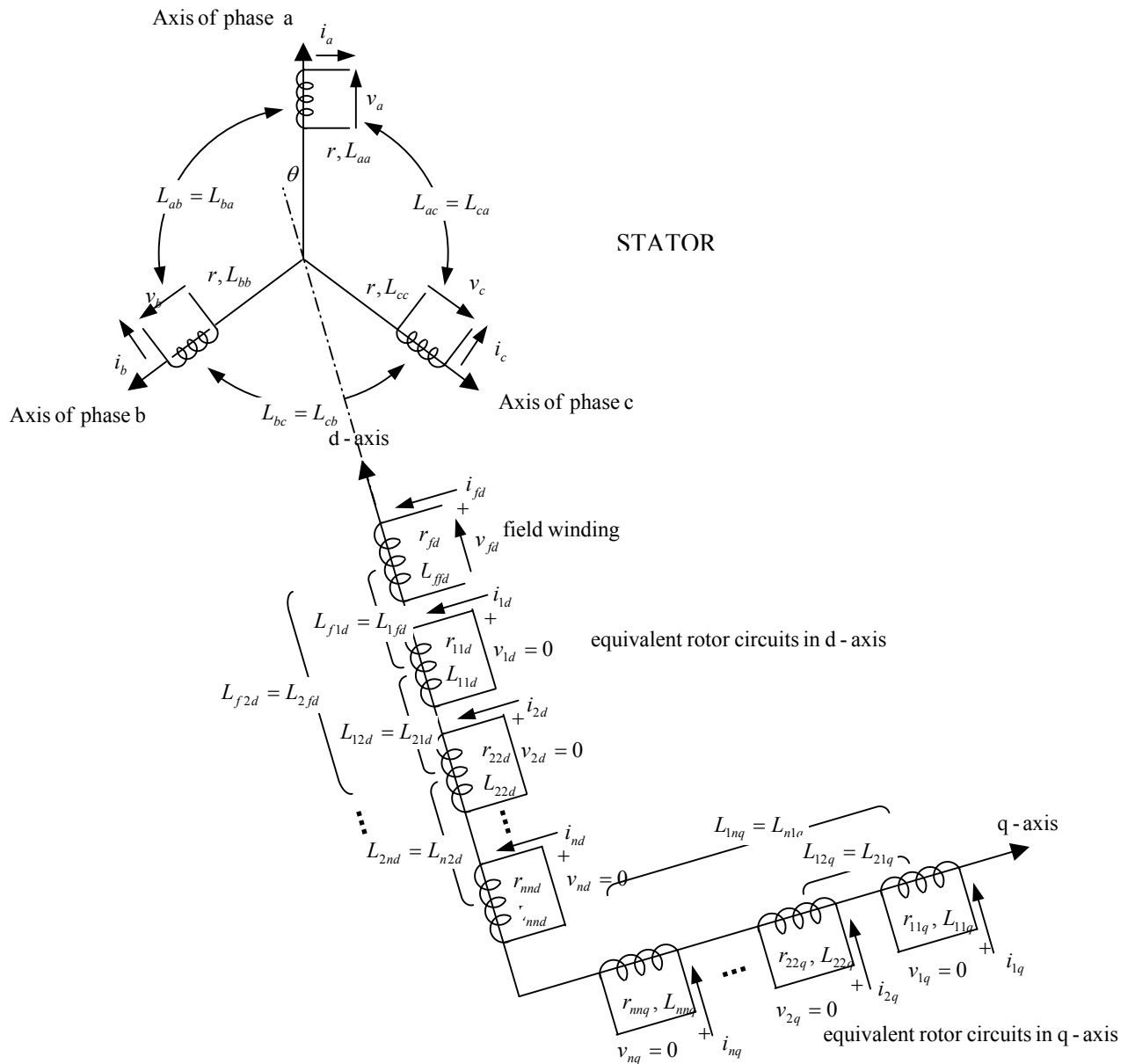
Figure 2-11 Synchronous machine representation for model development [23].

With reference to Figure 2-11, the voltage equations for the stator are [22, 23]:

$$\frac{d\psi_a}{dt} = -(v_a + ri_a)$$

$$\frac{d\psi_b}{dt} = -(v_b + ri_b) \tag{2-68}$$

$$\frac{d\psi_c}{dt} = -(v_c + r_{ic})$$

2.11.2 Rotor and stator voltage equations in abc frame

The voltage equations for the rotor (*d-axis*) are [23, 22]:

$$\frac{d\psi_{fd}}{dt} = \left(v_{fd} - r_{fd}i_{fd}\right)$$

$$\frac{d\psi_{1d}}{dt} = -\left(r_{11d}i_{1d} + r_{12d}i_{2d} + r_{13d}i_{3d} + \cdots + r_{1nd}i_{nd}\right) \tag{2-69}$$

$$\vdots$$

$$\frac{d\psi_{nd}}{dt} = -\left(r_{n1d}i_{1d} + r_{n2d}i_{2d} + r_{n3d}i_{3d} + \cdots + r_{nnd}i_{nd}\right)$$

The first equation corresponds to the field winding while the rest correspond to the *n* equivalent rotor circuits on the *d-* axis. Note that the equivalent rotor circuits on the *d* and *q*-axis representing the solid rotor body and damper windings are both inductance and resistance coupled. The resistances in eq. (2-69) denote the mutual effects between circuits. Under transient conditions, when the rotor is either accelerating or decelerating, slip frequency currents are induced in these equivalent rotor circuits and they contribute to electrical damping, helping to restore stable operation. During steady state, synchronous operation, the currents in these circuits are zero. Similarly, the voltage equations for the rotor (*q-axis*) are [23]:

$$\frac{d\psi_{1q}}{dt} = -\left(r_{11q}i_{1q} + r_{12q}i_{2q} + r_{13q}i_{3q} + \cdots + r_{1nq}i_{nq}\right)$$

$$\vdots \tag{2-70}$$

$$\frac{d\psi_{nq}}{dt} = -\left(r_{n1q}i_{1q} + r_{n2q}i_{2q} + r_{n3q}i_{3q} + \cdots + r_{nnq}i_{nq}\right)$$

From equation (2-61), the following is obtained[7] [23, 22]:

$$\frac{d\boldsymbol{\psi}}{dt} = \omega\mathbf{G}\mathbf{I} + \mathbf{L}\frac{d\mathbf{I}}{dt} \tag{2-71}$$

Where the matrix **G** exhibits rotating performance of the machine and is called the rotational inductance matrix. Up to this point, it has been assumed that there are *n* equivalent circuits on the rotor *d* and *q*-axes respectively. From this point onwards it is assumed that there is only one equivalent circuit on each rotor axis.

This gives the rotational inductance matrix as:

$$\mathbf{G} = \begin{bmatrix} 0 & 0 & 0 & -M_{afd}\sin\theta & -M_{ald}\sin\theta & M_{aq}\cos\theta \\ 0 & 0 & 0 & -M_{afd}\sin\left(\theta+\frac{2\pi}{3}\right) & -M_{ald}\sin\left(\theta+\frac{2\pi}{3}\right) & M_{aq}\cos\left(\theta+\frac{2\pi}{3}\right) \\ 0 & 0 & 0 & -M_{afd}\sin\left(\theta-\frac{2\pi}{3}\right) & -M_{ald}\sin\left(\theta-\frac{2\pi}{3}\right) & M_{aq}\cos\left(\theta-\frac{2\pi}{3}\right) \\ -M_{afd}\sin\theta & -M_{afd}\sin\left(\theta+\frac{2\pi}{3}\right) & -M_{afd}\sin\left(\theta-\frac{2\pi}{3}\right) & 0 & 0 & 0 \\ -M_{ald}\sin\theta & -M_{ald}\sin\left(\theta+\frac{2\pi}{3}\right) & -M_{ald}\sin\left(\theta-\frac{2\pi}{3}\right) & 0 & 0 & 0 \\ M_{aq}\cos\theta & M_{aq}\cos\left(\theta+\frac{2\pi}{3}\right) & M_{aq}\cos\left(\theta-\frac{2\pi}{3}\right) & 0 & 0 & 0 \end{bmatrix} \tag{2-72}$$

and the inductance matrix as:

---

[7] Refer to Appendix F for derivation of this equation.

$$\mathbf{L} = \begin{bmatrix} L_s & -M_s & -M_s & M_{afd}\cos\theta & M_{a1d}\cos\theta & M_{aq}\sin\theta \\ -M_s & L_s & -M_s & M_{afd}\cos\left(\theta-\frac{2\pi}{3}\right) & M_{a1d}\cos\left(\theta-\frac{2\pi}{3}\right) & M_{aq}\sin\left(\theta-\frac{2\pi}{3}\right) \\ -M_s & -M_s & L_s & M_{afd}\cos\left(\theta+\frac{2\pi}{3}\right) & M_{a1d}\cos\left(\theta+\frac{2\pi}{3}\right) & M_{aq}\sin\left(\theta+\frac{2\pi}{3}\right) \\ M_{afd}\cos\theta & M_{afd}\cos\left(\theta-\frac{2\pi}{3}\right) & M_{afd}\cos\left(\theta+\frac{2\pi}{3}\right) & L_f & M_{f1d} & 0 \\ M_{a1d}\cos\theta & M_{a1d}\cos\left(\theta-\frac{2\pi}{3}\right) & M_{a1d}\cos\left(\theta+\frac{2\pi}{3}\right) & M_{f1d} & L_{1d} & 0 \\ M_{aq}\sin\theta & M_{aq}\sin\left(\theta-\frac{2\pi}{3}\right) & M_{aq}\sin\left(\theta+\frac{2\pi}{3}\right) & 0 & 0 & L_q \end{bmatrix} \quad \textbf{(2-73)}$$

A set of electrical differential equations can therefore be derived as follows [23, 22]:

$$\mathbf{L}\mathbf{p}[\mathbf{i}] + \omega\mathbf{G}\mathbf{i} - \mathbf{R}\mathbf{i} = -\mathbf{V} \tag{2-74}$$

where $\mathbf{p}$ denotes the differential operator.

2.11.3 Rotor and stator voltage equations in the dqo frame [23]

The solution of the synchronous machine equations when expressed in terms of phase quantities is difficult due to the presence of time-varying coefficients in the governing equations. As for the induction motor model discussed in Appendix D, the solution of these equations is generally considered too difficult, or impossible [23]. These equations are usually simplified by means of Park's transform. This allows the phase quantities to be transformed into the *dqo* reference frame, eliminating the time-varying coefficients. Under power invariance the transformation is defined as follows [23]:

$$P = \sqrt{\frac{2}{3}} \begin{bmatrix} \cos\theta & \cos\left(\theta-\frac{2\pi}{3}\right) & \cos\left(\theta+\frac{2\pi}{3}\right) \\ \sin\theta & \sin\left(\theta-\frac{2\pi}{3}\right) & \sin\left(\theta+\frac{2\pi}{3}\right) \\ \frac{1}{\sqrt{2}} & \frac{1}{\sqrt{2}} & \frac{1}{\sqrt{2}} \end{bmatrix} \tag{2-75}$$

where θ denotes the rotor angle. Using vector-matrix notation phase voltages, currents and flux linkages in the *abc*-frame can be expressed in the *dqo*-frame:

$$\left.\begin{array}{l} \mathbf{v_{dqo}} = \mathbf{P}\mathbf{v_{abc}} \\ \mathbf{i_{dqo}} = \mathbf{P}\mathbf{i_{abc}} \\ \mathbf{\psi_{dqo}} = \mathbf{P}\mathbf{\psi_{abc}} \end{array}\right\} \tag{2-76}$$

where the vectors in the *dqo*-frame are defined as follows [23]:

$$\mathbf{v_{dqo}} \Rightarrow \begin{bmatrix} v_d \\ v_q \\ v_o \end{bmatrix}; \quad \mathbf{i_{dqo}} \Rightarrow \begin{bmatrix} i_d \\ i_q \\ i_o \end{bmatrix}; \quad \mathbf{\psi_{dqo}} \Rightarrow \begin{bmatrix} \psi_d \\ \psi_q \\ \psi_o \end{bmatrix} \tag{2-77}$$

The vectors $\mathbf{v_{dqo}}$, $\mathbf{i_{dqo}}$ and $\mathbf{\psi_{dqo}}$ are fictitious voltages, currents and flux linkages, all of which are instantaneous in the *dqo* frame of reference. Once the machine performance is obtained in terms of Park's variables, the original phase quantities can be obtained by the inverse transformation which is defined as [23]:

$$P^{-1} = P^T = \sqrt{\tfrac{2}{3}} \begin{bmatrix} \cos\theta & \sin\theta & \dfrac{1}{\sqrt{2}} \\[2mm] \cos\left(\theta - \dfrac{2\pi}{3}\right) & \sin\left(\theta - \dfrac{2\pi}{3}\right) & \dfrac{1}{\sqrt{2}} \\[2mm] \cos\left(\theta + \dfrac{2\pi}{3}\right) & \sin\left(\theta + \dfrac{2\pi}{3}\right) & \dfrac{1}{\sqrt{2}} \end{bmatrix} \tag{2-78}$$

where θ denotes the rotor angle. From this we get [23]:

$$\left.\begin{aligned} \mathbf{v_{abc}} &= \mathbf{P^T v_{dqo}} \\ \mathbf{i_{abc}} &= \mathbf{P^T i_{dqo}} \\ \mathbf{\psi_{abc}} &= \mathbf{P^T \psi_{dqo}} \end{aligned}\right\} \tag{2-79}$$

Equation (2-68) can be written in vector from as [23]:

$$\frac{d}{dt}\mathbf{\psi_{abc}} = -\left(\mathbf{v_{abc}} + r\mathbf{i_{abc}}\right) \tag{2-80}$$

This can be written in terms of *dqo*-variables by applying Park's transform as[8] [23]:

$$\frac{d}{dt}\mathbf{\psi_{dqo}} + \omega \begin{bmatrix} 0 & 1 & 0 \\ -1 & 0 & 0 \\ 0 & 0 & 0 \end{bmatrix} \mathbf{\psi_{dqo}} = -\left(\mathbf{v_{dqo}} + r\mathbf{i_{dqo}}\right) \tag{2-81}$$

or, after expanding and re-arranging terms [23]:

$$\left.\begin{aligned} \frac{d\psi_d}{dt} &= -\left(v_d + ri_d + \omega\psi_q\right) \\ \frac{d\psi_q}{dt} &= -\left(v_d + ri_q - \omega\psi_d\right) \\ \frac{d\psi_o}{dt} &= -\left(v_o + ri_o\right) \end{aligned}\right\} \tag{2-82}$$

Thus far, Park's transformation has been applied to stator variables expressed in phase quantities. The rotor variables remain unchanged allowing the rotor circuit variables to be augmented with the stator *dqo* variables. The transformation matrix can be augmented and partitioned for n rotor circuits as follows [23]:

$$\mathbf{P_A} \Rightarrow \left[\begin{array}{c:c:c} \mathbf{P_{3x3}} & \mathbf{O_{3x(n+1)}} & \mathbf{O_{3xn}} \\ \hdashline \mathbf{O_{(n+1)x3}} & \mathbf{I_{(n+1)x(n+1)}} & \mathbf{O_{(n+1)xn}} \\ \hdashline \mathbf{O_{nx3}} & \mathbf{O_{nx(n+1)}} & \mathbf{I_{nxn}} \end{array}\right] \tag{2-83}$$

Where $\mathbf{I}$ is the unit matrix and $\mathbf{O}$ is the zero matrix and subscripts denote matrix dimensions. The inverse of the augmented transformation matrix is given by:

$$\mathbf{P_A^{-1}} \Rightarrow \left[\begin{array}{c:c:c} \mathbf{P_{3x3}^T} & \mathbf{O_{3x(n+1)}} & \mathbf{O_{3xn}} \\ \hdashline \mathbf{O_{(n+1)x3}} & \mathbf{I_{(n+1)x(n+1)}} & \mathbf{O_{(n+1)xn}} \\ \hdashline \mathbf{O_{nx3}} & \mathbf{O_{nx(n+1)}} & \mathbf{I_{nxn}} \end{array}\right] \tag{2-84}$$

---

[8] Refer to Appendix F, 12.3 for detail derivation

The *dqo* flux linkages and currents can now be expressed in terms of *abc* flux linkages and currents using P_A. The inductance matrix in the *dqo*-frame is therefore given by [23]:

$$\mathbf{P_A L P_A^{-1}} = \begin{bmatrix} \mathbf{PL_S P^{-1}} & \vdots & \mathbf{PL_{SRd}} & \vdots & \mathbf{PL_{SRq}} \\ \hdashline \mathbf{L_{SRd}^T P^{-1}} & \vdots & \mathbf{L_{Rd}} & \vdots & \mathbf{O} \\ \hdashline \mathbf{L_{SRq}^T P^{-1}} & \vdots & \mathbf{O} & \vdots & \mathbf{L_{Rq}} \end{bmatrix} \tag{2-85}$$

The various sub-matrices of eq. (2-85) are given below:

$$\mathbf{PL_S P_A^{-1}} = \begin{bmatrix} L_d & 0 & 0 \\ 0 & L_q & 0 \\ 0 & 0 & L_0 \end{bmatrix} \tag{2-86}$$

where

$$L_d = \left(L_s + M_s + \tfrac{3}{2} L_m \right)$$

$$L_q = \left(L_s + M_s - \tfrac{3}{2} L_m \right)$$

$$L_0 = \left(L_s - 2M_s \right)$$

L_d denotes the *d*- axis synchronous inductance, L_q denotes the *q*- axis synchronous inductance and L_o denotes the zero-sequence inductance. In the case of a cylindrical rotor machine, L_m will be equal to zero in the above expressions [23]:

$$\mathbf{PL_{SRd}} = \sqrt{\frac{3}{2}} \begin{bmatrix} M_{afd} & M_{a1d} & \cdots & M_{and} \\ 0 & 0 & \cdots & 0 \\ 0 & 0 & \cdots & 0 \end{bmatrix}_{3x(n+1)} \tag{2-87}$$

and $\left[\mathbf{PL_{SRd}} \right]^T = \mathbf{L_{SRd}^T P^T} = \mathbf{L_{SRd}^T P^{-1}}$

$$\mathbf{PL_{SRq}} = \sqrt{\frac{3}{2}} \begin{bmatrix} 0 & 0 & \cdots & 0 \\ M_{a1q} & M_{a2q} & \cdots & M_{anq} \\ 0 & 0 & \cdots & 0 \end{bmatrix}_{3xn} \tag{2-88}$$

and $\left[\mathbf{PL_{SRq}} \right]^T = \mathbf{L_{SRq}^T P^T} = \mathbf{L_{SRq}^T P^{-1}}$

where *n* denotes the number of equivalent rotor circuits on the *d* and *q*- axes.

The above equations can now be used to determine the flux-current relationship in the *dqo*-frame. For example, if it is assumed that there is only one equivalent rotor circuit on each axis, the following equation is obtained:

$$\begin{bmatrix} \psi_d \\ \psi_q \\ \psi_0 \\ \hdashline \psi_{fd} \\ \psi_{1d} \\ \psi_{1q} \end{bmatrix} = \begin{bmatrix} L_d & 0 & 0 & \vdots & kM_{afd} & kM_{a1d} & \vdots & 0 \\ 0 & L_q & 0 & \vdots & 0 & 0 & \vdots & kM_{a1q} \\ 0 & 0 & L_0 & \vdots & 0 & 0 & \vdots & 0 \\ \hdashline kM_{afd} & 0 & 0 & \vdots & L_{ffd} & L_{f1d} & \vdots & 0 \\ kM_{a1d} & 0 & 0 & \vdots & L_{f1d} & L_{11d} & \vdots & 0 \\ \hdashline 0 & kM_{a1q} & 0 & \vdots & 0 & 0 & \vdots & L_{11q} \end{bmatrix} \begin{bmatrix} i_d \\ i_q \\ i_o \\ \hdashline i_{fd} \\ i_{1d} \\ ii_{1q} \end{bmatrix} \tag{2-89}$$

where $k = \sqrt{\tfrac{3}{2}}$.

The voltage equations are obtained as follows [23]:

$$
\left.
\begin{aligned}
\frac{d\psi_d}{dt} &= -\left(v_d + ri_d - \omega\psi_q\right) \\
\frac{d\psi_q}{dt} &= -\left(v_q + r_{iq} - \omega\psi_d\right) \\
\frac{d\psi_o}{dt} &= -\left(v_o + ri_0\right)
\end{aligned}
\right\} \text{Stator}
$$

$$
\left.
\begin{aligned}
\frac{d\psi_{fd}}{dt} &= \left(v_{fd} - r_{fd}i_{fd}\right) \\
\frac{d\psi_{1d}}{dt} &= -r_{11d}i_{1d}
\end{aligned}
\right\} \text{Rotor d - axis}
\qquad (2\text{-}90)
$$

$$
\left.
\frac{d\psi_{1q}}{dt} = -r_{11q}i_{1q}
\right\} \text{Rotor q - axis}
$$

2.11.4 Flux linkage equations in terms of reactances

Since manufacturers generally supply machine parameters in terms of reactances rather than inductances, it is convenient to express the flux linkage equations in terms of reactances rather than inductances. If both sides of equation (2-61) are multiplied by the rated angular frequency ω_0, the following is obtained [23]:

$$
\varphi \Rightarrow \omega_0\psi = \omega_0\mathbf{L}i = \mathbf{X}i
\qquad (2\text{-}91)
$$

where $\mathbf{X}$ is the rated-frequency reactance matrix of the machine with all elements expressed in ohms. Flux linkages are replaced by flux linkages per second having the unit of volt. The voltage equations given in (2-91) can be written as follows [23]:

$$
\left.
\begin{aligned}
\frac{d\varphi_d}{dt} &= -\omega_0\left(v_d + ri_d - \omega\psi_q\right) \\
\frac{d\varphi_q}{dt} &= -\omega_0\left(v_q + r_{iq} - \omega\psi_d\right) \\
\frac{d\varphi_o}{dt} &= -\omega_0\left(v_o + ri_0\right)
\end{aligned}
\right\} \text{Stator}
$$

$$
\left.
\begin{aligned}
\frac{d\varphi_{fd}}{dt} &= \omega_0\left(v_{fd} - r_{fd}i_{fd}\right) \\
\frac{d\varphi_{1d}}{dt} &= -\omega_0 r_{11d}i_{1d}
\end{aligned}
\right\} \text{Rotor d - axis}
\qquad (2\text{-}92)
$$

$$
\left.
\frac{d\varphi_{1q}}{dt} = -\omega_0 r_{11q}i_{1q}
\right\} \text{Rotor q - axis}
$$

The flux linkage relation in equation (2-91) with d- and q-axes decoupled is given by [23]:

$$
\begin{bmatrix}
\varphi_d \\
\varphi_{fd} \\
\varphi_{1d} \\
\varphi_q \\
\varphi_{1q}
\end{bmatrix}
=
\begin{bmatrix}
x_d & kx_{afd} & kx_{a1d} & 0 & 0 \\
kx_{afd} & x_{ffd} & kx_{f1d} & 0 & 0 \\
kx_{a1d} & kx_{f1d} & x_{11d} & 0 & 0 \\
0 & 0 & 0 & x_q & kx_{a1q} \\
0 & 0 & 0 & kx_{a1q} & x_{11q}
\end{bmatrix}
\begin{bmatrix}
i_d \\
i_{fd} \\
i_{1d} \\
i_q \\
i_{1q}
\end{bmatrix}
\qquad (2\text{-}93)
$$

2.12 Electrical Air-Gap Power And Torque

Under the power-invariant transform $\mathbf{P}$, the instantaneous 3-phase power output of the synchronous generator in terms of the dqo variables defined in eq. (2-76) is given by [23, 32]:

$$P_e = \mathbf{v}_{\mathbf{anc}}^{\mathbf{T}}\mathbf{i}_{\mathbf{abc}} = \mathbf{v}_{\mathbf{dqo}}^{\mathbf{T}}\mathbf{P}\mathbf{P}^{\mathbf{T}}\mathbf{i}_{\mathbf{dqo}} = \mathbf{v}_{\mathbf{dqo}}^{\mathbf{T}}\mathbf{i}_{\mathbf{dqo}}$$
$$= \left(v_d i_d + v_q i_q + v_o i_o\right) \tag{2-94}$$

Under balanced operation, the v_0, i_0 terms vanish. Substituting for v_d and v_q from (2-92) above gives the following:

$$P_e = \left(-ri_d - \frac{\omega}{\omega_0}\varphi_q - \frac{1}{\omega_0}\frac{d\varphi_d}{dt}\right)i_d + \left(-ri_q + \frac{\omega}{\omega_0}\varphi_d - \frac{1}{\omega_0}\frac{d\varphi_q}{dt}\right)i_q$$
$$= -r\left(i_d^2 + i_q^2\right) + \frac{\omega}{\omega_0}\left(\varphi_d i_q - \varphi_q i_d\right) - \frac{1}{\omega_0}\left(i_d \frac{d\varphi_q}{dt} = i_q \frac{d\varphi_d}{dt}\right) \tag{2-95}$$

The first and last terms of equation (2-95) represents the stator ohmic losses and rate of change of armature magnetic energy respectively. The power transferred across the airgap is given by the second term. The airgap power is designated P_g

$$P_g = \frac{\omega}{\omega_0}\left(\varphi_d i_q - \varphi_q i_d\right) \tag{2-96}$$

where ω = rotor speed, ω_0 = synchronous speed and the flux linkages φ_d and φ_q are defined in section 2.11.4. If it is assumed that the $\dfrac{d\varphi_d}{dt}$ and $\dfrac{d\varphi_q}{dt}$ terms are negligible, then the electrical power output is given by the air-gap power, P_g minus the stator ohmic losses. If the ohmic losses are also neglected, then $P_e = P_g$. The airgap power is related to the airgap torque by [23]:

$$P_g = T_g \omega_m = \frac{\omega}{\omega_0}\left(\varphi_d i_q - \varphi_q i_d\right) \tag{2-97}$$

where ω_{m} denotes the mechanical shaft speed and T_g the airgap torque.

2.12.1 Torque and power expressions in p.u.

The equations for the airgap power and torque, (2-96) and (2-97) may be normalised as:

$$P_{g(1\phi)}^* = \frac{\omega^*}{\omega_0^*}\left(\varphi_d^* i_q^* - \varphi_q^* i_d^*\right) \tag{2-98}$$

and

$$T_{g(1\phi)}^* = \left(\varphi_d^* i_q^* - \varphi_q^* i_d^*\right) \tag{2-99}$$

where The superscript * denotes normalised (per-unit) values. $P_{g(1\phi)}^*$ = p.u. airgap power, $T_{g(1\phi)}^*$ = p.u. torque, ω^* = p.u. rotor angular velocity[9], ω_0^* = p.u. synchronous speed and p.u. flux linkages and currents are as defined in section 2.11.4. Note $P_{g(1\phi)}^*$ and $T_{g(1\phi)}^*$ are obtained by choosing the base power equal to the rated stator power per phase. When using the p.u. air-

---

[9] Note that the p.u. angular velocity is the same whether expressed in mechanical or electrical form [23]

gap torque from eq.(2-99) above in the swing equation $T_{g(1\phi)}^*$ must be converted to a three phase power base since the p.u. quantities in the swing equation are obtained using three phase power base. The following change of base operation is required [23]:

$$\left.\begin{array}{l} \dfrac{T_g^*}{T_{g(1\phi)}^*} = \dfrac{\text{Base torque (1- phase basis)}}{\text{Base torque (3 - phase basis)}} = \dfrac{S_B}{S_{B(3\phi)}} = \dfrac{S_B}{3S_B} \\[3mm] \therefore T_g^* = T_{g(1\phi)}^*/3 \end{array}\right\} \qquad \textbf{(2-100)}$$

2.13 Machine Power System Interface

The synchronous generator models are based on the *d-q* frame which is rotating at the same speed as the field axis. The network equations defining voltages and currents in the power system are solved in the system frame of reference, which is rotating at synchronous speed. The voltages and currents obtained at the terminals of the machines from the load flow solution have to be interfaced with the generator *d-q* variables and vice versa.

The necessary transformations are obtained from Figure 2-12. The *q*-axis is shown to lag the *d*-axis and is taken as the reference for phasor representation. The system reference is defined by Real-Imaginary (Re,Im) axes, 90 electrical degrees apart to distinguish from the machine *d-q* axes. If $\bar{V}_t, \bar{I}_t$ and $\hat{V}_t, \hat{I}_t$ are the terminal voltage and current phasors with respect to the *d-q* and Re-Im axes respectively then

$$\bar{V}_t = \left(V_q + jV_d\right) \text{ and } \bar{I}_t = \left(I_q + jI_d\right)$$

and

$$\hat{V}_t = \left(V_{\text{Re}} + jV_{\text{Im}}\right) \text{ and } \hat{I}_t = \left(I_{\text{Re}} + jI_{\text{Im}}\right)$$

The terminal conditions at any generator, the phasor terminal voltage $V_t \angle \beta$ (rms phase value), the phasor terminal current $I_t \angle \gamma$, and the power factor angle ϕ are known from the load-flow solution prior to the disturbance. Figure 2-12 illustrates the relationship between the system frame of reference which is rotating at synchronous speed and the machine reference frame.

Figure 2-12 Machine-system interface relations [23].

V_{Re} and V_{Im}, V_d and V_q are the components of the terminal voltage along the d-q and Re-Im axes respectively. Similarly for I_{Re}, I_{Im} and I_d, I_q and the terminal current. δ denotes the instantaneous angle between the system and machine frames of reference. From Figure 2-12, the following relation can be derived [23]:

$$\begin{bmatrix} V_{Re} \\ V_{Im} \end{bmatrix} = \begin{bmatrix} \cos\delta & -\sin\delta \\ \sin\delta & \cos\delta \end{bmatrix} \begin{bmatrix} V_q \\ (-)V_d \end{bmatrix}$$

(2-101)

The inverse relation is:

$$\begin{bmatrix} V_q \\ (-)V_d \end{bmatrix} = \begin{bmatrix} \cos\delta & \sin\delta \\ -\sin\delta & \cos\delta \end{bmatrix} \begin{bmatrix} V_{Re} \\ V_{Im} \end{bmatrix}$$

(2-102)

Note that V_d, V_q, I_d and I_q are the rms stator equivalents of the rotor referenced magnitudes v_d, v_q, i_d and i_q respectively. Under balanced operation the relations are [23]:

$$\left. \begin{aligned} v_d = \sqrt{3}V_d \text{ and } v_q = \sqrt{3}V_q \\ i_d = \sqrt{3}I_d \text{ and } i_q = \sqrt{3}I_q \end{aligned} \right\}$$

(2-103)

2.13.1 Locating machine q-axis with respect to system reference

The phasor diagram in Figure 2-13 is used to obtain the initial rotor angle δ with respect to the synchronously rotating system reference. It is first necessary to locate the machine q-axis with respect to system reference. The internal machine angle is given by[23]:

$$\delta' = \tan^{-1} \frac{\left(x_q I_t \cos\phi - r I_t \sin\phi \right)}{\left(V_t + r I_t \cos\phi + x_q I_t \sin\phi \right)}$$

(2-104)

Figure 2-13 Locating machine axis with respect to system axis [23].

where all quantities are as defined in Figure 2-12.[10]

Since the magnitudes of the terminal voltage V_t, terminal current I_t, and power factor angle ϕ are known, the location of the machine q-axis can be fixed with the terminal voltage as

---

[10] Refer to Appendix F, 12.5 for detailed derivation

reference. For leading power factor conditions at the machine terminals the algebraic sign of I_t $\sin \phi$ in equation (2-104) has to be reversed. The rotor angle referred to the system reference is given by:

$$\delta = \delta' + \beta \tag{2-105}$$

where β is the phase angle of the terminal voltage with respect to the system reference[11]. It is taken as positive when measured from the system reference in a counter-clockwise direction and is determined from the load-flow solution.

2.14 Excitation System Modelling

For dynamic power system simulations of 1s or longer duration, it is necessary to include the effects of the machine controllers. The two principal controllers of a turbine generator are the automatic voltage regulator (AVR) and the speed governor.

2.14.1 Automatic voltage regulators

Many different AVR models have been developed to represent the different types of AVR's in use. It is however recommended that general purpose AVR models be used, which can revert to the desired type by using the correct parameters [21]. A commonly used model recommended by the IEEE is shown in Figure 2-14.
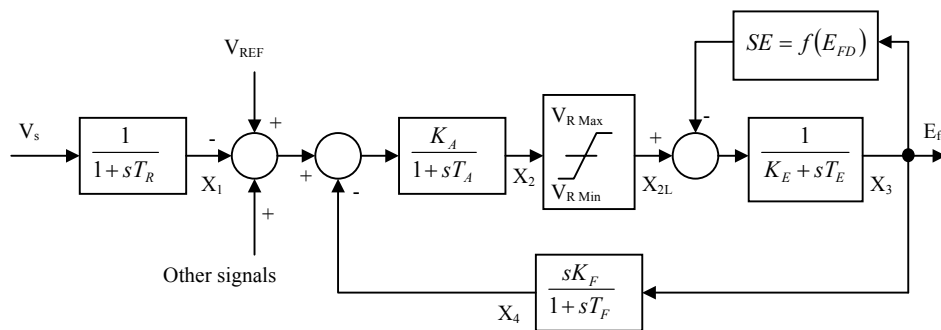
Figure 2-14 IEEE type 1 AVR model [23, 22].

The type 1 AVR model was selected for simulation purposes based on the available data for the main plant generator, 48GT101. With reference to Figure 2-14, the following are derived:

$$\frac{dX_1}{dt} = -\frac{X_1}{T_R} + \frac{V_S}{T_R} \tag{2-106}$$

$$\frac{dX_2}{dt} = -\frac{X_2}{T_A} + \frac{K_A}{T_A}\left(V_{REF} - X_1 - X_4\right) \tag{2-107}$$

define:

$$f = -\frac{X_2}{T_A} + \frac{K_A}{T_A}\left(V_{REF} - X_1 - X_4\right) \tag{2-108}$$

The regulator output is restricted by non-windup limits, thus X_{2L} is given by the following:

---

[11] The Swing Bus is taken as the system reference

- If $X_2 \geq V_{R\,Max}$ and $f > 0$, then $\dfrac{dX_{2L}}{dt}$ is set to zero

- If $X_2 \leq V_{R\,MIN}$ and $f < 0$, then $\dfrac{dX_{2L}}{dt}$ is set to zero

otherwise, $\dfrac{dX_{2L}}{dt} = f$ for $V_{R\,MIN} < X_2 < V_{R\,MAX}$

$$\frac{dE_{fd}}{dt} = -\frac{K_E}{T_E} E_{fd} + \frac{1}{T_E}\left(X_{2L} - SE\right) \tag{2-109}$$

The exciter saturation is specified at maximum field voltage E_{fdmax} and at 0.75 of maximum field voltage $E_{fd0.75}$ as per IEEE recommendations [21]. The exciter saturation function is then determined using linear interpolation for any value of field voltage as follows:

$$SE = \left(k_1 E_{fd} - k_2\right) E_{fd} \tag{2-110}$$

where

$$\left.\begin{aligned} k_1 &= \frac{4SE_{0.75}}{3E_{fdMax}} \\ k_2 &= 0 \end{aligned}\right\} \text{if } E_{fd} \leq 0.75 E_{fdMax}$$

or

$$\left.\begin{aligned} k_1 &= \frac{4\left(SE_{Max} - SE_{0.75}\right)}{E_{fdMax}} \\ k_2 &= 4SE_{0.75} - 3SE_{Max} \end{aligned}\right\} \text{if } E_{fd} > 0.75 E_{fdMax}$$

For the feedback loop the following is obtained:

$$\frac{dX_4}{dt} = -\frac{X_4}{T_F} + K_F \frac{dE_{fd}}{dt} \tag{2-111}$$

Substitution of equation (2-109) into the above gives:

$$\frac{dX_4}{dt} = \frac{-X_4}{T_F} + \frac{K_F}{T_F}\left(\frac{-K_E}{T_E} E_{fd} + \frac{1}{T_E}\left(X_{2L} - SE\right)\right) \tag{2-112}$$

The equations derived in this section are added to the synchronous machine electrical equations in order to model the AVR.

2.14.2 Machine excitation simulation interface

In order to include the effect of the AVR on machine performance the excitation system equations derived in section 2.14.1 have to be appended to the machine equations and solved simultaneously. The mathematical interface between these two is the field equation of the rotor which relates the time rate of change of field flux linkages to field voltage and current. For consistency between the excitation system and machine equations, it is necessary to convert the rotor quantities (field voltage, current or flux linkage) into an equivalent stator electromotive force (emf)[23].

The open-circuit instantaneous voltage of phase a according to eq. (2-68) is:

$$v_a = -\frac{d\psi_a}{dt} \tag{2-113}$$

The inductance-rotor position relation for ψ_a, L_{afd} is defined by[23, 21, 22]:

$$\psi_a = L_{afd} i_{fd} = \left(M_{afd} \cos\theta \right) i_{fd} \tag{2-114}$$

In steady state,

$$v_a = \left(\omega_0 M_{afd} i_{fd} \right) \sin\theta \tag{2-115}$$

The peak phase a voltage V_a is given by

$$V_a = \left(\omega_0 M_{afd} i_{fd} \right) = x_{afd} i_{fd} \tag{2-116}$$

If the rms value of this voltage is denoted by E_I known as *field excitation* then

$$V_a = x_{afd} i_{fd} = \sqrt{2} E_I \tag{2-117}$$

Since E_I is the rms per-phase value, it has to be multiplied by a factor k to express the above relationship in the *dqo* frame:

$$k x_{afd} i_{fd} = \sqrt{3} E_I \quad \text{where} \quad k = \sqrt{\tfrac{3}{2}} \tag{2-118}$$

kx_{afd} is the mutual reactance between stator and field in the *dqo* frame and $\sqrt{3}E_I$ corresponds to the d-axis stator voltage. The correspondence between field voltage and stator emf is determined as follows: In steady state [23]:

$$i_{fd} = \frac{v_{fd}}{r_{fd}} \tag{2-119}$$

This field current corresponds to a peak stator emf of $\frac{v_{fd}}{i_{fd}} x_{afd}$ volts (per phase) If the rms value of this voltage is denoted by E_{fd}, known as the *Exciter voltage referred to the stator*, then the *d*-axis stator emf ($\sqrt{3}E_{fd}$) corresponds to a field voltage v_{fd}, related by [23]:

$$v_{fd} \left(\frac{k x_{afd}}{r_{fd}} \right) = \sqrt{3} E_{fd} \tag{2-120}$$

Under steady state $E_{fd} = E_I$.

2.15 Rotor Dynamics

One of the most important aspects of transient stability studies is to analyse the behaviour of the synchronous machine rotor during the transient period. The differential equation describing this motion is called the *swing equation* because of the swinging nature, under disturbed conditions of the rotor angle with respect to an arbitrary synchronously rotating reference frame [23]. These equations are very well established and discussed in most references dealing with synchronous machines and/or electrical power systems [14, 22, 21, 23].

2.15.1 The swing equation

The motion of the machine is given by [23]:

$$T_{net} = J\alpha \tag{2-121}$$

where

$\quad\quad\quad \alpha \quad\quad\quad$ is the net acceleration or deceleration of the machine rotor

J is the machine rotor's moment of inertia.

T_{net} is the net torque responsible for α

For a synchronous generator, the generator rotor, exciter and prime mover turbine rotor normally form the rotating body and J is thus the combined moment of inertia of the prime mover-generator-exciter system.

The kinetic energy stored in this rotating body is given by:

$$E_{KE} = \tfrac{1}{2} J \omega_m^2 \tag{2-122}$$

where (In MKSA units):

T is expressed in Newton-metre or Joule/radian

J is expressed in kgm^2 or joule-sec^2/radian^2

ω_m is expressed in radians/sec

α is expressed in radians/sec^2

E_{KE} is expressed in joules

The net torque acting on the rotor of the machine is the algebraic sum of the following [23]:

- "The *electromagnetic* torque. This can be subdivided into two components. (i) The *synchronising torque* which is in phase with the rotor angle (also known as the air-gap torque) is equal to the electrical output torque plus the torque corresponding to electrical losses in the machine. This is equal to the rate of change, with respect to rotor angle, of the total stored electromagnetic energy. The time rate of change of this energy is the *synchronising power*. Let T_g denote this torque. (ii) The *damping torque* which is in phase with the rotor speed is produced by the equivalent rotor electrical circuits (i.e. dampers and solid cylindrical rotor body) due to asynchronous action. Let us denote it by T_{DD} "

- The *damping torques* contributed by the prime mover and its controls, generator controls, power system and load. This can be combined with T_{DD} to give one single damping torque, T_D. This torque is assumed to be proportional to rotor speed deviations.

- The *mechanical input* torque from the prime mover, corrected for rotational losses and denoted by T_m

The net torque responsible for acceleration or deceleration of the machine rotor under disturbance conditions is:

$$T_{net} = \left(T_m - T_g - T_D \right) \tag{2-123}$$

If the generator and turbine with controls are represented in detail, then T_D will not have any significance and can be omitted from equation (2-123) [23]. If the generator model includes the sub-transient effect of damper windings this coefficient is generally omitted [21]. This parameter can also be omitted when the generator model only includes transient effects of damper windings, at the expense of accuracy, particularly during the first 30-50msec following the disturbance being simulated [32]. Assuming that the rotor rotates with uniform angular velocity ω_{m0}, the rotor angle will go on increasing uniformly with time. The mechanical rotor angle is therefore measured with respect to a synchronously rotating reference frame. Thus:

$$\delta_m = \theta_m - \left(\omega_{m0} t + \theta_0 \right) \tag{2-124}$$

where

> δ_m = mechanical rotor angle measured with respect to a synchronously rotating reference frame, ω_{m0} = rated mechanical angular speed of the rotor, θ_m = rotor mechanical angle with respect to a stationary reference frame and θ_0 = constant angle equal to $\pi/2$ if the q-axis lags the d-axis.

The swing equation can be written in terms of torque as follows [23]:

$$J \frac{d^2\delta_m}{dt^2} = T_{net} = \left(T_m - T_g - T_D\right) \tag{2-125}$$

The swing equation can be written in terms of power by multiplying both sides of equation (2-125) by the instantaneous mechanical speed [23]:

$$J\omega_m \frac{d^2\delta_m}{dt^2} = \left(T_m - T_g - T_D\right)\omega_m \tag{2-126}$$

or

$$M \frac{d^2\delta_m}{dt^2} = P_m - P_g - P_D \tag{2-127}$$

where

P_m denotes the mechanical input power corrected for rotational losses and P_g denotes the electrical output power P_e + electrical losses. The mechanical input power from the turbine is converted into electromagnetic air-gap power. The electrical power output of the machine is determined from the air-gap power by subtracting electrical losses. If losses are neglected, P_g may be replaced by P_e. P_D denotes equivalent damping power proportional to slip velocity.

From the above equations:

$$M = J\omega_m$$

Since the deviations from the rated speed following a disturbance can be considered negligible [21, 23] the following approximation can be made [23]:

$$M = J\omega_{m0} \tag{2-128}$$

When formulating the swing equation, it is more convenient to use the rotor electrical angle, related to the mechanical angle by [23]:

$$\delta_e = \frac{p}{2}\delta_m \tag{2-129}$$

where $p/2$ is the number of pole pairs in the machine.

The swing equation in terms of the electrical angle is given by [23]:

$$\left(J \frac{N_0}{60} \frac{1}{f_0}\right)\frac{d^2\delta_e}{dt^2} = \left(T_m - T_g - T_D\right) \tag{2-130}$$

where

N_0 denotes the rated shaft speed of the machine in revolutions per minute and f_0 denotes the rated electrical frequency of the machine in Hz.

The inertia constant H, expressed in seconds, of the machine is defined as [23]:

$$H \triangleq \frac{\text{stored energy in (Mega)Joules at rated speed}}{\text{rating of machine in (Mega)volt - amperes}} \qquad \textbf{(2-131)}$$

The three phase MVA of the machine, denoted by $S_{B(3\phi)}$ gives

$$H = \frac{\frac{1}{2} J \omega_{m0}^2}{S_{B(3\phi)}} \qquad \textbf{(2-132)}$$

which allows the following form of the swing equation to be derived [23]:

$$\left(\frac{2HS_{b(3\phi)}}{\omega_{m0}} \cdot \frac{1}{2\pi f_0} \right) \frac{d^2 \delta_e}{dt^2} = \left(T_m - T_g - T_D \right) \qquad \textbf{(2-133)}$$

Assuming that under transient conditions, the shaft speed will not vary significantly from the rated speed, i.e. $\omega_m / \omega_{m0} \cong 1$, and also that the electrical losses are negligible gives the following:

$$M \frac{d^2 \delta_e}{dt^2} = P_m - P_e - P_D \qquad \textbf{(2-134)}$$

where M is given by an expression equivalent to equation (2-128) as:

$$M = \frac{HS_{B(3\phi)}}{\pi f_0} \qquad \textbf{(2-135)}$$

A damping coefficient D is defined as being related to the damping power by:

$$P_D \Rightarrow D \frac{d\delta_e}{dt} \qquad \textbf{(2-136)}$$

The swing equation can then be written [23]:

$$M \frac{d^2 \delta_e}{dt^2} + D \frac{d\delta_e}{dt} = \left(P_m - P_e \right) \qquad \textbf{(2-137)}$$

The swing equation above, employing powers is only an approximation due to the assumption that the rotor speed remains unchanged during the transient period. This form of the swing equation is widely used however, in particular in direct methods [23].

2.15.2 Swing equation in the p.u. system

The base torque (T_B), defined as the ratio of the 3-phase MVA rating of the machine to the rated angular speed ω_{m0}, can be used to normalise equation (2-133):

$$T_B \Rightarrow \frac{S_{B(3\phi)}}{\omega_{m0}} \qquad \textbf{(2-138)}$$

Dividing equation (2-133) by T_B and replacing $2\pi f_0$ by ω_0 gives the following:

$$\frac{2H}{\omega_0} \frac{d^2 \delta_e}{dt^2} = \left(T_m^* - T_g^* - T_D^* \right) \qquad \textbf{(2-139)}$$

The superscript * denotes normalised (per-unit) values. The base angle is defined as 1 electrical radian, base speed as 1 electrical rad/sec and base time as 1 second. Equation (2-139) is frequently used in time domain simulation studies [23]. The swing equation involving powers can also be normalised. as follows [23]:

$$M^* \frac{d^2 \delta_e}{dt^2} + D^* \frac{d\delta_e}{dt} = \left(P_m^* - P_e^* \right) \qquad \text{(2-140)}$$

M^* is the per-unit value of M normalised to machine rated power and can be expressed as

$$M^* = \frac{H}{\pi f_0}.$$

The damping coefficient D is not used when the machine model includes the subtransient and/or transient effects of the damper windings in the electrical equations [23]. When required, damping coefficient values of 1-2 p.u. may be used to account for the effects of the damper windings [32].

2.15.3 The inertia constant H

The constant H which appears in various forms of the swing equation is the combined inertia constant of the prime mover – generator – exciter system expressed in seconds. The value of H is generally in the range of 1-10 seconds for all types of machines and is based on the three-phase MVA rating of the particular machine. It may be necessary to normalise the machine H to the common MVA base chosen for the system in transient stability studies as follows [23]:

$$H_{msys} = \left(H_m MVA_m \right) / MVA_{sys} \ (\text{sec.}) \qquad \text{(2-141)}$$

2.16 Speed Governor Models

There is no data available for modelling the governor of the main plant generator. The generator is driven by a three stage steam turbine. Since the generator was originally commissioned, there have been continual adjustments to the governor control systems by operating personnel. In addition, the entire governor control system was refurbished during the last (2002) shutdown. The hydraulic servo valves were replaced and the operating sequence of the four main governor valves changed[12]. This will affect the overall dynamic response of the turbine, since the set of governor valves opening first in the current sequence admit steam to the nozzles designed for medium to full load operation, while the second set of valves which open admit steam to the nozzles for light running. It is therefore likely that even if the governor design data had been available, it would not accurately represent the operation of the machine. In view of this, the machine can either be modelled without a governor or an attempt can be made to implement a simple approximate governor model based on generic data.

Since the generator model being used for this work is fairly basic, implementing an elaborate governor-prime mover model, especially in view of the lack of data is not justified. The two possible approaches followed are discussed below.

2.16.1 Modelling generator without a governor

When the generator model state variables are initialised, the generator is assumed to be operating under steady-state conditions. The generator output power is assumed to be the same as that calculated during the initial loadflow solution. For steady-state operation, this implies that the mechanical input power to the generator is equal to the electrical output power[13]. If there are no further disturbances, the generator model state variables will remain

---

[12] These changes were necessitated by difficulties experienced in controlling the speed of the turbine during startup. It is suspected that one of the governor valves is not seating properly causing overspeeding whilst attempting to synchronise the generator. The intention is to correct this during the next major plant shutdown in 2006

[13] Friction and windage losses are ignored.

unchanged for the duration of the simulation. If system disturbances are modelled however, the generator rotor angle with respect to the system will change. If the mechanical input power exceeds the electrical output power, the rotor will accelerate and the rotor angle will increase with the converse true if mechanical input power is less than the electrical output power. For first-swing transient stability studies where the simulation time is in the range of 1-2 seconds the machine is represented by a simple model which does not take AVR and governor systems into consideration [21, 23]. This generally gives a slightly pessimistic indication of generator performance.

Since the simulations to be carried out will be for a period of 9-15 seconds, neglecting the governor will not give realistic results. One simple alternative is to increase the inertia constant H, to a high value which will restrict changes to the rotor angle to a negligible value [32]. This fictitiously high inertia results in the generator being disturbed very little and slowly from it's steady-state during transient conditions. In the case of large disturbances, this would produce inaccurate results since the effect of such disturbances on the system would be masked. In the case of small disturbances, this approach may be acceptable, since the generator prime-mover and governor response to such disturbances is likely to be minimal.

2.16.2 Approximate governor model

Due to the lack of data on the generator turbine and governor characteristics, a detailed implementation of a governor and prime mover model was not justified. The approach followed was to investigate the performance characteristics of typical systems and to attempt to derive a simple approximate model. Standard models for turbine and governor systems are discussed in the literature [21, 32, 23, 31, 33, 22]. The simplified model of a three-stage steam turbine and governor shown in Figure 2-15 was considered.
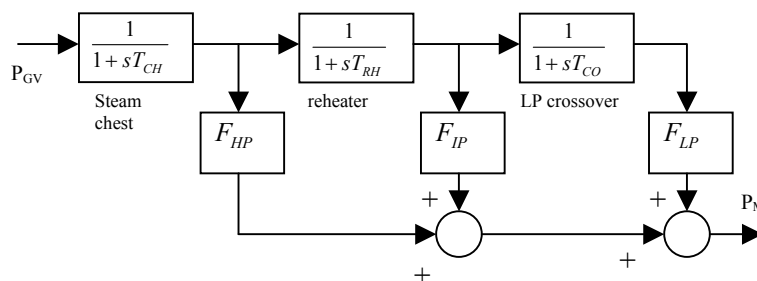
Figure 2-15 IEEE steam turbine model [21, 33, 22].

Table 2-2 gives typical parameters used for the model shown in Figure 2-15.

Table 2-2 Typical parameters used in detailed turbine model ©IEEE [21].

Parameter	Typical Values	Estimated
T_{CH}	0.1-0.4 (sec)	0.25 (sec)
T_{RH}	4-11 (sec)	7.5 (sec)
T_{CO}	0.3-0.5 (sec)	0.4 (sec)
F_{HP}	0.3 p.u.	0.3 p.u.
F_{IP}	0.4 p.u.	0.4 p.u.
F_{LP}	0.3 p.u.	0.3 p.u.

The shorter time constants would be applicable to smaller steam turbines. Since the generator being modelled is rated at 140MVA, the average values of the given time constants were considered a reasonable approximation for the steam turbine model. The governor was represented by the simplified model shown in Figure 2-16[23, 33]:
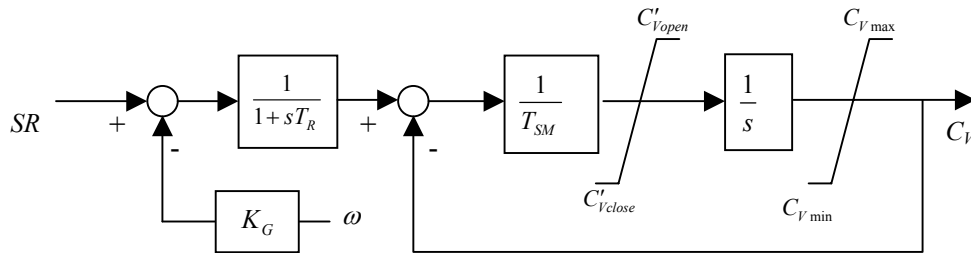
Figure 2-16 Block diagram representation of steam turbine governor system [23, 33].

The symbols in the model shown in Figure 2-16 are defined as [23]:

SR - Speed reference

ω - Rotor Speed

K_G - speed governor gain $= \dfrac{100}{(\% \text{ steady - state speed regulation})}$

T_{SR} - speed relay time constant

T_{SM} - valve positioning servomotor time constant

$\left. \begin{array}{l} C'_{Vopen} \\ C'_{Vclose} \end{array} \right\}$ - valve or servo rate limits

$\left. \begin{array}{l} C_{V\max} \\ C_{V\min} \end{array} \right\}$ - valve position limits

C_V - effective governor-controlled valve position

The relationship between valve position and power can be simply modelled as:

$$P_{GV} = C_V \cdot P_b \tag{2-142}$$

where P_b is the maximum output available from the boiler system. This is assumed to be a constant for the time duration of the studies considered in this work. Speed regulation for generators varies from about 5% to 1% with values of 4-5% being considered typical [14, 33, 32]. In order to derive an approximate governor model, the above models were implemented using Simulink and their response to a step input change investigated. For the governor, the default parameters listed in Table 2-3 were used.

Table 2-3 Default governor parameters for steam turbine [33].

Parameter	Value
K_G	25
T_{SR}	0.001s
T_{SM}	0.02s

At PetroSA, the generator power output is limited by steam availability. This is largely dependent on plant process conditions. The value of P_b in equation (2-142) is set to 1.1, to account for generator operation close to the maximum steam availability. This was modelled by setting the valve limits in the model between 0 and 1,1. The model used to investigate the governor-prime mover response to generator speed errors is shown in Figure 2-17.

Figure 2-17 Simulink governor-turbine model.

The response of the turbine-governor model to a step change in speed error was determined using the model shown in Figure 2-17. The response of this model to a 0.1% and a 1% step change in speed error is shown in Figure 2-18 and Figure 2-19.

Figure 2-18 Turbine-governor response to 0.1% speed error.
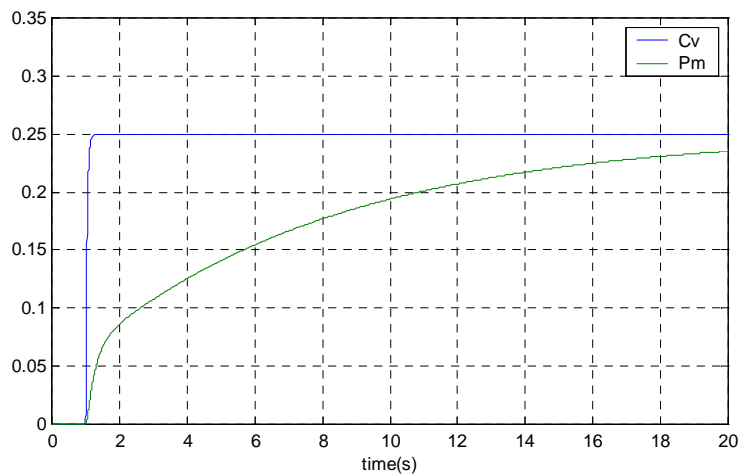
Figure 2-19 Turbine-governor response to 1% speed error.

From Figure 2-18 and Figure 2-19 it can be seen that the initial response is largely dictated by the high-pressure turbine followed by the slower response after 500ms of the intermediate and low pressure turbines. The turbine-governor system model was approximated with the simplified model shown in Figure 2-20.
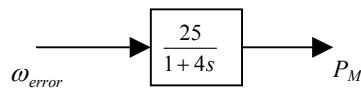
Figure 2-20 Approximate governor model.

Where $K_G = 25$ and $T_G = 4$ seconds. The approximate model shown in Figure 2-20 can be represented by the following differential equation:

$$\frac{dP_M}{dt} = -\frac{1}{T_G}P_M + \frac{K_G}{T_G}\omega_{error} \tag{2-143}$$

The response of the approximate model described by equation 2-143 was compared to that of the more elaborate model shown in Figure 2-17 giving the results shown in Figure 2-21 below:
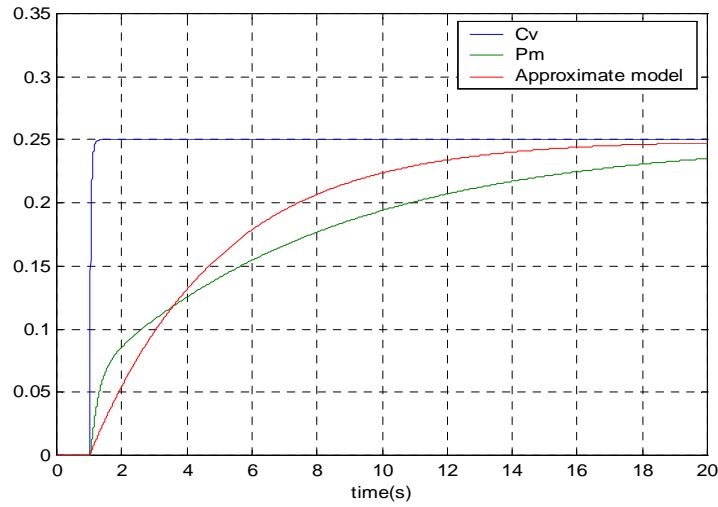
Figure 2-21 Approximate governor model response to 1% speed error.

The approximate model was therefore used to represent the steam turbine and governor.

2.17 Machine Modelling For Stability Studies

The detailed synchronous machine model presented in the preceding sections is not generally used for transient stability analysis. The stator transients are normally neglected and a simpler machine representation used in order to reduce the complexity of the system model [23].

2.17.1 Rate of change of field flux linkages

From equation (2-90), the basic field equation is given by:

$$\frac{d\psi_{fd}}{dt} = \left(v_{fd} - r_{fd}i_{fd}\right)$$
(2-144)

Multiplying on both sides with $\dfrac{\omega_0 M_{afd}}{r_{fd}}$ gives

$$\frac{\omega_0 M_{afd}}{r_{fd}}\frac{d\psi_{fd}}{dt} = \left(\frac{\omega_0 M_{afd}}{r_{fd}}v_{fd} - \omega_0 M_{afd}i_{fd}\right)$$
(2-145)

Using the relationships from section 2.14.2 allows the following expression to be derived[14]:

$$\frac{L_{ffd}}{r_{fd}}\frac{dE'_q}{dt} = \left(E_{fd} - E_I\right)$$
(2-146)

where L_{ffd} is the field self-inductance, r_{fd} is the field resistance, E_I is the field excitation voltage (rms), E_{fd} is the exciter voltage referred to the stator and E'_q is the *q*-axis component of the transient internal voltage. The *d*-axis open-circuit time constant is defined as [23]:

$$\frac{L_{ffd}}{r_{fd}} \overset{\Delta}{=} T'_{d0}$$

---

[14] Refer to Appendix F 12.7 for detailed derivation.

With this eq. (2-146) becomes:

$$T'_{d0} \frac{dE'_q}{dt} = \left(E_{fd} - E_I \right)$$

(2-147)

In the above equation E_{fd} can be constant (manual regulation) or can vary due to automatic voltage regulator action independently of the other variables in the equation. Excitation system dynamics are therefore taken into consideration through E_{fd}. In order to solve the above equation, E_I has to be expressed in terms of E'_q. It can be shown that [23]:

$$E_I = E'_q - \left(x_d - x'_d \right) \frac{i_d}{\sqrt{3}}$$

(2-148)

where x'_d is the d-axis transient reactance. Substituting the above into eq.(2-147) gives:

$$T'_{d0} \frac{dE'_q}{dt} = E_{fd} - E'_q + \left(x_d - x'_d \right) \frac{i_d}{\sqrt{3}}$$

Since $\frac{i_d}{\sqrt{3}} = I_d$, the d-axis component of terminal current (rms stator equivalent) we have the following equation for taking into account the field flux linkages [23]:

$$T'_{d0} \frac{dE'_q}{dt} = E_{fd} - E'_q + \left(x_d - x'_d \right) I_d$$

(2-149)

and eq.(2-148) becomes:

$$E_I = E'_q - \left(x_d - x'_d \right) I_d$$

(2-150)

2.17.2 Rate of change of q-axis rotor flux linkages

For solid round body rotor machines it is preferable to treat the changes in rotor flux linkages separately in each axis. This will give an additional differential equation for the q-axis to account for the damper and round body currents similar to eq. (2-149). For the q-axis, E_d and E'_d are related by [23]:

$$E_d = E'_d - \left(x_q - x'_q \right) I_q$$

(2-151)

where Since there is no excitation in the q-axis, by analogy with eq. (2-149) the following is obtained:

$$T'_{q0} \frac{dE'_d}{dt} = -E'_d - \left(x_q - x'_q \right) I_q$$

(2-152)

The voltage E'_d (like E'_q) is defined to be proportional to the q-axis equivalent rotor circuit flux linkages, ψ_{1q}. If only one equivalent circuit is considered in the q-axis the transient open circuit time constant T'_{q0} is equal to T''_{q0} and is given by L_{11q}/r_{11q} [23].

Since stator transients have been neglected, the differential equations given in (2-149) and (2-152) for the rotor will have to be augmented with two algebraic equations for the stator. If there are no stator transients, equation. (2-82) can be written:

$$\left(-v_d - ri_d - \omega \psi_q \right) = 0$$

(2-153)

$$\left(-v_q - ri_q - \omega \psi_d \right) = 0$$

(2-154)

The stator transient flux linkages are defined as [23]:

$$\psi'_d \Rightarrow \left(\psi_d - L'_d i_d\right) \text{ and } \quad \psi'_q \Rightarrow \left(\psi_q - L'_q i_q\right)$$

and the corresponding speed voltages defined as:

$$e'_d \Rightarrow -\omega \psi'_q \text{ and } e'_q \Rightarrow -\omega \psi'_d$$

If it is assumed that the rotor speed does not change appreciably during the transient, equations (2-153) and (2-154) can be written:

$$-v_d - ri_d - \omega_0\left(\psi'_q + L'_q i_q\right) = 0 \text{ and } -v_q - ri_q - \omega_0\left(\psi'_d + L'_d i_d\right) = 0$$

or

$$e'_d = v_d + ri_d + x'_q i_q \text{ and } e'_q = v_q + ri_q + x'_d i_d$$

The above equations are based on rotor-referenced quantities and can be expressed in rms stator equivalent quantities by dividing by $\sqrt{3}$ giving:

$$E'_d = V_d + rI_d + x'_q I_q \tag{2-155}$$

$$E'_q = V_q + rI_q - x'_d I_d \tag{2-156}$$

E'_d and E'_q are the components of the transient internal voltage $\overline{E}'$ along the d- and q-axes.

In order to account for the damper windings and other stray circuits in the rotor, the subtransient equations can be developed along similar lines as the above equations and are [21]:

$$T''_{d0} \frac{dE''_q}{dt} = E'_q - E''_q + \left(x'_d - x''_d\right)I_d \tag{2-157}$$

$$T''_{qo} \frac{dE''_d}{dt} = E'_d - E''_d - \left(x'_q - x''_q\right)I_q \tag{2-158}$$

$$E''_d = V_d + rI_d + x''_q I_q \tag{2-159}$$

$$E''_q = V_q + rI_q - x''_d I_d \tag{2-160}$$

where superscript " denotes subtransient voltages, reactances and time constants. These equations are based on the assumption that the subtransient time constants are small compared to the transient time constants.

2.17.3 Summary of generator models

Based on the above, models of varying complexity may be defined [21]:

Model 1: d-axis transient effects only. Equations (2-149), (2-155) and (2-156) are used[15].

Model 2: d and *q*-axis transient effects are considered. Equations (2-149),(2-152), (2-155) and (2-156) are used. Equations (2-155) and (2-156) can be written in terms of *d* and *q-axis* currents as follows:

---

[15] Note that when this model is used, it will be necessary to account for the effects of the damper bars by including the damping coefficient, *D* in the swing equation.

$$I_d = \frac{1}{r^2 + x_d' x_q'} \left[r\left(E_d' - V_d\right) + x_q'\left(V_q - E_q'\right) \right]$$

(2-161)

$$I_q = \frac{1}{r^2 + x_d' x_q'} \left[r\left(E_q' - V_q\right) + x_d'\left(V_q - E_q'\right) \right]$$

(2-162)

Model 3: d and *q*-axis sub-transient effects are considered. Equations (2-149), (2-152), and (2-157) through (2-160) are used. Equations (2-159) and (2-160) can be written in terms of *d* and *q*-axis currents as follows:

$$I_d = \frac{x_q''}{x_d'' x_q'' + r^2}\left(V_q - E_q''\right) + \frac{r}{x_d'' x_q'' + r^2}\left(E_d'' - V_d\right)$$

(2-163)

$$I_q = \frac{x_d''}{x_d'' x_q'' + r^2}\left(E_d'' - V_d\right) - \frac{r}{x_d'' x_q'' + r^2}\left(V_q - E_q''\right)$$

(2-164)

2.17.4 Power equations for two-axis model

The three phase electrical power output can be derived as follows for the two-axis model from equation (2-94) [23]:

$$\begin{aligned} P_e &= 3\left(E_d' I_d - x_q' I_d I_q + E_q' I_q + x_d' I_d I_q\right) \\ &= 3\left[\left\{E_q' + \left(x_d' - x_q'\right)I_d\right\}I_q + E_d' I_d\right] \end{aligned}$$

(2-165)

The above equation remains unchanged when expressed in p.u. on a single-phase power base. For use in the swing equation the p.u. electrical power output on a 3-phase power base has to be obtained which is given by [23]

$$P_e = \left\{E_q' + \left(x_d' - x_q'\right)I_d\right\}I_q + E_d' I_d \quad \text{p.u.}$$

(2-166)

2.17.5 Modelling of saturation

Modelling of saturation was considered. Saturation modelling generally requires more detailed knowledge of machine parameter data than was available for the PetroSA machines. Due to a lack of sufficiently accurate parametric data and the need to limit the scope of work, it was decided not to model saturation.

2.18 Review Of Numerical Methods For Solving Differential Equations

A major problem is the stiffness of the system of differential equations. This is due to the large variations in time constants associated with the system variables [21]. When synchronous machines are considered, rotor swing stability is the principal concern. The main time constants associated with the rotor are of the order of 1 to 10s. The electrical transmission network responds rapidly to changes and the time constants associated with the network variables are small enough to be taken as zero without significant loss of accuracy. The relevant differential equations for these rapidly changing variables are transformed into algebraic equations. When a time constant is large, or the disturbance is such that the variable will not change appreciably during the time frame being considered, the time constant may be assumed infinite and the variable becomes a constant. In the following section, the numerical methods usually employed for transient stability studies are discussed along with their properties. Matlab is equipped with built-in subroutines for solving ordinary differential equations (ODE's). Since the transient stability analysis software was developed using Matlab, these built in routines were used, rather than writing new routines. The review of numerical methods below was mainly carried out to gain an understanding of the application

of numerical methods to transient stability analysis and to aid in selecting the appropriate Matlab routines. Also note that although the various solution methods are discussed below in terms of single variables, all can readily be extended to a system of n first-order differential equations.

2.18.1 Accuracy and stability

Accuracy of the solution is affected by round-off and truncation errors. Round-off errors are caused by the computer's inability to represent numbers exactly. In lengthy calculations this type of error is extremely difficult to analyse and control. Carrying more decimal places in the intermediate calculations, than are required in the final answer is the usual practice to minimize round-off errors [20]. A word length of 48bits is normally considered acceptable for transient stability analysis. The difference between the true and calculated results is primarily determined by the truncation error. In order to compare the performance of various algorithms, *Big O* notation is used. This is defined as follows [20]:

A function, $f(n)=O(h(n))$, if and only if there exists an n_0 such that, for all $n>n_0$, we have $f(n) \leq K_1 h(n)$ for some $K_1>0$.

The truncation error is mainly a property of the numerical method chosen. In general terms, the truncation error of a method using a step length h is given by [21].

$$T(h) = O\left(h^{p+1}\right)$$
(2-167)

where p represents the order of accuracy of the method. The true solution $y(t_n)$ at t_n is therefore:

$$y(t_n) = y_n + O\left(h^{p+1}\right) + \varepsilon_n$$
(2-168)

where y_n is the value of y calculated by the method after n steps, and ε_n represents other possible errors.

Two types of instability occur in the solution of ordinary differential equations: inherent and induced instability. Inherent instability arises when the initial conditions are not known exactly. The solution will be affected to some extent, depending on the sensitivity of the differential equation. Inherent instability is not a problem with transient stability studies due to the form of the differential equations used [21]. Induced instability is related to the method used for the numerical solution of the differential equations. It is basically a measure of the difference between the true and approximate solutions as the number of steps becomes large.

Partial stability occurs when the step length *(h)* is critical to the solution and is particularly relevant when considering Runge-Kutta methods. A method with an infinite stability boundary is known as A-stable (unconditionally stable). Backward Euler and the trapezoidal method are A-stable, single-step methods. For a multi-step method to be A-stable, the order of accuracy cannot exceed $p = 2$. Implicit Runge-Kutta methods in which $p<2r$ may also be A-stable. (r = number of stages in the method)

2.18.2 Existence of unique solution

Generally all numerical methods will give some numerical results whether a solution exists or not. These numbers will however be meaningless if a solution does not exist. The following theorem on the existence and uniqueness of a solution for the initial value problem is required:

Theorem [20, 23]:

If $\dfrac{dy}{dt} = y' = f(y,t)$ is a scalar differential equation such that $f(y,t)$ is continuous in the region $0 \leq t \leq b$, and if there exists a constant L (called the Lipschitz constant) such that for any two numbers y_1 and y_s, and any $t \in [0,b]$,

$$\left|f(y_1,t) - f(y_2,t)\right| \leq L\left|y_1 - y_2\right| \tag{2-169}$$

then there exists a unique continuously differentiable function $y(t)$ such that

$$\frac{dy(t)}{dt} = f(y(t),t) \tag{2-170}$$

and $y(0) = y_0$ is the initial condition. The above inequality is known as the Lipschitz condition. In the non-scalar case vector norms replace the absolute values in the Lipschitz condition. Consider the vector differential equation:

$$\frac{d\underline{y}}{dt} = \underline{\dot{y}} = \underline{f}(\underline{y},t) \quad \text{with } \underline{y}(t_0) = \underline{y}_0 \tag{2-171}$$

where $\underline{y}$ is an m-dimensional column vector with elements $y_1,\ldots,y_m$, and $\underline{f}$ is also an m-dimensional vector with elements $f_1,\ldots,f_m$. Equation (2-171) is called non-autonomous because of the explicit dependence of $\underline{f}$ on t. This explicit dependence on t can be eliminated and an autonomous equation obtained by defining a new variable y_{m+1} as follows [23]:

$$\frac{dy_{m+1}}{dt} = \dot{y}_{m+1} = 1 \text{ with } y_{m+1}(t_0) = t_0 \tag{2-172}$$

Now define the following set of vectors [23]:

$$\underline{Z} \overset{\Delta}{=} \begin{bmatrix} \underline{y} \\ y_{m+1} \end{bmatrix} ; \; \underline{F} \overset{\Delta}{=} \begin{bmatrix} \underline{f} \\ 1 \end{bmatrix} ; \; \underline{Z}_0 \overset{\Delta}{=} \begin{bmatrix} \underline{y}_0 \\ t_0 \end{bmatrix} \tag{2-173}$$

With the following results:

$$\frac{d\underline{Z}}{dt} = \underline{\dot{Z}} = \underline{F}(\underline{Z}) \text{ and } \underline{Z}(t_0) = \underline{Z}_0 \tag{2-174}$$

Equation (2-174) is autonomous.

2.18.3 Explicit (open) Runge-Kutta single-step formulas

Consider the differential equation, $\dfrac{dy}{dt} = f(y,t)$

Examples are the following second-order two stage formulas [23]:

$$y_{n+1} = y_n + \frac{1}{2}(K_1 + K_2)$$
$$K_1 = hf(y_n, t_n)$$
$$K_2 = hf(y_n + K_1, t_n + h)$$

(2-175)

and the fourth-order four-stage formulas [23]:

$$y_{n+1} = y_n + \frac{1}{6}(K_1 + 2K_2 + 2K_3 + K_4)$$

with

$$K_1 = hf(y_n, t_n)$$
$$K_2 = hf\left(y_n + \frac{K_1}{2}, t_n + \frac{h}{2}\right)$$
$$K_3 = hf\left(y_n + \frac{K_2}{2}, t_n + \frac{h}{2}\right)$$
$$K_4 = hf(y_n + K_3, t_n + h)$$

(2-176)

All the above are *explicit* or *open single-step* formulas. These formulas are fairly stable for very small h. Errors committed in the calculation do not propagate and increase in amplitude but decrease as n increases. The small value required for h leads to excessive computation time. A rule of thumb is that h is generally chosen as one order less than the smallest time constant in the system. It is also possible that the numerical solution may not approximate the true solution of the differential equation even for this small h [23].

2.18.4 Implicit (closed) Runge-Kutta single-step formulas

An example of a second-order implicit Runge-Kutta method used to solve the autonomous equation $\dfrac{dy}{dt} = f(y)$ is given by [23, 20]:

$$K_1 = hf(y_n)$$
$$K_2 = hf\left(y_n + \frac{K_1}{2} + \frac{K_2}{2}\right)$$

and

$$y_{n+1} = y_n + \frac{1}{2}(K_1 + K_2)$$

(2-177)

This is also known as the *trapezoidal rule or modified Euler formula.*

For:

$$\frac{1}{2}(K_1 + K_2) = (y_{n+1} - y_n)$$

giving

$$K_2 = hf(y_{n+1})$$
$$\therefore y_{n+1} = y_n + \frac{h}{2}[f(y_n) + f(y_{n+1})]$$

(2-178)

This is obviously the trapezoidal rule. This is a very stable implicit single-step formula and is successfully implemented for transient stability [23].

The following implicit Runge-Kutta formula is also known as the *Milne form* for the non-autonomous differential equation (2-171) above:

$$K_1 = hf(y_n, t_n)$$
$$K_2 = hf\left(y_n + \tfrac{1}{4}K_1 + \tfrac{1}{4}K_2, t_n + \tfrac{1}{2}h\right)$$
$$K_3 = hf(y_n + K_2, t_n + h) \tag{2-179}$$

and

$$y_{n+1} = y_n + \tfrac{1}{6}(K_1 + 4K_2 + K_3)$$

From the above equations it can be seen that explicit Runge-Kutta methods employing open formulas are quite straightforward. Implicit methods employing closed formulas require the solution of a system of (generally) non-linear simultaneous equations at each step. Due to the non-linearity, these equations have to be solved by an iterative method which guarantees convergence for small enough h. Implicit methods provide increased accuracy and are considered very stable. The restriction on h is not as severe as with explicit methods. This is important when dealing with stiff systems of differential equations. The disadvantage when using these methods is the iterative solution of the non-linear simultaneous equations which is required [23].

2.18.5 Two-step Runge-Kutta open formulas

For the differential equation, $\dfrac{dy}{dt} = f(y,t)$, a two step Runge-Kutta system can be defined as follows [23]:

$$y_{n+1} = y_n + \sum_{i=1}^{r} s_i \ell_i(y_{n-1}) + \sum_{i=1}^{r} w_i K_i(y_n) \tag{2-180}$$

where r corresponds to the number of stages. A two-stage third-order approximation is give by the following [23]:

$$y_{n+1} = y_n + \tfrac{1}{240}\ell_1(y_{n-1}) - \tfrac{125}{240}\ell_2(y_n - 1) + \tfrac{239}{240}K_1(y_n) + \tfrac{125}{240}K_2(y_n) \tag{2-181}$$

where

$$\ell_1(y_{n-1}) = hf(y_{n-1}, t_{n-1})$$
$$\ell_2(y_{n-1}) = hf\left(y_{n-1} + \tfrac{4}{5}\ell_1, t_{n-1} + \tfrac{4}{5}h\right)$$
$$K_1(y_n) = hf(y_n, t_n) \tag{2-182}$$
$$K_2(y_n) = hf\left(y_n + \tfrac{4}{5}K_1, t_n + \tfrac{4}{5}h\right)$$

This method is not self starting since two consecutive values of y immediately preceding y_{n+1} are required.

2.18.6 Multi-step predictor corrector formulas

These methods use several values of the dependent variable and its derivative obtained at different preceding instants of time to calculate the dependent variable and its derivative at $t = t_{n+1}$. A multi-step method has two processes which are called the prediction and the correction. A predictor-corrector pair consists of an explicit (open) and an implicit (closed) formula. The predictor is used to obtain an approximate first value for y_{n+1} and then this value is used in the corrector to obtain a more accurate value of y_{n+1}. The closed formula is iterated until there is not further change in two successive values of y_{n+1}. The following is the Adams third order predictor-corrector set [23].

$$\bar{y}_{n+1} = y_n + \frac{h}{12}\left[23y'_n - 16y'_{n-1} + 5y'_{n-1}\right] \text{ (predictor)} \qquad \textbf{(2-183)}$$

(first approximate value)

$$y_{n+1} = y_n + \frac{h}{12}\left[5\overline{y'_{n+1}} + 8y'_n - y'_{n-1}\right] \text{(corrector)} \qquad \textbf{(2-184)}$$

where

$$y' = \frac{dy}{dt} = f(y,t) \qquad \textbf{(2-185)}$$

The values of derivatives at t_n, t_{n-1} and t_{n-2} used for calculating y at t_{n+1} may be obtained using Runge-Kutta open formulas. The Newton-Raphson method of solving the implicit multi-step formula in equation (2-184) is recommended for a stiff system of differential equations.

2.18.7 Matlab ODE solvers

Matlab is equipped with the ordinary differential equation (ODE) solvers given in table 2-4:

Table 2-4 Summary of Matlab ODE solver algorithms.

Function	*Description*
ode45	Based on an explicit Runge-Kutta (4,5) formula, the Dormand-Prince pair. This is a one-step solver. Best used as a "first try" for most problems
ode23	Based on an explicit Runge-Kutta (2,3) pair of Bogacki and Shampine. This is a one-step solver and may be more efficient than ode45 at crude tolerances and in the presence of mild stiffness
ode113	This is a variable-order Adams-Bashforth_Moulton solver. It may be more efficient than ode45 at stringent tolerances and when the ODE function is particularly expensive to evaluate. This is a multi-step solver, requiring solutions at several preceding time points to compute the current solution.
ode15s	This is a variable-order solver based on the numerical differentiation formulas. It can optionally, use the backward differentiation formulas (Gear's Method) that are usually less efficient. This is a multi-step solver. If a problem is stiff or if ode45 fails or was very inefficient, try ode15s
ode23s	This is based on a modified Rosenbrock formula of order 2. It is a one-step solver and may be more efficient than ode15s at crude tolerances. It can solve some kinds of problems for which ode15s is not effective.

2.18.8 Selection of differential equation solver

The following are some of the criteria that need to be considered when selecting and evaluating the performance of numerical methods for solving differential equations:

- The result should be as close to the desired goal as possible. The desired goal is the solution of the problem at the end of the interval with an error that falls within a specified tolerance.

- Minimum effort in program design and coding.

- Minimum effort on the computer in terms of computational burden.

- The method should be stable.

- The convergence of the method. Convergence ensures that the true solution can be approached arbitrarily closely for all $t \in [0,b]$ and for a step size $h = t/n$ with $n \to \infty$. Errors in the starting value y_0 are permitted.

For the given problem, the differential equation set will have to be integrated over a (relatively) long interval. Many steps will be required for the accuracy desired. In addition, the equations are likely to be stiff. Multi-step methods perform well for this type of problem with the Adams predictor-corrector set or the trapezoidal method being suggested for stiff problems [23].

Gerald and Wheatley[20] provide the comparison in table 2-5 of methods for solving ordinary differential equations:

Table 2-5 Comparison of methods for solving differential equations [20].

Method	Type	Local Error	Global Error	Function evaluations / step	Stability	Recom-mended?
Modified Euler	SS	$O(h^3)$	$O(h^2)$	2	Good	No
4th order Runge-Kutta	SS	$O(h^5)$	$O(h^4)$	4	Good	Yes
Runge-Kutta-Fehlberg	SS	$O(h^6)$	$O(h^5)$	6	Good	Yes
Milne	MS	$O(h^5)$	$O(h^4)$	2	Poor	No
Adams-Moulton	MS	$O(h^5)$	$O(h^4)$	2	Good	Yes
SS = single step, MS = multi-step						

Gear's method is a predictor-corrector method for use with stiff equations that has an $O(h^6)$ local error, but is computationally more efficient than Adams' method [20]. It is thus likely that the Matlab ode15s method would give the best overall performance when applied to solving the differential equation set for transient stability analysis.

2.19 Load Flow

The object of load-flow calculations is to determine the steady-state operating characteristics of the power generations/transmission system for a given set of busbar loads. The solution provides information on voltage magnitudes and angles, reactive and active power flows and the reactive power generated or absorbed at voltage controlled busses. The load-flow problem is formulated with the network represented by linear lumped parameters. The power and voltage constraints make the problem non-linear, and the numerical solution must therefore be iterative.

2.19.1 Nodal analysis

Mesh or nodal analysis may be used to derive a set of equations describing the distribution network. Nodal analysis is preferred [19, 21] due to the following advantages:

- The number of equations are generally less than obtained with mesh analysis

- There is no need to combine parallel branches before forming equations

- There is no difficulty in dealing with non-planar networks

- The admittance matrix is square (n x n)

- The nodal admittance matrix is symmetrical since $y_{ij} = y_{ji}$.

- Each off diagonal element is the negative of the branch admittance between nodes k and i and is frequently zero.

- Each diagonal element y_{kk} is the sum of the admittances of the branches which terminate on node k, including branches to ground.

- For practical networks, the nodal admittance matrix is highly sparse.
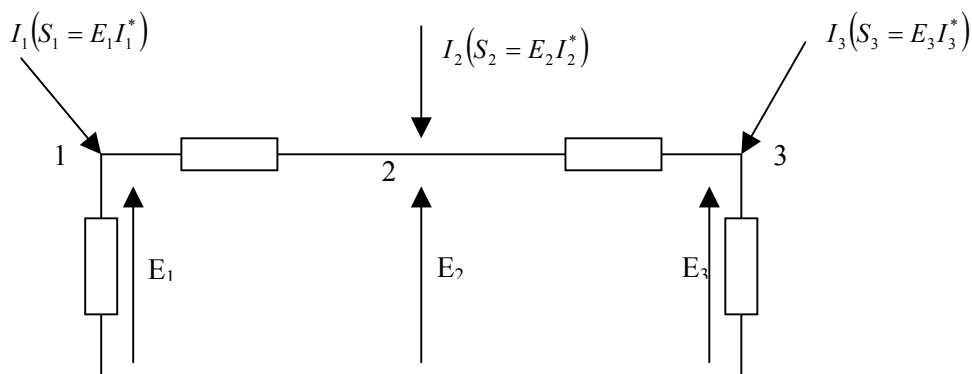
Figure 2-22 Simple network illustrating nodal quantities [21].

Two different references are usually chosen: For voltage magnitudes, the reference is ground and for voltage angles, one of the busbars is chosen as zero. A nodal current is the net current injected into the network at a given node from an external source and/or load. Current entering the network from a source is defined as positive and current leaving the network to a load is defined as negative. Nodal injected powers ($S=P+jQ$) are similarly defined. Figure 15-1 gives a simple network illustrating the various network quantities.

It is convenient to use branch admittances rather than impedances. The voltage of nodes k and i are denoted as E_k and E_i and the admittance of the branch between them by y_{ki}. The current flowing in this branch is given by [21]:

$$I_{ki} = y_{ki}\left(E_k - E_i\right) \tag{2-186}$$

For a network with n nodes, by Kirchoff's current law, the injected current into node k is given by:

$$I_k = \sum_{i=0}^{n} I_{ki} = \sum_{i=0}^{n} y_{ki}\left(E_k - E_i\right)$$

(2-187)

Since $E_0=0$, and if the system is linear:

$$I_k = \sum_{i=0\neq k}^{n} y_{ki}E_k - \sum_{i=1\neq k}^{n} y_{ki}E_i$$

(2-188)

If this equation is written for all nodes except the reference node[16] in the case of a power system network, then a complete set of equations defining the network is obtained of the following form [21]:

$$\begin{bmatrix} I_1 \\ I_2 \\ \vdots \\ I_n \end{bmatrix} = \begin{bmatrix} Y_{11} & Y_{12} & \cdots & Y_{1n} \\ Y_{21} & Y_{22} & & Y_{2n} \\ \vdots & & \ddots & \vdots \\ Y_{n1} & \cdots & \cdots & Y_{nn} \end{bmatrix} \begin{bmatrix} E_1 \\ E_2 \\ \vdots \\ E_n \end{bmatrix}$$

(2-189)

where

$$Y_{kk} = \sum_{i=0\neq k}^{n} y_{ki} = \text{self admittance of node k}$$

$$Y_{ki} = -y_{ki} = \text{mututal admittance between nodes k and i}$$

or:

$$I_k = \sum_{i=1}^{n} Y_{ki}E_i$$

(2-190)

One of the voltages in the network is usually specified in load flow studies, and instead the current at that busbar is unknown. Assuming that E_1 is the known voltage, it is eliminated as a variable from the nodal equations as follows [21].

$$\begin{bmatrix} I_1 \\ I_2 \\ \vdots \\ I_n \end{bmatrix} - \begin{bmatrix} Y_{11}E_1 \\ Y_{12}E_1 \\ \vdots \\ Y_{1n}E_1 \end{bmatrix} = \begin{bmatrix} Y_{21}E_2 & Y_{31}E_3 & \cdots & Y_{2n}E_n \\ Y_{22}E_2 & Y_{32}E_3 & & Y_{3n}E_n \\ \vdots & & \ddots & \vdots \\ Y_{n2}E_2 & Y_{n3}E_3 & \cdots & Y_{nn}E_n \end{bmatrix}$$

(2-191)

The first row of the above set of equations may now be eliminated leaving (*n-1*) equations in (*n-1*) unknowns:

$$\begin{bmatrix} I_2 - Y_{21}E_1 \\ \vdots \\ I_n - Y_{n1}E_1 \end{bmatrix} = \begin{bmatrix} Y_{22} & \cdots & Y_{2n} \\ \vdots & \ddots & \vdots \\ Y_{n2} & \cdots & Y_{nn} \end{bmatrix} \begin{bmatrix} E_2 \\ \vdots \\ E_n \end{bmatrix}$$

(2-192)

or $\mathbf{I} = \mathbf{Y} \cdot \mathbf{E}$.

The new matrix **Y** is obtained from the full admittance matrix by simply removing the row and column corresponding to the fixed-voltage busbar. In summation notation, the new equations are [21]:

$$I_k - Y_{k1}E_1 = \sum_{i=2}^{n} Y_{ki}E_i \quad \text{for } k = 2,\ldots,n$$

(2-193)

---

[16] The reference node designates ground (0V)

2.19.2 Load flow variables

The following four variables must be determined at each bus in the system in order to calculate power flows throughout the system.

- P – real (active) power
- Q – reactive (quadrature) power
- V – Voltage magnitude
- θ – Voltage phase angle

Three different bus conditions are defined based on steady-state assumptions of constant system frequency and constant voltages[17]:

2.19.3 Voltage-controlled bus

The total injected active power P is specified and the voltage magnitude V is maintained at a specified value by reactive power injection. This type of bus generally corresponds to a generator where P is fixed by turbine governor setting and V is fixed by automatic voltage regulators acting on the machine excitation.

2.19.4 Nonvoltage-controlled bus

The total injected power $P + jQ$ is specified at this bus. This corresponds to a load centre in a physical power system. Both P and Q are assumed to be unaffected by small variations in bus voltage.

2.19.5 Slack or swing bus.

This bus arises because system losses are not known precisely in advance of the load-flow calculation, therefore the total injected power cannot be specified at every bus. One of the available voltage controlled busses is chosen as slack, and its active power is regarded as unknown. The slack bus voltage is usually assigned as the system phase reference, and its complex voltage:

$$E = V \angle \theta$$

is specified. This represents the generating station that has the responsibility for system frequency control in a practical power system.

2.19.6 Newton-Raphson method of solving load flows

Various methods of solving the load-flow problem can be used. The Newton-Raphson method and derived techniques are used almost exclusively in commercial software packages for load-flow calculations [21]. Only the Newton-Raphson method will be used in this work.

The generalised Newton-Raphson method is an iterative algorithm for solving a set of simultaneous non-linear equations in an equal number of unknowns. At each iteration of the N-R method, the non-linear problem is approximated by a linear matrix equation. Consider the case of a single variable problem [21]:

$$f\left(x^p + \Delta x^p\right) = 0 \tag{2-194}$$

Where x^p is an approximation to the solution, with error Δx^p at iteration p. This can be expanded by Taylor's theorem:

---

[17] Where these quantities are controlled

$$f(x^p + \Delta x^p) = 0 = f(x^p) + \Delta x^p f'(x^p) + \frac{(\Delta x^p)^2}{2!} f''(x^p) + \cdots \tag{2-195}$$

Assuming that the error is small and neglecting all terms of higher powers gives [21]

$$f(x^p) + \Delta x^p f'(x^p) = 0 \tag{2-196}$$

or

$$\Delta x^p = \frac{-f(x^p)}{f'(x^p)} \tag{2-197}$$

The new value of the variable is then obtained from:

$$x^{p+1} = x^p + \Delta x^p \tag{2-198}$$

Equation (2-197) can be re-written as:

$$f(x^p) = -J\Delta x^p \tag{2-199}$$

This is readily extended to a set of N equations in N unknowns. J becomes the square Jacobian matrix of the first-order partial differentials of the functions $f_k(x_m)$ [21]:

$$J_{km} = \frac{\partial f_k}{\partial x_m} \tag{2-200}$$

2.19.7 Power system load flow equations

The power distribution network is described by the following equations [21]:

$$I_k = \sum_{m=0}^{n} y_{km} E_m \text{ for all } k \tag{2-201}$$

Where I_k denotes the current injected into a bus k and E_m denotes the complex voltage at bus m. The power at a bus is then given by [21]

$$\begin{aligned} S_k = P_k + jQ_k &= E_k I_k^* \\ &= E_k \sum_{m=0}^{n} y_{km}^* E_m^* \end{aligned} \tag{2-202}$$

where I_k^* denotes the complex conjugate of the current injected into bus k, P_k denotes real power and Q_k denotes reactive power. The complex loadflow equations are nonanalytic and cannot be differentiated in complex form. The problem has to be separated into real equations and variables using polar or rectangular co-ordinates for the bus voltages. this gives the following two equations [21]:

$$P_k = P(V, \theta) \text{ and } Q_k = Q(V, \theta) \tag{2-203}$$

The bus voltages and admittances are defined as [21]:

$$\begin{aligned} E_k &= V_k(\cos\theta_k + j\sin\theta_k) \\ y_{km}^* &= G_{km} - jB_{km} \\ E_m^* &= V_m(\cos\theta_m - j\sin\theta_m) \end{aligned} \tag{2-204}$$

Substitution of the above into equation 2-202 and separating the real and imaginary parts gives the following expressions for real and imaginary power in polar co-ordinates [21]:

$$P_k = \sum_{m \in k} V_k V_m \left(G_{km} \cos \theta_{km} + B_{km} \sin \theta_{km} \right)$$ **(2-205)**

$$Q_k = \sum_{m \in k} V_k V_m \left(G_{km} \sin \theta_{km} - B_{km} \cos \theta_{km} \right)$$ **(2-206)**

where

$$\theta_{km} = \theta_k - \theta_m$$ **(2-207)**

For small variations in the voltage and angle variables, the resulting equations are obtained by forming the total differentials [21]:

$$\Delta P_k = \sum_m \frac{\partial P_k}{\partial \theta_m} \Delta \theta_m + \sum_m \frac{\partial P_k}{\partial V_m} \Delta V_m$$ **(2-208)**

and

$$\Delta Q_k = \sum_m \frac{\partial Q_k}{\partial \theta_m} \Delta \theta_m + \sum_m \frac{\partial Q_k}{\partial V_m} \Delta V_m$$ **(2-209)**

- For a PQ busbar both equations are used
- For a PV busbar, only equation 2-208 is used since Q_k is not specified.
- For a slack busbar, no equations are required.

The complete set of defining equations is made up of two equations for each PQ busbar and one for each PV busbar. The voltage magnitudes for PV and slack busbars are not variables, since they are specified. Similarly, θ is fixed at the slack busbar. The number of variables is therefore equal to the number of equations giving [21]:

$$\begin{bmatrix} \Delta P^{p-1} \\ \Delta Q^{p-1} \end{bmatrix} = \begin{bmatrix} H^{p-1} & N^{p-1} \\ J^{p-1} & L^{p-1} \end{bmatrix} \begin{bmatrix} \Delta \theta^p \\ \dfrac{\Delta V^p}{V^{p-1}} \end{bmatrix}$$ **(2-210)**

where

ΔP^{p-1} = P mismatches for all PQ and PV busbars

ΔQ^{p-1} = Q mismatches for all PQ busbars

$\Delta \theta^p = \theta$ corrections for all PQ and PV busbars

$\Delta V^p / V^{p-1}$ = V corrections for all PQ busbars

The differences in bus powers are obtained from [21]

$$\Delta P_k = P_k^{SP} - P_k$$
$$\Delta Q_k = Q_k^{SP} - Q_k$$ **(2-211)**

The division of each ΔV^p by V^{p-1} does not affect the algorithm numerically, but simplifies some of the Jacobian matrix terms. The performance of the Newton-Raphson algorithm is closely related to problem non-linearity, with the best defining equations being the most linear. For busbars k and m the terms of the Jacobian matrix are given by [21]:

$$H_{km} = \frac{\partial P_k}{\partial \theta_m} = V_k V_m \left(G_{km} \sin \theta_{km} - B_{km} \cos \theta_{km} \right)$$

$$N_{km} = \frac{\partial P_k}{\partial V_m} = V_k V_m \left(G_{km} \cos \theta_{km} + B_{km} \sin \theta_{km} \right)$$

$$J_{km} = \frac{\partial Q_k}{\partial \theta_m} = -V_k V_m \left(G_{km} \cos \theta_{km} + B_{km} \sin \theta_{km} \right)$$

$$L_{km} = \frac{\partial Q_k}{\partial V_m} = V_k V_m \left(G_{km} \sin \theta_{km} - B_{km} \cos \theta_{km} \right)$$

(2-212)

and for *m=k* [21]

$$H_{kk} = \frac{\partial P_k}{\partial \theta_k} = -Q_k - B_{kk} V_k^2$$

$$N_{kk} = \frac{\partial P_k}{\partial V_k} = P_k + G_{kk} V_k^2$$

$$J_{kk} = \frac{\partial Q_k}{\partial \theta_k} = P_k - G_{kk} V_k^2$$

$$L_{kk} = \frac{\partial Q_k}{\partial V_k} = Q_k - B_{kk} V_k^2$$

(2-213)

These equations can also be expressed using voltages in rectangular form, but the polar co-ordinate representation is recommended since it has computational advantages over rectangular co-ordinates [21]. The polar co-ordinate representation was used for this work and rectangular co-ordinates are therefore not discussed further.

A further improvement is to replace the reactive power residual ΔQ in the Jacobian matrix equations by $\Delta Q/V$. If the system power equation is divided throughout by V_k, only one term on the right-hand side of the equation is non-linear in V_k.

The success of the Newton-Raphson method is highly dependent upon the formulation of the problem defining equations. Power mismatch representation is better than current mismatch representations [21].

2.19.8 Improvements to basic Newton-Raphson algorithm

The techniques that have been used to improve the efficiency of the Newton-Raphson method are centered around the efficient solution of the Jacobian matrix equation and reducing storage requirements by taking advantage of the sparsity of the system admittance and Jacobian matrices [21]. These techniques become very important when large systems[18] need to be analysed. For the present work, the system size will be approximately 100 – 200 busses. Since the main aim of the work is to investigate load behaviour, and not load- flow algorithms, the simplest solution providing accurate reliable results was used. Refinements are only implemented when absolutely necessary. In general, the following principles were adopted [21]:

- Use the basic Newton-Raphson algorithm as far as possible
- System size will be kept relatively small
- Computational efficiency is not considered a high priority
- Utilise the built-in Matlab functions wherever possible
- Decoupled load flow algorithms were not considered.

---

[18] A system with approximately 500 or more busses would be considered large

An overview of the basic loadflow algorithm is shown in Figure 2-23.
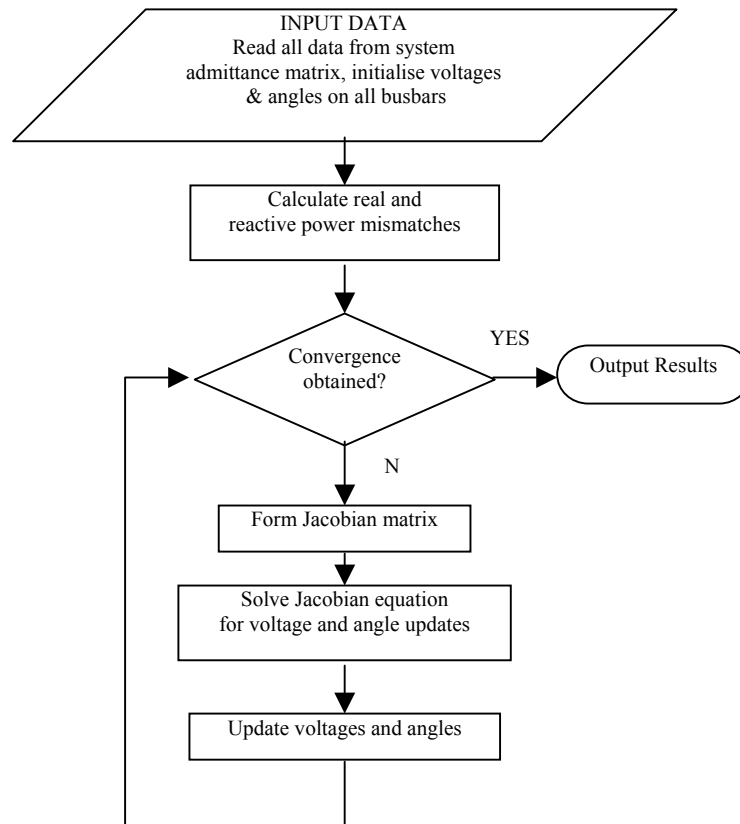
Figure 2-23 Basic load flow algorithm [21].

3 OVERVIEW OF SYSTEM COMPONENTS

3.1 PetroSA Electrical Distribution System Description

The PetroSA electrical distribution system consists of a primary 132kV distribution network feeding six main substations. From these substations, secondary distribution networks operating at 11 and 6.6kV supply power to the secondary substations. Electrical loads operating at 11, 6.6kV and 550V are supplied from main and secondary substations. The system also includes two generators. A 140MVA unit provides approximately half of the plant's power requirements from steam generated by waste heat. The second generator, rated at 14MVA, supplies power to the critical power system. This system supplies power to equipment that must remain operational to allow a controlled plant shutdown following a power outage on the Eskom supply network. The critical power system and 14MVA generator is automatically isolated from the rest of the distribution system whenever disturbances are detected[1] and continues operating in what is termed *"island mode"*.

3.1.1 Eskom network

Figure 3.1 is a simplified diagram of the Eskom network supplying PetroSA
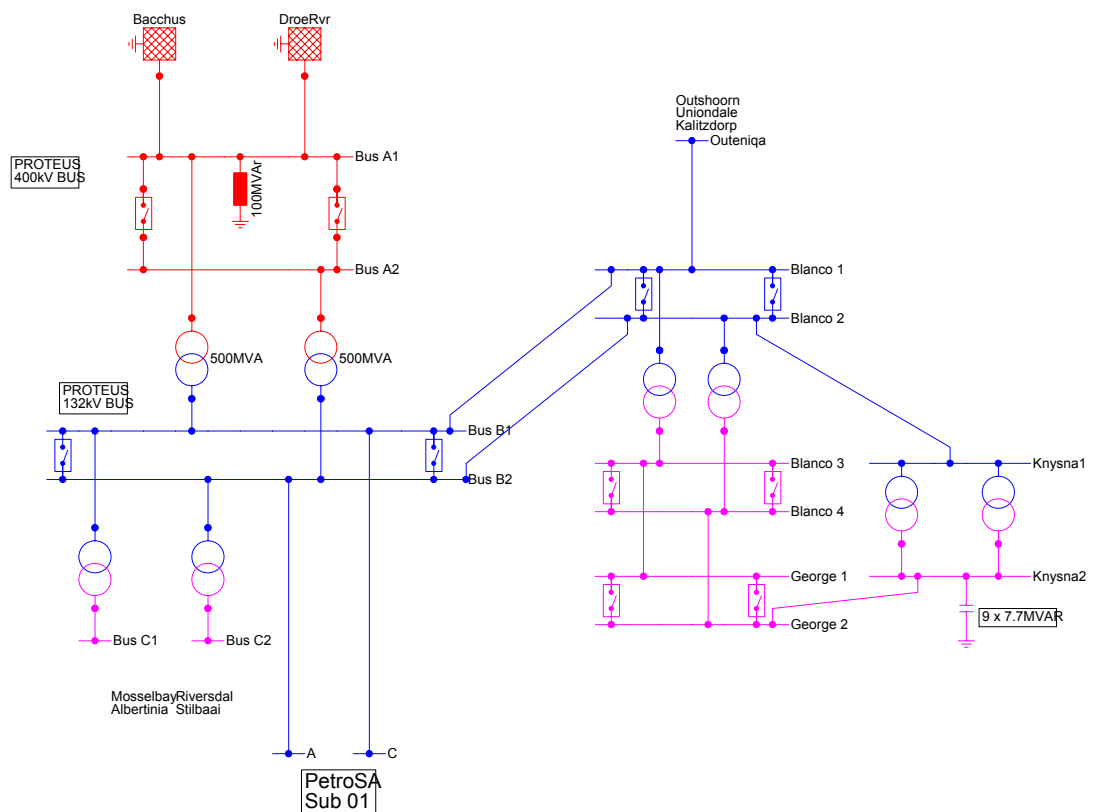
Figure 3-1 Eskom network supplying PetroSA.

The Eskom network supplying power to PetroSA consists of the following:

---

[1] The critical power system is manually re-synchronised with the remainder of the system after the cause of the electrical disturbance which caused the system to island has been determined and further disturbances are considered unlikely.

- Two 400kV lines. One line runs from Bacchus (Cape Town area) to Proteus Substation. The other line runs from Droe Rivier (Beaufort West area) to Proteus Substation.
- Proteus Substation is situated 15km away from PetroSA and incorporates two 500MVA, 400/132kV transformers.
- Two 132kV lines supply power to PetroSA Substation 01.

3.1.2 PetroSA system overview

The main power intake is located at Substation 01 (refer to Figure 3-4). From here, power is fed to the main substations 02, 03, 04, 05 and 06. The following is a summary of the major units supplied from these main substations.

- *Sub 02* (Figure 3-5) supplies the air separation unit where the major power consumers are the main air compressors (2 x 26MW synchronous machines) and the oxygen compressors (2 x 9.85MW induction machines) Most of the remaining loads are compressor auxiliaries and motorised valves. The main air compressors are also used for power factor correction.
- *Sub03* (not shown)supplies the catalyst preparation plant. The most significant load in this plant is the arc-furnace (7MW), ball-mill (132kW) and secondary catalyst crusher(110kW).
- *Sub 04* (not shown) supplies the Synthol unit. This is the largest substation on site feeding approximately 500 different loads. The most significant being the three total feed gas compressors (20MW each). These compressor motors are synchronous machines fed from variable speed drives. The variable speed drives (VSD's) are designed to 'ride through' a power dip of up to 180ms duration. When line voltage drops by 20% or more, the VSD cuts power to the motor and the compressor will start decelerating. If the line voltage recovers within 180ms, the VSD will re-accelerate the compressors to normal operating speed. If the duration of the power dip is longer than 180ms, the drive will shut down resulting in the synthol train shutting down. Under these circumstances, all three synthol trains usually trip followed by the downstream units, resulting in a total plant shutdown.
- *Sub05* (Figure 3-6) supplies mainly utility units. In addition, the critical power distribution system is fed from this substation. Some of the major loads are: tail gas processing and LNG storage refrigerant compressors (7MW each), main cooling water pumps and cooling tower fans. Four secondary substations are supplied from this substation, as well as all critical power. These secondary substations supply power to various utility units.
- *Sub06* (Figure 3-7) supplies power to the Methane reforming unit. The major loads are cooling fans and blowers and a number of pumps. Eight secondary sub stations are supplied from this substation. These secondary substations supply power to the refinery units, tank farm, water treatment and effluent handling units.

3.1.3 Critical power system

The plant is equipped with a critical power system. This consists of a 10MW generator and associated distribution network. Substations generally have 'A' and 'B' boards supplied from independent feeders to provide redundancy. The tie breaker between 'A' and 'B' boards is usually closed. A typical arrangement with normal and critical power supplies is shown in Figure 3-2 below:
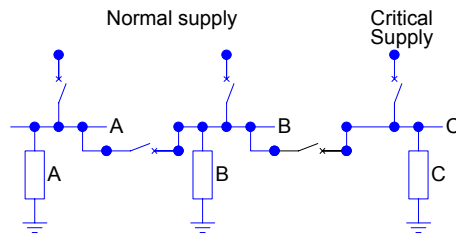
Figure 3-2 Typical substation critical supply arrangement.

The 'C' board is supplied from the critical generator and the tie breaker is usually open. If the critical generator is unavailable, the 'C' board can be fed from the 'B' board via the tie breaker. The layout of the critical power system showing the connection to the Eskom supply as well as the main plant generator (48GT101) is shown in Figure 3-3 below.
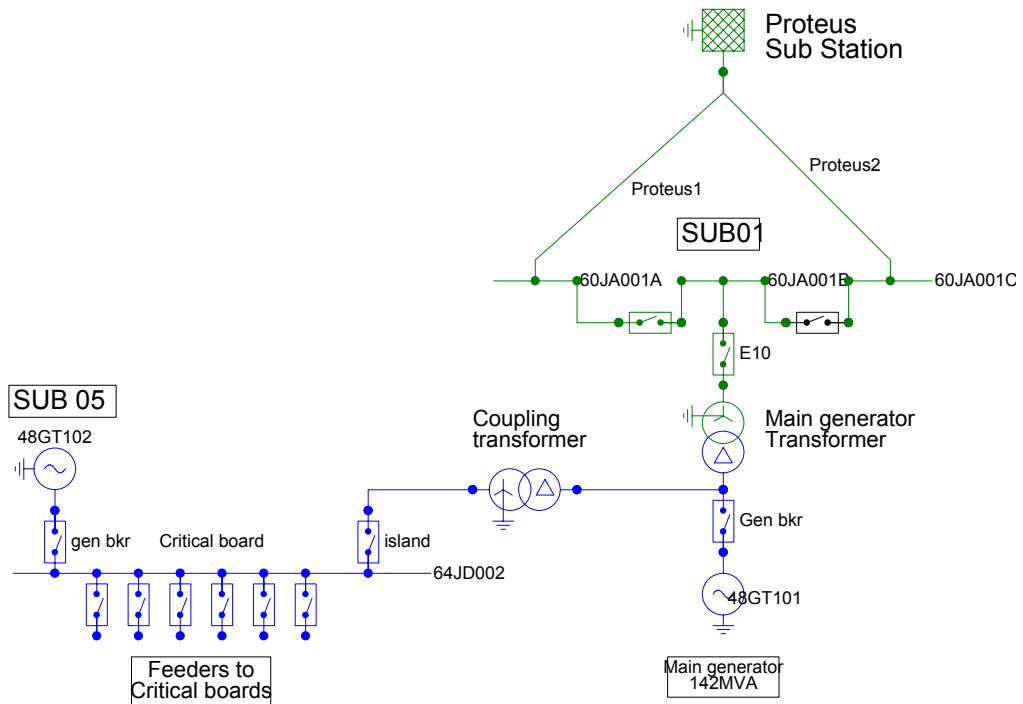
Figure 3-3 Critical power system

PetroSA is equipped with two generators, the main generator, 48GT101 and the Critical power generator, 48GT102 (refer Figure 3-4). The critical power generator is a 10MW unit and its primary purpose is to keep critical loads energised to permit a safe, controlled plant shutdown in the event of a major power outage or fault on the PetroSA distribution system. The critical generator feeds into the 11kV critical board in substation 05, and from here all critical loads throughout the factory are supplied. Most substations have a critical board,

supplied from substation 05 critical board. This board can be connected to the 'normal' boards in the substation via a tie breaker. This arrangement allows power to be supplied to the critical network in the event of a failure, or maintenance activities on the critical distribution system, During normal operation, all critical boards are supplied via the 11kV critical board in substation 05, and isolated from the rest of the electrical system. The only point of common coupling with the rest of the system is via the 'island' circuit breaker. The island circuit breaker is set up to trip instantaneously if any electrical disturbance is detected on the system. This isolates the critical power system from the rest of the PetroSA (and Eskom) system.

3.2   Modelling Of PetroSA Distribution Network

Modelling of the entire PetroSA distribution system is not practical. A portion of the system was modelled in detail, with the remainder of the system being represented by static loads. Where possible, equipment that could be omitted from the model was identified.

3.2.1   Selection of substation for modelling

For this initial analysis, selection of a secondary substation is preferable to one of the six main substations. System impedance will be higher at the secondary substations. Busbar voltage drops during starting of motors is likely to be more severe for these substations. The refinery units, which incorporate a large number of pumps normally remain on-line following a power dip. Optimal operation of the re-acceleration systems are essential to ensure that these units remain on-line. One of the refinery substations, substation 24, was selected for detailed modelling since the greatest potential for improvement exists within this area.

3.2.2   Transformer tap-changers

All distribution transformers are equipped with tap changers. These are not online tap-changers and thus play no role during system transients. There is rarely, if ever, a need to adjust tap-changer settings on transformers.

3.2.3   Distributed control system and power disturbances

The entire production process is controlled by a Distributed Control System (DCS). The DCS[2] equipment is located in the Central Control Room and in a number of Satellite buildings distributed around the site. Electrical drives are controlled by the DCS when in auto mode, or from manual stop/start stations in the field.

All DCS equipment is fed from 24VDC uninterruptible power supplies located in the Central Control Room and in each satellite building. The DCS and all field equipment will remain operational for at least one hour following a total power outage. Due to this arrangement, the DCS is not affected by, nor does it directly detect short duration power dips and or disturbances. The DCS will indirectly detect power dips due to flow and pressure changes that occur shortly after pump motors have tripped, and the possible shutdown of equipment such as compressors.

3.2.4   Compressors and compressor controls

Compressors are generally equipped with their own local control systems which interface to the DCS. Compressor response to power dip and duration will depend on the individual compressor control systems and varies. The four largest compressors on the plant usually trip following a power disturbance. The two main plant air compressors[3] (26MW synchronous

---

[2] Note that throughout this document, this control system will be referred to as the DCS

[3] The main plant air compressors, 03KC101 and 03KC201 and oxygen compressors 03KC102 amd 03KC202 are shown on Figure 3-5

motors) trip due to loss of excitation for power dips longer than 80ms. When these machines trip, process conditions force the two main oxygen compressors to trip within 10 to 15 seconds (9.85MW induction machines)

3.2.5 Pumps

During electrical transients, the DCS will continue to operate normally. Apart from small dosing pumps, most pumps either have no flow control or flow is regulated by control valves that restrict fluid flow. Since the chemical process time constants are long compared to those of electrical transients, control valve positions can be treated as constants during electrical power dips and for a short period thereafter. The period following a power dip during which control valve positions remain unchanged will differ from pump to pump. Although the DCS is not set up to explicitly detect and respond to a power dip, changes in flow rates will be detected after a power dip. This will take place during the period between which the motor is disconnected by the undervoltage relay, and the time that the re-acceleration circuit closes the contactor and the motor re-starts. In general, if a flow falls below the set point, the normal response of the DCS would be to open the associated control valve to restore normal flow. It is not feasible to determine the exact DCS response for individual pumps since this will depend on variables such as plant loading, tank levels, pressures etc. It is therefore assumed that all pump loads remain constant and equal to the pre-disturbance loading.

3.2.6 Motor operated valves

Motor operated valves only operate intermittently and are not considered.

3.3 Distribution System Model

The one-line diagrams of the system as modelled are presented in the following section. The substation chosen for detailed modelling (Sub 24, Figure 3-8 and Figure 3-9) is shown as well as the feeders and substations from the point of supply to Sub 24. The 6.6kV motors fed from Sub 24 were modelled and their behaviour and impact on the rest of the system investigated. The total load of the motors to be modelled is about 2MW or 1% of the total system load of approximately 200MW. The disturbances created by these motors will be relatively small, but busbar voltage drops will give an indication of the potential impact of much larger groups of motors being re-started simultaneously by the re-acceleration system. The remaining portions of the system will be modelled by constant impedances. The system voltage drops caused by the test motors will be small and these loads will remain relatively constant. Any of the more elaborate load models discussed in section 2.6 could have been used. Using these models could mask the effects of the test motors on the system, hence the choice of the simple constant impedance model. The PetroSA distribution system is equipped with a telemetry system that provides real time voltage, current and power measurements which was used to determine typical loads. Actual loads are usually about half the maximum theoretical connected load. This is due to most motors having an installed spare (e.g. "A" and "B" pumps) where only one of the two motors is operating at any given time. These lumped loads are indicated on the one-line diagrams.

The following applies to all diagrams:

- Node numbers are shown in a square near the bus
- Branch numbers[4] are shown next to the branch component. E.g. b23 = branch 23
- The system is shown in the normal mode of operation. Substation busbars generally have an 'A' and 'B' section with interconnecting tie breaker. Where these tie breakers are normally closed, the substation busbar is modelled as a single busbar and the tie breaker not shown. This is the usual arrangement for 11kV and 6.6kV busbars. 550V

---

[4] Node and branch numbers are the same as those used in the Matlab software.

MCC's are operated with tie breakers open and are equipped with a PLC controlled slow transfer scheme and 'A' and 'B' sections will be represented as separate busbars.

- Where a substation is modelled in more detail, only the substation number is indicated. If a load is shown along with a substation, that substation is not modelled and the given load represents that particular substation

3.3.1 Substation 01

The following figure shows the arrangement of the main substation, Sub 01:
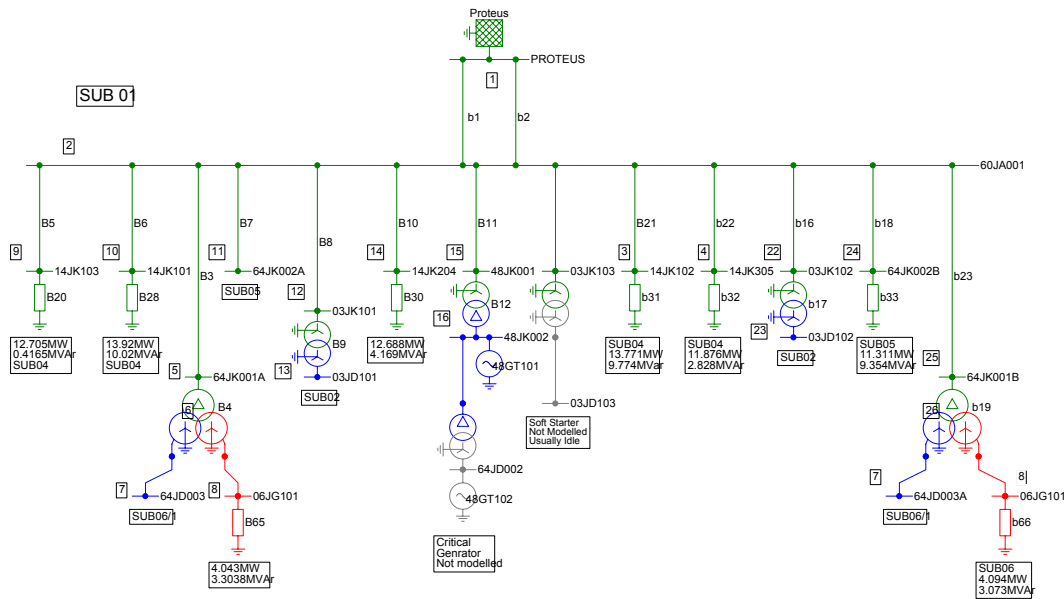
Figure 3-4. Substation 01 132kV (main substation).

The critical generator is not modelled. The only connection point between the critical power system and the remainder of the system is via the transformer between busses 64JD002 and 48JK002. If any voltage dip is detected, a breaker (not shown) instantaneously disconnects bus 64JD002 from the coupling transformer. The system normally operates with negligible current flow through the coupling transformer, i.e. the generator output equals the critical system power demand. The effect of the critical system is thus negligible before and after transients.

Only the 11kV bus of Sub06 is modelled since this feeds Sub24. The 6.6kV bus which is fed from the same three winding transformers (64JK001A/B) is modelled with a lumped load.

3.3.2 Substation 02

The following figure shows the arrangement of Sub 02. This substation supplies the air separation plant.
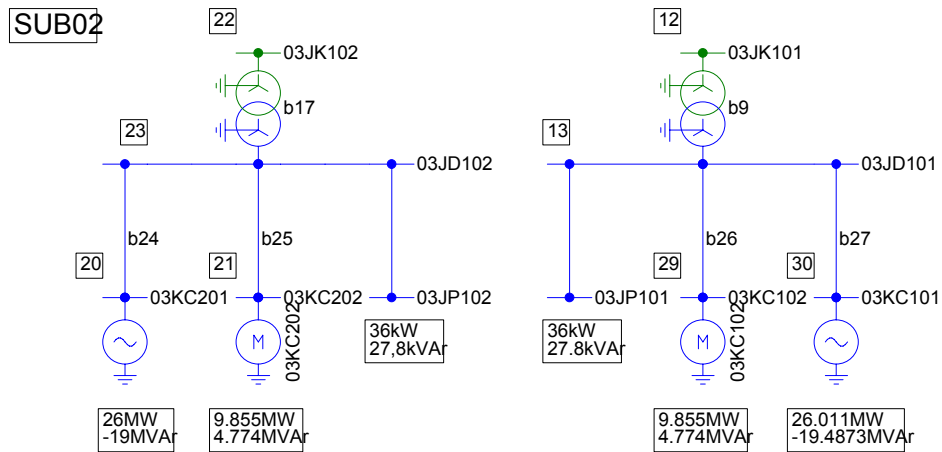
Figure 3-5 Substation 02 11kV distribution.

The soft starter which is fed from Sub01 via transformer 03JK103 is only used when starting the air separation plant compressor motors 03KC101/201 and is therefore not modelled. The air separation plant compressors are represented by constant power and reactive power loads applied to the relevant busbars as shown.

3.3.3 Substation 05

Substation 05 consists of two sections. The 11kV critical board (64JD002) shown in Figure 3-3 is not modelled, since this section of the distribution system is disconnected from the remainder of the system following a power supply disturbance. The medium voltage distribution is shown in Figure 3-6 below. Various other substations are fed from these 11kV

and 6.6kV boards. The normal loads on these boards are represented by equivalent static loads

SUB05
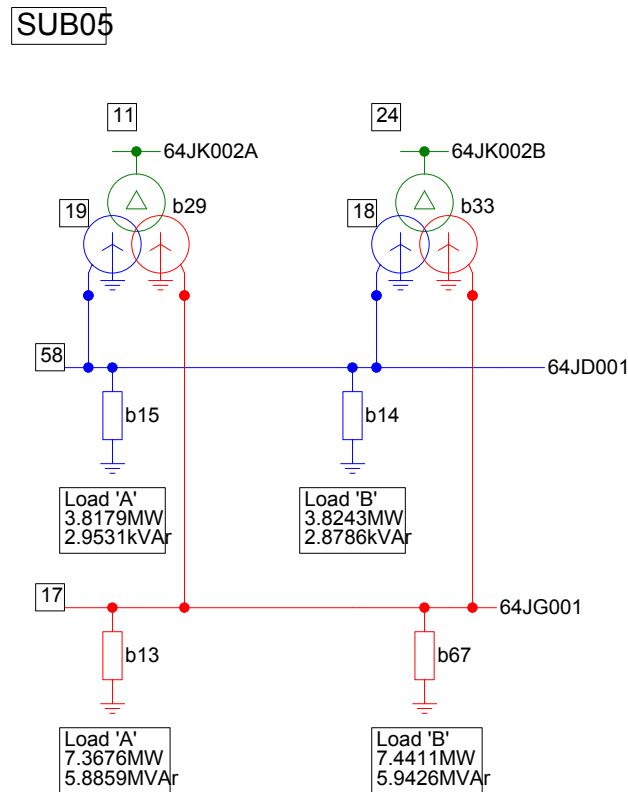
as shown.

Figure 3-6 Substation 05 MV distribution.

3.3.4 Substation 06

Substation 06 is one of the main substations on site. This was modelled in detail, since it supplies substation 24 which was chosen for detailed modelling of motor loads. A number of secondary substations are supplied from substation 06. The normal loads of these substations were represented by equivalent static loads as shown in Figure 3-7 below.

Figure 3-7 Substation 06 MV distribution.
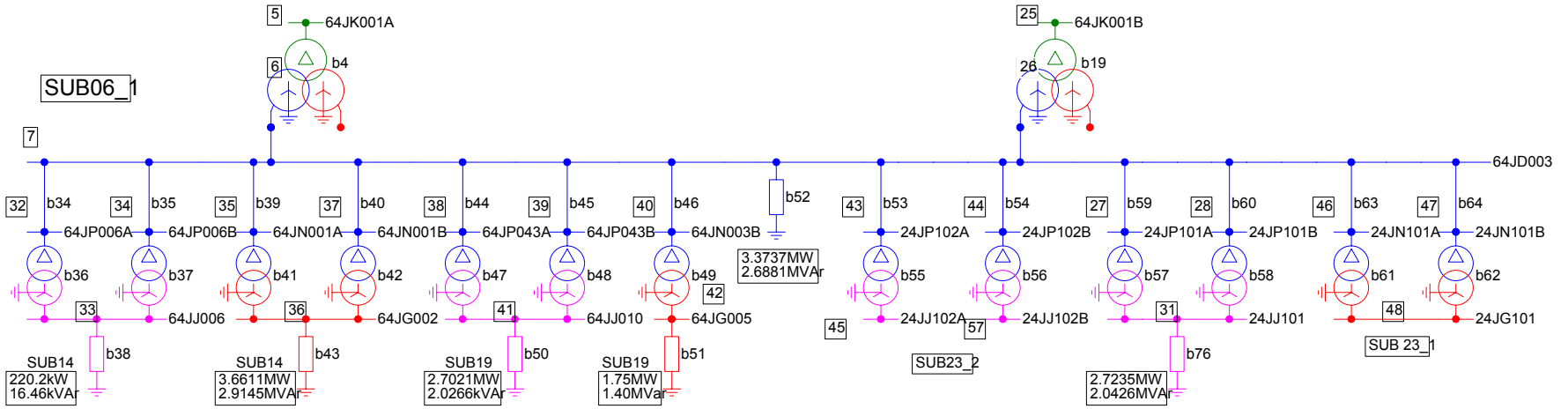
Load			Load		
64JP005A/B	61kW	45.6kVAr	64JN007B	194.7kW	147.6kVAr
63JP011	Off		64JN009B	299.4kW	234.7kVAr
63JP023	Off		64JP005B	30kW	22.8kVAr
64JP009A	Off		64JP007B	4kW	5kVAr
64JN008A	1135.2kW	908.2kVAr	64JP008B	1.367kW	1.108kVAr
64JN007A	193.6kW	147.0kVAr	64JP014A	55kW	41.5kVAr
64JP005A	30kW	22.5kVAr	64JP007A	4kW	5kVAr
			TOTAL	3.3737MW	2.6881MVAr

Notes:
64JD003A/B modelled as a single bus since B/C normally closed
A number of loads have been combined and are represented by load branch b52
Some feeders to Sub 14 & 19 have been modelled to examine the effect of load changes

3.3.5 Substation 24

This substation was chosen for detailed modelling of the 6.6kV induction motors. The 6.6kV layout is shown in Figure 3-8 and the 525V layout in Figure 3-9 on the following pages.

The motors modelled for simulation purposes are shown with their ratings and re-acceleration timer settings. Note that at any given time, only the 'A' or 'B' motor would be in operation. It is therefore only necessary to model the following four motors 24PC101A (300kW), 24PC102A(800kW), 24PC104A(300kW) and 24KC101A (550kW – no spare). Motor 24KC101 is a compressor motor with its own independent controls and is not part of the re-acceleration system.

The 525V motor loads are shown as lumped static loads grouped according to re-acceleration time setting.
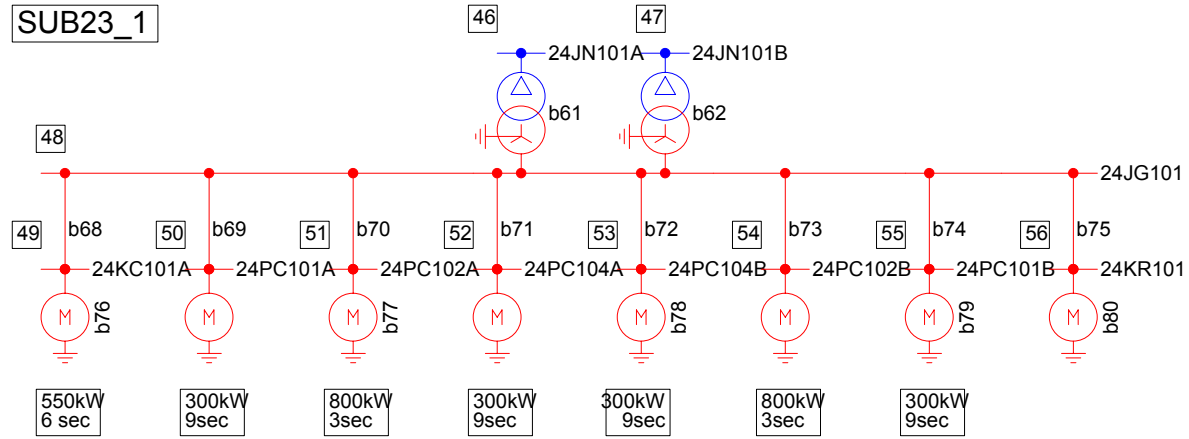
Figure 3-8 Substation 24 – 6.6kV.

Figure 3-9 Substation 24 - 550V.

3.4 System Data

This section introduces the data that was used as input for all simulations.

3.4.1 Bus data

The bus type is given by:

- 1 = Swing bus
- 2 = Voltage-controlled bus
- 3 = Load bus
- P_G, Q_G = Power and reactive power injected into system (generation) in p.u. on a 100MVA base.
- P_D, Q_D = Power and reactive power taken out of system (loads) in p.u.

Table 3-1 Bus data used for simulation.

Bus	Type	Vbus kV	P_G	Q_G	P_D	Q_D	Nominal Bus Voltage (KV)	
1	1	133	0	0	0	0	132	Swing Bus - Proteus
2	3	132	0	0	0	0	132	Sub01 - 60JA001A/B/C
3	3	132	0	0	0	0	132	Sub04 - 14JK102 - primary
4	3	132	0	0	0	0	132	Sub04 - 14JK305 - primary
5	3	132	0	0	0	0	132	Sub06 - 64JK001A - primary
6	3	132	0	0	0	0	132	64JK001A - internal modelling bus
7	3	11	0	0	0	0	11	Sub06 - 64JD003A/B
8	3	6.6	0	0	0	0	6.6	Sub06 - 06JG101A/B/C
9	3	132	0	0	0	0	132	Sub04 - 14JK103 - primary
10	3	132	0	0	0	0	132	Sub04 - 14JK101
11	3	132	0	0	0	0	132	Sub05 - 64JK002A - primary
12	3	132	0	0	0	0	132	Sub02 - 03JK101 - primary
13	3	11	0	0	0	0	11	Sub02 - 03JD101
14	3	132	0	0	0	0	132	Sub04 - 14JK204 - primary
15	3	132	0	0	0	0	132	Sub48 - 48JK001 - primary
16	3	11	56	41	0	0	11	Sub48 - 48JK002 - primary +GT101
17	3	6.6	0	0	0	0	6.6	Sub05 - 64JG001A/B
18	3	132	0	0	0	0	132	64JK002B - internal modelling bus
19	3	132	0	0	0	0	132	64JK002A - internal modelling bus
20	3	11	0	19.4873	26.0177	0	11	Sub03 - 03KC201
21	3	11	0	0	9.8551	4.774	11	Sub03 - 03KC202
22	3	132	0	0	0	0	132	Sub02 - 03JK102 - primary
23	3	11	0	0	0	0	11	Sub02 - 03JD102
24	3	132	0	0	0	0	132	Sub05 - 64JK002B - primary
25	3	132	0	0	0	0	132	Sub06 - 64JK001B - primary
26	3	132	0	0	0	0	132	64JK001B - internal modelling bus
27	3	11	0	0	0	0	11	Sub24 - 24JP101A - primary
28	3	11	0	0	0	0	11	Sub24 - 24JP101B - primary
29	3	11	0	0	9.8551	4.7784	11	Sub03 - 03KC102
30	3	11	0	19.4873	26.0177	0	11	Sub03 - 03KC101
31	3	0.55	0	0	0	0	0.55	Sub24 - 24JJ101A/B

Bus	Type	Vbus kV	P_G	Q_G	P_D	Q_D	Nominal Bus Voltage (KV)	
32	3	11	0	0	0	0	11	Sub14 - 64JP006A - primary
33	3	0.55	0	0	0	0	0.55	Sub14 - 64JJ006A/B
34	3	0.55	0	0	0	0	0.55	Sub14 - 64JP006B - primary
35	3	11	0	0	0	0	11	Sub14 - 64JN001A - primary
36	3	6.6	0	0	0	0	6.6	Sub14 - 64JG002A
37	3	11	0	0	0	0	11	Sub14 - 64JN001B - primary
38	3	11	0	0	0	0	11	Sub19 - 64JP043A - primary
39	3	11	0	0	0	0	11	Sub19 - 64JP043B - primary
40	3	11	0	0	0	0	11	Sub19 - 64JN003B - primary
41	3	0.55	0	0	0	0	0.55	Sub19 - 64JJ010A/B
42	3	6.6	0	0	0	0	6.6	Sub19 - 64JG005
43	3	11	0	0	0	0	11	Sub24 - 24JP102A - primary
44	3	11	0	0	0	0	11	Sub24 - 24JP102B - primary
45	3	0.55	0	0	0	0	0.55	Sub24 - 24JJ102A
46	3	11	0	0	0	0	11	Sub24 - 24JN101A - primary
47	3	11	0	0	0	0	11	Sub24 - 24JN101B - primary
48	3	6.6	0	0	0	0	6.6	Sub24 - 24JG101A/B
49	3	6.6	0	0	0	0	6.6	Sub24 - 24KC101M
50	3	6.6	0	0	0	0	6.6	Sub24 - 24PC101AM
51	3	6.6	0	0	0	0	6.6	Sub24 - 24PC102AM
52	3	6.6	0	0	0	0	6.6	Sub24 - 24PC104AM
53	3	6.6	0	0	0	0	6.6	Sub24 - 24PC104BM
54	3	6.6	0	0	0	0	6.6	Sub24 - 24PC102BM
55	3	6.6	0	0	0	0	6.6	Sub24 - 24PC101BM
56	3	6.6	0	0	0.1793	0.1344	6.6	Sub24 - 24KR101M
57	3	0.55	0	0	0	0	0.55	Sub24 - 24JJ102B
58	3	11	0	0	0	0	11	Sub05 - 64JD001A/B

3.4.2 Branch data

Branch data was obtained from the databases of the software currently used at PetroSA for fault current and loadflow analysis. This data is entered into a spreadsheet in a format suitable for import by the Matlab simulation software and is thus not tabulated here.

4 DETAILED SIMULATION STRATEGY

4.1 Software Selection

In order to investigate the transient behaviour of the PetroSA distribution system, various system models had to be developed. These models then had to be implemented on a suitable software platform. One of the objectives of this work is to investigate the application of 'general-purpose' software tools to the transient stability problem. The following were considered:

a) Spreadsheet application – MS-Excel

MS-Excel is equipped with an embedded Visual Basic programming capability. The combination of the programming facility with the spreadsheet user interface allows for very rapid software development, since the spreadsheet can be used to enter and pre-process data as well as present results in tabular or graph format. The Visual Basic application can focus on processing the data. The advantage is that very little time needs to be spent on developing a user interface and associated software allowing most of the time to be spent solving the problem at hand. The major disadvantage is that the Visual Basic application runs through an interpreter resulting in slow execution.

b) Develop a stand-alone application

All the required software could be developed using a standard programming language such as C++. This option will require a significant amount of time and effort to be spent on developing the user interface and support functions allowing less time to focus on the core problem. The time and effort required to develop an de-bug a stand-alone software application is not justified for this type of analysis and this option was not considered.

c) Engineering/scientific analysis software, Matlab.

The Matlab/Simulink environment incorporates an extensive mathematical and numerical analysis function set. The nature of the transient stability problem requires extensive use of matrix manipulation and calculation as well as numerical integration. It would thus be possible to develop the required transient stability analysis software and machine models by building on existing Matlab functionality.

Matlab was selected as the development platform based on the following considerations:

i)   Matrix manipulation functions and ODE solvers for stiff and non-stiff problems are built in. There would be no need to devote a significant programming effort to implementing these functions.

ii)   Matlab programming code executes somewhat faster than Visual Basic code embedded in Excel[1]

iii) Matlab has the ability to import and export data in spreadsheet format. Excel can therefore still be used for preparing system data and, if necessary presentation of results.

---

[1] Based on a crude test executing an arbitrary section of code a set number of times.

4.2   Simulation Of Faults

A review of voltage dips recorded at PetroSA substation 01 over a two year period was carried out. This data was obtained from a perturbograph installed at substation 01. The substation bus voltage was plotted against the dip duration in Figure 4-1.
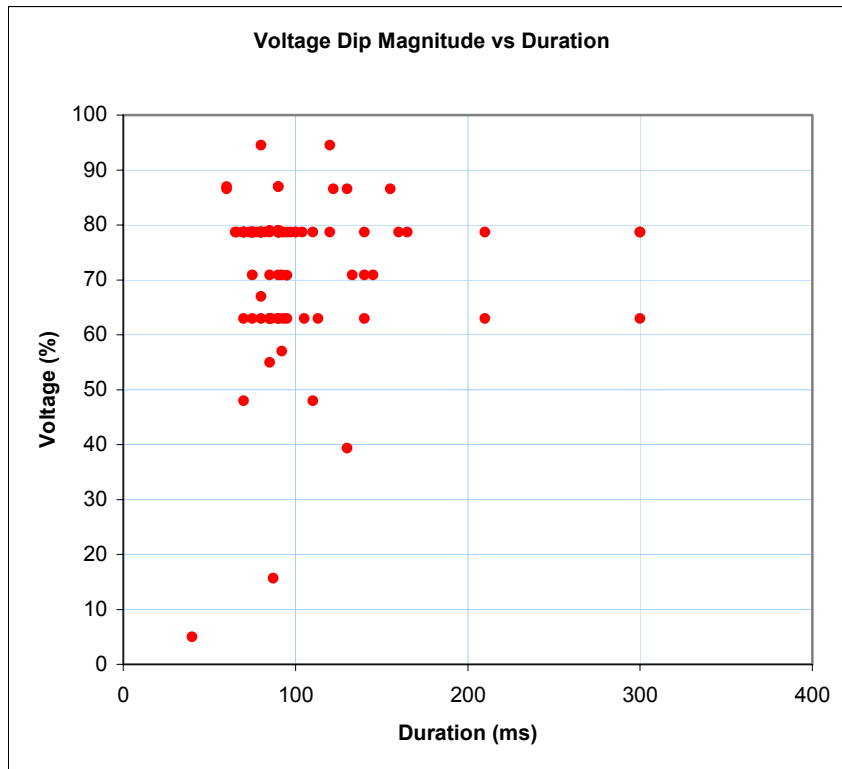
Figure 4-1 Voltage dip magnitude vs. duration.

It can be seen that the majority of the dips have a magnitude of less than 40% and a duration of between 50 to 150ms. Dips longer than about 180ms result in the total feedgas compressors' variable speed drives tripping leading to a plant outage. Voltage dips approaching 40% have been found to be more likely to cause plant outages for various reasons. Under these circumstances, the operation of the re-acceleration system is irrelevant and need not be considered. A voltage dip of 20% with 100ms duration will therefore be used to simulate a typical disturbance.

Figure 4-2 illustrates a recording of a typical voltage dip obtained from the perturbograph installed at substation 01. From Figure 4-2 it can be seen that the voltage dip only occurred on one phase (blue) and lasted about 73ms. The magnitude of the dip was approx. 20%. Although most voltage dips only occur on one phase, about 20-30% of the dips observed affect all three phases. For simulation purposes, a voltage dip on all three phases will be assumed since this is a more severe case. In order to more accurately analyse the effects of a single-phase voltage dip, a three-phase loadflow program and more complex component models would be required. Since the intent is to carry out an initial investigation, the additional complexity was considered beyond the scope of the present work.

A voltage dip on the Eskom supply is simulated by reducing the swing-bus voltage by 20% at the appropriate times during the system simulation.
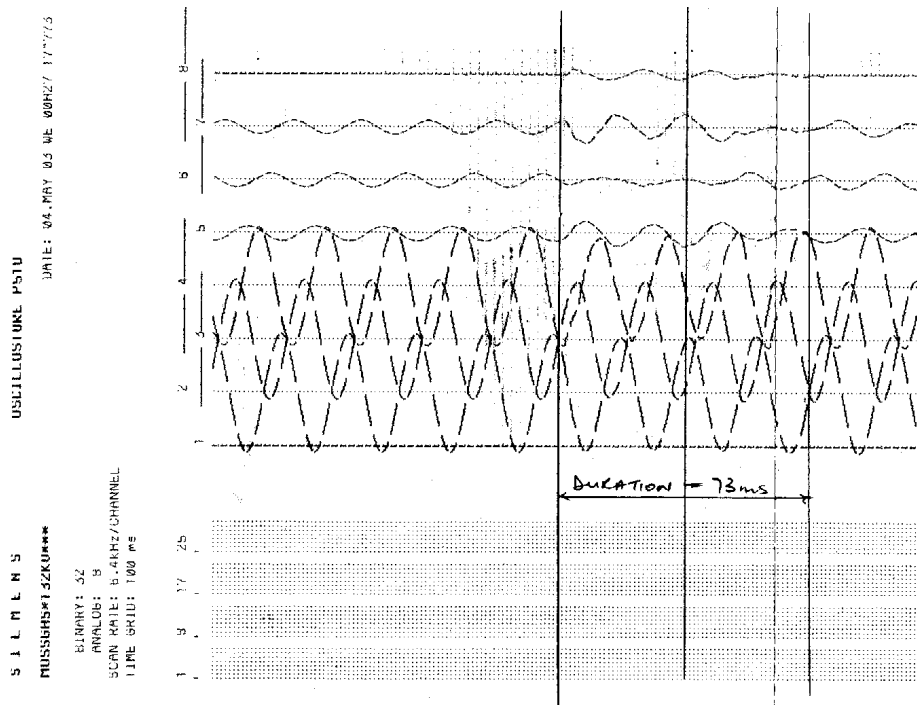
Figure 4-2 Recording of voltage dip on Eskom supply

4.2.1 Switching of motors

The switching of the motors being studied following a voltage dip needs to be simulated. This was done by changing the stator resistance in the model to a high value. This models the opening of the motor contactor, but allows simulation of the behaviour of the remaining model state variables such as rotor current and speed to continue. This will give a more accurate simulation of the motor behaviour when re-connected to the system. To simulate re-connection to the system, the stator resistance is returned to its normal value. For simulation purposes, motors will be tripped 80ms after the start of the voltage dip to simulate the time that it takes for the undervoltage relays to respond and the contactors to open.

The only other motors which trip during a voltage dip are the two 26MW air separation plant compressors(03KC101 and 03KC201)[2]. These motors are represented by a P,Q load applied to the relevant busbars. Tripping of these machines is simulated by setting these values to zero. These machines need to be manually re-started after tripping and thus no re-start needs to be simulated. The oxygen compressors (03KC201 and 03KC202)[2] will also trip if the air separation plant compressors trip due to process reasons. This typically takes about 15 seconds and is not simulated because the transient simulations will be carried out for periods less than 15 seconds. These machines are therefore assumed to remain connected to the network during the transient simulation.

4.3 Model Selection

The selection of the various system component models is dependent upon the transient stability study to be carried out. For practical reasons, it was necessary to model a sub-section of the entire PetroSA distribution network. The re-acceleration system performance will be investigated by considering the behaviour of four 6.6kV motors which comprise about 1% (2MW) of the total connected load. The main plant generator will also be modelled to determine its potential effect during transients.

---

[2] The location of these machines is shown on Figure 3-5

4.3.1 System component models

The distribution system component data is entered into a Excel spreadsheet. Visual Basic routines were developed to facilitate data entry. All data is entered via a menu and appropriate dialog boxes. Once entered, the Visual Basic routines process the data and write it in a standard format into the spreadsheet forming a branch data list. This branch data list is then used by the Matlab routines to generate the complex admittance matrix used for the loadflow calculations. The system component models to be used for network representation are the 'standard' models described in the literature [21, 23].

The PetroSA distribution system is represented by *Feeders, Loads, Two-winding transformers and Three-winding transformers*. All calculated values are converted to per-unit on a 100MVA base for use by the loadflow program. These components are discussed in the remainder of this section.

Feeders are represented by a complex series impedance: *Z=R=jX*. The feeder data entry dialog is shown in Figure 4-3.

Figure 4-3 Feeder data entry.

The feeder impedance is calculated using the length and feeder type[3] entered into the feeder data entry dialog box when preparing the branch data in spreadsheet format. This representation is acceptable in stability studies where the electromechanical transients are hundreds of times slower than the electromagnetic transients [23].

Loads are represented by a shunt admittance calculated from the real and reactive power.

Given *S=P+jQ* , the p.u. impedance is given by [21]:

$$Z = \frac{1}{S^* / 3} \tag{4-1}$$

Where S^* is the p.u. complex conjugate of the apparent power. The load data entry dialog box is shown in Figure 4-4.

---

[3] The data entry spreadsheet incorporates a look-up table listing the impedance per km for the various feeder cable types used.

This load model will not represent the behaviour of induction motor loads correctly when bus voltages change. In order to maintain a constant power output, the current drawn by an induction motor will increase when the bus voltage drops. For this load model, load current will decrease with decreasing bus voltage. It is therefore not possible to model the behaviour of a distribution system consisting mainly of induction motor loads correctly by using this model to represent the induction motors. During voltage dips or fault conditions, system bus voltages are depressed resulting in induction motors drawing increased currents. This in turn depresses bus voltages even further and can lead to system instability and voltage collapse with induction motors stalling. It is possible to model constant power loads by entering the appropriate values in the bus data list. (Table 3-1).

The major portion of the PetroSA distribution system load was however modelled as lumped loads represented by shunt admittances. This was justified by the fact that transient simulations would only involve dynamic modelling of a small portion of the induction machine load (approx 1% of the total load). The bus voltage drops would therefore be expected to be relatively small and the current drawn by the lumped loads would remain essentially unchanged. If system simulations show that this assumption is not justified, a more representative model can be used to represent induction motor loads. The main advantage of using this model is that the shunt admittances increase the coupling of the network to ground. This improves the performance of the basic Newton-Raphson algorithm that was used. If most of the system loads had been represented by constant loads in the bus data list, as discussed above, the coupling of the network to ground reference becomes weak. This results in an ill-conditioned system of equations and it becomes difficult to calculate a loadflow solution. The basic Newton-Raphson algorithm will converge slowly or fail to converge under these conditions [23].

Figure 4-4 Load data entry.

Two Winding Transformers: The transformer is represented analytically by its admittance matrix giving the following model presented by Arrilaga and Arnold[21]:

$$\begin{bmatrix} I_p \\ I_s \end{bmatrix} = \begin{bmatrix} \dfrac{Y}{\alpha_i \alpha_v} & \dfrac{-Y}{\alpha_i} \\ \dfrac{-Y}{\alpha_v} & Y \end{bmatrix} \begin{bmatrix} V_p \\ V_s \end{bmatrix} \qquad (4\text{-}2)$$

where α_v denotes the complex turns ratio for voltages and is given by $u+jv$, α_i denotes the complex turns ratio for currents given by $u - jv$ and u and v are defined by[21]:

$$v = r\cos(\beta), \qquad (4\text{-}3)$$

$$u = r\sin(\beta) \tag{4-4}$$

and

$$Y = \frac{1}{R + jX} \tag{4-5}$$

where r denotes the transformer turns ratio and β denotes the phase shift. The two winding transformer data entry dialog box is shown in Figure 4-5.

Figure 4-5 Two winding transformer data entry.

Three winding transformers are represented by a wye circuit with magnetising current neglected [23]. The resistance of each branch is made equal to the resistance of the corresponding winding. The sum of the reactances of any two branches of the wye is such that it equals the short-circuit reactance of the corresponding pair of windings with the remaining winding open, giving:

$$\begin{aligned} X_1 + X_2 &= X_{12} \\ X_1 + X_3 &= X_{13} \\ X_2 + X_3 &= X_{23} \end{aligned} \tag{4-6}$$

This gives the reactances of the wye circuit as [23]:

$$\begin{aligned} X_1 &= \frac{1}{2}(X_{12} + X_{13} - X_{23}) \\ X_2 &= \frac{1}{2}\left(X_{12} + X_{23} - X_{13}\right) \\ X_3 &= \frac{1}{2}\left(X_{13} + X_{23} - X_{12}\right) \end{aligned} \tag{4-7}$$

The three winding transformer data entry dialog box is shown in Figure 4-6. Note that although the transformer data entry dialog box makes provision for entering tap settings and phase shifts between windings, this data was not used for the current work. An imaginary bus is required for the common connection of the wye circuit. This is called the transformer model internal bus.

Figure 4-6 Three winding transformer data entry.

4.3.2 Induction machine models

Two aspects of the re-acceleration system need to be investigated. The impact on the motor itself, and the effect on the distribution system. The load models described in the literature [10, 11, 26, 29, 30, 34] fall into three categories: Models with little physical significance which are designed to represent aggregate loads where the composition is largely unknown, estimated, or based on measurements of load response to controlled perturbations [26]. Models based on physical considerations but simplified to represent aggregate loads consisting, for example, a combination of induction motors and static load [29] Induction motor models of varying degrees of complexity intended to represent both aggregate and single loads [21, 22, 23].

A model based on the direct solution of the machine equations as proposed by Smith and Chen [22] was selected. This model is referred to as the *abc* model and is described in section 2.9.4. The *d-q* models derived from the machine equations eliminate time dependent inductance terms, but are generally suited for balanced operation only [22]. The majority of the voltage dips observed are single-line to ground faults. For the purposes of this work, voltage dips were assumed to occur on all three phases. The performance of the *abc* model proposed above also needed to be compared with a simpler 'standard' model commonly used. A third-order dynamic induction motor model [21] was selected for this purpose. This model is referred to as the *d-q* model, described in section 2.9.2.

Although detailed data is available for some of the larger motors at PetroSA, the majority would have to be modelled using nameplate data. Machine models can be developed which are able to represent saturation effects.[1,3,4,5] Due to a lack of knowledge of the PetroSA machines' saturation curves, it is of little use to include saturation in the machine models since the necessary parameters needed to make use of the saturation model were unavailable. Due to this and the need to limit the scope of work, modelling of saturation was excluded.

Both models are of single cage rotor machines, whilst the machines at PetroSA are double cage, or deep-bar machines. In the case of the *abc* model, the second rotor cage could be modelled directly, leading to three additional differential equations for modelling the electrical behaviour. Such a complex model could not be justified. A simpler approach adopted was to modify the rotor resistance and reactance as a function of rotor speed to approximate the effect of the second rotor cage [22].

The *d-q* model does not take rotor parameter variations into account. This model was kept as simple as possible, to allow comparison of results obtained with a relatively simple, approximate induction motor model, to those obtained form a more complex model.

The *d-q* induction motor is modelled as follows:

d-q model electrical equations:

$$V_{\text{Re}} - E'_{\text{Re}} = r_s I_{\text{Re}} - x' I_{\text{Im}}, \tag{4-8}$$

$$V_{\text{Im}} - E'_{\text{Im}} = r_s I_{\text{Im}} + x' I_{\text{Re}}, \tag{4-9}$$

$$\frac{dE'_{\text{Re}}}{dt} = 2\pi f_0 S E'_{\text{Im}} - \left(E'_{\text{Re}} + \left(x_0 - x'\right) I_{\text{Im}}\right) / T'_0, \tag{4-10}$$

and

$$\frac{dE'_{\text{Im}}}{dt} = -2\pi f_0 S E'_{\text{Re}} - \left(E'_{\text{Im}} - \left(x_0 - x'\right) I_{\text{Re}}\right) / T'_0 \tag{4-11}.$$

d-q model mechanical equations:

$$S = \frac{(\omega_0 - \omega)}{\omega_0}$$

(4-12)

$$\frac{dS}{dt} = \frac{T_m - T_e}{2H_m}$$

(4-13)

$$T_m \propto (speed)^k$$

(4-14)

with *k = 1* for fan-type loads and *k=2* for centrifugal pumps

Refer to 2.9.2 and 2.9.3 for a detailed description of these equations.

The *abc* induction motor is modelled as follows:

abc model electrical equations:

$$[V_s] = [R_s][I_s] + [L_{ss}]p[I_s] + [L_{sr}]p[I_r] + \omega_r[G_{ss}][I_s] + \omega_r[G_{sr}][I_r]$$

(4-15)

$$[V_r] = [R_r][I_r] + [L_{rs}]p[I_s] + [L_{rr}]p[I_r] + \omega_r[G_{rs}][I_s] + \omega_r[G_{rr}][I_r]$$

(4-16)

$$T_e = [I]^T[G][I].$$

(4-17)

$$P_e = V_{as}I_{as} + V_{bs}I_{bs} + V_{cs}I_{cs}$$

(4-18)

$$Q_e = \tfrac{1}{\sqrt{3}}\left(V_{as}(I_{bs} - I_{cs}) + V_{bs}(I_{cs} - I_{as}) + V_{cs}(I_{as} - I_{bs})\right)$$

(4-19)

abc model mechanical equations

$$\tfrac{d}{dt}\omega_r = \frac{1}{2H}(T_e - T_m)$$

(4-20)

$$H = \frac{J\omega_{base(m)}^2}{2P_{base}} = (n)^2 \cdot \frac{J\omega_{base(e)}^2}{2P_{base}}$$

(4-21)

$$T_m \propto (speed)^k$$

(4-22)

Refer to 2.9 for a detailed discussion of the above equations.

4.3.3 Synchronous machine model selection

Since the voltage dips and subsequent re-starting of motors being investigated takes place over a period of up to 12-15 seconds, sub-transient phenomena can be excluded. A Generator model taking transient effects into account was selected (Model 2 section 2.17.3).

The primary aim is to investigate the behaviour of induction motors. Only a limited group of motors will be modelled and it is expected that the generator response to system disturbances emanating from these motors will be small. In addition, the generator turbine and governor are not accurately represented. The relatively simple generator model should be able to give a good indication of how the generator affects the re-acceleration system (and vice versa). Saturation effects were therefore not modelled.

The main plant generator is modelled as follows:

Generator Electrical Equations:

$$T'_{d0} \frac{dE'_q}{dt} = E_{fd} - E'_q + (x_d - x'_d)I_d \tag{4-23}$$

$$T'_{q0} \frac{dE'_d}{dt} = -E'_d - (x_q - x'_q)I_q \tag{4-24}$$

$$E'_d = V_d + rI_d + x'_q I_q \tag{4-25}$$

$$E'_q = V_q + rI_q - x'_d I_d \tag{4-26}$$

$$I_d = \frac{1}{r^2 + x'_d x'_q} \left[r(E'_d - V_d) + x'_q (V_q - E'_q) \right] \tag{4-27}$$

Rather than use equation (2-164) to determine I_q, it is simpler to use equation (4-26):

$$I_q = \frac{1}{r} \left(E'_q - V_q + x'_d I_d \right) \tag{4-28}$$

$$P_e = V_d I_d + V_q I_q \tag{4-29}$$

Note that the above expression for power takes the stator resistance into account. The expression which neglects rotor resistance (equation (2-166)) was found to give unacceptable cumulative errors during simulations.

Type 1 AVR:

$$\frac{dX_1}{dt} = -\frac{X_1}{T_R} + \frac{V_S}{T_R} \tag{4-30}$$

$$\frac{dX_2}{dt} = -\frac{X_2}{T_A} + \frac{K_A}{T_A} \left(V_{REF} - X_1 - X_4 \right) \tag{4-31}$$

Define f as:

$$f = -\frac{X_2}{T_A} + \frac{K_A}{T_A} \left(V_{REF} - X_1 - X_4 \right) \tag{4-32}$$

The regulator output is restricted by non-windup limits, thus X_{2L} is given by the following:

If $X_2 \geq V_{R\,Max}$ and $f > 0$, then $\dfrac{dX_{2L}}{dt}$ is set to zero

If $X_2 \leq V_{R\,MIN}$ and $f < 0$, then $\dfrac{dX_{2L}}{dt}$ is set to zero

otherwise, $\dfrac{dX_{2L}}{dt} = f$ for $V_{R\,MIN} < X_2 < V_{R\,MAX}$

$$\frac{dE_{fd}}{dt} = -\frac{K_E}{T_E} E_{fd} + \frac{1}{T_E} \left(X_{2L} - SE \right) \tag{4-33}$$

The exciter saturation is specified at maximum field voltage E_{fdmax} and at 0.75 of maximum field voltage $E_{fd0.75}$ as per IEEE recommendations [21]. The exciter saturation function is then determined using linear interpolation for any value of field voltage as follows:

$$SE = (k_1 E_{fd} - k_2) E_{fd}$$ (4-34)

where

$$\left. \begin{array}{l} k_1 = \dfrac{4 SE_{0.75}}{3 E_{fdMax}} \\ k_2 = 0 \end{array} \right\} \text{if } E_{fd} \leq 0.75 E_{fdMax}$$

or

$$\left. \begin{array}{l} k_1 = \dfrac{4(SE_{Max} - SE_{0.75})}{E_{fdMax}} \\ k_2 = 4 SE_{0.75} - 3 SE_{Max} \end{array} \right\} \text{if } E_{fd} > 0.75 E_{fdMax}$$

$$\frac{dX_4}{dt} = \frac{-X_4}{T_F} + \frac{K_F}{T_F} \left(\frac{-K_E}{T_E} E_{fd} + \frac{1}{T_E} (X_{2L} - SE) \right)$$ (4-35)

Mechanical equations:

The generator rotor motion is given by the swing equation:

$$M \frac{d^2 \delta_e}{dt^2} + D \frac{d\delta_e}{dt} = (P_m - P_e)$$ (4-36)

which is modelled as two first-order differential equations with the damping constant $D = 0$:

$$\frac{d\omega_e}{dt} = \frac{1}{M} (P_m - P_e)$$ (4-37)

$$\frac{d\delta_e}{dt} = \omega_e$$ (4-38)

Governor:

$$\frac{dP_M}{dt} = -\frac{1}{T_G} P_m + \frac{K_G}{T_G} \omega_{error}$$ (4-39)

where

$$\omega_{error} = \omega_0 - \omega_e$$ (4-40)

Note that the model does not take generator pole pairs into account. Since the only machine being modelled is a 2-pole machine, mechanical and electrical angles are the same.

4.3.4 Generator model initialisation

At the start of the simulation, it is assumed that the generator is operating in a steady state condition. All derivatives are thus assumed to be zero. From the initial loadflow solution, the terminal voltage, voltage angle, power and reactive power are known. By applying the equations developed in section 2.13.1, the angle between the system real axis and the generator q- axis and hence V_d, V_q, I_d and I_q can be determined. Since the rotor position with respect to the system axis (δ_e) is constant, the rotor speed with respect to the system axis (ω_e) equals zero. When operating in steady state, the electrical power output must equal the

mechanical power input to the generator. The electrical power output is determined from the initial loadflow solution, and the initial mechanical power input is set to this value. The AVR set point, V_{ref} is set equal to the generator terminal voltage determined from the initial loadflow solution.

The model differential equations, with derivatives set to zero are then used to determine the initial values of the remaining model state variables. Note all variables have a 'zero' subscript added to indicate initial values.

From equation (4-24):

$$E'_{d0} = \left(x_{q0} - x'_{q0}\right)I_{q0} \tag{4-41}$$

From equation (4-26):

$$E'_{q0} = V_{q0} + rI_{q0} - x'_d I_{d0} \tag{4-42}$$

From equation (4-30):

$$X_{10} = V_{S0} \tag{4-43}$$

Where V_{S0} = initial terminal voltage from the loadflow solution.

From equation (4-23):

$$E_{fd0} = E'_{q0} - \left(x_d - x'_d\right)I_{d0} \tag{4-44}$$

Note that the above value of E_{fd0} is in p.u. on the generator p.u. base. To convert to the exciter/AVR p.u. base this value has to be divided by a scaling factor of 0.94364 (refer to section 9.2.1) This voltage is referred to as V_{fd0} for clarity in the equations that follow. The exciter saturation function is then determined as follows:

$$SE_0 = \left(k_1 V_{fd0} - k_2\right)V_{fd0}$$

where

$$\left. \begin{array}{l} k_1 = \dfrac{4SE_{0.75}}{3E_{fdMax}} \\ k_2 = 0 \end{array} \right\} \text{if } V_{fd0} \le 0.75 E_{fdMax}$$

or

$$\left. \begin{array}{l} k_1 = \dfrac{4\left(SE_{Max} - SE_{0.75}\right)}{E_{fdMax}} \\ k_2 = 4SE_{0.75} - 3SE_{Max} \end{array} \right\} \text{if } V_{fd0} > 0.75 E_{fdMax}$$

From equation (4-33):

$$X_{2L0} = K_E V_{fd0} + SE$$

From equation (4-31):

$$X_{40} = \left(V_{ref0} - X_{10}\right) - \frac{X_{20}}{K_A}$$

4.4 Program Structure

All analysis software has been developed on Matlab. Where possible, use has been made of Matlab's built–in functions. The system loadflow is calculated using a Newton Raphson Algorithm. The induction motor models are solved using the built-in ODE solver functions in Matlab. Listings of all programs used have been included in Appendix B. The program is described by the flowcharts in Figure 4-7, Figure 4-8, Figure 4-9 and Figure 4-10.
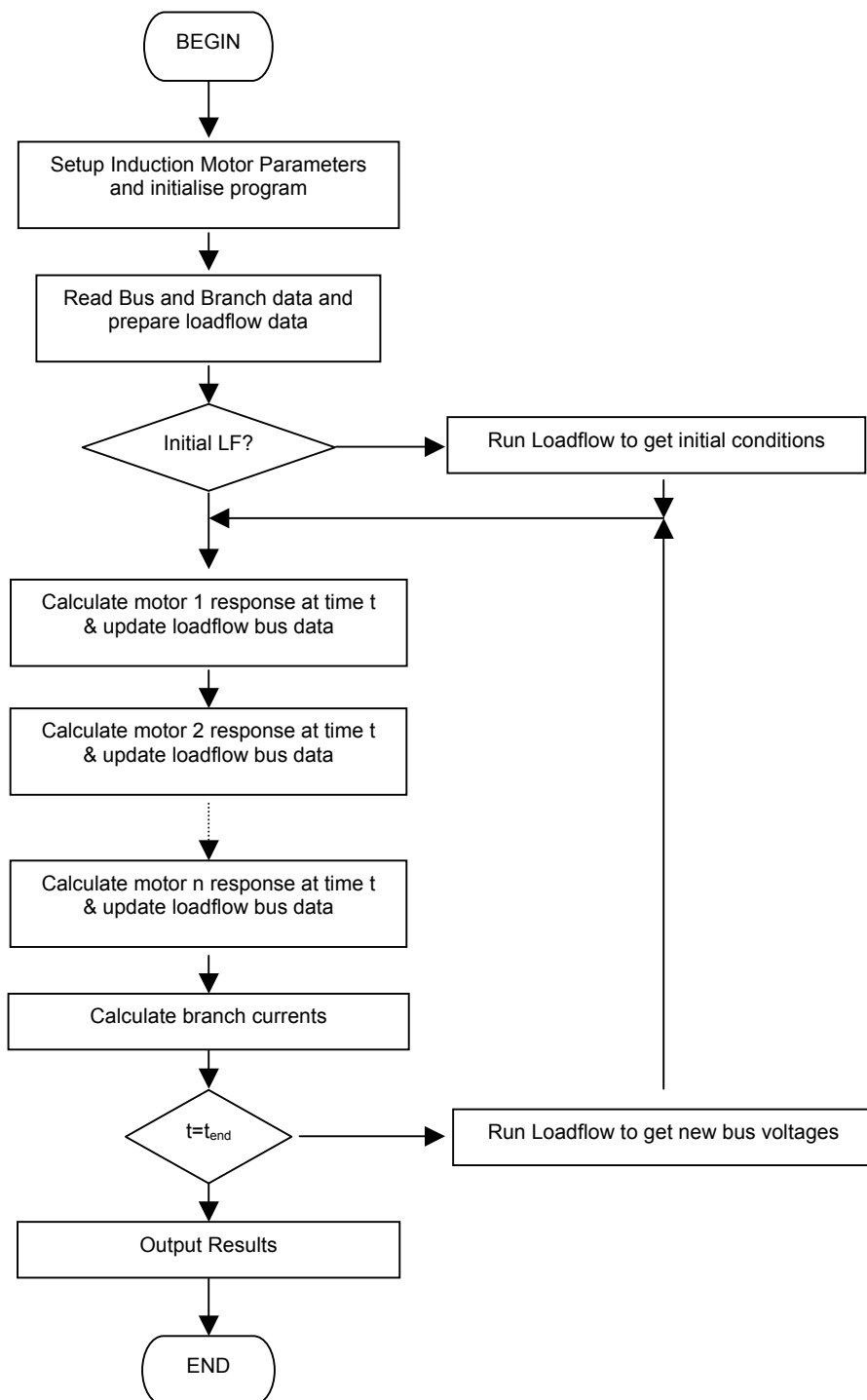
Figure 4-7 Simulation software overview.

The following flowchart gives a detailed summary of the simulation program:
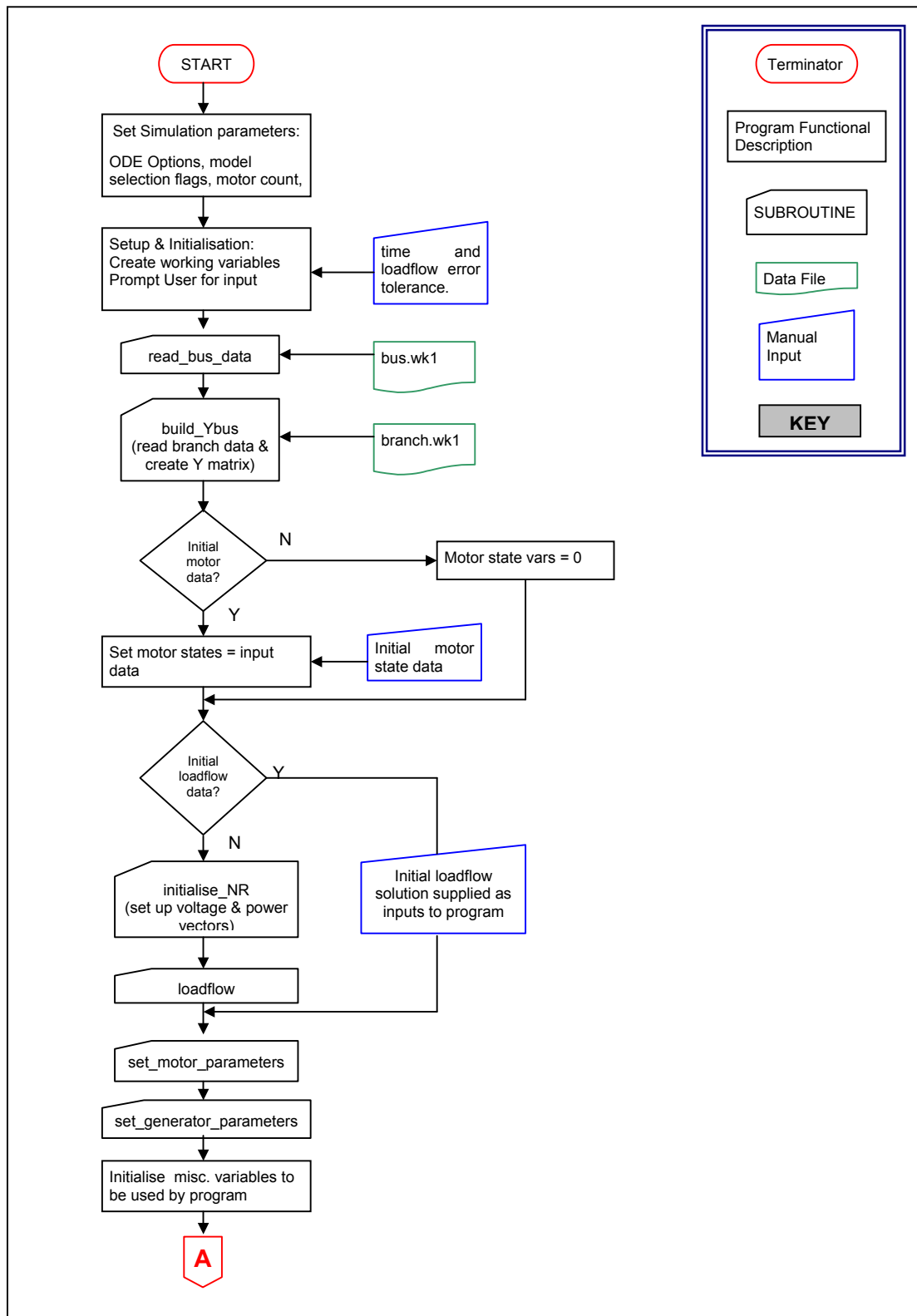
Figure 4-8 Simulation program detail flowchart A.
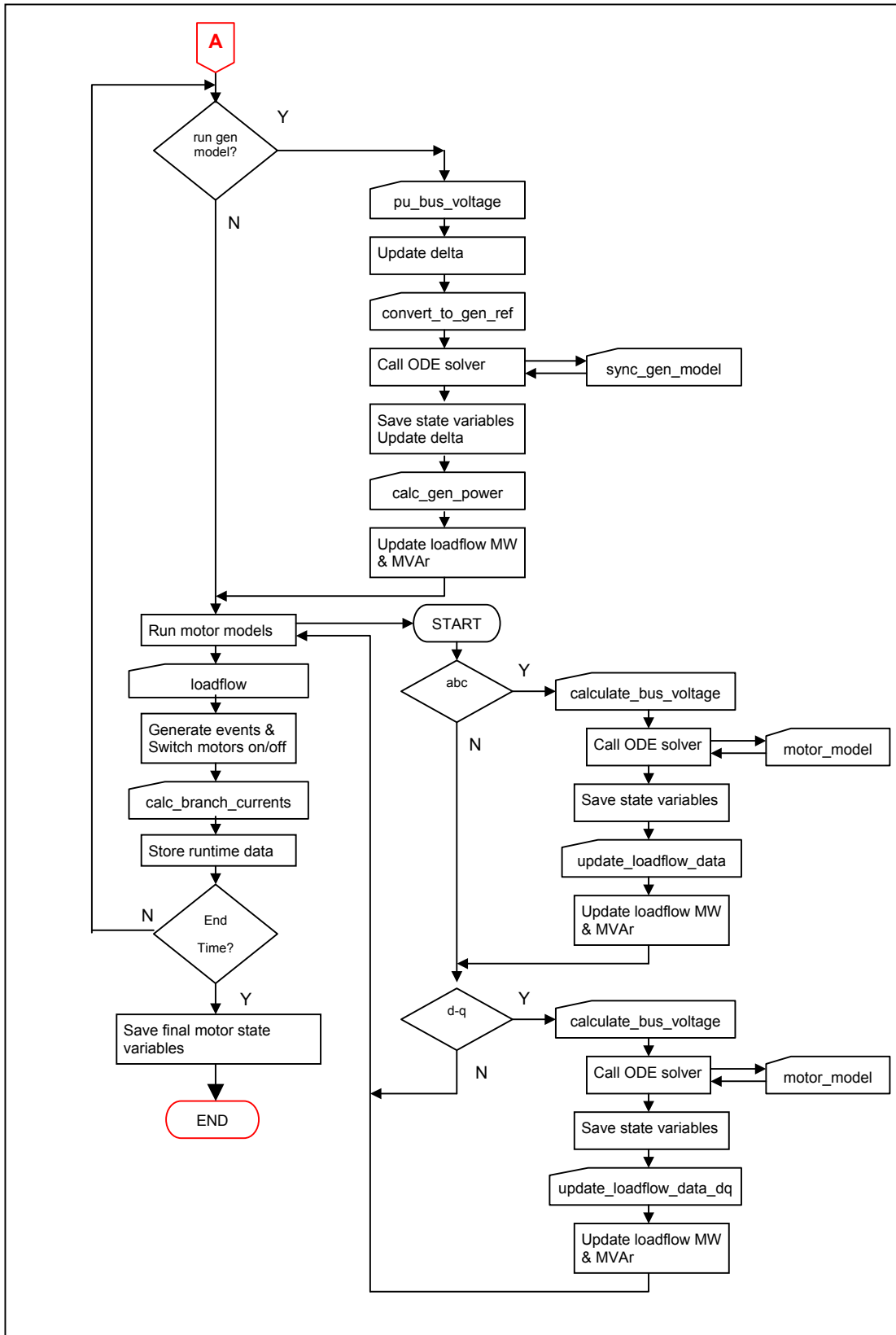
Figure 4-9 Simulation program detail flowchart B.
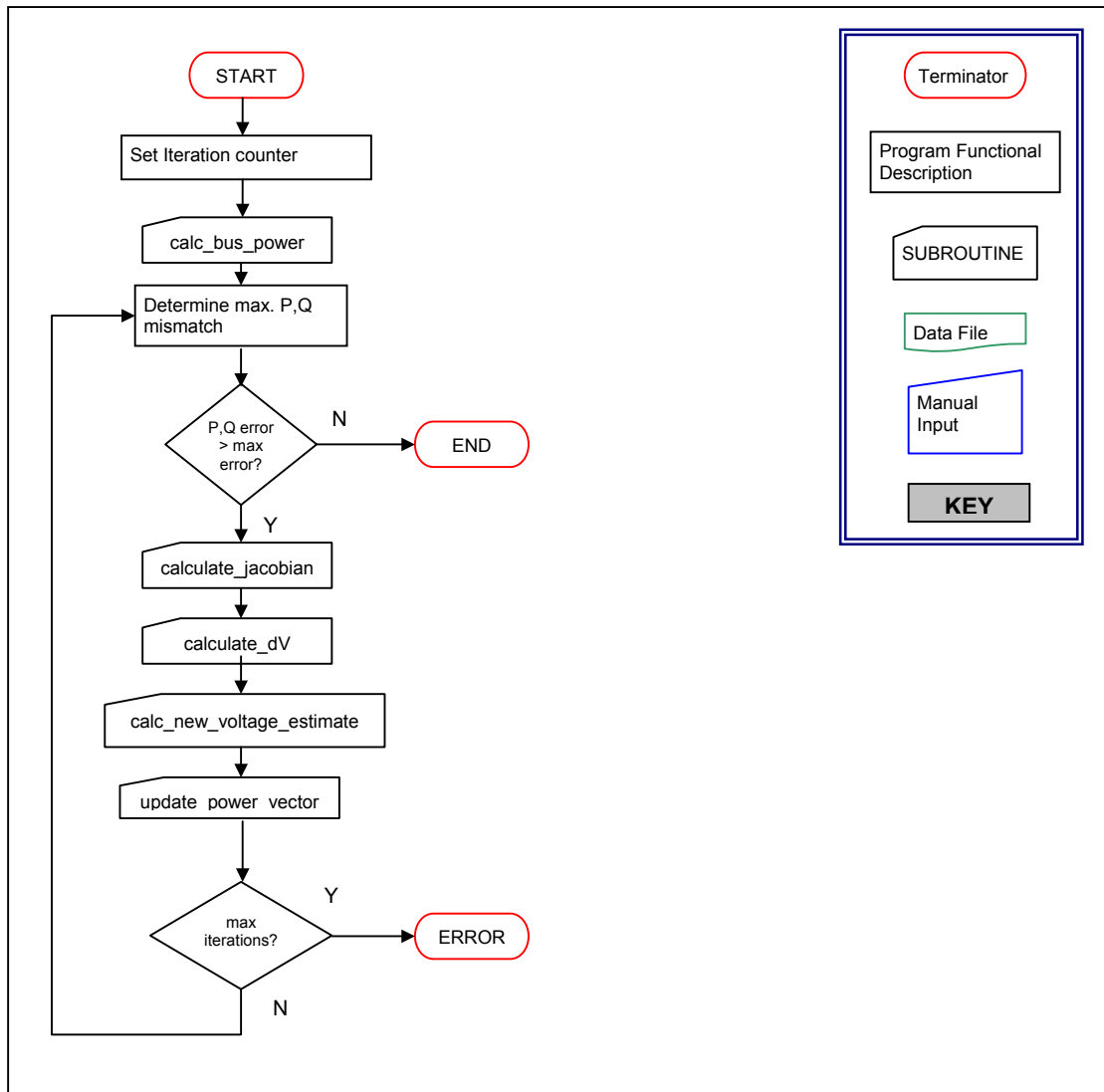
Figure 4-10 Loadflow detailed flowchart.

4.4.1 Summary of subroutines

The various program subroutines are summarised in Table 4-1, along with a brief functional description and relevant cross references. Listings of all software appears in Appendix B

Table 4-1 Summary of program subroutines

Name	Functional Description	Cross Reference
simtrans.m	Main simulation program. Called from the Matlab command line.	pg. 201
read_bus_data.m	Read the bus data from the input file "bus.wk1" and save data in variable 'bus_data' Also returns vector Pvbus which indicates voltage controlled bus	pg. 216
build_Ybus.m	Generates the system admittance matrix from the file "branch.wk1" and generates a data table used for calculating branch currents.	pg. 218
write_load_data	Add impedance used to represent static loads to admittance matrix.	sub-function of build_Ybus.m
write_feeder_data	Add feeder impedance to admittance matrix., Admittance is added to diagonal elements and subtracted from off-diagonal elements	sub-function of build_Ybus.m
write_transformer_data	Add two-winding transformer impedances to admittance matrix. Transformer is modelled as an ideal transformer with a complex ratio feeding the transformer impedance[21]: $$\begin{bmatrix} I_p \\ I_s \end{bmatrix} = \begin{bmatrix} \dfrac{Y}{(a_i a_v)} & \dfrac{-Y}{a_i} \\ \dfrac{-Y}{a_v} & Y \end{bmatrix} \begin{bmatrix} V_p \\ V_s \end{bmatrix}$$ where a_v = complex turns ratio for voltages (*u+jv*) a_i = complex turns ratio for currents *(u-jv)* *v=r*cos*(Beta)*, *u=r*sin*(Beta)* *r* = turns ratio, *Beta* = phase shift	sub-function of build_Ybus.m
write_transformer3_data	Add three-winding transformer impedances to admittance matrix. Modelled as a Y-connected network of impedances[23] where $$Y_1 = \frac{2}{Z_{ps} + Z_{pt} - Z_{st}}, Y_2 = \frac{2}{Z_{ps} + Z_{st} - Z_{pt}}, Y_3 = \frac{2}{Z_{pt} + Z_{st} - Z_{ps}}$$	sub-function of build_Ybus.m
initialise_NR.m	Load initial data into vectors used to store power and voltage for all busses to prepare for first loadflow solution	pg. 222
set_motor_parameters.m	Set up motor model parameter matrix. All model data is saved in one matrix for use during the simulation	pg. 223
set_generator_parameters.m	Set up generator model parameter vector	pg. 228
set_motor_state_vector.m	Set up motor model initial state according to model used	pg. 229
locate_gen_axis.m	Locate generator q-axis with respect to system (swing bus) axis	refer to section 2.13.1 pg. 229
init_gen_state.m	Calculate initial values for all generator state variables before simulation starts	refer to section 4.3.4 pg. 230
pu_bus_voltage.m	Gets specified bus voltage from latest loadflow data and returns $V_t = (V_r + jV_m)$ where V_r = real component of bus voltage, V_m = imaginary component of bus voltage	pg. 231
convert_to_gen_ref.m	Convert X_r, X_m from system reference frame to X_d, X_q in the generator reference frame	see equation (12-34)
calc_gen_power.m	Calculate generator active and reactive power from generator model state variables and terminal voltage. I_d and I_q are calculated, giving I_r and I_m from which power is obtained: $S = (P + jQ) = V_t(I_r - jI_m)$	see equations: (4-27), (4-28) and (4-29)
calculate_bus_voltage.m	Get voltage and phase angle for specified bus from loadflow and return as a vector [V_{bus}, V_{angle}] – used by induction motor models	pg. 232
update_loadflow_data.m	Used with the abc motor model. Calculates the following from the motor model state variables: P_{pu}, Q_{pu} – per unit power and reactive power *P, Q* – power and reactive power in W and Var I_m – instantaneous rms motor current (A) *omega* – motor speed (p.u.)	see equations: (2-41) and (2-42)

Name	Functional Description	Cross Reference
calc_abc_tmnl_voltage.m	Calculate the three instantaneous phase voltages	used by *update_loadflow_data* pg. 233
update_loadflow_data_dq_model.m	Used with the d-q motor model. Calculates the following from the motor model state variables: P_{pu}, Q_{pu} – per unit power and reactive power P, Q – power and reactive power in W and Var I_m – instantaneous rms motor current (A) *omega* – motor speed (p.u.)	pg. 233
calc_branch_currents.m	Calculate branch currents using bus voltages calculated by loadflow	pg. 234
calc_feeder_current	Calculates the current in a feeder	sub function of calc_branch_currents.m
calc_transformer_current	Calculate primary and secondary currents for a two winding transformer	sub function of calc_branch_currents.m
calc_3wtransformer_current	Calculate primary, secondary and tertiary currents for a three winding transformer	sub function of calc_branch_currents.m
calc_load_current	Calculate load current, MVA and MVAr for a load	sub function of calc_branch_currents.m
loadflow.m	Execute Newton-Raphson loadflow	pg. 238
calc_bus_power	Calculate active and reactive power for all busses	sub function of loadflow.m
calc_new_voltage_estimate	Calculate new estimate for bus voltage magnitudes and angles	sub function of loadflow.m
calculate_dV	Calculate delta-V values for bus voltages	sub function of loadflow.m
update_power_vector	Copy newly calculate P & Q values to prepare for next NR iteration	sub function of loadflow.m
calculate_jacobian.m	Calculates the Jacobian matrix for the NR loadflow.	pg. 243
delete_blanks	Delete rows and columns corresponding to VC busses from the Jacobian	sub function of calculate_jacobian
dP_dth	Calculate $\dfrac{dP}{d\theta}$	sub function of calculate_jacobian
dP_dV	Calculate $\dfrac{dP}{dV}$	sub function of calculate_jacobian
dQ_dth	Calculate $\dfrac{dQ}{d\theta}$	sub function of calculate_jacobian
dQ_dV	Calculate $\dfrac{dQ}{dV}$	sub function of calculate_jacobian
test_motor_model.m	Function used to run simulations of *abc* induction motor models independently of the transient simulation program	pg. 246

4.5 Simulation Strategy

The following is an overview of the simulations that were conducted. The results of these simulations are presented and discussed in the following chapter. All motors were assumed to be driving pumps, implying that the load torque is proportional to the square of the speed. Estimation of the load applied to a motor following a power dip is difficult, since this depends on plant process conditions, and the control system response. Random observations carried out on site indicate that motor loads generally fall within 60-90% of rated output.[4] When the PetroSA plant was originally commissioned, the starting currents for most of the 6.6kV and 11kV motors was recorded under normal plant operating conditions. A review of these records revealed that motors take between 1 to 5 seconds to start. A range of arbitrary load values shown in Table 4-2 were chosen and load parameters calculated accordingly. The intention was not to perform a direct comparison between the *abc* and *d-q* motor models with these tests. This was done when the motor models were compared to motor performance measured during tests. The model parameters could have been chosen to simulate the motor performance measured during the startup tests as closely as possible. It is unlikely that this would have resulted in the simulations representing actual motor behaviour following a power dip any more than any other arbitrary chosen set of parameters. For this reason, two sets of arbitrary parameters were chosen for the *abc* and *d-q* models to give a range of starting times similar to that observed on the PetroSA plant with a bias towards the longer times. The tests carried out during commissioning were carried out under similar conditions as the motor starting tests done for this work.

Table 4-2 Load values for motor models.

Motor	Rating	abc model load	d-q model Load
24PC101A	300kW	70%	93%
24PC104A	300kW	80%	93%
24KC101A	550kW	97%	75%
24PC102A	800kW	75%	63%

The inertia constants for the motor models were chosen to give starting times of between 3 and 4.5 seconds. Motor loads were arbitrarily chosen to represent typical loads observed on site. The shorter (1 – 2 second) times were not simulated since motors should be running with normal load during and after a voltage dip, and acceleration times can be expected to be longer. In some cases, when motors are started under controlled conditions, there is minimal load on the motor as a result of control system actions resulting in some of the shorter starting times being recorded. Inertia constants are assumed to represent the motor and driven load. In summary, the parameters were chosen to give two arbitrary test cases using the *abc* and *d-q* models respectively, that would simulate conditions believed to exist following a power dip.

The remainder of this section discusses some aspects of the simulation strategy in more detail.

---

[4] Generally these observations refer to the larger 6.6kV and 11kV motors where the switchgear in the substations is equipped with metering allowing motor input power to be determined. It is not possible to measure power input to individual 415V motors under operational conditions since only the incomers on the MCC panels are equipped with ammeters and power factor indication. Access to individual MCC buckets whilst energised is not permitted for safety reasons. As a result of these restrictions, 6.6kV motors were selected for the initial simulations carried out for this work.

4.5.1 Motor parameter estimation

Although more detailed data was available for some motors, it was decided to use motor nameplate data for parameter estimation. The parameter estimation scheme proposed in section 2.10.4 was used to derive parameters for the *d-q* and *abc* models. Simulations were carried out to determine the validity of the parameter estimates. A DOL start of the 300kW, 550kW and 800kW motors was simulated using both the *abc* and *d-q* models and results compared to startup tests carried out on the actual machines in the plant. The load and inertia parameters for the *abc* and *d*-q models were adjusted for these tests so that the simulated starting times and loads were similar to that of the measured data. The intent here was to determine how accurate the motor models are and to compare the models with each other.

4.5.2 Alternating solution errors

The algebraic and differential equations need to be solved simultaneously and the alternating solution approach will introduce cumulative errors. In order to try to evaluate the magnitude of these errors, a motor start was simulated using only the motor model. A constant bus voltage was assumed and the test was continuous, i.e. the ODE solver was not interrupted to run the loadflow and adjust parameters. A second test is then carried out with the loadflow and motor model equations being solved alternately and results compared. The effect of varying integration step lengths was also investigated.

4.5.3 Voltage dips and switching effects on motor operation

During a voltage dip motors are disconnected from the supply and re-started several seconds later. Different re-connection intervals are investigated as well as the effects of leaving the motor connected to the system.

4.5.4 Effect of plant generator

The simultaneous startup of four motors is investigated with and without the generator model. Various configurations of the generator model are simulated: constant excitation and power, constant power and variable power and excitation. The aim was to investigate the impact of the generator and if the generator model can be omitted.

4.5.5 Examine effects of voltage dips and re-acceleration system

The effect of voltage dips on the PetroSA distribution system are investigated as well as the impact of the re-acceleration system

5   PRESENTATION OF RESULTS

Where possible, related data is presented using similar scales for the x and y axis to facilitate comparison. In some cases different scales have been used to show detail more clearly.

5.1   Matlab ODE Solver Performance

The alternating solution approach adopted requires that the ODE solver is repeatedly used to perform numerical integration over short intervals with the final state of the previous step being used as the initial state for the next integration interval. Since the ODE solvers are normally used to calculate a solution over a longer interval, it was necessary to determine if the repeated use of the solver over short intervals yields different results to those obtained when integration is carried out in a single step over a longer period.

For the purpose of this discussion, the repeated use of the ODE solver over short intervals is referred to as '*step mode*' whilst the use of the solver to integrate over the entire period of interest in a single step is referred to as '*continuous mode*'[1]

Note that for all these tests an infinite bus was assumed, no loadflow calculations carried out and the parameters for a 550kW 6.6kV motor[2] with a load of 20% used. The default values were used for the Matlab ODE solver relative and absolute error tolerance parameters.[3]

When comparing test results, plotting data points only obscures the detail due to the large number of points to be plotted. For detail plots, data points for one data set are plotted to allow comparison with the second data set.

The results of this investigation are summarized in this section, for a detailed review of all tests carried out, refer to Appendix J.

5.1.1   Stepped vs. Continuous use of ODE solvers

The Matlab ODE solver ode45 was used for these tests since this is recommended as a 'first try' for most problems in the Matlab documentation. The results obtained when using the ODE solvers in continuous and stepped mode were compared. The more complex abc model was used for all tests unless stated otherwise. The abc model which requires a greater number of calculations to obtain a numerical solution was chosen since it is likely that any inaccuracies will be more readily observed. The motor startup from standstill was simulated using the ode45 solver in continuous and stepped mode. The results are compared in Figure 5-1. It can be seen that there is a clear discrepancy between the results obtained.

---

[1] Even though this mode is referred to as continuous, the Matlab ODE solver algorithms are using multiple internal steps at time intervals dictated mainly by the relative and absolute error tolerance parameters RelTol and AbsTol to calculate the solution over the specified time interval.

[2] Motor model parameters used are as for 550kW motor no. 24KC101M

[3] Matlab documentation states that the error at each integration step is required to be less than an acceptable error which is a function of two user defined tolerances RelTol and AbsTol. RelTol controls the number of correct digits in the answer (the default, 1e-3, corresponds to 0.1% accuracy) and AbsTol is the threshold below which solution components are unimportant. The absolute error tolerance determines the accuracy when the solution approaches zero (default 1e-6)

Figure 5-1 ODE Solver test: abc model, stepped vs. continuous solution, 1ms step interval.

It was suspected that using the ode solver in stepped mode was introducing errors and the relative tolerance parameter was changed from 1e-3 to 1e-5. The motor startup was again simulated in stepped mode using RelTol = 1e-5, but the results remained unchanged. A further test was carried out where the motor start was simulated using the ODE solver in continuous mode with RelTol = 1e-5.
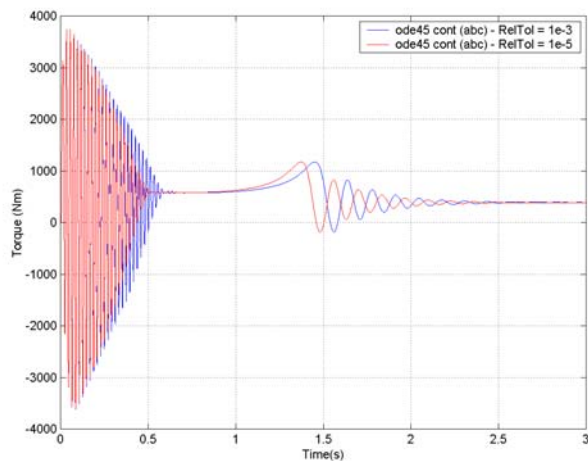
Figure 5-2 ODE Solver test: abc model, continuous mode with RelTol changed.

The effect of changing RelTol when using the ODE solver to carry out the integration in continuous mode is shown in Figure 5-2. It was found that using values of 1e-5 and smaller for RelTol gave identical solutions. As RelTol becomes larger, the solutions obtained start to differ. Matlab documentation states that the Ode solvers deliver less accuracy for problems integrated over "long" intervals and for problems that are moderately unstable. It was found that the default error tolerance parameters do not result in a sufficiently accurate solution when using the ODE solver to integrate in continuous mode over an interval of 0 to 3 seconds.
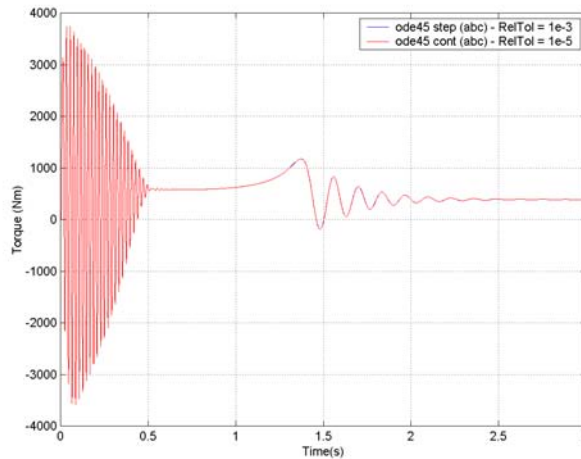
Figure 5-3 ODE Solver test: abc model, stepped vs. continuous solution

The results obtained using the ODE solver in continuous mode with RelTol = 1e-5 were then compared to the results obtained using the ODE solver in stepped mode with RelTol = 1e-3. It can be seen from Figure 5-3 that the results compare well. The above tests show that when the Matlab ODE solvers are used over short intervals, accurate results are obtained with the default error tolerance parameters. When using the solver over 'longer' intervals, the relative tolerance parameter has to be made smaller to obtain an accurate solution

5.1.2 Comparison of ODE solver performance

The different Matlab ODE solvers were then compared to each other. All tests were carried out using the abc motor model, with the same parameters as used for the tests in 5.1.1, above. RelTol was 1e-5.

The different ODE solver algorithms all gave similar results with varying efficiencies. The results are summarised in Table 5-1

Table 5-1 ODE Solver test: Comparison of solution times

Solver	Solution time
ode45	36s
ode23	47s
ode113	10s
ode15s	26s
ode23s	722s
ode23t	77s
ode23tb	108s

5.1.3 Summary of ODE Solver Test Results

The Matlab ODE solvers were tested using the same motor model and parameters. Initially it appeared as if the use of the Matlab ODE solvers in a stepped mode caused errors since the solution obtained differed from that obtained by using the ODE solver to integrate over a continuous interval. It was found that the solver was in fact, giving inaccurate results when

integrating over a 'long' interval. The accuracy can be improved by changing the relative tolerance parameter of the ODE solver algorithm from its default value of 1e-3 to a smaller value. A value of 1e-5 for RelTol was found to give acceptable results.

Using the solver in stepped mode gave accurate results, even with the default tolerance parameters. According to the Matlab documentation, the ODE solver algorithms will give more accurate results over 'short' intervals and the default tolerance parameters might not result in acceptable accuracy of solutions over 'long' intervals. Using the solvers over multiple short intervals (1ms) in step mode gives accurate results even with the default tolerance parameters. If the step size approaches 10ms in stepped mode, it was found that RelTol <= 1e-5 needs to be used as for the continuous solution.

The various ODE solvers all produced similar results when used with the correct relative tolerance. The main difference observed was the time taken to compute a solution with ode113, a non-stiff solver, being the most efficient and one of the stiff solvers, ode23s being extremely inefficient. The performance of the stiff equation solvers can possibly be improved if the motor model ODE file is modified to return the Jacobian of the system of equations. This was not investigated further since the speed and efficiency with which solutions are obtained is not a primary objective of the present work. This would be a topic for investigation in future work if the size and complexity of the distribution system and motor models is increased.

In summary:

- If using the ODE solver in stepped mode, accurate results are obtained with RelTol <= 1e-3 (default value) and a step length of 1ms or less.

- If the ODE solver is used in stepped mode with a step length greater than 1ms, RelTol should preferably be <= 1e-5 to obtain accurate results

If using the ode solver to integrate continuously over a 'long' interval, a value for RelTol <= 1e-5 must be used. All system simulations were carried out using the ODE solvers in stepped mode with default tolerance parameters and a step interval of 1ms.

5.2   Review Of Motor Parameter Estimation Accuracy

Due to the difficulties in obtaining detailed data on the majority of the motors installed at PetroSA, it was desirable that model parameters be estimated based on nameplate data. The *abc* and *d-q* models were used to simulate a DOL start using the parameters derived from the parameter estimation schemes developed in section 2.10. The models gave unrealistic results with motor starting currents and torque being about 50% lower than expected.

A 40% reduction in the calculated values for the rotor and stator leakage reactances was found to give a more realistic estimate of starting conditions with models predicting starting currents of 4 to 5 times full load current. The simple parameter estimation scheme is inaccurate and will need to be improved for future work. More accurate parameter estimation methods have been developed by other researchers and should be considered for use.[25] The simple parameter estimation scheme used was mainly adopted to limit the scope of work.

Since the *d-q* model is a single-cage rotor model, the starting torque predicted by this model would be less than that developed by a double cage motor.

When compared to the known motor parameters, the estimated stator resistance is higher than the measured resistance since, in the parameter derivation, iron losses are assumed to be accounted for by the stator resistance.

Since the motors being modelled have double-cage rotors, the *abc* model was modified to allow variation of rotor parameters with speed[22]. The variation of rotor resistance and reactance with rotor speed can be reasonably well approximated by a linear function. The

variation or parameters differs between motors and approximate values had to be chosen [33, 25]. The starting rotor resistance was assumed to be three times the value at rated speed. The rotor reactance at rated speed was assumed to be twice that at starting.

The performance of the *abc* and *d-q* models with the calculated parameters was investigated by simulating a direct-on-line start on an infinite bus. No loadflow calculations were executed for these tests.

Figure 5-4 shows the stator current calculated by the *abc* motor model using the parameters listed in Appendix C for motor 24PC101A.
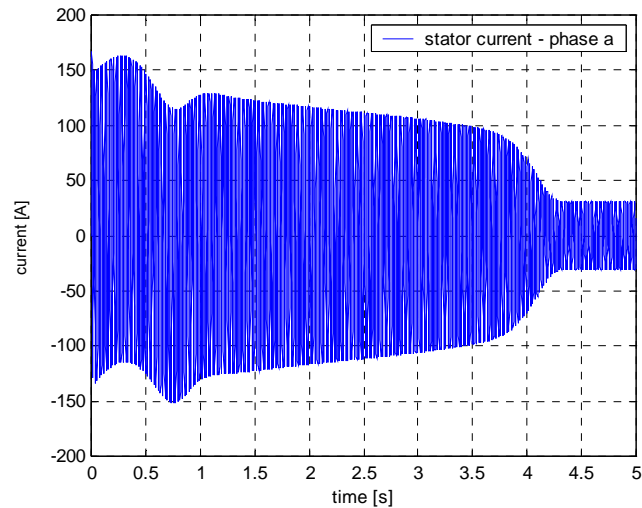
Figure 5-4 300kW motor stator current – *abc* model

Figure 5-5 shows the stator current calculated by the *d-q* motor model using the parameters listed in Appendix C for motor 24PC101A. The stator current of the *d-q* model remains constant until the rotor speed reaches about 0.8 p.u. This is due to rotor parameters remaining constant in this model. The rotor parameter variation can be clearly seen during the *abc* model startup simulation. The gradual reduction in stator current is due to the variation in rotor resistance and reactance with rotor speed.
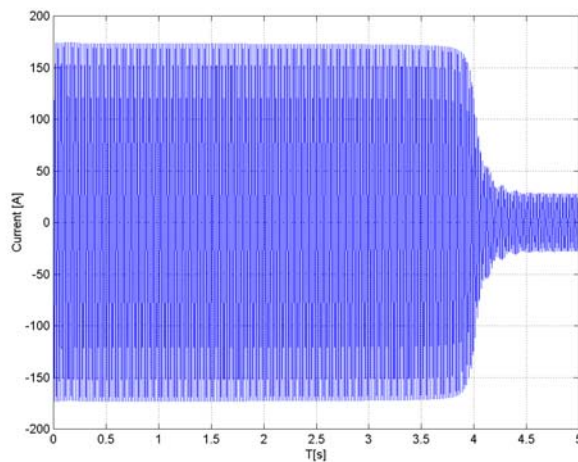
Figure 5-5 300kW motor stator current – *d-q* model

The *d-q* model predicts a higher starting current than the *abc* model. Figure 5-6 and Figure 5-8 show the motor torques calculated using the *d-q* and *abc* models.
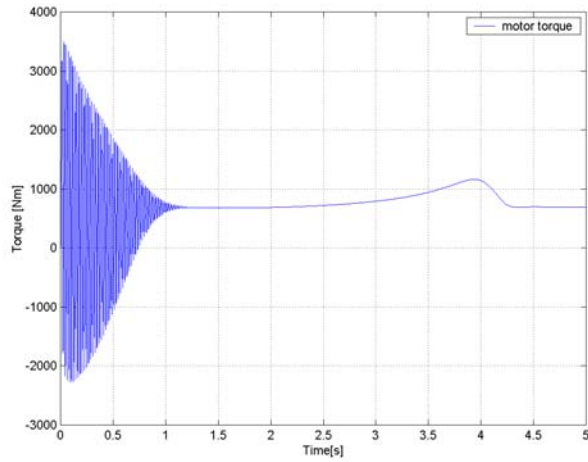
Figure 5-6 300kW motor DOL start: electromagnetic torque (*abc* model)
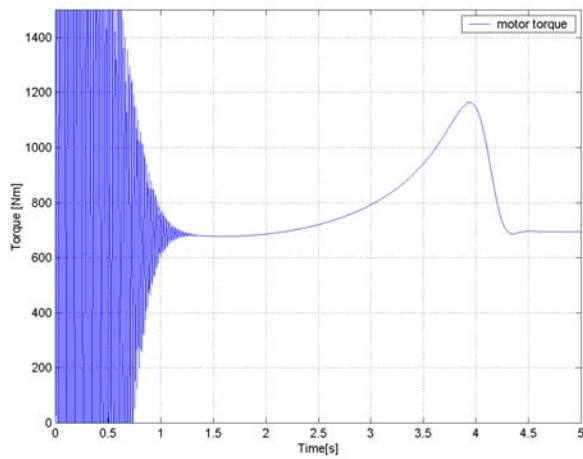
Figure 5-7 Detail of Figure 5-6
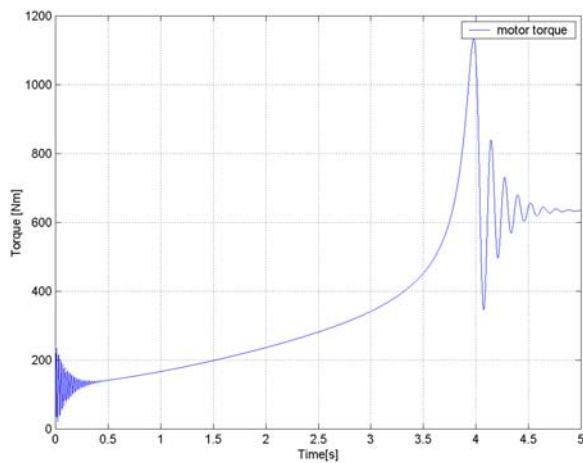
Figure 5-8 300kW motor DOL start: electromagnetic torque (*d-q* model)

The peak torques predicted by the models agree fairly well, but the initial 50Hz torque transients predicted by the models differ quite significantly. The 50Hz torque transients typically attain magnitudes of 2 to 3 times the pull-out torque of the motor.[36] It therefore appears as if the *abc* model predicts the maximum value of the transient torques more accurately than the *d-q* model.

From Figure 5-8 it can be seen that the d-q model exhibits torque fluctuations as the accelerating rotor reaches full speed, overshoots, decelerates and continues to oscillate around the steady-state speed before settling. These oscillations are attributable to the lower inertia constant used for the *d-q* model and the difference in speed torque characteristics between the *abc* and *d-q* models. The *d-q* model does not incorporate varying rotor parameters to approximate the behaviour of a double-cage rotor machine and thus a different (lower) torque characteristic is simulated. A lower inertia constant is therefore used with this model to ensure that the time taken to accelerate to full speed is the same as for the *abc* model.

Figure 5-6 was compared to test results obtained by Smith and Chen[22] using a similar model. These test results have been reproduced in Figure 5-9 and Figure 5-10. It can be seen by comparing these figures with Figure 5-6 and Figure 5-8 that the stator current and torques predicted by the models exhibit similar characteristics to those obtained by Smith and Chen.
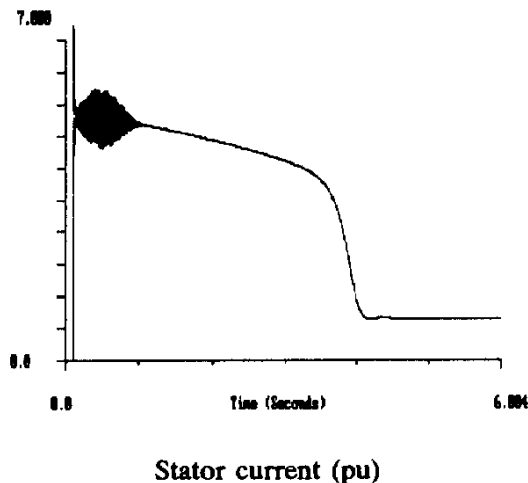
Stator current (pu)

Figure 5-9 Induction motor stator current [22][4]

---

[4] Figure 5-9 and Figure 5-10 have been reproduced from figure 3-7 on page 44 of "Three Phase Electrical Machine Systems Computer Simulation"[22]

Electro-magnetic torque (pu)
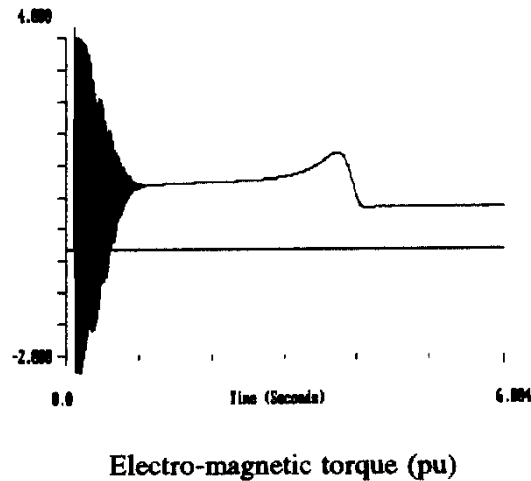
Figure 5-10 Electro-magnetic torque [22]

An attempt was made to simulate a motor start with the *abc* model using the induction motor model parameters used by Smith and Chen in order to compare the results obtained with those shown in Figure 5-9 and Figure 5-10. It was however found that the model was unstable when using these parameters with the state variables tending to infinity at about t = 50ms. Parameters were also calculated for other motors on the PetroSA plant for which data was available using the estimation scheme presented in section 2.10.4. In all these cases, the *abc* model was found to be stable, giving results similar to those shown in Figure 5-6 and Figure 5-8.[5] This issue was never resolved, and it is probable that there is an error in the parameter values presented by Smith and Chen, or that the data was misinterpreted.

5.3   Motor Starting Tests

In order to check the accuracy of the models used, the starting currents and bus voltages were measured for the motors in substation 24 (refer to Figure 3-8, page 99). These values were then compared with the results obtained using the *abc* and *d-q* models. It is obviously not possible to simulate a voltage dip on the PetroSA system to check the validity of simulation results. A motor start was the only transient event that could be measured on the physical system and compared to the theoretical results. As mentioned elsewhere, most motors have an installed spare. In order to prevent problems such as brinelling of bearings and pump corrosion, motors are switched over weekly. The standby motor is started and the motor that was running will be stopped. The load on the motor will be different during a controlled start-up than that following a voltage dip and subsequent re-connection. This will result in different starting times. The model parameters were used as derived and no attempt was made to adjust these parameters to match the machine startup as measured. Three of the motors on the 6.6kV bus in substation 24 could be tested and results obtained are shown below:

---

[5] These tests have not been included here since they do not add any value to the discussion. They were conducted to try to determine if there was an error in the model resulting in instability with differing parameter sets. The fact that these tests did not result in instability does not prove conclusively that there is no problem with the model or that there is an error with parameters presented by Smith and Chen. The *abc* model equations are discussed in detail by several authors and verification that the equations implemented in the Matlab code are a correct representation of these equations is a simple exercise. The Matlab ode solvers used are widely used, thus there is sufficient justification for accepting that the model is mathematically correct and correctly implemented. The accuracy of results predicted by the model will obviously depend on accuracy of model parameters, but based on the aforementioned considerations it was reasonable to conclude that the model instability was due to a parameter error, rather than an inherent flaw in the model.

Measurements were made using the following equipment:

- Yokogawa Digital Storage Oscilloscope Model DL775

- Kyoritsu Current Probe, model 8111 range 10mA/mV

- 250:1 Attenuator – Strike Technologies (Model Unknown)

The attenuator unit is simply a resistor divider and was required because the secondary voltage of the bus voltage transformer (110VAC) exceeds the maximum input voltage ratings of the oscilloscope. Currents were measured on the current transformer secondaries.

5.3.1 Comparison Of Test Results With Simulated Results

The load on each motor was estimated from the measured running current and the simulated load for each model set to the same value. The inertia constant was also adjusted so that the simulated starting times were approximately the same as the measured starting times. Since the *d-q* model is included as a reference model, the characteristics of the model are compared to the *abc* model, but not analysed or model behaviour discussed in any detail.
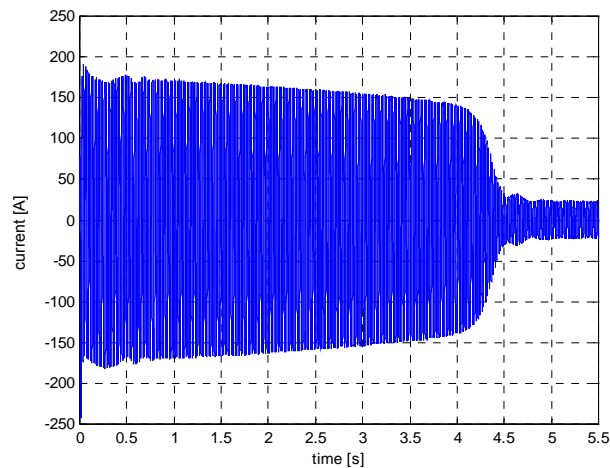
Figure 5-11 300 kW pump motor (24PC101A) stator current – measured.
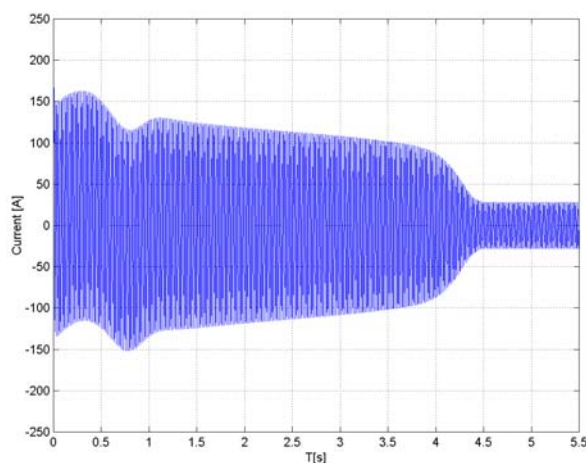
Figure 5-12 300kW pump motor (24PC101A) stator current – *abc* model.

Comparing the *abc* model (Figure 5-12) with the measured results (Figure 5-11) shows that the initial transient stator currents are smaller and decay faster than the measured currents. When voltage is initially applied to a stationary machine, phase fluxes begin to build up at

rates proportional to the instantaneous voltages. The stationary rotor develops corresponding opposition currents which initially maintain the motor starting condition of zero linkages.[14] These currents decay in the rotor circuit at a rate determined by the rotor circuit parameters. These currents, whilst present also give rise to the 50Hz torque transients observed when the motor starts. This can be seen from Figure 5-4 and Figure 5-6, above where the 50Hz torque transients can be seen to decay as the stator current transients decay.

In the real machine, saturation of the machine during the initial current inrush would limit the magnetic flux in the machine. This in turn would limit the magnitude of the opposition currents developed in the rotor, also reducing the time taken for these transient currents to decay. The 50Hz transient torque fluctuations would therefore also decay more rapidly than predicted by the *abc* model.

The *abc* model does not predict the starting current correctly, The variation of rotor parameters with motor speed is incorrect in the model, since the simulated stator current shown in Figure 5-12 decays more rapidly than the measured current in Figure 5-11. This needs to be corrected by improved parameter estimation
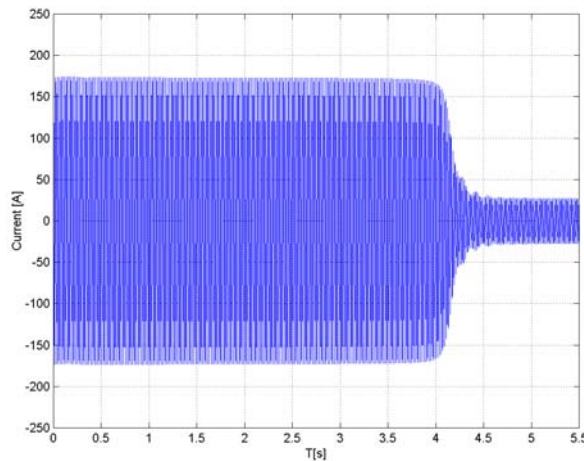
Figure 5-13 300kW pump motor (24PC101A) stator current – *d-q* model.

The stator current simulated by the *d-q* model (Figure 5-13) is greater than the measured current and the transient current fluctuations almost non-existent.
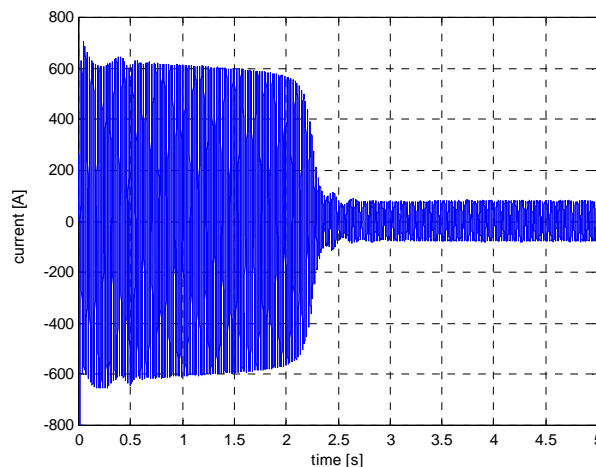
Figure 5-14 800 kW pump motor (24PC102A) stator current – measured.
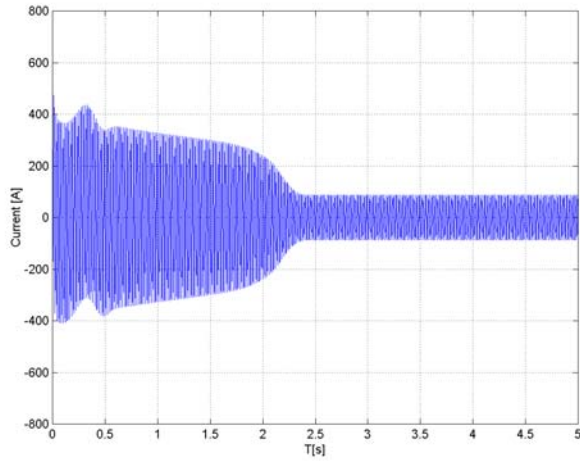
Figure 5-15 800 kW pump motor (24PC102A) stator current – *abc* model.

Comparing Figure 5-14 and Figure 5-15 shows that there is an even greater error between the measured motor starting current and the current simulated by the *abc* model than for the 300kW motor discussed above. The starting current simulated by the *d-q* model (Figure 5-16) is greater than that given by the *abc* model, but still less than the measured current.
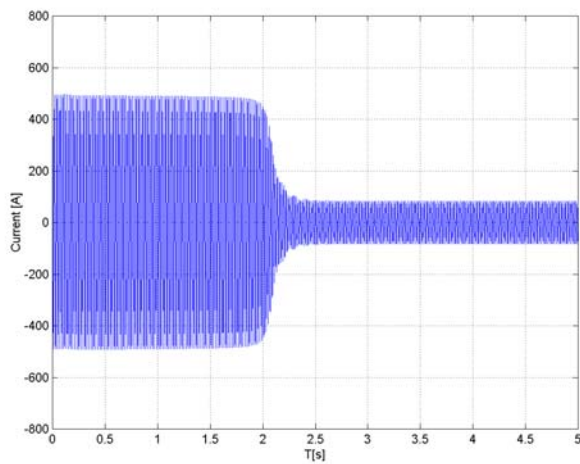
Figure 5-16 800 kW pump motor (24PC102A) stator current – *d-q* model.
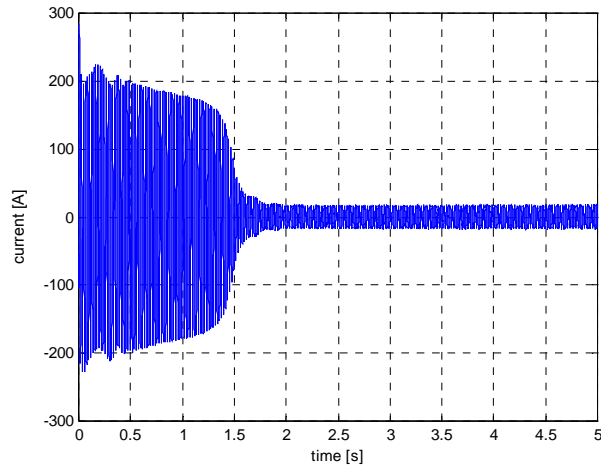
Figure 5-17 550 kW pump motor (24PC104A) stator current – measured.
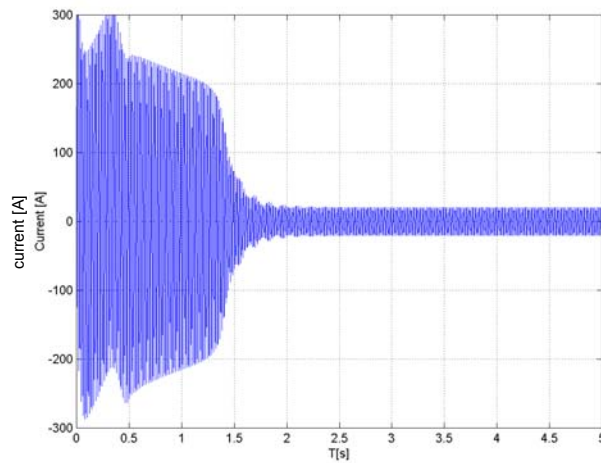
Figure 5-18 550 kW pump motor (24PC104A) stator current – *abc* **model.**
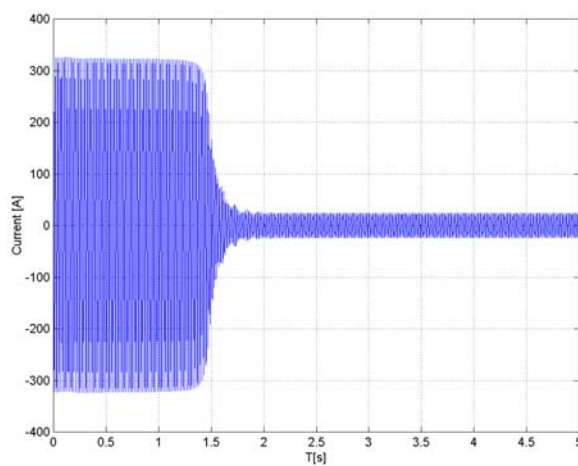
Figure 5-19 550 kW pump motor (24PC104A) stator current – *d-q* **model.**

From Figure 5-17, Figure 5-18 and Figure 5-19 it can be seen that both the *abc* and *d-q* models predicted starting currents greater than the current measured for the 550kW motor.

The test results have shown that the parameter estimation scheme used to obtain model parameters is unsatisfactory and will need to be improved before future work is carried out. The errors resulting form the inaccurate model parameters were also inconsistent. For the 550kW motor, simulated currents were greater than measured, whilst for the 800kW motor, simulated currents were less than measured. The *abc* model will need to be extended to include saturation in order to represent the 50Hz transient torque fluctuations on startup more accurately. The motor data required for modelling saturation would need to be obtained.

5.3.2 System bus voltage

From Figure 5-20 it can be seen that there is noise present on the measured bus voltages. This is mainly due to thyristor controlled[6] heaters installed in the same substation. It was difficult to accurately estimate the bus voltage drops while the motors were starting, because the system bus voltage continually fluctuates. This can be seen in Figure 5-20. where the voltage increased in the period between 2 and 4 seconds, although the motor had not yet finished accelerating.
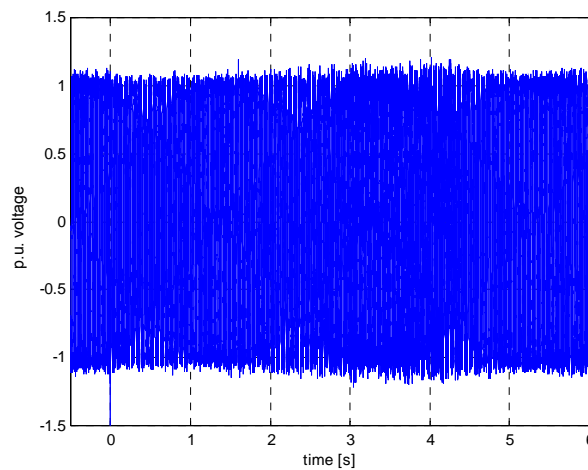
Figure 5-20 300 kW pump motor (24PC101A) bus voltage – measured.

Figure 5-21 shows a magnified portion of the recorded bus voltage. The initial bus voltage is approximately 1.1 p.u. Immediately after the motor is started, the bus voltage drops to about 1.06 p.u., giving an estimated drop of approximately 0.04 p.u.

---

[6] The voltage fluctuations were observed to change in sympathy with the continual switching of the thyristor heater controllers. (6 x 500kW electrical heaters)
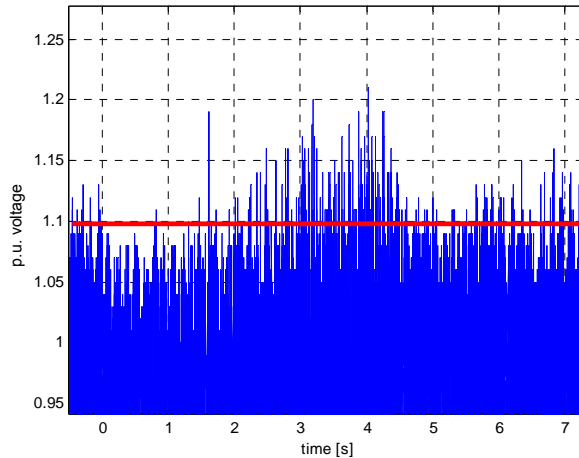
Figure 5-21 300 kW pump motor (24PC101A) Bus voltage – detail.

Figure 5-22 shows the system bus voltage measured during the startup of the 800kW pump motor. In this case the voltage drop is approximately 0.07 p.u.
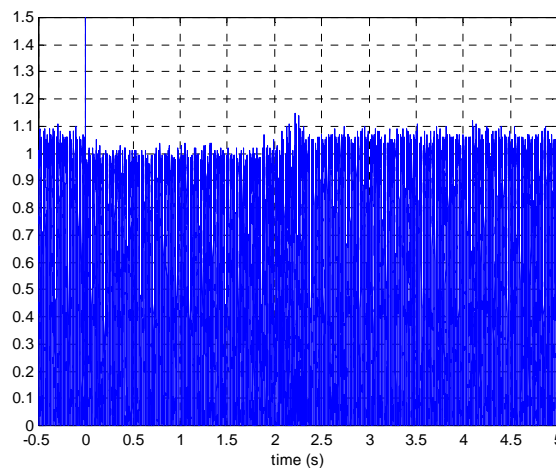
Figure 5-22 800 kW pump motor (24PC102A) Bus voltage – measured.

The parameters for the *d-q* model were changed to approximate the measured starting current for the 800kW motor, 24PC102A. A system simulation was then carried out with only this motor starting. The *d-q* model was selected since the parameters are easily adjusted by trial and error to give simulated stator currents and acceleration times closely approximating the values measured for the 800kW motor. The 800kW motor was chosen for the simulation since starting this motor results in the largest bus voltage drop. The generator model was disabled for this simulation with a constant 56MW and 41MVAr injected at the generator bus.

The simulated motor starting current is shown in Figure 5-23. Note that the motor start is simulated from time t = 0.01s. This allows the system bus voltage before the motor start to be clearly seen when simulation results are plotted.
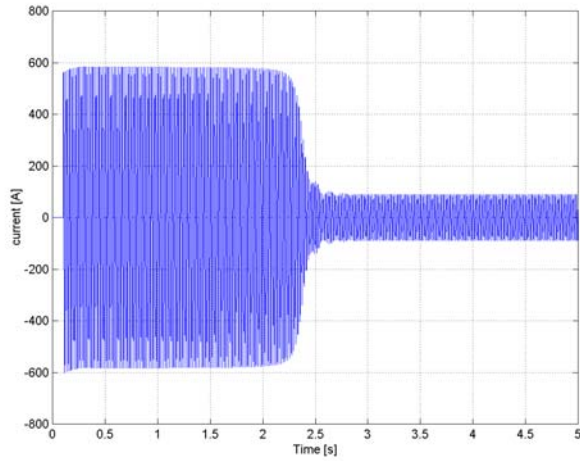
Figure 5-23 800kW pump motor (24PC102A) Stator current – simulated
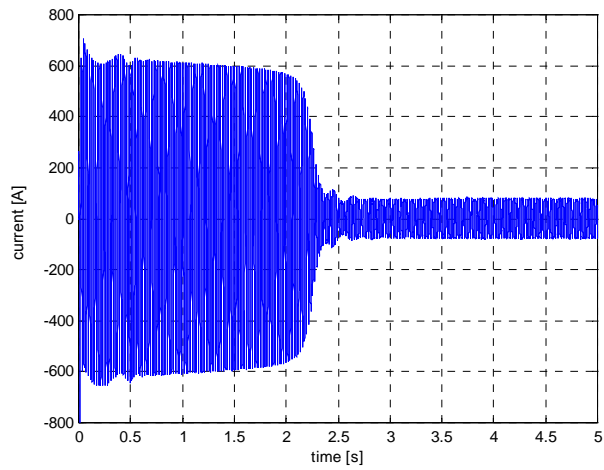
Figure 5-24 800kW pump motor (24PC102A) Stator current – measured

Comparing Figure 5-23 and Figure 5-24 shows that the *d-q* model approximates the measured motor startup currents reasonably well.
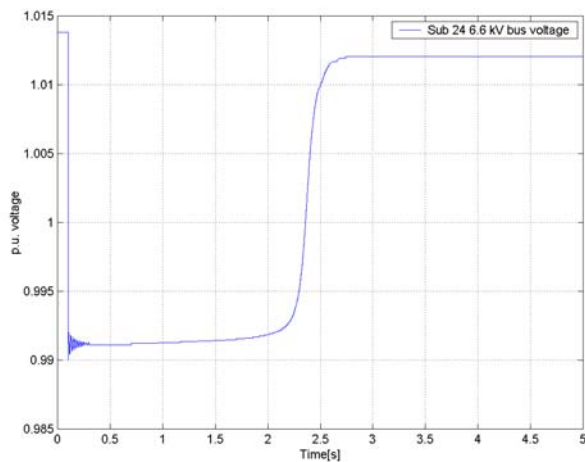
Figure 5-25 800kW pump motor (24PC102A) Bus voltage - simulated

The simulated substation bus voltage is shown in Figure 5-25. The bus voltage drop when the motor starts is approximately 0.02 p.u. From Figure 5-22, it can be seen that the bus voltage drop measured when the 800kW motor was started was approximately 0.07 p.u.

These results show that the PetroSA system is not as stiff as indicated by the system model. The two most probable sources of error are the representation of the Eskom supply and inaccurate modelling of the PetroSA distribution system.

The most likely cause of this error are inaccuracies in the parameters used for modelling the distribution system. These parameters were obtained from the database of the loadflow analysis software currently used by PetroSA.[7] Transformer impedance data in this database was obtained from the manufacturer's data sheets and should be accurate. Feeder cable impedances were obtained from standard libraries included with this software, and these values are the most probable source of error. There are two likely sources of error: The impedances of the cables in the software libraries differ from those of the actual feeders. The feeder lengths and types could have been incorrectly entered when the database was developed. The most probable source of error is the first since the test results indicate that the system impedances in the model are too low. Incorrect entry of feeder lengths and types, although probably present, is likely to result in random errors with some feeder impedances being too high and some being too low, whilst the error observed appears to be due to impedance values throughout the system being too low. The accuracy of this data needs to be verified before attempting to investigate or identify any other potential sources of error.

Notwithstanding the above, the magnitude of the error needs to be considered in practical terms. The difference between the measured and simulated results is about 0.05 p.u. or 5% A 5%. reduction in bus voltage will not result in any significant change in the running or starting performance of this 800kW motor. The normal bus voltages on the PetroSA plant are usually above 1 p.u. (Typical range is 1.05-1.1p.u.) During normal operation of the plant bus voltage variations of the order of 0.05 p.u. occur continuously.

The 132kV bus at Proteus substation from which the PetroSA plant is supplied is modelled as the swing bus. The impedance of the two 11km 132kV lines supplying the plant are included in the model. This was considered a reasonable approximation since the total motor load being modelled under transient conditions is approximately 1% of the plant load of 200MW. Prior tests carried out on site (not related to this work) showed that it was difficult to detect a drop in bus voltage on the 132kV bus at the main substation[8] when one of the main cooling water pumps (2.2MW) is started. It would therefore even have been reasonable to assume that the main substation 132kV bus is a swing bus. If the investigation into the feeder impedance parameters suggested above does not resolve the problem, the representation of the Eskom system should be reviewed, followed by a review of the transformer impedance data.

Investigation and rectification of the model errors will be necessary if further studies are carried out and the complexity of the model is increased by modelling the remainder of the system in greater detail and adding additional dynamic motor models. As more motor models are added to the system, the simulation of these motors starting simultaneously or in sequence will result in more significant bus voltage drops which have the potential to adversely affect the performance the various motors. Under these circumstances, it is critical that the system model predicts bus voltage drops correctly.

For this work the relatively small transient load being simulated was considered along with the need to restrict the scope of work, and the remaining simulations carried out using the unchanged parameters.

---

[7] Dapper and Captor

[8] Substation 01

5.3.3 Summary of Findings

The parameter estimation scheme is inaccurate and needs to be reviewed. This results in the errors between simulated and measured results being unacceptably large. The omission of saturation from the *abc* model has resulted in inaccurate modelling of the 50Hz torque transients. The amplitude of the torque transients predicted by the *abc* model agrees with results obtained by other researchers[22,36] but could not be verified against any real, measured results. At best, this should be treated as an estimate of the 50Hz torque transient amplitude. The duration of the torque transients and associated stator current transients predicted by the *abc* model is greater than that observed on the actual machines.[9] The inclusion of saturation effects in the *abc* model will permit more accurate simulation of the 50Hz transient torques and stator current transients. The revised models would also need to be benchmarked against known and accepted results to establish that they are working correctly.

The simulated bus voltage drop was less than that measured during the motor starting tests. Incorrect feeder parameter data used for the distribution system model is the most probable cause of this error which should be rectified if the model is to be extended for further studies.

5.4 Voltage Dips And Switching Effects On Motor Operation

The following simulations were carried out using the *abc* and *d-q* motor models. The behaviour of the motor model was simulated assuming connection to an infinite bus. Simulation was carried out using only the motor model with no alternating loadflow calculations. Except for test 6, the *abc* model was used. Table 5-2 gives a summary of the simulations carried out

Table 5-2 Summary of motor response studies.

Simulation	Description	Comments
1	20%, 100ms 3-phase voltage dip. 550kW induction motor	Determine effect of leaving motor connected to the supply during the voltage dip
2	20%, 100ms 3-phase voltage dip. 550kW induction motor. Disconnect 80ms after voltage dip and reconnect 0.25s later	Determine effects of reconnecting motor after a voltage dip at different times. Note, the motor is disconnected 80ms after the start of the voltage dip to simulate the time taken for the contactor to drop out.
3	20%, 100ms 3-phase voltage dip. 550kW induction motor. Disconnect 80ms after voltage dip and reconnect 0.4s later	
4	20%, 100ms 3-phase voltage dip. 550kW induction motor. Disconnect 80ms after voltage dip and reconnect 1s later	
5	20%, 200ms 3-phase voltage dip. 550kW induction motor	Determine effect of leaving motor connected during longer voltage dip
6	20%, 100ms 3-phase voltage dip. 550kW induction motor – *d-q* model	Compare with results obtained from *abc* model

When the terminal voltage or current of an induction machine is abruptly changed, the theorem of constant linkage[10] implies that the magnetic flux linkages within the machine cannot change instantaneously. If a running motor is disconnected, the stator currents are forced to zero. The motor maintains its flux linkages by a unidirectional current in the rotor. This gives rise to a trapped or frozen flux which is carried around with the rotor as it decays. This flux induces rotational e.m.f.'s in the stator windings. If the stator windings are re-

---

[9] The torque transients on the actual machines could obviously not be measured. The 50Hz torque transients will however decay as the stator current transients decay.

[10] The *Theorem of constant linkage* states that in a closed circuit of zero resistance, the algebraic sum of its magnetic linkages remains constant. In a practical circuit with low resistance, as in an induction motor, the linkage remains effectively constant immediately after a sudden change because it takes time for stored magnetic energy to be altered, usually approximating a timed-exponential rise or decay[14].

connected to the supply during this period, transient currents and torques are induced. If the induced stator e.m.f.'s have phase opposition to the supply voltages at the instant of re-connection, transient currents and torques may be severe with the torque possibly having a retarding (negative) peak. In the worst case, the first peak may reach 15 times full-load torque with stator currents typically 5-7 times full load current. [14].

If the motor terminal voltage is reduced, a similar unidirectional rotor current component is set up which induces stator e.m.f.'s resulting in transient currents and torques being produced. The motor speed will fall during this period. When the terminal voltage returns to normal, the motor will re-accelerate placing reactive power demands on the system.

5.4.1 Effect of voltage dip duration

Simulations 2, 3 and 4 show the effects of disconnecting and re-connecting a motor to the supply with increasing time delay. Comparing Figure 5-26, Figure 5-27 and Figure 5-28 shows that the rotor torque following re-connection of the supply is dependent on the position of the trapped rotor flux with respect to the stator flux that is established when line voltage is re-connected. The rotor phase angle in turn is dependent upon factors such as the motor load, duration of the interruption, and magnitude of the initial voltage dip.
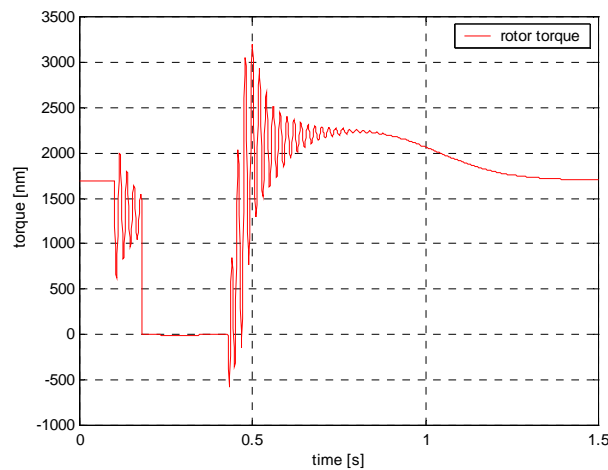
Figure 5-26 550kW motor rotor torque (simulation 2).
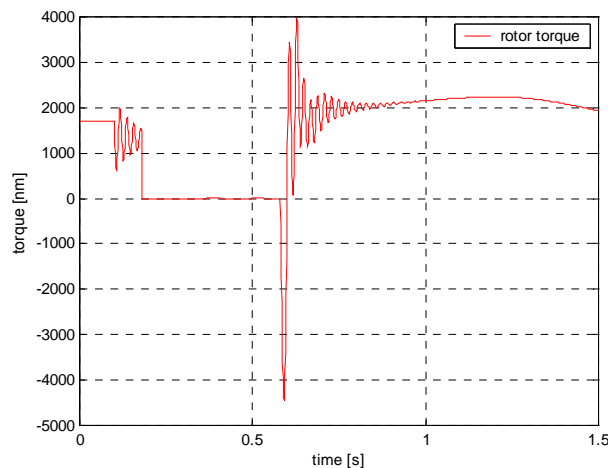
Figure 5-27 550kW motor rotor torque(simulation 3).
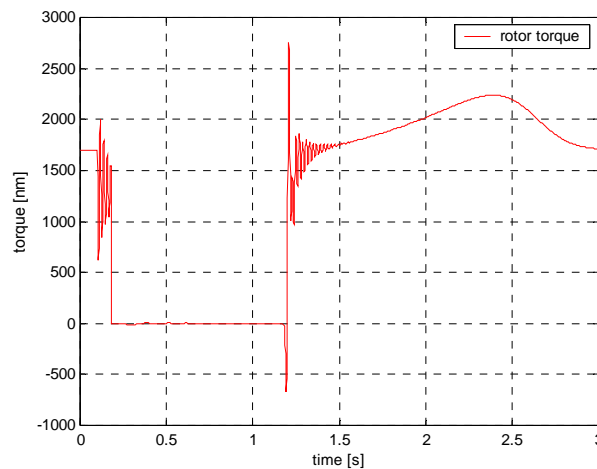
Figure 5-28 550kW motor rotor torque (simulation 4).

 If the stator e.m.f happens to be in phase with the line voltages when re-connected, the torque and current transients will be relatively small. Simulation 3 happens to show a case where the phase misalignment resulted in a negative transient torque of about 2.5 p.u.. This is still significantly less than torques of up to 15 p.u. which can be generated [14] under these conditions. The effect of this negative torque can be seen in Figure 5-29 where a sudden deceleration of the rotor is observed at the instant of re-connection. It must be borne in mind that these transients are not accurately represented by the a*bc* model and that they will decay more rapidly than predicted by the model. Absolute accuracy of the current and torque magnitudes predicted by the models has not been established, but a comparison of different tests gives and indication of the variation in magnitude expected under different conditions.
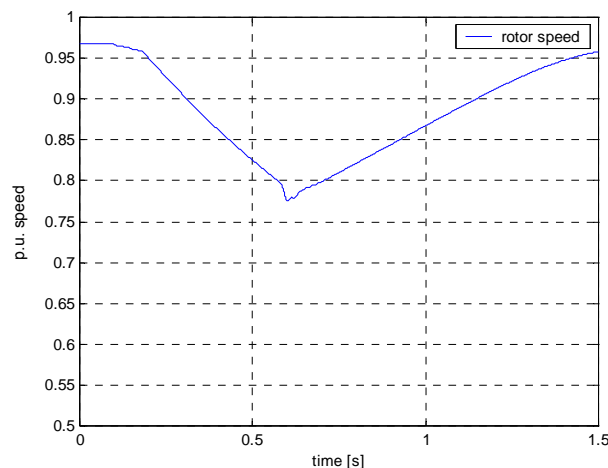
Figure 5-29 550kW motor rotor speed (simulation 4).

The magnitude of the initial stator transient currents is relatively independent of the time period before the motor is re-connected to the supply. Comparing Figure 5-30, Figure 5-31 and Figure 5-32 shows that the magnitude of the current following the initial transient can be seen to increase as the delay before re-connection of the supply increases. This is due to the motor slowing down and having to be re-accelerated. Stator current is also drawn for a longer period of time as the rotor re-accelerates. As discussed above, the magnitude of the stator

current on re-connection is also influenced by the degree of misalignment between the trapped rotor flux and the stator flux at the instant of re-connection. In this case, the highest transient current at the instant the motor was re-connected was almost 300A which occurred during simulation 2, where the motor was re-connected after only 0.25s - Figure 5-30. It is important that the transient stator current and torque magnitudes are not directly related to the time delay before the motor is reconnected to the supply. The design of the PetroSA re-acceleration system is partly based on the assumption that motor currents magnitudes will always increase as the delay before reconnection after a power dip increases.
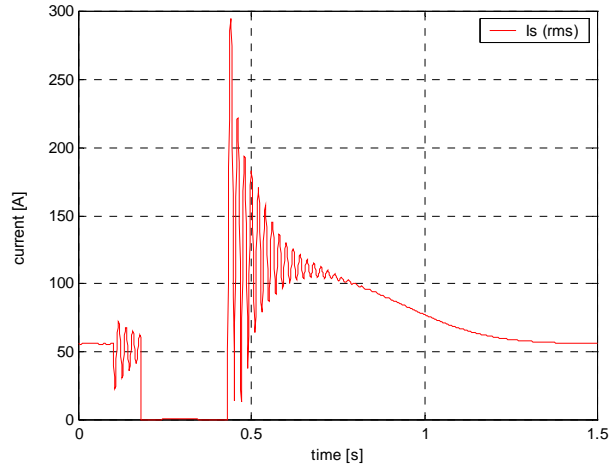
Figure 5-30 550kW motor rms stator current (simulation 2).
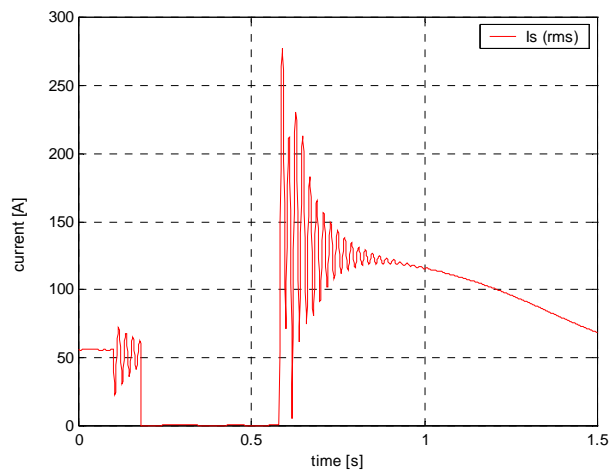
Figure 5-31 550kW motor rms stator current (simulation 3).
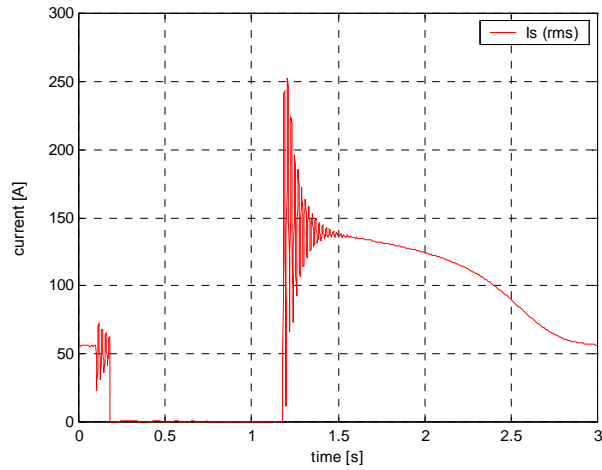
Figure 5-32 550kW motor rms stator current (simulation 4).

If the behaviour of a motor that remains connected to the supply during a short voltage dip is compared to that of a motor which is disconnected, and then reconnected to the supply, it can be seen that the amplitude of the stator current transients is lower. This can be seen, for example, by comparing Figure 5-33 with Figure 5-30, Figure 5-31 and Figure 5-32.
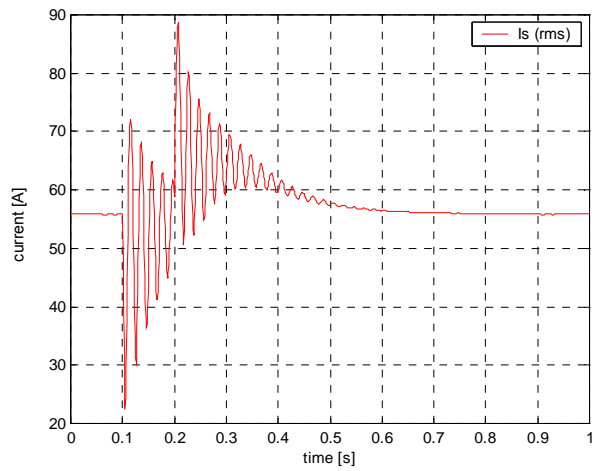
Figure 5-33 550kW motor rms stator current (simulation 1).
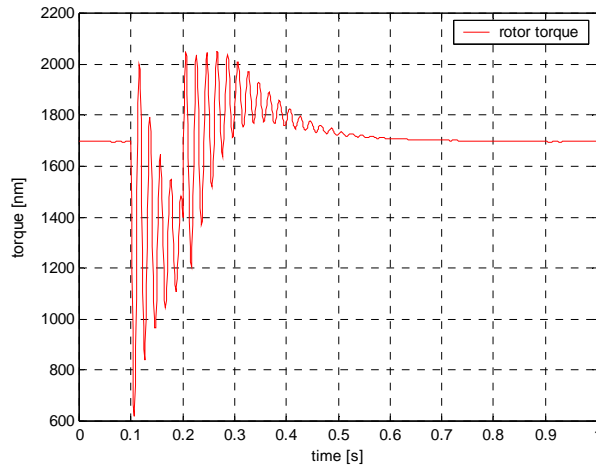
Figure 5-34 550kW motor rotor torque (simulation 1).
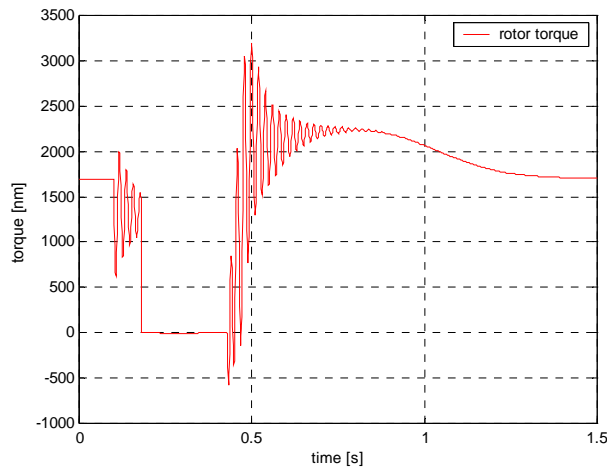
Figure 5-35 550kW motor rotor torque (simulation 2).

Comparing Figure 5-34 and Figure 5-35 shows that the rotor transient torque amplitude is also greater when the motor is disconnected from the supply following a voltage dip and then reconnected.

When disconnecting and then re-connecting a motor, the torque transients generated are variable, depending on factors such as the rotor position, speed, motor load and instant of reconnection. The generation of 'worst case' transients is random and might explain some isolated cases where motor couplings have failed at PetroSA. The duration of the 50Hz torque transients is shorter than predicted by the model and the rotor inertia and elasticity of the machine rotor and shaft assembly generally absorb most of these transients before they are transmitted to the motor shaft[14]. It should not just be assumed that the transient torques are responsible for these failures without careful investigation of the driven machine, operating conditions, etc.

The simulation results indicate that the voltage level at which the re-acceleration system disconnects motors could be reduced, allowing motors to remain online during the less severe voltage dips which occur most frequently. This would result in decreased current being drawn by motors after the voltage dip.

5.4.2 abc vs. d-q induction motor model

Comparison of simulations 1 and 6 shows that the *d-q* model can provide a reasonable estimate of stator current and torque transients. Comparing Figure 5-36 with Figure 5-37 shows that the 50Hz current transients are not shown by the *d-q* model. The peak current of about 77A which occurs when motor voltage recovers compares reasonably well with the peak of about 90A predicted by the *abc* model.
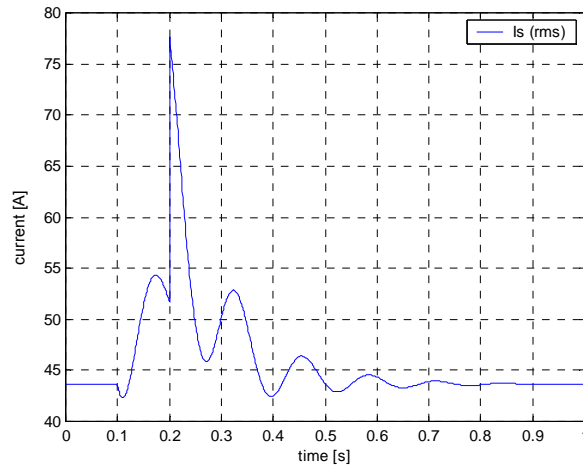
Figure 5-36 550kW motor rms stator current (simulation 6).
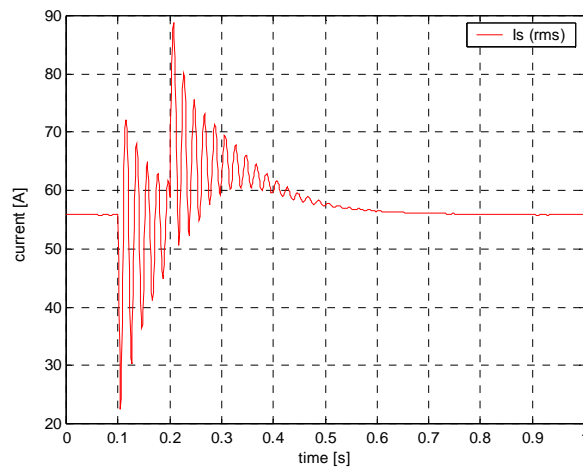
Figure 5-37 550kW motor rms stator current (simulation 1).
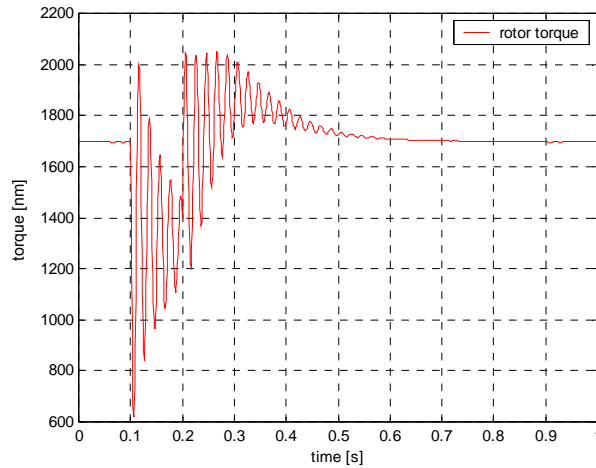
Figure 5-38 550kW motor rotor torque (simulation 2).
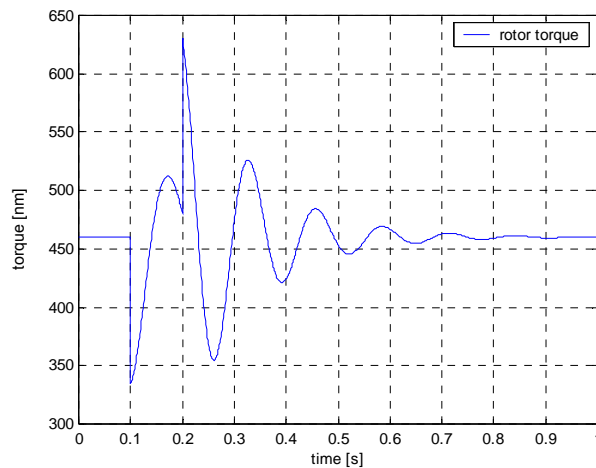
Figure 5-39 550kW motor rotor torque (simulation 7).

Comparing Figure 5-38 and Figure 5-39 shows that 50Hz torque transients during the voltage dip are not well represented. The peak torque of about 1875Nm on voltage recovery predicted by the *d-q* model appears to give some indication of the magnitudes of the torque peaks that could be expected when compared to the 2050Nm predicted by the *abc* model. This needs to be carefully investigated if the *d-q* model is to be used to investigate transient stator currents and rotor torques during system disturbances. The torque oscillations following voltage recovery that are shown in Figure 5-39 are suspected to be caused by mechanical oscillations of the rotor following the voltage dip. These oscillations are due to the lower inertia values that had to be used for the *d-q* model which were discussed in paragraph 5.2

Comparison of the two models shows that the *abc* model should be used when the 50Hz torque transients and stator transient currents need to be examined. The *d-q* model is not recommended for investigation of the 50Hz transient torques or currents.

5.5 Generator And Distribution System Behaviour

Table 5-3 gives an overview of the simulation studies that were carried out. Selected loadflow results are tabulated in Appendix G and give an overview of system bus voltages and branch current flows. Motors were modelled using the parameters discussed in section 4.5

Note: For location of motors on the electrical distribution system, refer to Figure 3-8

Table 5-3 Summary of system studies

Study	Description	System Conditions
1	Simultaneous DOL start of four 6.6kV motors: 24PC101 – 300kW, 24PC104 – 300kW, 24KC101 – 550kW, 24PC102 – 800kW abc model used	Generator not modelled. Generator bus = load bus with P = 56MW, Q = 41MVAr.
2	Simultaneous DOL start of four 6.6kV motors: 24PC101 – 300kW, 24PC104 – 300kW, 24KC101 – 550kW, 24PC102 – 800kW d-q model used	Generator not modelled. Generator bus = load bus with P = 56MW, Q = 41MVAr.
3	Simultaneous DOL start of four 6.6kV motors: 24PC101 – 300kW, 24PC104 – 300kW, 24KC101 – 550kW, 24PC102 – 800kW abc model used	Generator modelled with fixed excitation and mechanical input power, P = 56MW
4	Simultaneous DOL start of four 6.6kV motors: 24PC101 – 300kW, 24PC104 – 300kW, 24KC101 – 550kW, 24PC102 – 800kW d-q model used	Generator modelled with fixed excitation and mechanical input power, P = 56MW
5	Simultaneous DOL start of four 6.6kV motors: 24PC101 – 300kW, 24PC104 – 300kW, 24KC101 – 550kW, 24PC102 – 800kW abc model used	Generator modelled with AVR and governor enabled. Initial mech. power, P = 56MW
6	Simultaneous DOL start of four 6.6kV motors: 24PC101 – 300kW, 24PC104 – 300kW, 24KC101 – 550kW, 24PC102 – 800kW d-q model used	Generator modelled with AVR enabled and constant mech power input. Initial mech. power, P = 56MW
7	Simultaneous DOL start of four 6.6kV motors: 24PC101 – 300kW, 24PC104 – 300kW, 24KC101 – 550kW, 24PC102 – 800kW abc model used	Generator modelled with AVR enabled and constant mech power input. Initial mech. power, P = 56MW
8	Examine effect of 20%, 100ms voltage dip on Eskom supply. Motor initial conditions from Study case 6 final state. All 6.6kV motors remain online. d-q model used	Generator modelled with AVR enabled and constant mech power input. Initial mech. power, P = 56MW. No other system changes
9	Examine effect of 20%, 100ms voltage dip on Eskom supply. Motor initial conditions from Study case 7 final state. All 6.6kV motors remain online. abc model used	Generator modelled with AVR enabled and constant mech power input. Initial mech. power, P = 56MW. No other system changes
10	Examine effect of 20%, 100ms voltage dip on Eskom supply. Motor initial conditions from Study case 6 final state. All 6.6kV motors remain online. d-q model used	Generator modelled with AVR enabled and constant mech power input. Initial mech. power, P = 56MW. Two 26MW compressors at air separation plant tripped 80ms after start of voltage dip
11	Examine effect of 20%, 100ms voltage dip on Eskom supply. Motor initial conditions from Study case 7 final state. All 6.6kV motors trip and re-start sequentially. abc model used	Generator not modelled. Generator bus = load bus with P = 56MW, Q = 41MVAr. Two 26MW compressors at air separation plant tripped 80ms after start of voltage dip
12	Examine effect of 20%, 100ms voltage dip on Eskom supply. Motor initial conditions from Study case 7 final state. All 6.6kV motors trip and re-start immediately. abc model used	Generator not modelled. Generator bus = load bus with P = 56MW, Q = 41MVAr. Two 26MW compressors at air separation plant tripped 80ms after start of voltage dip

The simultaneous start of the four test motors was simulated to determine the impact on the distribution system as well as the plant generator. Since the intent of this work is to investigate induction motor behaviour, the generator model was kept relatively simple. The main plant generator is the largest single machine connected to the PetroSA system. It could not be excluded from the system and was modelled to determine its impact during transients. From practical experience, it is known that the plant will successfully recover after a voltage

dip whether the generator is online or not. It is however necessary to try to determine what influence the main generator has on the ability of the plant to recover following a voltage dip.

The overall system response using the two different induction machine models as well as the influence of the generator model is examined. Bus voltage drops throughout the system are investigated. Apart from the main substation bus voltages (Sub 01 and 06) the voltage drop on the 525V supply at one of the other secondary substations (Sub 19) was also examined to investigate how transient events at one substation affects other parts of the system.

5.5.1 Study 1 and 2: abc and d-q models

Study	Description	System Conditions
1	Simultaneous DOL start of four 6.6kV motors: 24PC101 – 300kW, 24PC104 – 300kW, 24KC101 – 550kW, 24PC102 – 800kW abc model used	Generator not modelled. Generator bus = load bus with P = 56MW, Q = 41MVAr.
2	Simultaneous DOL start of four 6.6kV motors: 24PC101 – 300kW, 24PC104 – 300kW, 24KC101 – 550kW, 24PC102 – 800kW d-q model used	Generator not modelled. Generator bus = load bus with P = 56MW, Q = 41MVAr.

Figure 5-40 Distribution system bus voltages (study 1).

The transient bus voltage fluctuations occurring between 0 and 0.5 seconds (Figure 5-40) are caused by the transient stator currents. In practice, these transients decay more rapidly than predicted by the *abc* model. These transients are absent when the *d-q* model is used, as can be seen from Figure 5-41
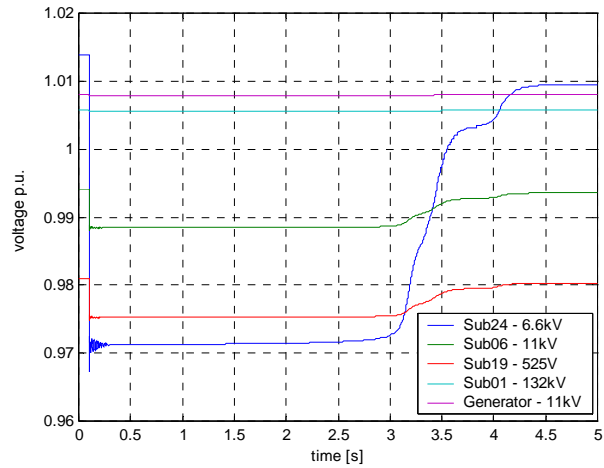
Figure 5-41 Distribution system bus voltages (study 2).

It is important to note that in both tests, a voltage drop is also observed on substation19 525V bus. This indicates that even the relatively minor transient simulated here has the potential to affect the entire system. This is particularly important considering that the system is not as stiff as the models indicate, and these voltage drops can be expected to be 2-3 times greater in practice.

Since rotor parameter changes are not modelled in the *d-q* model, the motor starting currents do not decay during the starting period as with the *abc* model. This can be seen by comparing Figure 5-42 and Figure 5-43. As a result, bus voltages remain depressed for longer and the *d-q* model simulates a more severe starting condition than would occur in practice.

Figure 5-42 Motor and substation feeder currents (study1).
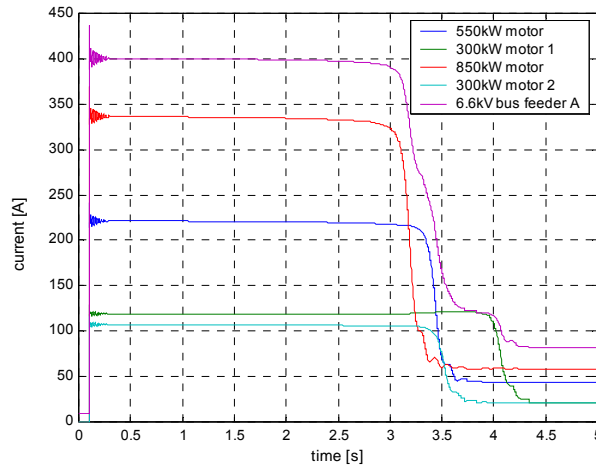
Figure 5-43 Motor and substation feeder currents (study 2).

Figure 5-42 and Figure 5-43 shows that there is little interaction between individual motors with stator currents not varying significantly during the period between 3 and 4.5 seconds. The bus feeder current is simply the sum of the individual motor currents. Note that there are two feeders in parallel with only feeder A current being shown.

5.5.2 Study 1 and 3: effect of generator model when abc motor model is used

Study	Description	System Conditions
1	Simultaneous DOL start of four 6.6kV motors: 24PC101 – 300kW, 24PC104 – 300kW, 24KC101 – 550kW, 24PC102 – 800kW abc model used	Generator not modelled. Generator bus = load bus with P = 56MW, Q = 41MVAr. No system disturbances
3	Simultaneous DOL start of four 6.6kV motors: 24PC101 – 300kW, 24PC104 – 300kW, 24KC101 – 550kW, 24PC102 – 800kW abc model used	Generator modelled with fixed excitation and mechanical input power, P = 56MW

Figure 5-44 and Figure 5-45 show that bus voltages are not affected by the inclusion of the generator model.
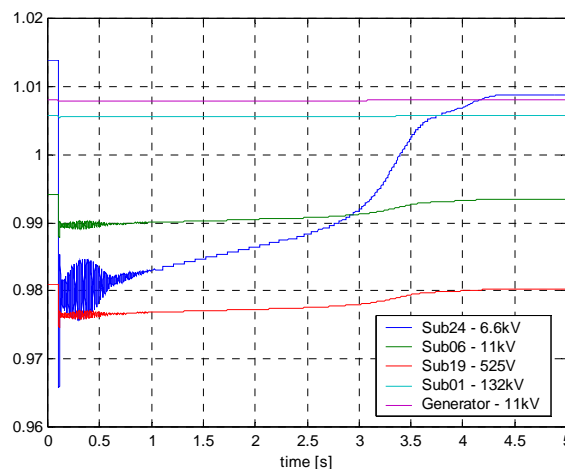
Figure 5-44 Distribution system bus voltages (study 1).
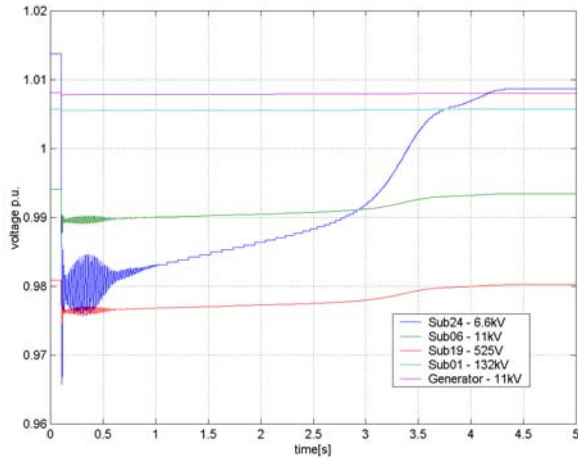
Figure 5-45 Distribution system bus voltages (study 3).

Comparing Figure 5-46 and Figure 5-47 shows that motor and feeder currents are also unchanged by the inclusion of the generator dynamic model.
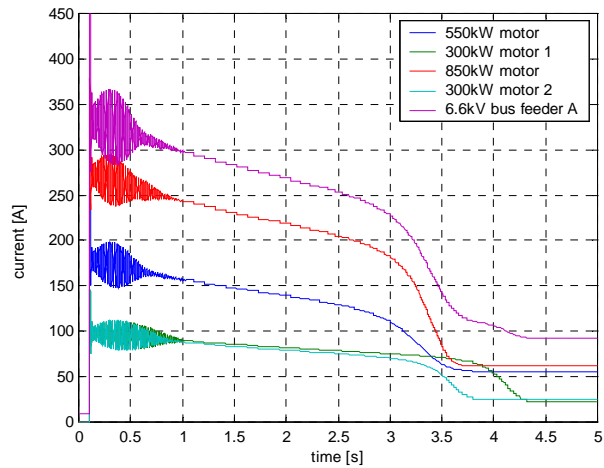
Figure 5-46 Motor and substation feeder currents (study 1).
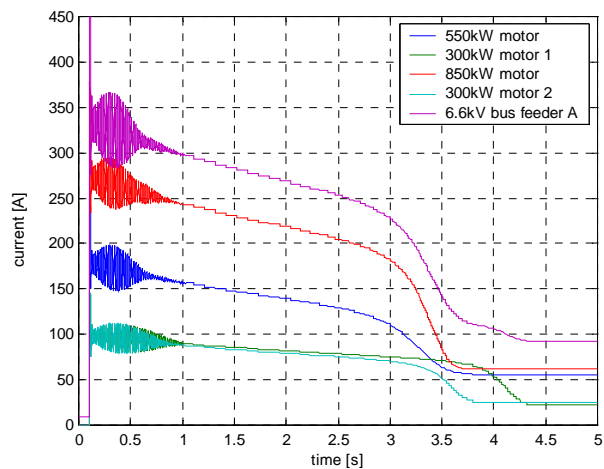
Figure 5-47 Motor and substation feeder currents (study 3).

Figure 5-48 shows that generator rotor angle variations were negligible.
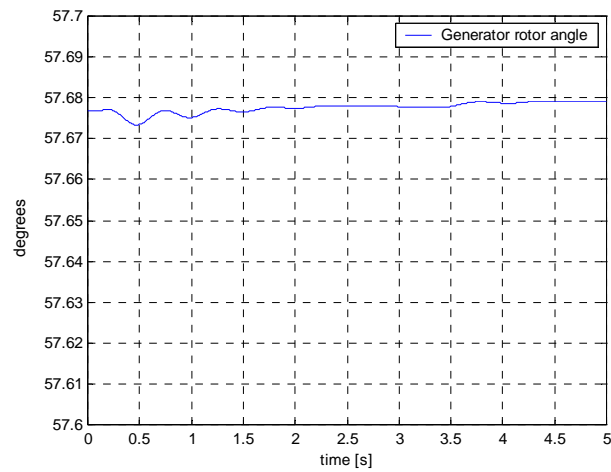
Figure 5-48 Generator rotor angle (study 3).

The above results show that the generator model can be omitted and the generator represented by constant power and reactive power injection on the generator bus without affecting the transient simulation results. This is to be expected since the system disturbance that was simulated is relatively small when compared to the load on the rest of the PetroSA distribution system. In practice, motors in the 300kW to 1MW range are stopped and started during normal plant operation with little or no impact observed on the distribution network.

5.5.3 Study 2 and 4: effect of generator model when d-q motor model is used

Study	Description	System Conditions
2	Simultaneous DOL start of four 6.6kV motors: 24PC101 – 300kW, 24PC104 – 300kW, 24KC101 – 550kW, 24PC102 – 800kW d-q model used	Generator not modelled. Generator bus = load bus with P = 56MW, Q = 41MVAr.
4	Simultaneous DOL start of four 6.6kV motors: 24PC101 – 300kW, 24PC104 – 300kW, 24KC101 – 550kW, 24PC102 – 800kW d-q model used	Generator modelled with fixed excitation and mechanical input power, P = 56MW

Figure 5-49 and Figure 5-50 show that the inclusion of the generator dynamic model has a negligible impact on the calculated system bus voltages.
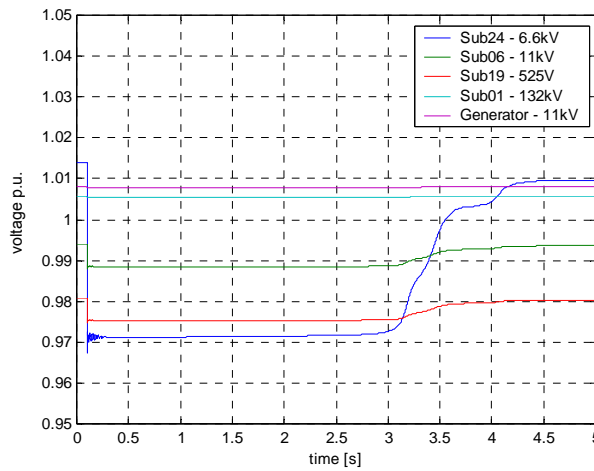
Figure 5-49 Distribution system bus voltages (study 2).
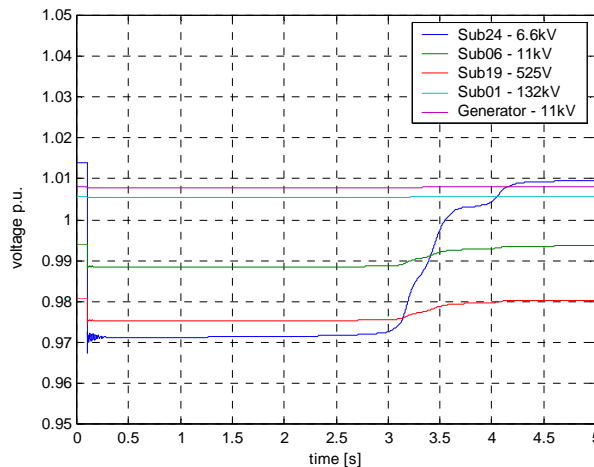
Figure 5-50 Distribution system bus voltages (study 4).
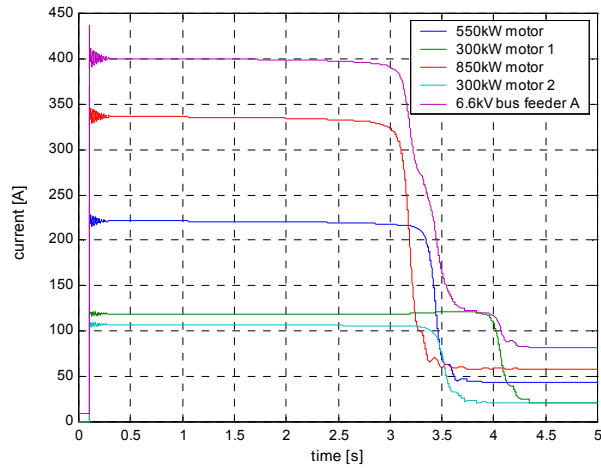
Figure 5-51 Motor and substation feeder currents (study 2).
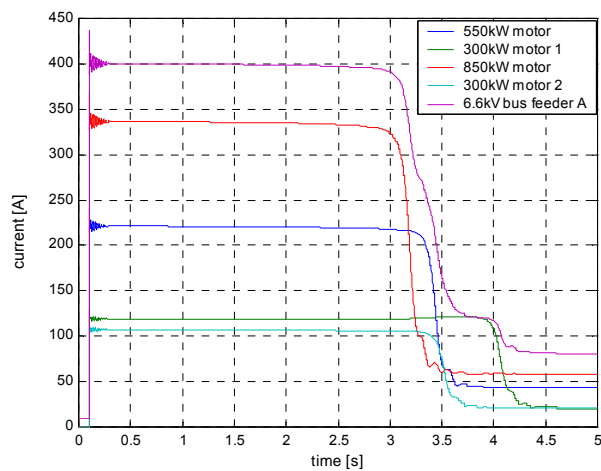
Figure 5-52 Motor and substation feeder currents (study 4).

Figure 5-51 and Figure 5-52 show that there are negligible changes to the motor and bus currents.

As for Studies 1 and 3, above, the inclusion of the generator model has not significantly affected the results obtained for system bus voltages and motor starting currents when using the *d-q* model.
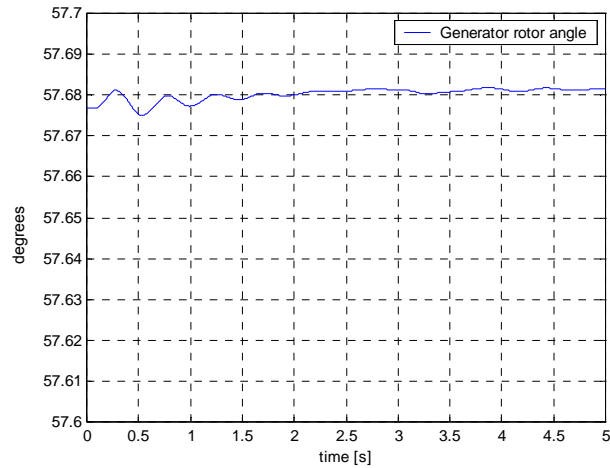
Figure 5-53 Generator rotor angle (study 4).

Generator rotor angle variations are negligible as can be seen from Figure 5-53.

For small disturbances, such as the starting of the motors which was simulated, it is acceptable to represent the generator by fixed power and reactive power injection at the generator bus. In studies 3 and 4, the generator was modelled with fixed mechanical power input and excitation, which gives a pessimistic estimate of rotor angle variations. In practice the disturbances to the generator caused by the motors starting would be expected to be negligible as predicted by the model.

5.5.4 Study 1, 5 and 7: effect of generator model with AVR and governor when abc motor model is used

Study	Description	System Conditions
1	Simultaneous DOL start of four 6.6kV motors: 24PC101 – 300kW, 24PC104 – 300kW, 24KC101 – 550kW, 24PC102 – 800kW abc model used	Generator not modelled. Generator bus = load bus with P = 56MW, Q = 41MVAr. No system disturbances
5	Simultaneous DOL start of four 6.6kV motors: 24PC101 – 300kW, 24PC104 – 300kW, 24KC101 – 550kW, 24PC102 – 800kW abc model used	Generator modelled with AVR and governor enabled. Initial mech. power, P = 56MW
7	Simultaneous DOL start of four 6.6kV motors: 24PC101 – 300kW, 24PC104 – 300kW, 24KC101 – 550kW, 24PC102 – 800kW abc model used	Generator modelled with AVR enabled and constant mech power input. Initial mech. power, P = 56MW

Comparing Figure 5-54, Figure 5-55 and Figure 5-56 shows that the inclusion of the generator model with governor/AVR models has had a negligible effect on the calculated system bus voltages. The motor currents also remained unchanged. This can be seen by referring to Appendix H. The motor and bus current plots are omitted here for brevity.
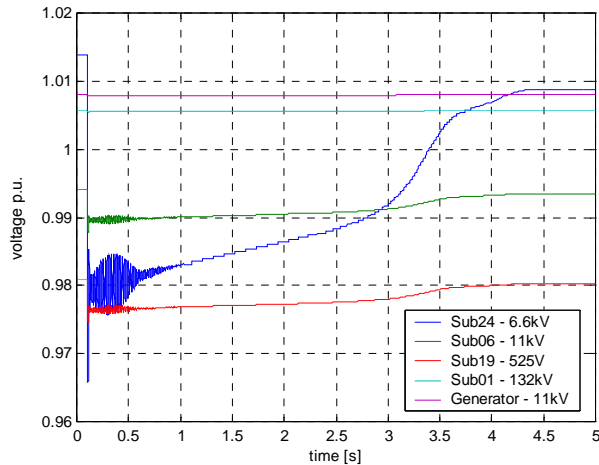
Figure 5-54 Distribution system bus voltages (study 1).
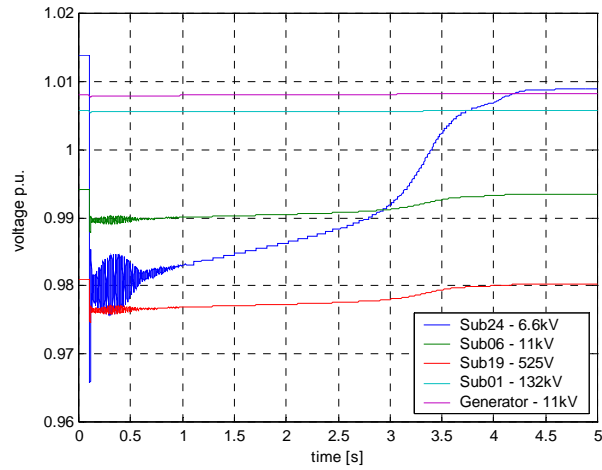
Figure 5-55 Distribution system bus voltages (study 5).
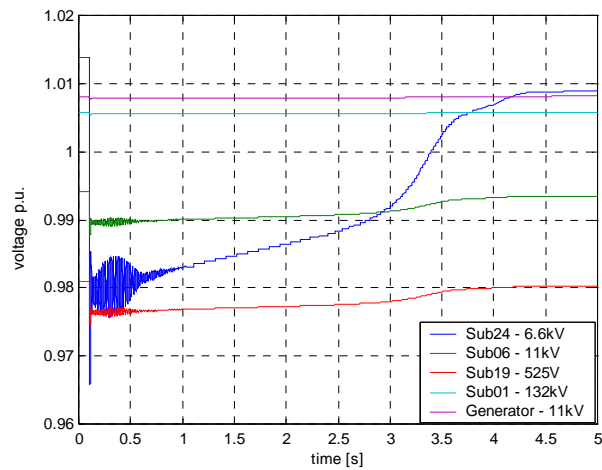
Figure 5-56 Distribution system bus voltages (study 7).

The above results show that again the inclusion of the generator model has negligible effect on the results obtained for the motor startup simulation. Modelling of the generator, AVR and governor did not have any significant effect on the results obtained.

5.5.5 Study 2 and 6: effect of generator model with AVR and governor when d-q motor model is used

Study	Description	System Conditions
2	Simultaneous DOL start of four 6.6kV motors: 24PC101 – 300kW, 24PC104 – 300kW, 24KC101 – 550kW, 24PC102 – 800kW d-q model used	Generator not modelled. Generator bus = load bus with P = 56MW, Q = 41MVAr.
6	Simultaneous DOL start of four 6.6kV motors: 24PC101 – 300kW, 24PC104 – 300kW, 24KC101 – 550kW, 24PC102 – 800kW d-q model used	Generator modelled with AVR enabled and constant mech power input. Initial mech. power, P = 56MW.

Comparing Figure 5-57 and Figure 5-58 shows that the inclusion of the generator dynamic model has a negligible effect on calculated system bus voltages when the *d-q* induction motor model is used. The motor and bus currents also remain unaffected. This can be seen by referring to Appendix H. The motor and bus current plots are omitted here for brevity.
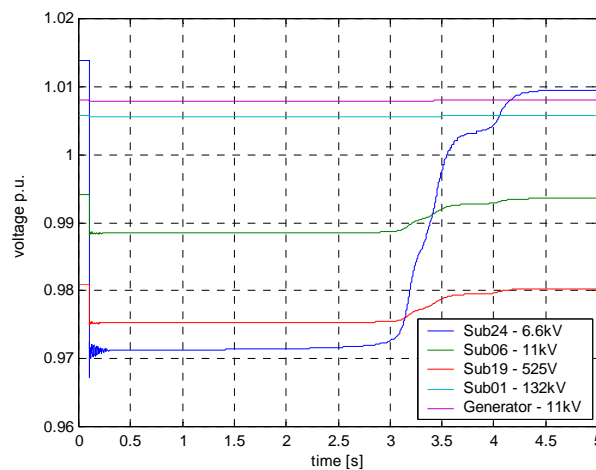
Figure 5-57 Distribution system bus voltages (study 2).
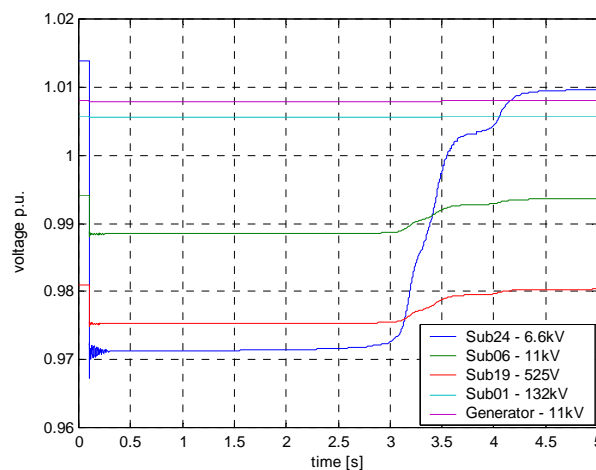
Figure 5-58 Distribution system bus voltages (study 6).

The above results confirm that inclusion of the generator model has a negligible effect on the motor starting simulation when the *d-q* induction motor model is used. For small

disturbances, such as the starting of the motors, the generator may be represented by fixed power and reactive power injection at the generator bus.

5.5.6 Comments on generator model performance.

The generator model incorporates an AVR and an approximate governor model. The governor model will adjust mechanical input power if the generator speed deviates from synchronous speed. Power will be increased or decreased as appropriate to return the machine to synchronous speed.

The AVR will increase excitation in response to a voltage drop on the generator terminals. It was found that the AVR initially increases excitation to compensate for the slight voltage drop due to the motors starting. As the motors start, and bus voltages return to normal (at approx. t = 3.5s), the generator bus voltage is slightly above set point due to the increased excitation. The AVR then starts reducing excitation to return the bus voltage to set point. This behaviour can be seen in Figure 5-59 and Figure 5-60 where the field voltage suddenly decreases after approx. 3.25s.
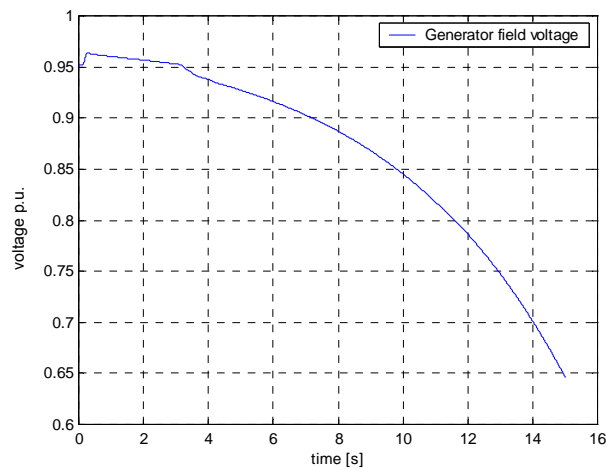
Figure 5-59 Generator field voltage – extended time (study 6).
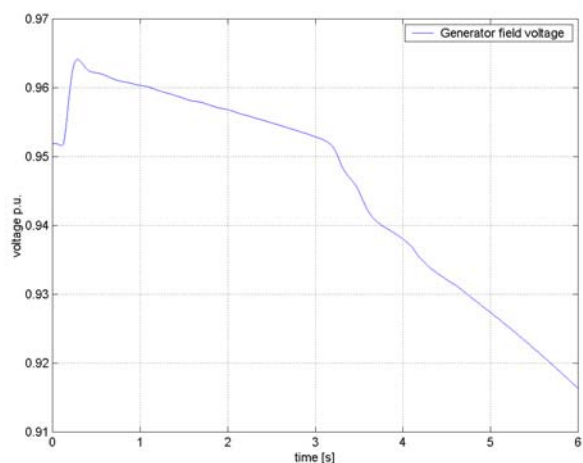
Figure 5-60 Generator field voltage - detail (study 6).
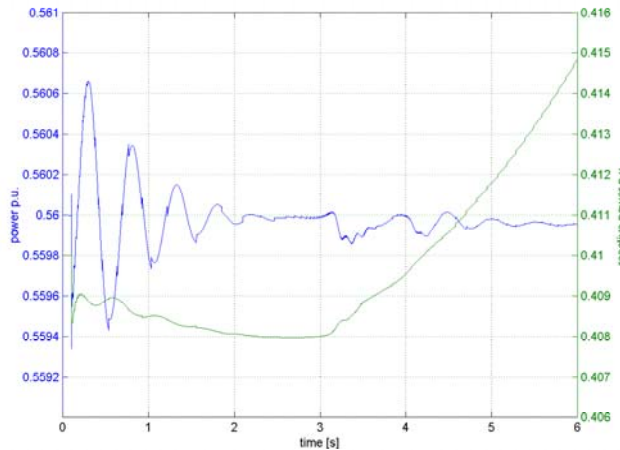
Figure 5-61 Generator power and reactive power (study 6)

From Figure 5-61 a steady increase in reactive power output caused by the reduction in field voltage can be seen. This implies that the generator is running under-excited in this study and not generating reactive power, but absorbing reactive power from the system. As the field current is decreased, the generator absorbs more reactive power from the system. This is incorrect, since this generator should supply reactive power to the PetroSA system. Under these conditions, the reduction in field voltage and increase in reactive power consumption should result in the generator terminal voltage reducing to the set value. The AVR should then settle to a new steady-state. From Figure 5-60 and Figure 5-61 it can be seen that the AVR does not do this but continues reducing excitation.

The generator model response is clearly incorrect.

The initial reduction in rotor angle seen in Figure 5-62 is caused by increased load on the generator due to the motors starting.
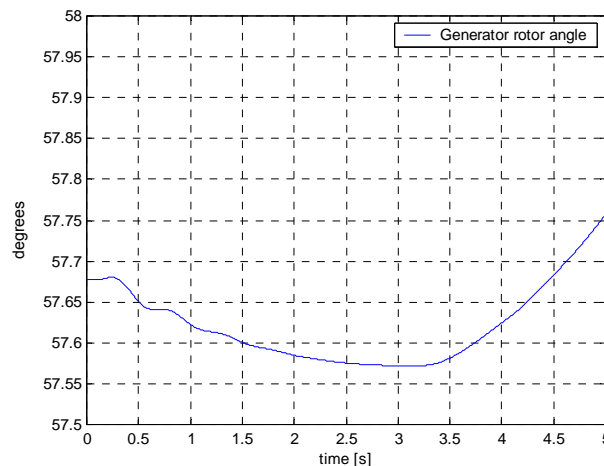
Figure 5-62 Generator rotor angle (study 6).

At about 3.5 seconds, when the motors have started, the rotor angle starts increasing. This is due to the reduction in field voltage caused by the AVR response. As field voltage is reduced, the electrical power output of the generator reduces. The rotor angle will then keep increasing, because the fixed mechanical power input exceeds the electrical power output. Due to the incorrect model behaviour described above, the system will not settle to a new equilibrium position.

5.5.7 Study 8 and 9: comparison of d-q and abc motor model performance following a 20% voltage dip

Study	Description	System Conditions
8	Examine effect of 20%, 100ms voltage dip on Eskom supply. Motor initial conditions from Study case 6 final state. All 6.6kV motors remain online. d-q model used	Generator modelled with AVR enabled and constant mech power input. Initial mech. power, P = 56MW. No other system changes
9	Examine effect of 20%, 100ms voltage dip on Eskom supply. Motor initial conditions from Study case 7 final state. All 6.6kV motors remain online. abc model used	Generator modelled with AVR enabled and constant mech power input. Initial mech. power, P = 56MW. No other system changes

Although the previous studies showed that the generator model can be omitted for relatively small disturbances such as the starting of a few motors, the behaviour for larger disturbances needs to be determined. A system-wide volt drop was considered a large disturbance. The AVR model is based on manufacturer's parameters and should be relatively accurate, while the governor model is based on assumed parameters. It is more important to investigate the generator electrical transients rather than the mechanical transients. The generator was therefore modelled with constant power input and variable excitation. The substation bus voltage drops as predicted by the *d-q* and *abc* models are relatively consistent, apart form the *d-q* model not predicting the rapid transient voltage fluctuations as discussed earlier. This can be seen by comparing Figure 5-63 and Figure 5-64
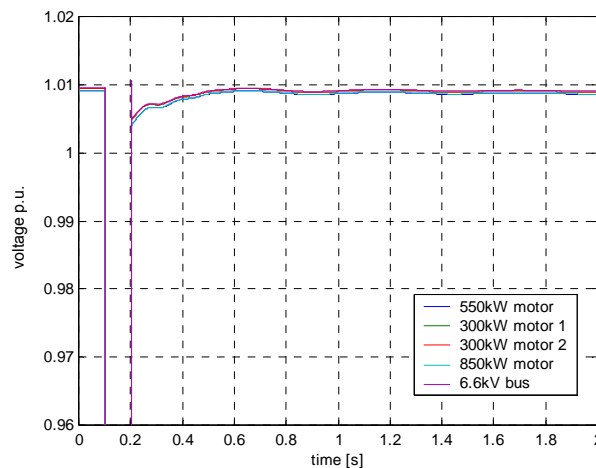
Figure 5-63 Motor terminal and bus voltages (study 8).
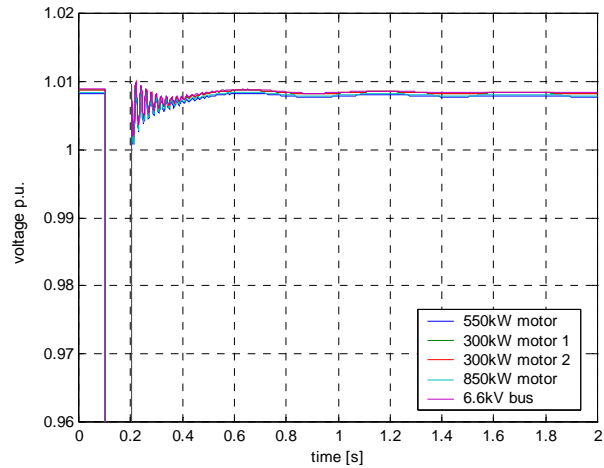
Figure 5-64 Motor terminal and bus voltages (study 9).

From Figure 5-65 and Figure 5-66 it can be seen that the generator rotor angle fluctuations resulting from the voltage dip remain the same, irrespective of the motor model being used. Rotor angle variation in the model is mainly caused by the simulated voltage dip. The re-starting of the motors does not significantly affect the generator as was seen in studies 3 and 4 where generator rotor angle variations were negligible. These variations will not be negligible if the model is extended to represent more of the system with additional motor models being added. It would not be possible to neglect the generator and the problems identified with the generator model in section 5.5.6 would have to be corrected.
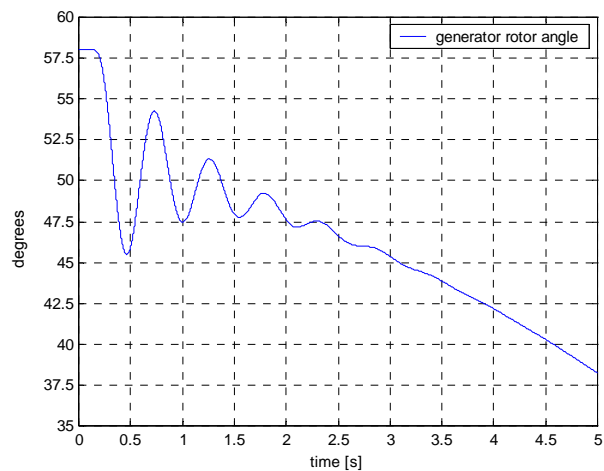
Figure 5-65 Generator rotor angle (study 8).
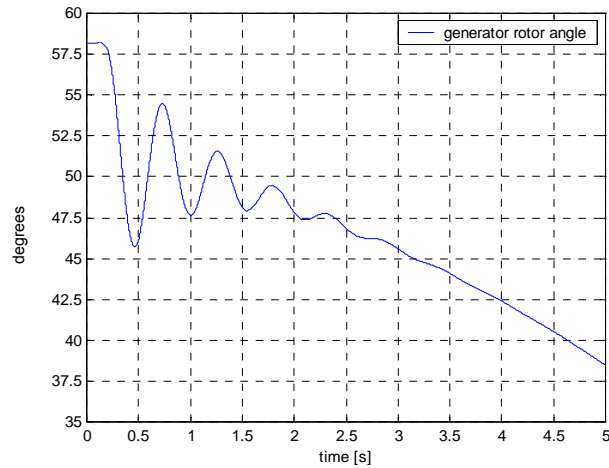
Figure 5-66 Generator rotor angle (study 9).

The response of the generator rotor angle shows the characteristics of a generator becoming unstable due to a lack of synchronising torque. This is due to the generator being strongly under-excited at the beginning of the simulation as discussed in section 5.5.6. Due to the under-excitation, the rotor magnetic field is weak resulting in the rotor drifting out of step with the synchronously rotating stator field.
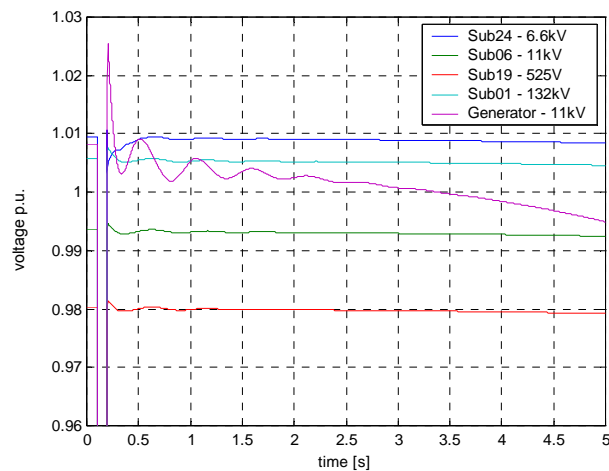
Figure 5-67 Distribution system bus voltages (study 8).
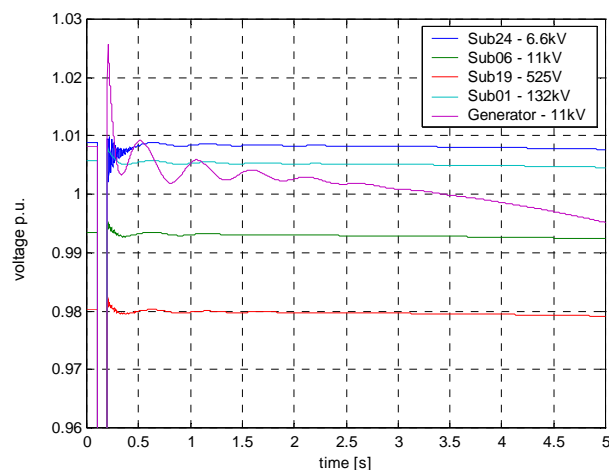
Figure 5-68 Distribution system bus voltages (study 9).

Following the voltage dip, the AVR continues to increase excitation. As the excitation is increased, the generator bus voltage should increase. Figure 5-67 and Figure 5-68 show the generator voltage decreasing which is incorrect. This error needs to be investigated with the most probable cause being incorrect sign conventions for reactive power between the generator dynamic model and the loadflow calculation. As the excitation is increased, the power output increases and reactive power output decreases as can be seen in Figure 5-69 and Figure 5-70. This indicates that the generator is absorbing reactive power and that the reactive power being absorbed is decreasing. As for study 6 discussed in section 5.5.6 above, the generator is running underexcited and the model is behaviour is clearly incorrect..
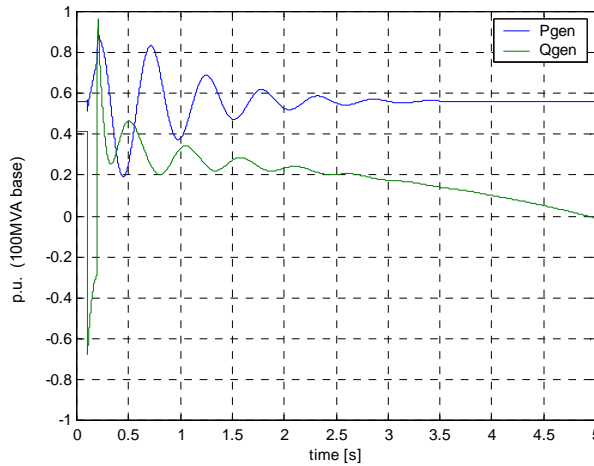
Figure 5-69 Generator power and reactive power output (study8).
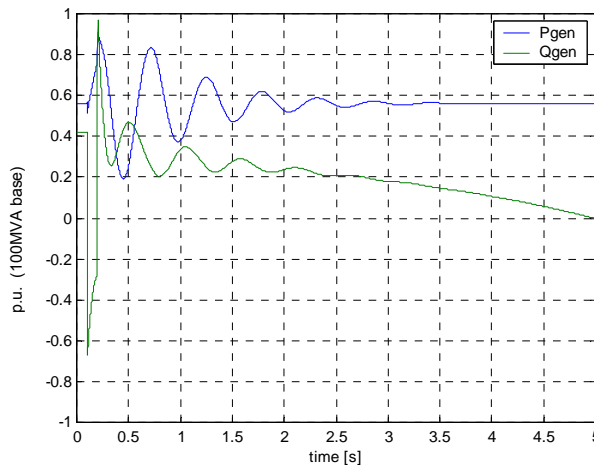
Figure 5-70 Generator power and reactive power output (study 9).

During the voltage dip, the reactive power absorbed by the generator becomes negative. The generator is in fact supplying reactive power to the system at this time. During the dip, the generator which was running underexcited, suddenly becomes overexcited resulting in the observed change in reactive power.

The problems with the generator model could be caused by one or more of the following:

- Incorrect steady state initialisation of the model
- Incorrect or unrealistic initial operating conditions

- The sign conventions used for reactive power at the generator terminals between the generator dynamic model and the load flow calculation are incorrect

There is a slight voltage fluctuation observed throughout the system, due to the generator rotor oscillation following the voltage dip, but this does not significantly affect the motor behaviour. This rotor oscillation results from incorrect generator model response and no definite conclusions regarding the behaviour of the system can be made on the basis of these results.

Comparison of the results obtained using the *abc* and *d-q* models shows that the *d-q* model gives an acceptably accurate simulation of system bus voltages. From Figure 5-71 and Figure 5-72 the absence of fast transient currents in the *d-q* model solution can be seen when compared to the *abc* model. Accurate simulation of bus voltage behaviour is more important since this will give an indication of whether motors will successfully re-start following a disturbance. The *d-q* model is able to give a reasonably accurate estimate of bus voltage behaviour.
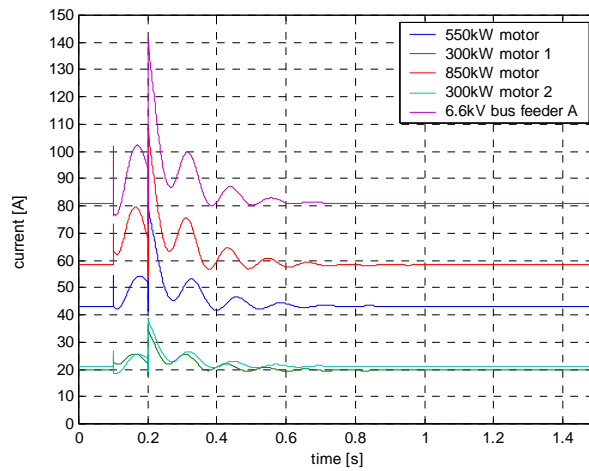
Figure 5-71 Motor and substation feeder currents (study 8).
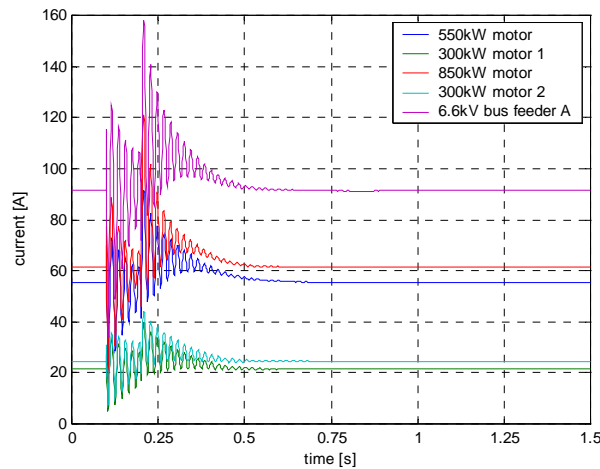
Figure 5-72 Motor and substation feeder currents (study 9).

As discussed previously, both models have problems which need to be resolved before further more detailed work is attempted. The *d-q* model produces low frequency stator current oscillations caused by mechanical oscillations of the rotor following a disturbance. This is due to the difference in torque speed characteristics between the models and the lower inertia constants used with the *d-q* model. The *abc* model appears to give an reasonable indication peak stator current and torque amplitudes which could be expected in practice. These transients take too long to decay though. These problems need to be resolved by extending this model to include saturation, correct parameter estimation and benchmarking of the model against known accurate results.

5.5.8 Study 8 and 10: effect of main plant air compressor trip following voltage dip.

Study	Description	System Conditions
8	Examine effect of 20%, 100ms voltage dip on Eskom supply. Motor initial conditions from Study case 6 final state. All 6.6kV motors remain online. d-q model used	Generator modelled with AVR enabled and constant mech power input. Initial mech. power, P = 56MW. No other system changes
10	Examine effect of 20%, 100ms voltage dip on Eskom supply. Motor initial conditions from Study case 6 final state. All 6.6kV motors remain online. d-q model used	Generator modelled with AVR enabled and constant mech power input. Initial mech. power, P = 56MW. Two 26MW compressors at air separation plant tripped 80ms after start of voltage dip

The two main plant air compressors are synchronous machines and are used to assist with the generation of reactive power. If these machines trip there is a loss of about 38MVAr, but this is offset to some extent by a load reduction of about 52MW on the PetroSA distribution system. This load reduction is due to the two plant air compressors themselves tripping. As can be seen by comparing Figure 5-73 and Figure 5-74, there is a slight reduction in bus voltages following the loss of the two plant air compressors.
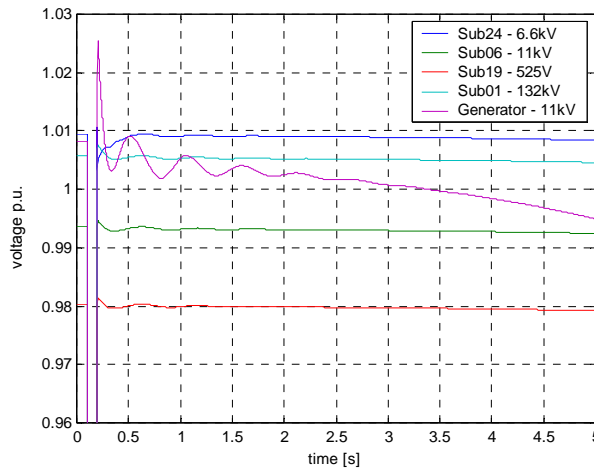
Figure 5-73 Distribution system bus voltages (study 8).
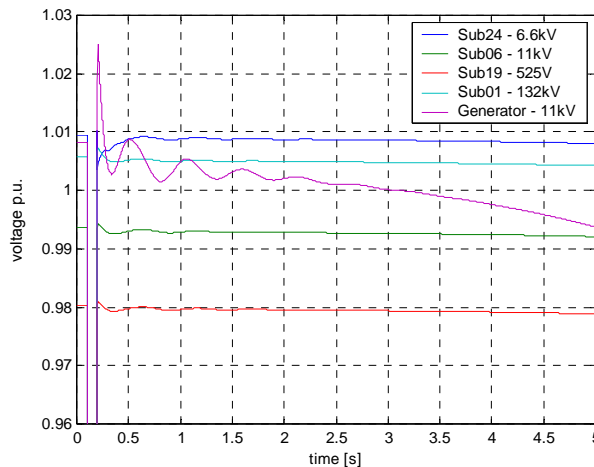
Figure 5-74 Distribution system bus voltages (study 10).

Comparing Figure 5-75 and Figure 5-76 shows that the effect on the motor and substation feeder currents is negligible.
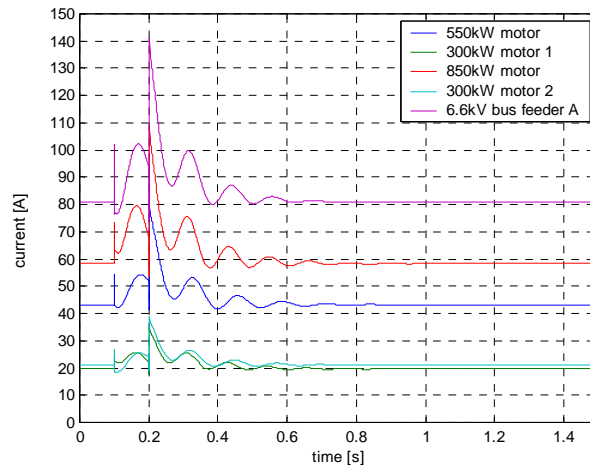
Figure 5-75 Motor and substation feeder currents (study 8).
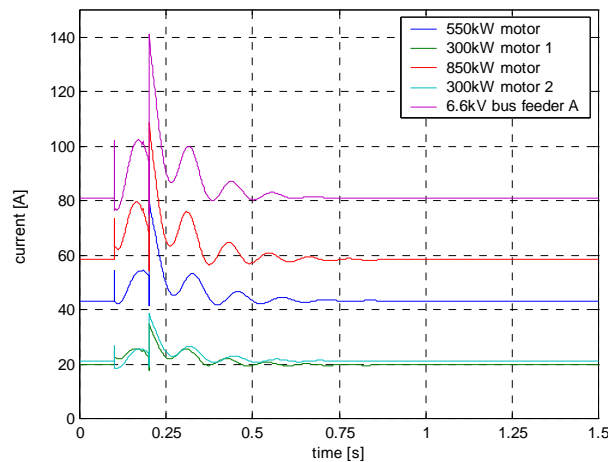
Figure 5-76 Motor and substation feeder currents (study 10).

Comparison of results shows that modelling the tripping of the two main 26MW air separation compressors following a voltage dip has a negligible effect on the results obtained.

It is not possible to determine the generator impact on the system following large disturbances. The rotor angle is continually decreasing in all cases due to incorrect behaviour of the generator model. The electrical transients due to rotor oscillation are possibly exaggerated due to the drifting instability described earlier, particularly in the first 2 seconds after the voltage dip. It is reasonable to expect that the rotor angle deviations would be less severe if the generator is not under-excited and thus the voltage fluctuations observed on the generator busbar would be reduced. This comment is speculative however, since the problems with the generator model will need to be addressed before studies can be performed allowing the generator response following a voltage dip to be examined.

The effect of the generator is once again minimal as far as the simulation of motor performance is concerned. The generator model can therefore be omitted and replaced with fixed power and reactive power injection on the generator bus. This would however not be possible if the scope of the simulation is extended to include a large portion of the installed induction motors.

5.5.9 Study 11: motor re-acceleration following a voltage dip

Study	Description	System Conditions
11	Examine effect of 20%, 100ms voltage dip on Eskom supply. Motor initial conditions from Study case 7 final state. All 6.6kV motors trip and re-start sequentially. abc model used	Generator not modelled. Generator bus = load bus with P = 56MW, Q = 41MVAr. Two 26MW compressors at air separation plant tripped 80ms after start of voltage dip

The sequential re-acceleration of motors following a voltage dip is simulated. The motors were re-started in the following sequence during the simulation:

- one 550kW 6.6kV motor – 2 seconds after voltage recovery.

- two 300kW 6.6kV motors – 4 seconds after voltage recovery.

- one 850kW 6.6kV motor – 6 seconds after voltage recovery.

These motors are shown in Figure 3-8. Note that only the motors on the 'A' busbar are assumed to be re-accelerating. This is due to only the 'A' or 'B' motor being in service at any given time. The re-acceleration times shown in Figure 3-8 are the times as set in the plant. This study has only considered motors starting at 2 second intervals. In reality motors are re-started at 3 second intervals with some being re-started after 12 – 15 seconds. This was not simulated, since it would amount to a sequential re-starting of motors from standstill. The startup sequence time delays were reduced for this study to investigate the effects of motor starting 'overlapping'- i.e. the next motor starting while the predecessor is still busy accelerating.

When Figure 5-78 is compared to study 1 (Figure 5-77) it can be seen that motor currents during re-acceleration are almost the same as DOL starting currents, particularly in the motors starting later in the sequence.
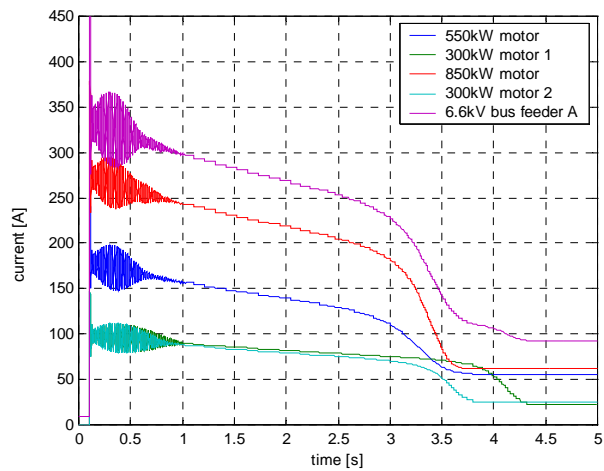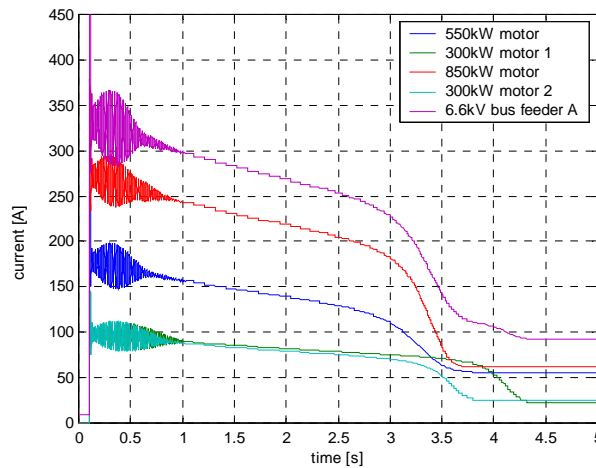

Figure 5-77 Motor and substation feeder currents (Study 1).
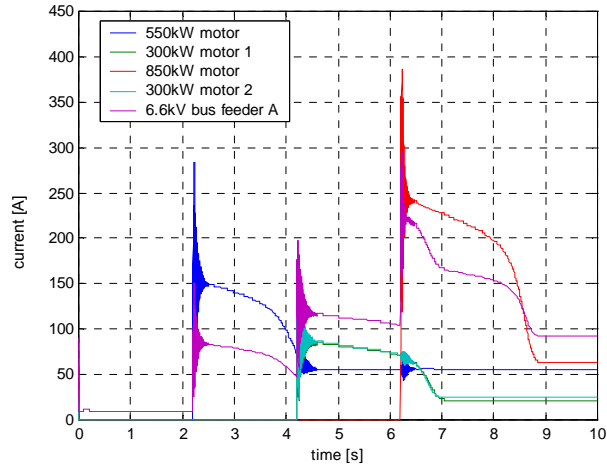
Figure 5-78 Motor and substation feeder currents (Study 11).

From Figure 5-78 and Figure 5-79 it can be seen that the 300kW motors are unaffected by the 850kW motor starting. It can also be seen that the motors which are starting, cause slight current (and torque) transients on the running motors.
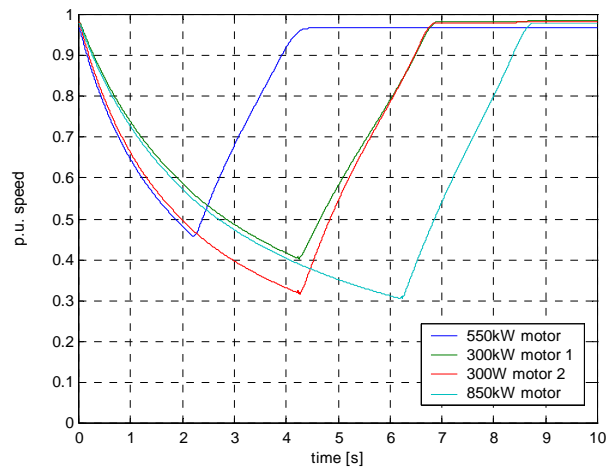
Figure 5-79 Motor shaft speeds (study 11).

Figure 5-80 shows that the system bus voltage drops are less severe than those resulting from a simultaneous start of all four motors as shown in Figure 5-41. This is in agreement with what is intuitively expected.
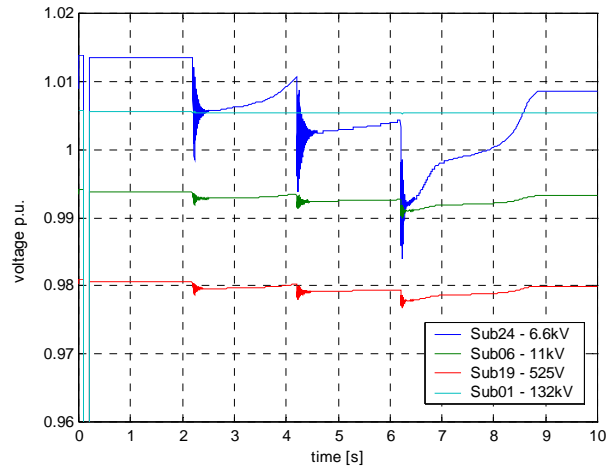
Figure 5-80 Distribution system bus voltages (study 11).

It would be possible to carry out various simulations of sequential re-starting of motors using different time delays, but the results would vary between a simultaneous re-start of all four motors and starting up of motors sequentially with one motor only starting after the predecessor as finished starting. This last case would be a variation of studies 1 and 2 with less severe starting conditions since only one motor is starting at a time instead of four. The simultaneous re-start of all four motors is investigated in study 12**.**

5.5.10 Study 12: effect of all motors re starting after a voltage dip

Study	Description	System Conditions
12	Examine effect of 20%, 100ms voltage dip on Eskom supply. Motor initial conditions from Study case 7 final state. All 6.6kV motors trip and re-start immediately. abc model used	Generator not modelled. Generator bus = load bus with P = 56MW, Q = 41MVAr. Two 26MW compressors at air separation plant tripped 80ms after start of voltage dip

Disconnecting all four motors and re-starting immediately after the voltage dip leads to higher transient current, when compared to a sequential re-start. This can be seen by comparing Figure 5-81 and Figure 5-82.
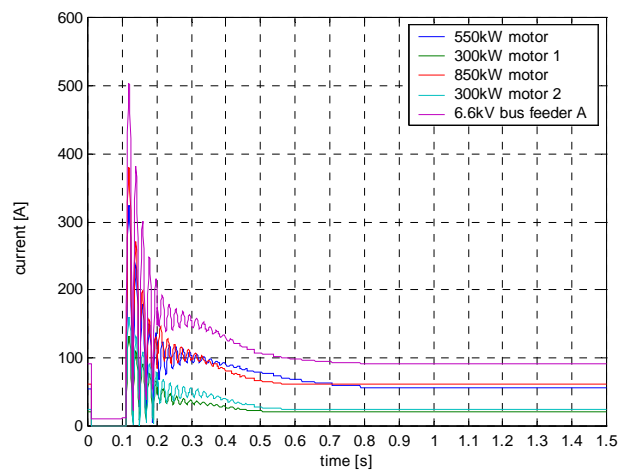
Figure 5-81 Motor and substation feeder currents (study 12).
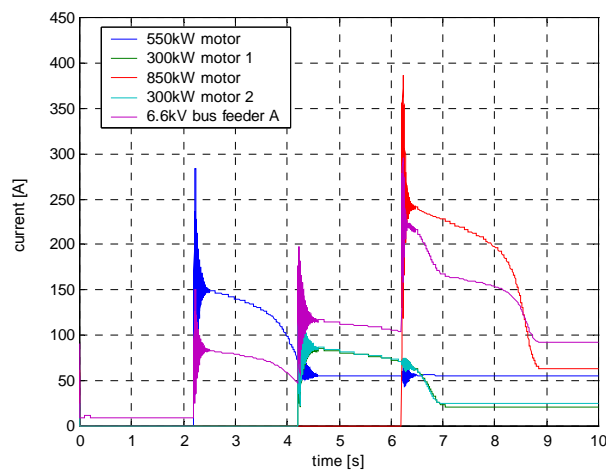
Figure 5-82 Motor and substation feeder currents (study 11).

Comparing Figure 5-83 and Figure 5-84 shows that the duration of the disturbance is much shorter following the voltage dip and the bus voltage drop is less than for a sequential re-start.
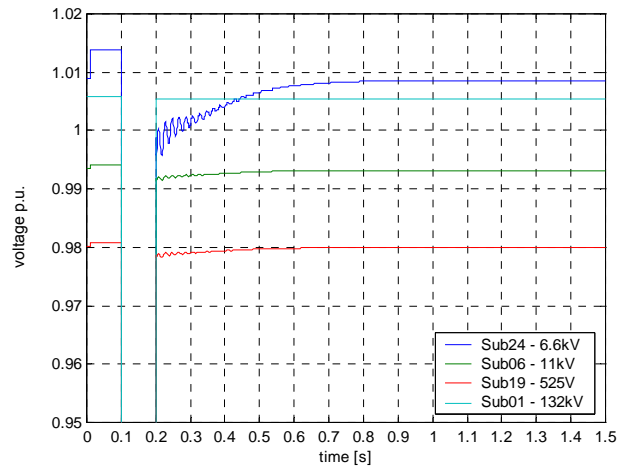
Figure 5-83 Distribution system bus voltages (study 12).
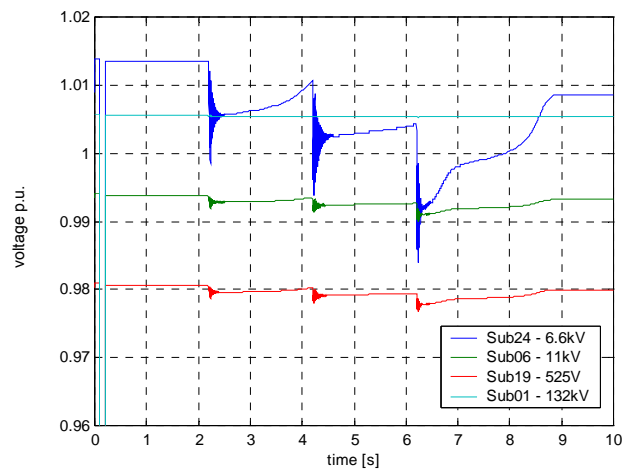
Figure 5-84 Distribution system bus voltages (study 11).

6 CONCLUSIONS AND RECOMMENDATIONS

The transient behaviour of the PetroSA electrical distribution system and associated loads was investigated. The majority of the motors installed at PetroSA are equipped with a re-acceleration system which disconnects them from the supply when a voltage dip takes place and re-connects them to the supply a short time later. The design intent is to sequentially re-start motors following a voltage dip, whilst reducing the impact on the distribution system. This research was prompted by the following considerations:

- Optimizing the performance of the re-acceleration system does not require any capital investment or equipment modifications.

- Although the system performance is satisfactory at present, continued expansion in the Mossel Bay area will lead to increasing demands on the Eskom supply and an inevitable deterioration in quality of supply[11]. This could lead to plant outages which may be prevented by a timely review and optimization of the re-acceleration system performance.

- Before physical changes are implemented, detailed transient studies may need to be carried out. This work will require a significant financial outlay and effort in terms of manpower. An initial investigation is required to determine if this is justified. The initial investigation might also identify some improvements which can be implemented before detailed simulation studies are carried out.

The topics to be investigated were initially defined as:

1. Re-acceleration system optimization

2. Faults due to Veldt Fires

3. Software development

Each topic is discussed below and the results obtained are reviewed.

6.1 Re-acceleration System Optimization

Optimization of the re-acceleration system requires an investigation of the transient behaviour of the PetroSA distribution system during the re-acceleration sequence as well as investigating the effects on individual motors and loads. A review of transient stability studies carried out during the design of the plant confirmed that the performance of the re-acceleration system had never been investigated.

The initial investigation of the system performance required the development of transient stability analysis software with appropriate dynamic and static equipment models.

6.1.1 Induction motor models

Investigation of motor behaviour required dynamic induction motor models. A detailed model was developed and performance compared to a relatively simple induction motor model that is widely used in commercial transient analysis software.

The main problems encountered were a lack of data on the motors to be modelled and uncertainties about the motor operating conditions following a voltage dip. Although detailed data was available for some machines, it was decided to try to estimate motor parameters based on nameplate data. The estimation of motor parameters needs to be improved before

---

[11] The Quality of Supply at PetroSA's main substation is currently significantly better than that stipulated by the NER.

further studies are carried out. More accurate parameter estimation schemes can be implemented [25]. A relatively simple scheme was adopted to limit the scope of work. It was reasonably easy to establish some simple rules of thumb for adjusting the values of the calculated parameters for use with the two induction motor models. Parameter estimates appeared more realistic for the 300kW motors than for the 800kW motor. This observation might be due to the characteristics of the particular motors chosen for the tests and no general conclusions can be made. The use of an elaborate model such as the *abc* model is not justified if the model parameters are not accurate. The model should also be extended to include saturation. It was relatively easy to adjust the *abc* model parameters to closely match the characteristics of the actual machine by trial and error. This approach was not used though, and all simulations were carried out using the parameters as calculated.

Both induction machine modes tended to give starting currents that were lower than the measured currents. This was attributable to the approximate parameters used. Saturation was initially modeled but omitted to limit the scope of work and due to a lack of motor data. Based on the results of the various simulations, the following is suggested:

The *abc* model is recommended for investigating individual machine performance. Transients are more realistically simulated. An improvement in parameter estimation as well as modelling of saturation is necessary. The models need to be benchmarked against known results to establish their validity. The *abc* model is capable of giving very accurate results [22, 33] if these shortcomings are addressed. The use of this model is recommended when the performance or interaction of individual machines is being investigated.

The *d-q* model gives results which are accurate enough for investigating overall system behaviour, particularly when the behaviour of individual machines is less important. The *d-q* model behaviour differed significantly from the *abc* model during transient conditions due to the difference in torque speed characteristics and inertia parameters which had to be used. When using approximate motor models, results obtained should be carefully evaluated before interpretation.

As discussed earlier, the exact loading on motors following a voltage dip cannot be determined. Two arbitrary sets of model parameters were chosen to represent what was believed to be typical motor loads following a voltage dip. Although the chosen parameters resulted in the simulated motors (particularly the *abc* model) drawing less current than the actual motors, the scale of the simulation was such that voltage collapse phenomena and system instability would not be observed considering the relatively minor disturbance imposed by the simulated motors starting.

6.1.2 Synchronous generator model

A relatively simple generator model was implemented.It was found that the literature devotes a lot of attention to in depth analysis of synchronous machines from the electrical point of view and little, if any attention is paid to generator controls. Authors tend to oversimplify the modelling of generator controls [21, 23, 32, 22]. The generator model performance was unsatisfactory, exhibiting unstable operation. The most probable causes of the problems being incorrect initialization of the model, incorrect sign conventions for reactive power between the generator model and the loadflow calculation or unrealistic initial operating conditions. The problems with the generator model need to be addressed as part of any future work that may be carried out.

During simulations, it was found that motor behaviour during transients is not significantly affected by the generator. This was mainly due to the limited scale of the simulation, resulting in relatively small system perturbations. It was found that the generator could be adequately represented by active and reactive power injection on the generator bus.

6.1.3 PetroSA distribution system model

In deriving a suitable model of the electrical distribution system, it was possible to immediately exclude a significant amount of equipment from the model based on an evaluation of the system operation and response to transient conditions. The critical power system and generator could easily be eliminated, as well as the seven largest motors on site. A secondary substation and associated motors were chosen for detailed modelling with the remainder of the system represented by lumped equivalent loads. A constant impedance load model was chosen rather than a constant power load model based on the considerations discussed in sections 2.6.3 and 3.3. The major error attributable to the distribution system modelling identified by comparing simulated results with test results was the underestimation of bus voltage drops.

Measured bus voltage drops were greater than simulated. This can be attributed to one, or both of the following: Feeder cable impedances were underestimated and secondly the representation of the Eskom supply can be improved. Feeder data was obtained from the loadflow and fault calculation software database in use at PetroSA. Transformer impedances should be accurate, having been obtained from vendor specifications.

The system model is far too simple and limited in scope to provide anything more than an indication of voltage drops and current distributions during the transient conditions that were simulated. A far more extensive and accurate model will be required to properly investigate the behaviour of the entire system under transient conditions.

6.1.4 Optimization of re-acceleration system

Based on simulation results, it was established that the re-acceleration system introduces unnecessary transients. Most power dips are of approximately 100ms duration with about a 20% volt drop. Simply leaving induction motors connected to the supply during such a dip results in lower system disturbances, than disconnecting motors from the supply and re-starting in sequence. The undervoltage relays can be set to 30% instead of the current 20%. No further studies are required to ensure that this is feasible. The current and voltage transients will be less than with the existing settings. In addition, motor speed fluctuations, and hence the risk of process upsets are reduced.

As a further action, the load distribution due to the re-acceleration system was examined. The total load being re-connected to the distribution system by the re-acceleration system was calculated by adding up the re-acceleration loads for each substation as given in Appendix A. These results are shown in Table 6-1 with all values in kW.

Table 6-1 Overall re-acceleration loads

SUB	0 sec	3 sec	6 sec	9 sec	Other	Static
02	208	532.5	0	0	0	1012.7
03	0	0	0	0	0	666.65
04	1346.54	12682.74	5338.61	7404.14	7214	2404
05	331	7656.8	340.6	0	11412	2265.23
06	20.2	5338	4424	0	0	1089.2
10	326	8124	4650	3350	8000	739.65
11	30	974	233.04	0	0	208
13	80.418	290	222	0	0	764.5
14	479.77	1630	1391	1018	0	779.9
15	270.94	612	149	148	0	1283
17	0	0	0	0	0	275.74
18	0	0	0	0	0	506.84
19	0	5.14	0	0	0	261
20	150	511	410.5	723.5	0	883.25
23	9	1600	1212.4	1443	0	3756.9
24	1.1	762.7	1069	0	0	691.27
25	0	0	0	0	0	34
48	121.74	103.25	383.8	441	0	347.41
Totals [kW]	3374.708	40822.13	19823.95	14527.64	26626	17969.24

The figures in Table 6-1 are based on the total connected load. Almost all motors at PetroSA are spared. Thus, at any given time only half of the motors are running. There are a number of installations where three or four motors are installed with one always being idle. Taking this into account along with the fact that motors are not running at maximum rated load allows the above loads to be estimated at approximately half the calculated value.

It can therefore be seen that the largest load being connected is approximately 20MW at 3 seconds followed by 10MW at 6 seconds. Changing re-acceleration times will allow re-connection of a load of about 10MW every 3 seconds which will reduce the maximum load being started simultaneously by about half.

6.1.5 Recommendations for future work

The review carried out on the transient stability studies performed during the design of the plant, showed that typical parameters were used in most cases and the system layout greatly simplified with lumped equivalent load models being used. In addition, the loading of the Eskom system supplying power to PetroSA has changed significantly. At present, plant operation is stable with minimal outages attributable to electrical disturbances. Detailed transient stability studies would be justified if:

1. Any major plant expansion takes place. The electrical system was designed with spare capacity. The point has been reached where this has all been utilised for minor modifications and additions to the plant. Any significant expansion will require the construction of a new substation.

2. The proposed Peak power Generation Station is constructed adjacent to PetroSA.

3. The quality of supply deteriorates significantly from what is currently being received.

6.2 Faults Due To Veldt Fires

This topic was prompted by the assumption that the re-acceleration system significantly reduces the impact of re-starting motors following a voltage dip, as opposed to re-starting from standstill. The concern was that repeated voltage dips, due to veldt fires would re-start the re-acceleration sequence and that motor speeds would reduce, resulting in essentially re-starting motors from standstill. An induction motor will draw a high starting current until the rotor speed is above about 80-90% of rated speed. Initial investigations into the operation of the system showed that due to motor loads remaining unchanged following a voltage dip, the motors would decelerate fairly rapidly. The first motors are only re-started after three seconds. At that stage the rotor speed has reduced significantly resulting in the motor drawing currents close to that required for a startup from standstill. The motors being re-started after 6s, 9s and longer delays can be considered as starting from standstill and drawing full starting current. Re-starting the re-acceleration sequence does not therefore result in a significantly greater demands on the system. This topic did not merit further investigation.

6.3 Software Development

6.3.1 Matlab

The use of Matlab greatly accelerated the software development process. The use of the built-in matrix arithmetic functions and ODE solvers permitted rapid software development, allowing time to be spent on developing the transient simulation program and the various models rather than matrix arithmetic functions and ODE solvers. If one of the other software options had been used, a great deal of additional time and effort would have been spent on writing these functions.

Since Matlab is equipped with a number of different ODE solver routines, it was easy to experiment with and investigate the performance of the different solvers. This made it relatively easy to select the ODE solver which performed the best in terms of accuracy and solution speed. It was established that the correct error tolerance parameters need to be set when using the ode solvers since the default parameters did not give accurate results in all cases. A step length of 1ms was chosen for simulations since this allowed system response to be accurately represented. When using the ode solvers alternately with the loadflow calculations, default error tolerance parameters gave correct results.

The Matlab matrix functions proved very useful for implementing both the *abc* motor model as well as the Newton-Raphson loadflow routines. Due to the relatively small size of the system, the basic Newton-Raphson method was found to be capable of giving accurate results without convergence problems. Step voltage changes of up to 40% could be simulated on the swing bus without the loadflow algorithm failing to converge. For larger voltage changes, or simulation of short circuits, it would be necessary to provide appropriate initial estimates of bus voltages and angles to ensure convergence.

6.3.2 Simulink

The Simulink environment within Matlab was found to be extremely useful for development and testing of the *d-q* motor and generator model. The AVR and governor responses could also be easily evaluated. The major advantage is the speed with which a model can be implemented and tested. The power systems block set was excluded on the basis of tests which showed that the component models were unwieldy to use. Another restriction on the

use of the power systems block set is that the model of the PetroSA distribution system, as used for simulations would be cumbersome and difficult to implement.

6.3.3 Execution times

Although the speed of software execution was not considered very important for this work, it will become a factor if the transient simulation program is extended to include more dynamic motor models. The execution times of simulations with similar time steps and time durations were compared. When using the ODE solvers to evaluate the motor models independently, simulation of a motor starting from t = 0 to 5s took about 4 seconds for the *d-q* model, compared to the *abc* model which took about 40s on average. The generator model simulation time was comparable to the *d-q* motor model

The transient simulation program was tested with four motor models and the generator model enabled. Simulation of the four motors starting at t=0 to 5s, takes about 30 minutes when using the *abc* motor model and 15 minutes when using the *d-q* model. The loadflow calculations take a major portion of this time. The use of the more complex motor model does result in increased program execution times, but additional execution times are not prohibitive.

6.4   Topics For Further Investigation

This initial investigation into the re-acceleration system has yielded useful results and immediate changes can be implemented with will significantly reduce system transients due to the action of the re-acceleration system. Although system bus voltage drops were underestimated by the simulations, the motor startup tests allowed this error to be determined. It will be necessary to review feeder data and include more detailed modelling of the Eskom system before further simulations are conducted. Underestimation of bus voltage drops could lead to overly optimistic results when motor startup simulations are carried out, particularly where system performance is marginal.

The generator model problems need to be addressed. Saturation effects, excluded to limit the scope of work, should be included. If more detailed studies are carried out, investigating the behaviour of a larger number of induction motors, the generator model will definitely need to be included.

The use of a more elaborate induction machine model is only really justified when parameters can be accurately estimated or the behaviour of individual machines needs to be determined. For investigation of distribution system transient response, the simpler *d-q* models have proven adequate, provided their inherent limitations are appreciated. The more detailed model is useful for investigating motor behaviour and the effects on the driven load under transient conditions. This model needs to be extended to include saturation effects. This would be useful for evaluating peak torques under transient conditions, particularly where mechanical failures have taken place on couplings and driven machinery. If further more detailed studies are to be attempted, models need to be benchmarked and the errors in parameter estimation addressed.

Further work on the PetroSA system will require a detailed representation of the entire system with the majority of the motors represented by dynamic models or lumped equivalent motors. The generator will have to be accurately modelled. It will only be possible to fully investigate the behaviour of the system under transient conditions if the entire system is correctly represented. The bus voltage drops under these conditions will no longer be relatively insignificant and phenomena such as motors stalling and voltage collapse can be properly investigated. In order to proceed further the use of commercially available software such as DigSilent is essential. This will also permit the behaviour of the protection systems to be modelled and incorporates sophisticated routines to estimate parameters of equipment based on 'nameplate' data.. The time and effort required to extend the system models developed for this work is not justified if the capabilities of commercial software which is the result of

considerable research and development effort[12] is considered. The models developed for this work are considered as a 'first try' at investigating system behaviour. Continuing development of these models to further investigate the PetroSA system in detail will require an investment in time and effort that is not justified.

If the problems identified with the models are corrected and saturation effects included, it will be possible to carry out further investigations using the existing models. The behaviour of the generator can be properly investigated and unresolved problems addressed. Additional dynamic motor models can be added to extend the scope of the simulation, but at some stage, the time taken to run the computer simulation will become prohibitive and further work will have to be carried out using commercially available software as suggested above.

---

[12] Commercial software packages are typically the result of tens, if not hundreds of man-years of research and development effort.

ACKNOWLEDGEMENTS

I would like to thank my wife, Lindi, for her patience and support during this project. I realise that at times it seemed as if the work would never end, and that my overly optimistic estimates of the completion date were a source of great frustration. Without her understanding, encouragement and support this project would never have been completed and is as much her achievement as mine.

I would also like to thank Prof. Ron Herman for his assistance and guidance during the initial stages of this project, but a special word of thanks goes to Dr. Johan Vermeulen for all the assistance, guidance and valuable advice he has given me during the finalisation of this work.

Andre Claassens,

February 2008.

REFERENCES

[1]   D. Bispio, L.M. Neto, J.T. de Resende and D. A. de Andrae, "A New Strategy for Induction Machine Modelling Taking into Account the Magnetic Saturation", IEEE Trans. on Industry Applications, Vol. 37, No. 6, November/December 2001, pp. 1710-1719

[2]   M.E. Baran and A.J. Goetze, "Equivalent Circuits of AC Machines Based on Field Analysis", IEEE Trans. on Power Systems, Vol. 9, No. 2, May 1994, pp. 565-571

[3]   Y. He and T.A. Lipo, "Computer Simulation of an Induction Machine With Spatially Dependent Saturation", IEEE Trans. on Power Apparatus and Systems, Vol. PAS-103, No. 4, April 1984, pp. 707-714

[4]   K.P. Kovacs, "On the Theory of Cylindrical Rotor A.C. Machines, Including Main Flux Saturation", IEEE Trans. on Power Apparatus and Systems, Vol. PAS-103, No. 4, April 1984, pp. 754-757

[5]   J.C. Moreira and T.A. Lipo, "Modelling of Saturated AC Machines Including Air Gap Flux Harmonic Components", IEEE Trans. on Industry Applications, Vol. 28, No. 2, March/April 1992, pp. 343-349

[6]   K. Czernek, W. Koczara and Z. Szulc, "Construction of Induction Motor's Mathematical Model On the Basis of its Nominal Parameters", Modelling and Simulation of Electrical Machines and Power Systems, J. Roberts and K. Tran (Editors), Elsevier Science Publishers (North-Holland), ©IMACS, 1988, pp 185-195

[7]   J. Robert, "A Simplified Method for the Study of Saturation in AC Machines", Modelling and Simulation of Electrical Machines and Power Systems, J. Roberts and K. Tran (Editors), Elsevier Science Publishers (North-Holland), ©IMACS, 1988, pp 129-136

[8]   M.S. Garrido, L. Pierrat and E. Dejaeger, "The Matrix Analysis of Saturated Electrical Machines", Modelling and Simulation of Electrical Machines and Power Systems, J. Roberts and K. Tran (Editors), Elsevier Science Publishers (North-Holland), ©IMACS, 1988, pp 137-144

[9]   J. Esteves and J. Santana, "Application of a Saturated Induction Machines Dynamic Model", Modelling and Simulation of Electrical Machines and Power Systems, J. Roberts and K. Tran (Editors), Elsevier Science Publishers (North-Holland), ©IMACS, 1988, pp 145-150

[10]   IEEE Task force on Load Representation for Dynamic Performance, "Standard Load Models for Power Flow and Dynamic Performance Simulation", IEEE Trans. on Power Systems, Vol. 10, No 3, August 1995

[11]   IEEE Task force on Load Representation for Dynamic Performance, "Load Representation For Dynamic Performance Analysis", IEEE Trans. on Power Systems, Vol. 8, No. 2, May 1993

[12]   L. M. Hajagos and B. Danai, "Laboratory Measurements and Models of Modern Loads and Their Effect on Voltage Stability Studies", IEEE Trans. on Power Systems, Vol. 13, No. 2, May 1998

[13]   C.D. Vournas and G.A. Manos, "Modelling of Stalling Motors During Voltage Stability Studies", IEEE Trans. on Power Systems, Vol. 13, No. 3, August 1998

[14]   M.G. Say, "Alternating Current Machines", 5th Ed., Longman Scientific & Technical, 1983

[15]   A.E. Fitzgerald, C. Kingsley and A. Kusko, "Electric Machinery". 3rd Ed., McGraw-Hill, 1971

[16]   R.E. Steven, "Electrical Machines and Power Electronics", 1st Ed., Van Nostrand Reinhold (UK) Co. Ltd, 1983

[17]   L. S. Bobrow, "Elementary Linear Circuit Analysis", 1st Ed., Holt-Saunders Japan, Ltd, 1981

[18]   J.D. Kraus, "Electromagnetics", 3rd Ed., McGraw-Hill, 1985

[19]   A.E. Guile and W. Paterson, "Electrical Power Systems, Vol. 1 and 2", 2nd Ed., Pergamon Press, 1986

[20]   C.F. Gerald and P.O. Wheatley, "Applied Numerical Analysis", 6th Ed., Addison-Wesley, 1999

[21]   J. Arrilaga and C.P. Arnold, "Computer Analysis of Power Systems", 1st Ed., John Wiley and Sons Ltd. England., 1990

[22]   J.R. Smith and M. Chen, "Three Phase Electrical Machine Systems Computer Simulation", 1st Ed., Research Studies Press Ltd. John Wiley and Sons Ltd., 1990

[23]   M. Pavella and P.G. Murthy, "Transient Stability of Power Systems: Theory and Practice", 1st Ed., John Wiley & Sons Ltd. England, 1994

[24]   P. Vas, "Vector Control of AC Machines", Oxford University Press, Oxford, 1990

[25]   R. Babau and I. Boldea, "Parameter Identification For Large Induction Machines Using Direct On Line Startup Test", Workshop on Electrical Machines Parameters, Technical University of Cluj-Napoca, Romania, 26th May 2001

[26]   K.P. Wong, W.D. Humpage, T.T. Nguyen and K.K.K. Ho, "Dynamic Load Model Synthesis", IEE Proceedings, Vol.132, Pt.C, No. 4, July 1985

[27]   Merz and McLellan (SA) Consulting Engineers, "Mossel Bay Onshore Project Final Report: Initial Transient Stability Studies - Proposed Factory Distribution Scheme", Feb 1989

[28]   Powerplan Systems Analysis (PTY) Ltd, "Mossel Bay Onshore Project: Supplementary Power System Studies For Refinery Electrical System", Dec. 1988

[29]   A. Borghetti, R. Caldon, A. Mari and C.A. Nucci, "On Dynamic Load Models for Voltage Stability Studies", IEEE Trans. on Power Systems, Vol. 12, No. 1, February 1997

[30]   L. Pereira, D. Kosterev, P. Mackin, D. Davies, J. Undrill and W. Zhu, "An Interim Dynamic Induction Motor Model for Stability Studies in the WSCC", IEEE Trans. on Power Systems, Vol. 17, No. 4, Nov. 2002

[31]   A.W. Ordys, A.W. Pike, M.A. Johnson, R.M. Katebi and M.J. Grimble, "Modelling and Simulation of Power Generation Plants", 1st Ed., Springer-Verlag London Ltd., 1994

[32]   P.W. Sauer and M.A. Pai, "Power System Dynamics and Stability", 1st Ed., Prentice-Hall Inc., 1998

[33]   M. Buamud, M.J. Chen, J.R. Smith and D.M. Grant, "Industrial Electrical Power Systems Software", 1st Ed., Chapman & Hall, London, 1997

[34]   B.C. Lesieutre, P.W. Sauer and M.A. Pai, "Development and Comparative Study Of Induction Machine Based Dynamic P, Q Load Models", IEEE Trans. on Power Systems, Vol. 10, No. 1, February 1995

[35]   R. Babau, I. Boldea, "Parameter Identification for Large Induction Machines Using Direct On Line Startup Test", Workshop on Electrical Machines' Parameters, Technical University of Cluj-Napoca, 26th May 2001

[36]   R.C.H. Richardson, "The Commissioning Of Electrical Plant", 4th Ed., Chapman & Hall Ltd, 1962

7 Appendix A: MOTOR RE-ACCELERATION GROUPS

The following is a list of all motor re-acceleration groups per substation. For Medium voltage only motors are considered for re-acceleration. For LV, all loads are considered. Units supplied by substations are listed with the substations.

7.1 Substation 02

Unit 03: Air Separation

Description	NO Re-acc (kW)	0sec (kW)	3sec (kW)	6sec (kW)	9sec (kW)	Other re-acc setting (kW)	(sec)	Static Loads (kW)
03KC101M	26000							
03KC102M	9850							
03KC201M	26000							
03KC202M	9850							
03JJ101	182.21	41	224					559.6
03JJ102	167.2	41	224					408.1
03JJ103C	83.33	126	84.5					45
Sub totals	72132.74	208	532.5	0	0	0		1012.7
							TOTAL kW	73885.94

Note – 03KCxxx motors are all 11kV motors

7.2 Substation 03

Unit 10: Catalyst Preparation and Arc Furnace

Description	NO Re-acc (kW)	0sec (kW)	3sec (kW)	6sec (kW)	9sec (kW)	Other re-acc setting (kW)	(sec)	Static Loads (kW)
Arc Furnace								
10JJ001A	274.89							199
10JJ001B	168.14							172
10JJ001C	180							67.55
10JJ002A	386.9							110.1
10JJ002B	604.31							118
Sub totals	1614.24	0	0	0	0	0		666.65
							TOTAL kW	2280.89

7.3 Substation 04

Unit 11: Catalyst Reduction

Unit 14: Synthol

Unit 16: Alcohol Recovery

Description	NO Re-acc (kW)	0sec (kW)	3sec (kW)	6sec (kW)	9sec (kW)	Other re-acc setting (kW)	(sec)	Static Loads (kW)
14KC120AM			5660					
14KC120BM					5660			
11KC101M						4660	12	
VSD1	19920							
VSD1 Filter								
VSD2	19920							
VSD2 Filter								
VSD3	19920							
VSD3 Filter								
14PC101AM			300					
14PC101BM			300					
14PC101CM			300					
14PC103M					200			
14PC111AM			220					
14PC111BM			220					
14PC111CM			220					
14PC122AM			200					
14PC122BM			200					
14PC201AM			300					
14PC201BM			300					
14PC201CM			300					
14PC211AM			220					
14PC211BM			220					
14PC211CM			220					
14PC301AM			300					
14PC301BM			300					
14PC301CM			300					
14PC311AM			220					
14PC311BM			220					
14PC311CM			220					
14KC130AM				1700				
14KC130BM				1700				
14KR125AM			300					
14KR125BM			300					
16KC110M						2554	12	
14JJ101		93.37	129.5	137.5				320.5

Description	NO Re-acc (kW)	0sec (kW)	3sec (kW)	6sec (kW)	9sec (kW)	Other re-acc setting (kW)	(sec)	Static Loads (kW)
14JJ102			148	111				28
14JJ107		41	184.87	283.52	278.1			64
14JJ108		211	249.87	321.72	264.04			59.5
14JJ109C	141.18	500.4			4			95
14JJ110	54		5.5					474
14JJ111	54		5.5					324
14JJ112C	21	19.4	37		4			332
14JJ113	5	60						
14JJ203	317	93	37	119.37	92.5			317
14JJ204	25.5	15	74	92.5	92.5			10.5
14JJ214		60						
14JJ305	317	93.37	37	137.5	92.5			317
14JJ306	25.5	15	74	92.5	92.5			10.5
14JJ315		60						
16JJ101		37	213.5	292	312.5			26
16JJ102			147	351	311.5			6
16JJ103C	6.11	48						20
Sub totals	**60726.29**	**1346.54**	**12682.74**	**5338.61**	**7404.14**	**7214**		**2404**
							TOTAL kW	**97116.32**

7.4 Substation 05

This substation supplies critical power to units throughout the site.

Unit 01: NGL Recovery

Unit 19: Tail gas Processing

Unit 41: Fuel Gas System

Unit 47: Boiler Feed water

Unit 48: Steam/condensate and Power Generation

Unit 49: Boilers

Description	NO Re-acc (kW)	0sec (kW)	3sec (kW)	6sec (kW)	9sec (kW)	Other re-acc setting (kW)	(sec)	Static Loads (kW)
01KR101M	410							
02KC101M						7032	12	
19KC103M			7300					
47PC101AM						250	20	
47PC101BM						250	16	
48PC111M	350							
49KB301M	350							
49PC101AM						250	12	
49PC101BM						250	16	
49PC101CM						250	25	
49PC101DM						250	25	
49PC103AM						720	17.5	
49PC103BM						720	16	

49PC103CM						720	15	
49PC103DM						720	16	
64JJ002A	332.6	15		225.3				514.15
64JJ002B	188.75		352	115.3				1111.2
64JJ015C	232.9	316	4.8					639.88
Sub totals	**1864.25**	**331**	**7656.8**	**340.6**	**0**	**11412**		**2265.23**
							TOTAL kW	**23869.88**

7.5　Substation 06

Unit 04: H_2 Purification

Unit 06: Methane Reforming

Unit 08: CO_2 Removal

Description	NO Re-acc (kW)	0sec (kW)	3sec (kW)	6sec (kW)	9sec (kW)	Other re-acc setting (kW)	(sec)	Static Loads (kW)
06PC101BM				3900				
06PC102AM			250					
06PC102BM			250					
06KB101M			375					
06KB102M			300					
06KB201M			375					
06KB202M			300					
06KB301M			375					
06KB302M			300					
08PC101AM			1100					
08PC101BM			1100					
06JJ101A	18.5		206.75	180				282
06JJ101B	17		206.75	180				320.6
06JJ102A		1.5	98.5	82				188.3
06JJ102B			101	82				
06JJ103C	25.85	18.7						298.3
Sub totals	61.35	20.2	5338	4424	0	0		1089.2
							TOTAL kW	10932.75

7.6　Substation 10

Unit 40: Factory flare gas system

Unit 42: Plant and instrument air

Unit 43: Process cooling water

Unit 50: Gas and condensate metering

Unit 53: Air sep Cooling Water

Unit 99: Gas and Condensate Pig Receiver

Description	NO Re-acc (kW)	0sec (kW)	3sec (kW)	6sec (kW)	9sec (kW)	Other re-acc setting (kW)	(sec)	Static Loads (kW)
42KC101AM			400					
42KC101BM			400					

42KC102AM			1300					
42KC102BM				1300				
43PC101AM			2000					
43PC101BM				2000				
43PC101CM						2000	12	
43PC101DM						2000	15	
43PC102AM						2000	12	
43PC102BM					2000			
43PC102CM			2000					
53PC101AM			750					
53PC101BM					750			
53PC101CM			750					
64JJ003A	49.42	3	437		400			63.4
64JJ003B	19.17	163	37	200		400	12	504.25
64JJ003B						200	15	
64JJ017C	51.1	160	400		200	200	15	172
64JJ024A			200	200		200	12	
64JJ024A						200	15	
64JJ024A						200	21	
64JJ024B			200	200		200	12	
64JJ024B						200	15	
64JJ024B						200	21	
Sub totals	119.69	326	8124	4650	3350	8000		739.65
							TOTAL kW	25309.34

7.7 Substation 11

Unit 45: Raw water treatment

Unit 56: Fire water

Description	NO Re-acc (kW)	0sec (kW)	3sec (kW)	6sec (kW)	9sec (kW)	Other re-acc setting		Static Loads (kW)
						(kW)	(sec)	
56PC102M			375					
56PC202M			375					
64JJ004A	218.32		187	71.52				40
64JJ004B	218.1		37	161.52				142
64JJ021C	6.2	30						26
Sub totals	442.62	30	974	233.04	0	0		208
							TOTAL kW	1887.66

7.8 Substation 13

Unit 01: NGL Recovery

Unit 19: Tail Gas processing

Unit 48: Steam/condensate and power generation

Description	NO Re-acc (kW)	0sec (kW)	3sec (kW)	6sec (kW)	9sec (kW)	Other re-acc setting (kW)	(sec)	Static Loads (kW)
64JJ001A	425	37.048	145	111				335.5
64JJ001B	144	0.37	145	111				336
64JJ016C	9.3	43						93
Sub totals	578.3	80.418	290	222	0	0		764.5
							TOTAL kW	1935.218

7.9 Substation 14

Unit 27: HF Alkylation

Unit 29: Napthahydrogenation

Unit 33: Platformer

Unit 54: Alkylation Cooling Water

Description	NO Re-acc (kW)	0sec (kW)	3sec (kW)	6sec (kW)	9sec (kW)	Other re-acc setting (kW)	(sec)	Static Loads (kW)
29PC101AM	320							
29PC101BM	320							
29KR101AM				600				
29KR101BM				600				
33KC101M			1000					
33KR101AM	1060							
33KR101BM	1060							
33KR102AM	1300							
33KR102BM	1300							
54PC101AM			300					
54PC101BM			300					
64JJ005A	251.85	30	15	88	322			129.65
64JJ005B	197.08	30.37	15	88	322			228.15
64JJ006A	187.87	110		7.5	187			145.4
64JJ006B	135.2	110		7.5	187			140.2
64JJ018C	17.82	199.4						136.5
Sub totals	6149.82	479.77	1630	1391	1018	0		779.9
							TOTAL kW	11448.49

7.10 Substation 15

Unit 25: Butamer

Unit 31: Penex

Unit 35: Distillate hydrotreater

EE-17-12: Central Control Room

Description	NO Re-acc (kW)	0sec (kW)	3sec (kW)	6sec (kW)	9sec (kW)	Other re-acc setting		Static Loads (kW)
						(kW)	(sec)	
35KR101AM			230					
35KR101BM			230					
35PC101AM	450							
35PC101BM	450							
64JJ007A	284.12	4	43	30	30			367
64JJ007B	219.02	4	43	30	30			279
64JJ014A	250.25	55		44.5	44			255
64JJ014B	190.25			44.5	44			112
64JJ019C	107.14	207.94	66					270
Sub totals	1950.78	270.94	612	149	148	0		1283
							TOTAL kW	4413.72

7.11 Substation 17

Unit 51: Tank Farm

Description	NO Re-acc (kW)	0sec (kW)	3sec (kW)	6sec (kW)	9sec (kW)	Other re-acc setting		Static Loads (kW)
						(kW)	(sec)	
64JJ008A	1319.8							
64JJ008B	1348.3							275.74
Sub totals	2668.1	0	0	0	0	0		275.74
							TOTAL kW	2943.84

7.12 Substation 18

Unit 51: Tank Farm

Description	NO Re-acc (kW)	0sec (kW)	3sec (kW)	6sec (kW)	9sec (kW)	Other re-acc setting		Static Loads (kW)
						(kW)	(sec)	
64JJ009A	1110.8							82.84
64JJ009B	1457.7							424
Sub totals	2568.5	0	0	0	0	0		506.84
							TOTAL kW	3075.34

7.13 Substation 19

Unit 18: Reaction water treatment

Unit 58: Liquid effluent

Unit 59: Solid effluent handling

Description	NO Re-acc (kW)	0sec (kW)	3sec (kW)	6sec (kW)	9sec (kW)	Other re-acc setting		Static Loads (kW)
						(kW)	(sec)	
18KB101M	550							
18KB201M	550							
64JJ010A	1400.4		2.2					50
64JJ010B	1107.3		2.2					140
64JJ022C	185		0.74					71
Sub totals	3792.7	0	5.14	0	0	0		261
							TOTAL kW	4058.84

7.14 Substation 20

Unit 20: NGL Fractionation

Unit 21: SLO Fractionation

Unit 49: Steam/condensate and power generation

Description	NO Re-acc (kW)	0sec (kW)	3sec (kW)	6sec (kW)	9sec (kW)	Other re-acc setting		Static Loads (kW)
						(kW)	(sec)	
64JJ011A	185.12		255.5	196	371			149
64JJ011B	191		255.5	214.5	352.5			640.35
64JJ020C	15.9	150						93.9
Sub totals	392.02	150	511	410.5	723.5	0		883.25
							TOTAL kW	3070.27

7.15 Substation 24

Unit 24: C.O. D.

Description	NO Re-acc (kW)	0sec (kW)	3sec (kW)	6sec (kW)	9sec (kW)	Other re-acc setting		Static Loads (kW)
						(kW)	(sec)	
24KC101M				550				
24PC101AM					300			
24PC101BM					300			
24PC102AM			800					
24PC102BM			800					
24PC104AM					300			
24PC104BM					300			
24KR101M	220							
24JJ101A								1791

Description							
24JJ101B							1790
24JJ102A	116.42	6		331.2	118.5		99.8
24JJ102B	85.2	3		331.2	124.5		66.1
24JJ103C	6.6						10
Sub totals	428.22	9	1600	1212.4	1443	0	3756.9
						TOTAL kW	8449.52

7.16 Substation 25

Unit 02: LNG Storage

Description	NO Re-acc (kW)	0sec (kW)	3sec (kW)	6sec (kW)	9sec (kW)	Other re-acc setting		Static Loads (kW)
						(kW)	(sec)	
02KB102M			290					
02PS103M				280				
02PS104M				600				
02JJ101A	12		170	134				374
02JJ101B	2.11		227.7	55				183.87
02JJ101C	7.5	1.1	75					133.4
Sub totals	21.61	1.1	762.7	1069	0	0		691.27
							TOTAL kW	2545.68

7.17 Substation 26

Unit 10: Catalyst preparation

Description	NO Re-acc (kW)	0sec (kW)	3sec (kW)	6sec (kW)	9sec (kW)	Other re-acc setting		Static Loads (kW)
						(kW)	(sec)	
10JJ103	358.51							34
Sub totals	358.51	0	0	0	0	0		34
							TOTAL kW	392.51

7.18 Substation 48

Main generator utilities

Description	NO Re-acc (kW)	0sec (kW)	3sec (kW)	6sec (kW)	9sec (kW)	Other re-acc setting		Static Loads (kW)
						(kW)	(sec)	
48JJ006A	3	55.37	37.5	196	242			64
48JJ006B	8.2	55.37	43.75	185	110			174.04
48JJ026C	29.9	11	22	2.8	89			109.37

48JJ110C	38.75							
Sub totals	**79.85**	**121.74**	**103.25**	**383.8**	**441**	**0**		**347.41**
							TOTAL kW	**1477.05**

8   Appendix B: SOFTWARE LISTINGS

The following is a summary of the subroutines used in the Matlab simulation software

Table 8-1 Summary of program subroutines

Name	Functional Description	Cross Reference
simtrans.m	Main simulation program. Called from the Matlab command line.	pg. 201
read_bus_data.m	Read the bus data from the input file "bus.wk1" and save data in variable 'bus_data' Also returns vector Pvbus which indicates voltage controlled bus	pg. 216
build_Ybus.m	Generates the system admittance matrix from the file "branch.wk1" and generates a data table used for calculating branch currents.	pg. 218
write_load_data	Add impedance used to represent static loads to admittance matrix.	sub-function of build_Ybus.m
write_feeder_data	Add feeder impedance to admittance matrix., Admittance is added to diagonal elements and subtracted from off-diagonal elements	sub-function of build_Ybus.m
write_transformer_data	Add two-winding transformer impedances to admittance matrix. Transformer is modelled as [21]: $$\begin{bmatrix} I_p \\ I_s \end{bmatrix} = \begin{bmatrix} \dfrac{Y}{(a_i a_v)} & \dfrac{-Y}{a_i} \\ \dfrac{-Y}{a_v} & Y \end{bmatrix}\begin{bmatrix} V_p \\ V_s \end{bmatrix}$$ where a_v = complex turns ratio for voltages $(u+jv)$ a_i = complex turns ratio for currents $(u-jv)$ $v=r\cos(Beta)$, $u=r\sin(Beta)$ r = turns ratio, $Beta$ = phase shift	sub-function of build_Ybus.m
write_transformer3_data	Add three-winding transformer impedances to admittance matrix. Modelled as a Y-connected network of impedances[23] where $$Y_1 = \frac{2}{Z_{ps} + Z_{pt} - Z_{st}} , Y_2 = \frac{2}{Z_{ps} + Z_{st} - Z_{pt}} , Y_3 = \frac{2}{Z_{pt} + Z_{st} - Z_{ps}}$$	sub-function of build_Ybus.m
initialise_NR.m	Load initial data into vectors used to store power and voltage for all busses to prepare for first loadflow solution	pg. 222
set_motor_parameters.m	Set up motor model parameter matrix. All model data is saved in one matrix for use during the simulation	pg. 223
set_generator_parameters.m	Set up generator model parameter vector	pg. 228
set_motor_state_vector.m	Set up motor model initial state according to model used	pg. 229
locate_gen_axis.m	Locate generator q-axis with respect to system (swing bus) axis	refer to section 2.13.1
init_gen_state.m	Calculate initial values for all generator state variables before simulation starts	refer to section 4.3.4 pg. 230
pu_bus_voltage.m	Gets specified bus voltage from latest loadflow data and returns $V_t = (V_r + jV_m)$ where V_r = real component of bus voltage, V_m = imaginary component of bus voltage	pg. 231
convert_to_gen_ref.m	Convert X_r, X_m from system reference frame to X_d, X_q in the generator reference frame	see equation (12-34) pg. 231
calc_gen_power.m	Calculate generator active and reactive power from generator model state variables and terminal voltage. I_d and I_q are calculated, giving I_r and I_m from which power is obtained: $S = (P + jQ) = V_t(I_r - jI_m)$	see equations: (4-27), (4-28) and (4-29)
calculate_bus_voltage.m	Get voltage and phase angle for specified bus from loadflow and return as a vector [V_{bus}, V_{angle}] – used by induction motor models	pg. 232
update_loadflow_data.m	Used with the abc motor model. Calculates the following from the motor model state variables: P_{pu}, Q_{pu} – per unit power and reactive power P, Q – power and reactive power in W and Var I_m – instantaneous rms motor current (A)	see equations: (2-41) and (2-42)

Name	Functional Description	Cross Reference
	omega – motor speed (p.u.)	
calc_abc_tmnl_voltage.m	Calculate the three instantaneous phase voltages	used by *update_loadflow_data* pg. 233
update_loadflow_data_dq_model.m	Used with the d-q motor model. Calculates the following from the motor model state variables: P_{pu}, Q_{pu} – per unit power and reactive power P, Q – power and reactive power in W and Var I_m – instantaneous rms motor current (A) *omega* – motor speed (p.u.)	pg. 233
calc_branch_currents.m	Calculate branch currents using bus voltages calculated by loadflow	pg. 234
calc_feeder_current	Calculates the current in a feeder	sub function of calc_branch_currents.m
calc_transformer_current	Calculate primary and secondary currents for a two winding transformer	sub function of calc_branch_currents.m
calc_3wtransformer_current	Calculate primary, secondary and tertiary currents for a three winding transformer	sub function of calc_branch_currents.m
calc_load_current	Calculate load current, MVA and MVAr for a load	sub function of calc_branch_currents.m
loadflow.m	Execute Newton-Raphson loadflow	pg. 238
calc_bus_power	Calculate active and reactive power for all busses	sub function of loadflow.m
calc_new_voltage_estimate	Calculate new estimate for bus voltage magnitudes and angles	sub function of loadflow.m
calculate_dV	Calculate delta-V values for bus voltages	sub function of loadflow.m
update_power_vector	Copy newly calculate P & Q values to prepare for next NR iteration	sub function of loadflow.m
calculate_jacobian.m	Calculates the Jacobian matrix for the NR loadflow.	pg. 243
delete_blanks	Delete rows and columns corresponding to VC busses from the Jacobian	sub function of calculate_jacobian
dP_dth	Calculate $\dfrac{dP}{d\theta}$	sub function of calculate_jacobian
dP_dV	Calculate $\dfrac{dP}{dV}$	sub function of calculate_jacobian
dQ_dth	Calculate $\dfrac{dQ}{d\theta}$	sub function of calculate_jacobian
dQ_dV	Calculate $\dfrac{dQ}{dV}$	sub function of calculate_jacobian
test_motor_model.m	Function used to run simulations of *abc* induction motor models independently of the transient simulation program	pg. 246

8.1 Flowcharts

The following is an overview of the simulation program operation.
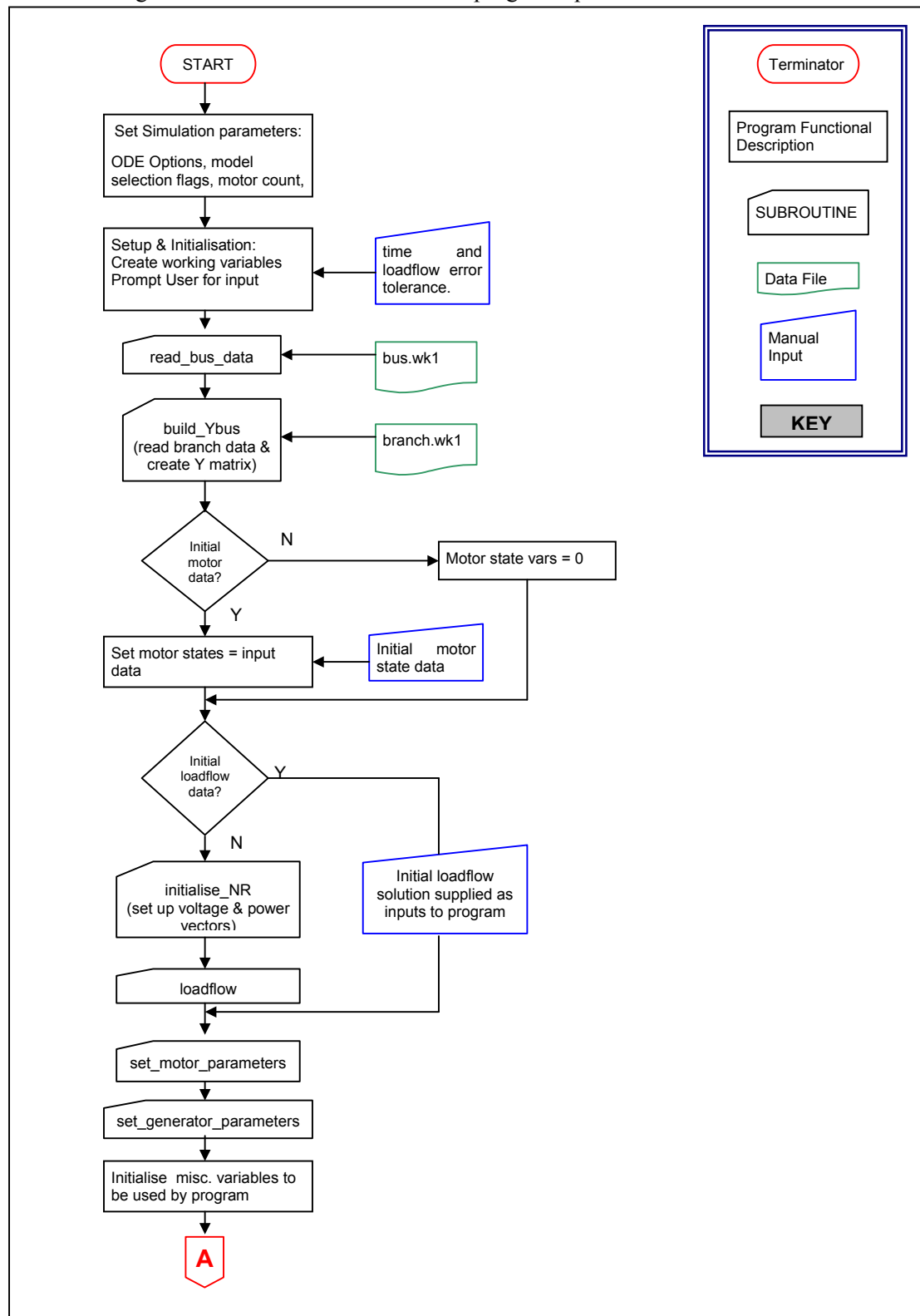
Figure 8-1 Simulation program detail flowchart A
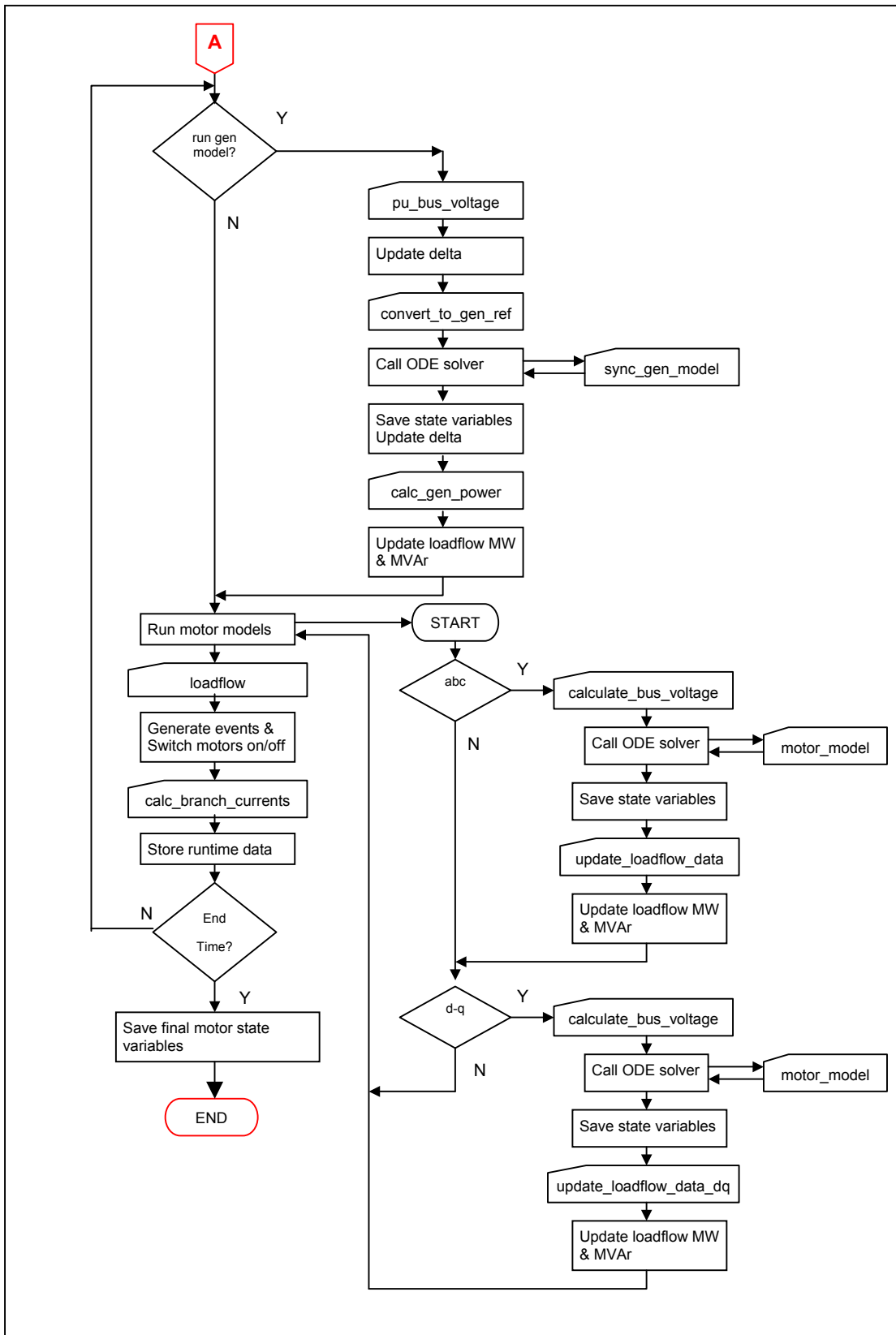
Figure 8-2 Simulation program detail flowchart B
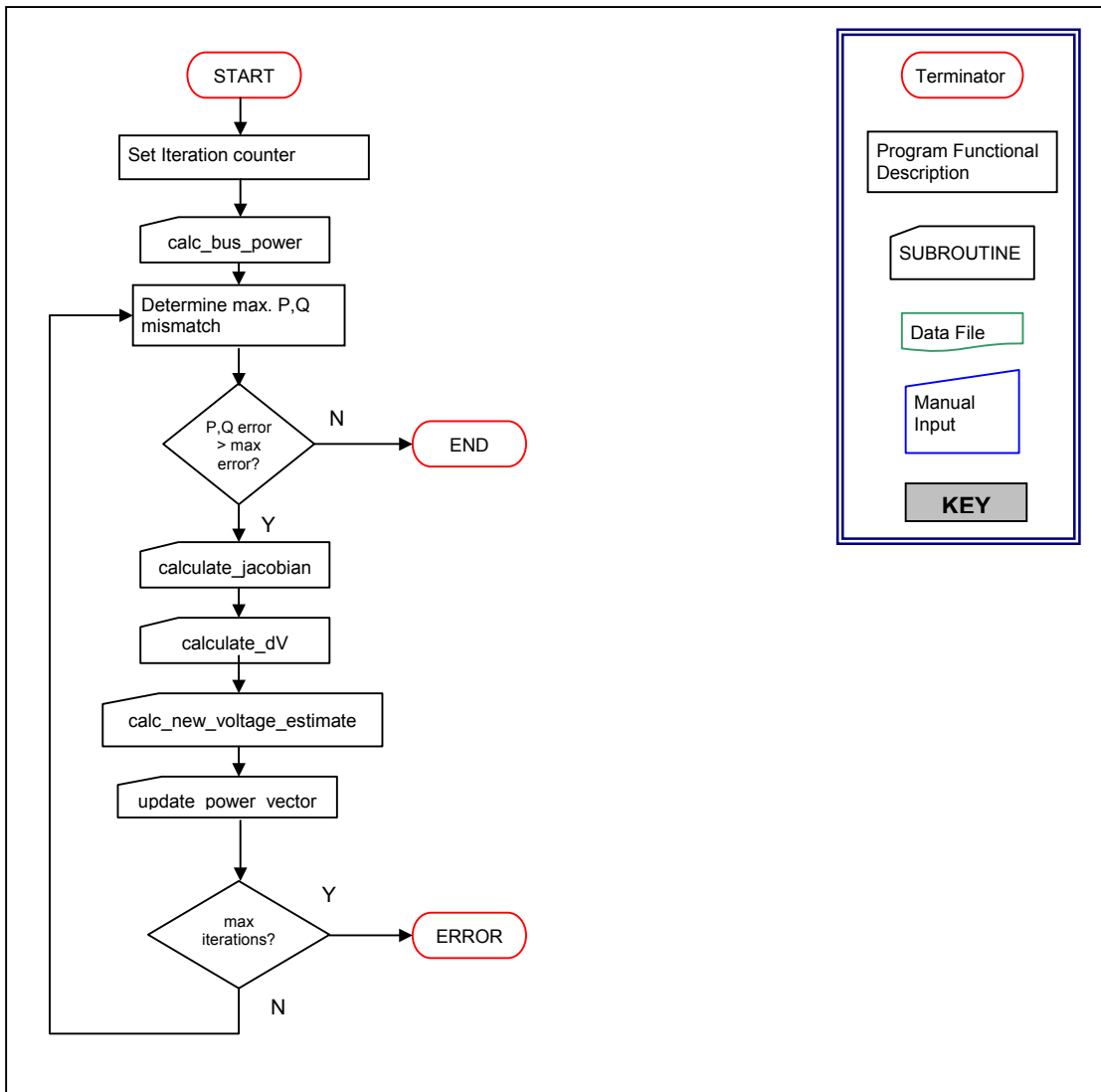
Figure 8-3 Loadflow detailed flowchart

8.2 Program Listings

8.2.1 simtrans.m

```
function [INIT_IM, V, S0, SDAT] = simtrans (INIT_IM, V0, SI)
```

% Transient response simulation [INIT_IM, INIT_LF, SDAT] = simtrans (INIT_IM, V0, SI)

% INIT_IM = initial state vectors for induction motors with following format:

% INIT_IM = [M1 M2 ... Mn] where Mx = initial state variables for motor model

% x refers to the motor

% Mx = [8 x 1] vector - refer to induction motor model for format

% This data is to be set up manually before running the simulation with all

% motors stable at time = T0 which is the starting time for the transient simulation.

% When completed, the simulation data will be written to INIT_IM

% If INIT_IM is omitted, a default initialisation matrix with all values = 0 will

% be generated

% V0, SI = data to initialise loadflow - if omitted - loadflow will be run

% with default bus power values. Returned on completion of simulation

%

%###

% LAST PRINT: 05/08/2005

% Revision History

% 26/06/05 - Used as basis for adding synchronous machine model

% 29/07/05 - Updated functions to initialise generator model and to

%   pass information between system and generator ref frames

% 29/07/05 - AVR changed to lower field when bus voltage drops - Init

%   function updated - gen model functional.

% 30/07/05 - Add governor functions

% 31/07/05 - Correct rotor angle simulation

% 01/08/05 - Changed governor function, sync gen init routine and parameters

%   to gen model

% 02/08/05 - Added network event function to generate faults

% 03/08/05 - Added single rotor induction machine model

% 05/08/05 - General cleanup and moving of subroutines to separate m-files

%###

% Subroutine usage

% The following files are called:

% set_motor_parameters.m

```
% set_motor_state_vector.m
% adjust_state_vecor_lengths.m
% update_loadflow_data.m
% update_loadflow_data_dq_model.m
% calc_abc_tmnl_voltage.m
% calculate_bus_voltage.m
% read_bus_data.m
% build_Ybus.m
% initialise_NR.m
% loadflow.m
% calc_branch_currents.m
% calculate_jacobian.m
% set_generator_parameters.m
% init_gen_state.m
% locate_gen_axis.m
% pu_bus_voltage.m
% calc_gen_power.m
% convert_to_gen_ref.m
% induction_motor_0X.m
% sync_gen_model_0X.m
%####################################################################
% Structure of global variables
% mvab = MVA base = 100
% n = number of busses
% bus_data = (NB At later stage remove bus number col? - not used)
% Col Data
%  1  Bus number (integer) NB bus zero = ground
%  2  Bus type: 1 = swing bus, 2 = VC bus, 3 = load bus
%  3  Bus voltage: Vb (kV)
%  4  Bus voltage angle: theta (degrees)
%  5  Pg = generated power MW
%  6  Qg = generated reactive power MVAr
%  7  Pd = demand power (load) MW
%  8  Qd = demand reactive power (load) MVAr
%  9  Vn = nominal bus operating voltage (kV)


% branch_data =
% Col Feeder     Transformer     3wdg Transformer     Shunt Load
%  1  Type=1     Type=2          Type = 3             Type = 4
%  2  Bus1       pri-bus         pri-bus              bus
%  3  Bus2       sec-bus         sec-bus              MVA(pu)
%  4  R          R               ter-bus             MVAr(pu)
%  5  X          X               internal (model) bus -
```

```
%  6   Voltage   pri-con(D/Y)   R_ps            -
%  7   -         sec-con(D/Y)   X_ps            -
%  8   -         phase shift    R_pt            -
%  9   -         V-pri(kv)      X_pt            -
%  10  -         V-sec(kV)      R_st            -
%  11  -         Pri Tap        X_st            -
%  12  -         -              MVA-pri         -
%  13  -         -              MVA-sec         -
%  14  -         -              MVA-ter         -
%  15  -         -              pri Tap         -
%  16  -         -              ter Tap         -
%  17  -         -              V-pri(kV)       -
%  18  -         -              V-sec(kV)       -
%  19  -         -              V-ter(kV)       -
%  20  -         -              pri-con(D/Y)    -
%  21  -         -              sec-con(D/Y)    -
%  22  -         -              ter_con(D/Y)    -
%  23  -         -              ps-phase shift  -
%  24  -         -              pt-phase shift  -
%
% V = loadflow voltage vector
% V = [ theta1, ..., theta_n, V1, ... ,Vn] (transposed)
% S0 = [ P1, .. , Pn, Q1, .. , Qn ] (transposed)
% Voltage angles are assumed to be in radians
% Ymag = Magnitudes of admittance matrix data
% Yang = Argument of admittance matrix data
% GP = matrix of generator parameters


global mvab n bus_data branch_data  V S0 PV_bus Ymag Yang GP Y SDAT


%######################################################################
################
% Simulation parameter Setup
%######################################################################
###############
mvab = 100; %Set Base MVA

motor_count = 4; %Number of motors - used to generate correct size
initialisation matrix

gen_bus = 16; %Generator bus

% Set flag to model the generator: 1 = enable, 0 = ignore

% When set to ignore, P & Q as set in loadflow will be modelled for
the generator bus

enable_gen = 0;

% Set the type of AVR

% Mode 1: Increases excitation when bus voltage low
```

```
% Mode 2: Reduces excitation when bus voltage low giving increased
VARs

AVR_mode = 1; % Flag is used to select correct initialisation of AVR
state
                % variables


%==================================================================
% Set up motors to be modelled
%==================================================================
% 0 = ignore, 1 = abc model, 2 = dq model
%==================================================================
%MOTOR 01 - 24KC101AM 550kW - bus 49 - 6sec reacc
motor1_model = 1;
%MOTOR 02 - 24PC101AM 300kW - bus 50 - 9sec - reacc
motor2_model = 1;
%MOTOR 03 - 24PC104AM 300kW - bus 52 - 9sec - reacc
motor3_model = 1;
%MOTOR 04 - 24PC102AM 800kW - bus 51 - 3sec - reacc
motor4_model = 1;
%==================================================================
% Set list of branch currents to be calculated
%==================================================================
% 68 = feeder to 24KC101M
% 69 = feeder to 24PC101AM
% 70 = feeder to 24PC102AM
% 71 = feeder to 24PC104AM
% 61 = incomer from 24JN101A to 24JG101A/B (Sub 24 6.6kV board)
% 62 = incomer from 24JN101B to 24JG101A/B
% 11 = feeder to 48GT101
% 1  = Proteus feeder
% 19 = Transformer 64JK001B
%
% Calculated branch currents are returned as follows
% Ib = complex matrix with current corresponding to each element with
the following
% format: (All values in MKSA)
% col:           1                 2         3
% feeder:      If (b1 - b2)    0             0
% transformer: Ip              Is            0
% 3 wdg trfmr: Ip              Is            It
% Load         Il              MVA           MVAr


branch_list = [68 69 70 71 61 11 1 19];


%==================================================================
```

```matlab
%Set ODE options
% AbsTol determines the accuracy of the ODE when the solution
approaches zero
% the default is 1e-6
% RelTol determines (approximately) the number of correct digits in
the
% answer. The default 1e-3 corresponds to 0.1% accuracy
options = odeset('AbsTol', 1e-6, 'RelTol', 1e-3);
%####################################################################
################
% End of parameter setup
%####################################################################
################


%====================================================================
% Setup and initialisation
%====================================================================

w0 = 100*pi;
a = (2*pi)/3;
root3 = sqrt(3);
motor1 = zeros(1,7);
motor2 = zeros(1,7);
motor3 = zeros(1,7);
motor4 = zeros(1,7);
Pgen = 0;
Qgen = 0;
tinit = input('Start time? ');  %All motor init state vars to
correspond to this time
time_step = input('Time step? ');
end_time = input('End time? ');
half_step = time_step/2; %Used to set ODE solver to return only three
data values
%Create output data matrix
data_points = ceil((end_time - tinit)/time_step);
SDAT = zeros(data_points,48);
% The following functions run once to prepare for the loadflow
solution
max_error = input('Maximum Power error tolerance for loadflow? (kVA)
')/(mvab*1e3);
PV_bus = read_bus_data;  %read bus data, create bus_data and mark VC
busses for loadlfow
% Also sets value of global n = number of busses (Definition below)
Y = build_Ybus; %Calculate admittance matrix for loadlfow - reads
branch.wk1
Ymag = abs(Y); %Create matrix containing absolute values of
admittances
```

```matlab
Yang = angle(Y); %Create matrix containing admittance  angles
switch nargin
case 1 %Only initialisation data for motors supplied
    % If no loadflow initialisation data, run loadflow to get initial
values
    [V, S0] = initialise_NR; %Initialise the voltage vector and power
vectors for loadflow
    loadflow(10, max_error); %Run loadflow to get initial solution
case 0 %No data supplied
    % If no loadflow initialisation data, run loadflow to get initial
values
    [V, S0] = initialise_NR; %Initialise the voltage vector and power
vectors for loadflow
    loadflow(10, max_error); %Run loadflow to get initial solution
    INIT_IM = zeros(8,motor_count); %Generate default initialisation
matrix
    % Set default initial values for d-q models if used.
    if motor1_model == 2
        INIT_IM(3,1) = 1; %Slip = 1 - standstill
    end
    if motor2_model == 2
        INIT_IM(3,2) = 1; %Slip = 1 - standstill
    end
    if motor3_model == 2
        INIT_IM(3,3) = 1; %Slip = 1 - standstill
    end
    if motor4_model == 2
        INIT_IM(3,4) = 1; %Slip = 1 - standstill
    end
case 3 % All data supplied
    V = V0; %Initialise variables
    S0 = SI;
otherwise
    % Invalid number of arguments
    error('Invalid number of arguments supplied')
end
%==================================================================
%Load motor model parameters and set initial state vectors
% MOTOR_BUS = list of motor connection busses
[MP, MOTOR_BUS] = set_motor_parameters(motor_count);
MP0 = MP; %Save a copy - used when simulating motor switching
state_motor1 = set_motor_state_vector( INIT_IM, 1, motor1_model);
state_motor2 = set_motor_state_vector( INIT_IM, 2, motor2_model);
state_motor3 = set_motor_state_vector( INIT_IM, 3, motor3_model);
state_motor4 = set_motor_state_vector( INIT_IM, 4, motor4_model);
```

```matlab
%==================================================================
% Load initial values for generator model 01
GP = set_generator_parameters;
% Set generator mech input power and bus voltage
Pm = S0(gen_bus)*3; % Set mech power = loadflow solution
Vref = V(gen_bus+n); %AVR setpoint = init. loadflow
% Initialise state variables for generator model
[delta, It, Vt] = locate_gen_axis (gen_bus);
YG0 = init_gen_state(Vref, Vt, It, delta, Pm);
Beta_old = V(gen_bus); %Save bus voltage angle
end_sim = 0; %Flag to determine end of simulation
t = tinit;
r = 1; %pointer to index output data matrix
%==================================================================
% Temp code to delay motor startup
%motor1_model = 0;
%motor2_model = 0;
%motor3_model = 0;
%motor4_model = 0;


%==================================================================
% Main program loop
%==================================================================
while end_sim ~= 1
    t2 = t + time_step;
    tspan = [t t+half_step t2]; %Set tspan to only return three values
    tspan = [t t2];

%==================================================================
    % Run Generator model

%==================================================================
    if enable_gen == 1
        % Get voltage from loadflow
        Vt = pu_bus_voltage(gen_bus);
        % Calculate Vd, Vq  wrt system
        delta = delta - Beta_old + V(gen_bus);
        Beta_old = V(gen_bus); %Update with new loadflow angle
        [Vd, Vq] = convert_to_gen_ref( delta, real(Vt), imag(Vt));
        % YG0 and YG1 are the generator initial and final state vectors
        [T,YG1] = ode23s( 'sync_gen_model_01', tspan, YG0, options, GP,
Vref, Vd, Vq, Pm);
        YG0 = YG1(end,:)'; %Get initial variables for the next step
        %Update rotor angle with value calculated by gen model
        delta = YG0(3,1); %Update rotor angle wrt system
```

```matlab
    %Calculate generator output power
    [Pgen, Qgen]=calc_gen_power(YG0, Vt, Vd, Vq, delta);
    S0(gen_bus)  =  Pgen/3;%(Pgen  -  Perr)/3;  %Update  loadflow
generator power output
    S0(gen_bus+n) = Qgen/3;%(Qgen  -  Perr)/3;  %Update  loadflow
generator reactive power output
  end


%=================================================================
  % Run motor models

%=================================================================
  %MOTOR 01 - 24KC101AM 550kW - bus 49 - 6sec reacc
  switch motor1_model
  case 1 %abc model
    vbus = calculate_bus_voltage(MOTOR_BUS(1)); %Get   motor 1 bus
voltage from loadflow
    [T,Y]  =  ode23s(  'induction_motor_01',  tspan,  state_motor1,
options, vbus, MP(1,:));
    state_motor1 = Y(end,:)'; %Get initial state variables for next
step
    %Convert data from motor model and update loadflow data
    motor1 = update_loadflow_data(t2, vbus, state_motor1);
    %  The  motor  power  calculated  by  the  motor  model  is  now
transferred to
    %  the  loadflow  model  to  recalculate  system  conditions.  The  S0
vector
    % is updated to reflect the new load on the motor bus.
    S0(MOTOR_BUS(1)) = -motor1(1); %Motor pu instantaneous power
    S0(n+MOTOR_BUS(1)) = -motor1(2); %Motor pu instantaneous reactive
power
  case 2 %dq model
    vbus = calculate_bus_voltage(MOTOR_BUS(1)); %Get   motor 1 bus
voltage from loadflow
    [T,Y]= ode23s('induction_motor_03', tspan, state_motor1, options,
vbus, MP(5,:));
    state_motor1 = Y(end,:)';
    motor1  =  update_loadflow_data_dq_model(state_motor1,  vbus,
MP(5,:), t2);
    S0(MOTOR_BUS(1)) = -motor1(1); %Motor pu instantaneous power
    S0(n+MOTOR_BUS(1)) = -motor1(2); %Motor pu instantaneous reactive
power
  end


%=================================================================
  %MOTOR 02 - 24PC101AM 300kW - bus 50 - 9sec - reacc
  switch motor2_model
  case 1 %abc model
```

```matlab
    vbus = calculate_bus_voltage(MOTOR_BUS(2)); %Get motor 2 bus
voltage from loadflow
    [T,Y] = ode23s( 'induction_motor_01', tspan, state_motor2,
options, vbus, MP(2,:));
    state_motor2 = Y(end,:)'; %Get initital state vars for next step
    motor2 = update_loadflow_data(t2, vbus, state_motor2);
    S0(MOTOR_BUS(2)) = -motor2(1); %Motor pu instantaneous power
    S0(n+MOTOR_BUS(2)) = -motor2(2); %Motor pu instantaneous reactive
power
    case 2
    vbus = calculate_bus_voltage(MOTOR_BUS(2)); %Get  motor 1 bus
voltage from loadflow
    [T,Y]= ode23s('induction_motor_03', tspan, state_motor2, options,
vbus, MP(6,:));
    state_motor2 = Y(end,:)';
    motor2 =  update_loadflow_data_dq_model(state_motor2,  vbus,
MP(6,:), t2);
    S0(MOTOR_BUS(2)) = -motor2(1); %Motor pu instantaneous power
    S0(n+MOTOR_BUS(2)) = -motor2(2); %Motor pu instantaneous reactive
power
    end

%=====================================================================
    %MOTOR 03 - 24PC104BM 300kW - bus 52 - 9sec - reacc
    switch motor3_model
    case 1
    vbus = calculate_bus_voltage(MOTOR_BUS(3)); %Get motor 3 bus
voltage from loadflow
    [T,Y] = ode23s( 'induction_motor_01', tspan, state_motor3,
options, vbus, MP(3,:));
    state_motor3 = Y(end,:)'; %Get initital state vars for next step
    motor3 = update_loadflow_data(t2, vbus, state_motor3);
    S0(MOTOR_BUS(3)) = -motor3(1); %Motor pu instantaneous power
    S0(n+MOTOR_BUS(3)) = -motor3(2); %Motor pu instantaneous reactive
power
    case 2
    vbus = calculate_bus_voltage(MOTOR_BUS(3)); %Get  motor 3 bus
voltage from loadflow
    [T,Y]= ode23s('induction_motor_03', tspan, state_motor3, options,
vbus, MP(7,:));
    state_motor3 = Y(end,:)';
    motor3 =  update_loadflow_data_dq_model(state_motor3,  vbus,
MP(7,:), t2);
    S0(MOTOR_BUS(3)) = -motor3(1); %Motor pu instantaneous power
    S0(n+MOTOR_BUS(3)) = -motor3(2); %Motor pu instantaneous reactive
power
    end

    %=================================================================
==
```

```matlab
    %MOTOR 04 - 24PC102AMM 800kW - bus 51 - 3sec - reacc
    switch motor4_model
    case 1
     vbus = calculate_bus_voltage(MOTOR_BUS(4)); %Get motor 4 bus
voltage from loadflow
     [T,Y] = ode23s( 'induction_motor_01', tspan, state_motor4,
options, vbus, MP(4,:));
     state_motor4 = Y(end,:)'; %Get initital state vars for next step
     motor4 = update_loadflow_data(t2, vbus, state_motor4);
     S0(MOTOR_BUS(4)) = -motor4(1); %Motor pu instantaneous power
     S0(n+MOTOR_BUS(4)) = -motor4(2); %Motor pu instantaneous reactive
power
    case 2
     vbus = calculate_bus_voltage(MOTOR_BUS(4)); %Get  motor 4 bus
voltage from loadflow
     [T,Y]= ode23s('induction_motor_03', tspan, state_motor4, options,
vbus, MP(8,:));
     state_motor4 = Y(end,:)';
     motor4   =   update_loadflow_data_dq_model(state_motor4,   vbus,
MP(8,:), t2);
     S0(MOTOR_BUS(4)) = -motor4(1); %Motor pu instantaneous power
     S0(n+MOTOR_BUS(4)) = -motor4(2); %Motor pu instantaneous reactive
power
    end

    %================================================================
==
    t = t2; %Increment time
    loadflow(10, max_error); %Run loadflow

%==================================================================
    % Generate events

%==================================================================
    % Motor switching is specified here
    % Disconnection of motor simulated by increasing stator resistance
and modifying
    % state variables where required.

%==================================================================
    % DOL start of motors at t=0.1 sec
    %if (t>=0.1)&(t<=0.102)
     %  motor1_model = 2;
     %  motor2_model = 2;
     %  motor3_model = 2;
     %  motor4_model = 2;
    %end
    % Simulate motors tripping and re-starting
```

```matlab
    if (t>=0.01)&(t<=0.012)
        %NB - this will not work if all motors are not modelled using
the same model
        % For all simulatione either abc or d-q model used so OK
        switch motor1_model
        case 1 %abc model - all motors off line
            MP(1,6) = 1e6; %set high stator resistance
            MP(2,6) = 1e6;
            MP(3,6) = 1e6;
            MP(4,6) = 1e6;
        case 2 %d-q model - all motors offline
            MP(5,4) = 1e6; %set stator resistance high
            MP(6,4) = 1e6;
            MP(7,4) = 1e6;
            MP(8,4) = 1e6;
        end
    end
    if (t>=0.11)&(t<0.112) %Restart after dip
        switch motor1_model
        case 1 %abc model
            MP(1,6) = MP0(1,6);
            MP(2,6) = MP0(2,6);
            MP(3,6) = MP0(3,6);
            MP(4,6) = MP0(4,6);
        case 2 %d-q model
            MP(5,4) = MP0(5,4); %restore original value
            MP(6,4) = MP0(6,4);
            MP(7,4) = MP0(7,4);
            MP(8,4) = MP0(8,4);
        end
    end


%====================================================================
    % Changes to network specified here

%====================================================================
    % Simulate 20% voltage dip at Proteus for 100ms
    if (t>= 0.1)&(t<=0.2)
        V(n+1) = 0.8;
    else
        V(n+1) = bus_data(1,3); %restore original value
    end
```

```matlab
    % Simulate trip on main 26MW air compressors - assume about 80ms
for breakers to open
    if (t>=0.18)&(t<=0.182)
        S0(20) = 0;     %set 03KC201 power = 0
        S0(20+n) = 0;   %set 03KC201 vars = 0
        S0(30) = 0;     %set 03KC201 power = 0
        S0(30+n) = 0;   %set 03KC201 vars = 0
    end



%===================================================================
    % Store runtime data

%===================================================================
    I_branch = calc_branch_currents(branch_list);
    %save each step data here
    SDAT(r,1) = t;
    SDAT(r,2) = V(n+MOTOR_BUS(1));%24KC101AM voltage
    SDAT(r,3) = V(n+MOTOR_BUS(2));%24PC104AM voltage
    SDAT(r,4) = V(n+MOTOR_BUS(3));%24PC104AM voltage
    SDAT(r,5) = V(n+MOTOR_BUS(4));%24PC102AM voltage
    SDAT(r,6) = motor1(5); %24KC101AM instantaneous current
    SDAT(r,7) = motor2(5); %24PC101AM instantaneous current
    SDAT(r,8) = motor3(5); %24PC104AM instantaneous current
    SDAT(r,9) = motor4(5); %24PC102AM instantaneous current
    SDAT(r,10) = motor1(3)/1000; %24KC101AM power (kW)
    SDAT(r,11) = motor2(3)/1000; %24PC101AM power (kW)
    SDAT(r,12) = motor3(3)/1000; %24PC104AM power (kW)
    SDAT(r,13) = motor4(3)/1000; %24PC102AM power (kW)
    SDAT(r,14) = motor1(4)/1000; %24KC101AM Reactive power (kVa)
    SDAT(r,15) = motor2(4)/1000; %24PC101AM Reactive power (kVa)
    SDAT(r,16) = motor3(4)/1000; %24PC104AM Reactive power (kVa)
    SDAT(r,17) = motor4(4)/1000; %24PC102AM Reactive power (kVa)
    SDAT(r,18) = motor1(6); %24PC101AM speed pu
    SDAT(r,19) = motor2(6); %24KC101AM speed pu
    SDAT(r,20) = motor3(6); %24PC104AM speed pu
    SDAT(r,21) = motor4(6); %24PC102AM speed pu
    SDAT(r,22) = V(n+2); %Sub01
    SDAT(r,23) = V(n+48); %Sub24 24JG101A
    SDAT(r,24) = abs(I_branch(1,1)); %Proteus incomer A current
    SDAT(r,25) = abs(I_branch(11,1)); %48GT101 feeder current
    SDAT(r,26) = delta*57.2957; %48GT101 rotor angle
    SDAT(r,27) = Pgen; %48GT101 power output
    SDAT(r,28) = Qgen; %48GT101 reactive power output
    SDAT(r,29) = V(n+gen_bus); %48GT101 bus voltage
```

```matlab
        SDAT(r,30) = YG0(7); %Field voltage
        SDAT(r,31) = V(n+7); %Sub 06 11kV busbar
        SDAT(r,32) = V(41+n); %Sub 19 525V bus
        SDAT(r,33) = abs(I_branch(19,1)); %64JK001B primary
        SDAT(r,34) = abs(I_branch(19,2)); %64JK001B secondary
        SDAT(r,35) = abs(I_branch(19,3)); %64JK001B tertiary
        SDAT(r,36) = abs(I_branch(68,1)); %24KC101 current
        SDAT(r,37) = abs(I_branch(69,1)); %24PC101 current
        SDAT(r,38) = abs(I_branch(70,1)); %24PC104 current
        SDAT(r,39) = abs(I_branch(71,1)); %24PC102 current
        SDAT(r,40) = abs(I_branch(61,2)); %24JK101A secondary current
        SDAT(r,41) = motor1(7); %Save phase a current
        SDAT(r,42) = motor2(7);
        SDAT(r,43) = motor3(7);
        SDAT(r,44) = motor4(7);
        SDAT(r,45) = YG0(4)*57.2957; %Gen rotor angular speed
        SDAT(r,46) = YG0(9); %Pm
        SDAT(r,47) = S0(gen_bus)*3; %Loadflow power
        SDAT(r,48) = S0(gen_bus+n)*3; %LF Q

    %====================================================================
        print_runtime_data(SDAT,r);
        r = r+1; %increment pointer
        if t >= end_time
            end_sim = 1; %Check for end of simulation
        end
    end % End of main simulation loop
    %====================================================================
figure(1);
plotsim(SDAT);
figure(2);
plotgen(SDAT, end_time);
%Before saving to workspace, all induction motor state variables are
set to the same length
state_motor1 = adjust_state_vecor_lengths(state_motor1);
state_motor2 = adjust_state_vecor_lengths(state_motor2);
state_motor3 = adjust_state_vecor_lengths(state_motor3);
state_motor4 = adjust_state_vecor_lengths(state_motor4);
INIT_IM = [state_motor1 state_motor2 state_motor3 state_motor4];
DATESTR(NOW) %End time to console


%####################################################################
###############
% END OF MAIN PROGRAM
```

```matlab
%################################################################
################

function print_runtime_data(SDAT,r)

%fprintf('t=%6.4f s',SDAT(r,1)); %time
%fprintf('%6.4f Vgen',SDAT(r,29)); %Gen voltage
%fprintf('%6.3f Pgout',SDAT(r,27));
%fprintf('%6.3f Qgout',SDAT(r,28));
%fprintf('%7.2f delta ',SDAT(r,26));
%fprintf('%7.3f omega ', SDAT(r,45));%rotor speed
%fprintf('%5.3f Pm ', SDAT(r,46)); %Mechanical power
%fprintf('%5.3f Plf ', SDAT(r,47));
%fprintf('%5.3f Qlf ', SDAT(r,48));
%fprintf('\n');



fprintf('t=%6.4f s ',SDAT(r,1)); %time
fprintf('%6.4f Vgen ',SDAT(r,29)); %Gen voltage
fprintf('%6.2f Im1 ',SDAT(r,6));
fprintf('%6.2f Im2 ',SDAT(r,7));
fprintf('%6.2f Im3 ',SDAT(r,8));
fprintf('%7.2f Im4 ', SDAT(r,9));
fprintf('%4.3f Pg ', SDAT(r,27));
fprintf('%4.3f Qg ', SDAT(r,28));
fprintf('%7.3f delta', SDAT(r,26));
fprintf('\n');
```

8.2.2 Event simulation – code section

This is the code added to *simtrans.m* to generate the events for case study 11.

```matlab
%======================================================================
%                              Generate                        events
%======================================================================
   % Motor switching is specified here
   % Disconnection of motor simulated by increasing stator resistance
and modifying
   %           state          variables          where          required.
%======================================================================
   % DOL start of motors at t=0.1 sec
   %if (t>=0.1)&(t<=0.102)
    %  motor1_model = 2;
    %  motor2_model = 2;
    %  motor3_model = 2;
    %  motor4_model = 2;
   %end
   % Simulate motors tripping and re-starting
   if (t>=0.01)&(t<=0.012)
      %NB - this will not work if all motors are not modelled using
the same model
      % For all simulatione either abc or d-q model used so OK
      switch motor1_model
      case 1 %abc model - all motors off line
         MP(1,6) = 1e6; %set high stator resistance
         MP(2,6) = 1e6;
         MP(3,6) = 1e6;
         MP(4,6) = 1e6;
      case 2 %d-q model - all motors offline
         MP(5,4) = 1e6; %set stator resistance high
         MP(6,4) = 1e6;
         MP(7,4) = 1e6;
         MP(8,4) = 1e6;
      end
   end
   if (t>=2.2)&(t<2.202) %24KC101 - 6sec delay (use 2 sec)
      switch motor1_model
      case 1 %abc model
         MP(1,6) = MP0(1,6);
      case 2 %d-q model
         MP(5,4) = MP0(5,4); %restore original value
      end
```

```matlab
   end
   if (t>=4.2)&(t<4.202) %24PC101 & 104 - 9sec delay (use 4 sec)
      switch motor1_model
      case 1 %abc model
         MP(2,6) = MP0(2,6);
         MP(3,6) = MP0(3,6);
      case 2 %d-q model
         MP(6,4) = MP0(6,4); %restore original value
         MP(7,4) = MP0(7,4);
      end
   end
   if (t>=6.2)&(t<6.202) %24PC102 - 3sec delay ( use 6 sec)
      switch motor1_model
      case 1 %abc model
         MP(4,6) = MP0(4,6);
      case 2 %d-q model
         MP(8,4) = MP0(8,4); %restore original value
      end
   end



%=====================================================================
%        Changes        to       network       specified        here
%=====================================================================
   % Simulate 20% voltage dip at Proteus for 100ms
   if (t>= 0.1)&(t<=0.2)
      V(n+1) = 0.8;
   else
      V(n+1) = bus_data(1,3); %restore original value
   end


   % Simulate trip on main 26MW air compressors - assume about 80ms
for breakers to open
   if (t>=0.18)&(t<=0.182)
      S0(20) = 0;     %set 03KC201 power = 0
      S0(20+n) = 0;   %set 03KC201 vars = 0
      S0(30) = 0;     %set 03KC201 power = 0
      S0(30+n) = 0;   %set 03KC201 vars = 0
   end
```

8.2.3 read_bus_data.m

```matlab
function PVbus = read_bus_data()


%####################################################################
```

```
% REV 01 - 22/08/2004 - Global variables and return variables changed
%#############################################################
% Read the bus data from bus.wk1 and mark Voltage controlled busses
% before running loadflow for the first time
% Return vector PVbus indicating PV busses - used when constructing
Jacobian
% bus.wk1 must have the following structure:
% Col Data
%  1  Bus number (integer) NB bus zero = ground
%  2  Bus type: 1 = swing bus, 2 = VC bus, 3 = load bus
%  3  Bus voltage: Vb (kV)
%  4  Bus voltage angle: theta (degrees)
%  5  Pg = generated power MW
%  6  Qg = generated reactive power MVAr
%  7  Pd = demand power (load) MW
%  8  Qd = demand reactive power (load) MVAr
%  9  Vn = nominal bus operating voltage (kV)


% Bus type and specified data:
%
%                 V   delta    Pg    Qg    Pd    Qd
% 1: swing bus :  Y   Y        N     N     Y     Y
% 2: VC bus:      Y   N        Y     N     Y     Y
% 3: Load bus:    N   N        Y     Y     Y     Y
%
% PVbus = [ b2, b3, ...bn ]
%       where bi = 0 for PQ bus and 1 for PV bus


global mvab bus_data n

 bus_data  =  wk1read('bus.wk1',1,0);  %read  file  bus.wk1  omitting
headings
 n = size(bus_data,1); %determine number of busses
 PVbus = zeros(1,n);
 mvab3 = 3*mvab; %Used to convert Bus power to pu
 for row = 1:n
    switch bus_data(row,2)
        %Note - All values which are to be ignored for the different
bus types
        %       are set to zero.
        %     - All MW and MVA values are divided by 3 for per-phase
representation
    case 1 % swing bus
        bus_data(row,3)  =  bus_data(row,3)/bus_data(row,9);  %convert
voltage to pu
```

```
        bus_data(row,4) = bus_data(row,4)*(pi/180); %convert voltage
angle to radians

        bus_data(row,5) = 0;

        bus_data(row,6) = 0;

        bus_data(row,7) = bus_data(row,7)/mvab3; %convert to pu

        bus_data(row,8) = bus_data(row,8)/mvab3;
    case 2 % voltage controlled bus
        bus_data(row,3) = bus_data(row,3)/bus_data(row,9);  %convert
voltage to pu

        bus_data(row,4) = 0;

        bus_data(row,5) = bus_data(row,5)/mvab3;
        bus_data(row,6) = 0;

        bus_data(row,7) = bus_data(row,7)/mvab3;

        bus_data(row,8) = bus_data(row,8)/mvab3;

        PVbus(1,row) = 1; %set flag to indicate PV bus

    case 3 % load bus
        bus_data(row,3) = 0;

        bus_data(row,4) = 0;

        bus_data(row,5) = bus_data(row,5)/mvab3;

        bus_data(row,6) = bus_data(row,6)/mvab3;

        bus_data(row,7) = bus_data(row,7)/mvab3;

        bus_data(row,8) = bus_data(row,8)/mvab3;

    end %switch
end %for
```

8.2.4 build_Ybus.m

```
function Y =  build_Ybus()
% Y = build_Ybus() Y = admittance matrix
%####################################################################
% REV 01 - 22/08/2004 - global variable usage and function parameters
modified
%####################################################################
% Builds the Ybus matrix from the data in the file branch.wk1
% Also returns the branch data matrix for use when calculating
% branch currents
% branch.wk1 must have the following structure:
%
% Each non-blank row has the following format:
% All Resistance/Reactance values are pu
%
% Col Feeder     Transformer     3wdg Transformer      Shunt Load
%  1  Type=1     Type=2          Type = 3              Type = 4
%  2  Bus1       pri-bus         pri-bus               bus
%  3  Bus2       sec-bus         sec-bus               MVA(pu)
%  4  R          R               ter-bus               MVAr(pu)
```

```
%  5   X         X               internal (model) bus -
%  6   Voltage   pri-con(D/Y)    R_ps                  -
%  7   -         sec-con(D/Y)    X_ps                  -
%  8   -         phase shift     R_pt                  -
%  9   -         V-pri(kv)       X_pt                  -
%  10  -         V-sec(kV)       R_st                  -
%  11  -         Pri Tap         X_st                  -
%  12  -         -               MVA-pri               -
%  13  -         -               MVA-sec               -
%  14  -         -               MVA-ter               -
%  15  -         -               pri Tap               -
%  16  -         -               ter Tap               -
%  17  -         -               V-pri(kV)             -
%  18  -         -               V-sec(kV)             -
%  19  -         -               V-ter(kV)             -
%  20  -         -               pri-con(D/Y)          -
%  21  -         -               sec-con(D/Y)          -
%  22  -         -               ter_con(D/Y)          -
%  23  -         -               ps-phase shift        -
%  24  -         -               pt-phase shift        -
%  25  comment   comment         comment         comment
% All values are assumed to be in pu or radians as appropriate


global branch_data n Y

branch_data = wk1read( 'branch.wk1');
Y = zeros(n);         %create Y matrix
elements = size(branch_data,1);  %Determine number of branch elements
for row = 1:elements
    component_type = branch_data(row,1); %Read component type
    switch component_type
        case 1 %Feeder
            write_feeder_data (row);
        case 2 %Two winding transformer
            write_transformer_data(row);
        case 3 %Three winding transformer
            write_transformer3_data(row);
        case 4 %Shunt connected load
            write_load_data(row)
        otherwise
            error('Undefined component type in branch list')
    end %case
end %For loop to read in all branch components
```

```matlab
%###############################################################

function write_load_data(row)
% Write load data to Y_matrix

global branch_data Y

% Given pu apparent power Spu, the pu impedance = 1/(S*pu/3) where
% S*pu = complex conjugate of pu Apparent power. This is divided by 3
% for per/phase representation
% thus the admittance is simply 1/Zpu = S*pu/3
Yl = complex(branch_data(row,3), branch_data(row,4));
bus = branch_data(row,2);
Y(bus,bus) = Y(bus,bus) + (conj(Yl)/3); %Conjugate needed since P =
VI*


%###############################################################

function write_feeder_data(row)
% Write feeder data to Y matrix

global branch_data Y

Yn = 1/complex(branch_data(row,4), branch_data(row,5)); %Create Y
bus1 = branch_data(row,2);
bus2 = branch_data(row,3);
Y(bus2,bus2) = Y(bus2,bus2) + Yn;
Y(bus1,bus1) = Y(bus1,bus1) + Yn;
Y(bus1,bus2) = Y(bus1,bus2) - Yn; %subtract off-diagonal elements
Y(bus2,bus1) = Y(bus2,bus1) - Yn;


%###############################################################

function write_transformer_data(row)
%Write two-winding transformer data to Y matrix
%Transformenr is modelled as an ideal transforemr with a complex
ratio feeding
%the transformer impedance, giving the admittance matrix:
%
% [Ip]  [ Y/(ai*av)  -Y/ai  ][ Vp ]
```

```matlab
%  [Is] =[ -Y/av        Y     ][ Vs ]
% where
% av = complex turns ratio for voltages = u + jv
% ai = complex turns ratio for currents = u - jv
% v = r*cos(beta), u = r*sin(beta)
% r = turns ratio and beta = phase shift

global branch_data Y


bus1 = branch_data(row,2); %primary bus
bus2 = branch_data(row,3); %secondary bus
Yt = 1/complex(branch_data(row,4),branch_data(row,5));   %Transformer
admittance
%Calculate the complex turns ratio
alpha = complex(cos(branch_data(row,8)),sin(branch_data(row,8)));
alpha = alpha * branch_data(row,11); %multiply by tap value
Y1 = Yt/(alpha* conj(alpha)); %Calculate primary node admittance
Y(bus1,bus1) = Y(bus1,bus1) + Y1;
Y1 = Yt/conj(alpha); %Calculate pri-sec admittance
Y(bus1,bus2) = Y(bus1,bus2) - Y1;
Y1 = Yt/alpha; %sec-pri admittance
Y(bus2,bus1) = Y(bus2,bus1) - Y1;
Y(bus2,bus2) = Y(bus2,bus2) + Yt; %secondary node admittance



%#############################################################


function write_transformer3_data(row)
%Write three winding transformer data

global branch_data Y


bus1 = branch_data(row,2); %primary bus
bus2 = branch_data(row,3); %secondary bus
bus3 = branch_data(row,4); %tertiary bus
bus4 = branch_data(row,5); %Imaginary internal bus used to model the
transformer
Zps  = complex(branch_data(row,6),branch_data(row,7));   %primary/sec
impedance
Zpt  = complex(branch_data(row,8),branch_data(row,9));   %primary/ter
impedance
Zst  = complex(branch_data(row,10),branch_data(row,11));   %sec/ter
impedance
Y1 = 2/(Zps + Zpt - Zst); %admittances used to model transformer
Y(bus1,bus1) = Y(bus1,bus1) + Y1;
```

```
Y(bus1,bus4) = Y(bus1,bus4) - Y1;
Y(bus4,bus1) = Y(bus4,bus2) - Y1;
Y(bus4,bus4) = Y(bus4,bus4) + Y1;
Y1 = 2/(Zps + Zst - Zpt);
Y(bus2,bus2) = Y(bus2,bus2) + Y1;
Y(bus2,bus4) = Y(bus2,bus4) - Y1;
Y(bus4,bus2) = Y(bus4,bus2) - Y1;
Y(bus4,bus4) = Y(bus4,bus4) + Y1;
Y1 = 2/(Zst + Zpt - Zps);
Y(bus3,bus3) = Y(bus3,bus3) + Y1;
Y(bus3,bus4) = Y(bus3,bus4) - Y1;
Y(bus4,bus3) = Y(bus4,bus3) - Y1;
Y(bus4,bus4) = Y(bus4,bus4) + Y1;
```

8.2.5 initialise_NR.m

```
function [V, S0] = initialise_NR
% Initialise the voltage and power vector
%####################################################################
% REV 01 - Added functions to reload results from previous loadflow
% REV 02 - Removed functions to reload data - easier to do in main
%          prog. since S0 and V0 can be directly set as desired
%####################################################################
% V = [ theta1, ..., theta_n, V1, ... ,Vn] (transposed)
% S0 = [ P1, .. , Pn, Q1, .. , Qn ] (transposed)
% Voltage angles are assumed to be in radians

global bus_data n

V = zeros( 2*n , 1); %initialise voltage vector
S0 = V;
V(n+1:end) = 1; %set all voltages = 1pu
for row = 1:n
   switch bus_data(row,2)
   case 1  %swing bus
      V(row) = bus_data(row,4); %swing bus voltage angle
      V(row+n) = bus_data(row,3); %swing bus voltage
      S0(row) = -bus_data(row,7); %Pd (-ve)
      S0(row+n) = -bus_data(row,8); %Qd (-ve)
   case 2 %voltage controlled bus
      V(row+n) = bus_data(row,3); %controlled bus voltage
      S0(row) = bus_data(row,5)-bus_data(row,7); %Pg-Pd
      S0(row+n) = -bus_data(row,8); %Qd (-ve)
   case 3 %load bus
```

```
        S0(row) = bus_data(row,5)-bus_data(row,7); %Pg-Pd
        S0(row+n) = bus_data(row,6)-bus_data(row,8); %Pg-Pd
    end %switch
end %for
```

8.2.6 set_motor_parameters.m

```
function [MP, MOTOR_BUS] = set_motor_parameters(motor_count)
%[MP, MOTOR_BUS] = set_motor_parameters()
%Set up induction motor model parameters

% MP = motor model parameters
% All inductance and resistance values are in MKSA units
% MP = [Lsl, Lsm, Lsrm, Lrm, Lrl, Rs, Rr H, LC, LT, P, Tf, tds, tde,
dt, dp1, dp2]
% MP(1) = Lsl = Stator leakage inductance
% MP(2) = Lsm = Stator mutual induxctance
% MP(3) = Lsrm = Stator/rotor mutual inductance - set according to
model
%          Vas gives Lsrm = 2/3Lsm = 2/3Lrm
% MP(4) = Lrm = rotor mutual inductance
% MP(5) = Lrl = rotor leakage inductance
% MP(6) = Rs = stator resistance
% MP(7) = Rr = rotor resistance
% MP(8) = H = inertia constant
% MP(9) = L = load constant
% MP(10) = LT = load type: 1=load proportional to speed
%                          2=load proportional to speed^2
% MP(11) = number of pole pairs
% MP(12) = Torque due to friction and windage at rated speed.
% MP(13) = Rotor resistance variation factor Rr at standstill =
Rr*(1+(factor*slip))
% MP(14) = Rotor reactance variation factor Xr at standstill = Xr*(1-
(factor*slip))
% MP(15) to MP(21) - not used
% MOTOR_BUS = loadflow motor bus


%======================================================================
% Revision History
% 2005/08/02 - Added parameters for simple single-cage induction
motor model
%======================================================================

MP = zeros(motor_count*2, 21);
MOTOR_BUS = zeros(motor_count,1);
```

```
%=====================================================================
% Parameters for abc model
%
% Note: MOTOR_BUS is an array storing the connection bus numbers of
the
% motors to be simulated. There is no value stored for the d-q model
% since this simply uses the abc model data


%=====================================================================
% MOTOR 01 - 24KC101AM 550kW - bus 49
%=====================================================================
MOTOR_BUS(1) = 49; %Motor 1 bus number


MP(1,1) = 0.03592; %Lsl = Stator leakage inductance (=equiv. ckt
param)
MP(1,2) = 0.8726; %Lsm = Stator magnetising inductance
MP(1,3) = MP(1,2); %Lsrm = Stator/rotor mutual inductance
MP(1,4) = MP(1,2); %Lrm = rotor mutual inductance
MP(1,5) = 0.05389; %Lrl = rotor leakage inductance
MP(1,6) = 1.1895; %Rs = stator resistance
MP(1,7) = 1.941; %Rr = rotor resistance
MP(1,8) = 5.5; %H = inertia constant
MP(1,9) = 0.018; %L = load constant approx 95% of 550kW load
MP(1,10) = 2;%LT = load type: 1= proportional to speed 2=
proportional to speed^2
MP(1,11) = 1; %pole pairs
MP(1,12) = 37.93; %Torque due to friction and Windage at rated speed
(Nm)
MP(1,13) = 2; %Rr standstill = 3Rr
MP(1,14) = 0.5; %Xr standstill = 0.5*Xr


%=====================================================================
% MOTOR 02 - 24PC101AM 300kW - bus 50
%=====================================================================
MOTOR_BUS(2) = 50; %Motor 2 bus number


MP(2,1) = 0.0671; %Lsl = Stator leakage inductance (=equiv. ckt
param)
MP(2,2) = 1.844; %Lsm = Stator magnetising inductance
MP(2,3) = MP(2,2); %Lsrm = Stator/rotor mutual inductance
MP(2,4) = MP(2,2); %Lrm = rotor mutual inductance
MP(2,5) = 0.1005; %Lrl = rotor leakage inductance
MP(2,6) = 1.456; %Rs = stator resistance
MP(2,7) = 2.739; %Rr = rotor resistance
MP(2,8) = 3.3; %H = inertia constant
```

```
MP(2,9) = 7e-3; %L = load constant  70% of load

MP(2,10) = 2;%LT = load type: 1= proportional to speed 2=
proportional to speed^2

MP(2,11) = 1; %pole pairs

MP(2,12) = 27; %Torque due to friction and Windage at rated speed

MP(2,13) = 2; %Rr standstill = 2.5Rr

MP(2,14) = 0.5; %Xr standstill = 0.5*Xr




%===================================================================
% MOTOR 03 - 24PC104AM 300kW - bus 52
%===================================================================
MOTOR_BUS(3) = 52; %Motor 3 bus number


MP(3,1) = 0.0671; %Lsl = Stator leakage inductance (=equiv. ckt
param)

MP(3,2) = 1.844; %Lsm = Stator magnetising inductance

MP(3,3) = MP(2,2); %Lsrm = Stator/rotor mutual inductance

MP(3,4) = MP(2,2); %Lrm = rotor mutual inductance

MP(3,5) = 0.1005; %Lrl = rotor leakage inductance

MP(3,6) = 1.456; %Rs = stator resistance

MP(3,7) = 2.739; %Rr = rotor resistance

MP(3,8) = 2.6; %6.3 H = inertia constant

MP(3,9) = 8e-3; %L = load constant 80% of load

MP(3,10) = 2;%LT = load type: 1= proportional to speed 2=
proportional to speed^2

MP(3,11) = 1; %pole pairs

MP(3,12) = 27; %Torque due to friction and Windage at rated speed

MP(3,13) = 2; %Rr standstill = 4Rr

MP(3,14) = 0.5; %Xr standstill = 0.5*Xr




%===================================================================
% MOTOR 04 - 24PC102AM 850kW - bus 51
%===================================================================
MOTOR_BUS(4) = 51; %Motor 4 bus number


MP(4,1) = 0.023393; %Lsl = Stator leakage inductance (=equiv. ckt
param)

MP(4,2) = 0.7080; %Lsm = Stator magnetising inductance

MP(4,3) = MP(4,2); %Lsrm = Stator/rotor mutual inductance

MP(4,4) = MP(4,2); %Lrm = rotor mutual inductance

MP(4,5) = 0.03509; %Lrl = rotor leakage inductance

MP(4,6) = 1.2555; %Rs = stator resistance

MP(4,7) = 1.133; %Rr = rotor resistance

MP(4,8) = 9; %H = inertia constant
```

```
MP(4,9) = 0.02064; %L = load constant 80% of load

MP(4,10) = 2;%LT = load type: 1= proportional to speed 2=
proportional to speed^2

MP(4,11) = 1; %pole pairs

MP(4,12) = 24; %Torque due to friction and Windage at rated speed
(Nm)

MP(4,13) = 2; %Rr standstill = 3Rr

MP(4,14) = 0.5; %Xr standstill = 0.5*Xr


%################################################################
% Parameters for simplified motor models
%################################################################
% MP = motor model parameters in MKSA
%
% MP = [X', T'o, Xo, R1, Hm, L, LT, tds, tde, dt, dp1, dp2]
% MP(1) = X': Transient reactance
% MP(2) = T'o: open circuit time constant
% MP(3) = Xo: open circuit reactance
% MP(4) = R1: Stator resistance
% MP(5) = Hm = inertia constant
% MP(6) = L = load constant
% MP(7) = LT = load type: 1=load proportional to speed
%                         2=load proportional to speed^2
% MP(8) = bus voltage (kV)
% MP(9) = not used
% MP(10) = not used
% MP(11) = not used
% MP(12) = not used
% MP(13) = Motor base MVA
% MP(14) - MP(21) are not used for this model


%===================================================================
% MOTOR 01 - 24KC101AM 550kW - bus 49
%===================================================================
R1 = 1.189;

X1 = 6.771;

Xm = 274;

X2 = 10.16;

R2 = 0.647;


MP(5,1) = X1 + ((X2*Xm)/(X2+Xm));   %Transient reactance

MP(5,2) = (X2+Xm)/(100*pi*R2);   %open circuit time constant

MP(5,3) = X1+Xm;                 %open circuit reactance

MP(5,4) = R1;                    %Stator resistance
```

```
MP(5,5) = 160;              %H, inertia constant
MP(5,6) = 4.73e-3;            %load constant 80% load
MP(5,7) = 2;           %Load type
MP(5,8) = 6.6;         %bus voltage (kv)
MP(5,13) = 0.55; %Sb(MVA) for motor


%===================================================================
% MOTOR 02 - 24PC101AM 300kW - bus 50
%===================================================================
R1 = 1.456;
X1 = 12.64;
Xm = 579;
X2 = 18.96;
R2 = 0.913;


MP(6,1) = X1 + ((X2*Xm)/(X2+Xm));   %Transient reactance
MP(6,2) = (X2+Xm)/(100*pi*R2);   %open circuit time constant
MP(6,3) = X1+Xm;                 %open circuit reactance
MP(6,4) = R1;                    %Stator resistance
MP(6,5) = 70;        %H, inertia constant
MP(6,6) = 2.162e-3;  %load constant 80% load
MP(6,7) = 2;             %Load type
MP(6,8) = 6.6;         %bus voltage (kv)
MP(6,13) = 0.3; %Sb(MVA) for motor


%===================================================================
% MOTOR 03 - 24PC104AM 300kW - bus 52
%===================================================================

R1 = 3.464;
X1 = 14.09;
Xm = 420.6;
X2 = 21.14;
R2 = 1.259;


MP(7,1) = X1 + ((X2*Xm)/(X2+Xm));   %Transient reactance
MP(7,2) = (X2+Xm)/(100*pi*R2);   %open circuit time constant
MP(7,3) = X1+Xm;                 %open circuit reactance
MP(7,4) = R1;                    %Stator resistance
MP(7,5) = 70;        %H, inertia constant
MP(7,6) = 2.162e-3;       %load constant 80% load
MP(7,7) = 2;             %Load type
MP(7,8) = 6.6;         %bus voltage (kv)
```

```matlab
MP(7,13) = 0.3; %Sb(MVA) for motor


%=================================================================
% MOTOR 04 - 24PC102AM 800kW - bus 51
%=================================================================



R1 = 1.255;
X1 = 4.409;
Xm = 222.4;
X2 = 6.614;
R2 = 0.377;


MP(8,1) = X1 + ((X2*Xm)/(X2+Xm));   %Transient reactance
MP(8,2) = (X2+Xm)/(100*pi*R2);   %open circuit time constant
MP(8,3) = X1+Xm;                 %open circuit reactance
MP(8,4) = R1;                    %Stator resistance
MP(8,5) = 200;        %H, inertia constant
MP(8,6) = 6.485e-3;   %load constant 80% load
MP(8,7) = 2;          %Load type
MP(8,8) = 6.6;        %bus voltage (kv)
MP(8,13) = 0.8; %Sb(MVA) for motor
```

8.2.7 set_generator_parameters.m

```matlab
function GEN_PAR = set_generator_parameters
% [GEN_PAR] = set_generator_parameters creates matrix with generator
parameters
%
% GP = [Rs Xd X'd T'do Xq X'd T'qo AVR_mode]
% 48GT101 prameters - use with model sync_gen_01,02
% Note all pu values have been referred to 100MVA base
% AVR parameters are not listed here but are coded into AVR DE's.
     GEN_PAR = zeros(1,7);
     GEN_PAR(1)  = 0.003; % Stator winding resistance - ASSUMED
VALUE
     % d - axis parameters
     GEN_PAR(2)  = 1.421; % Synchronous reactance Xd
     GEN_PAR(3)  = 0.1571;% Transient reactance X'd
     GEN_PAR(4)  = 9.5;   % Open circuit transient time constant
T'do
     % q - axis parameters
     GEN_PAR(5)  = 1.3143;% Synchronous reactance Xq
     GEN_PAR(6)  = 0.2;   % Transient reactance X'q - ASSUMED VALUE
```

```
      GEN_PAR(7)  = 0.5;   %  Open  circuit  transient  time  constant
T'qo - ASSUMED VALUE

      % Inertia constant is set in the model - no need to change this
value thus

      % not included here
```

8.2.8 set_motor_state_vector.m

```
function SM = set_motor_state_vector( INIT_IM, motor_no, model )
```

```
% Sets up the initial motor model state vectors from the imput state
vector matrix
```

```
% based on the model selected
```

```
SM = INIT_IM(:,motor_no); %Default abc model uses full state vector
```

```
if model == 2 %d-q model only uses first three variables
```

```
   SM = SM(1:3,1);
```

```
end
```

8.2.9 locate_gen_axis.m

```
function [delta, It, Vt] = locate_gen_axis (gen_bus)
```

```
% Locate generator axis wrt system axis.
```

```
global n V GP S0
```

```
% Determine generator complex power - Loadflow power is on per phase
```

```
% basis and must be multiplied by three
```

```
Sgen = complex(S0(gen_bus), S0(gen_bus+n))*3;
```

```
% Calculate phase angle
```

```
phi = angle(Sgen);
```

```
% Take complex conjugate of Sgen to ensure that Q is negative for
```

```
% leading power factor and positive for lagging so that the phase
```

```
% angle of the current is correct
```

```
Sgen = conj(Sgen);
```

```
% Get terminal voltage
```

```
V_magnitude = V(gen_bus+n);
```

```
V_angle = V(gen_bus); %Angle wrt swing bus
```

```
Vre = V_magnitude*cos(V_angle); % Real part of voltage
```

```
Vim = V_magnitude*sin(V_angle); % Imaginary part of voltage
```

```
Vt = complex(Vre, Vim); % Complex voltage
```

```
It = conj(Sgen/Vt); %Terminal current
```

```
% Calculate internal voltage angle
```

```
% temp1 = (xq*cos(phi)+r*sin(phi))*|It|
```

```
temp1 = (GP(5)*cos(phi)+GP(1)*sin(phi))*abs(It);
```

```
% temp2 = |Vt|+|It|(r*cos(phi)-xq*sin(phi))
```

```
temp2 = V_magnitude + ( abs(It)*(GP(1)*cos(phi)-GP(5)*sin(phi)));
```

```
d_int = atan(temp1/temp2); %Internal voltage angle
delta = d_int + V_angle;
```

8.2.10 init_gen_state.m

```
function YG0 = init_gen_state(Vref, Vt, It, delta, Pref)
% This is called after the first loadflow solution to determine
% generator initial state variables
% Vt = complex terminal voltage
% It = complex terminal current
% delta = machine ref frame angle wrt system reference frame
% Pm0 = initial steady-state mechanical input power

global GP

% Calculate voltage and current dq components
[Vd, Vq] = convert_to_gen_ref(delta, real(Vt), imag(Vt));
[Id, Iq] = convert_to_gen_ref(delta, real(It), imag(It));
% Calculate initial values of state variables
% E'do = (x'q-xq)Iq
Ed_t0 = (GP(6)-GP(5))*Iq;
% E'qo = Vq + rIq - x'd*Id
Eq_t0 = Vq + GP(1)*Iq - GP(3)*Id;
delta_e0 = delta;
omega_e0 = 0;
% Efdo = (E'qo - (xd - x'd)*Id)/0.9436
Efd0 = (Eq_t0 - (GP(2)-GP(3))*Id)/0.9436;
X10 = abs(Vt);
% Calculate the exciter saturation function
if Efd0 > 4.06
      %Use SE2
      SE = ((0.2292*Efd0)-1)*Efd0;
   else
      %Use SE1
      SE = Efd0^2*0.4757;
   end
% X20 = SE + KE*Vfd, but KE = 1
X20 = SE + Efd0;
% X40 = Vref-X1-(X2/KA), KA = 1762
X40 = Vref - X10 - (X20 / 1762);
Pm0 = Pref; % omega_e0 = 0
YG0 = [Ed_t0; Eq_t0; delta_e0; omega_e0; X10; X20; Efd0; X40; Pm0];
```

8.2.11 pu_bus_voltage.m

```
function Vt = pu_bus_voltage(gen_bus)
% Reads generator bus voltage from loadflow and returns as a complex
% variable Vt = (Vr+JVm) where Vr = real bus voltage, Vm = imaginary
% bus voltage. This routine is used for the generator model and the
% single-cage induction machine model

global n V

V_magnitude = V(gen_bus+n);
V_angle = V(gen_bus); %Angle wrt swing bus
Vre = V_magnitude*cos(V_angle); % Real part of voltage
Vim = V_magnitude*sin(V_angle); % Imaginary part of voltage
Vt = complex(Vre, Vim); % Complex voltage
```

8.2.12 convert_to_gen_ref.m

```
function [Xd, Xq] = convert_to_gen_ref( delta, Xre, Xim )
% Convert voltage or current from system reference frame to
% the generator reference frame

Xd = -sin(delta)*Xre + cos(delta)*Xim;
Xq =  cos(delta)*Xre + sin(delta)*Xim;
```

8.2.13 calc_gen_power.m

```
function [Pg, Qg]=calc_gen_power(YG1, Vt, Vd, Vq, delta )
% Calculate generator output power and vars to update loadflow.
% YG1 = state variable from solution of generator model
% Vt = complex bus voltage (system reference)
% Vd, Vq = bus voltage (generator model reference)

global GP

% Calculate Id, Iq
% temp = (r^2+xd'*xq')
temp = GP(3)*GP(6)+GP(1)^2;
% Id = (r(E'd-Vd)+x'q(Vq-E'q))/temp
Id = ((GP(1)*(YG1(1,1)-Vd))+(GP(6)*(Vq-YG1(2,1))))/temp;
% Iq = (E'd-Vd-r*Id)/x'q
Iq = (YG1(1,1)-Vd-GP(1)*Id)/GP(6);
% Convert current to system reference
Ire = cos(delta)*Iq - sin(delta)*Id;
Iim = sin(delta)*Iq + cos(delta)*Id;
It = complex(Ire, Iim);
S = Vt*conj(It); %Complex power
```

```
Pg = real(S);
Qg = -imag(S);
```

8.2.14 calculate_bus_voltage.m

```
function vbus = calculate_bus_voltage(bus)
% Get phase rms bus voltage from loadflow
% vbus = calculate_bus_voltage(bus)
% bus = bus number
% vbus = [vbus, angle]
% vb = bus voltage
% va = voltage angle (rad) calculated during loadflow solution
% Multiply bus voltage by 1000 since branch data values in kV

global n bus_data V

vb = (V(n+bus)*bus_data(bus,9))*1000; %l-l rms bus voltage
angle = V(bus); % bus voltage angle
vbus = [ vb angle ];
```

8.2.15 update_loadflow_data.m

```
function S_motor = update_loadflow_data(t, vmot, MSV)
% S_motor = update_loadflow_data(t, vmot, MSV)
% t = time
% vmot = motor terminal voltage
% MSV = motor state variables
%
% This function is used with the abc Induction motor model
% Smot = [Ppu Qpu P Q Im omega, Ia]
% Ppu = inst. motor power (pu) (per-phase)
% Qpu = inst. motor reactive power (pu) (per-phase)
% P = inst motor power (W) (3-phase)
% Q = inst motor reactive power (3-phase)
% Im = inst. rms motor current (A)
% omega = motor_speed (pu)
% Ia = phase A instantaneous motor current

global mvab

S_motor = zeros(1,7);
S_motor(6) = MSV(8)/(100*pi); %Since all motors are single pole this
% calculation ignores the number of motor poles
% Calculate instantaneous motor voltages in abc reference frame
Vm = calc_abc_tmnl_voltage(vmot,t);
%Calculate instantaneous bus power
```

```
S_motor(3) = Vm(1)*MSV(1)+Vm(2)*MSV(2)+Vm(3)*MSV(3);

S_motor(1) = S_motor(3)/(3e6*mvab); %convert to pu and divide by 3

%Instantaneous reactive power

%The calculated value will be -ve for lagging power factor, invert

%to get positive value since +ve values are assumed to be power input

%into the machine.

temp1 = MSV(2)-MSV(3); %Ibs - Ics

temp2 = MSV(3)-MSV(1); %Ics - Ias

temp3 = MSV(1)-MSV(2); %Ias - Ibs

S_motor(4) = -(Vm(1)*temp1+Vm(2)*temp2+Vm(3)*temp3)/sqrt(3);

S_motor(2) = S_motor(4)/(3e6*mvab); %convert to pu and divide by 3

%Calculate the instantaneous rms motor current.

S_motor(5) = sqrt((1/3)*(MSV(1)^2+MSV(2)^2+MSV(3)^2));

S_motor(7) = MSV(1); %Phase a inst. stator current
```

8.2.16 calc_abc_tmnl_voltage.m

```
function Vinst = calc_abc_tmnl_voltage(v,t)

% % Calculate the three instantaneous phase voltages to allow motor power

% to be determined. The voltages are in the abc reference frame

% v = [Vt Va] = motor terminal rms line voltage and angle

% The phase p-p voltage is calculated and the 30degree phase shift between

% phase and line voltage taken into account


Vinst = zeros(3,1);


TWOpi3 = 2*pi/3;

v_angle = v(2)-(pi/6); %Voltage angle from loadflow - 30degrees

% a = instantaneus bus voltage angle

a = (100 * pi * t) + v_angle;

vpeak = v(1)*sqrt(2/3);

Vinst(1,1) = vpeak*cos( a );

Vinst(2,1) = vpeak*cos( a - TWOpi3);

Vinst(3,1) = vpeak*cos( a + TWOpi3);
```

8.2.17 update_loadflow_data_dq_model.m

```
function  Smot = update_loadflow_data_dq_model(SV, vbus, MP, t)

% Calculate the real and reactive power for the single cage induction

% motor model

% SV = model state variables SV = [E'r, E'm, S]

% vbus = [|vbus| angle_vbus ]

% MP = motor model parameters

% Smot = [Ppu Qpu P Q Im omega, Ia]
```

```matlab
% Ppu = inst. motor power (pu) (per-phase)

% Qpu = inst. motor reactive power (pu) (per-phase)

% P = inst motor power (W) (3-phase)

% Q = inst motor reactive power (3-phase)

% Im = rms motor current (A)

% omega = motor_speed (pu)

% Ia = phase A instantaneous motor current


global mvab


Smot = zeros(1,7);


temp = vbus(1)/sqrt(3);

Vr = temp*cos(vbus(2));

Vm = temp*sin(vbus(2));

% Ir = (R1(Vr-E'r)+X'(Vm-E'm))/(R1^2+X'^2)

Ir = ((MP(4)*(Vr-SV(1,1)))+(MP(1)*(Vm-SV(2,1))))/(MP(4)^2+MP(1)^2);

% Im = (Vm-E'm-X'Ir)/R1

Im = (Vm-SV(2,1)-(MP(1)*Ir))/MP(4);

It = complex(Ir,Im);

Vt = complex(Vr, Vm);

Sm = Vt*conj(It);

Smot(3) = real(Sm)*3; %Save Power

Smot(4) = imag(Sm)*3; %Save reactive power

% Change to system base

Smot(1) = Smot(3)/(mvab*3e6);

Smot(2) = Smot(4)/(mvab*3e6);

%Convert to pu (motor base)

Smot(5) = abs(It); %rms current (A)

Smot(6) = (1-SV(3,1)); %Calculate speed pu

Smot(7)  =   abs(It)*1.414*cos((100*pi*t)+angle(It));   %Calculate
instantaneous phase a current
```

8.2.18 calc_branch_currents.m

```matlab
function Ib = calc_branch_currents( branch_list )
```

% Ib = calc_branch_currents(branch_list) Calculates the branch
currents

%##

%REV 01 - Added load power calculations - 13/08/2004

%REV 02 - Added functions to calculate only selected branch currents
- 28/08/2004

%##

% If the vector branch_list is omitted, values are calculated for all
branches

% If the vector branch_list is present, values are only calculated
for the branches

```matlab
% listed in the branch_list vector
% branch_list = [b1 b2 .... bn]
% V = bus voltage matrix
% Data is returned in Ib with row n = branch n
% When branch_list is specified, currents are only calculated for the
specific branches
% the rest are left = 0
% Ib = complex matrix with current corresponding to each element with
the following
% format: (All values in MKSA)
% col:            1                 2         3
% feeder:      If (b1 – b2)   0             0
% transformer: Ip             Is            0
% 3 wdg trfmr: Ip             Is            It
% Load         Il             MVA           MVAr
% n = number of busses
% mvab = base mva
global Ib mvab n bus_data branch_data V
elements = size(branch_data,1); %Determine the number of branch
elements
Ib = zeros(elements,3); %Create branch current matrix
if nargin == 0
    %Calculate all branch currents
    for row = 1:elements
        component_type = branch_data(row,1); %Read component type
        switch component_type
            case 1 %Feeder
                calc_feeder_current(row, n, V, branch_data, mvab);
            case 2 %Two winding transformer
                calc_transformer_current(row, n, V, branch_data, mvab);
            case 3 %Three winding transformer
                calc_3wtransformer_current(row, n, V, branch_data, mvab);
            case 4 %Shunt connected load
                calc_load_current(row,  n,  V,  branch_data,  bus_data,
mvab);
            otherwise
                error('Undefined component type in branch list')
            end %case
    end %for loop to read all elements
 else
   %Calculate only selected branch currents
   for row = branch_list
        component_type = branch_data(row,1); %Read component type
        switch component_type
            case 1 %Feeder
```

```matlab
                    calc_feeder_current(row, n, V, branch_data, mvab);
            case 2 %Two winding transformer
                    calc_transformer_current(row, n, V, branch_data, mvab);
            case 3 %Three winding transformer
                    calc_3wtransformer_current(row, n, V, branch_data, mvab);
            case 4 %Shunt connected load
                    calc_load_current(row,   n,   V,   branch_data,   bus_data,
mvab);
            otherwise
                    error('Undefined component type in branch list')
        end %cas
    end %for loop to read selected elements
    end %If nargin


%###############################################################


function calc_feeder_current(row, n, V, branch_data, mvab)
%Calculate feeder current from bus 1 to bus 2


global  Ib


Z   =   complex(branch_data(row,4),   branch_data(row,5));   %Feeder
impedance
bus1 = branch_data(row,2);
bus2 = branch_data(row,3);
% Calculate complex bus voltages
V1 = V(bus1+n)*complex(cos(V(bus1)),sin(V(bus1)));
V2 = V(bus2+n)*complex(cos(V(bus2)),sin(V(bus2)));
%Calculate base current
Ibase = (mvab*1000)/branch_data(row,6)* sqrt(3);
Ib(row,1) = ((V1-V2)/Z)*Ibase;  %Save branch current


%###############################################################


function calc_transformer_current(row, n, V, branch_data, mvab)
%Calculate transformer primary and secondary currents


global  Ib


bus1 = branch_data(row,2); %primary bus
bus2 = branch_data(row,3); %secondary bus
Yt = 1/complex(branch_data(row,4),branch_data(row,5));   %Transformer
impedance
%Calculate the complex turns ratio
alpha = complex(cos(branch_data(row,8)),sin(branch_data(row,8)));
```

```matlab
alpha = alpha * branch_data(row,11); %multiply by tap value

Y11 = Yt/(alpha* conj(alpha)); %Calculate primary node admittance

Y12 = -Yt/conj(alpha); %Calculate pri-sec admittance

Y21 = -Yt/alpha; %sec-pri admittance

Vp = V(bus1+n)*complex(cos(V(bus1)),sin(V(bus1)));

Vs = V(bus2+n)*complex(cos(V(bus2)),sin(V(bus2)));

Ibase = (mvab*1000)/branch_data(row,9)* sqrt(3);

Ib(row,1) = (Y11*Vp + Y12*Vs)*Ibase; %Primary current

Ibase = (mvab*1000)/branch_data(row,10)* sqrt(3);

Ib(row,2) = -(Y21*Vp + Yt*Vs)*Ibase; %Secondary current

%Note the negative of the secondary current is taken since the model
assumes
%current flow into the transformer


%###############################################################


function calc_3wtransformer_current(row, n, V, branch_data, mvab)
%Calculate transformer primary secondary and tertiary currents


global  Ib


bus1 = branch_data(row,2); %primary bus
bus2 = branch_data(row,3); %secondary bus
bus3 = branch_data(row,4); %tertiary bus
bus4 = branch_data(row,5); %Imaginary internal bus used to model the
transformer
Zps  = complex(branch_data(row,6),branch_data(row,7));  %primary/sec
impedance
Zpt  = complex(branch_data(row,8),branch_data(row,9));  %primary/ter
impedance
Zst  = complex(branch_data(row,10),branch_data(row,11));  %sec/ter
impedance
Zp = (Zps + Zpt - Zst)/2; %impedances used to model transformer

Zs = (Zps + Zst - Zpt)/2;

Zt = (Zst + Zpt - Zps)/2;

Vp = V(bus1+n)*complex(cos(V(bus1)),sin(V(bus1))); %Bus voltages

Vs = V(bus2+n)*complex(cos(V(bus2)),sin(V(bus2)));

Vt = V(bus3+n)*complex(cos(V(bus3)),sin(V(bus3)));

Vm = V(bus4+n)*complex(cos(V(bus4)),sin(V(bus4))); %Internal bus used
to model transformer
Ibase = (mvab*1000)/branch_data(row,17)* sqrt(3); %Calc base current

Ib(row,1) = ((Vp - Vm)/Zp)*Ibase; %Calculate primary,secondary and
tertiary currents
Ibase = (mvab*1000)/branch_data(row,18)* sqrt(3);
```

```matlab
%The secondary and tertiary currents are calculated assuming flow out
of the transformer
Ib(row,2) = ((Vm - Vs)/Zs)*Ibase;

Ibase = (mvab*1000)/branch_data(row,19)* sqrt(3);

Ib(row,3) = ((Vm - Vt)/Zt)*Ibase;


%####################################################################



function calc_load_current(row, n, V, branch_data, bus_data, mvab)
%Calculate bus load current


global  Ib


% Given pu apparent power Spu, the pu impedance = 1/(S*pu/3)
% * denotes complex conjugate, and S*pu is divided by three for
per/phase representation
Zl = 3/conj(complex(branch_data(row,3), branch_data(row,4)));
bus = branch_data(row,2);
Vb  = V(bus+n)*complex(cos(V(bus)),sin(V(bus)));  %Calculated  Bus
voltage in pu
Ibase = (mvab*1000)/bus_data(bus,9)* sqrt(3); %Base current
Ib(row,1) = (Vb*Ibase) / Zl; %Load current in amps
Vb = Vb * bus_data(bus,9); %Bus voltage in kV
VA = sqrt(3)*Vb*conj(Ib(row,1))/1000; %Apparenr power in MVA
Ib(row,2) = real(VA); %MW
Ib(row,3) = imag(VA); %MVAr
```

8.2.19 loadflow.m

```matlab
function loadflow(maxloops, max_error)
% [V, S0] = loadflow(maxloops, max_error, PV_bus, Y, S0)
%####################################################################
% REV 01 - 22/08/2004 - smaller functions added to end of this file
% REV 02 - 22/08/2004 - modified to be called from simtrans
% REV 03 - 02/08/2005 - removed mvab, bus_data & branch_data from
%                       global variables - not used
%####################################################################


% Data is read from the following files:
% branch.wk1: Branch data for constructing [Y]
% bus.wk1: Bus data defining swing bus (bus 1), load and constant
voltage busses


% Variables used
```

```
% mvab = constant - base MVA

% Y = bus admittance matrix - all values in pu

% Ymag - magnitutes of bus admittances

% Yang - bus admittance angles

% bus_data = System bus data - read in from file "bus.wk1' - refer to
read_bus_data.m for format

% branch_data = system branch data - read in from file "branch.wk1" -
refer to build_Ybus.m for format

% PVbus = Vector used to keep track of voltage-controlled busses -
used when calculating the

%         Jacobian matrix

% n = number of system busses

% V = bus voltage vector - refer to initialise_NR.m for format

% S0 = Current estimate of bus power - refer to initialise_NR.m for
format

% S1 = bus power estimate based on current voltage values

% J = Jacobian matrix


global  n V Ymag Yang S0 PV_bus


% Loop starts here

q = 0; %quit flag

loopcount = 0; %Used to count iterations

while q == 0

S1 = calc_bus_power(Ymag,Yang); %Calculate Active & reactive powers
at all busses

deltaS = S0 - S1;

%Determine power mismatch

mismatch = max(abs(deltaS)); %Get value of the largest mismatch
element.

if mismatch < max_error

   q = 1; %stop interation

else

   q = 0; %Continue iteration

end

if q == 0

 J = calculate_jacobian(S1,PV_bus);  %Calculate the Jacobian matrix

 deltaV = calculate_dV(deltaS,J,PV_bus); %Calculate the new delta-V
values

 %Calculate new voltage estimate. The last two parameters allow
limiting of the deltaV and

 %delta@ values - can improve convergence where phase shifting
transformers present

 %lv = 0.05 and lt = 0.5 (30degrees) reduces iterations by 1

 calc_new_voltage_estimate(deltaV,PV_bus,0,0);

 S0 = update_power_vector(S1,S0,PV_bus);

 loopcount = loopcount + 1;
```

```matlab
  if loopcount > maxloops
    error('Load flow did not converge');
    q = 1; %Stop program
end
end
end %while loop




%#####################################################################
% End of main function
%#####################################################################


function S1 = calc_bus_power(Ymag, Yang )
%S1 = calc_bus_power(Ymag, Yang, V)
%Calculate Pi and Qi based on the current value of V
% V = [@1, @2,...,@n,V1,V2,...,Vn] (@ = theta)
% S1 = [P1, ..Pn, Q1, ..Qn](transpose)
%
% Si = Pi + JQi
% Pi = sum: j = 1 to n : |Vi||Vj||Yij|cos(@j-@i+&ij) & = delta =
complex admittance angle
% Qi = sum: j = 1 to n :-|Vi||Vj||Yij|sin(@j-@i+&ij)


global n V

S1 = zeros(2*n,1);
for i = 1:n
    %Loop to calculate the i'th P and Q value
    sigmaQ = 0; %Variables to store the summation terms
    sigmaP = 0;
    for j = 1:n
     theta = V(j) - V(i) + Yang(i,j); %Calculate angle
     sigmaQ  =  sigmaQ  +  (V(j+n)*Ymag(i,j)*sin(theta));%Vj*sin(@j-
Qi+&ij)
     sigmaP = sigmaP + V(j+n)*Ymag(i,j)*cos(theta);%Vj*cos(@j-Qi+&ij)
    end %for 'j' loop
  S1(i+n) = sigmaQ * (-V(i + n)); %multiply by -|vi|
  S1(i) = sigmaP * V(i + n); %multiply by |vi|
end   %end 'i' loop




%#####################################################################


function calc_new_voltage_estimate(deltaV,PVbus,lv,lt)
```

```matlab
% calc_new_voltage_estimate(deltaV,PVbus,lv,lt)
% lv = deltaV limit - ignored if zero - in pu
% lt = delta@ limit - ignored if zero - in radians
% If necessary the voltage magnitudes of deltaV  and delta@ can be limited if the
% N-R solution does not converge
%
% Calculates V1 = V0 + deltaV.
% deltaV does not contain V and @ values for bus 1 or V values for voltage controlled
% busses since V is already known(specified)
%
% Update voltage angles - all angles from @2 to @n are present as elements 1 to n-1
% in deltaV, this index i ranges from 2 to n
% There are no voltage magnitude entries for VC busses. Thus j is used to keep track of the
% index position for updating Voltage magnitudes
%
% V = [ @1, @2,...,@n,V2,...Vn ]
% dV= [ @2, @3,...,@n,V?,V?] V?


global  n V


j = n; %init j to n since @1 does not exist in deltaV
for i = 2:n %i is used to index V
   if lt ~= 0
       %Execute if phase angles are to be limited
       if abs(deltaV(i-1))>lt
          V(i) = V(i) + lt * sign(deltaV(i-1)); %Limit voltage phase angle
       else
          V(i)  =  V(i)  +  deltaV(i-1);  %Calculate  new  voltage  phase angle
       end
   else
       %Execute if no limiting of phase angles
       V(i) = V(i) + deltaV(i-1); %Calculate new voltage phase angle
   end
   if PVbus(i) == 0 %only add deltaV for Load busses
       if lv ~= 0
          %Execute if voltage magnitude changes are to be limited
          if abs(deltaV(j))>lv
             V(i+n)=  V(i+n)  +  sign(deltaV(j))*lv;  %Limit  voltage magnitude change
          else
```

```matlab
                V(i+n)  =  V(i+n)  +  deltaV(j);  %Calculate  next  voltage
estimate
            end
        else
            %Execute if no limiting of Voltage magnitude changes
            V(i+n) = V(i+n) + deltaV(j);
        end
        j = j+1; %If deltaV value copied, set to next index position
    end
end


%###############################################################


function deltaV = calculate_dV(deltaS, J, PVbus )
% deltaV = calculate_dV(deltaS, J, PVbus )
% Calculate new delta values for voltage vector.
% deltaS = power mismatch vector
% J = jacobian
% n = number of busses
% PVbus  =  vector  indicating  voltage  controlled  busses,used  to
determine which
% of the deltaS values are to be deleted.


global n


for  i  =  n:-1:1  %start  from  end  of  matrix  to  ensure  index  remains
correct
    if PVbus(i) == 1
        %If bus i = Voltage controlled bus, delete row containing Qi
        deltaS(i+n,:)=[]; %delete row containing Qi
    end
end
deltaS(1+n,:)=[]; %delete Q1
deltaS(1,:) = []; %delete P1
deltaV = J\deltaS;


%###############################################################


function S0 = update_power_vector(S1,S0,PVbus)
%Transfer newly calculated P & Q values to prepare for next iteration
%For swing bus, transfer both values
%For voltage controlled bus, only transfer Q, since P is specified
%For load busses, no transfer, since P and Q specified


global n
```

```matlab
S0(1) = S1(1); %Copy P1 (swing bus power)

S0(1+n) = S1(1+n); %copy Q1 (swing bus reactive power)

for i = 2:n

    if PVbus(i) == 1 %VC bus

        S0(i+n) = S1(i+n); %copy new Qi,Pi remains unchanged at the
specified value

    end

end
```

%##

8.2.20 calculate_jacobian.m

```matlab
function J = calculate_jacobian(S1, PVbus)

% J = calculate_jacobian(S1, PVbus) Calculate the Jacobian matrix for
loadflow

%##########################################################################
% REV 01 - global variable usage changed

%##########################################################################
% Assume that bus 1 = swing bus

% The Jacobian is initialised to full size and row and columns
corresponding

% to Voltage controlled busses deleted before returning to calling
program

% Elements are not calculated for the rows/columns to be deleted

%

% let @= voltage angle and & = admittance angle

% i and m index step from 2 to n, to access V, Ymag and Yang

% row and col step from 1 to n-1 to access the four suu matrices
making up the jacobian

% matrix as follows:

% J = [J1 J2]

%     [J3 J4]

% i = 2, m = 2 -> set row = i-1, col = m-1

% eg. 1 = 2, j = 2, row = 1, col = 1

% dp2/d@2  -> J1(1,1)   dp2/dV2** -> J2(1,1)

% dq2/d@2* -> J3(1,1)   dq2/dv2* -> J4(1,1)

% row = 2, col = 3, row = 1 col = 2

% dp2/d@3  -> J(1,2)    dp2/dV3** -> J2(1,2)

% dq2/d@3* -> J3(1,2)   dq2/dV3* -> J4(1,2) ... etc.

% * -> do not calculate if i = vc bus

% ** -> do not calculate if j = vc bus

%

% sub-functions are used to calculate the derivatives with all
parameters being passed as
```

```matlab
% follows:
% P = [ Vi, Vm, Yim, @i, @m, &im, Pi, Qi]


global V P i m n Ymag Yang



J1 = zeros(n-1); %initialise Jacobian sub-matrices leaving out row
and column for bus 1
J2 = J1;
J3 = J1;
J4 = J1;
P = zeros(1,8);  %initialise parameter matrix
for i = 2:n %loop to step through rows of Y and V
    row = i-1; %set correct index for J - (rows 1 to n-1)
    for m = 2:n %loop to step through columns of Y and V
        col = m-1; %set correct index for J
        P(1) = V(i+n);     %Vi
        P(2) = V(m+n);     %Vm
        P(3) = Ymag(i,m); %Yim
        P(4) = V(i);       %@i
        P(5) = V(m);       %@m
        P(6) = Yang(i,m); %&im
        P(7) = S1(i);      %Pi
        P(8) = S1(i+n);    %Qi
        J1(row,col) = dP_dth; %dp wrt theta - always calculated
        if PVbus(m) == 0 %If VC bus, then delta-V = 0 - do not
calculate the column in J
            J2(row,col) = dP_dV;
        end
        if PVbus(i) == 0 %For VC bus i, Qi is not known, do not
calculate this row in the jacobian
            J3(row,col) = dQ_dth;
            if PVbus(m) == 0  %Fro VC bus i, delta-V = 0, thus do not
calculate the corresponding column
                J4(row,col) = dQ_dV;
            end
        end
    end %i loop
end %m loop
J = [J1 J2; J3 J4]; %Combine submatrices to form jacobian
J = delete_blanks(J, n, PVbus);  %delete unwanted rows and columns


%################################################################
% END OF MAIN FUNCTION
%################################################################
```

```matlab
% Delete rows/columns corresponding to VC busses from J

function J = delete_blanks(J,n,PVbus)

for i = n:-1:2
    if PVbus(i)== 1
        % delete row
        J(i+n-2,:) = [];
        %delete column
        J(:,i+n-2) = [];
    end
end

%##############################################################

function dp = dP_dth()
%Calculate dP wrt theta

global P i m

if i == m
    dp = P(1)^2*P(3)*sin(P(6)); %vi^2*yim*sin&ii
    dp = -P(8) - dp; %-Qi - vi^2*yim*sin&ii
else
    dp = sin(P(5)-P(4)+P(6)); %sin(@m-@i+&im)
    dp = (-P(1))*P(2)*P(3)*dp; %-Vi*Vm*yim*sin(@m-@i+&im)
end

%##############################################################

function dp = dP_dV()
%Calculate dP wrt V

global P i m
if i == m
    dp = P(1)*P(3)*cos(P(6)); %Vi*Yii*cos(&ii)
    dp = P(7)/P(1) + dp; %Pi/Vi + %Vi*Yii*cos(&ii)
else
    dp = cos(P(5)-P(4)+P(6)); %cos(Vm -Vi + &im)
    dp = P(1)*P(3)*dp;%Vi*Yim*cos(Vm -Vi + &im)
end
```

```matlab
%##############################################################

function dq = dQ_dth()
%Calculate dQ wrt theta

global P i m
if i == m
   dq = P(1)^2*P(3)*cos(P(6)); %Vi^2*Yii*cos(&ii)
   dq = P(7) - dq; %Pi - Vi^2*Yii*cos(&ii)
else
   dq = cos(P(5)-P(4)+P(6)); %cos(Vm-Vi+&im)
   dq = (-P(1))*P(2)*P(3)*dq; %-Vi*Vm*yim*cos(Vm-Vi+&im
end


%##############################################################

function dq = dQ_dV()
%Calculate dQ wrt V

global P i m
if i == m
   dq = P(1)*P(3)*sin(P(6)); %Vi*Yii*sin(&ii)
   dq = P(8)/P(1) - dq; %Qi/Vi-Vi*Yii*sin(&ii)
else
   dq = sin(P(5)-P(4)+P(6)); %sin(Vm-Vi+&im)
   dq = (-P(1))*P(3)*dq; %-Vi*Yim*sin(Vm-Vi+&im)
end
```

8.2.21 test_motor_model.m

```matlab
function [t_final,s_final,T,Y] = test_motor_model(tstart, tstep, tstop, motor_num, odeslv, s_init)
%[t_final,s_final] = test_motor_model(tstart, tstep, tstop, motor_num, odeslv, s_init)
%Test motor model independently of loadflow
%s_init = optional initial state vector

global IM1 T Y


motor_count = 4;
v1 = [6600 0]; %Motor rms line voltage
%Initial state vector
if nargin == 5
   S0 = zeros(8,1);
else
```

```matlab
    S0 = s_init; %Load initial values
end
[MP,  MB]  =  set_motor_parameters(motor_count);  %Set  up  simtrans
parametere
tspan = [tstart:tstep:tstop];
switch motor_num
case 1
   IM1 = MP(1,:);
   ode_model = 'induction_motor_01';
case 2
   IM1 = MP(2,:);
   ode_model = 'induction_motor_01';
case 3
   IM1 = MP(3,:);
   ode_model = 'induction_motor_01';
case 4
   IM1 = MP(4,:);
   ode_model = 'induction_motor_01';
end


%Set ODE options
options = odeset('AbsTol', 1e-6, 'RelTol', 1e-5);
fprintf(1,DATESTR(NOW)); %Print start of ODE solution
switch odeslv
case 1
   [T,Y] = ode23( ode_model, tspan, S0, options, v1, IM1);
case 2
   %More efficient for transients
   [T,Y] = ode15s( ode_model, tspan, S0, options, v1, IM1);
end
fprintf(1,'\n');
fprintf(1,DATESTR(NOW)); %End of ODE solution
fprintf(1,'\n');
TRQ = calc_torque;
t_final = T(end); %Get end time
s_final = Y(end,:)'; %Get final state variables
tp3 = (2*pi)/3;
A = (T*100*pi) - (pi/6) + v1(2);
%Calculate motor stator voltages
vpk = v1(1)*sqrt(2/3);
VA = vpk*cos(A);
VB = vpk*cos(A-tp3);
VC = vpk*cos(A+tp3);
```

```matlab
%Input Power
PWR = ((VA.*Y(:,1))+(VB.*Y(:,2))+(VC.*Y(:,3)))/1e3; %kW
VAR     =      -(VA.*(Y(:,2)-Y(:,3))+VB.*(Y(:,3)-Y(:,1))+VC.*(Y(:,1)-
Y(:,2)))/(1e3*sqrt(3));
ISTAT  =  sqrt((1/3)*(Y(:,1).^2+Y(:,2).^2+Y(:,3).^2));  %Stator  rms
current
%Calculate torque

%Plot Data
yy = 350;
xx = tstop;
figure(1);
subplot(3,1,1);
h = plot(T,Y(:,1));
legend('stator current - phase a');
xlabel('time (s)');
grid on;
axis([0 xx -yy yy]);
set(h,{'Color'},{'r'});
subplot(3,1,2);
h=plot(T,Y(:,2));
legend('stator current - phase b');
xlabel('time (s)');
grid on;
axis([0 xx -yy yy]);
set(h,{'Color'},{'b'});
subplot(3,1,3);
h=plot(T,Y(:,3));
legend('stator current - phase c');
xlabel('time (s)');
set(h,{'Color'},{'g'});
grid on;
axis([0 xx -yy yy]);

figure(2);
% Plot Stator and rotor current
plot(T,ISTAT,'r');
legend('Is (rms)');
xlabel('time (s)');
grid on;
figure(3);
% Plot Active and Reactive Power
plot(T,PWR, '-r',T,VAR);
legend('kW', 'kVAr');
```

```matlab
xlabel('time (s)');
grid on;
% Plot motor torque and speed
figure(4)
plot(T,Y(:,8)/(IM1(11)*314.1592));
xlabel('time (s)');
legend('rotor speed');
grid on;
figure(5);
plot(T,TRQ,'-r');
xlabel('time (s)');
legend('rotor torque');
grid on;


%##################################################################
#################

function TRQ = calc_torque()
%Calculate motor inst. torque

global IM1 T Y

points = size(T,1);
TRQ = zeros(points,1);
for index = 1:points
    MC = Y(index,1:6); %get currents
    r_angle = Y(index,7);
    G = calculate_G(r_angle, IM1);
    TRQ(index) = (IM1(11)/2)*MC*G*MC';
end




%##################################################################
#################
% This function is only needed in the induction motor ODE solver
program when calculating
% system transient response - only used in the test program to
calculate instantaneous motor
% torque for plotting


function G = calculate_G(rotor_angle, MP)
% G = calculate_rotational_inductance_matrix(rotor_angle, MP)
% rotor_angle = rotor electrical angle
% MP(1) = Lsl = Stator leakage inductance - not used here
```

```matlab
% MP(2) = Lsm = Stator mutual inductance - not used here
% MP(3) = Lsrm = Stator/rotor mutual inductance
% MP(4) = Lrm = rotor mutual inductance - not used here
% MP(5) = Lrl = rotor leakage inductance - not used here


TWOpi3 = (2*pi)/3;


G = zeros(6); %Create empty array
temp = -MP(3) * sin(rotor_angle);
for i = 1:3
    G(i,i+3) = temp; %Gsr diagonal
    G(i+3,i) = temp; %Grs diagonal
end
% Calc Gsr and Grs off diagonal elements for rotor angle - 120
temp = -MP(3) * sin(rotor_angle - TWOpi3);
G(1,6) = temp;
G(2,4) = temp;
G(3,5) = temp;
G(4,2) = temp;
G(5,3) = temp;
G(6,1) = temp;
%Calc Gsr & Grs off diagonal elements for theta + 120
temp = -MP(3) * sin(rotor_angle + TWOpi3);
G(1,5) = temp;
G(2,6) = temp;
G(3,4) = temp;
G(4,3) = temp;
G(5,1) = temp;
G(6,2) = temp;
```

8.2.22 induction_motor_01.m

```matlab
function  dS = induction_motor_01(t, S, flag, v_mot, MP)
% ODE Function to simulate induction motor performance
% abc reference frame model:
% Does not model saturation
% Models friction and windage with a constant torque proportional to
speed^2
%################################################################
% Rev | Comment
% ----+----------------------------------------------------------
% 00  | Corrected error in friction and windage torque calculation
% 01  | Added function to reduce rotor resistance and increase rotor
%     | reactance as a function of slip to give approximation of a
```

```
%      | double cage rotor
%################################################################
% Use with ODE solver as follows:
% [T,Y] = odeXX( 'induction_motor_01', tspan, S1_IM1, options, vbus,
MP(1,:));
%
% tspan = [t0 tfinal]
% S = motor model state variables
% S = [isa; isb; isc; ira; irb; irc; rotor_angle; rotor_speed]
% S(1,1) = isa - stator currents
% S(2,1) = isb
% S(3,1) = isc
% S(4,1) = ira - rotor currents
% etc
% S(7,1) = rotor_angle is in radians
% S(8,1) = rotor_speed is in rad/sec
%
% flag - used to set ODE solver return values:
% '' = F(t,S) (emply flag)
%
% v_mot = rms line voltage and phase angle on motor connection bus
from loadflow
%
%
% MP = motor model parameters
% All inductance and resistance values are in MKSA units
% MP = [Lsl, Lsm, Lsrm, Lrm, Lrl, Rs, Rr H, LC, LT, P, Tf, tds, tde,
dt, dp1, dp2]
% MP(1) = Lsl = Stator leakage inductance
% MP(2) = Lsm = Stator mutual induxctance
% MP(3) = Lsrm = Stator/rotor mutual inductance - set according to
model
%           Vas gives Lsrm = 2/3Lsm = 2/3Lrm
% MP(4) = Lrm = rotor mutual inductance
% MP(5) = Lrl = rotor leakage inductance
% MP(6) = Rs = stator resistance
% MP(7) = Rr = rotor resistance
% MP(8) = H = inertia constant
% MP(9) = L = load constant
% MP(10) = LT = load type: 1=load proportional to speed
%                          2=load proportional to speed^2
% MP(11) = number of pole pairs
% MP(12) = Torque due to friction and windage at rated speed.
% MP(13) = Rotor resistance variation factor
% MP(14) = Rotor reactance variation factor
```

```matlab
% MP(15) to MP(21) = not used
%###############################################################

global TWOpi3

if isempty(flag)
    %Return dS/dt = F(t,S)
    TWOpi3 = 2*pi/3;
    %Keep rotor angle value between zero and 2*pi
    rotor_angle = S(7,1);
    if rotor_angle > (2*pi)
        rotor_angle = rotor_angle - (2*pi);
    end
    % Make adjustment to rotor resistance and reactance to account for
    % double cage rotor
    sync_spd = 100*pi/MP(11);
    slip = (sync_spd - S(8))/sync_spd;
    % Adjust rotor resistance
    MP(7) = MP(7)*(1 + (MP(13)*slip));
    % Adjust rotor reactance
    MP(5) = MP(5)*(1 - (MP(14)*slip));
    I = S(1:6,1); %Extract rotor and stator currents
    V = calculate_voltage_vector(v_mot,t);
    L = calculate_inductance_matrix(rotor_angle, MP);
    G = calculate_rotational_inductance_matrix(rotor_angle, MP);
    R = create_resistance_matrix(MP);
    Linv = inv(L); %Invert inductance matrix
    %Calculate [V] - [R]*[I]
    dI = V - R*I;
    %Calculate [V]-[R][I]-rotor_speed*[G][I]
    dI = dI - (S(8)*G*I);
    %Calculate dI = 1/[L]*([V]-[R][I]-rotor_speed*[G][I])
    dI = Linv * dI;
    % rate of change of rotor angle = rotor speed
    % thus d/dt rotor_angle = rotor speed
    % calculate and return d/dt rotor_speed
    rotor_accel = calc_rotor_acceleration(I,G,S(8,1),MP);
    dS = [dI; S(8,1); rotor_accel];
else
    %The flag argument is not used
    error('Motor model requires initial values');
end
```

```
%###################################################################
% END OF MAIN FUNCTION
%###################################################################


function dw = calc_rotor_acceleration(I,G,rotor_speed,MP)
% Calculate rotor acceleration
% Note to take pole pairs into account - multiply Te by the number
% of pole pairs (MP(11). Since rotor speed in electrical radians, the
load
% torque calculations must also take pole pairs into account
% Friction and windage loss torque is assumed to increase with the
square of the
% rotor speed up to the maximum value given by MP(12). To simplify
the calculation
% it is assumed that the maximum speed = synchronous speed, thus the
friction and
% windage torque is not strictly accurate since it would be
determined at motor
% rated speed. The value is an estimate, so slight error does not
really mattter

% Calculate airgap electrical torque = 1/2*P*I'*G*I (Vas)
Te = (MP(11)/2)*I'*G*I;
% Calculate friction and windage torque
Tfw = MP(12)*((rotor_speed)/(100*pi))^2;
%Calculate load torque
switch MP(10)
case 1
    % Load proportional to speed * load constant
    Tl = MP(9) * (rotor_speed/MP(11));
case 2
    % Load proportional to speed^2
    Tl = MP(9) * (rotor_speed/MP(11))^2;
end
%Calculate acceleration = (Te - Tl)/(2*H) where H = MP(8) = inertia
constant
dw = (Te- Tfw - Tl)/(2*MP(8));



%###################################################################


function V = calculate_voltage_vector(v,t)
% Calculate instantaneous motor voltages
```

```matlab
% It is assumed that the motor is connected in star. v = the rms line
voltage at the
% motor connection bus. The 30degree phase shift between Vline and
Vphase is taken
% into account here and the phase (l-g) p-p voltage used in the model
is calculated
% The phase voltage lags the line voltage by 30deg(pi/6) This is
subtracted from the
% loadflow voltage angle to get the actual phase voltage angle.
% Vphase = Vline/sqrt(3) and Vpp = Vphase*sqrt(2)


global TWOpi3


V = zeros(6,1);
v_angle = v(2)-(pi/6); %Voltage angle from loadflow - 30degrees
% a = instantaneous bus voltage angle
a = (100 * pi * t)+ v_angle;
vpeak = v(1)*sqrt(2/3);
V(1,1) = vpeak*cos( a );
V(2,1) = vpeak*cos( a - TWOpi3);
V(3,1) = vpeak*cos( a + TWOpi3);




%################################################################


function L = calculate_inductance_matrix(rotor_angle, MP)
% L = calculate_inductance_matrix(S(3), MP) - calculate motor
inductance matrix
% MP(1) = Lsl = Stator leakage inductance
% MP(2) = Lsm = Stator mutual inductance
% MP(3) = Lsrm = Stator/rotor mutual inductance - this is set
accoring to model
% MP(4) = Lrm = rotor mutual inductance
% MP(5) = Lrl = rotor leakage inductance


global TWOpi3


L = zeros(6); %Create empty array
temp = MP(1) + MP(2); % Lsm + Lsl - Smith/chen
for i = 1:3
    L(i,i)=temp; %Lss diagonal elements
end
temp = MP(4) + MP(5); %Lrm + Lrl - Smith/Chen
for i = 4:6
    L(i,i) = temp; %Lrr diagonal
end
```

```matlab
temp = -MP(2)/2; %Lss off diagonal elements = -Lsm/2
for i = 1:3
    for j = 1:3
        if i ~= j
            L(i,j) = temp;
        end
    end
end
temp = -MP(4)/2; %Lrr off diagonal elements = -Lrm/2
for i = 4:6
    for j = 4:6
        if i ~= j
            L(i,j) = temp;
        end
    end
end
temp = cos(rotor_angle)* MP(3); %cos(@)*Lsrm
for i = 1:3
    L(i,i+3) = temp; %Lsr diagonal
    L(i+3,i) = temp; %Lrs diagonal
end
% Calc Lsr off diagonal elements
temp = cos(rotor_angle - TWOpi3)*MP(3);
L(2,4) = temp;
L(3,5) = temp;
L(1,6) = temp;
L(4,2) = temp;
L(5,3) = temp;
L(6,1) = temp;
temp = cos(rotor_angle + TWOpi3)*MP(3);
L(1,5) = temp;
L(2,6) = temp;
L(3,4) = temp;
L(4,3) = temp;
L(5,1) = temp;
L(6,2) = temp;


%################################################################

function G = calculate_rotational_inductance_matrix(rotor_angle, MP)
% G = calculate_rotational_inductance_matrix(rotor_angle, MP)
% rotor_angle = rotor electrical angle
% MP(1) = Lsl = Stator leakage inductance - not used here
```

```matlab
% MP(2) = Lsm = Stator mutual inductance - not used here
% MP(3) = Lsrm = Stator/rotor mutual inductance
% MP(4) = Lrm = rotor mutual inductance - not used here
% MP(5) = Lrl = rotor leakage inductance - not used here

global TWOpi3

G = zeros(6); %Create empty array
temp = -MP(3) * sin(rotor_angle);
for i = 1:3
   G(i,i+3) = temp; %Gsr diagonal
   G(i+3,i) = temp; %Grs diagonal
end
% Calc Gsr and Grs off diagonal elements for rotor angle - 120
temp = -MP(3) * sin(rotor_angle - TWOpi3);
G(1,6) = temp;
G(2,4) = temp;
G(3,5) = temp;
G(4,2) = temp;
G(5,3) = temp;
G(6,1) = temp;
%Calc Gsr & Grs off diagonal elements for theta + 120
temp = -MP(3) * sin(rotor_angle + TWOpi3);
G(1,5) = temp;
G(2,6) = temp;
G(3,4) = temp;
G(4,3) = temp;
G(5,1) = temp;
G(6,2) = temp;


%####################################################################

function R = create_resistance_matrix(MP)
% Create resistance matrix using Rs and Rr

R = eye(6);
Rs = R(1:3,:)*MP(6); %Enter Rs values into array
Rr = R(4:6,:)*MP(7); %Enter Rr values into array
R = [Rs;Rr]; %Form complete matrix
```

8.2.23 induction_motor_03.m

```matlab
function  dS = induction_motor_03(t, S, flag, v_mot, MP)
% ODE Function to simulate induction motor performance
```

```
% Simplified Equivalent Circuit d-q model cf Arrilaga pg. 212
% Does not model saturation
%
####################################################################
% Rev | Comment
% ----+--------------------------------------------------------
% 00  | Initial version
%
####################################################################
% Use with ODE solver as follows:
% [T,Y] = solver('induction_motor_01', tspan , Y0,'',busdata, MP)
%
% tspan = [t0 tfinal]
% S = motor model state variables
% S = [ E'r; E'm; S; ]
%  S(1,1) = E'r - Thevinin  equivalent  circuit  voltage  (real  axis
component)
% S(2,1) = E'm - Thevinin equivalent circuit voltage (imaginary axis
component)
% S(3,1) = Slip
%
% flag - used to set ODE solver return values:
% '' = F(t,S) (emply flag)
%
% v_mot = [Vbus V_angle] where Vbus = rms l-l Bus voltage(kV)
%
% MP = motor model parameters in MKSA
%
% MP = [X', T'o, Xo, R1, Hm, L, LT, tds, tde, dt, dp1, dp2]
% MP(1) = X': Transient reactance
% MP(2) = T'o: open circuit time constant
% MP(3) = Xo: open circuit reactance
% MP(4) = R1: Stator resistance
% MP(5) = Hm = inertia constant
% MP(6) = L = load constant
% MP(7) = LT = load type: 1=load proportional to speed
%                         2=load proportional to speed^2
% MP(8) = Disturbance start time - not used
% MP(9) = Disturbance end time - not used
% MP(10) = Disturbance type - not used
% MP(11) = Distrubance parameter 1 - not used
% MP(12) = Disturbance parameter 2 - not used
% MP(13) = Motor base MVA
% MP(14) - MP(21) are not used for this model
```

```matlab
if isempty(flag)
   %Return dS/dt = F(t,S)
   % Use variables Vr,Vm, wo to simplify code


   temp = v_mot(1) / sqrt(3); %convert to phase voltage
   Vr = temp*cos(v_mot(2));
   Vm = temp*sin(v_mot(2));
   wo = 100*pi; %omega_o
   % Ir = (R1(Vr-E'r)+X'(Vm-E'm))/(R1^2+X'^2)
   Ir = ((MP(4)*(Vr-S(1,1)))+(MP(1)*(Vm-S(2,1))))/(MP(4)^2+MP(1)^2);
   % Im = (Vm-E'm-X'Ir)/R1
   Im = (Vm-S(2,1)-(MP(1)*Ir))/MP(4);
   %temp = X0-X'
   temp = MP(3)-MP(1);
   %dE'r/dt=2*pi*fo*S*E'm-(E'r+(X0-X')Im)/T'o
   dEr = wo*S(3,1)*S(2,1)-(S(1,1)+(temp*Im))/MP(2);
   %dE'm/dt=-2*pi*fo*E'r-(E'm-(X0-X')Ir)/T'o
   dEm = -wo*S(3,1)*S(1,1)-(S(2,1)-(temp*Ir))/MP(2);
   % Electrical torque Te
   Te = ((S(1,1)*Ir)+(S(2,1)*Im))/wo;
   % Mechanical torque
   if MP(7) == 1
      Tm = MP(6)*wo*(1-S(3,1)); %load proportional to speed (fan)
   else
      Tm = MP(6)*(wo*(1-S(3,1)))^2; %Load prop. to speed^2 (pumps)
   end
   % Slip
   %dSl/dt = (Tm-Te)/2*Hm
   dSl = (Tm-Te)/(2*MP(5));
   dS = [dEr; dEm; dSl;];
else
   % Flag argument not used
   error('Model requires initial values');
end
```

8.2.24 sync_gen_model_01.m

```matlab
function dS = sync_gen_model_01 (t, S, flag, GP, Vref, Vd, Vq, Pref )
% ODE Function to simulate synchronous generator
% Implements d-q model with d and q axis transient effects
% IEEE Type I AVR model used with exciter saturation taken into
account
```

```
%
%
######################################################################
###
%  Rev | Comment
% -----+--------------------------------------------------------------
----
% 00  | Initial version - used for debugging
% 01  | Minor changes to input parameters and calculation of Pe
corrected
% 02  | AVR changed to reduce field when bus voltage low
% 03  | Governor functions added
% 04  | Limits added to governor function and swing equation
parameters
%     | corrected
% 05  | Governor function changed Pref added to argument list
% 06  | Changed governor time constant
%
######################################################################
###


% Use with ODE solver as follows:
% [T,Y] = solver('sync_gen_model_01', tspan, Y0, '', GP, Pm, Vref,
Vd, Vq)
%
% GP = generator model parameters
% GP = [Rs Xd X'd T'do Xq X'd T'qo]
% Vref = voltage setpoint
% Vd, Vq =  generator d-q terminal voltage
% Pref = Generator power reference setting
% tspan = [t0 tfinal]
% Y0 = initial state variable values
%
% S = model state variables (Note all quantities are in pu)
% S = [E'd; E"d; E'q; E"q; delta_e; omega_e; X1; X2; Efd; X5; X6]
% S(1,1) = E'd - d-axis transient rms voltage
% S(2,1) = E'q - q-axis transient rms voltage
% S(3,1) = delta_e - rotor elect angle wrt ref frame rotating at
synchronous speed
% S(4,1) = omega_e - rotor elect angular speed wrt to rotating
reference frame
% S(5,1) = X1 - AVR internal variable (Stator voltage after input
filter)
% S(6,1) = X2 - AVR internal variable (Regulator amplifier ouput)
% S(7,1) = Efd - AVR output (Field voltage)
% S(8,1) = X4 - AVR internal variable (Feedback signal)
% S(9,1) = Pm - Mechanical input power - controlled by governor
%
```

```matlab
% flag - used to set ODE solver return value: '' = F(t,S) (empty
flag)
%
%###################################################################



%###################################################################
% Main function
%###################################################################


if isempty(flag)
    % Calculate Id, Iq
    % temp = (r^2+xd'*xq')
    temp = GP(3)*GP(6)+GP(1)^2;
    % Id = (r(E'd-Vd)+x'q(Vq-E'q))/temp
    Id = (GP(1)*(S(1,1)-Vd)+GP(6)*(Vq-S(2,1)))/temp;
    % Iq = (E'd-Vd-r*Id)/x'q
    Iq = (S(1,1)-Vd-GP(1)*Id)/GP(6);
    % d-axis transient voltage E'd
    % dE'd/dt = (-E'd-(xq-xq')Iq)/T'q0
    dEd_t = (-S(1,1)-((GP(5)-GP(6))*Iq))/GP(7);
    % q-axis transient voltage E'q
    % dE'q/dt = (Efd-E'q+(xd-x'd)Id)/T'd0
    % Note Efd is multiplied by a scaling factor of 0.9436 when used
in the
    % generator model equation
    dEq_t = ((S(7,1)*0.9436)-S(2,1)+((GP(2)-GP(3))*Id))/GP(4);
    % AVR model
    %dX1/dt = (Vs - X1)/Tr, where Vs = stator RMS voltage
    Vs = abs(complex(Vd,Vq)); %Get rms magnitude of stator voltage
    dX1 = (Vs - S(5,1))/0.02; % TR = 0.02
    % dX2/dt = (KA(Vref-X1-X4)-X2)/Ta
    dX2 = ((Vref-S(5,1)-S(8,1))*1762-S(6,1))/0.04; %KA = 1762, TA =
0.04
    if (S(7,1)> 17.5) & (dX2 > 0)
        dX2 = 0; %Efd has reached the positive limit
    end
    if (S(7,1)< -14) & (dX2 < 0)
        dX2 = 0; %Efd has reached the negative limit
    end
    % Calculate the saturation function SE
    if S(7,1) > 4.06
        %Use SE2
        SE = ((0.2292*S(7,1))-1)*S(7,1);
```

```matlab
    else
        %Use SE1
        SE = S(7,1)^2*0.4757;
    end
    %dEfd/dt = (X2-SE-KE*Efd)/TE
    temp = S(6,1)-SE-S(7,1); %X2-SE-KE*Efd
    dEfd = temp/1.95; %TE = 1.95
    %dX4/dt = 1/TF(-X4+(KF/TE)(-KE*Efd+X2-SE))
    dX4 = (0.05528*temp-S(8,1))/5; %TF=5
    % Electrical power output
    % Pe = (VdId+VqIq)
    Pe = (Vd*Id)+(Vq*Iq);
    % Swing equation
    % dw_e/dt = 1/M(Pm-Pe) where 1/M = fo*pi/H = 50*pi/4.55 = 34.523
    d_omega_e = 34.523*(S(9,1)-Pe);
    d_delta_e = S(4,1);
    % Governor DE
    % dPm/dt = (Pref-Pm-omega*Kg)/Tg
    % The governor model is a simple approximation of a typical
governor model
    % this was used in the absence of any detailed information on the
generator
    % This approximates the governor and turbine response. Kg = 25, Tg
= 5
    % Tg increased from estimated 2.4 to 7 to give more reasonable
response
    % Limit the power output between 0 and 1.1pu
    d_Pm = (Pref - S(9,1) - S(4,1)*25)/4;
    if (S(9,1) < 0) & (d_Pm < 0)
        d_Pm = 0;
    end
    if (S(9,1) > 1.1) & (d_Pm > 0)
        d_Pm = 0;
    end
    dS = [dEd_t; dEq_t; d_delta_e; d_omega_e; dX1; dX2; dEfd; dX4;
d_Pm];
else
    % The flag argument is not used
    error('Generator model does not use the flag argument')
end
```

9 Appendix C: MACHINE DATA AND PARAMETER ESTIMATES

9.1 Induction Motor Data

Table 9-1 300kW 6.6kV Induction motor data

Nameplate Data			24PC101	
Power (kw)	300	Voltage (V)	6600	
Current (A)	30	Speed (rpm)	2976	
cosφ	0.91	Starting current ratio I_a/I_n	5.85	
Starting torque ratio M_a/M_n	0.9	Pull-out torque ratio M_k/M_n	2.4	

Test Data				
	Phase			
	u	v	w	
Stator Resistance (Ω)	1.646	1.648	1.65	
No-load Test				
Voltage (V)	6636			
Current (A)	6.3			
Input power (kw)	8.89			
cosφ				
Locked Rotor Test				
Voltage (V)	3845			
Current (A)	90.9	89.6	90.5	
Power(kW)	105.5			

Load Test	Voltage	Current	Pout (kw)	Pin (kVA)	cosφ	Slip(rpm)
125% load	6642	38.1	392	438.3	0.75	20.7
100% load	6655	30.2	312.7	348.1	0.9	19.8
75% load	6602	22.9	235.3	261.9	0.9	14.4
50% load	6616	15.8	156.7	181.1	0.87	9.6
25% load	6616	9.6	78.5	110	0.71	4.5
0% load	6636	6.34	8.9	72.9	0.12	
	Time after switch-off					
	1min	2min	4min	6min	8min	
Stator Resistance - hot (Ω)	2.148	2.141	2.125	2.11	2.097	
	Load(%)					
Losses	104	99.5	74.2	48.6	23	
Friction & Windage (kW)	8.755	8.755	8.755	8.755	8.755	
Copper Loss (kW)	4.498	2.826	1.625	0.774	0.286	
Additional Loss (kW)	1.645	1.569	1.177	0.784	0.392	
Rotor Loss (kW)	2.167	1.984	1.074	0.469	0.104	
Output: (kW)	311.9	298.6	222.7	145.9	68.9	
Efficiency (%)	94.81	95.18	94.63	95.32	87.85	
cosφ	0.75	0.9	0.9	0.87	0.71	

Mechanical Data				
Stator Length (mm)	535	Stator inside diameter (mm)	350	
Rotor Length (mm)	534	Rotor outside diameter (mm)	343.988	
Calculated Airgaps (mm)	3.006	Rotor Inertia (kgm^2)	6.3	
(per side)		Load power input (kW)	246.4	

Based on the nameplate data, the following parameters were calculated:

Table 9-2 300kW motor parameters based on nameplate data

Nameplate Data		
Rated Power (Pn)	300000	W
Terminal Voltage (Vt)	3811	V
Full load Current (Ifl)	30	A
eff	0.9518	
pf	0.91	
Pole Pairs	1	
Full Load Speed	2976	rpm
Friction & Windage loss	2.91	%
No-load current	6.3	A
No-load input power	8890	W
Calculated Data		
Power (shaft)	297076.6726	W
Slip	0.008	
Synchronous Speed (rpm)	3000	rpm
Full load torque	953.2504219	Nm
Airgap Power	308187.1006	W
Rotor Copper Loss	2465.496805	W
Stator Input Power	312120.9	W
Stator Losses	3933.799402	W
Rotor power	305721.6038	W
Equivalent Circuit Parameters		
Stator Resistance: Rs	1.456962741	Ohm
Rotor Resistance: Rr	0.913146965	Ohm
Nema Class B		
Stator reactance: Xs	21.06762715	Ohm
Rotor reactance: X'r	31.60144073	Ohm
Magnetising reactance Xm	579.2277716	Ohm
Stator inductance: Ls	0.06706034	H
Rotor inductance: Lr	0.10059051	H
Magnetising inductance: Lm	1.84373926	H

Table 9-3 850kW 6.6kV Induction motor data

Nameplate Data			24PC102	
Power (kw)	850	Voltage (V)	6600	
Current (A)	86	Speed (rpm)	2971	
cosφ	0.91	Starting current ratio I_a/I_n		
Starting torque ratio M_a/M_n		Pull-out torque ratio M_k/M_n		

Test Data				
	Phase			
	u	v	w	
Stator Resistance (Ω)	0.6856	0.6850	0.6850	
No-load Test				
Voltage (V)	6629			
Current (A)	16.36	16.07	17.22	
Input power (kw)	19.22			
cosφ				
Locked Rotor Test				
Voltage (V)				
Current (A)				
Power(kW)				

Load Test	Voltage	Current	Pout (kw)	Pin (kVA)	cosφ	Slip(rpm)
125% load						
100% load						
75% load						
50% load						
25% load						
0% load						
	Time after switch-off					
	1min	2min	4min	6min	8min	
Stator Resistance - hot (Ω)						
	Load(%)					

Losses					
Friction & Windage (kW)					
Copper Loss (kW)					
Additional Loss (kW)					
Rotor Loss (kW)					
Output: (kW)					
Efficiency (%)					
cosφ					

Mechanical Data				
Stator Length (mm)	600	Stator inside diameter (mm)	370	
Rotor Length (mm)	600	Rotor outside diameter (mm)	364	
Calculated Airgaps (mm)	3	Load power input (kW)	654	

Table 9-4 550kW Motor parameters based on nameplate data

Nameplate Data		
Rated Power (Pn)	550000	W
Terminal Voltage (Vt)	3811	V
Full load Current (Ifl)	56	A
eff	0.95	
pf	0.91	
Pole Pairs	1	
Full Load Speed	2968	rpm
Friction & Windage loss	2.14	%
No-load current	13.31	A
No-load input power	12130	W
Calculated Data		
Power (shaft)	553494.396	W
Slip	0.010666667	
Synchronous Speed (rpm)	3000	rpm
Full load torque	1780.822825	Nm
Airgap Power	571434.4772	W
Rotor Copper Loss	6095.30109	W
Stator Input Power	582625.68	W
Stator Losses	11191.20284	W
Rotor power	565339.1761	W
Equivalent Circuit Parameters		
Stator Resistance: Rs	1.189541118	Ohm
Rotor Resistance: Rr	0.647884895	Ohm
Nema Class B		
Stator reactance: Xs	11.28622883	Ohm
Rotor reactance: X'r	16.92934325	Ohm
Magnetising reactance Xm	274.1287387	Ohm
Stator inductance: Ls	0.035925182	H
Rotor inductance: Lr	0.053887773	H
Magnetising inductance: Lm	0.872578876	H

Table 9-5 550kW 6.6kV Induction motor Data

Nameplate Data			24KC101	
Power (kw)	550	Voltage (V)	6600	
Current (A)	56	Speed (rpm)	2968	
$\cos\varphi$	0.91	Starting current ratio I_a/I_n	5.53	
Starting torque ratio M_a/M_n	0.95	Pull-out torque ratio M_k/M_n	2.3	

Test Data				
	Phase			
	u	v	w	
Stator Resistance (Ω)	1.229	1.229	1.230	
No-load Test				
Voltage (V)	6657			
Current (A)	12.31			
Input power (kw)	12.13			
$\cos\varphi$				
Locked Rotor Test				
Voltage (V)	3305			
Current (A)	106.5			
Power(kW)	128.9			

Load Test	Voltage	Current	Pout (kw)	Pin (kVA)	cosj	Slip(rpm)
125% load	6593	73	700.0	833.6	0.84	250
100% load	6643	57	570.6	655.8	0.88	183
75% load	6640	42.9	434.7	493.4	0.88	137
50% load	6642	29.7	289.7	341.7	0.85	91
25% load	6639	18.1	115.0	208.1	0.70	44
0% load	6657	12.31	12.1	141.9	0.09	

	Time after switch-off					
	1min	2min	4min	6min	8min	
Stator Resistance - hot (Ω)	1.615	1.613	1.607	1.603	1.599	
	Load(%)					
Losses	120.3	98.6	75.1	49.7	23.9	
Friction & Windage (kW)	11.789	11.789	11.789	11.489	11.789	
Copper Loss (kW)	11.981	7.305	4.138	1.983	0.737	
Additional Loss (kW)	3.5	2.853	2.173	1.449	0.725	
Rotor Loss (kW)	11.212	6.365	3.249	1.318	0.303	
Output: (kW)	661.5	542.3	413.3	273.2	131.4	
Efficiency (%)	94.5	95.04	95.09	94.29	90.65	
$\cos\varphi$	0.84	0.87	0.88	0.85	0.7	

Mechanical Data				
Stator Length (mm)	530	Stator inside diameter (mm)	330	
Rotor Length (mm)	530	Rotor outside diameter (mm)	327.3	
Calculated Airgaps (mm)	1.35	Rotor inertia (kgm^2)	5	
		Load power input (kW)	504	

Table 9-6 850kW Motor parameters based on nameplate data

Nameplate Data		
Rated Power (Pn)	850000	W
Terminal Voltage (Vt)	3811	V
Full load Current (Ifl)	86	A
eff	0.95	
pf	0.91	
Pole Pairs	1	
Full Load Speed	2971	rpm
No-load current	16.5	A
No-load input power	19220	W
Calculated Data		
Power (shaft)	850009.3	W
Slip	0.009667	
Synchronous Speed (rpm)	3000	rpm
Full load torque	2732.074	Nm
Airgap Power	866889.3	W
Rotor Copper Loss	8379.93	W
Stator Input Power	894746.6	W
Stator Losses	27857.31	W
Rotor power	858509.3	W
Equivalent Circuit Parameters		
Stator Resistance: Rs	1.25551229	Ohm
Rotor Resistance: Rr	0.37767845	Ohm
Nema Class B		
Stator reactance: Xs	7.349172	Ohm
Rotor reactance: X'r	11.02376	Ohm
Magnetising reactance Xm	222.4186	Ohm
Stator inductance: Ls	0.023393	H
Rotor inductance: Lr	0.03509	H
Magnetising inductance: Lm	0.70798	H

9.2　Main Plant Generator Data

Table 9-7 Main Plant Generator Data

Parameter Description	Value
Output (base)	140[1]@0.8pf
Rated Voltage (kV)	11
Rated speed (rpm)	3000
Machine type	Round rotor
Reactances (pu on machine base)	
Synchronous (Xd) sat/unsat	-/1.99
Transient (X'd) sat/unsat.	0.17/0.22
Sub-transient (X''d) sat/unsat	0.12/0.17
Synchronous (Xq)	1.84
Sub-transient (X''q)	0.12
Stator resistance (Ra)	
Negative sequence reactance (X2)	0.17
Zero sequence reactance (X0)	0.087
Stator stray synchronous reactance (Xl)	0.13
Time constants (sec)	
D-axis, open circuit transient (T'do)	9.5
D-axis, short circuit transient (T''d)	0.69
D-axis, short circuit sub-transient (T''q)	0.017
Armature short circuit (T'a)	0.34
Inertia	
Inertia constant (set)(H) $\left(kWs/kVA \right)$	3.25

---

[1] Exact value = 139.421MVA

Table 9-8 Exciter and AVR parameters

Parameter Description	Value
Exciter Rated Voltage and Current @ rated terminal output	
Voltage (V)	185
Current (A)	1710
Ceiling voltage (% of rated voltage)	195
AVR Parameters	
T_r (s)	0.02
K_a	1762
T_a (s)	0.04
$V_{r\,max}$ (V)	17.5
$V_{r\,min}$ (V)	-14
$E_{fd\,max}$ (V)	5.41
$E_{fd\,min}$ (V)	0
$E_{fd\,0.75}$ (V)	4.06
K_f	0.1078
K_e	1
T_e (s)	1.95
SE_{max}	2.24
$SE\,0.75_{max}$	1.93
1 p.u. E_{fd} (V)	66.54

Table 9-9 Generator Open Circuit Test

Stator Volts A-B	Stator Volts A-B	Rotor Current	x_{afd} (Ω)
1244	1236	70	25.1
2490	2485	134	26.2
3357	3353	174	27.3
5113	5110	269	26.9
6441	6440	339	26.9
8262	8263	440	26.6
9469	9471	513	26.1
11114	11116	627	25.1
12418	12419	754	23.3
13954	13952	1037	19.0

9.2.1 Scaling factor between generator and AVR pu systems

In the generator model, it is assumed that 1p.u. field voltage will result in 1p.u. generator terminal voltage. Since the AVR and generator p.u systems differ, a scaling factor is required to convert from the one to the other.

The rotor field resistance is calculated from the exciter rated voltage and current as:

$$r_{fd} = \frac{185V}{1710A} = 0.10817\Omega$$

The stator open circuit rms voltage E_{fd} is related to the exciter voltage v_{fd} by equation (2-120) as:

$$v_{fd}\left(\frac{\sqrt{\frac{3}{2}}x_{afd}}{r_{fd}}\right) = \sqrt{3}E_{fd}$$

From Table 9-9 data, the mutual rotor-stator reactance is estimated $x_{afd} = 26.8\ \Omega$ giving the following:

$$E_{fd} = 175.91 \cdot v_{fd}$$

Thus for rated stator voltage of 11kV, a field voltage of

$$v_{fd} = \frac{E_{fd}}{175.91} = \frac{11kV}{175.91} = 62.79V$$

is required. Now 1p.u. field voltage is 66.54V, thus 1p.u. field voltage needs to be multiplied by a factor of:

$$\frac{62.79}{66.54} = 0.9436$$

Thus the AVR model field voltage must be multiplied by 0.9346 before being used in the generator model equations.

10 Appendix D: INDUCTION MOTOR MODELS – ADDITIONAL DATA

10.1 Derivation Of Equation (2-27)

By implication, the derivatives of these inductances with respect to time are present in the machine equations. Substitution of equation (2-21) into equation (2-20) gives the following [22]:

$$
\begin{aligned}
[V] &= [R][I] + p[L][I] \\
&= [R][I] + \frac{d[L]}{dt}[I] + [L]\frac{d[I]}{dt} \\
&= [R][I] + \frac{d[L]}{d\theta} \cdot \frac{d\theta}{dt} + [L]\frac{d[I]}{dt} \\
&= [R][I] + \omega_r \frac{d[L]}{d\theta} + [L]\frac{d[I]}{dt}
\end{aligned}
\tag{10-1}
$$

10.2 Derivation Of Equation (2-46)

The Thevenin equivalent circuit is determined for the portion of the circuit to the left of A-A, in Figure 2-8 with the Thevenin equivalent voltage being given by E_{TH} in Figure 10-1:
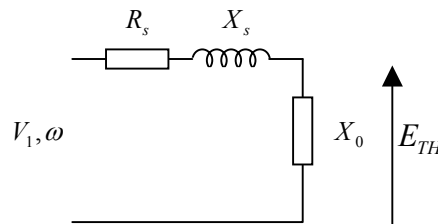
Figure 10-1 Derivation of Thevenin equivalent circuit

The Thevenin voltage is given by [16]:

$$
E_{TH} = \frac{V_1 jX_0}{R_s + j(X_s + X_0)}
\tag{10-2}
$$

The Thevenin impedance is:

$$
\begin{aligned}
Z_{th} &= \frac{E_{TH}}{I_{sc}} \qquad I_{sc} = \frac{V_1}{R_s + jX_s} \\
Z_{th} &= \frac{V_1 jX_0}{R_s + j(X_s + X_0)} \cdot \frac{R_s + jX_s}{V_1} \\
&= \frac{jX_0(R_s + jX_s)}{R_s + j(X_s + X_0)} \\
&= R_{TH} + jX_{TH}
\end{aligned}
\tag{10-3}
$$

Where I_{sc} is the 'short circuit' current that would flow if X_0 was equal to zero.

This gives the equivalent circuit shown in Figure 10-2:
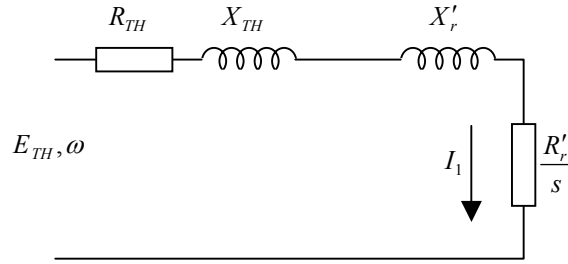
Figure 10-2 Thevenin equivalent circuit [16].

Now,

$$I_1 = \frac{E_{TH}}{\left(R_{TH} + \frac{R'_r}{s}\right) + j(X_{TH} + X'_r)}$$

(10-4)

The rotor power/phase is given by:

$$P_{ph} = \frac{(I'_r)^2 R'_r}{s}$$

$$= \frac{R'_r}{s} \cdot \frac{E_{TH}^2}{\left(R_{TH} + \frac{R'_r}{s}\right)^2 + (X_{TH} + X'_r)^2}$$

(10-5)

Thus for m phases, rotor power = mP_{ph}.

Gross torque is given by:

$$\tau = \frac{1}{\omega_s} p$$

$$= \frac{mE_{TH}^2 R'_r}{s\omega_s\left[\left(R_{TH} + \frac{R'_r}{s}\right)^2 + (X_{TH} + X'_r)^2\right]} Nm$$

(10-6)

10.3 Derivation Of Equation (2-49)

The maximum torque is given when: $\frac{d\tau}{ds} = 0$ and equation (2-46) can be rewritten:

$$\tau = \frac{KR'_r}{s} \cdot \frac{1}{\left[\left(R_{TH} + \frac{R'_r}{s}\right)^2 + X^2\right]}$$

$$= KR'_r \cdot \frac{1}{sR_{TH}^2 + 2R_{TH}R'_r + \frac{R'^2_r}{s} + sX^2}$$

(10-7)

where

$$K = \frac{mE_{TH}^2}{\omega_s} \quad and \quad X = X_{TH} + X'_r$$

and

$$\frac{d}{ds}\left(sR_{TH}^2 + 2R_{TH}R_r' + \frac{R_r'^2}{s} + sX^2\right) = R_{TH}^2 - \frac{R_r'^2}{s^2} + X^2.$$

For maximum torque, this gives [16]:

$$\frac{d\tau}{ds} = \frac{KR_r'\left[R_{TH}^2 - \frac{R_r'^2}{s^2} + X^2\right]}{D^2} = 0 \tag{10-8}$$

where D is the denominator of equation (10-7). Equation (10-8) is only zero where:

$$\left(\frac{R_r'}{s}\right)^2 = R_{TH}^2 + X^2$$

$$or$$

$$\frac{R_r'}{s} = \pm\sqrt{R_{TH}^2 + (X_{TH} + X_r')^2}$$

$$\therefore \tag{10-9}$$

$$s_m = \pm\frac{R_r'}{\sqrt{R_{TH}^2 + (X_{TH} + X_r')^2}}$$

$$= \pm\frac{R_r'}{\sqrt{R_{TH}^2 + X^2}}$$

where s_m is the slip at which maximum torque is produced. Substituting eq. (10-9) into the torque equation (10-6) gives [16]:

$$\tau_{MAX} = \frac{KR_r'}{s_m} \cdot \frac{1}{\left(R_{TH} + \frac{R_r'}{s_m}\right)^2 + X^2}$$

$$= \frac{K}{2\left[\left(R_{TH}^2 + X^2\right)^{\frac{1}{2}} + R_{TH}\right]} \tag{10-10}$$

where

$$X = X_{TH} + X_r'$$

and

$$K = \frac{mE_{TH}}{\omega_s}$$

11 Appendix E: REVIEW OF EXISTING TRANSIENT STABILITY STUDIES

Two transient stability studies were carried out during the design of the PetroSA (then Mossgas) onshore facility. These studies were conducted by Merz and McLellan. In addition, a supplementary study was carried out by Powerplan Systems Analysis.

11.1 Merz & McLellan Study: 23 December 1988

To date, no copies of this study could be located. This study is referred to in the two remaining studies discussed below, which were essentially carried out to verify and examine further the results of this study.

11.2 Powerplan Study: 22 December 1988 28

The scope of this study was to undertake a series of supplementary power systems analyses in conjunction with Merz & McLellan in order to validate key results of the Merz & McLellan studies27 and identify any potential problem areas in the proposed design of the PetroSA electrical power system. It was necessary to assume typical data for most equipment parameters since vendor data was not yet available. This study did not analyse the performance of the re-acceleration system.

11.2.1 Summary of main conclusions and study recommendations

- For all 100ms fault and system conditions specified, recovery of all induction motors is possible.

- The local generators are stable for the specified fault conditions

- The 26MW synchronous motors are stable for the specified fault conditions, but become unstable when subjected to a 400kV fault longer than 200ms.

- The 26MW synchronous machine should be equipped with an AVR, which controls the local 11kV voltage. This aids in plant recovery following a fault.

- Stability for all machines for the 100ms fault condition is achieved by a wide margin. The impedances of the 132kV step-down transformers can be increased to more normal values.

11.2.2 Basic system details.

The Eskom power system was represented as follows:

Powerplan Study
Eskom Network
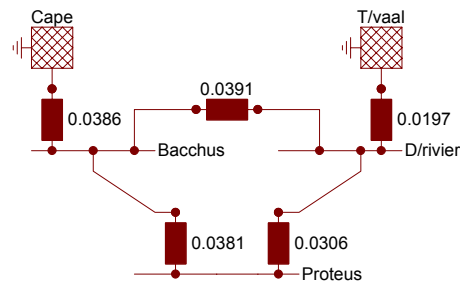
Figure 11-1: Eskom representation

The PetroSA system was represented as shown in Fig. 12-3 at the end of this section. Numerous cables were ignored and low voltage transformers represented by equivalent lumped models. The validity of the combined equivalents could not be evaluated.

The lumped LV and HV motors were assumed to run at a load torque of 85% of full load torque, based on the rating of the motor. Typical HV and LV motor characteristics were used to represent numerous equivalent or lumped motors. The larger HV machines were represented by the equivalent HV motor. The 10MW oxygen compressor motors at the air separation plant were represented by different model parameters due to their performance characteristics being very different from the typical HV model used for the other motors. Due to the approximate nature of the modelling data, a simple equivalent circuit model, shown below was used.
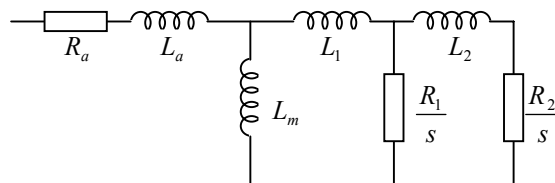
Figure 11-2 Equivalent circuit for induction motors

Synchronous machines were also modelled using typical data. The models were detailed and included a full d-q axis representation taking transient, sub-transient and saturation effects into account.

Variable speed drives were modelled simply as constant power loads.

Reactive power compensation was represented by the following:

- Operation of the 26MW synchronous machines (03KC101/201) at 0.95 leading power factor.

- 4 MVAr filters at the catalyst preparation furnace. (Note – no such filters were ever installed)

- 10MVAr filters at each of the three variable speed drives, (Note: There are no details of the data used to model these filters. The filters installed consist of five filters connected in parallel tuned to the 5th,7th, 11th, 23rd and 25th harmonics. During tests related to a different problem, these filter banks were energised without the associated variable speed drives running. They were observed to have a negligible effect on the

11kV distribution system voltages and currents and no significant impact on reactive power consumption.)

- Operation of the main generator (48GT101) to reduce MVAr import from Eskom to a low value.

11.2.3 Study cases

Stability studies were carried out as follows:

- 100ms solid 3-phase fault on the main 132kV busbar (Sub01) with one Eskom 400/132kV transformer tripped

- 100ms solid 3-phase fault on the 400kV Proteus busbar with the Proteus-Droerivier line tripped

- 100ms solid 3-phase fault applied to the 11kV busbars of one of the air separation trains

- 100ms solid 3-phase fault on the main 132kV busbar (Sub01) with the main generator tripped.

It was assumed that all loads' (motor, static loads and drives) contactors remain held in during low control voltage conditions and ride through the fault even if the busbar voltage falls to zero. This represents the most severe recovery condition, which is prevented in practice by the re-acceleration system.

It was also assumed that no busbars are isolated by disconnecting network branches after the fault.

11.2.4 Summary of Data Used

Table 11-1 400kV Fault levels on Eskom system (1988)

Substation	Contingency	Fault Level (MVA)
Bacchus		4295
Droerivier		6375
Proteus	With all Cape generation including Koeberg	3291
	With all Cape generation & outage of Bacchus-Proteus 400kV Line	2162
	With all Cape generation & outage on Droerivier-Proteus line	1628
	With no generation at Koeberg & Palmiet	2425

Table 11-2 Derived Induction motor parameters

Machine Parameters	Equivalent Large HV Motor (2)	10MW Motor (Airsep)	Equivalent LV Motor
No. of poles	4	4	4
Full load slip (pu)	0.011	0.007	0.020
Full load power factor (pu)	0.870	0.900	0.850
Full load efficiency (pu)	0.962	0.974	0.900
Pull out torque (pu)	2.100	2.000	2.350
Slip at pull out (pu)	0.050	0.030	0.090
Torque at 50% speed (pu)	1.000	0.620	1.900
Starting Torque (pu)	0.650	0.450	2.100
Starting current (pu)	5.000	4.400	6.000
Starting power factor (pu)	0.170	0.120	0.350
Base MVA (MVA)	varies	11.240	Varies
Inertia constant $\left(\frac{kW.s}{kVA}\right)$	Varies	2.350	Varies
Stator R (pu)	0.0065	0.0050	0.005
Stator X (pu)	0.1050	0.1200	0.100
Magnetising X (pu)	3.9000	3.8800	209.
First rotor R (pu)	0.0400	0.0261	0.085
First rotor X (pu)	0.0800	0.0900	0.020
Second rotor R (pu)	0.0160	0.0070	0.020
Second rotor X (pu)	0.0800	0.0400	0.130

Table 11-3 Synchronous machine parameters

	Main Generator
Primary Ratings	
Output (base)	140[1]@0.8pf
Rated Voltage (kV)	11
Rated speed (rpm)	3000
Machine type	Round rotor
Reactances (pu on machine base)	
Synchronous (Xd) sat/unsat	-/1.99
Transient (X'd) sat/unsat.	0.17/0.22
Sub-transient (X''d) sat/unsat	0.12/0.17
Synchronous (Xq)	1.84
Sub-transient (X''q)	0.12
Stator resistance (Ra)	
Negative sequence reactance (X2)	0.17
Zero sequence reactance (X0)	0.087
Stator stray synchronous reactance (Xl)	0.13
Time constants (sec)	
D-axis, open circuit transient (T'do)	9.5
D-axis, short circuit transient (T''d)	0.69
D-axis, short circuit sub-transient (T"q)	0.017
Armature short circuit (T'a)	0.34
Inertia	
Inertia constant (set)(H) $\left(kWs/kVA \right)$	3.25

---

[1] Exact value = 139.421MVA

Figure 11-3 PetroSA system representation

Note: The original drawing is illegible in some places, this diagram is only included to illustrate the degree of complexity of the system model used for simulations.

11.3 Merz and McLellan Study: 3 Feb 1989 [27]

The report covers study results for the final stability studies as well as those carried out in the 23 December 1988 study.

The studies additional to those of 23 December 1988 cover a modified base case comprising a two transformer supply arrangement to the Synthol medium voltage switchboards. A variation entailed modelling the distribution system with standard impedance transformers throughout the plant. Studies were also carried out modelling Proteus distribution station 40km further away than the then envisaged position 11km away from the plant. Certain studies performed for the preliminary report were repeated.

The purpose of the studies were to determine whether the plant with (then) proposed distribution system would recover satisfactorily after a 100ms supply interruption, or any short circuit in the distribution system that is cleared within 100ms.

11.3.1 Eskom equivalent source representation

The following reference data was used:

PetroSA-Proteus Overhead line

Length = 11km

Line construction: 2 x Single circuit, single conductor 'Zebra', 132kV

Parameters: R = 0.000487 pu/km   (100MVA base)

                 X = 0.00229 pu/km

                 B = 0.00057 pu/km

Note: The 'Zebra' line was never installed and was replaced with the 'Wolf' line described below.

Proteus 400/132kV step-down transformers

Rating: 2 x 250MVA

Nominal impedance: 13.5%

X/R ratio: 46.5 (45 used in the model)

Droerivier – Proteus and Bacchus- Proteus 400kV overhead lines

Length: 243km Bacchus-Proteus

                 230km Droerivier-Proteus

Line construction: Single circuit, quad 'Wolf' conductor

Parameters: R = 29.8 e-6 pu/km (100mVA base)

                 X = 171e-6 pu/km

                 B = 6834e-6 pu/km

Droerivier and Bacchus Distribution Substation Fault Levels

Source: Eskom Simmerpan, 1988-12-07

Bacchus 400kV -   max 3ph : 7271A (5038 MVA)

                       min 3ph : 5555A (3848 MVA)

Droerivier 400kV -   max 3ph : 9623A (6667 MVA)

                       min 3ph : 7190A (4981 MVA)

11.3.2 Proteus 400kV fault levels

Information from Eskom 12-September 1988

Contingency	Fault Level (MVA)
With all Cape generation including Koeberg	3291 (4.75kA)
With all Cape generation except 1 set at Koeberg	3083 (4.45kA)
With all Cape generation except Koeberg	3007 (4.34kA)
With all Cape generation except 1 set at Palmiet	3118 (4.50kA)
With all Cape generation & outage of Bacchus-Proteus 400kV Line	2162 (3.12kA)
With all Cape generation & outage on Droerivier-Proteus line	1628 (2.35kA)
With no generation at Koeberg & Palmiet	2425 (3.50kA)

Table 11-4 Proteus 400kV fault levels (1988)

For modelling purposes the estimated infeeds from Bacchus and Droerivier were calculated neglecting shunt reactors and shunt capacitances of overhead lines and the summated infeed at Proteus 400kV was 3405MVA.

11.3.3 Fault clearance times

400kV Network - Main 1 Protection: 58 – 85 ms

      - Main 2 Protection   58 – 85 ms

      - Back-up Protection: Zone 2 – 400ms

                Zone 3 – 1s

                IDMT Earth Fault +/- 3s

132kV Network - Main 1 Protection: 70 – 100 ms

      - Main 2 Protection   70 – 100 ms

      - Back-up Protection: Zone 2 – 400ms

                Zone 3 – 1s

                IDMT Earth Fault +/- 3s

Probability of main protection clearance: 400kV – 97%

                  132kV – 90%

11.3.4 Eskom 'infinite' generator representation

Rated Power: 9000MVA

Stored energy co-efficient H: 100 kWs/kVA

Transient reactance: 0.01 pu

11.3.5 PetroSA plant data

When these studies were carried out, vendor data on drives was minimal. Typical data was therefore assumed throughout with regard to motor load characteristics and drive inertias.

Information on the Total Feed Compressor variable speed drives was not firm and these were represented as a constant power (PQ) type load.. This load was assumed to be switched out during the period the fault persisted and switched in after fault clearance. Note that this assumption was correct, since the variable speed drives will block firing pulses to the inverter thyristors during a voltage dip, effectively disconnecting the drives from the 11kV supply. If the bus voltage returns to normal within 180ms, normal operation is restored. In practice, the impact on the system is relatively minor with the variable speed drive smoothly accelerating the compressor motor to its pre-fault speed and load.

In general, summated equivalent loads based on available load lists were used. An effort was also made to bring the databases used by Merz and McLellan and Powerplan into closer agreement. This was largely done, except in the way rotating machines are modelled, The induction machine parameters, AVR and governor models differ significantly.

11.3.6 Synchronous machines

Some parameters for the 33MVA Air separation machines were available from preliminary bid data. Typical data had to be assumed for the plant generators with regard to machine parameters, AVR and governor data.

A *dqo* axis model is used which includes saturation and transients. A simple first order governor model featuring 4% droop and 5s time delay was used for the generators. The governor representation was not considered important since it only becomes significant when assessing machine performance 5 seconds or more after a disturbance. The influence on transient stability was considered small, since it is readily apparent after 1-2sec duration if the system will recover or not.

Different AVR models for the Air separation machines were used and performance discussed. The machine parameters used were similar to those used by Powerplan.

11.3.7 Induction machines

Where possible, preliminary data was used for modelling MV induction machines. This mainly applied to the duty cycle and inertia constant. Real equivalent machine model data was only available for the oxygen compressors (03KC102/202)

LV machines were treated a lumped machines of an equivalent summated loading. Small HV machines where no data was available were similarly modelled as lumped machines.

Induction machine modelling is based on a simple equivalent linear impedance model. Saturation is not taken into account and only rotor resistance is changed as a function of slip.

11.4 Study Results

From the load flow study the estimated infeed from Eskom was 102.5MW + 2.7MVAr (lagging) assuming 80MW generation on the main generator and 7.76MW on the critical generator. The reactive power delivered by the synchronous machines was calculated as follows:

120MVA generator 48GT101   -   55MVAr (max. 72)

12.5MVA generator 48GT102   -   5MVAr (max. 8)

33 MVA motors 03KC101/201 -   7.9MVAr (max. 19.5)

From the above figures, it is evident that adequate spare reactive power capacity is available to limit reactive power drawn from Eskom. It was concluded that the PetroSA system would recover satisfactorily after a 100ms supply interruption, or any short circuit in the distribution system that is cleared within 100ms.

12 Appendix F: SYNCHRONOUS MACHINE MODELS – ADDITIONAL INFORMATION

12.1 Derivation Of Equation (2-71)

$$
\begin{aligned}
\frac{d\psi}{dt} &= \frac{dL}{dt}I + L\frac{dI}{dt} \\
&= \frac{dL}{d\theta}\frac{d\theta}{dt}I + L\frac{dI}{dt} \\
&= \omega\frac{dL}{d\theta}I + L\frac{dI}{dt} \\
&= \omega GI + L\frac{dI}{dt}
\end{aligned}
\tag{12-1}
$$

12.2 Derivation Of Rotational Inductance Matrix G

It is assumed that there is only one equivalent circuit on each rotor axis.

From eq.(2-62) we get:

$$
\frac{dL_{SRd}}{d\theta} = G_{SRd} = -\begin{bmatrix}
M_{afd}\sin\theta & M_{a1d}\sin\theta \\
M_{afd}\sin(\theta+\frac{2\pi}{3}) & M_{a1d}\sin(\theta+\frac{2\pi}{3}) \\
M_{afd}\sin(\theta-\frac{2\pi}{3}) & M_{a1d}\sin(\theta-\frac{2\pi}{3})
\end{bmatrix}
\tag{12-2}
$$

and

$$
\frac{dL_{SRq}}{d\theta} = G_{SRq} = \begin{bmatrix}
M_{a1q}\cos\theta \\
M_{a1q}\cos(\theta+\frac{2\pi}{3}) \\
M_{a1q}\cos(\theta-\frac{2\pi}{3})
\end{bmatrix}
\tag{12-3}
$$

The remainder of the sub-matrices being constants, are zero when differentiated with respect to θ. This gives the rotational inductance matrix as:

$$
G = \begin{bmatrix}
0 & 0 & 0 & -M_{afd}\sin\theta & -M_{a1d}\sin\theta & M_{aq}\cos\theta \\
0 & 0 & 0 & -M_{afd}\sin(\theta+\frac{2\pi}{3}) & -M_{a1d}\sin(\theta+\frac{2\pi}{3}) & M_{aq}\cos(\theta+\frac{2\pi}{3}) \\
0 & 0 & 0 & -M_{afd}\sin(\theta-\frac{2\pi}{3}) & -M_{a1d}\sin(\theta-\frac{2\pi}{3}) & M_{aq}\cos(\theta-\frac{2\pi}{3}) \\
-M_{afd}\sin\theta & -M_{afd}\sin(\theta+\frac{2\pi}{3}) & -M_{afd}\sin(\theta-\frac{2\pi}{3}) & 0 & 0 & 0 \\
-M_{a1d}\sin\theta & -M_{a1d}\sin(\theta+\frac{2\pi}{3}) & -M_{a1d}\sin(\theta-\frac{2\pi}{3}) & 0 & 0 & 0 \\
M_{aq}\cos\theta & M_{aq}\cos(\theta+\frac{2\pi}{3}) & M_{aq}\cos(\theta-\frac{2\pi}{3}) & 0 & 0 & 0
\end{bmatrix}
\tag{12-4}
$$

12.3 Derivation Of Equation (2-81)

Equation (2-80) can be written in vector from as:

$$
\frac{d}{dt}\psi_{abc} = -(v_{abc} + ri_{abc})
\tag{12-5}
$$

This can be written in *dqo*-variables using the inverse Park transform:

$$
\frac{d}{dt}\left[P^T\psi_{dqo}\right] = -\left(P^T v_{dqo} + rP^T i_{dqo}\right)
\tag{12-6}
$$

Since P^T is a function of θ,

$$\frac{d}{dt}\left[\mathbf{P}^{\mathbf{T}}\boldsymbol{\psi}_{\mathbf{dqo}}\right] = \mathbf{P}^{\mathbf{T}}\frac{d}{dt}\boldsymbol{\psi}_{\mathbf{dqo}} + \left[\frac{d}{dt}\mathbf{P}^{\mathbf{T}}\right]\boldsymbol{\psi}_{\mathbf{dqo}}$$

(12-7)

where

$$\frac{d}{dt}\left[\mathbf{P}^{\mathbf{T}}\right] = \omega\sqrt{\frac{2}{3}}\begin{bmatrix} -\sin\theta & \cos\theta & 0 \\ -\sin\left(\theta - \frac{2\pi}{3}\right) & \cos\left(\theta - \frac{2\pi}{3}\right) & 0 \\ -\sin\left(\theta + \frac{2\pi}{3}\right) & \cos\left(\theta + \frac{2\pi}{3}\right) & 0 \end{bmatrix}$$

(12-8)

and $\omega = d\theta/dt$ is the electrical speed of the rotor. Equation (12-6) can thus be written as

$$\mathbf{P}^{\mathbf{T}}\frac{d}{dt}\boldsymbol{\psi}_{\mathbf{dqo}} + \omega\sqrt{\frac{2}{3}}\begin{bmatrix} -\sin\theta & \cos\theta & 0 \\ -\sin\left(\theta - \frac{2\pi}{3}\right) & \cos\left(\theta - \frac{2\pi}{3}\right) & 0 \\ -\sin\left(\theta + \frac{2\pi}{3}\right) & \cos\left(\theta + \frac{2\pi}{3}\right) & 0 \end{bmatrix}\boldsymbol{\psi}_{\mathbf{dqo}} = -\left(\mathbf{P}^{\mathbf{T}}\mathbf{v}_{\mathbf{dqo}} + r\mathbf{P}^{\mathbf{T}}\mathbf{i}_{\mathbf{dqo}}\right)$$

(12-9)

If both sides of equation (12-9) are pre-multiplied with **P**, then we get:

$$\frac{d}{dt}\boldsymbol{\psi}_{\mathbf{dqo}} + \omega\begin{bmatrix} 0 & 1 & 0 \\ -1 & 0 & 0 \\ 0 & 0 & 0 \end{bmatrix}\boldsymbol{\psi}_{\mathbf{dqo}} = -\left(\mathbf{v}_{\mathbf{dqo}} + r\mathbf{i}_{\mathbf{dqo}}\right)$$

(12-10)

12.4 Derivation Of Equation (2-85)

The *dqo* flux linkages and currents can be expressed in terms of *abc* flux linkages and currents using $\mathbf{P_A}$:

$$\begin{bmatrix} \boldsymbol{\psi}_{\mathbf{dqo}} \\ \hline \boldsymbol{\psi}_{\mathbf{Rd}} \\ \hline \boldsymbol{\psi}_{\mathbf{Rq}} \end{bmatrix} = \mathbf{P_a}\begin{bmatrix} \boldsymbol{\psi}_{\mathbf{S}} \\ \hline \boldsymbol{\psi}_{\mathbf{Rd}} \\ \hline \boldsymbol{\psi}_{\mathbf{Rq}} \end{bmatrix} ; \quad \begin{bmatrix} \mathbf{i}_{\mathbf{dqo}} \\ \hline \mathbf{i}_{\mathbf{Rd}} \\ \hline \mathbf{i}_{\mathbf{Rq}} \end{bmatrix} = \mathbf{P_A}\begin{bmatrix} \mathbf{i}_{\mathbf{S}} \\ \hline \mathbf{i}_{\mathbf{Rd}} \\ \hline \mathbf{i}_{\mathbf{Rq}} \end{bmatrix}$$

(12-11)

The inverse relations are given by

$$\begin{bmatrix} \boldsymbol{\psi}_{\mathbf{S}} \\ \hline \boldsymbol{\psi}_{\mathbf{Rd}} \\ \hline \boldsymbol{\psi}_{\mathbf{Rq}} \end{bmatrix} = \mathbf{P_A^{-1}}\begin{bmatrix} \boldsymbol{\psi}_{\mathbf{dqo}} \\ \hline \boldsymbol{\psi}_{\mathbf{Rd}} \\ \hline \boldsymbol{\psi}_{\mathbf{Rq}} \end{bmatrix} ; \quad \begin{bmatrix} \mathbf{i}_{\mathbf{S}} \\ \hline \mathbf{i}_{\mathbf{Rd}} \\ \hline \mathbf{i}_{\mathbf{Rq}} \end{bmatrix} = \mathbf{P_A^{-1}}\begin{bmatrix} \mathbf{i}_{\mathbf{dqo}} \\ \hline \mathbf{i}_{\mathbf{Rd}} \\ \hline \mathbf{i}_{\mathbf{Rq}} \end{bmatrix}$$

(12-12)

The $\psi - i$ relationships in the *dqo* frame can now be obtained by substituting equation (12-12) into (2-62) giving:

$$\mathbf{P_A^{-1}}\begin{bmatrix} \boldsymbol{\psi}_{\mathbf{dqo}} \\ \hline \boldsymbol{\psi}_{\mathbf{Rd}} \\ \hline \boldsymbol{\psi}_{\mathbf{Rq}} \end{bmatrix} = \mathbf{L}\mathbf{P_A^{-1}}\begin{bmatrix} \mathbf{i}_{\mathbf{dqo}} \\ \hline \mathbf{i}_{\mathbf{Rd}} \\ \hline \mathbf{i}_{\mathbf{Rq}} \end{bmatrix}$$

(12-13)

After pre-multiplying both sides of eq. (12-13) with $\mathbf{P_A}$ the following is obtained:

$$\begin{bmatrix} \underline{\boldsymbol{\psi}}_{\mathbf{dqo}} \\ \overline{\underline{\boldsymbol{\psi}}_{\mathbf{Rd}}} \\ \overline{\boldsymbol{\psi}_{\mathbf{Rq}}} \end{bmatrix} = \mathbf{P_A L P_A^{-1}} \begin{bmatrix} \mathbf{i}_{\mathbf{dqo}} \\ \overline{\mathbf{i}_{\mathbf{Ra}}} \\ \overline{\mathbf{i}_{\mathbf{Rq}}} \end{bmatrix}$$

(12-14)

The inductance matrix in the *dqo*-frame is therefore given by [23]:

$$\mathbf{P_A L P_A^{-1}} = \begin{bmatrix} \mathbf{PL_S P^{-1}} & \mathbf{PL_{SRd}} & \mathbf{PL_{SRq}} \\ \mathbf{L_{SRd}^T P^{-1}} & \mathbf{L_{Rd}} & \mathbf{O} \\ \mathbf{L_{SRq}^T P^{-1}} & \mathbf{O} & \mathbf{L_{Rq}} \end{bmatrix}$$

(12-15)

12.5 Derivation Of Equation (2-104)

The phasor diagram in Figure 12-1 is used to obtain the initial rotor angle δ with respect to the synchronously rotating system reference. It is first necessary to locate the machine q-axis with respect to system reference.

From Figure 12-1, taking the terminal voltage as reference:

$$\overline{E}_{qt} = \overline{V}_t + (r_t + jx_q)\overline{I}_t$$

(12-16)

Also note that:

$$\overline{I}_t = (I_t \cos\phi - jI_t \sin\phi)$$

(12-17)

giving:

$$\begin{aligned} \overline{E}_{qt} &= V_t + (r + jx_q)(I_t \cos\phi - jI_t \sin\phi) \\ &= (V_t + rI_t \cos\phi + x_q I_t \sin\phi) + j(x_q I_t \cos\phi - rI_t \sin\phi) \end{aligned}$$

(12-18)

The internal machine angle is therefore given by [23]:

$$\delta' = \tan^{-1} \frac{(x_q I_t \cos\phi - rI_t \sin\phi)}{(V_t + rI_t \cos\phi + x_q I_t \sin\phi)}$$

(12-19)
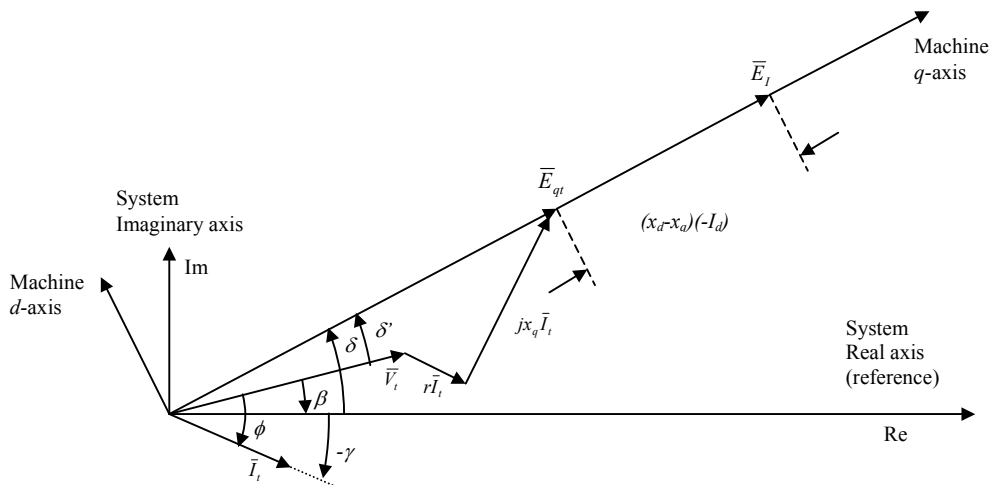
Figure 12-1 Locating machine axis with respect to system axis [23].

12.6 Derivation Of Equation (2-130)

When formulating the swing equation, it is more convenient to use the rotor electrical angle, related to the mechanical angle by:

$$\delta_e = \frac{p}{2} \delta_m \tag{12-20}$$

where *p/2* is the number of pole pairs in the machine. Substituting into equation (2-124) gives:

$$\delta_e = \frac{p}{2} \delta_m = \theta_e - \left(\omega_0 t + \theta_0' \right) \tag{12-21}$$

where

$$\theta_e = \frac{p}{2} \delta_m; \quad \omega_0 = \frac{p}{2} \omega_{m0} \tag{12-22}$$

The following quantities are more convenient to use than the number of pole pairs:

N_0 – The rated shaft speed of the machine in revolutions per minute

f_0 – The rated electrical frequency of the machine in Hz.

These quantities give:

$$f_0 = \frac{N_0}{60} \frac{p}{2}$$

or $\tag{12-23}$

$$\frac{p}{2} = \frac{60 f_0}{N_0}$$

and

$$\omega_{m0} = \frac{2\pi N_0}{60} \tag{12-24}$$

Substituting eq. (12-23) into eq. (12-20) for p/2 gives:

$$\delta_e = \frac{60 f_0}{N_0} \delta_m \tag{12-25}$$

Differentiating equation (12-25) twice with respect to time and substituting for δ_m in equation (2-125) gives the swing equation in terms of the electrical angle [23]:

$$\left(I \frac{N_0}{60} \frac{1}{f_0} \right) \frac{d^2 \delta_e}{dt^2} = \left(T_m - T_g - T_D \right) \tag{12-26}$$

12.7 Derivation Of Equation (2-146)

From equation (2-90), the basic field equation is:

$$\frac{d\psi_{fd}}{dt} = \left(v_{fd} - r_{fd} i_{fd} \right) \tag{12-27}$$

Multiplying on both sides with $\dfrac{\omega_0 M_{afd}}{r_{fd}}$ gives

$$\frac{\omega_0 M_{afd}}{r_{fd}} \frac{d\psi_{fd}}{dt} = \left(\frac{\omega_0 M_{afd}}{r_{fd}} v_{fd} - \omega_0 M_{afd} i_{fd} \right) \tag{12-28}$$

From equations (2-116) and (2-117) we get:

$$\omega_0 M_{afd} i_{fd} = x_{afd} i_{fd} \Rightarrow \sqrt{2} E_I \tag{12-29}$$

E_I in rms (per phase value) is the field excitation referred to the stator and is directly proportional to the field current. Also from equation (2-120) we define:

$$\frac{\omega_0 M_{afd}}{r_{fd}} v_{fd} \Rightarrow \sqrt{2} E_{fd} \tag{12-30}$$

where E_{fd} is the exciter voltage referred to the stator and is directly proportional to the field voltage v_{fd}. E'_q is the (fictitious) internal stator voltage and is the rms (per phase) voltage that is directly proportional to the field flux linkages and is defined [23]:

$$\omega_0 M_{afd} \frac{\psi_{fd}}{L_{ffd}} \Rightarrow \sqrt{2} E'_q \tag{12-31}$$

Differentiating (12-31) will result in:

$$\frac{d\psi_{fd}}{dt} = \frac{\sqrt{2} L_{ffd}}{\omega_0 M_{afd}} \frac{dE'_q}{dt} \tag{12-32}$$

Substituting equations (12-29), (12-30) and (12-32) into eq.(12-28) gives:

$$\frac{L_{ffd}}{r_{fd}} \frac{dE'_q}{dt} = \left(E_{fd} - E_I \right) \tag{12-33}$$

12.8 Derivation Of Equation (2-166)

The three phase electrical power output can be derived as follows for the two-axis model. From equation (2-94) the following can be derived:

$$P_e = 3\left(V_d I_d + V_q I_q \right) \tag{12-34}$$

From equations (2-155) and (2-156), V_d and V_q can be obtained after neglecting the armature resistance[1] as:

$$V_d = \left(E'_d - x'_q I_q \right)$$
$$V_q = \left(E'_q + x'_d I_d \right)$$

Substituting for V_d and V_q in equation (12-34) gives:

$$\begin{aligned} P_e &= 3\left(E'_d I_d - x'_q I_d I_q + E'_q I_q + x'_d I_d I_q \right) \\ &= 3\left[\left\{ E'_q + \left(x'_d - x'_q \right) I_d \right\} I_q + E'_d I_d \right] \end{aligned} \tag{12-35}$$

Equation (12-35) remains unchanged when expressed in p.u. on a single-phase power base. For use in the swing equation the p.u. electrical power output on a 3-phase power base has to be obtained which is given by [23]:

$$P_e = \left\{ E'_q + \left(x'_d - x'_q \right) I_d \right\} I_q + E'_d I_d \quad \text{p.u.} \tag{12-36}$$

---

[1] The armature resistance is small and ignoring this resistance introduces a negligible error when calculating the machine output power.

13 Appendix G: LOAD FLOW RESULTS

The following loadflow solutions were obtained prior to and after running various studies.

13.1 Initial Loadflow Solution

Used as initial conditions for Study cases 1, 2, 3, 4, 5, 6 and 7

```
Number of iterations:   4   Max Power mismatch:    10.0kVA
```

Bus	Voltage(l-l)	Voltage(pu)	Angle	P(bus)	Q(bus)
1	133.0000 kV	1.0076	0.00 deg.	127.7015 MW	1.5441 MVAr
2	132.7620 kV	1.0058	-0.20 deg.	0.0000 MW	0.0000 MVAr
3	132.7580 kV	1.0057	-0.20 deg.	0.0000 MW	0.0000 MVAr
4	132.7596 kV	1.0058	-0.20 deg.	0.0000 MW	0.0000 MVAr
5	132.7555 kV	1.0057	-0.20 deg.	0.0000 MW	0.0000 MVAr
6	131.2591 kV	0.9944	-0.92 deg.	0.0000 MW	0.0000 MVAr
7	10.9354 kV	0.9941	-0.95 deg.	0.0000 MW	0.0000 MVAr
8	6.5371 kV	0.9905	-1.19 deg.	0.0000 MW	0.0000 MVAr
9	132.7594 kV	1.0058	-0.20 deg.	0.0000 MW	0.0000 MVAr
10	132.7581 kV	1.0057	-0.20 deg.	0.0000 MW	0.0000 MVAr
11	132.7585 kV	1.0057	-0.20 deg.	0.0000 MW	0.0000 MVAr
12	132.7609 kV	1.0058	-0.20 deg.	0.0000 MW	0.0000 MVAr
13	11.1524 kV	1.0139	-1.59 deg.	0.0000 MW	0.0000 MVAr
14	132.7593 kV	1.0058	-0.20 deg.	0.0000 MW	0.0000 MVAr
15	132.7774 kV	1.0059	-0.19 deg.	0.0000 MW	0.0000 MVAr
16	11.0890 kV	1.0081	0.69 deg.	56.0000 MW	41.0000 MVAr
17	6.5434 kV	0.9914	-1.13 deg.	0.0000 MW	0.0000 MVAr
18	131.8298 kV	0.9987	-0.62 deg.	0.0000 MW	0.0000 MVAr
19	131.8266 kV	0.9987	-0.62 deg.	0.0000 MW	0.0000 MVAr
20	11.1353 kV	1.0123	-1.66 deg.	-26.0177 MW	19.4873 MVAr
21	11.1500 kV	1.0136	-1.59 deg.	-9.8551 MW	-4.7740 MVAr
22	132.7610 kV	1.0058	-0.20 deg.	0.0000 MW	0.0000 MVAr
23	11.1525 kV	1.0139	-1.59 deg.	0.0000 MW	0.0000 MVAr
24	132.7589 kV	1.0057	-0.20 deg.	0.0000 MW	0.0000 MVAr
25	132.7557 kV	1.0057	-0.20 deg.	0.0000 MW	0.0000 MVAr
26	131.2584 kV	0.9944	-0.92 deg.	0.0000 MW	0.0000 MVAr
27	10.9205 kV	0.9928	-1.01 deg.	0.0000 MW	0.0000 MVAr
28	10.9214 kV	0.9929	-1.01 deg.	0.0000 MW	0.0000 MVAr
29	11.1499 kV	1.0136	-1.59 deg.	-9.8551 MW	-4.7784 MVAr
30	11.1351 kV	1.0123	-1.66 deg.	-26.0177 MW	19.4873 MVAr
31	0.5569 kV	1.0125	-1.70 deg.	0.0000 MW	0.0000 MVAr
32	10.9348 kV	0.9941	-0.96 deg.	0.0000 MW	0.0000 MVAr
33	0.5606 kV	1.0194	-1.03 deg.	0.0000 MW	0.0000 MVAr
34	0.5467 kV	0.9941	-0.96 deg.	0.0000 MW	0.0000 MVAr
35	10.9331 kV	0.9939	-0.95 deg.	0.0000 MW	0.0000 MVAr
36	6.5242 kV	0.9885	-1.28 deg.	0.0000 MW	0.0000 MVAr
37	10.9309 kV	0.9937	-0.95 deg.	0.0000 MW	0.0000 MVAr
38	10.9086 kV	0.9917	-1.06 deg.	0.0000 MW	0.0000 MVAr
39	10.9086 kV	0.9917	-1.06 deg.	0.0000 MW	0.0000 MVAr
40	10.9031 kV	0.9912	-1.08 deg.	0.0000 MW	0.0000 MVAr
41	0.5395 kV	0.9809	-1.76 deg.	0.0000 MW	0.0000 MVAr
42	6.4520 kV	0.9776	-1.89 deg.	0.0000 MW	0.0000 MVAr
43	10.9300 kV	0.9936	-0.97 deg.	0.0000 MW	0.0000 MVAr
44	10.9305 kV	0.9937	-0.97 deg.	0.0000 MW	0.0000 MVAr
45	0.5581 kV	1.0147	-1.27 deg.	0.0000 MW	0.0000 MVAr
46	10.9345 kV	0.9940	-0.96 deg.	0.0000 MW	0.0000 MVAr
47	10.9345 kV	0.9940	-0.96 deg.	0.0000 MW	0.0000 MVAr
48	6.6911 kV	1.0138	-0.99 deg.	0.0000 MW	0.0000 MVAr
49	6.6911 kV	1.0138	-0.99 deg.	0.0000 MW	0.0000 MVAr
50	6.6911 kV	1.0138	-0.99 deg.	0.0000 MW	0.0000 MVAr
51	6.6911 kV	1.0138	-0.99 deg.	0.0000 MW	0.0000 MVAr
52	6.6911 kV	1.0138	-0.99 deg.	0.0000 MW	0.0000 MVAr

```
53      6.6911 kV      1.0138        -0.99 deg.    0.0000 MW      0.0000 MVAr
54      6.6911 kV      1.0138        -0.99 deg.    0.0000 MW      0.0000 MVAr
55      6.6911 kV      1.0138        -0.99 deg.    0.0000 MW      0.0000 MVAr
56      6.6904 kV      1.0137        -0.99 deg.   -0.1793 MW     -0.1344 MVAr
57      0.5584 kV      1.0152        -1.24 deg.    0.0000 MW      0.0000 MVAr
58     10.9681 kV      0.9971        -0.73 deg.    0.0000 MW      0.0000 MVAr

Branch currents:
 1     feeder: 280.9241A    -0.69 deg.
 2     feeder: 273.4660A    -0.69 deg.
 3     feeder:  65.2359A   -38.61 deg.
 4     3wtrnf: Ip: 65.2359A       -38.61 deg. Is:519.9523A  -38.86 deg.
          It:438.1562A   -38.11 deg.
 5     feeder:  58.7953A   -18.36 deg.
 6     feeder:  75.8448A   -36.07 deg.
 7     feeder:  61.8355A   -39.19 deg.
 8     feeder: 167.5266A    20.66 deg.
 9     transf: Ip:167.5266A        20.66 deg. Is:2010.3195A  20.66 deg.
10     feeder:  58.7506A   -18.39 deg.
11     feeder: 298.1480A   144.48 deg.
12     transf: Ip:298.1480A       144.48 deg. Is:3613.5533A 144.48 deg.
13      Load: 817.8449A   -39.75 deg.    7.2419MVA     5.7855MVAr
14      Load: 250.5037A   -37.70 deg.    3.8022MVA     2.8619MVAr
15      Load: 252.6026A   -38.45 deg.    3.7958MVA     2.9360MVAr
16     feeder: 167.5316A    20.67 deg.
17     transf: Ip:167.5316A        20.67 deg. Is:2010.3793A  20.67 deg.
18     feeder:  62.2644A   -39.17 deg.
19     3wtrnf: Ip: 65.1073A       -38.62 deg. Is:515.1753A  -38.89 deg.
          It:443.5490A   -38.09 deg.
20      Load:  58.7953A   -18.36 deg.   12.8465MVA     4.2131MVAr
21     feeder:  74.7976A   -36.12 deg.
22     feeder:  53.7025A   -13.59 deg.
23     feeder:  65.1073A   -38.62 deg.
24     feeder: 1685.4276A   35.17 deg.
25     feeder: 567.0198A   -27.44 deg.
26     feeder: 567.1266A   -27.45 deg.
27     feeder: 1685.4498A   35.17 deg.
28      Load:  75.8448A   -36.07 deg.   14.1329MVA    10.2184MVAr
29     3wtrnf: Ip: 61.8355A       -39.19 deg. Is:251.3735A  -38.09 deg.
          It:817.8705A   -39.75 deg.
30      Load:  58.7506A   -18.39 deg.   12.8344MVA     4.2171MVAr
31      Load:  74.7976A   -36.12 deg.   13.9291MVA    10.0893MVAr
32      Load:  53.7025A   -13.59 deg.   12.0128MVA     2.8606MVAr
33     3wtrnf: Ip: 62.2644A       -39.17 deg. Is:251.7219A  -38.07 deg.
          It:825.8688A   -39.74 deg.
34     feeder:   6.0585A    -5.30 deg.
35     feeder:   6.0585A    -5.30 deg.
36     transf: Ip:  6.0585A        -5.30 deg. Is:118.1411A   -5.30 deg.
37     transf: Ip:  6.0585A        -5.30 deg. Is:118.1411A   -5.30 deg.
38      Load: 236.2822A    -5.30 deg.    0.2288MVA     0.0171MVAr
39     feeder: 123.2117A   -40.27 deg.
40     feeder: 119.5833A   -39.31 deg.
41     transf: Ip:123.2117A       -40.27 deg. Is:205.3528A  -40.27 deg.
42     transf: Ip:119.5833A       -39.31 deg. Is:199.3056A  -39.31 deg.
43      Load: 404.6440A   -39.80 deg.    3.5774MVA     2.8479MVAr
44     feeder:  86.9446A   -38.63 deg.
45     feeder:  86.9446A   -38.63 deg.
46     feeder: 114.9956A   -40.48 deg.
47     transf: Ip: 86.9446A       -38.63 deg. Is:1738.8920A -38.63 deg.
48     transf: Ip: 86.9446A       -38.63 deg. Is:1738.8920A -38.63 deg.
49     transf: Ip:114.9956A       -40.48 deg. Is:191.6594A  -40.48 deg.
50      Load: 3477.7841A  -38.63 deg.    2.5997MVA     1.9498MVAr
51      Load: 191.6594A   -40.48 deg.    1.6740MVA     1.3361MVAr
52      Load: 225.0797A   -39.50 deg.    3.3342MVA     2.6566MVAr
53     feeder:  36.7044A   -38.17 deg.
54     feeder:  33.3359A   -38.14 deg.
55     transf: Ip: 36.7044A       -38.17 deg. Is:715.7361A  -38.17 deg.
56     transf: Ip: 33.3359A       -38.14 deg. Is:650.0502A  -38.14 deg.
```

```
57      transf: Ip: 92.9532A        -38.54 deg.  Is:1803.2914A -38.54 deg.
58      transf: Ip: 93.5505A        -38.59 deg.  Is:1814.8788A -38.59 deg.
59      feeder:  92.9532A   -38.54 deg.
60      feeder:  93.5505A   -38.59 deg.
61      transf: Ip:  5.9403A        -37.87 deg.  Is:  9.7024A  -37.87 deg.
62      transf: Ip:  5.8988A        -37.81 deg.  Is:  9.6347A  -37.81 deg.
63      feeder:   5.9403A   -37.87 deg.
64      feeder:   5.8988A   -37.81 deg.
65       Load: 438.1754A    -38.11 deg.   3.9663MVA     2.9804MVAr
66       Load: 443.5298A    -38.08 deg.   4.0164MVA     3.0147MVAr
67       Load: 825.8945A    -39.74 deg.   7.3141MVA     5.8412MVAr
68      feeder:   0.0000A    0.00 deg.
69      feeder:   0.0000A   -103.32 deg.
70      feeder:   0.0000A   -166.23 deg.
71      feeder:   0.0000A   -103.32 deg.
72      feeder:   0.0000A   -103.32 deg.
73      feeder:   0.0000A   -166.23 deg.
74      feeder:   0.0000A   -103.32 deg.
75      feeder:  19.3371A   -37.84 deg.
76       Load: 3618.1698A   -38.57 deg.   2.7918MVA     2.0938MVAr
77       Load:    6.3912A   -38.14 deg.   0.0049MVA     0.0037MVAr
78       Load: 352.7996A    -38.17 deg.   0.2727MVA     0.2048MVAr
79       Load: 126.2270A    -38.17 deg.   0.0976MVA     0.0733MVAr
80       Load: 124.0110A    -38.17 deg.   0.0959MVA     0.0720MVAr
81       Load: 106.3073A    -38.17 deg.   0.0822MVA     0.0617MVAr
82       Load:  70.4365A    -38.13 deg.   0.0545MVA     0.0409MVAr
83       Load:   3.1970A    -38.11 deg.   0.0025MVA     0.0019MVAr
84       Load: 352.9542A    -38.14 deg.   0.2730MVA     0.2049MVAr
85       Load: 132.6738A    -38.14 deg.   0.1026MVA     0.0770MVAr
86       Load:  90.7887A    -38.14 deg.   0.0702MVA     0.0527MVAr
```

13.2 Study Case 1 – Final State

Bus voltages and currents calculated on completion of simulation.

```
Number of iterations:   1   Max Power mismatch:    10.0kVA

 Bus  Voltage(l-l)  Voltage(pu)     Angle         P(bus)        Q(bus)
  1    133.0000 kV    1.0076      0.00 deg. 129.3276 MW     2.5233 MVAr
  2    132.7555 kV    1.0057     -0.20 deg.   0.0000 MW     0.0000 MVAr
  3    132.7515 kV    1.0057     -0.20 deg.   0.0000 MW     0.0000 MVAr
  4    132.7532 kV    1.0057     -0.20 deg.   0.0000 MW     0.0000 MVAr
  5    132.7487 kV    1.0057     -0.20 deg.   0.0000 MW     0.0000 MVAr
  6    131.1745 kV    0.9937     -0.97 deg.   0.0000 MW     0.0000 MVAr
  7     10.9282 kV    0.9935     -1.01 deg.   0.0000 MW     0.0000 MVAr
  8      6.5329 kV    0.9898     -1.24 deg.   0.0000 MW     0.0000 MVAr
  9    132.7530 kV    1.0057     -0.20 deg.   0.0000 MW     0.0000 MVAr
 10    132.7517 kV    1.0057     -0.20 deg.   0.0000 MW     0.0000 MVAr
 11    132.7521 kV    1.0057     -0.20 deg.   0.0000 MW     0.0000 MVAr
 12    132.7545 kV    1.0057     -0.20 deg.   0.0000 MW     0.0000 MVAr
 13     11.1518 kV    1.0138     -1.59 deg.   0.0000 MW     0.0000 MVAr
 14    132.7529 kV    1.0057     -0.20 deg.   0.0000 MW     0.0000 MVAr
 15    132.7710 kV    1.0058     -0.19 deg.   0.0000 MW     0.0000 MVAr
 16     11.0885 kV    1.0080      0.69 deg.  56.0000 MW    41.0000 MVAr
 17      6.5431 kV    0.9914     -1.13 deg.   0.0000 MW     0.0000 MVAr
 18    131.8234 kV    0.9987     -0.62 deg.   0.0000 MW     0.0000 MVAr
 19    131.8203 kV    0.9986     -0.63 deg.   0.0000 MW     0.0000 MVAr
 20     11.1347 kV    1.0122     -1.67 deg. -26.0177 MW    19.4873 MVAr
 21     11.1495 kV    1.0136     -1.59 deg.  -9.8551 MW    -4.7740 MVAr
 22    132.7546 kV    1.0057     -0.20 deg.   0.0000 MW     0.0000 MVAr
 23     11.1520 kV    1.0138     -1.59 deg.   0.0000 MW     0.0000 MVAr
 24    132.7525 kV    1.0057     -0.20 deg.   0.0000 MW     0.0000 MVAr
 25    132.7490 kV    1.0057     -0.20 deg.   0.0000 MW     0.0000 MVAr
 26    131.1738 kV    0.9937     -0.97 deg.   0.0000 MW     0.0000 MVAr
 27     10.9133 kV    0.9921     -1.07 deg.   0.0000 MW     0.0000 MVAr
 28     10.9142 kV    0.9922     -1.07 deg.   0.0000 MW     0.0000 MVAr
 29     11.1494 kV    1.0136     -1.59 deg.  -9.8551 MW    -4.7784 MVAr
```

```
30      11.1346 kV      1.0122      -1.66 deg.  -26.0177 MW      19.4873 MVAr
31       0.5565 kV      1.0118      -1.75 deg.    0.0000 MW       0.0000 MVAr
32      10.9276 kV      0.9934      -1.02 deg.    0.0000 MW       0.0000 MVAr
33       0.5603 kV      1.0187      -1.08 deg.    0.0000 MW       0.0000 MVAr
34       0.5464 kV      0.9934      -1.02 deg.    0.0000 MW       0.0000 MVAr
35      10.9259 kV      0.9933      -1.01 deg.    0.0000 MW       0.0000 MVAr
36       6.5199 kV      0.9879      -1.33 deg.    0.0000 MW       0.0000 MVAr
37      10.9237 kV      0.9931      -1.01 deg.    0.0000 MW       0.0000 MVAr
38      10.9014 kV      0.9910      -1.12 deg.    0.0000 MW       0.0000 MVAr
39      10.9014 kV      0.9910      -1.12 deg.    0.0000 MW       0.0000 MVAr
40      10.8959 kV      0.9905      -1.13 deg.    0.0000 MW       0.0000 MVAr
41       0.5391 kV      0.9802      -1.81 deg.    0.0000 MW       0.0000 MVAr
42       6.4477 kV      0.9769      -1.94 deg.    0.0000 MW       0.0000 MVAr
43      10.9228 kV      0.9930      -1.03 deg.    0.0000 MW       0.0000 MVAr
44      10.9232 kV      0.9930      -1.03 deg.    0.0000 MW       0.0000 MVAr
45       0.5577 kV      1.0141      -1.33 deg.    0.0000 MW       0.0000 MVAr
46      10.9209 kV      0.9928      -1.05 deg.    0.0000 MW       0.0000 MVAr
47      10.9205 kV      0.9928      -1.05 deg.    0.0000 MW       0.0000 MVAr
48       6.6582 kV      1.0088      -1.40 deg.    0.0000 MW       0.0000 MVAr
49       6.6544 kV      1.0082      -1.44 deg.   -0.5449 MW      -0.3305 MVAr
50       6.6575 kV      1.0087      -1.40 deg.   -0.2203 MW      -0.1134 MVAr
51       6.6555 kV      1.0084      -1.43 deg.   -0.6365 MW      -0.3115 MVAr
52       6.6576 kV      1.0087      -1.40 deg.   -0.2495 MW      -0.1338 MVAr
53       6.6582 kV      1.0088      -1.40 deg.    0.0000 MW       0.0000 MVAr
54       6.6582 kV      1.0088      -1.40 deg.    0.0000 MW       0.0000 MVAr
55       6.6582 kV      1.0088      -1.40 deg.    0.0000 MW       0.0000 MVAr
56       6.6575 kV      1.0087      -1.40 deg.   -0.1793 MW      -0.1344 MVAr
57       0.5580 kV      1.0145      -1.30 deg.    0.0000 MW       0.0000 MVAr
58      10.9676 kV      0.9971      -0.73 deg.    0.0000 MW       0.0000 MVAr


Branch currents:
 1     feeder: 284.5295A     -1.11 deg.
 2     feeder: 276.9756A     -1.11 deg.
 3     feeder:  69.3028A    -38.13 deg.
 4     3wtrnf: Ip: 69.3028A         -38.13 deg. Is:568.8969A  -38.12 deg.
           It:437.8951A    -38.16 deg.
 5     feeder:  58.7925A    -18.36 deg.
 6     feeder:  75.8412A    -36.07 deg.
 7     feeder:  61.8325A    -39.19 deg.
 8     feeder: 167.5346A     20.66 deg.
 9     transf: Ip:167.5346A         20.66 deg. Is:2010.4154A   20.66 deg.
10     feeder:  58.7478A    -18.39 deg.
11     feeder: 298.1620A    144.48 deg.
12     transf: Ip:298.1620A        144.48 deg. Is:3613.7236A 144.48 deg.
13      Load: 817.8054A    -39.75 deg.   7.2412MVA     5.7849MVAr
14      Load: 250.4916A    -37.70 deg.   3.8018MVA     2.8617MVAr
15      Load: 252.5904A    -38.45 deg.   3.7954MVA     2.9357MVAr
16     feeder: 167.5396A     20.67 deg.
17     transf: Ip:167.5396A         20.67 deg. Is:2010.4751A   20.67 deg.
18     feeder:  62.2614A    -39.18 deg.
19     3wtrnf: Ip: 69.1659A         -38.14 deg. Is:564.0458A  -38.14 deg.
           It:443.2420A    -38.14 deg.
20      Load:  58.7925A    -18.36 deg.  12.8453MVA     4.2127MVAr
21     feeder:  74.7940A    -36.12 deg.
22     feeder:  53.6999A    -13.59 deg.
23     feeder:  69.1659A    -38.14 deg.
24     feeder: 1685.5080A    35.17 deg.
25     feeder: 567.0467A    -27.44 deg.
26     feeder: 567.1536A    -27.46 deg.
27     feeder: 1685.5302A    35.17 deg.
28      Load:  75.8412A    -36.07 deg.  14.1316MVA    10.2174MVAr
29     3wtrnf: Ip: 61.8325A         -39.19 deg. Is:251.3614A  -38.09 deg.
           It:817.8311A    -39.75 deg.
30      Load:  58.7478A    -18.39 deg.  12.8332MVA     4.2167MVAr
31      Load:  74.7940A    -36.12 deg.  13.9278MVA    10.0883MVAr
32      Load:  53.6999A    -13.59 deg.  12.0116MVA     2.8604MVAr
33     3wtrnf: Ip: 62.2614A         -39.18 deg. Is:251.7098A  -38.07 deg.
           It:825.8290A    -39.74 deg.
```

```
34    feeder:   6.0545A    -5.36 deg.
35    feeder:   6.0545A    -5.36 deg.
36    transf: Ip:  6.0545A        -5.36 deg. Is:118.0631A   -5.36 deg.
37    transf: Ip:  6.0545A        -5.36 deg. Is:118.0631A   -5.36 deg.
38     Load: 236.1263A   -5.36 deg.  0.2285MVA    0.0171MVAr
39    feeder: 123.1304A  -40.33 deg.
40    feeder: 119.5044A  -39.37 deg.
41    transf: Ip:123.1304A        -40.33 deg. Is:205.2173A  -40.33 deg.
42    transf: Ip:119.5044A        -39.37 deg. Is:199.1741A  -39.37 deg.
43     Load: 404.3770A  -39.86 deg.  3.5727MVA    2.8442MVAr
44    feeder:  86.8872A  -38.69 deg.
45    feeder:  86.8872A  -38.69 deg.
46    feeder: 114.9198A  -40.54 deg.
47    transf: Ip: 86.8872A        -38.69 deg. Is:1737.7447A -38.69 deg.
48    transf: Ip: 86.8872A        -38.69 deg. Is:1737.7447A -38.69 deg.
49    transf: Ip:114.9198A        -40.54 deg. Is:191.5329A  -40.54 deg.
50     Load: 3475.4894A -38.69 deg.  2.5963MVA    1.9472MVAr
51     Load: 191.5329A  -40.54 deg.  1.6718MVA    1.3343MVAr
52     Load: 224.9312A  -39.55 deg.  3.3298MVA    2.6531MVAr
53    feeder:  36.6802A  -38.22 deg.
54    feeder:  33.3139A  -38.20 deg.
55    transf: Ip: 36.6802A        -38.22 deg. Is:715.2638A  -38.22 deg.
56    transf: Ip: 33.3139A        -38.20 deg. Is:649.6213A  -38.20 deg.
57    transf: Ip: 92.8918A        -38.60 deg. Is:1802.1015A -38.60 deg.
58    transf: Ip: 93.4887A        -38.65 deg. Is:1813.6813A -38.65 deg.
59    feeder:  92.8918A  -38.60 deg.
60    feeder:  93.4887A  -38.65 deg.
61    transf: Ip: 55.8861A        -30.67 deg. Is: 91.2807A  -30.67 deg.
62    transf: Ip: 55.4960A        -30.61 deg. Is: 90.6435A  -30.61 deg.
63    feeder:  55.8861A  -30.67 deg.
64    feeder:  55.4960A  -30.61 deg.
65     Load: 437.8931A  -38.16 deg.  3.9612MVA    2.9765MVAr
66     Load: 443.2441A  -38.13 deg.  4.0112MVA    3.0108MVAr
67     Load: 825.8546A  -39.74 deg.  7.3134MVA    5.8406MVAr
68    feeder:  55.2912A  -32.68 deg.
69    feeder:  21.4862A  -28.64 deg.
70    feeder:  61.4772A  -27.51 deg.
71    feeder:  24.5522A  -29.60 deg.
72    feeder:   0.0000A   76.68 deg.
73    feeder:   0.0000A -166.23 deg.
74    feeder:   0.0000A -103.32 deg.
75    feeder:  19.4326A  -38.26 deg.
76     Load: 3615.7825A -38.62 deg.  2.7881MVA    2.0910MVAr
77     Load:   6.3870A  -38.20 deg.  0.0049MVA    0.0037MVAr
78     Load: 352.5668A  -38.22 deg.  0.2724MVA    0.2045MVAr
79     Load: 126.1437A  -38.23 deg.  0.0974MVA    0.0732MVAr
80     Load: 123.9291A  -38.22 deg.  0.0957MVA    0.0719MVAr
81     Load: 106.2371A  -38.22 deg.  0.0821MVA    0.0616MVAr
82     Load:  70.3901A  -38.19 deg.  0.0544MVA    0.0408MVAr
83     Load:   3.1949A  -38.17 deg.  0.0025MVA    0.0019MVAr
84     Load: 352.7213A  -38.20 deg.  0.2726MVA    0.2047MVAr
85     Load: 132.5863A  -38.20 deg.  0.1025MVA    0.0769MVAr
86     Load:  90.7288A  -38.19 deg.  0.0701MVA    0.0526MVAr
```

13.3   Study Case 2 – Final State

Bus voltages and currents calculated on completion of simulation.

```
Number of iterations:   1   Max Power mismatch:    10.0kVA
```

Bus	Voltage(l-l)	Voltage(pu)	Angle	P(bus)	Q(bus)
1	133.0000 kV	1.0076	0.00 deg.	129.1434 MW	2.3913 MVAr
2	132.7564 kV	1.0057	-0.20 deg.	0.0000 MW	0.0000 MVAr
3	132.7524 kV	1.0057	-0.20 deg.	0.0000 MW	0.0000 MVAr
4	132.7541 kV	1.0057	-0.20 deg.	0.0000 MW	0.0000 MVAr
5	132.7496 kV	1.0057	-0.20 deg.	0.0000 MW	0.0000 MVAr
6	131.1868 kV	0.9938	-0.96 deg.	0.0000 MW	0.0000 MVAr
7	10.9293 kV	0.9936	-1.00 deg.	0.0000 MW	0.0000 MVAr

```
 8        6.5335 kV      0.9899      -1.24 deg.     0.0000 MW      0.0000 MVAr
 9      132.7538 kV      1.0057      -0.20 deg.     0.0000 MW      0.0000 MVAr
10      132.7526 kV      1.0057      -0.20 deg.     0.0000 MW      0.0000 MVAr
11      132.7529 kV      1.0057      -0.20 deg.     0.0000 MW      0.0000 MVAr
12      132.7554 kV      1.0057      -0.20 deg.     0.0000 MW      0.0000 MVAr
13       11.1519 kV      1.0138      -1.59 deg.     0.0000 MW      0.0000 MVAr
14      132.7538 kV      1.0057      -0.20 deg.     0.0000 MW      0.0000 MVAr
15      132.7719 kV      1.0058      -0.19 deg.     0.0000 MW      0.0000 MVAr
16       11.0886 kV      1.0081       0.69 deg.    56.0000 MW     41.0000 MVAr
17        6.5432 kV      0.9914      -1.13 deg.     0.0000 MW      0.0000 MVAr
18      131.8243 kV      0.9987      -0.62 deg.     0.0000 MW      0.0000 MVAr
19      131.8211 kV      0.9986      -0.62 deg.     0.0000 MW      0.0000 MVAr
20       11.1348 kV      1.0123      -1.66 deg.   -26.0177 MW     19.4873 MVAr
21       11.1496 kV      1.0136      -1.59 deg.    -9.8551 MW     -4.7740 MVAr
22      132.7554 kV      1.0057      -0.20 deg.     0.0000 MW      0.0000 MVAr
23       11.1520 kV      1.0138      -1.59 deg.     0.0000 MW      0.0000 MVAr
24      132.7534 kV      1.0057      -0.20 deg.     0.0000 MW      0.0000 MVAr
25      132.7499 kV      1.0057      -0.20 deg.     0.0000 MW      0.0000 MVAr
26      131.1860 kV      0.9938      -0.97 deg.     0.0000 MW      0.0000 MVAr
27       10.9144 kV      0.9922      -1.06 deg.     0.0000 MW      0.0000 MVAr
28       10.9152 kV      0.9923      -1.06 deg.     0.0000 MW      0.0000 MVAr
29       11.1494 kV      1.0136      -1.59 deg.    -9.8551 MW     -4.7784 MVAr
30       11.1346 kV      1.0122      -1.66 deg.   -26.0177 MW     19.4873 MVAr
31        0.5565 kV      1.0119      -1.75 deg.     0.0000 MW      0.0000 MVAr
32       10.9287 kV      0.9935      -1.01 deg.     0.0000 MW      0.0000 MVAr
33        0.5603 kV      1.0188      -1.08 deg.     0.0000 MW      0.0000 MVAr
34        0.5464 kV      0.9935      -1.01 deg.     0.0000 MW      0.0000 MVAr
35       10.9270 kV      0.9934      -1.00 deg.     0.0000 MW      0.0000 MVAr
36        6.5205 kV      0.9880      -1.33 deg.     0.0000 MW      0.0000 MVAr
37       10.9247 kV      0.9932      -1.00 deg.     0.0000 MW      0.0000 MVAr
38       10.9024 kV      0.9911      -1.11 deg.     0.0000 MW      0.0000 MVAr
39       10.9024 kV      0.9911      -1.11 deg.     0.0000 MW      0.0000 MVAr
40       10.8969 kV      0.9906      -1.13 deg.     0.0000 MW      0.0000 MVAr
41        0.5392 kV      0.9803      -1.81 deg.     0.0000 MW      0.0000 MVAr
42        6.4483 kV      0.9770      -1.94 deg.     0.0000 MW      0.0000 MVAr
43       10.9238 kV      0.9931      -1.02 deg.     0.0000 MW      0.0000 MVAr
44       10.9243 kV      0.9931      -1.02 deg.     0.0000 MW      0.0000 MVAr
45        0.5578 kV      1.0142      -1.32 deg.     0.0000 MW      0.0000 MVAr
46       10.9228 kV      0.9930      -1.04 deg.     0.0000 MW      0.0000 MVAr
47       10.9225 kV      0.9930      -1.04 deg.     0.0000 MW      0.0000 MVAr
48        6.6630 kV      1.0095      -1.35 deg.     0.0000 MW      0.0000 MVAr
49        6.6602 kV      1.0091      -1.38 deg.    -0.4405 MW     -0.2333 MVAr
50        6.6623 kV      1.0094      -1.35 deg.    -0.2010 MW     -0.1044 MVAr
51        6.6604 kV      1.0092      -1.38 deg.    -0.6093 MW     -0.2858 MVAr
52        6.6624 kV      1.0095      -1.35 deg.    -0.2032 MW     -0.1340 MVAr
53        6.6630 kV      1.0095      -1.35 deg.     0.0000 MW      0.0000 MVAr
54        6.6630 kV      1.0095      -1.35 deg.     0.0000 MW      0.0000 MVAr
55        6.6630 kV      1.0095      -1.35 deg.     0.0000 MW      0.0000 MVAr
56        6.6623 kV      1.0094      -1.35 deg.    -0.1793 MW     -0.1344 MVAr
57        0.5580 kV      1.0146      -1.29 deg.     0.0000 MW      0.0000 MVAr
58       10.9677 kV      0.9971      -0.73 deg.     0.0000 MW      0.0000 MVAr

Branch currents:
 1    feeder: 284.0984A     -1.05 deg.
 2    feeder: 276.5560A     -1.05 deg.
 3    feeder:  68.7807A    -38.15 deg.
 4    3wtrnf: Ip: 68.7807A        -38.15 deg. Is:562.6085A  -38.15 deg.
          It:437.9333A    -38.15 deg.
 5    feeder:  58.7929A    -18.36 deg.
 6    feeder:  75.8417A    -36.07 deg.
 7    feeder:  61.8329A    -39.19 deg.
 8    feeder: 167.5335A     20.66 deg.
 9    transf: Ip:167.5335A        20.66 deg. Is:2010.4025A   20.66 deg.
10    feeder:  58.7482A    -18.39 deg.
11    feeder: 298.1601A    144.48 deg.
12    transf: Ip:298.1601A       144.48 deg. Is:3613.7007A 144.48 deg.
13     Load: 817.8107A    -39.75 deg.    7.2413MVA     5.7850MVAr
14     Load: 250.4932A    -37.70 deg.    3.8018MVA     2.8617MVAr
```

```
15      Load: 252.5920A   -38.45 deg.   3.7955MVA     2.9358MVAr
16    feeder: 167.5385A    20.67 deg.
17    transf: Ip:167.5385A        20.67 deg. Is:2010.4622A   20.67 deg.
18    feeder:  62.2618A   -39.18 deg.
19    3wtrnf: Ip: 68.6449A        -38.15 deg. Is:557.7667A   -38.16 deg.
             It:443.2862A   -38.13 deg.
20      Load:  58.7929A   -18.36 deg.  12.8455MVA     4.2127MVAr
21    feeder:  74.7945A   -36.12 deg.
22    feeder:  53.7002A   -13.59 deg.
23    feeder:  68.6449A   -38.15 deg.
24    feeder: 1685.4971A   35.17 deg.
25    feeder: 567.0431A   -27.44 deg.
26    feeder: 567.1500A   -27.46 deg.
27    feeder: 1685.5193A   35.17 deg.
28      Load:  75.8417A   -36.07 deg.  14.1318MVA    10.2175MVAr
29    3wtrnf: Ip: 61.8329A        -39.19 deg. Is:251.3630A   -38.09 deg.
             It:817.8364A   -39.75 deg.
30      Load:  58.7482A   -18.39 deg.  12.8333MVA     4.2167MVAr
31      Load:  74.7945A   -36.12 deg.  13.9279MVA    10.0884MVAr
32      Load:  53.7002A   -13.59 deg.  12.0118MVA     2.8604MVAr
33    3wtrnf: Ip: 62.2618A        -39.18 deg. Is:251.7114A   -38.07 deg.
             It:825.8344A   -39.74 deg.
34    feeder:   6.0551A    -5.35 deg.
35    feeder:   6.0551A    -5.35 deg.
36    transf: Ip:  6.0551A         -5.35 deg. Is:118.0745A    -5.35 deg.
37    transf: Ip:  6.0551A         -5.35 deg. Is:118.0745A    -5.35 deg.
38      Load: 236.1490A    -5.35 deg.   0.2286MVA     0.0171MVAr
39    feeder: 123.1422A   -40.32 deg.
40    feeder: 119.5159A   -39.36 deg.
41    transf: Ip:123.1422A        -40.32 deg. Is:205.2370A   -40.32 deg.
42    transf: Ip:119.5159A        -39.36 deg. Is:199.1932A   -39.36 deg.
43      Load: 404.4159A   -39.85 deg.   3.5734MVA     2.8447MVAr
44    feeder:  86.8956A   -38.68 deg.
45    feeder:  86.8956A   -38.68 deg.
46    feeder: 114.9308A   -40.53 deg.
47    transf: Ip: 86.8956A        -38.68 deg. Is:1737.9117A -38.68 deg.
48    transf: Ip: 86.8956A        -38.68 deg. Is:1737.9117A -38.68 deg.
49    transf: Ip:114.9308A        -40.53 deg. Is:191.5513A   -40.53 deg.
50      Load: 3475.8234A  -38.68 deg.   2.5968MVA     1.9476MVAr
51      Load: 191.5513A   -40.53 deg.   1.6721MVA     1.3346MVAr
52      Load: 224.9528A   -39.55 deg.   3.3304MVA     2.6536MVAr
53    feeder:  36.6837A   -38.22 deg.
54    feeder:  33.3171A   -38.19 deg.
55    transf: Ip: 36.6837A        -38.22 deg. Is:715.3325A   -38.22 deg.
56    transf: Ip: 33.3171A        -38.19 deg. Is:649.6838A   -38.19 deg.
57    transf: Ip: 92.9008A        -38.59 deg. Is:1802.2747A -38.59 deg.
58    transf: Ip: 93.4977A        -38.64 deg. Is:1813.8556A -38.64 deg.
59    feeder:  92.9008A   -38.59 deg.
60    feeder:  93.4977A   -38.64 deg.
61    transf: Ip: 49.5498A        -30.04 deg. Is: 80.9313A   -30.04 deg.
62    transf: Ip: 49.2039A        -29.98 deg. Is: 80.3664A   -29.98 deg.
63    feeder:  49.5498A   -30.04 deg.
64    feeder:  49.2039A   -29.98 deg.
65      Load: 437.9340A   -38.16 deg.   3.9620MVA     2.9771MVAr
66      Load: 443.2855A   -38.13 deg.   4.0119MVA     3.0114MVAr
67      Load: 825.8600A   -39.74 deg.   7.3135MVA     5.8407MVAr
68    feeder:  43.2081A   -29.29 deg.
69    feeder:  19.6275A   -28.79 deg.
70    feeder:  58.3399A   -26.51 deg.
71    feeder:  21.0907A   -34.76 deg.
72    feeder:   0.0000A    76.68 deg.
73    feeder:   0.0000A    13.77 deg.
74    feeder:   0.0000A  -103.32 deg.
75    feeder:  19.4187A   -38.21 deg.
76      Load: 3616.1300A  -38.62 deg.   2.7886MVA     2.0914MVAr
77      Load:   6.3876A   -38.19 deg.   0.0049MVA     0.0037MVAr
78      Load: 352.6007A   -38.22 deg.   0.2724MVA     0.2045MVAr
79      Load: 126.1558A   -38.22 deg.   0.0975MVA     0.0732MVAr
```

```
80      Load: 123.9410A    -38.22 deg.   0.0958MVA     0.0719MVAr
81      Load: 106.2473A    -38.22 deg.   0.0821MVA     0.0616MVAr
82      Load:  70.3968A    -38.18 deg.   0.0544MVA     0.0408MVAr
83      Load:   3.1952A    -38.16 deg.   0.0025MVA     0.0019MVAr
84      Load: 352.7552A    -38.19 deg.   0.2727MVA     0.2047MVAr
85      Load: 132.5990A    -38.19 deg.   0.1025MVA     0.0770MVAr
86      Load:  90.7375A    -38.19 deg.   0.0701MVA     0.0527MVAr
```

13.4   Study Case 3 – Final State

Bus voltages and currents calculated on completion of simulation.

```
Number of iterations:   1   Max Power mismatch:    10.0kVA

 Bus  Voltage(l-l)  Voltage(pu)      Angle           P(bus)        Q(bus)
  1     133.0000 kV    1.0076      0.00 deg. 129.3266 MW      2.5245 MVAr
  2     132.7555 kV    1.0057     -0.20 deg.   0.0000 MW      0.0000 MVAr
  3     132.7515 kV    1.0057     -0.20 deg.   0.0000 MW      0.0000 MVAr
  4     132.7532 kV    1.0057     -0.20 deg.   0.0000 MW      0.0000 MVAr
  5     132.7487 kV    1.0057     -0.20 deg.   0.0000 MW      0.0000 MVAr
  6     131.1745 kV    0.9937     -0.97 deg.   0.0000 MW      0.0000 MVAr
  7      10.9282 kV    0.9935     -1.01 deg.   0.0000 MW      0.0000 MVAr
  8       6.5329 kV    0.9898     -1.24 deg.   0.0000 MW      0.0000 MVAr
  9     132.7530 kV    1.0057     -0.20 deg.   0.0000 MW      0.0000 MVAr
 10     132.7517 kV    1.0057     -0.20 deg.   0.0000 MW      0.0000 MVAr
 11     132.7521 kV    1.0057     -0.20 deg.   0.0000 MW      0.0000 MVAr
 12     132.7545 kV    1.0057     -0.20 deg.   0.0000 MW      0.0000 MVAr
 13      11.1518 kV    1.0138     -1.59 deg.   0.0000 MW      0.0000 MVAr
 14     132.7529 kV    1.0057     -0.20 deg.   0.0000 MW      0.0000 MVAr
 15     132.7710 kV    1.0058     -0.19 deg.   0.0000 MW      0.0000 MVAr
 16      11.0885 kV    1.0080      0.69 deg.  55.9999 MW     40.9982 MVAr
 17       6.5431 kV    0.9914     -1.13 deg.   0.0000 MW      0.0000 MVAr
 18     131.8234 kV    0.9987     -0.62 deg.   0.0000 MW      0.0000 MVAr
 19     131.8203 kV    0.9986     -0.63 deg.   0.0000 MW      0.0000 MVAr
 20      11.1347 kV    1.0122     -1.67 deg. -26.0177 MW     19.4873 MVAr
 21      11.1495 kV    1.0136     -1.59 deg.  -9.8551 MW     -4.7740 MVAr
 22     132.7545 kV    1.0057     -0.20 deg.   0.0000 MW      0.0000 MVAr
 23      11.1520 kV    1.0138     -1.59 deg.   0.0000 MW      0.0000 MVAr
 24     132.7525 kV    1.0057     -0.20 deg.   0.0000 MW      0.0000 MVAr
 25     132.7490 kV    1.0057     -0.20 deg.   0.0000 MW      0.0000 MVAr
 26     131.1738 kV    0.9937     -0.97 deg.   0.0000 MW      0.0000 MVAr
 27      10.9133 kV    0.9921     -1.07 deg.   0.0000 MW      0.0000 MVAr
 28      10.9142 kV    0.9922     -1.07 deg.   0.0000 MW      0.0000 MVAr
 29      11.1494 kV    1.0136     -1.59 deg.  -9.8551 MW     -4.7784 MVAr
 30      11.1346 kV    1.0122     -1.66 deg. -26.0177 MW     19.4873 MVAr
 31       0.5565 kV    1.0118     -1.75 deg.   0.0000 MW      0.0000 MVAr
 32      10.9276 kV    0.9934     -1.02 deg.   0.0000 MW      0.0000 MVAr
 33       0.5603 kV    1.0187     -1.08 deg.   0.0000 MW      0.0000 MVAr
 34       0.5464 kV    0.9934     -1.02 deg.   0.0000 MW      0.0000 MVAr
 35      10.9259 kV    0.9933     -1.01 deg.   0.0000 MW      0.0000 MVAr
 36       6.5199 kV    0.9879     -1.33 deg.   0.0000 MW      0.0000 MVAr
 37      10.9237 kV    0.9931     -1.01 deg.   0.0000 MW      0.0000 MVAr
 38      10.9014 kV    0.9910     -1.12 deg.   0.0000 MW      0.0000 MVAr
 39      10.9014 kV    0.9910     -1.12 deg.   0.0000 MW      0.0000 MVAr
 40      10.8959 kV    0.9905     -1.13 deg.   0.0000 MW      0.0000 MVAr
 41       0.5391 kV    0.9802     -1.81 deg.   0.0000 MW      0.0000 MVAr
 42       6.4477 kV    0.9769     -1.94 deg.   0.0000 MW      0.0000 MVAr
 43      10.9228 kV    0.9930     -1.03 deg.   0.0000 MW      0.0000 MVAr
 44      10.9232 kV    0.9930     -1.03 deg.   0.0000 MW      0.0000 MVAr
 45       0.5577 kV    1.0141     -1.33 deg.   0.0000 MW      0.0000 MVAr
 46      10.9209 kV    0.9928     -1.05 deg.   0.0000 MW      0.0000 MVAr
 47      10.9205 kV    0.9928     -1.05 deg.   0.0000 MW      0.0000 MVAr
 48       6.6582 kV    1.0088     -1.40 deg.   0.0000 MW      0.0000 MVAr
 49       6.6544 kV    1.0082     -1.44 deg.  -0.5449 MW     -0.3305 MVAr
 50       6.6575 kV    1.0087     -1.40 deg.  -0.2203 MW     -0.1134 MVAr
 51       6.6555 kV    1.0084     -1.43 deg.  -0.6365 MW     -0.3115 MVAr
 52       6.6576 kV    1.0087     -1.40 deg.  -0.2495 MW     -0.1338 MVAr
 53       6.6582 kV    1.0088     -1.40 deg.   0.0000 MW      0.0000 MVAr
```

```
54      6.6582 kV      1.0088      -1.40 deg.    0.0000 MW      0.0000 MVAr
55      6.6582 kV      1.0088      -1.40 deg.    0.0000 MW      0.0000 MVAr
56      6.6575 kV      1.0087      -1.40 deg.   -0.1793 MW     -0.1344 MVAr
57      0.5580 kV      1.0145      -1.30 deg.    0.0000 MW      0.0000 MVAr
58     10.9676 kV      0.9971      -0.73 deg.    0.0000 MW      0.0000 MVAr

Branch currents:
 1    feeder: 284.5298A     -1.11 deg.
 2    feeder: 276.9759A     -1.11 deg.
 3    feeder:  69.3028A    -38.13 deg.
 4    3wtrnf: Ip: 69.3028A       -38.13 deg. Is:568.8969A  -38.12 deg.
          It:437.8951A   -38.16 deg.
 5    feeder:  58.7925A    -18.36 deg.
 6    feeder:  75.8412A    -36.07 deg.
 7    feeder:  61.8325A    -39.19 deg.
 8    feeder: 167.5346A     20.66 deg.
 9    transf: Ip:167.5346A       20.66 deg. Is:2010.4155A  20.66 deg.
10    feeder:  58.7478A    -18.39 deg.
11    feeder: 298.1574A    144.48 deg.
12    transf: Ip:298.1574A      144.48 deg. Is:3613.6674A 144.48 deg.
13     Load: 817.8053A    -39.75 deg.    7.2412MVA     5.7849MVAr
14     Load: 250.4916A    -37.70 deg.    3.8018MVA     2.8617MVAr
15     Load: 252.5904A    -38.45 deg.    3.7954MVA     2.9357MVAr
16    feeder: 167.5396A     20.67 deg.
17    transf: Ip:167.5396A       20.67 deg. Is:2010.4752A  20.67 deg.
18    feeder:  62.2614A    -39.18 deg.
19    3wtrnf: Ip: 69.1659A       -38.14 deg. Is:564.0458A  -38.14 deg.
          It:443.2420A   -38.14 deg.
20     Load:  58.7925A    -18.36 deg.   12.8453MVA     4.2127MVAr
21    feeder:  74.7940A    -36.12 deg.
22    feeder:  53.6999A    -13.59 deg.
23    feeder:  69.1659A    -38.14 deg.
24    feeder: 1685.5081A    35.17 deg.
25    feeder: 567.0468A    -27.44 deg.
26    feeder: 567.1536A    -27.46 deg.
27    feeder: 1685.5303A    35.17 deg.
28     Load:  75.8412A    -36.07 deg.   14.1316MVA    10.2174MVAr
29    3wtrnf: Ip: 61.8325A       -39.19 deg. Is:251.3614A  -38.09 deg.
          It:817.8310A   -39.75 deg.
30     Load:  58.7478A    -18.39 deg.   12.8331MVA     4.2167MVAr
31     Load:  74.7940A    -36.12 deg.   13.9278MVA    10.0883MVAr
32     Load:  53.6999A    -13.59 deg.   12.0116MVA     2.8604MVAr
33    3wtrnf: Ip: 62.2614A       -39.18 deg. Is:251.7098A  -38.07 deg.
          It:825.8289A   -39.74 deg.
34    feeder:   6.0545A     -5.36 deg.
35    feeder:   6.0545A     -5.36 deg.
36    transf: Ip:  6.0545A        -5.36 deg. Is:118.0631A   -5.36 deg.
37    transf: Ip:  6.0545A        -5.36 deg. Is:118.0631A   -5.36 deg.
38     Load: 236.1263A     -5.36 deg.    0.2285MVA     0.0171MVAr
39    feeder: 123.1304A    -40.33 deg.
40    feeder: 119.5044A    -39.37 deg.
41    transf: Ip:123.1304A       -40.33 deg. Is:205.2173A  -40.33 deg.
42    transf: Ip:119.5044A       -39.37 deg. Is:199.1741A  -39.37 deg.
43     Load: 404.3770A    -39.86 deg.    3.5727MVA     2.8442MVAr
44    feeder:  86.8872A    -38.69 deg.
45    feeder:  86.8872A    -38.69 deg.
46    feeder: 114.9197A    -40.54 deg.
47    transf: Ip: 86.8872A       -38.69 deg. Is:1737.7446A -38.69 deg.
48    transf: Ip: 86.8872A       -38.69 deg. Is:1737.7446A -38.69 deg.
49    transf: Ip:114.9197A       -40.54 deg. Is:191.5329A  -40.54 deg.
50     Load: 3475.4892A  -38.69 deg.    2.5963MVA     1.9472MVAr
51     Load: 191.5329A    -40.54 deg.    1.6718MVA     1.3343MVAr
52     Load: 224.9312A    -39.55 deg.    3.3298MVA     2.6531MVAr
53    feeder:  36.6802A    -38.22 deg.
54    feeder:  33.3139A    -38.20 deg.
55    transf: Ip: 36.6802A       -38.22 deg. Is:715.2638A  -38.22 deg.
56    transf: Ip: 33.3139A       -38.20 deg. Is:649.6213A  -38.20 deg.
57    transf: Ip: 92.8918A       -38.60 deg. Is:1802.1014A -38.60 deg.
```

```
58    transf: Ip: 93.4887A        -38.65 deg. Is:1813.6812A -38.65 deg.
59    feeder:  92.8918A    -38.60 deg.
60    feeder:  93.4887A    -38.65 deg.
61    transf: Ip: 55.8861A        -30.67 deg. Is: 91.2807A   -30.67 deg.
62    transf: Ip: 55.4960A        -30.61 deg. Is: 90.6435A   -30.61 deg.
63    feeder:  55.8861A    -30.67 deg.
64    feeder:  55.4960A    -30.61 deg.
65     Load: 437.8931A    -38.16 deg.   3.9612MVA      2.9765MVAr
66     Load: 443.2441A    -38.13 deg.   4.0112MVA      3.0108MVAr
67     Load: 825.8546A    -39.74 deg.   7.3134MVA      5.8406MVAr
68    feeder:  55.2912A    -32.68 deg.
69    feeder:  21.4862A    -28.64 deg.
70    feeder:  61.4772A    -27.51 deg.
71    feeder:  24.5522A    -29.60 deg.
72    feeder:   0.0000A   -103.32 deg.
73    feeder:   0.0000A   -166.23 deg.
74    feeder:   0.0000A   -103.32 deg.
75    feeder:  19.4326A    -38.26 deg.
76     Load: 3615.7823A   -38.62 deg.   2.7881MVA      2.0910MVAr
77     Load:    6.3870A   -38.20 deg.   0.0049MVA      0.0037MVAr
78     Load: 352.5668A    -38.22 deg.   0.2724MVA      0.2045MVAr
79     Load: 126.1437A    -38.23 deg.   0.0974MVA      0.0732MVAr
80     Load: 123.9291A    -38.22 deg.   0.0957MVA      0.0719MVAr
81     Load: 106.2371A    -38.22 deg.   0.0821MVA      0.0616MVAr
82     Load:  70.3901A    -38.19 deg.   0.0544MVA      0.0408MVAr
83     Load:   3.1949A    -38.17 deg.   0.0025MVA      0.0019MVAr
84     Load: 352.7213A    -38.20 deg.   0.2726MVA      0.2047MVAr
85     Load: 132.5863A    -38.20 deg.   0.1025MVA      0.0769MVAr
86     Load:  90.7288A    -38.19 deg.   0.0701MVA      0.0526MVAr
```

13.5 Study Case 4 – Final State

Bus voltages and currents calculated on completion of simulation.

```
Number of iterations:   1   Max Power mismatch:    10.0kVA

 Bus  Voltage(l-l)  Voltage(pu)     Angle          P(bus)        Q(bus)
  1    133.0000 kV    1.0076     0.00 deg. 129.1329 MW    2.3638 MVAr
  2    132.7564 kV    1.0057    -0.20 deg.   0.0000 MW    0.0000 MVAr
  3    132.7524 kV    1.0057    -0.20 deg.   0.0000 MW    0.0000 MVAr
  4    132.7541 kV    1.0057    -0.20 deg.   0.0000 MW    0.0000 MVAr
  5    132.7496 kV    1.0057    -0.20 deg.   0.0000 MW    0.0000 MVAr
  6    131.1868 kV    0.9938    -0.96 deg.   0.0000 MW    0.0000 MVAr
  7     10.9293 kV    0.9936    -1.00 deg.   0.0000 MW    0.0000 MVAr
  8      6.5335 kV    0.9899    -1.24 deg.   0.0000 MW    0.0000 MVAr
  9    132.7538 kV    1.0057    -0.20 deg.   0.0000 MW    0.0000 MVAr
 10    132.7526 kV    1.0057    -0.20 deg.   0.0000 MW    0.0000 MVAr
 11    132.7529 kV    1.0057    -0.20 deg.   0.0000 MW    0.0000 MVAr
 12    132.7554 kV    1.0057    -0.20 deg.   0.0000 MW    0.0000 MVAr
 13     11.1519 kV    1.0138    -1.59 deg.   0.0000 MW    0.0000 MVAr
 14    132.7538 kV    1.0057    -0.20 deg.   0.0000 MW    0.0000 MVAr
 15    132.7719 kV    1.0058    -0.19 deg.   0.0000 MW    0.0000 MVAr
 16     11.0886 kV    1.0081     0.69 deg.  56.0000 MW   41.0018 MVAr
 17      6.5432 kV    0.9914    -1.13 deg.   0.0000 MW    0.0000 MVAr
 18    131.8243 kV    0.9987    -0.62 deg.   0.0000 MW    0.0000 MVAr
 19    131.8211 kV    0.9986    -0.62 deg.   0.0000 MW    0.0000 MVAr
 20     11.1348 kV    1.0123    -1.66 deg. -26.0177 MW   19.4873 MVAr
 21     11.1496 kV    1.0136    -1.59 deg.  -9.8551 MW   -4.7740 MVAr
 22    132.7554 kV    1.0057    -0.20 deg.   0.0000 MW    0.0000 MVAr
 23     11.1520 kV    1.0138    -1.59 deg.   0.0000 MW    0.0000 MVAr
 24    132.7534 kV    1.0057    -0.20 deg.   0.0000 MW    0.0000 MVAr
 25    132.7499 kV    1.0057    -0.20 deg.   0.0000 MW    0.0000 MVAr
 26    131.1860 kV    0.9938    -0.97 deg.   0.0000 MW    0.0000 MVAr
 27     10.9144 kV    0.9922    -1.06 deg.   0.0000 MW    0.0000 MVAr
 28     10.9152 kV    0.9923    -1.06 deg.   0.0000 MW    0.0000 MVAr
 29     11.1494 kV    1.0136    -1.59 deg.  -9.8551 MW   -4.7784 MVAr
 30     11.1346 kV    1.0122    -1.66 deg. -26.0177 MW   19.4873 MVAr
 31      0.5565 kV    1.0119    -1.75 deg.   0.0000 MW    0.0000 MVAr
```

```
32      10.9287 kV      0.9935        -1.01 deg.      0.0000 MW       0.0000 MVAr
33       0.5603 kV      1.0188        -1.08 deg.      0.0000 MW       0.0000 MVAr
34       0.5464 kV      0.9935        -1.01 deg.      0.0000 MW       0.0000 MVAr
35      10.9270 kV      0.9934        -1.00 deg.      0.0000 MW       0.0000 MVAr
36       6.5205 kV      0.9880        -1.33 deg.      0.0000 MW       0.0000 MVAr
37      10.9247 kV      0.9932        -1.00 deg.      0.0000 MW       0.0000 MVAr
38      10.9024 kV      0.9911        -1.11 deg.      0.0000 MW       0.0000 MVAr
39      10.9024 kV      0.9911        -1.11 deg.      0.0000 MW       0.0000 MVAr
40      10.8969 kV      0.9906        -1.13 deg.      0.0000 MW       0.0000 MVAr
41       0.5392 kV      0.9803        -1.81 deg.      0.0000 MW       0.0000 MVAr
42       6.4483 kV      0.9770        -1.94 deg.      0.0000 MW       0.0000 MVAr
43      10.9238 kV      0.9931        -1.02 deg.      0.0000 MW       0.0000 MVAr
44      10.9243 kV      0.9931        -1.02 deg.      0.0000 MW       0.0000 MVAr
45       0.5578 kV      1.0142        -1.32 deg.      0.0000 MW       0.0000 MVAr
46      10.9228 kV      0.9930        -1.04 deg.      0.0000 MW       0.0000 MVAr
47      10.9225 kV      0.9930        -1.04 deg.      0.0000 MW       0.0000 MVAr
48       6.6630 kV      1.0095        -1.35 deg.      0.0000 MW       0.0000 MVAr
49       6.6602 kV      1.0091        -1.38 deg.     -0.4405 MW      -0.2333 MVAr
50       6.6623 kV      1.0094        -1.35 deg.     -0.2010 MW      -0.1044 MVAr
51       6.6604 kV      1.0092        -1.38 deg.     -0.6093 MW      -0.2859 MVAr
52       6.6624 kV      1.0095        -1.35 deg.     -0.2032 MW      -0.1340 MVAr
53       6.6630 kV      1.0095        -1.35 deg.      0.0000 MW       0.0000 MVAr
54       6.6630 kV      1.0095        -1.35 deg.      0.0000 MW       0.0000 MVAr
55       6.6630 kV      1.0095        -1.35 deg.      0.0000 MW       0.0000 MVAr
56       6.6623 kV      1.0094        -1.35 deg.     -0.1793 MW      -0.1344 MVAr
57       0.5580 kV      1.0146        -1.29 deg.      0.0000 MW       0.0000 MVAr
58      10.9677 kV      0.9971        -0.73 deg.      0.0000 MW       0.0000 MVAr


Branch currents:
 1      feeder: 284.0984A     -1.05 deg.
 2      feeder: 276.5560A     -1.05 deg.
 3      feeder:  68.7808A    -38.15 deg.
 4      3wtrnf: Ip: 68.7808A        -38.15 deg. Is:562.6097A  -38.15 deg.
            It:437.9333A   -38.15 deg.
 5      feeder:  58.7929A    -18.36 deg.
 6      feeder:  75.8417A    -36.07 deg.
 7      feeder:  61.8329A    -39.19 deg.
 8      feeder: 167.5335A     20.66 deg.
 9      transf: Ip:167.5335A        20.66 deg. Is:2010.4024A  20.66 deg.
10      feeder:  58.7482A    -18.39 deg.
11      feeder: 298.1643A    144.48 deg.
12      transf: Ip:298.1643A        144.48 deg. Is:3613.7517A 144.48 deg.
13       Load: 817.8107A    -39.75 deg.   7.2413MVA     5.7850MVAr
14       Load: 250.4932A    -37.70 deg.   3.8019MVA     2.8617MVAr
15       Load: 252.5921A    -38.45 deg.   3.7955MVA     2.9358MVAr
16      feeder: 167.5385A     20.67 deg.
17      transf: Ip:167.5385A        20.67 deg. Is:2010.4621A  20.67 deg.
18      feeder:  62.2618A    -39.18 deg.
19      3wtrnf: Ip: 68.6450A        -38.15 deg. Is:557.7679A  -38.17 deg.
            It:443.2862A   -38.13 deg.
20       Load:  58.7929A    -18.36 deg.  12.8455MVA     4.2127MVAr
21      feeder:  74.7945A    -36.12 deg.
22      feeder:  53.7002A    -13.59 deg.
23      feeder:  68.6450A    -38.15 deg.
24      feeder: 1685.4971A    35.17 deg.
25      feeder: 567.0431A    -27.44 deg.
26      feeder: 567.1499A    -27.46 deg.
27      feeder: 1685.5193A    35.17 deg.
28       Load:  75.8417A    -36.07 deg.  14.1318MVA    10.2175MVAr
29      3wtrnf: Ip: 61.8329A        -39.19 deg. Is:251.3630A  -38.09 deg.
            It:817.8364A   -39.75 deg.
30       Load:  58.7482A    -18.39 deg.  12.8333MVA     4.2167MVAr
31       Load:  74.7945A    -36.12 deg.  13.9279MVA    10.0884MVAr
32       Load:  53.7002A    -13.59 deg.  12.0118MVA     2.8604MVAr
33      3wtrnf: Ip: 62.2618A        -39.18 deg. Is:251.7114A  -38.07 deg.
            It:825.8344A   -39.74 deg.
34      feeder:   6.0551A     -5.35 deg.
35      feeder:   6.0551A     -5.35 deg.
```

```
36    transf: Ip:  6.0551A          -5.35 deg. Is:118.0745A    -5.35 deg.
37    transf: Ip:  6.0551A          -5.35 deg. Is:118.0745A    -5.35 deg.
38     Load: 236.1490A    -5.35 deg.   0.2286MVA     0.0171MVAr
39    feeder: 123.1422A   -40.32 deg.
40    feeder: 119.5159A   -39.36 deg.
41    transf: Ip:123.1422A          -40.32 deg. Is:205.2370A   -40.32 deg.
42    transf: Ip:119.5159A          -39.36 deg. Is:199.1932A   -39.36 deg.
43     Load: 404.4159A    -39.85 deg.   3.5734MVA     2.8447MVAr
44    feeder:  86.8956A   -38.68 deg.
45    feeder:  86.8956A   -38.68 deg.
46    feeder: 114.9308A   -40.53 deg.
47    transf: Ip: 86.8956A          -38.68 deg. Is:1737.9117A -38.68 deg.
48    transf: Ip: 86.8956A          -38.68 deg. Is:1737.9117A -38.68 deg.
49    transf: Ip:114.9308A          -40.53 deg. Is:191.5513A   -40.53 deg.
50     Load: 3475.8234A  -38.68 deg.   2.5968MVA     1.9476MVAr
51     Load: 191.5513A   -40.53 deg.   1.6721MVA     1.3346MVAr
52     Load: 224.9528A   -39.55 deg.   3.3304MVA     2.6536MVAr
53    feeder:  36.6837A   -38.22 deg.
54    feeder:  33.3171A   -38.19 deg.
55    transf: Ip: 36.6837A          -38.22 deg. Is:715.3325A   -38.22 deg.
56    transf: Ip: 33.3171A          -38.19 deg. Is:649.6838A   -38.19 deg.
57    transf: Ip: 92.9008A          -38.59 deg. Is:1802.2747A -38.59 deg.
58    transf: Ip: 93.4977A          -38.64 deg. Is:1813.8556A -38.64 deg.
59    feeder:  92.9008A   -38.59 deg.
60    feeder:  93.4977A   -38.64 deg.
61    transf: Ip: 49.5508A          -30.04 deg. Is: 80.9329A   -30.04 deg.
62    transf: Ip: 49.2049A          -29.98 deg. Is: 80.3680A   -29.98 deg.
63    feeder:  49.5508A   -30.04 deg.
64    feeder:  49.2049A   -29.98 deg.
65     Load: 437.9340A    -38.16 deg.   3.9620MVA     2.9771MVAr
66     Load: 443.2855A    -38.13 deg.   4.0119MVA     3.0114MVAr
67     Load: 825.8601A    -39.74 deg.   7.3135MVA     5.8407MVAr
68    feeder:  43.2089A   -29.29 deg.
69    feeder:  19.6284A   -28.80 deg.
70    feeder:  58.3407A   -26.52 deg.
71    feeder:  21.0914A   -34.77 deg.
72    feeder:   0.0000A  -103.32 deg.
73    feeder:   0.0000A  -166.23 deg.
74    feeder:   0.0000A  -103.32 deg.
75    feeder:  19.4187A   -38.21 deg.
76     Load: 3616.1300A  -38.62 deg.   2.7886MVA     2.0914MVAr
77     Load:   6.3876A   -38.19 deg.   0.0049MVA     0.0037MVAr
78     Load: 352.6007A   -38.22 deg.   0.2724MVA     0.2045MVAr
79     Load: 126.1558A   -38.22 deg.   0.0975MVA     0.0732MVAr
80     Load: 123.9410A   -38.22 deg.   0.0958MVA     0.0719MVAr
81     Load: 106.2473A   -38.22 deg.   0.0821MVA     0.0616MVAr
82     Load:  70.3968A   -38.18 deg.   0.0544MVA     0.0408MVAr
83     Load:   3.1952A   -38.16 deg.   0.0025MVA     0.0019MVAr
84     Load: 352.7552A   -38.19 deg.   0.2727MVA     0.2047MVAr
85     Load: 132.5990A   -38.19 deg.   0.1025MVA     0.0770MVAr
86     Load:  90.7375A   -38.19 deg.   0.0701MVA     0.0527MVAr
```

13.6 Study Case 5 – Final State

Bus voltages and currents calculated on completion of simulation.

```
Number of iterations:   1   Max Power mismatch:    10.0kVA

  Bus  Voltage(l-l)  Voltage(pu)       Angle         P(bus)        Q(bus)
   1    133.0000 kV    1.0076       0.00 deg. 130.3709 MW     1.5078 MVAr
   2    132.7573 kV    1.0057      -0.20 deg.   0.0000 MW     0.0000 MVAr
   3    132.7533 kV    1.0057      -0.20 deg.   0.0000 MW     0.0000 MVAr
   4    132.7549 kV    1.0057      -0.20 deg.   0.0000 MW     0.0000 MVAr
   5    132.7504 kV    1.0057      -0.20 deg.   0.0000 MW     0.0000 MVAr
   6    131.1762 kV    0.9938      -0.97 deg.   0.0000 MW     0.0000 MVAr
   7     10.9283 kV    0.9935      -1.01 deg.   0.0000 MW     0.0000 MVAr
   8      6.5330 kV    0.9898      -1.24 deg.   0.0000 MW     0.0000 MVAr
```

```
 9     132.7547 kV      1.0057        -0.20 deg.     0.0000 MW       0.0000 MVAr
10     132.7534 kV      1.0057        -0.20 deg.     0.0000 MW       0.0000 MVAr
11     132.7538 kV      1.0057        -0.20 deg.     0.0000 MW       0.0000 MVAr
12     132.7562 kV      1.0057        -0.20 deg.     0.0000 MW       0.0000 MVAr
13      11.1520 kV      1.0138        -1.59 deg.     0.0000 MW       0.0000 MVAr
14     132.7546 kV      1.0057        -0.20 deg.     0.0000 MW       0.0000 MVAr
15     132.7729 kV      1.0059        -0.20 deg.     0.0000 MW       0.0000 MVAr
16      11.0917 kV      1.0083         0.67 deg.    54.9602 MW      41.9991 MVAr
17       6.5432 kV      0.9914        -1.13 deg.     0.0000 MW       0.0000 MVAr
18     131.8251 kV      0.9987        -0.63 deg.     0.0000 MW       0.0000 MVAr
19     131.8220 kV      0.9987        -0.63 deg.     0.0000 MW       0.0000 MVAr
20      11.1349 kV      1.0123        -1.67 deg.   -26.0177 MW      19.4873 MVAr
21      11.1496 kV      1.0136        -1.59 deg.    -9.8551 MW      -4.7740 MVAr
22     132.7563 kV      1.0057        -0.20 deg.     0.0000 MW       0.0000 MVAr
23      11.1521 kV      1.0138        -1.59 deg.     0.0000 MW       0.0000 MVAr
24     132.7542 kV      1.0057        -0.20 deg.     0.0000 MW       0.0000 MVAr
25     132.7507 kV      1.0057        -0.20 deg.     0.0000 MW       0.0000 MVAr
26     131.1755 kV      0.9938        -0.97 deg.     0.0000 MW       0.0000 MVAr
27      10.9135 kV      0.9921        -1.07 deg.     0.0000 MW       0.0000 MVAr
28      10.9143 kV      0.9922        -1.07 deg.     0.0000 MW       0.0000 MVAr
29      11.1495 kV      1.0136        -1.59 deg.    -9.8551 MW      -4.7784 MVAr
30      11.1347 kV      1.0122        -1.67 deg.   -26.0177 MW      19.4873 MVAr
31       0.5565 kV      1.0118        -1.76 deg.     0.0000 MW       0.0000 MVAr
32      10.9278 kV      0.9934        -1.02 deg.     0.0000 MW       0.0000 MVAr
33       0.5603 kV      1.0187        -1.09 deg.     0.0000 MW       0.0000 MVAr
34       0.5464 kV      0.9934        -1.02 deg.     0.0000 MW       0.0000 MVAr
35      10.9261 kV      0.9933        -1.01 deg.     0.0000 MW       0.0000 MVAr
36       6.5200 kV      0.9879        -1.33 deg.     0.0000 MW       0.0000 MVAr
37      10.9238 kV      0.9931        -1.01 deg.     0.0000 MW       0.0000 MVAr
38      10.9015 kV      0.9910        -1.12 deg.     0.0000 MW       0.0000 MVAr
39      10.9015 kV      0.9910        -1.12 deg.     0.0000 MW       0.0000 MVAr
40      10.8960 kV      0.9905        -1.14 deg.     0.0000 MW       0.0000 MVAr
41       0.5391 kV      0.9802        -1.82 deg.     0.0000 MW       0.0000 MVAr
42       6.4478 kV      0.9769        -1.95 deg.     0.0000 MW       0.0000 MVAr
43      10.9229 kV      0.9930        -1.03 deg.     0.0000 MW       0.0000 MVAr
44      10.9234 kV      0.9930        -1.03 deg.     0.0000 MW       0.0000 MVAr
45       0.5577 kV      1.0141        -1.33 deg.     0.0000 MW       0.0000 MVAr
46      10.9210 kV      0.9928        -1.05 deg.     0.0000 MW       0.0000 MVAr
47      10.9206 kV      0.9928        -1.05 deg.     0.0000 MW       0.0000 MVAr
48       6.6583 kV      1.0088        -1.41 deg.     0.0000 MW       0.0000 MVAr
49       6.6545 kV      1.0083        -1.44 deg.    -0.5449 MW      -0.3305 MVAr
50       6.6576 kV      1.0087        -1.40 deg.    -0.2203 MW      -0.1134 MVAr
51       6.6555 kV      1.0084        -1.43 deg.    -0.6365 MW      -0.3115 MVAr
52       6.6577 kV      1.0087        -1.40 deg.    -0.2495 MW      -0.1338 MVAr
53       6.6583 kV      1.0088        -1.41 deg.     0.0000 MW       0.0000 MVAr
54       6.6583 kV      1.0088        -1.41 deg.     0.0000 MW       0.0000 MVAr
55       6.6583 kV      1.0088        -1.41 deg.     0.0000 MW       0.0000 MVAr
56       6.6576 kV      1.0087        -1.40 deg.    -0.1793 MW      -0.1344 MVAr
57       0.5580 kV      1.0145        -1.30 deg.     0.0000 MW       0.0000 MVAr
58      10.9677 kV      0.9971        -0.74 deg.     0.0000 MW       0.0000 MVAr

Branch currents:
 1     feeder: 286.7961A    -0.66 deg.
 2     feeder: 279.1821A    -0.66 deg.
 3     feeder:  69.3035A   -38.14 deg.
 4     3wtrnf: Ip: 69.3035A       -38.14 deg. Is:568.9021A  -38.13 deg.
          It:437.9008A   -38.16 deg.
 5     feeder:  58.7932A   -18.36 deg.
 6     feeder:  75.8422A   -36.07 deg.
 7     feeder:  61.8333A   -39.19 deg.
 8     feeder: 167.5325A    20.66 deg.
 9     transf: Ip:167.5325A        20.66 deg. Is:2010.3897A  20.66 deg.
10     feeder:  58.7485A   -18.39 deg.
11     feeder: 297.0714A   143.29 deg.
12     transf: Ip:297.0714A       143.29 deg. Is:3600.5059A 143.29 deg.
13      Load: 817.8159A   -39.75 deg.   7.2414MVA     5.7851MVAr
14      Load: 250.4948A   -37.71 deg.   3.8019MVA     2.8617MVAr
15      Load: 252.5937A   -38.46 deg.   3.7955MVA     2.9358MVAr
```

```
16     feeder: 167.5375A    20.66 deg.
17     transf: Ip:167.5375A        20.66 deg.  Is:2010.4495A   20.66 deg.
18     feeder:  62.2622A   -39.18 deg.
19     3wtrnf: Ip: 69.1666A        -38.14 deg.  Is:564.0510A   -38.14 deg.
              It:443.2478A   -38.14 deg.
20      Load:  58.7932A   -18.36 deg.   12.8456MVA    4.2128MVAr
21     feeder:  74.7949A   -36.12 deg.
22     feeder:  53.7006A   -13.60 deg.
23     feeder:  69.1666A   -38.14 deg.
24     feeder: 1685.4865A   35.17 deg.
25     feeder: 567.0395A   -27.44 deg.
26     feeder: 567.1464A   -27.46 deg.
27     feeder: 1685.5087A   35.17 deg.
28      Load:  75.8422A   -36.07 deg.   14.1320MVA   10.2176MVAr
29     3wtrnf: Ip: 61.8333A        -39.19 deg.  Is:251.3646A   -38.09 deg.
              It:817.8416A   -39.76 deg.
30      Load:  58.7485A   -18.39 deg.   12.8335MVA    4.2168MVAr
31      Load:  74.7949A   -36.12 deg.   13.9281MVA   10.0886MVAr
32      Load:  53.7006A   -13.60 deg.   12.0119MVA    2.8604MVAr
33     3wtrnf: Ip: 62.2622A        -39.18 deg.  Is:251.7130A   -38.07 deg.
              It:825.8397A   -39.74 deg.
34     feeder:   6.0546A    -5.36 deg.
35     feeder:   6.0546A    -5.36 deg.
36     transf: Ip:  6.0546A         -5.36 deg.  Is:118.0647A    -5.36 deg.
37     transf: Ip:  6.0546A         -5.36 deg.  Is:118.0647A    -5.36 deg.
38      Load: 236.1293A    -5.36 deg.    0.2285MVA    0.0171MVAr
39     feeder: 123.1320A   -40.33 deg.
40     feeder: 119.5060A   -39.37 deg.
41     transf: Ip:123.1320A        -40.33 deg.  Is:205.2200A   -40.33 deg.
42     transf: Ip:119.5060A        -39.37 deg.  Is:199.1766A   -39.37 deg.
43      Load: 404.3823A   -39.86 deg.    3.5728MVA    2.8443MVAr
44     feeder:  86.8884A   -38.69 deg.
45     feeder:  86.8884A   -38.69 deg.
46     feeder: 114.9212A   -40.54 deg.
47     transf: Ip: 86.8884A        -38.69 deg.  Is:1737.7672A -38.69 deg.
48     transf: Ip: 86.8884A        -38.69 deg.  Is:1737.7672A -38.69 deg.
49     transf: Ip:114.9212A        -40.54 deg.  Is:191.5354A   -40.54 deg.
50      Load: 3475.5345A  -38.69 deg.    2.5964MVA    1.9473MVAr
51      Load: 191.5354A   -40.54 deg.    1.6718MVA    1.3344MVAr
52      Load: 224.9341A   -39.56 deg.    3.3299MVA    2.6532MVAr
53     feeder:  36.6807A   -38.23 deg.
54     feeder:  33.3143A   -38.20 deg.
55     transf: Ip: 36.6807A        -38.23 deg.  Is:715.2731A   -38.23 deg.
56     transf: Ip: 33.3143A        -38.20 deg.  Is:649.6298A   -38.20 deg.
57     transf: Ip: 92.8930A        -38.60 deg.  Is:1802.1249A -38.60 deg.
58     transf: Ip: 93.4899A        -38.65 deg.  Is:1813.7049A -38.65 deg.
59     feeder:  92.8930A   -38.60 deg.
60     feeder:  93.4899A   -38.65 deg.
61     transf: Ip: 55.8848A        -30.67 deg.  Is: 91.2786A   -30.67 deg.
62     transf: Ip: 55.4947A        -30.61 deg.  Is: 90.6414A   -30.61 deg.
63     feeder:  55.8848A   -30.67 deg.
64     feeder:  55.4947A   -30.61 deg.
65      Load: 437.8988A   -38.17 deg.    3.9613MVA    2.9766MVAr
66      Load: 443.2498A   -38.14 deg.    4.0113MVA    3.0109MVAr
67      Load: 825.8653A   -39.74 deg.    7.3136MVA    5.8408MVAr
68     feeder:  55.2893A   -32.68 deg.
69     feeder:  21.4860A   -28.64 deg.
70     feeder:  61.4760A   -27.51 deg.
71     feeder:  24.5515A   -29.60 deg.
72     feeder:   0.0000A    76.68 deg.
73     feeder:   0.0000A  -166.23 deg.
74     feeder:   0.0000A  -103.32 deg.
75     feeder:  19.4324A   -38.26 deg.
76      Load: 3615.8294A  -38.63 deg.    2.7882MVA    2.0911MVAr
77      Load:   6.3871A   -38.20 deg.    0.0049MVA    0.0037MVAr
78      Load: 352.5714A   -38.23 deg.    0.2724MVA    0.2045MVAr
79      Load: 126.1454A   -38.23 deg.    0.0975MVA    0.0732MVAr
80      Load: 123.9307A   -38.23 deg.    0.0957MVA    0.0719MVAr
```

```
81      Load: 106.2385A   -38.23 deg.   0.0821MVA    0.0616MVAr
82      Load:  70.3910A   -38.19 deg.   0.0544MVA    0.0408MVAr
83      Load:   3.1949A   -38.17 deg.   0.0025MVA    0.0019MVAr
84      Load: 352.7259A   -38.20 deg.   0.2726MVA    0.2047MVAr
85      Load: 132.5880A   -38.20 deg.   0.1025MVA    0.0769MVAr
86      Load:  90.7300A   -38.20 deg.   0.0701MVA    0.0526MVAr
```

13.7 Study Case 6 – Final State

Bus voltages and currents calculated on completion of simulation. This was used as the initial state for study cases 8 and 10.

```
Number of iterations:   1   Max Power mismatch:    10.0kVA

 Bus  Voltage(l-l)  Voltage(pu)      Angle           P(bus)         Q(bus)
  1    133.0000 kV    1.0076      0.00 deg. 129.1399 MW     1.9070 MVAr
  2    132.7581 kV    1.0057     -0.20 deg.   0.0000 MW     0.0000 MVAr
  3    132.7541 kV    1.0057     -0.20 deg.   0.0000 MW     0.0000 MVAr
  4    132.7558 kV    1.0057     -0.20 deg.   0.0000 MW     0.0000 MVAr
  5    132.7513 kV    1.0057     -0.20 deg.   0.0000 MW     0.0000 MVAr
  6    131.1884 kV    0.9939     -0.97 deg.   0.0000 MW     0.0000 MVAr
  7     10.9294 kV    0.9936     -1.00 deg.   0.0000 MW     0.0000 MVAr
  8      6.5336 kV    0.9899     -1.24 deg.   0.0000 MW     0.0000 MVAr
  9    132.7555 kV    1.0057     -0.20 deg.   0.0000 MW     0.0000 MVAr
 10    132.7543 kV    1.0057     -0.20 deg.   0.0000 MW     0.0000 MVAr
 11    132.7546 kV    1.0057     -0.20 deg.   0.0000 MW     0.0000 MVAr
 12    132.7571 kV    1.0057     -0.20 deg.   0.0000 MW     0.0000 MVAr
 13     11.1520 kV    1.0138     -1.59 deg.   0.0000 MW     0.0000 MVAr
 14    132.7554 kV    1.0057     -0.20 deg.   0.0000 MW     0.0000 MVAr
 15    132.7737 kV    1.0059     -0.19 deg.   0.0000 MW     0.0000 MVAr
 16     11.0902 kV    1.0082      0.69 deg.  55.9956 MW    41.4845 MVAr
 17      6.5433 kV    0.9914     -1.13 deg.   0.0000 MW     0.0000 MVAr
 18    131.8259 kV    0.9987     -0.62 deg.   0.0000 MW     0.0000 MVAr
 19    131.8228 kV    0.9987     -0.63 deg.   0.0000 MW     0.0000 MVAr
 20     11.1349 kV    1.0123     -1.67 deg. -26.0177 MW    19.4873 MVAr
 21     11.1497 kV    1.0136     -1.59 deg.  -9.8551 MW    -4.7740 MVAr
 22    132.7571 kV    1.0057     -0.20 deg.   0.0000 MW     0.0000 MVAr
 23     11.1522 kV    1.0138     -1.59 deg.   0.0000 MW     0.0000 MVAr
 24    132.7551 kV    1.0057     -0.20 deg.   0.0000 MW     0.0000 MVAr
 25    132.7516 kV    1.0057     -0.20 deg.   0.0000 MW     0.0000 MVAr
 26    131.1877 kV    0.9938     -0.97 deg.   0.0000 MW     0.0000 MVAr
 27     10.9145 kV    0.9922     -1.06 deg.   0.0000 MW     0.0000 MVAr
 28     10.9154 kV    0.9923     -1.06 deg.   0.0000 MW     0.0000 MVAr
 29     11.1496 kV    1.0136     -1.59 deg.  -9.8551 MW    -4.7784 MVAr
 30     11.1348 kV    1.0123     -1.66 deg. -26.0177 MW    19.4873 MVAr
 31      0.5565 kV    1.0119     -1.75 deg.   0.0000 MW     0.0000 MVAr
 32     10.9288 kV    0.9935     -1.01 deg.   0.0000 MW     0.0000 MVAr
 33      0.5603 kV    1.0188     -1.08 deg.   0.0000 MW     0.0000 MVAr
 34      0.5464 kV    0.9935     -1.01 deg.   0.0000 MW     0.0000 MVAr
 35     10.9271 kV    0.9934     -1.00 deg.   0.0000 MW     0.0000 MVAr
 36      6.5206 kV    0.9880     -1.33 deg.   0.0000 MW     0.0000 MVAr
 37     10.9248 kV    0.9932     -1.00 deg.   0.0000 MW     0.0000 MVAr
 38     10.9026 kV    0.9911     -1.11 deg.   0.0000 MW     0.0000 MVAr
 39     10.9026 kV    0.9911     -1.11 deg.   0.0000 MW     0.0000 MVAr
 40     10.8971 kV    0.9906     -1.13 deg.   0.0000 MW     0.0000 MVAr
 41      0.5392 kV    0.9803     -1.81 deg.   0.0000 MW     0.0000 MVAr
 42      6.4484 kV    0.9770     -1.94 deg.   0.0000 MW     0.0000 MVAr
 43     10.9240 kV    0.9931     -1.02 deg.   0.0000 MW     0.0000 MVAr
 44     10.9244 kV    0.9931     -1.02 deg.   0.0000 MW     0.0000 MVAr
 45      0.5578 kV    1.0142     -1.32 deg.   0.0000 MW     0.0000 MVAr
 46     10.9230 kV    0.9930     -1.04 deg.   0.0000 MW     0.0000 MVAr
 47     10.9226 kV    0.9930     -1.04 deg.   0.0000 MW     0.0000 MVAr
 48      6.6631 kV    1.0096     -1.35 deg.   0.0000 MW     0.0000 MVAr
 49      6.6603 kV    1.0091     -1.38 deg.  -0.4405 MW    -0.2333 MVAr
 50      6.6624 kV    1.0095     -1.35 deg.  -0.2010 MW    -0.1044 MVAr
 51      6.6605 kV    1.0092     -1.38 deg.  -0.6093 MW    -0.2859 MVAr
 52      6.6625 kV    1.0095     -1.35 deg.  -0.2032 MW    -0.1340 MVAr
 53      6.6631 kV    1.0096     -1.35 deg.   0.0000 MW     0.0000 MVAr
```

```
54        6.6631 kV      1.0096       -1.35 deg.     0.0000 MW      0.0000 MVAr
55        6.6631 kV      1.0096       -1.35 deg.     0.0000 MW      0.0000 MVAr
56        6.6623 kV      1.0094       -1.35 deg.    -0.1793 MW     -0.1344 MVAr
57        0.5580 kV      1.0146       -1.29 deg.     0.0000 MW      0.0000 MVAr
58       10.9678 kV      0.9971       -0.73 deg.     0.0000 MW      0.0000 MVAr

Branch currents:
 1     feeder: 284.0982A    -0.84 deg.
 2     feeder: 276.5558A    -0.84 deg.
 3     feeder:  68.7816A   -38.15 deg.
 4     3wtrnf: Ip: 68.7816A        -38.15 deg. Is:562.6160A  -38.15 deg.
           It:437.9388A   -38.15 deg.
 5     feeder:  58.7936A   -18.36 deg.
 6     feeder:  75.8426A   -36.07 deg.
 7     feeder:  61.8337A   -39.19 deg.
 8     feeder: 167.5314A    20.66 deg.
 9     transf: Ip:167.5314A         20.66 deg. Is:2010.3772A  20.66 deg.
10     feeder:  58.7489A   -18.39 deg.
11     feeder: 299.3350A   144.16 deg.
12     transf: Ip:299.3350A        144.16 deg. Is:3627.9405A 144.16 deg.
13       Load: 817.8211A   -39.75 deg.    7.2415MVA     5.7851MVAr
14       Load: 250.4964A   -37.70 deg.    3.8019MVA     2.8618MVAr
15       Load: 252.5953A   -38.46 deg.    3.7956MVA     2.9358MVAr
16     feeder: 167.5364A    20.67 deg.
17     transf: Ip:167.5364A         20.67 deg. Is:2010.4369A  20.67 deg.
18     feeder:  62.2626A   -39.18 deg.
19     3wtrnf: Ip: 68.6458A        -38.16 deg. Is:557.7742A  -38.17 deg.
           It:443.2918A   -38.13 deg.
20       Load:  58.7936A   -18.36 deg.   12.8458MVA     4.2128MVAr
21     feeder:  74.7954A   -36.12 deg.
22     feeder:  53.7009A   -13.60 deg.
23     feeder:  68.6458A   -38.16 deg.
24     feeder: 1685.4759A   35.17 deg.
25     feeder: 567.0360A   -27.44 deg.
26     feeder: 567.1428A   -27.46 deg.
27     feeder: 1685.4981A   35.17 deg.
28       Load:  75.8426A   -36.07 deg.   14.1321MVA    10.2178MVAr
29     3wtrnf: Ip: 61.8337A        -39.19 deg. Is:251.3662A  -38.09 deg.
           It:817.8468A   -39.75 deg.
30       Load:  58.7489A   -18.39 deg.   12.8336MVA     4.2169MVAr
31       Load:  74.7954A   -36.12 deg.   13.9283MVA    10.0887MVAr
32       Load:  53.7009A   -13.60 deg.   12.0121MVA     2.8605MVAr
33     3wtrnf: Ip: 62.2626A        -39.18 deg. Is:251.7146A  -38.07 deg.
           It:825.8449A   -39.74 deg.
34     feeder:   6.0552A    -5.35 deg.
35     feeder:   6.0552A    -5.35 deg.
36     transf: Ip:  6.0552A         -5.35 deg. Is:118.0760A   -5.35 deg.
37     transf: Ip:  6.0552A         -5.35 deg. Is:118.0760A   -5.35 deg.
38       Load: 236.1520A    -5.35 deg.    0.2286MVA     0.0171MVAr
39     feeder: 123.1438A   -40.32 deg.
40     feeder: 119.5174A   -39.36 deg.
41     transf: Ip:123.1438A        -40.32 deg. Is:205.2396A  -40.32 deg.
42     transf: Ip:119.5174A        -39.36 deg. Is:199.1957A  -39.36 deg.
43       Load: 404.4210A   -39.85 deg.    3.5734MVA     2.8448MVAr
44     feeder:  86.8967A   -38.68 deg.
45     feeder:  86.8967A   -38.68 deg.
46     feeder: 114.9323A   -40.53 deg.
47     transf: Ip: 86.8967A        -38.68 deg. Is:1737.9337A -38.68 deg.
48     transf: Ip: 86.8967A        -38.68 deg. Is:1737.9337A -38.68 deg.
49     transf: Ip:114.9323A        -40.53 deg. Is:191.5538A  -40.53 deg.
50       Load: 3475.8675A  -38.68 deg.    2.5969MVA     1.9477MVAr
51       Load: 191.5538A   -40.53 deg.    1.6721MVA     1.3346MVAr
52       Load: 224.9556A   -39.55 deg.    3.3305MVA     2.6537MVAr
53     feeder:  36.6842A   -38.22 deg.
54     feeder:  33.3175A   -38.19 deg.
55     transf: Ip: 36.6842A        -38.22 deg. Is:715.3416A  -38.22 deg.
56     transf: Ip: 33.3175A        -38.19 deg. Is:649.6920A  -38.19 deg.
57     transf: Ip: 92.9019A        -38.59 deg. Is:1802.2976A -38.59 deg.
```

```
58    transf: Ip: 93.4989A        -38.64 deg. Is:1813.8787A -38.64 deg.
59    feeder:  92.9019A   -38.59 deg.
60    feeder:  93.4989A   -38.64 deg.
61    transf: Ip: 49.5505A        -30.04 deg. Is: 80.9325A   -30.04 deg.
62    transf: Ip: 49.2046A        -29.98 deg. Is: 80.3675A   -29.98 deg.
63    feeder:  49.5505A   -30.04 deg.
64    feeder:  49.2046A   -29.98 deg.
65     Load: 437.9395A    -38.16 deg.   3.9621MVA      2.9772MVAr
66     Load: 443.2911A    -38.13 deg.   4.0120MVA      3.0115MVAr
67     Load: 825.8705A    -39.74 deg.   7.3137MVA      5.8409MVAr
68    feeder:  43.2087A   -29.29 deg.
69    feeder:  19.6283A   -28.80 deg.
70    feeder:  58.3403A   -26.52 deg.
71    feeder:  21.0914A   -34.77 deg.
72    feeder:   0.0000A  -103.32 deg.
73    feeder:   0.0000A  -166.23 deg.
74    feeder:   0.0000A   152.64 deg.
75    feeder:  19.4185A   -38.21 deg.
76     Load: 3616.1759A   -38.62 deg.   2.7887MVA      2.0915MVAr
77     Load:   6.3877A    -38.19 deg.   0.0049MVA      0.0037MVAr
78     Load: 352.6052A    -38.22 deg.   0.2724MVA      0.2045MVAr
79     Load: 126.1574A    -38.22 deg.   0.0975MVA      0.0732MVAr
80     Load: 123.9426A    -38.22 deg.   0.0958MVA      0.0719MVAr
81     Load: 106.2487A    -38.22 deg.   0.0821MVA      0.0616MVAr
82     Load:  70.3977A    -38.18 deg.   0.0544MVA      0.0408MVAr
83     Load:   3.1952A    -38.16 deg.   0.0025MVA      0.0019MVAr
84     Load: 352.7597A    -38.19 deg.   0.2727MVA      0.2047MVAr
85     Load: 132.6007A    -38.19 deg.   0.1025MVA      0.0770MVAr
86     Load:  90.7387A    -38.19 deg.   0.0701MVA      0.0527MVAr
```

13.8 Study Case 7 – Final State

Bus voltages and currents calculated on completion of simulation. This was used as the initial state for study cases 9, 11 and 12.

```
Number of iterations:   1   Max Power mismatch:    10.0kVA

  Bus  Voltage(l-l)  Voltage(pu)      Angle          P(bus)          Q(bus)
   1    133.0000 kV    1.0076      0.00 deg. 129.3357 MW     1.7911 MVAr
   2    132.7582 kV    1.0057     -0.20 deg.   0.0000 MW     0.0000 MVAr
   3    132.7542 kV    1.0057     -0.20 deg.   0.0000 MW     0.0000 MVAr
   4    132.7559 kV    1.0057     -0.20 deg.   0.0000 MW     0.0000 MVAr
   5    132.7513 kV    1.0057     -0.20 deg.   0.0000 MW     0.0000 MVAr
   6    131.1772 kV    0.9938     -0.97 deg.   0.0000 MW     0.0000 MVAr
   7     10.9284 kV    0.9935     -1.01 deg.   0.0000 MW     0.0000 MVAr
   8      6.5330 kV    0.9899     -1.24 deg.   0.0000 MW     0.0000 MVAr
   9    132.7556 kV    1.0057     -0.20 deg.   0.0000 MW     0.0000 MVAr
  10    132.7544 kV    1.0057     -0.20 deg.   0.0000 MW     0.0000 MVAr
  11    132.7547 kV    1.0057     -0.20 deg.   0.0000 MW     0.0000 MVAr
  12    132.7572 kV    1.0057     -0.20 deg.   0.0000 MW     0.0000 MVAr
  13     11.1520 kV    1.0138     -1.59 deg.   0.0000 MW     0.0000 MVAr
  14    132.7555 kV    1.0057     -0.20 deg.   0.0000 MW     0.0000 MVAr
  15    132.7739 kV    1.0059     -0.19 deg.   0.0000 MW     0.0000 MVAr
  16     11.0911 kV    1.0083      0.69 deg.  55.9950 MW    41.7600 MVAr
  17      6.5433 kV    0.9914     -1.13 deg.   0.0000 MW     0.0000 MVAr
  18    131.8260 kV    0.9987     -0.62 deg.   0.0000 MW     0.0000 MVAr
  19    131.8229 kV    0.9987     -0.63 deg.   0.0000 MW     0.0000 MVAr
  20     11.1349 kV    1.0123     -1.67 deg. -26.0177 MW    19.4873 MVAr
  21     11.1497 kV    1.0136     -1.59 deg.  -9.8551 MW    -4.7740 MVAr
  22    132.7572 kV    1.0057     -0.20 deg.   0.0000 MW     0.0000 MVAr
  23     11.1522 kV    1.0138     -1.59 deg.   0.0000 MW     0.0000 MVAr
  24    132.7552 kV    1.0057     -0.20 deg.   0.0000 MW     0.0000 MVAr
  25    132.7516 kV    1.0057     -0.20 deg.   0.0000 MW     0.0000 MVAr
  26    131.1764 kV    0.9938     -0.97 deg.   0.0000 MW     0.0000 MVAr
  27     10.9135 kV    0.9921     -1.07 deg.   0.0000 MW     0.0000 MVAr
  28     10.9144 kV    0.9922     -1.07 deg.   0.0000 MW     0.0000 MVAr
  29     11.1496 kV    1.0136     -1.59 deg.  -9.8551 MW    -4.7784 MVAr
  30     11.1348 kV    1.0123     -1.66 deg. -26.0177 MW    19.4873 MVAr
```

```
31      0.5565 kV      1.0118        -1.76 deg.     0.0000 MW      0.0000 MVAr
32     10.9278 kV      0.9934        -1.02 deg.     0.0000 MW      0.0000 MVAr
33      0.5603 kV      1.0187        -1.08 deg.     0.0000 MW      0.0000 MVAr
34      0.5464 kV      0.9934        -1.02 deg.     0.0000 MW      0.0000 MVAr
35     10.9261 kV      0.9933        -1.01 deg.     0.0000 MW      0.0000 MVAr
36      6.5200 kV      0.9879        -1.33 deg.     0.0000 MW      0.0000 MVAr
37     10.9239 kV      0.9931        -1.01 deg.     0.0000 MW      0.0000 MVAr
38     10.9016 kV      0.9911        -1.12 deg.     0.0000 MW      0.0000 MVAr
39     10.9016 kV      0.9911        -1.12 deg.     0.0000 MW      0.0000 MVAr
40     10.8961 kV      0.9906        -1.14 deg.     0.0000 MW      0.0000 MVAr
41      0.5391 kV      0.9802        -1.82 deg.     0.0000 MW      0.0000 MVAr
42      6.4478 kV      0.9769        -1.95 deg.     0.0000 MW      0.0000 MVAr
43     10.9230 kV      0.9930        -1.03 deg.     0.0000 MW      0.0000 MVAr
44     10.9235 kV      0.9930        -1.03 deg.     0.0000 MW      0.0000 MVAr
45      0.5578 kV      1.0141        -1.33 deg.     0.0000 MW      0.0000 MVAr
46     10.9211 kV      0.9928        -1.05 deg.     0.0000 MW      0.0000 MVAr
47     10.9207 kV      0.9928        -1.05 deg.     0.0000 MW      0.0000 MVAr
48      6.6584 kV      1.0088        -1.40 deg.     0.0000 MW      0.0000 MVAr
49      6.6546 kV      1.0083        -1.44 deg.    -0.5449 MW     -0.3305 MVAr
50      6.6577 kV      1.0087        -1.40 deg.    -0.2203 MW     -0.1134 MVAr
51      6.6556 kV      1.0084        -1.43 deg.    -0.6365 MW     -0.3115 MVAr
52      6.6577 kV      1.0087        -1.40 deg.    -0.2495 MW     -0.1338 MVAr
53      6.6584 kV      1.0088        -1.40 deg.     0.0000 MW      0.0000 MVAr
54      6.6584 kV      1.0088        -1.40 deg.     0.0000 MW      0.0000 MVAr
55      6.6584 kV      1.0088        -1.40 deg.     0.0000 MW      0.0000 MVAr
56      6.6576 kV      1.0087        -1.40 deg.    -0.1793 MW     -0.1344 MVAr
57      0.5580 kV      1.0145        -1.30 deg.     0.0000 MW      0.0000 MVAr
58     10.9678 kV      0.9971        -0.73 deg.     0.0000 MW      0.0000 MVAr


Branch currents:
 1     feeder: 284.5252A     -0.78 deg.
 2     feeder: 276.9714A     -0.78 deg.
 3     feeder:  69.3040A    -38.13 deg.
 4     3wtrnf: Ip: 69.3040A         -38.13 deg. Is:568.9053A  -38.12 deg.
            It:437.9039A   -38.16 deg.
 5     feeder:  58.7937A    -18.36 deg.
 6     feeder:  75.8427A    -36.07 deg.
 7     feeder:  61.8337A    -39.19 deg.
 8     feeder: 167.5313A     20.66 deg.
 9     transf: Ip:167.5313A         20.66 deg. Is:2010.3757A   20.66 deg.
10     feeder:  58.7490A    -18.39 deg.
11     feeder: 300.0151A    143.98 deg.
12     transf: Ip:300.0151A         143.98 deg. Is:3636.1834A 143.98 deg.
13      Load: 817.8217A    -39.75 deg.    7.2415MVA     5.7851MVAr
14      Load: 250.4966A    -37.70 deg.    3.8020MVA     2.8618MVAr
15      Load: 252.5955A    -38.46 deg.    3.7956MVA     2.9358MVAr
16     feeder: 167.5363A     20.67 deg.
17     transf: Ip:167.5363A         20.67 deg. Is:2010.4354A   20.67 deg.
18     feeder:  62.2626A    -39.18 deg.
19     3wtrnf: Ip: 69.1671A         -38.14 deg. Is:564.0541A  -38.14 deg.
            It:443.2509A   -38.14 deg.
20      Load:  58.7937A    -18.36 deg.   12.8458MVA     4.2128MVAr
21     feeder:  74.7955A    -36.12 deg.
22     feeder:  53.7009A    -13.60 deg.
23     feeder:  69.1671A    -38.14 deg.
24     feeder: 1685.4747A    35.17 deg.
25     feeder: 567.0356A    -27.44 deg.
26     feeder: 567.1424A    -27.46 deg.
27     feeder: 1685.4969A    35.17 deg.
28      Load:  75.8427A    -36.07 deg.   14.1322MVA    10.2178MVAr
29     3wtrnf: Ip: 61.8337A         -39.19 deg. Is:251.3664A  -38.09 deg.
            It:817.8474A   -39.75 deg.
30      Load:  58.7490A    -18.39 deg.   12.8337MVA     4.2169MVAr
31      Load:  74.7955A    -36.12 deg.   13.9283MVA    10.0887MVAr
32      Load:  53.7009A    -13.60 deg.   12.0121MVA     2.8605MVAr
33     3wtrnf: Ip: 62.2626A         -39.18 deg. Is:251.7148A  -38.07 deg.
            It:825.8455A   -39.74 deg.
34     feeder:   6.0546A     -5.36 deg.
```

```
35    feeder:   6.0546A    -5.36 deg.
36    transf: Ip:  6.0546A       -5.36 deg. Is:118.0655A    -5.36 deg.
37    transf: Ip:  6.0546A       -5.36 deg. Is:118.0655A    -5.36 deg.
38     Load: 236.1310A   -5.36 deg.   0.2285MVA    0.0171MVAr
39    feeder: 123.1329A   -40.33 deg.
40    feeder: 119.5068A   -39.37 deg.
41    transf: Ip:123.1329A       -40.33 deg. Is:205.2214A   -40.33 deg.
42    transf: Ip:119.5068A       -39.37 deg. Is:199.1781A   -39.37 deg.
43     Load: 404.3851A   -39.86 deg.   3.5728MVA    2.8443MVAr
44    feeder:  86.8890A   -38.69 deg.
45    feeder:  86.8890A   -38.69 deg.
46    feeder: 114.9221A   -40.54 deg.
47    transf: Ip: 86.8890A       -38.69 deg. Is:1737.7796A -38.69 deg.
48    transf: Ip: 86.8890A       -38.69 deg. Is:1737.7796A -38.69 deg.
49    transf: Ip:114.9221A       -40.54 deg. Is:191.5368A   -40.54 deg.
50     Load: 3475.5592A  -38.69 deg.   2.5964MVA    1.9473MVAr
51     Load: 191.5368A   -40.54 deg.   1.6719MVA    1.3344MVAr
52     Load: 224.9357A   -39.56 deg.   3.3299MVA    2.6532MVAr
53    feeder:  36.6809A   -38.23 deg.
54    feeder:  33.3146A   -38.20 deg.
55    transf: Ip: 36.6809A       -38.23 deg. Is:715.2782A   -38.23 deg.
56    transf: Ip: 33.3146A       -38.20 deg. Is:649.6344A   -38.20 deg.
57    transf: Ip: 92.8937A       -38.60 deg. Is:1802.1377A -38.60 deg.
58    transf: Ip: 93.4906A       -38.65 deg. Is:1813.7177A -38.65 deg.
59    feeder:  92.8937A   -38.60 deg.
60    feeder:  93.4906A   -38.65 deg.
61    transf: Ip: 55.8844A       -30.66 deg. Is: 91.2779A   -30.66 deg.
62    transf: Ip: 55.4943A       -30.61 deg. Is: 90.6407A   -30.61 deg.
63    feeder:  55.8844A   -30.66 deg.
64    feeder:  55.4943A   -30.61 deg.
65     Load: 437.9019A   -38.16 deg.   3.9614MVA    2.9767MVAr
66     Load: 443.2530A   -38.13 deg.   4.0113MVA    3.0110MVAr
67     Load: 825.8712A   -39.74 deg.   7.3137MVA    5.8409MVAr
68    feeder:  55.2889A   -32.68 deg.
69    feeder:  21.4858A   -28.64 deg.
70    feeder:  61.4756A   -27.51 deg.
71    feeder:  24.5514A   -29.60 deg.
72    feeder:   0.0000A    76.68 deg.
73    feeder:   0.0000A   136.41 deg.
74    feeder:   0.0000A  -103.32 deg.
75    feeder:  19.4322A   -38.26 deg.
76     Load: 3615.8551A  -38.62 deg.   2.7882MVA    2.0911MVAr
77     Load:   6.3871A   -38.20 deg.   0.0049MVA    0.0037MVAr
78     Load: 352.5739A   -38.23 deg.   0.2724MVA    0.2045MVAr
79     Load: 126.1463A   -38.23 deg.   0.0975MVA    0.0732MVAr
80     Load: 123.9316A   -38.23 deg.   0.0957MVA    0.0719MVAr
81     Load: 106.2393A   -38.22 deg.   0.0821MVA    0.0616MVAr
82     Load:  70.3915A   -38.19 deg.   0.0544MVA    0.0408MVAr
83     Load:   3.1950A   -38.17 deg.   0.0025MVA    0.0019MVAr
84     Load: 352.7284A   -38.20 deg.   0.2726MVA    0.2047MVAr
85     Load: 132.5889A   -38.20 deg.   0.1025MVA    0.0769MVAr
86     Load:  90.7306A   -38.20 deg.   0.0701MVA    0.0526MVAr
```

14 Appendix H: TRANSIENT SIMULATION RESULTS

The results of all the system transient simulations carried out are shown in this appendix. These simulations were all carried out by means of the alternating solution method described in 2.8.1.

Table 14-1 Summary of System Studies

Note: For location of motors on the electrical distribution system, refer to Figure 3-8

Study	Description	System Conditions
1	Simultaneous DOL start of four 6.6kV motors: 24PC101 – 300kW, 24PC104 – 300kW, 24KC101 – 550kW, 24PC102 – 800kW abc model used	Generator not modelled. Generator bus = load bus with P = 56MW, Q = 41MVAr. No system disturbances
2	Simultaneous DOL start of four 6.6kV motors: 24PC101 – 300kW, 24PC104 – 300kW, 24KC101 – 550kW, 24PC102 – 800kW d-q model used	Generator not modelled. Generator bus = load bus with P = 56MW, Q = 41MVAr. No system disturbances
3	Simultaneous DOL start of four 6.6kV motors: 24PC101 – 300kW, 24PC104 – 300kW, 24KC101 – 550kW, 24PC102 – 800kW abc model used	Generator modelled with fixed excitation and mechanical input power, P = 56MW
4	Simultaneous DOL start of four 6.6kV motors: 24PC101 – 300kW, 24PC104 – 300kW, 24KC101 – 550kW, 24PC102 – 800kW d-q model used	Generator modelled with fixed excitation and mechanical input power, P = 56MW
5	Simultaneous DOL start of four 6.6kV motors: 24PC101 – 300kW, 24PC104 – 300kW, 24KC101 – 550kW, 24PC102 – 800kW abc model used	Generator modelled with AVR and governor enabled. Initial mech. power, P = 56MW
6	Simultaneous DOL start of four 6.6kV motors: 24PC101 – 300kW, 24PC104 – 300kW, 24KC101 – 550kW, 24PC102 – 800kW d-q model used	Generator modelled with AVR enabled and constant mech power input. Initial mech. power, P = 56MW
7	Simultaneous DOL start of four 6.6kV motors: 24PC101 – 300kW, 24PC104 – 300kW, 24KC101 – 550kW, 24PC102 – 800kW abc model used	Generator modelled with AVR enabled and constant mech power input. Initial mech. power, P = 56MW
8	Examine effect of 20%, 100ms voltage dip on Eskom supply. Motor initial conditions from Study case 6 final state. All 6.6kV motors remain online. d-q model used	Generator modelled with AVR enabled and constant mech power input. Initial mech. power, P = 56MW. No other system changes
9	Examine effect of 20%, 100ms voltage dip on Eskom supply. Motor initial conditions from Study case 7 final state. All 6.6kV motors remain online. abc model used	Generator modelled with AVR enabled and constant mech power input. Initial mech. power, P = 56MW. No other system changes
10	Examine effect of 20%, 100ms voltage dip on Eskom supply. Motor initial conditions from Study case 6 final state. All 6.6kV motors remain online. d-q model used	Generator modelled with AVR enabled and constant mech power input. Initial mech. power, P = 56MW. Two 26MW compressors at air separation plant tripped 80ms after start of voltage dip
11	Examine effect of 20%, 100ms voltage dip on Eskom supply. Motor initial conditions from Study case 7 final state. All 6.6kV motors trip and re-start sequentially. abc model used	Generator not modelled. Generator bus = load bus with P = 56MW, Q = 41MVAr. Two 26MW compressors at air separation plant tripped 80ms after start of voltage dip
12	Examine effect of 20%, 100ms voltage dip on Eskom supply. Motor initial conditions from Study case 7 final state. All 6.6kV motors trip and re-start immediately. abc model used	Generator not modelled. Generator bus = load bus with P = 56MW, Q = 41MVAr. Two 26MW compressors at air separation plant tripped 80ms after start of voltage dip

14.1 Study 1
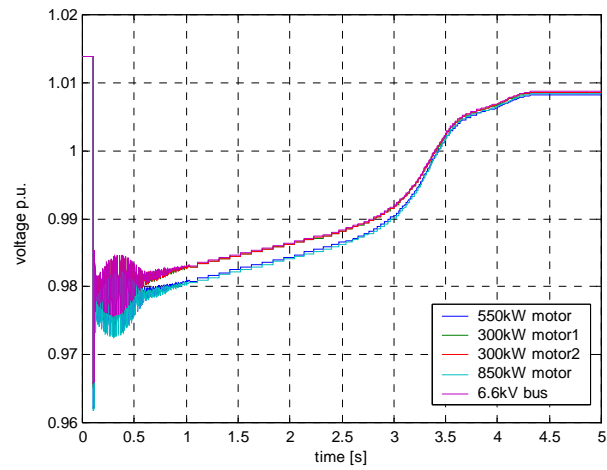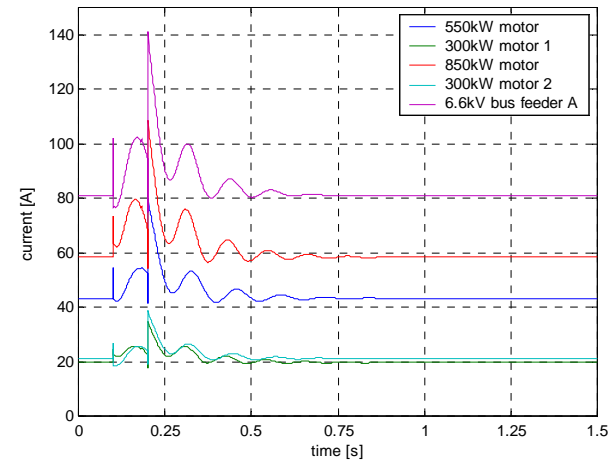

Figure 14-1 Motor terminal and bus voltages (1).
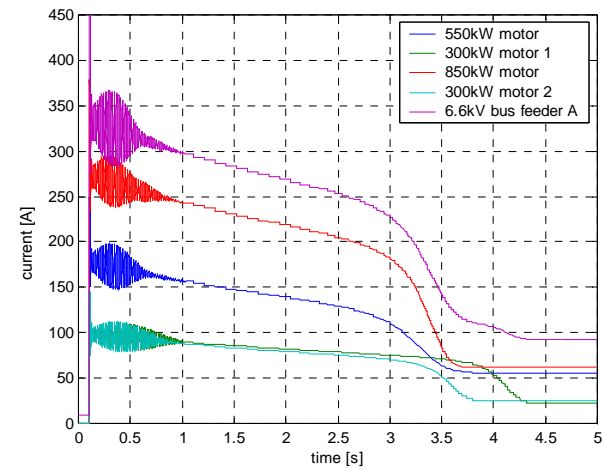
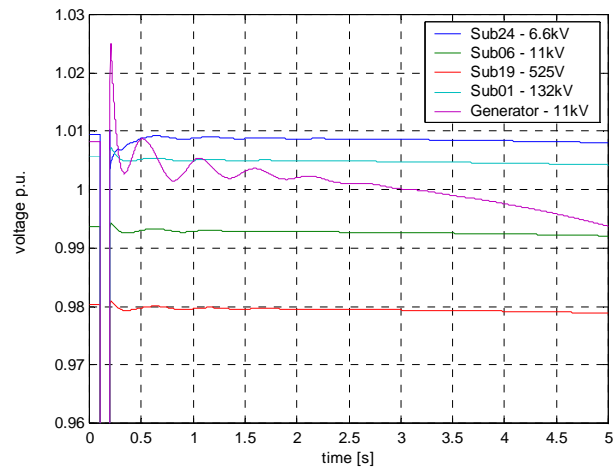
Figure 14-3 Motor and substation feeder currents (1).
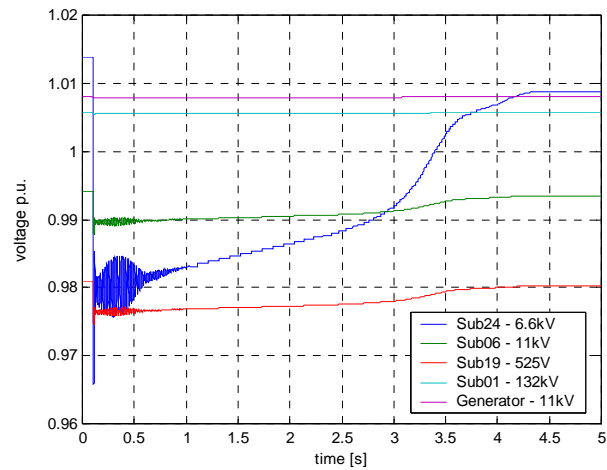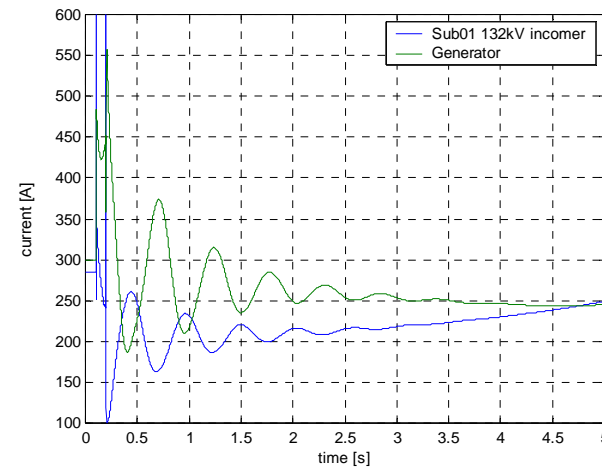

Figure 14-2 Distribution system bus voltages (1).
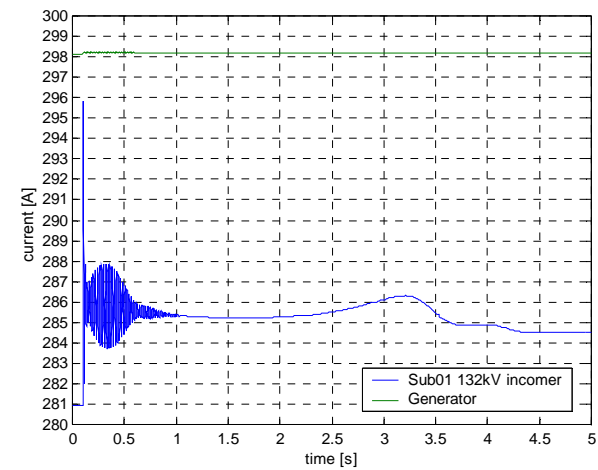
Figure 14-4 Main generator and Eskom feeder currents (1).
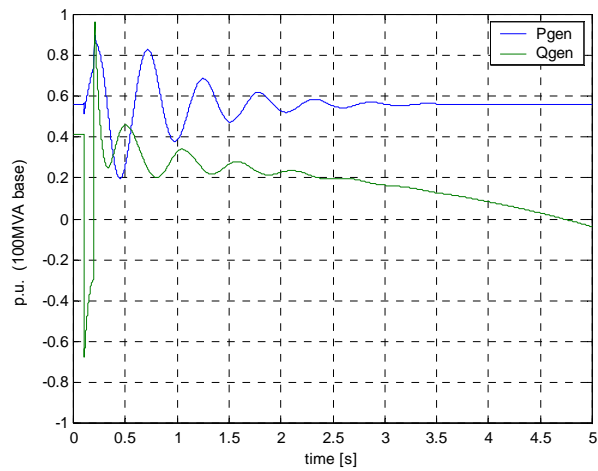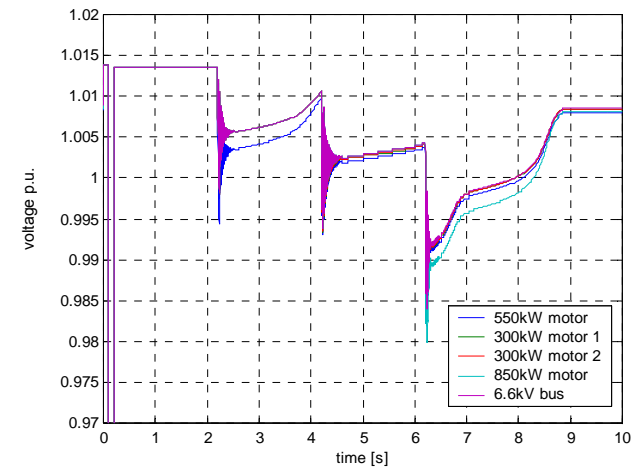
14.2 Study 2
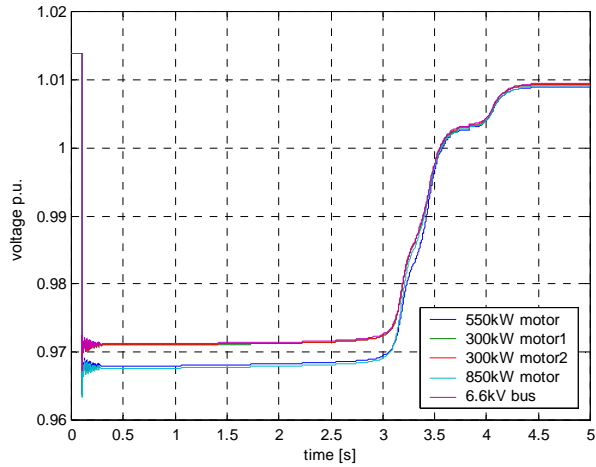
Figure 14-5 Motor terminal and bus voltages (2).

Figure 14-6 Distribution system bus voltages (2).
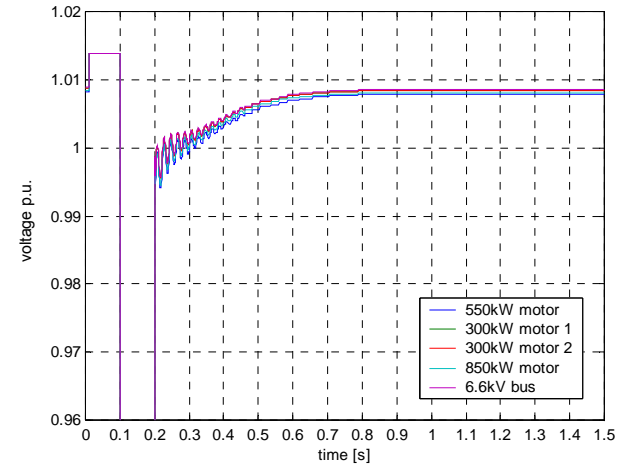

Figure 14-7 Motor and substation feeder currents (2).
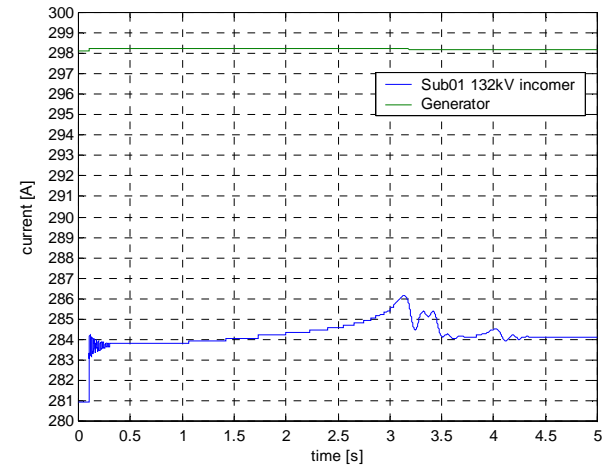
Figure 14-8 Main generator and Eskom feeder currents (2).

14.3 Study 3
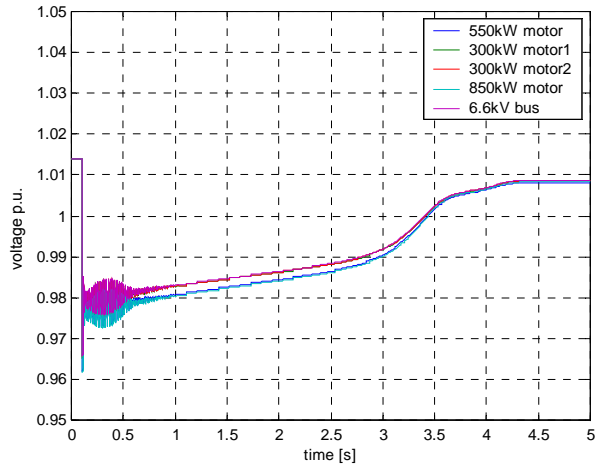
Figure 14-9 Motor terminal and bus voltages (3).
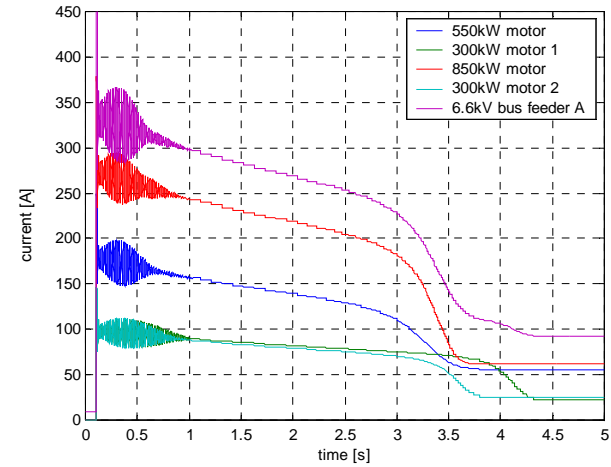
Figure 14-11 Motor and substation feeder currents (3).
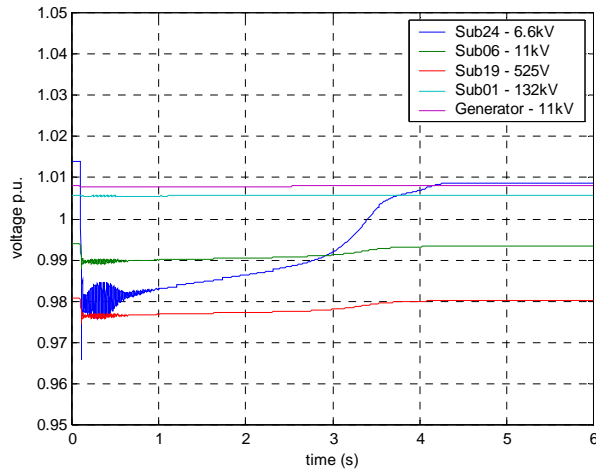
Figure 14-10 Distribution system bus voltages (3).
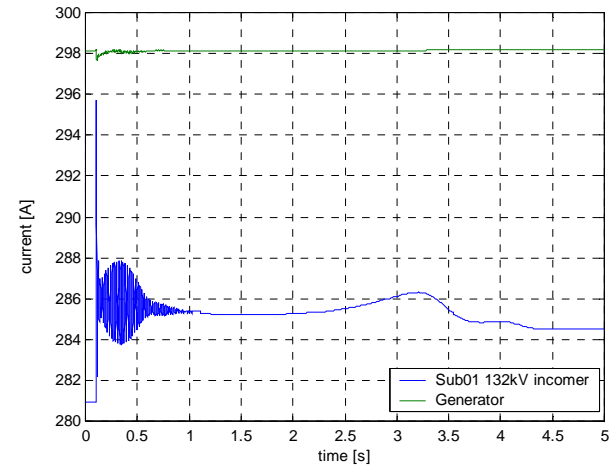
Figure 14-12 Main generator and Eskom feeder currents (3).

14.4 Study 4
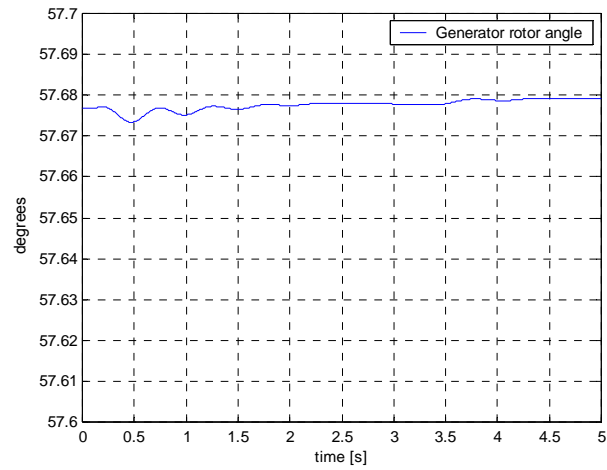
Figure 14-13 Generator rotor angle (3).
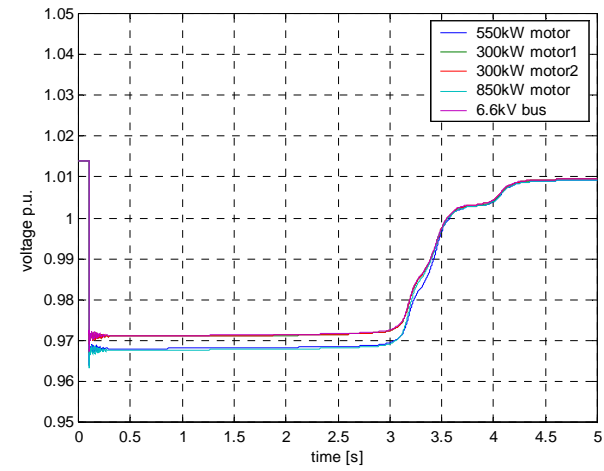
Figure 14-14 Motor terminal and bus voltages (4).
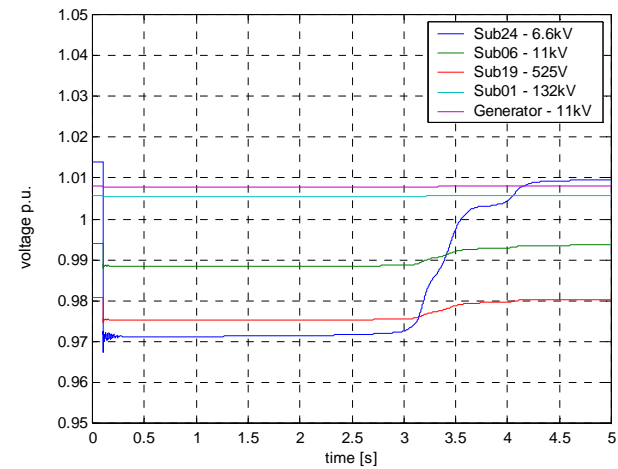
Figure 14-15 Distribution system bus voltages (4).
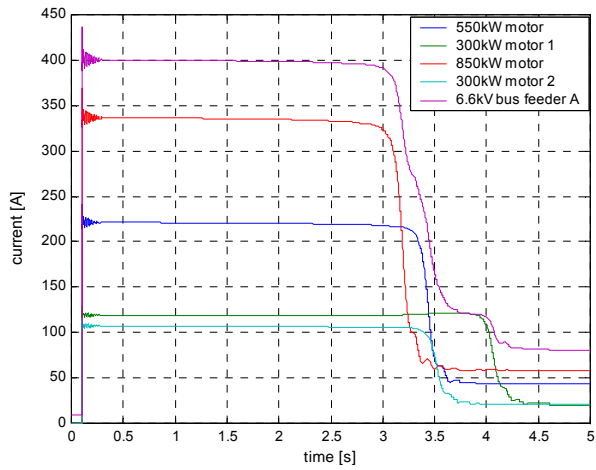
Figure 14-16 Motor and substation feeder currents (4).
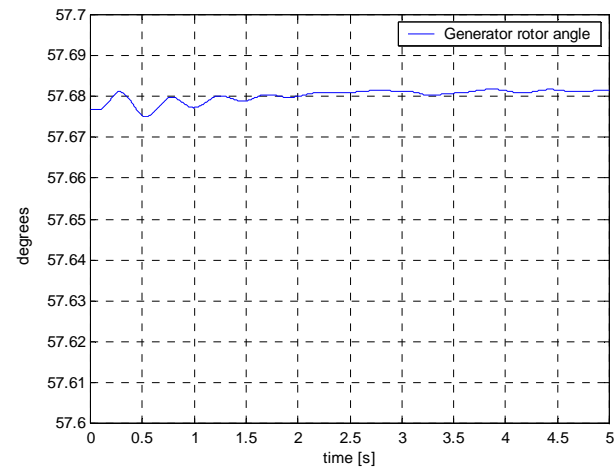
Figure 14-18 Generator rotor angle (4).
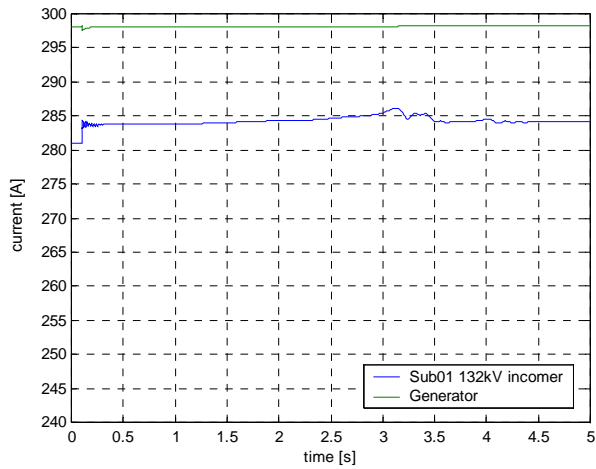
Figure 14-17 Main generator and Eskom feeder currents (4).

14.5 Study 5
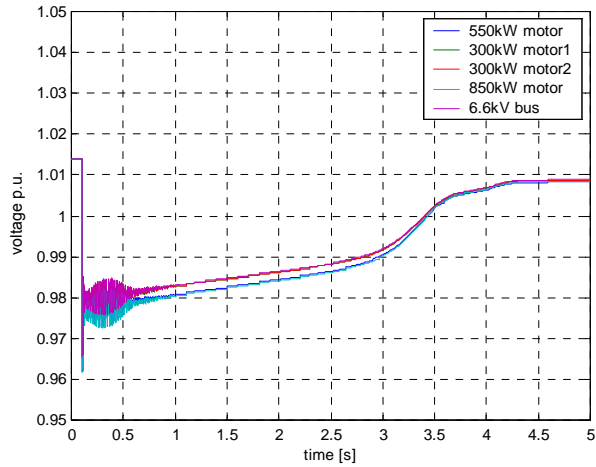
Figure 14-19 Motor terminal and bus voltages (5).
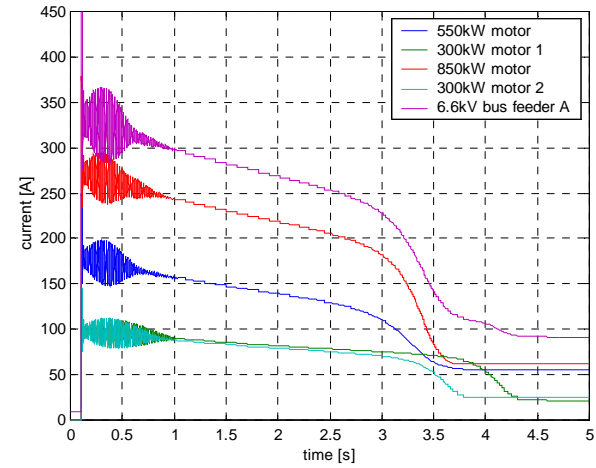
Figure 14-21 Motor and substation feeder currents (5).
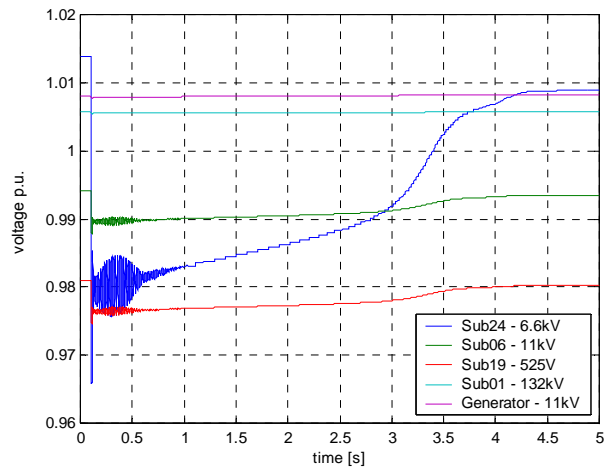
Figure 14-20 Distribution system bus voltages (5).
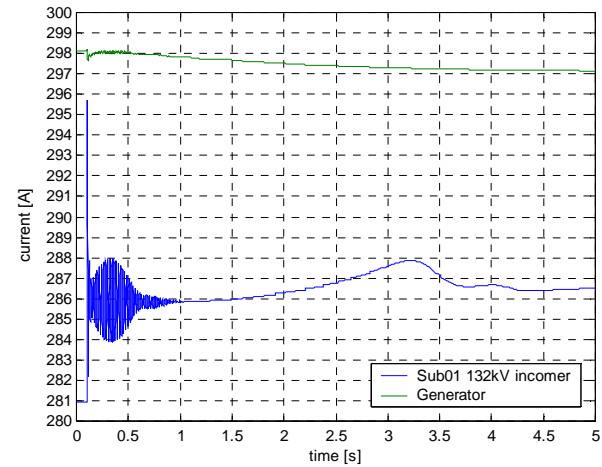
Figure 14-22 Main generator and Eskom feeder currents (5).
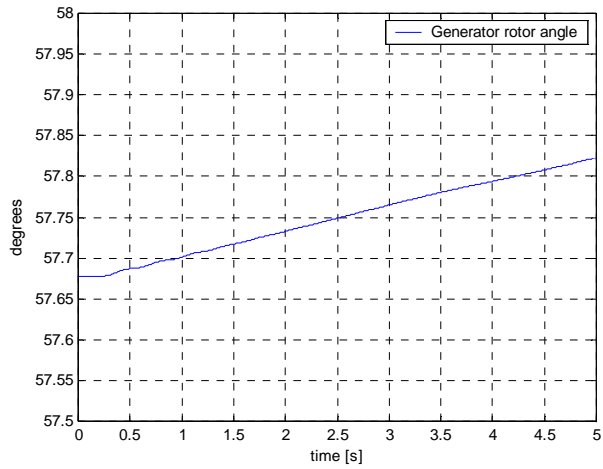
Figure 14-23 Generator rotor angle (5).
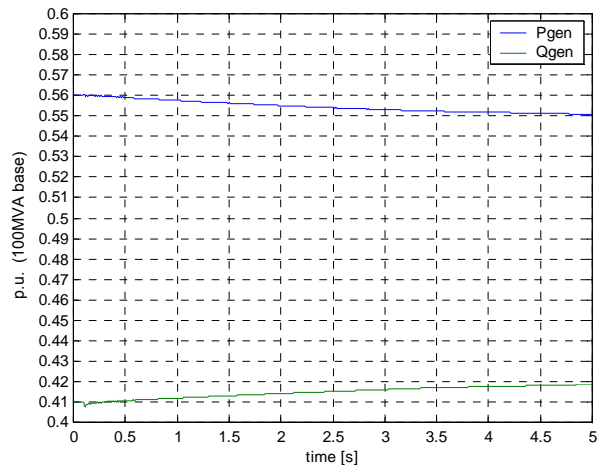
Figure 14-24 Generator power and reactive power output (5).

14.6 Study 6
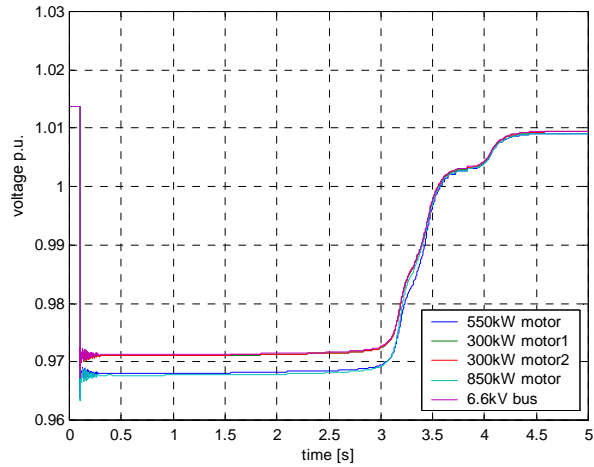
Figure 14-25 Motor terminal and bus voltages (6).
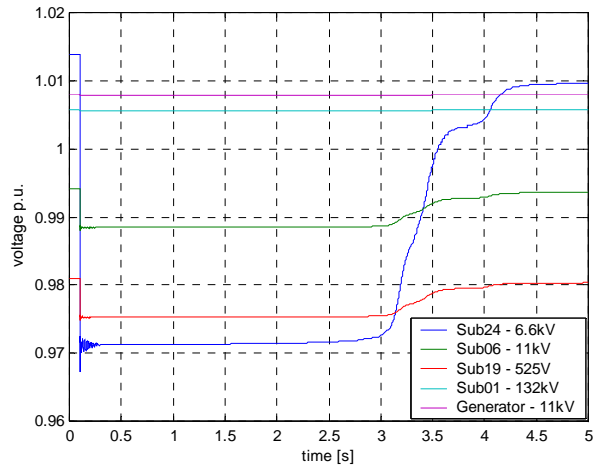
Figure 14-26 Distribution system bus voltages (6).
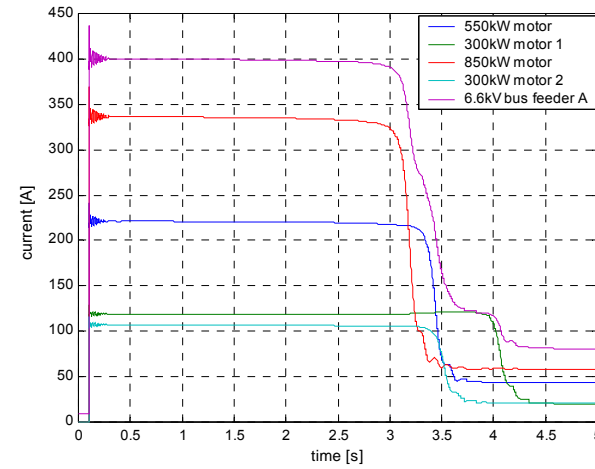
Figure 14-27 Motor and substation feeder currents (6).
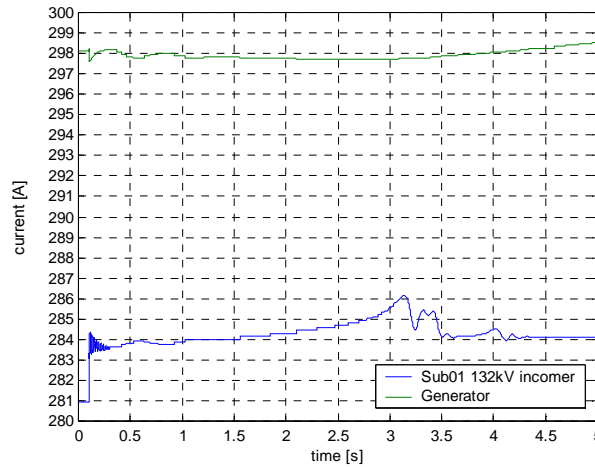
Figure 14-28 Main generator and Eskom feeder currents (6).
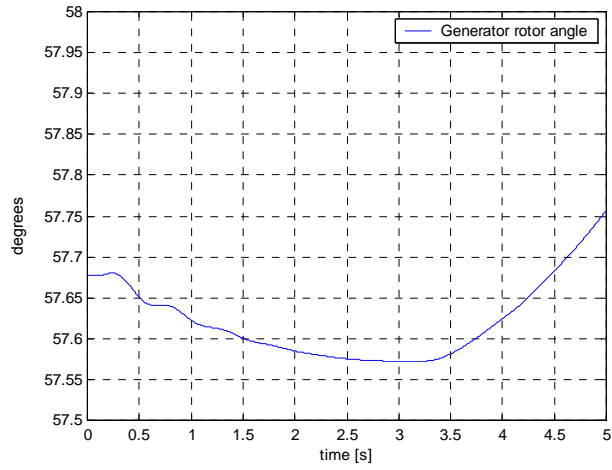
Figure 14-29 Generator rotor angle (6).
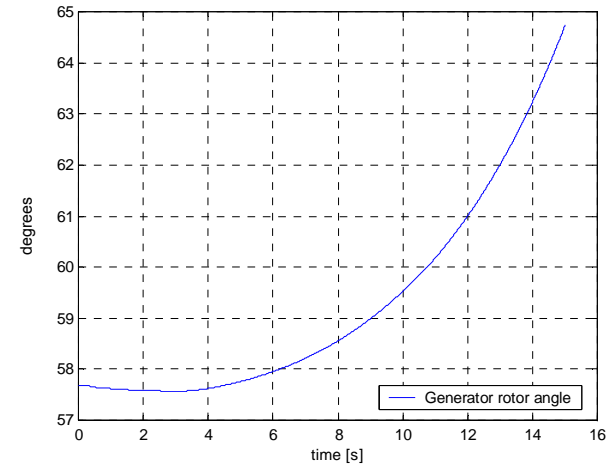
Figure 14-31 Generator rotor angle –extended time (6).
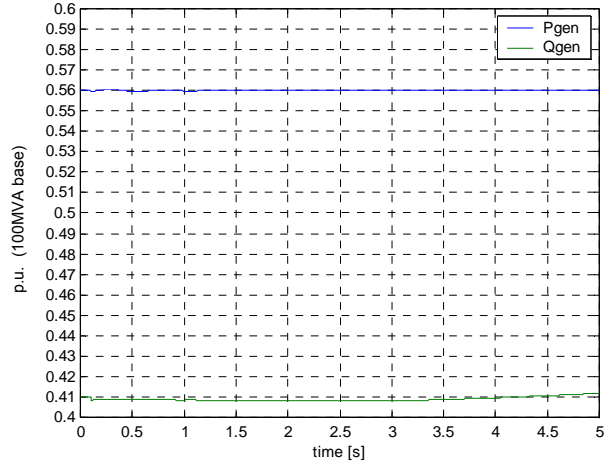
Figure 14-30 Generator power and reactive power output (6).
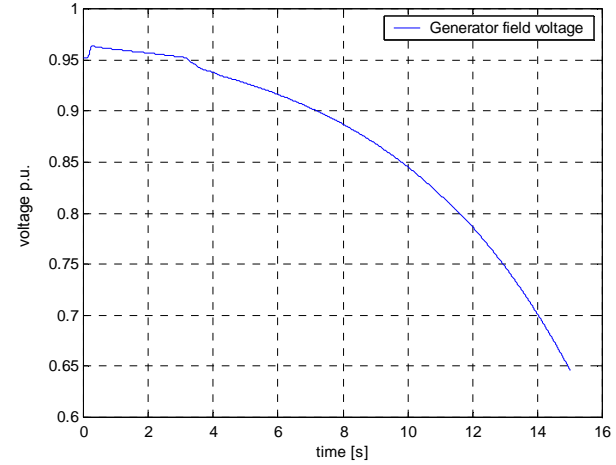
Figure 14-32 Generator field voltage – extended time (6).
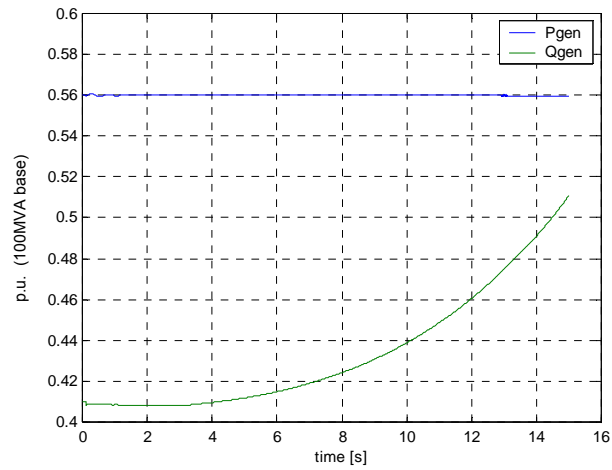
Figure 14-33 Generator power and reactive power output – extended time (6).
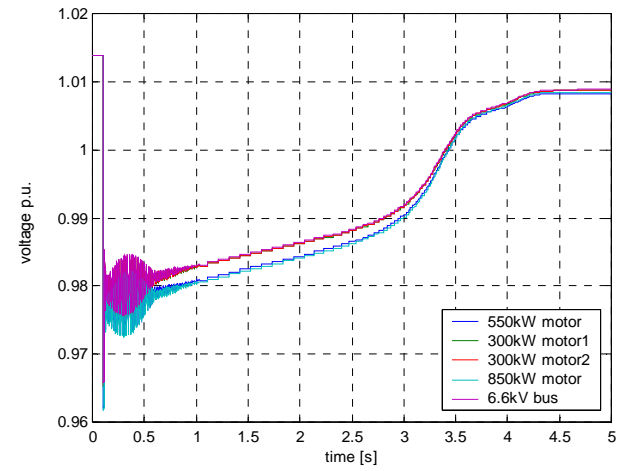
Figure 14-34 Motor terminal and bus voltages (7).
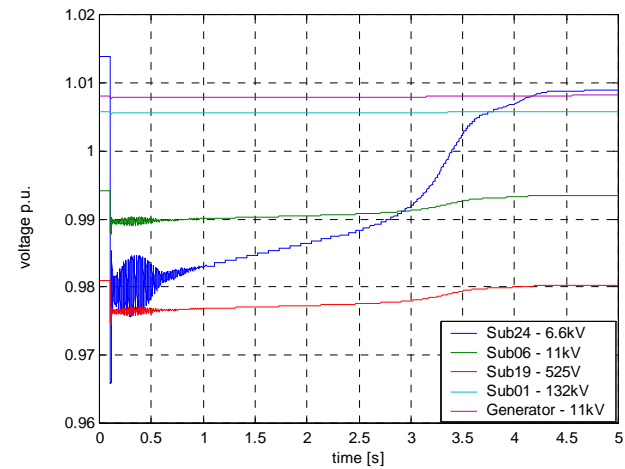
Figure 14-35 Distribution system bus voltages (7).
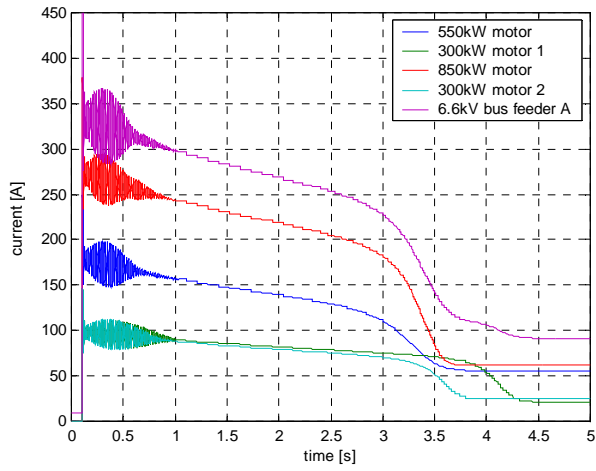
Figure 14-36 Motor and substation feeder currents (7).
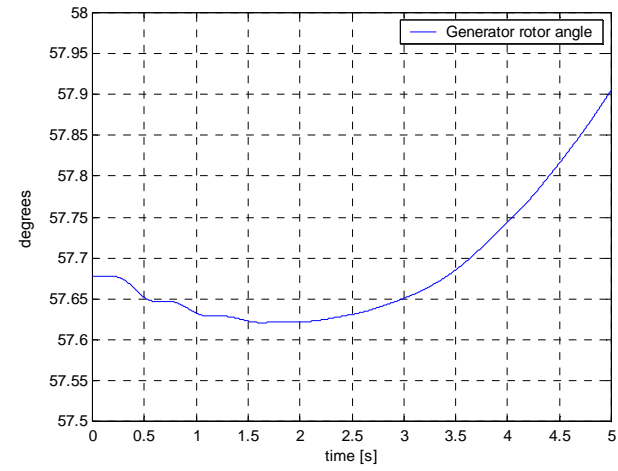
Figure 14-38 Generator rotor angle (7).
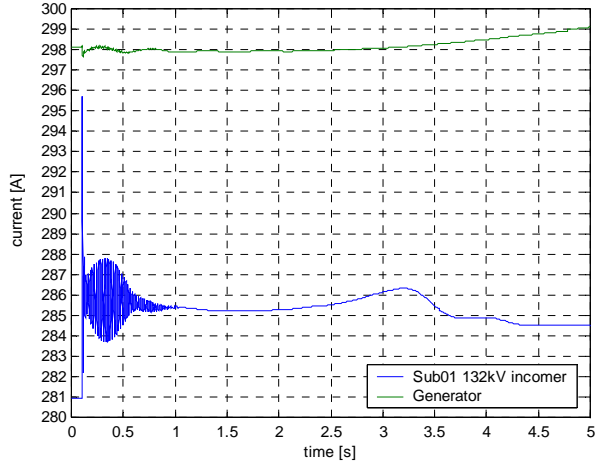
Figure 14-37 Main generator and Eskom feeder currents (7).
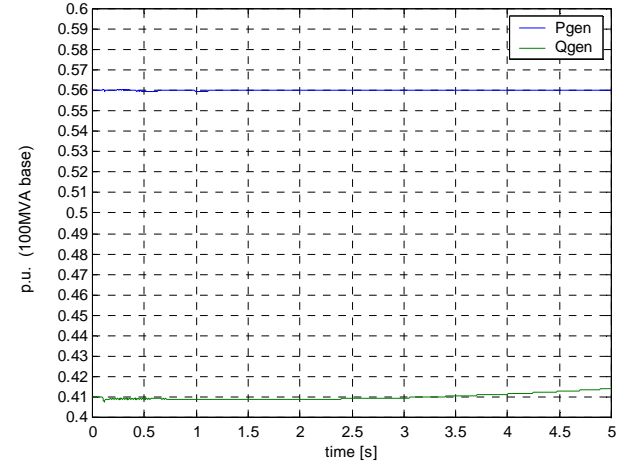
Figure 14-39 Generator power and reactive power output (7).

14.8   Study 8
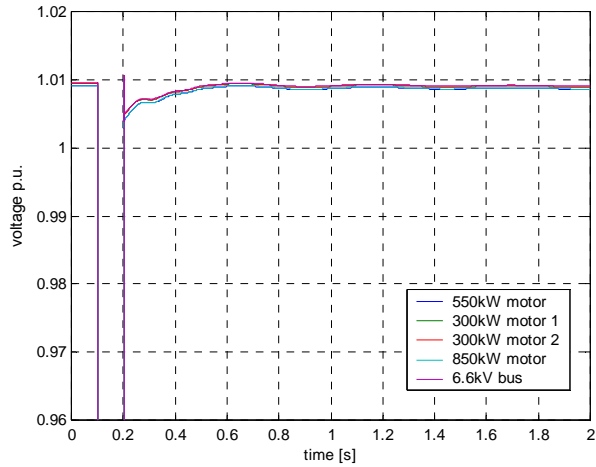
Figure 14-40 Motor terminal and bus voltages (8).

Figure 14-41 Distribution system bus voltages (8).

Figure 14-42 Motor and substation feeder currents (8).
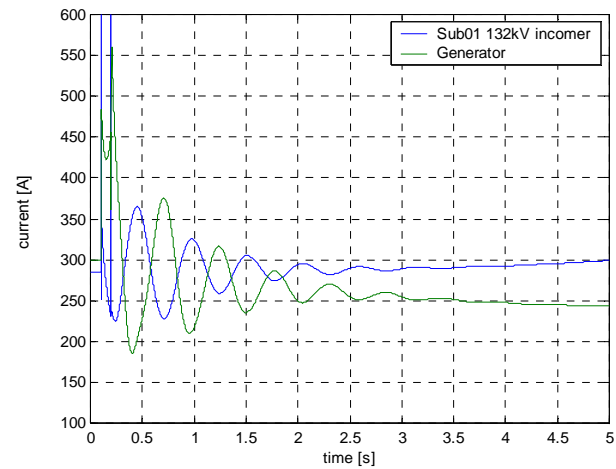
Figure 14-43 Main generator and Eskom feeder currents (8).

14.9 Study 9
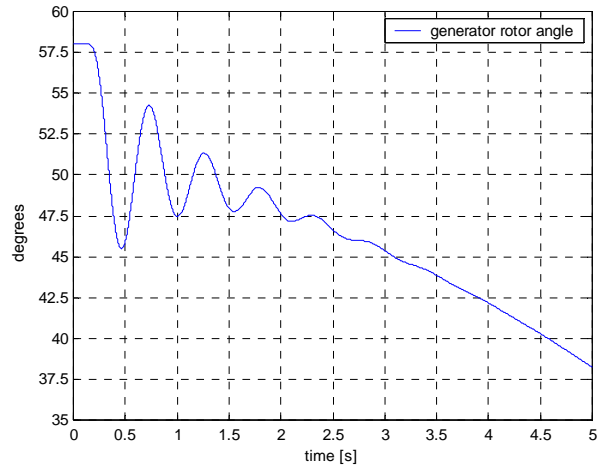
Figure 14-44 Generator rotor angle (8).
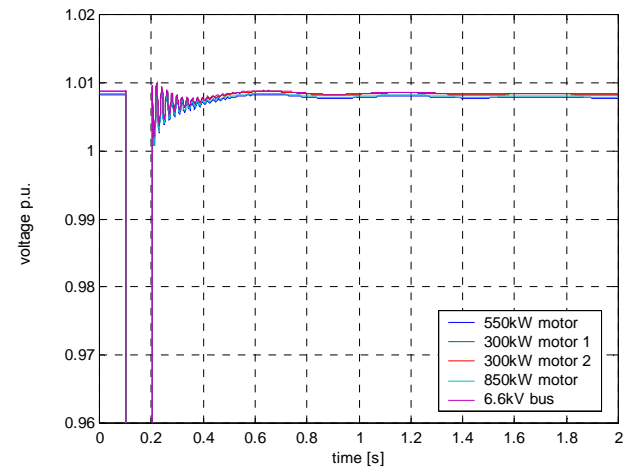
Figure 14-46 Motor terminal and bus voltages (9).
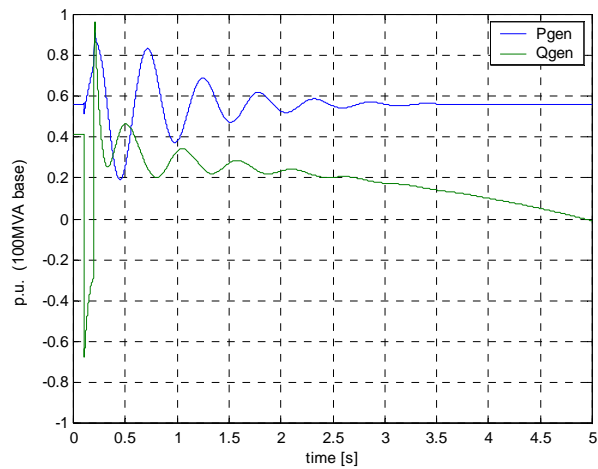
Figure 14-45 Generator power and reactive power output (8).
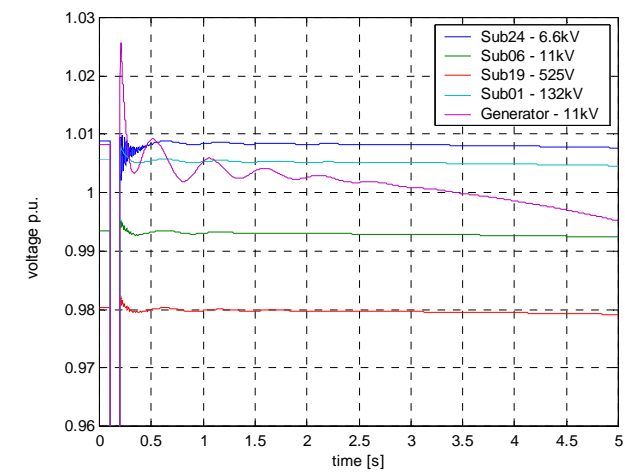
Figure 14-47 Distribution system bus voltages (9).
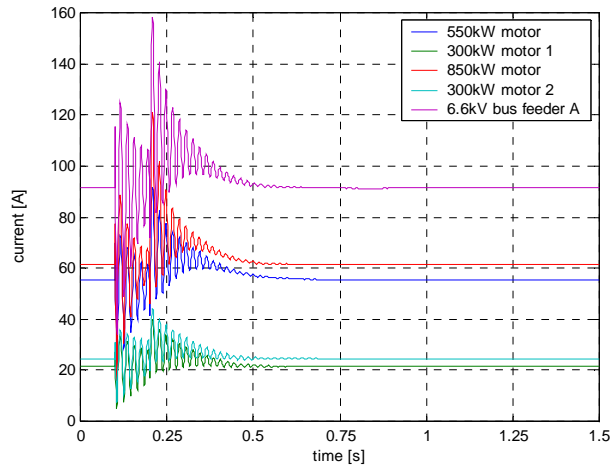
Figure 14-48 Motor and substation feeder currents (9).
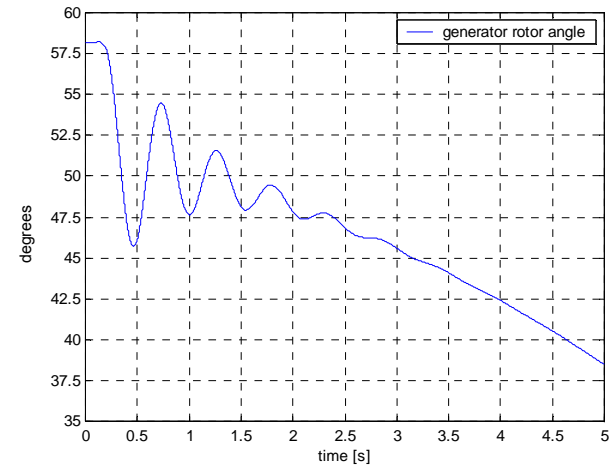
Figure 14-50 Generator rotor angle (9).
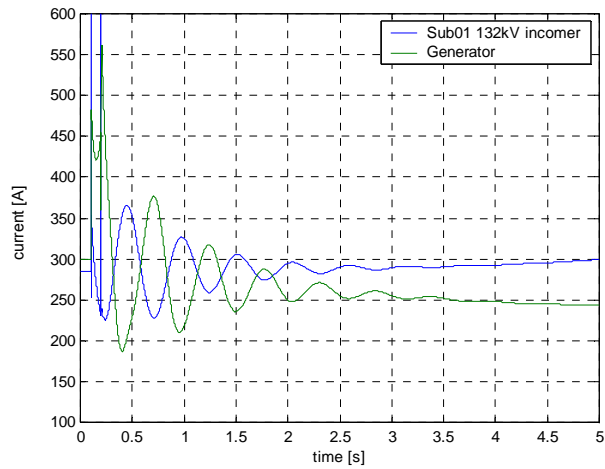
Figure 14-49 Main generator and Eskom feeder currents (9).
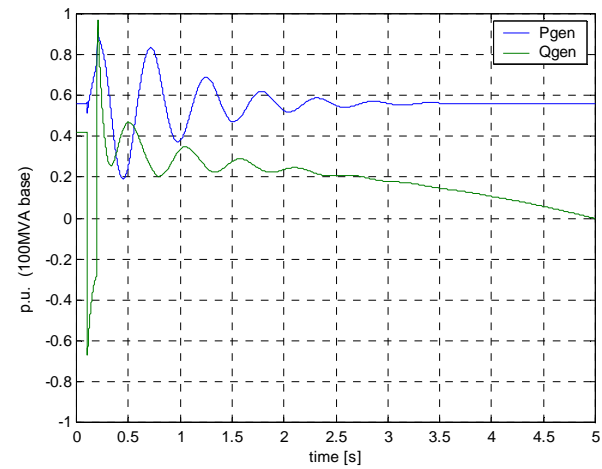
Figure 14-51 Generator power and reactive power output (9).

14.10 Study 10
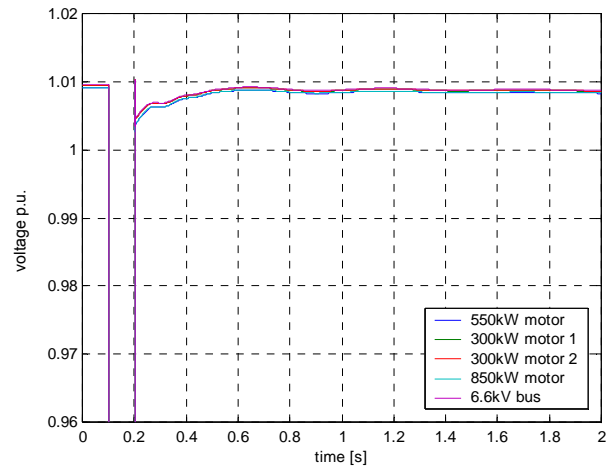
Figure 14-52 Motor terminal and bus voltages (10).

Figure 14-53 Distribution system bus voltages (10).

Figure 14-54 Motor and substation feeder currents (10).

Figure 14-55 Main generator and Eskom feeder currents (10).
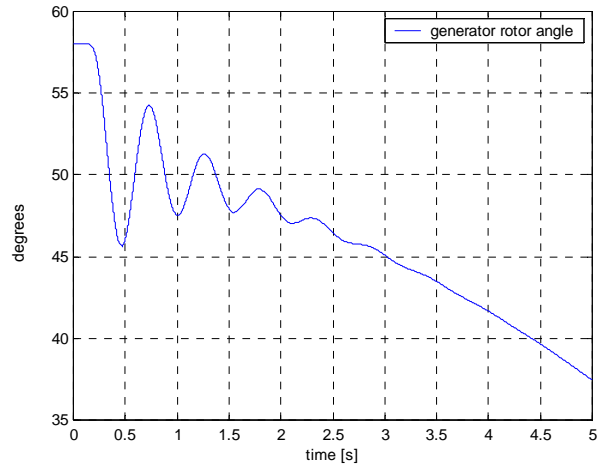
Figure 14-56 Generator rotor angle (10).

Figure 14-57 Generator power and reactive power output (10).

14.11 Study 11

Figure 14-58 Motor terminal and bus voltages (11).
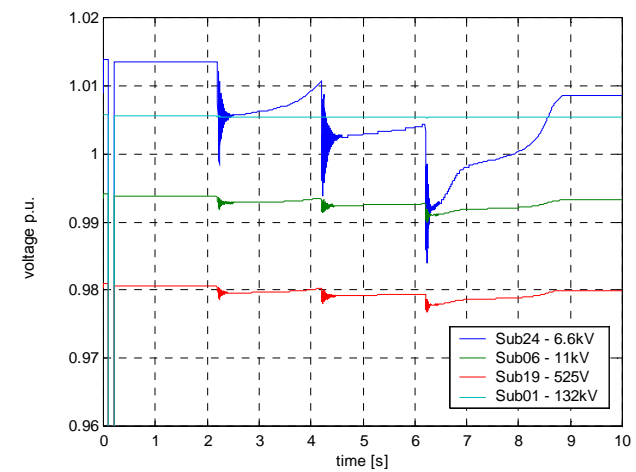
Figure 14-59 Distribution system bus voltages (11).
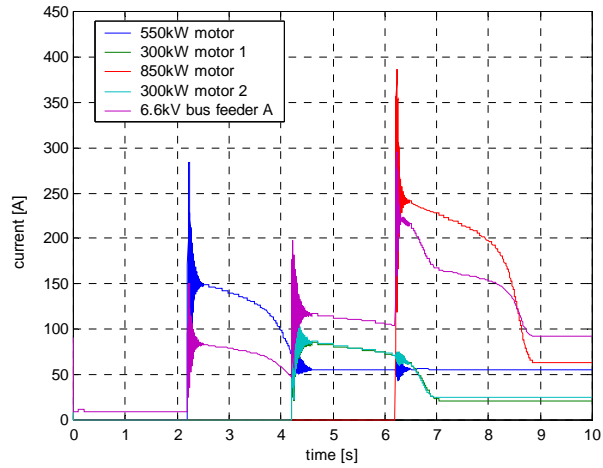
Figure 14-60 Motor and substation feeder currents (11).

Figure 14-61 Motor shaft speeds (11).

14.12 Study 12

Figure 14-62 Motor and terminal bus voltages (12).
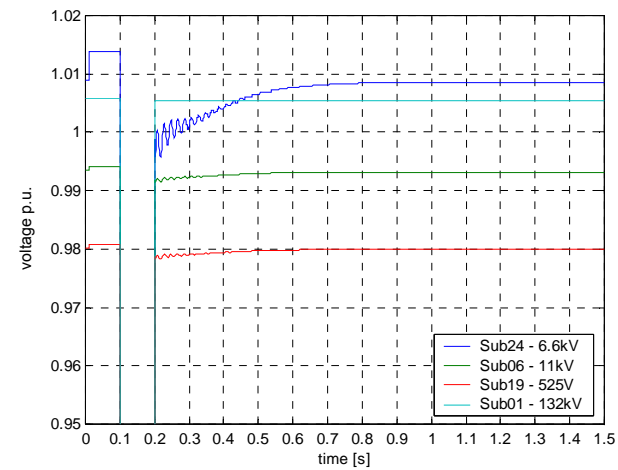
Figure 14-63 Distribution system bus voltages (12).
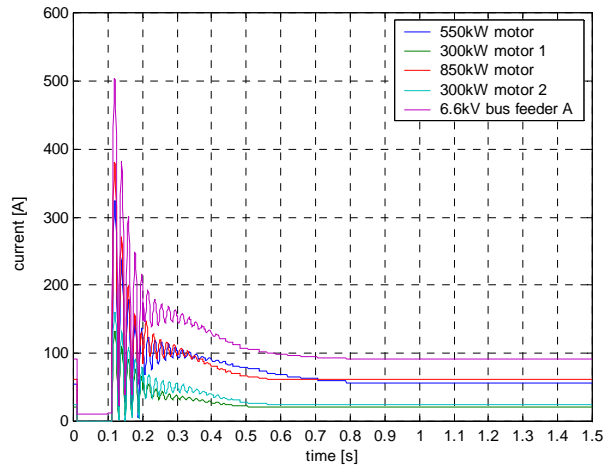
Figure 14-64 Motor and substation feeder currents (12).

15 Appendix I: INDUCTION MOTOR MODEL SIMULATIONS

The results of all induction motor model simulations carried out are shown in this appendix.

Table 15-1 Induction motor model simulations

Simulation	Description	Comments
1	20%, 100ms 3-phase voltage dip. 550kW induction motor	Determine effect of leaving motor connected to the supply during the voltage dip
2	20%, 100ms 3-phase voltage dip. 550kW induction motor. Disconnect 80ms after voltage dip and reconnect 0.25s later	Determine effects of reconnecting motor after a voltage dip at different times. Note, the motor is disconnected 80ms after the start of the voltage dip to simulate the time taken for the contactor to drop out.
3	20%, 100ms 3-phase voltage dip. 550kW induction motor. Disconnect 80ms after voltage dip and reconnect 0.4s later	
4	20%, 100ms 3-phase voltage dip. 550kW induction motor. Disconnect 80ms after voltage dip and reconnect 1s later	
5	20%, 200ms 3-phase voltage dip. 550kW induction motor	Determine effect of leaving motor connected during longer voltage dip
6	20%, 100ms 3-phase voltage dip. 550kW induction motor – *d-q* model	Compare with results obtained from *abc* model

15.1 Simulation 1
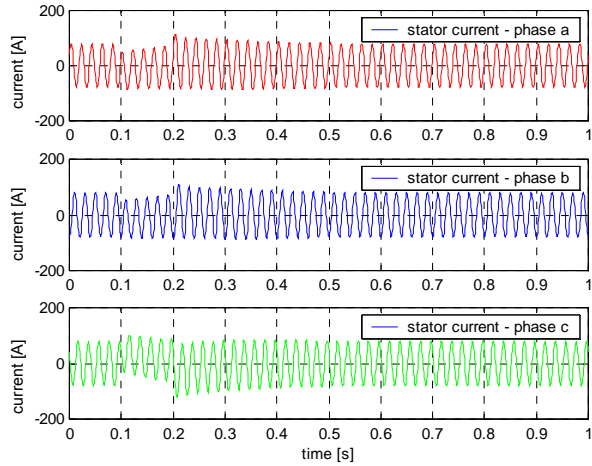
Figure 15-1 Stator currents.
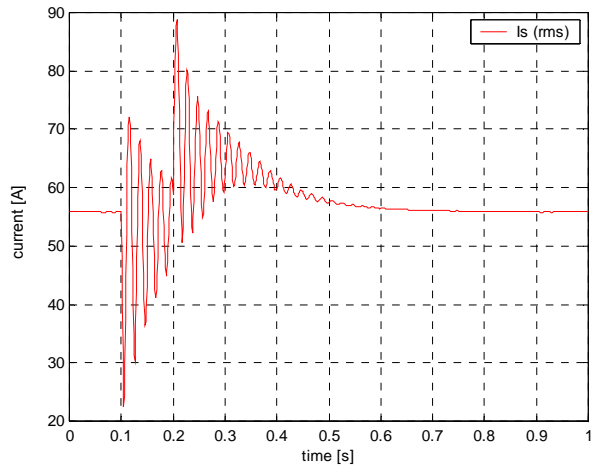
Figure 15-2 RMS Stator current.
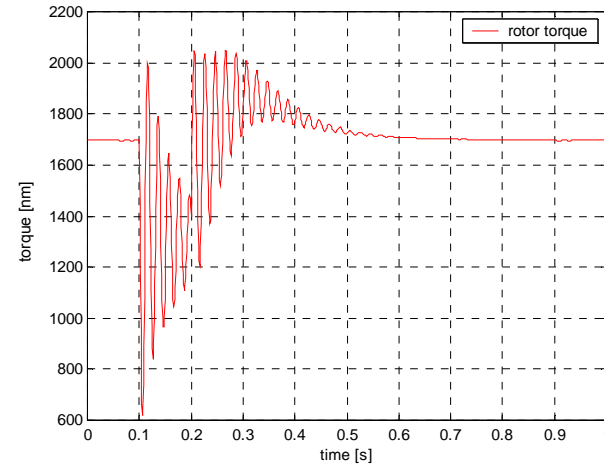
Figure 15-3 Rotor torque.
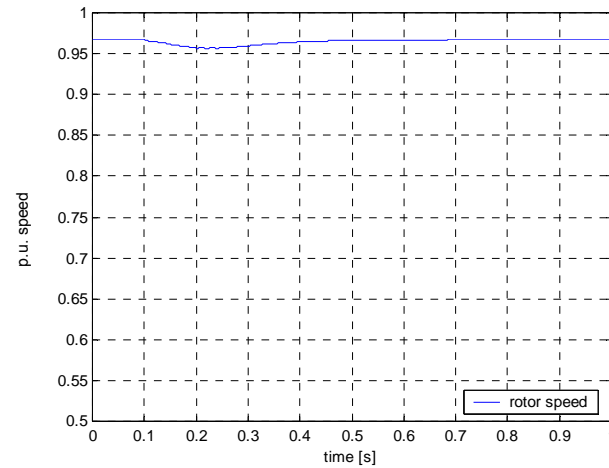
Figure 15-4 Rotor Speed.
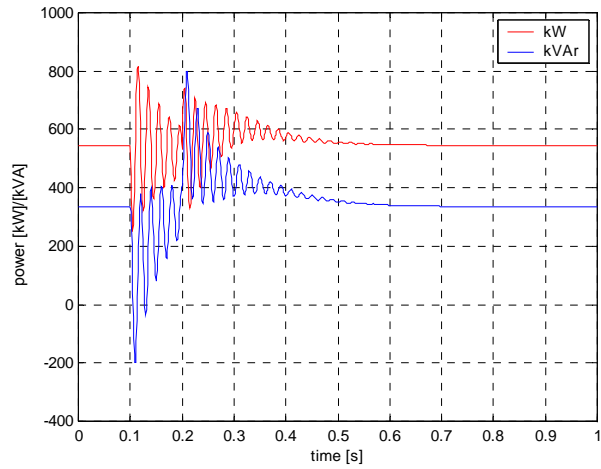
Figure 15-5 Active and reactive power.

15.2 Simulation 2
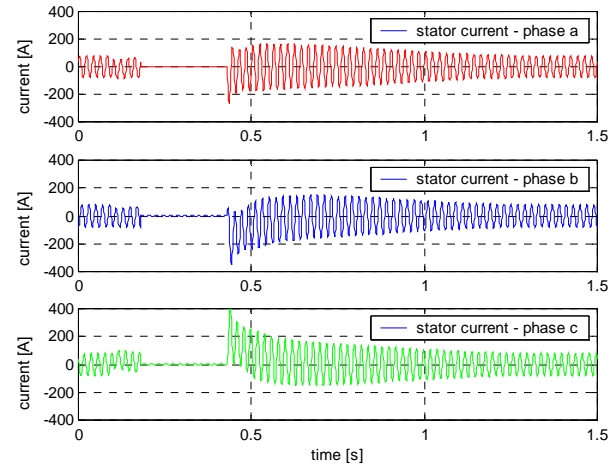
Figure 15-6 Stator currents.
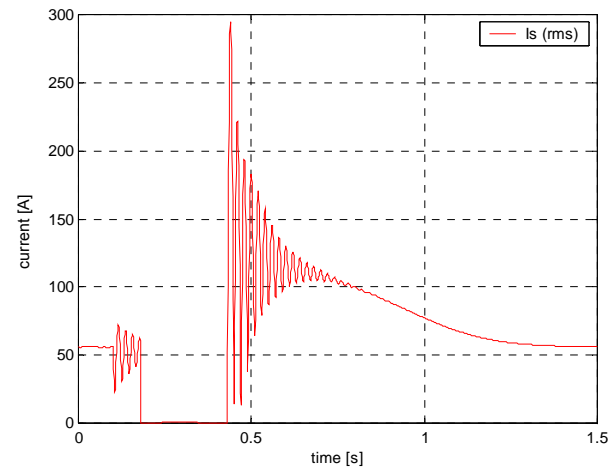
Figure 15-7 RMS stator current.
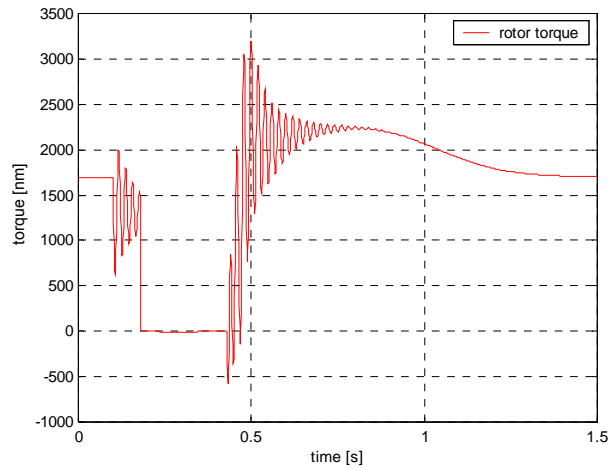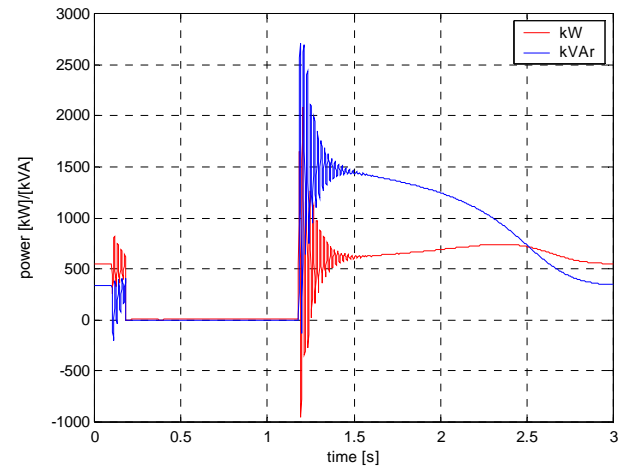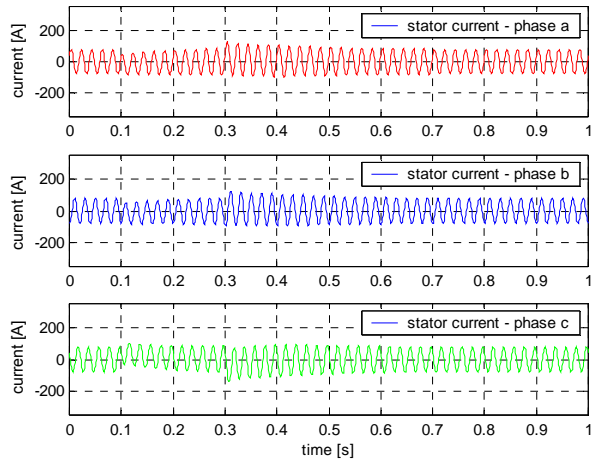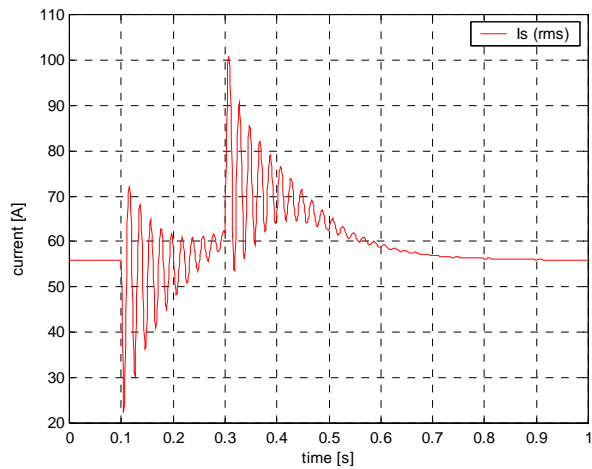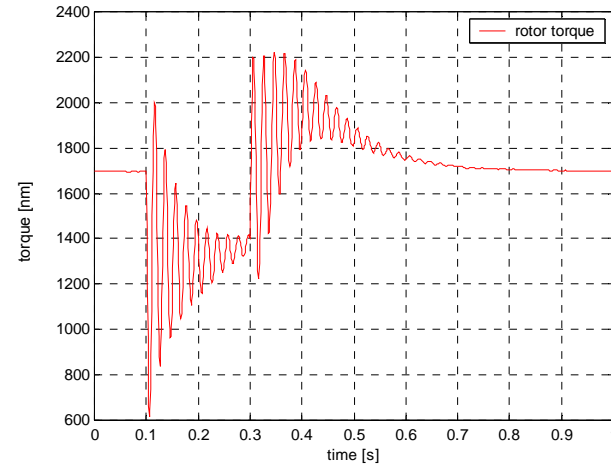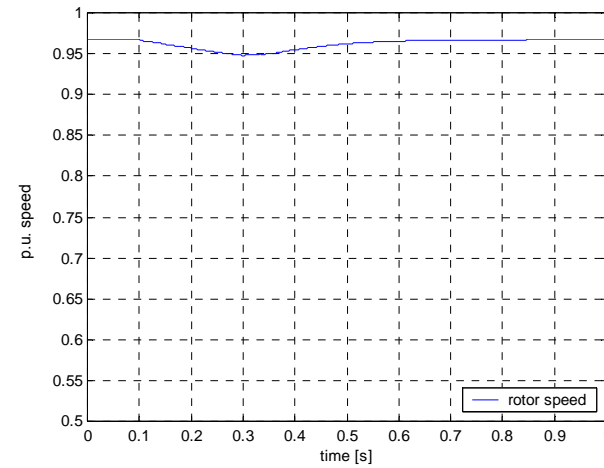
Figure 15-8 Rotor torque.
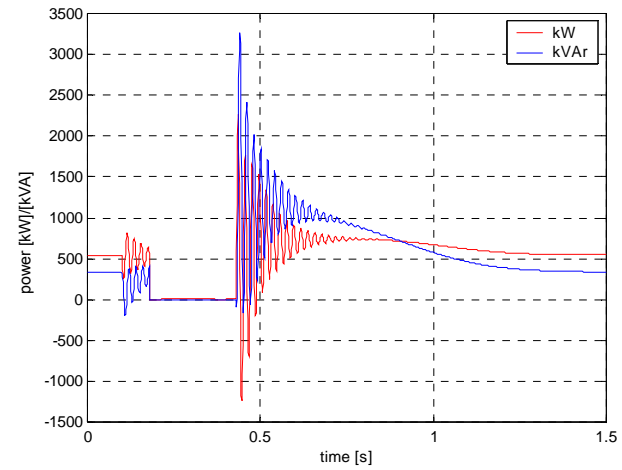
Figure 15-10 Active and reactive power.
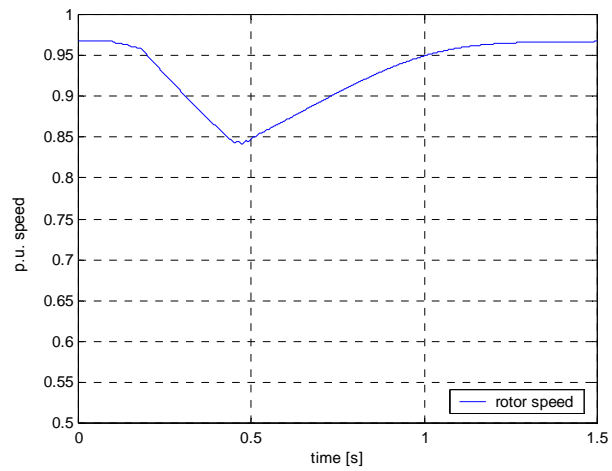
Figure 15-9 Rotor speed.

15.3 Simulation 3
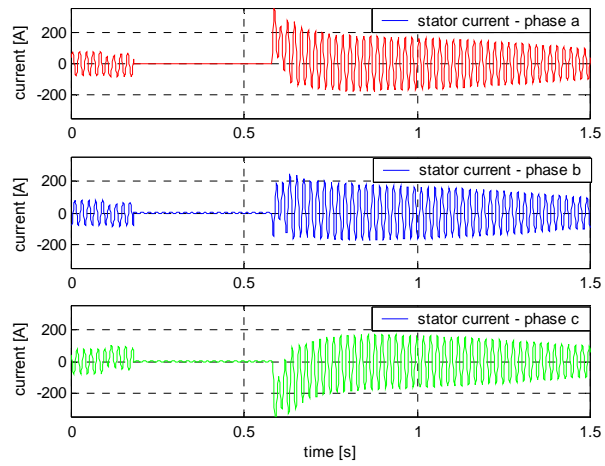
Figure 15-11 Stator currents.
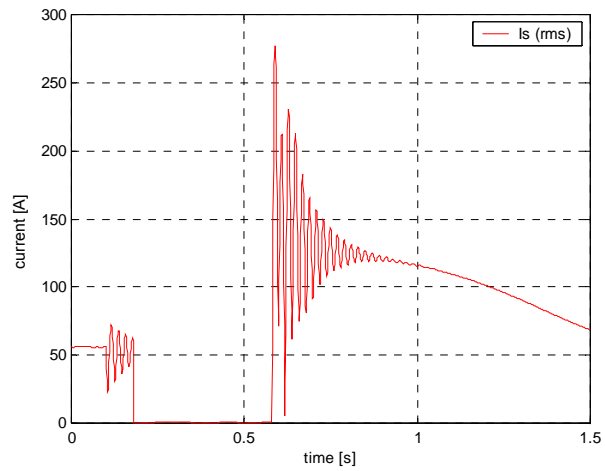
Figure 15-12 RMS stator current.
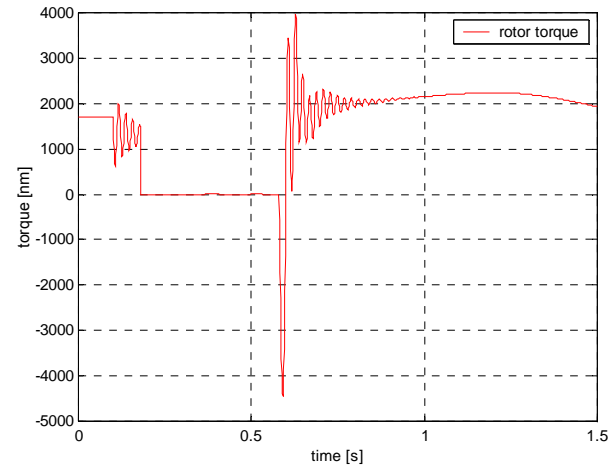
Figure 15-13 Rotor torque.
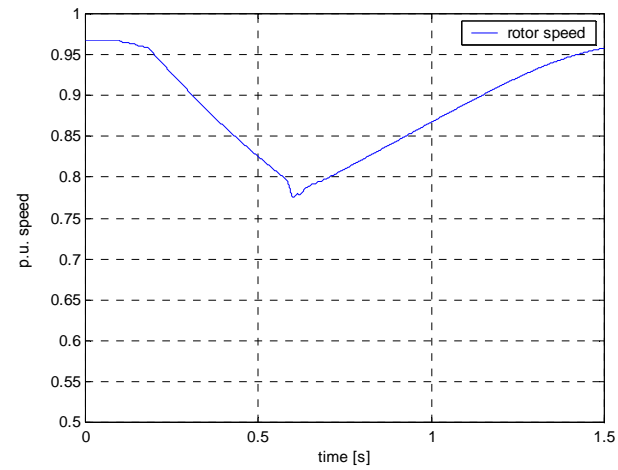
Figure 15-14 Rotor speed.
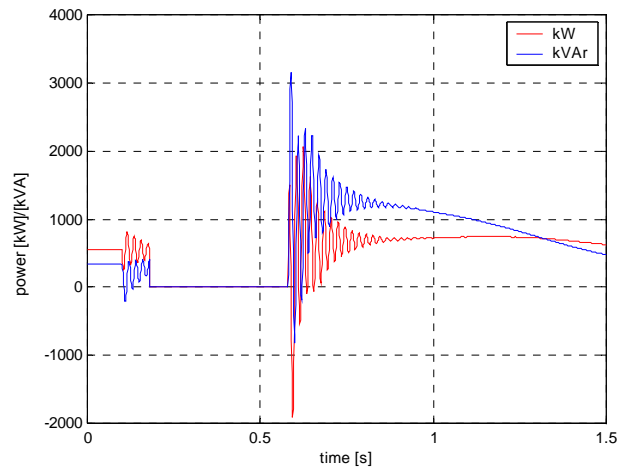
Figure 15-15 Power and reactive power.

15.4 Simulation 4
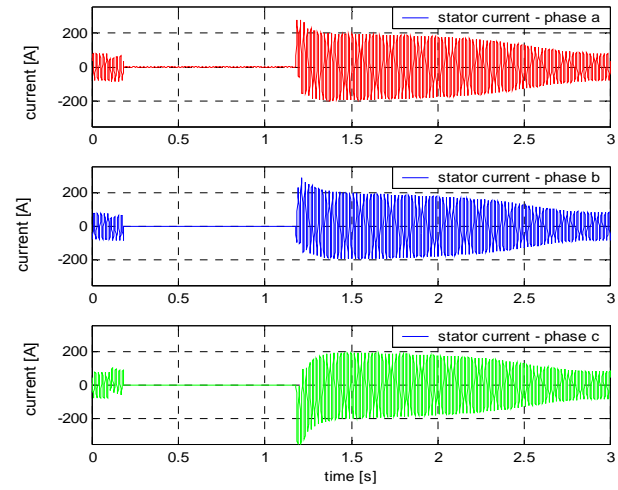
Figure 15-16 Stator currents.
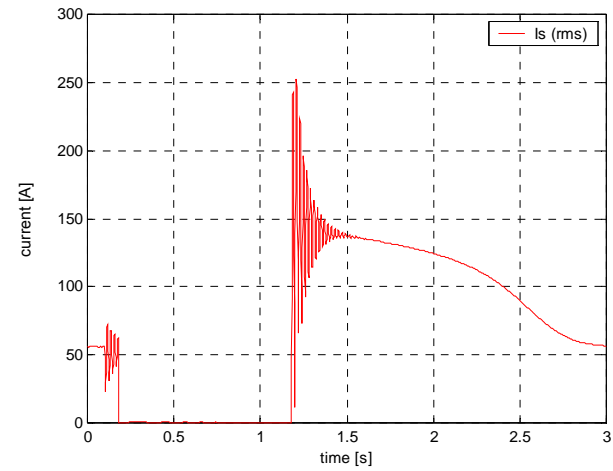
Figure 15-17 RMS stator current.
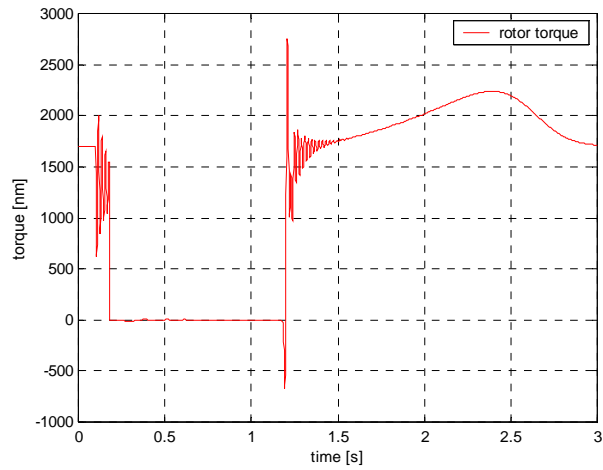
Figure 15-18 Rotor torque.

Figure 15-20 Active and reactive power.
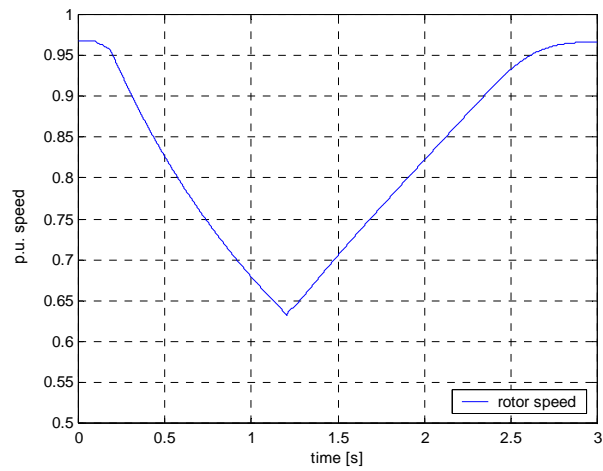
Figure 15-19 Rotor speed.

15.5 Simulation 5

Figure 15-21 Stator currents.

Figure 15-22 RMS stator current.

Figure 15-23 Rotor torque.

Figure 15-24 Rotor Speed.
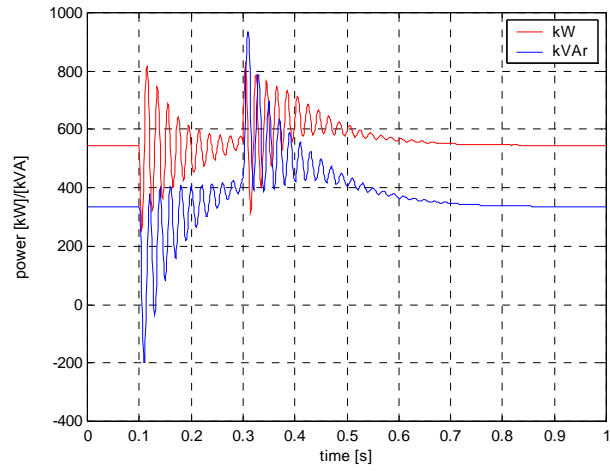
Figure 15-25 Active and reactive power.

15.6 Simulation 6
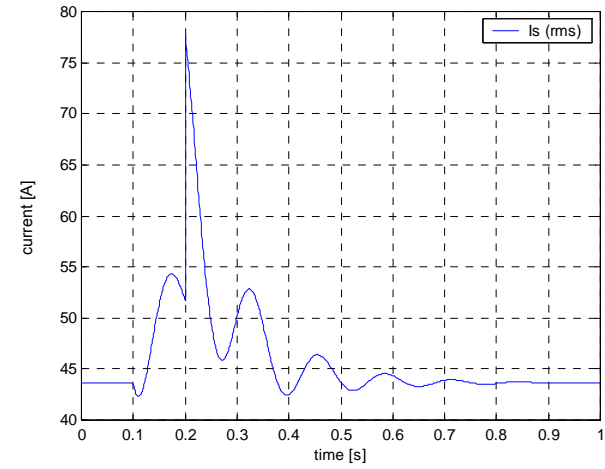
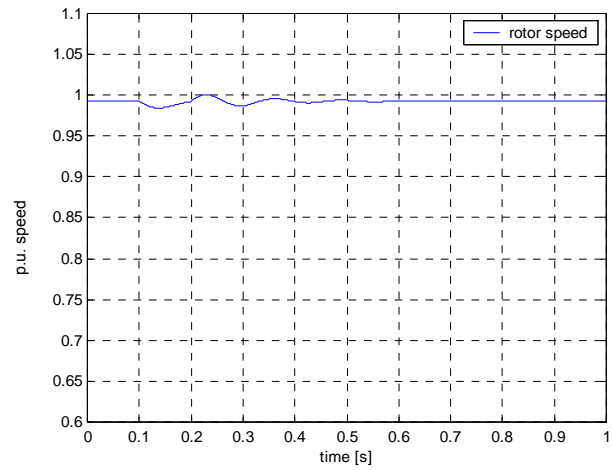**Figure 15-26 RMS stator current.**
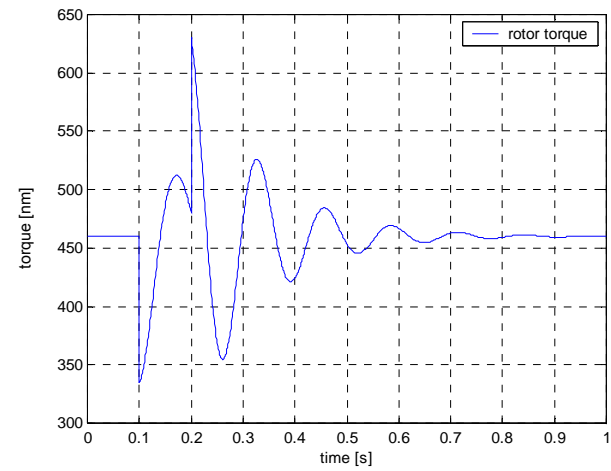
Figure 15-27 Rotor torque.

Figure 15-28 Rotor Speed.

16 Appendix J: MATLAB ODE SOLVER PERFORMANCE

The alternating solution approach adopted requires that the ODE solver is repeatedly used to perform numerical integration over short intervals with the final state of the previous step being used as the initial state for the next integration interval. Since the ODE solvers are normally used to calculate a solution over a longer interval, it was necessary to determine if the repeated use of the solver over short intervals yields different results to those obtained when integration is carried out in a single step over a longer period.

For the purpose of this discussion, the repeated use of the ODE solver over short intervals is referred to as '*step mode*' whilst the use of the solver to integrate over the entire period of interest in a single step is referred to as '*continuous mode*'[1]

Note that for all these tests an infinite bus was assumed, no loadflow calculations carried out and the parameters for a 550kW 6.6kV motor[2] with a load of 20% used. The default values were used for the Matlab ODE solver relative and absolute error tolerance parameters.[3]

When comparing test results, plotting data points only obscures the detail due to the large number of points to be plotted. For detail plots, data points for one data set are plotted to allow comparison with the second data set.

16.1 Stepped vs. Continuous use of ODE solvers

The d-q model was used to simulate the motor starting from standstill. For the first test, the solver was set to return data points at 1ms intervals and for the second, at 10ms. The Matlab ODE solver ode45 was used since this is recommended as a 'first try' for most problems in the Matlab documentation.
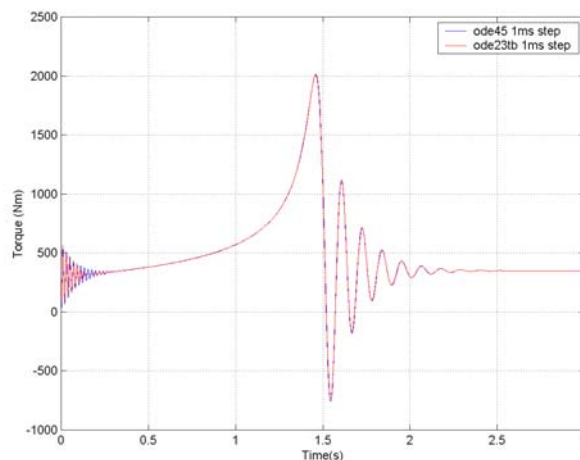

Figure 16-1 ODE solver test: d-q model using continuous integration with different step lengths.

---

[1] Even though this mode is referred to as continuous, the Matlab ODE solver algorithms are using multiple internal steps at time intervals dictated mainly by the relative and absolute error tolerance parameters RelTol and AbsTol to calculate the solution over the specified time interval.

[2] Motor model parameters used are as for 550kW motor no. 24KC101M

[3] Matlab documentation states that the error at each integration step is required to be less than an acceptable error which is a function of two user defined tolerances RelTol and AbsTol. RelTol controls the number of correct digits in the answer (the default, 1e-3, corresponds to 0.1% accuracy) and AbsTol is the threshold below which solution components are unimportant. The absolute error tolerance determines the accuracy when the solution approaches zero (default 1e-6)

The test results are compared in Figure 16-1 and the initial torque transients as well as the torque transients as the machine reaches full speed are shown in more detail in Figure 16-2 and Figure 16-3. For clarity, only the data points returned by the ODE solver at 10ms intervals are shown. It can be seen that the results obtained are identical at the returned data points. The results are therefore not affected by the time interval at which data points are returned by the ODE solvers when using the solvers to integrate continuously over a time period.[4]
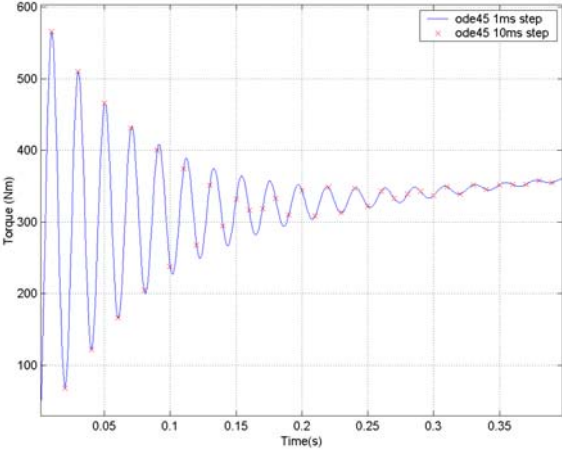

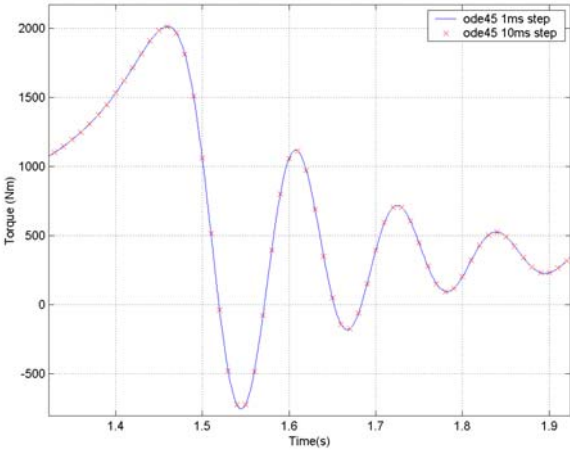**Figure 16-2 ODE solver test: Detail view of Figure 16-1.**

Figure 16-3 ODE solver test: Detail view of Figure 16-1.

The same test as above was carried out using the abc motor model. The abc model was used to simulate the motor starting from standstill. For the first test, the solver was set to return data points at 1ms intervals and for the second, at 10ms.

---

[4] This is in agreement with the Matlab documentation which states that the definition (or omission) of specific time points at which to obtain solutions does not affect the internal time steps the solvers use or the accuracy of results obtained.
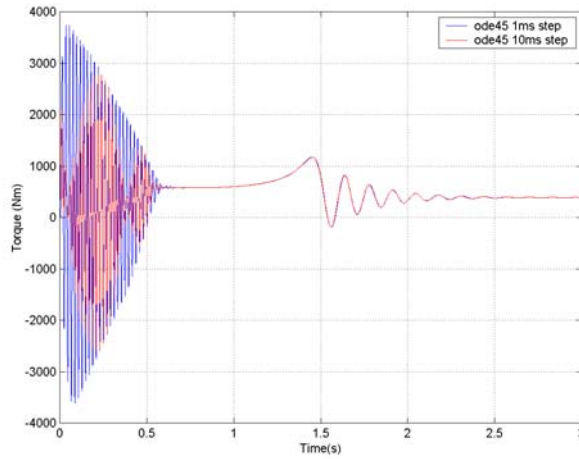
Figure 16-4 ODE solver test: abc model using continuous integration with different step lengths.
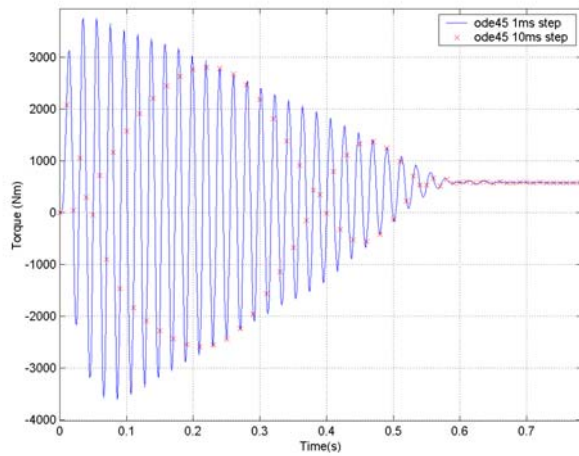

Figure 16-5 ODE solver test: Detail view of Figure 16-4.
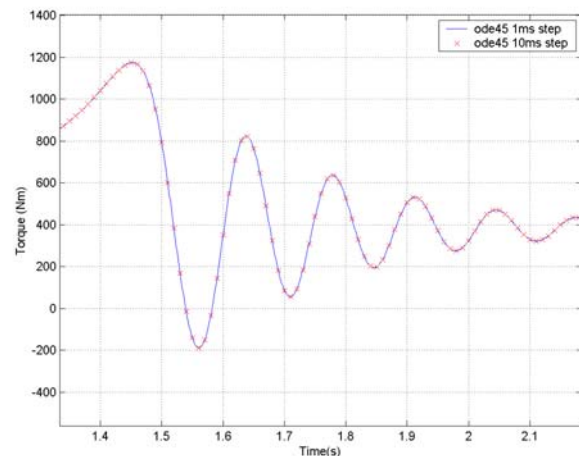

Figure 16-6 ODE solver test: Detail view of Figure 16-4.

Figure 16-4 shows that the results are not affected by the selection of step length, as for the d-q model. Figure 16-5 and Figure 16-6 show that the data points returned at the 10ms intervals are the same as the data points returned at 1ms intervals. As for the d-q model, the results are not affected by the time

interval at which data points are returned by the ODE solvers when using the solvers to integrate continuously over a time period. Using a step interval of 10ms however does not allow the 50Hz torque transients during motor startup to be accurately plotted since insufficient data points are available. The slower torque transients occurring as the motor accelerates to its steady running speed[5] can be displayed in sufficient detail – refer to Figure 16-4.

The results obtained when using the ODE solvers in continuous and stepped mode were compared. The more complex abc model was used for all tests unless stated otherwise. The abc model which requires a greater number of calculations to obtain a numerical solution was chosen since it is likely that any inaccuracies will be more readily observed. The motor startup from standstill was simulated using the ode45 solver in continuous and stepped mode. The results are compared in Figure 16-7. It can be seen that there is a clear discrepancy between the results obtained.
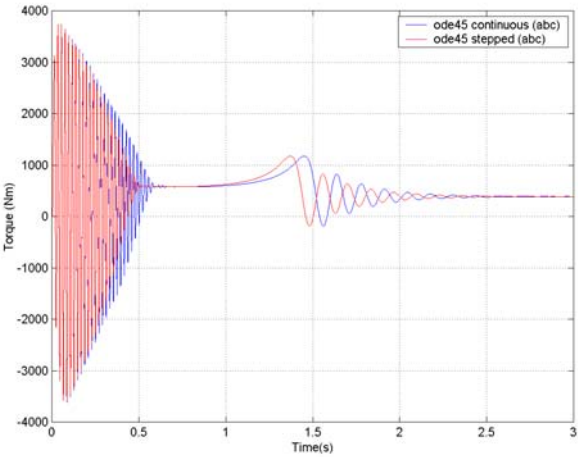

Figure 16-7 ODE solver test: abc model, stepped vs. continuous solution, 1ms step interval.

It was suspected that using the ode solver in stepped mode was introducing errors and the relative tolerance parameter was changed from 1e-3 to 1e-5. The motor startup was again simulated in stepped mode using RelTol = 1e-5.
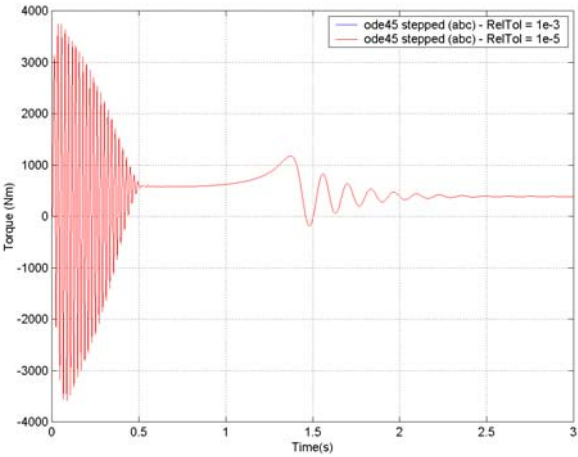
Figure 16-8 ODE solver test: abc model, stepped solution with RelTol parameter varied.

---

[5] These torque pulsations are due to rotor and load inertia and the degree of damping that exists in the mechanical load being driven by the motor. The rotor will initially accelerate past the steady-state speed and may exceed synchronous speed. Under these conditions the motor acts as a generator and output torque will be negative. The rotor speed (and torque) will continue oscillating until the motor and load reach a steady state.

The solution obtained using RelTol = 1e-5 was compared to that obtained using RelTol = 1e-3 and found to be identical. This can be seen in Figure 16-8 and Figure 16-9 where only the data points for the solution obtained using RelTol = 1e-5 have been plotted.
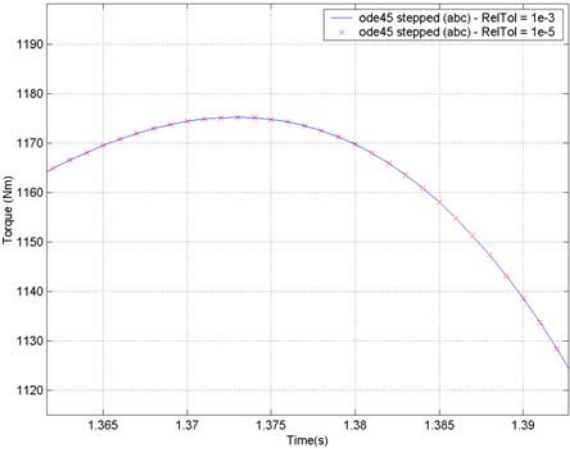

Figure 16-9 ODE solver test: Detail view of Figure 16-8.

A further test was carried out where the motor start was simulated using the ODE solver in continuous mode with RelTol = 1e-5.
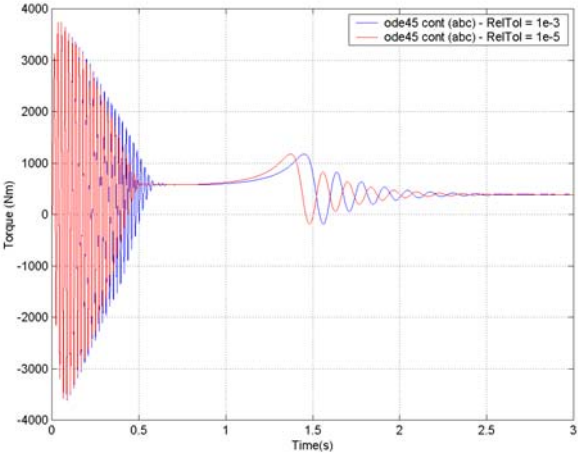
Figure 16-10 ODE solver test: abc model, continuous mode with RelTol changed.

The effect of changing RelTol when using the ODE solver to carry out the integration in continuous mode is shown in Figure 16-10. It was found that using values of 1e-5 and smaller for RelTol gave identical solutions. As RelTol becomes larger, the solutions obtained start to differ as seen in Figure 16-10. Matlab documentation states that the Ode solvers deliver less accuracy for problems integrated over "long" intervals and for problems that are moderately unstable. It is therefore clear that the default error tolerance parameters do not result in a sufficiently accurate solution when using the ODE solver to integrate in continuous mode over an interval of 0 to 3 seconds.

Figure 16-11 ODE solver test: abc model, stepped vs. continuous solution.

Figure 16-12 ODE solver test: Detail view of Figure 16-11.

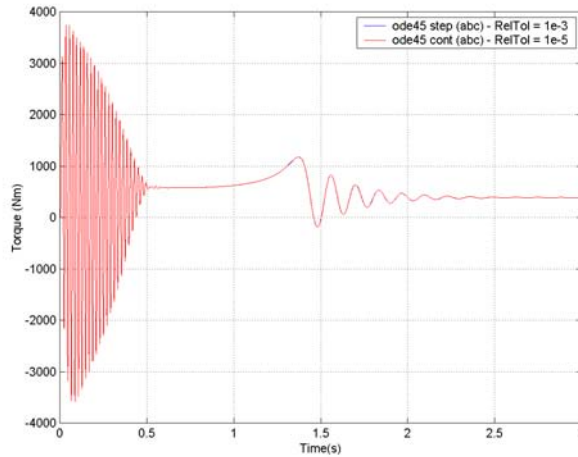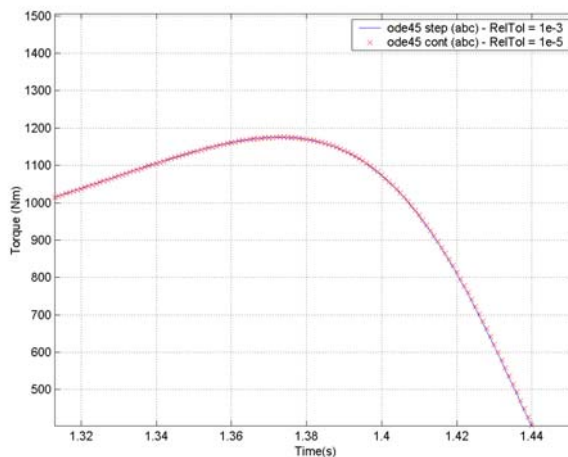The results obtained using the ODE solver in continuous mode with RelTol = 1e-5 were then compared to the results obtained using the ODE solver in stepped mode with RelTol = 1e-3. It can be seen from Figure 16-11 and Figure 16-12, that the results compare well. The above tests show that when the Matlab ODE solvers are used over short intervals, accurate results are obtained with the default error tolerance parameters. When using the solver over 'longer' intervals, the relative tolerance parameter has to be made smaller to obtain an accurate solution. For the purposes of this work, a solution was considered 'accurate' if further changes in parameters (e.g. reduced time step or smaller tolerance) did not result in significant changes to the solutions obtained.

16.2 Comparison of ODE solver performance

The different Matlab ODE solvers were then compared to each other to determine if the value of RelTol used above yields identical solutions to those obtained using ode45, above. The various Matlab ODE solvers are listed in Table 16-1 for reference. All tests were carried out using the abc motor model, with the same parameters as used for the tests in 16.1, above. RelTol was 1e-5.

Table 16-1 Summary of Matlab ODE solver algorithms.

Function	*Description*
ode45	Based on an explicit Runge-Kutta (4,5) formula, the Dormand-Prince pair. This is a one-step solver. Best used as a "first try" for most problems
ode23	Based on an explicit Runge-Kutta (2,3) pair of Bogacki and Shampine. This is a one-step solver and may be more efficient than ode45 at crude tolerances and in the presence of mild stiffness
ode113	This is a variable-order Adams-Bashforth_Moulton solver. It may be more efficient than ode45 at stringent tolerances and when the ODE function is particularly expensive to evaluate. This is a multi-step solver, requiring solutions at several preceding time points to compute the current solution.
ode15s	This is a variable-order solver based on the numerical differentiation formulas. It can optionally, use the backward differentiation formulas (Gear's Method) that are usually less efficient. This is a multi-step solver. If a problem is stiff or if ode45 fails or was very inefficient, try ode15s
ode23s	This is based on a modified Rosenbrock formula of order 2. It is a one-step solver and may be more efficient than ode15s at crude tolerances. It can solve some kinds of problems for which ode15s is not effective.

The solution obtained using ode23 is compared to that obtained using ode45.
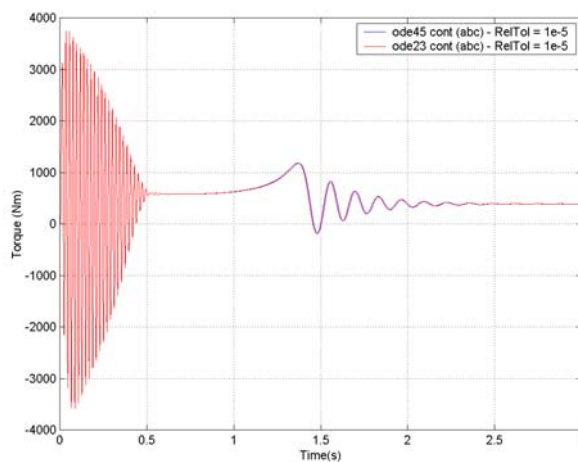
Figure 16-13 ODE Solver test: Compare ode45 and ode23.

From Figure 16-13 it can be seen that the solutions are not identical. Additional tests (not shown) showed that this discrepancy can be further reduced by using smaller error tolerance values. Solver ode23 is less efficient than ode 45 and was not considered further.
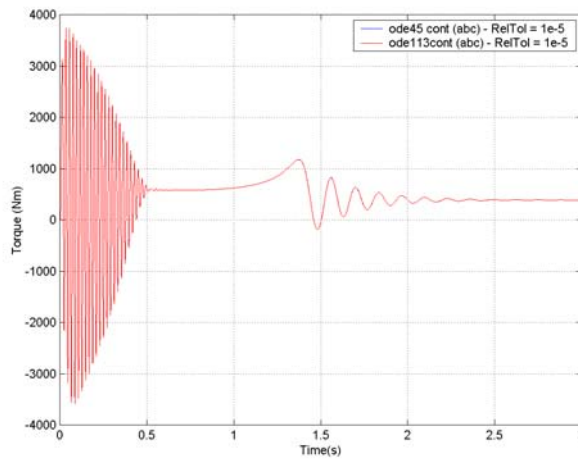
Figure 16-14 ODE Solver test: Compare ode45 and ode113.

From Figure 16-14 it can be seen that results obtained using ode113 agree well with those obtained using ode45. A portion of Figure 16-14 is shown in Figure 16-15 with only the data points returned by ode113 plotted for clarity.
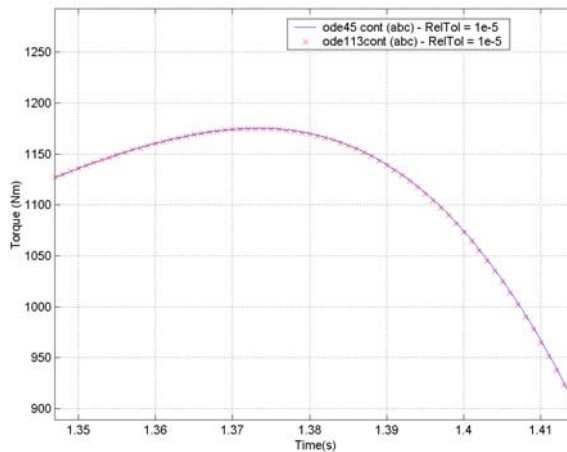
Figure 16-15 Detail view of Figure 16-14.
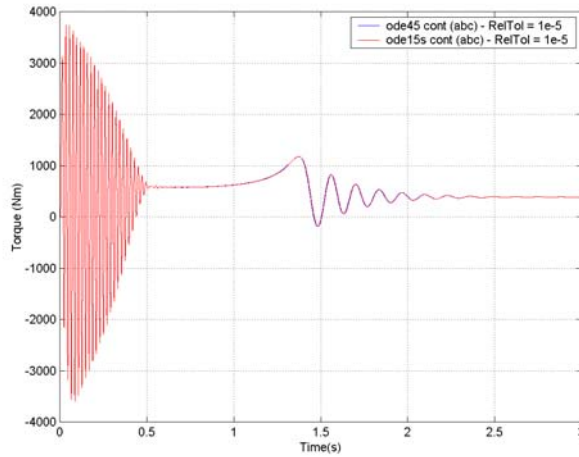
Figure 16-16 ODE solver test: Compare ode45 and ode15s.
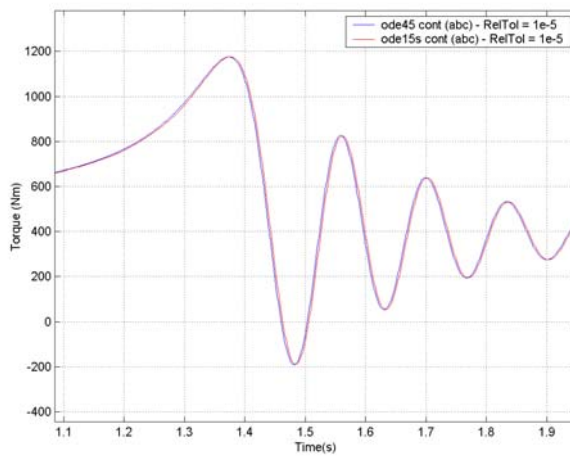
Figure 16-17 Detail view of Figure 16-16.

Figure 16-16 and Figure 16-17 show that the results obtained using ode15s compare reasonably well with those obtained form ode45.
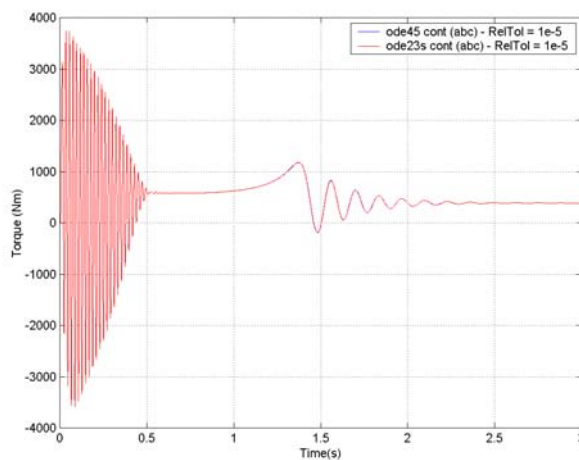
Figure 16-18 ODE Solver test: Compare ode45 and ode23s.
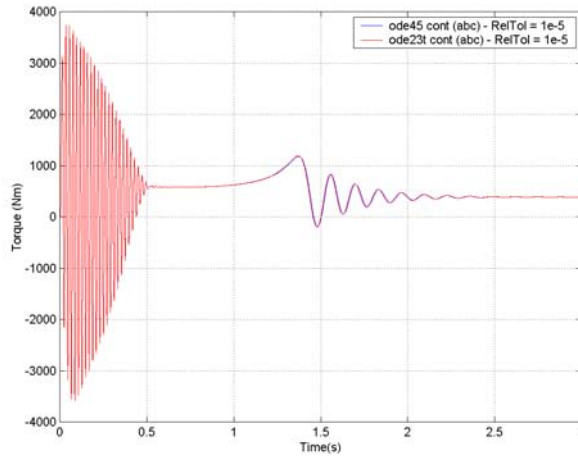
Figure 16-19 ODE Solver test: Compare ode45 and ode23t.
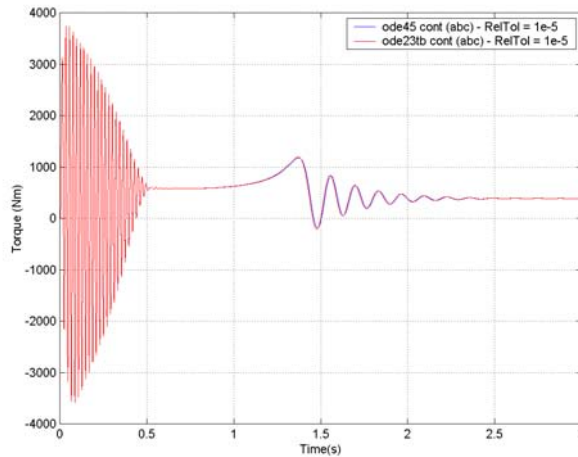
Figure 16-20 ODE Solver test: Compare ode45 to ode23tb.

Figure 16-18, Figure 16-19 and Figure 16-20 show comparisons of the solutions obtained using ode23s, ode23t and ode23tb with that obtained using ode45. It can be seen that RelTol <= 1e-5 needs to be used to obtain consistent solutions when using the Matlab ode solvers. Using larger values of RelTol results in differences between the solutions obtained from the different ode solvers, similar to that shown in Figure 16-10. The time taken to compute a solution varied significantly between solvers.

It was interesting to note that the stiff equation solvers were not particularly efficient. This can probably be attributed to the fact that the 'Jacobian' option was not set. According to the Matlab documentation, the use of this option along with coding the solver ODE file to evaluate the Jacobian for the problem analytically often increases the speed and reliability of the solution. Without this option, ode15s and ode23s evaluate the Jacobian numerically. It was found that the ode113 solver was the most efficient algorithm giving a solution in an acceptable time. As discussed above, the possibility exists that the performance of the ode5s solver will be improved by modifying the solver ODE file to be able to evaluate the Jacobian, but the additional complexity was not considered justified and this was not investigated further.

Table 16-2 ODE Solver test: Comparison of solution times.

Solver	Solution time
ode45	36s
ode23	47s
ode113	10s
ode15s	26s
ode23s	722s
ode23t	77s
ode23tb	108s

16.3 ODE Solver performance when using stepped solution

From the previous tests it has been determined that the Matlab ODE solvers can give inaccurate results when the tolerance parameters, in this case RelTol, are not set correctly. This occurs when integrating over 'long' periods and under these conditions the default values are not acceptable. When the transient response of the PetroSA distribution system is calculated, the alternating solution approach adopted results in the ode solvers being used to calculate system response over a large number of 'short' time periods. It was found that the solvers give acceptable results when used in this manner with the default tolerance parameters when the time step length was 1ms. It is therefore necessary to determine what value of RelTol should be used with longer step lengths to ensure that simulation results remain accurate.

The abc motor model was used with the same parameters as for the previous tests discussed in this appendix. ODE solver ode113 was used for all of the following tests.
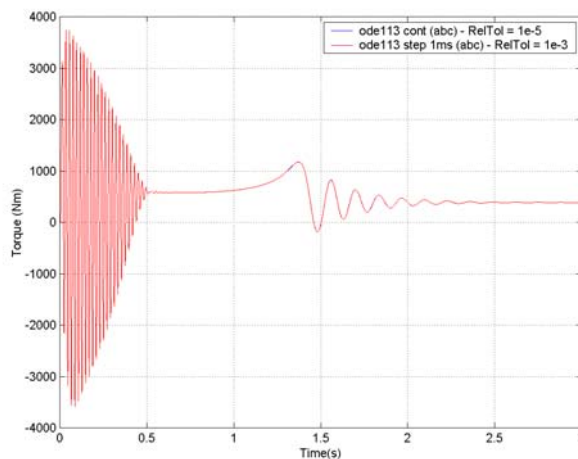
Figure 16-21 ODE Solver test: ode113 stepped vs. continuous solution.
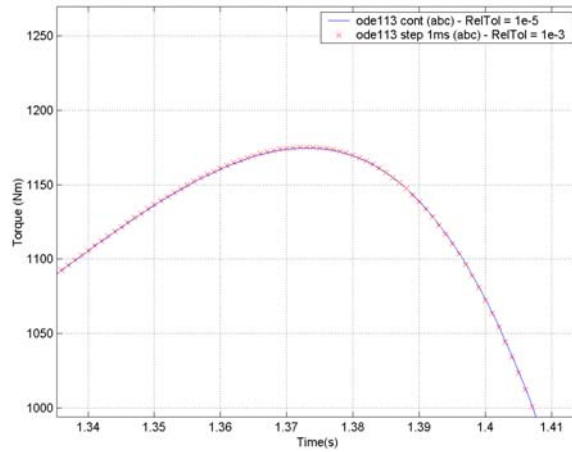
Figure 16-22 Detail view of Figure 16-21.

Figure 16-21 and Figure 16-22 show that the results obtained from the stepped and continuous methods are the same.
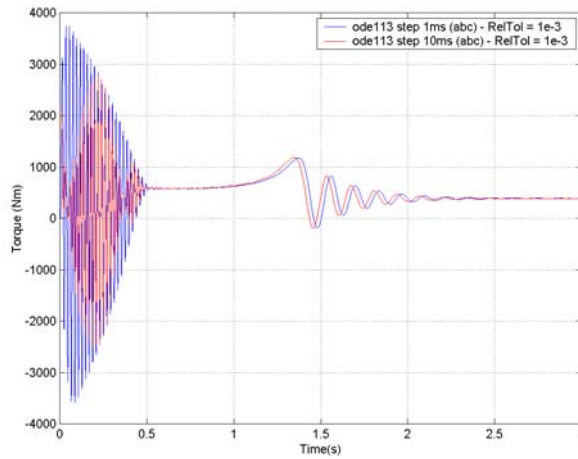
Figure 16-23 ODE Solver test: ode113 comparison of solutions with different step lengths.
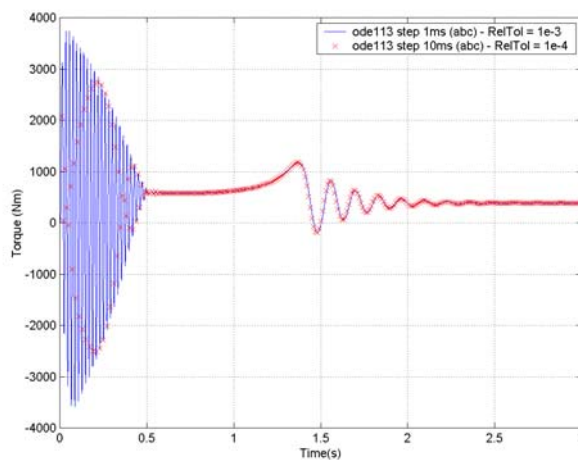
Figure 16-24 ODE Solver test: ode113 comparison of solutions with RelTol change.
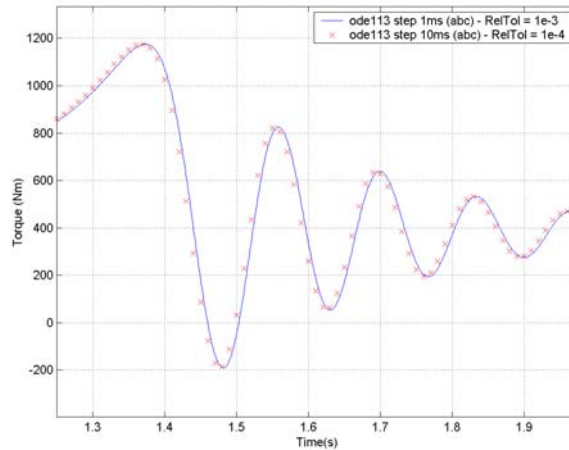
Figure 16-25 Detail view of Figure 16-24.

It can be seen from Figure 16-24 and Figure 16-25 that the error between the two sets of results has been reduced, but that RelTol <= 1e-5 should be used in step mode if step sizes of the order of 10ms or greater are used.
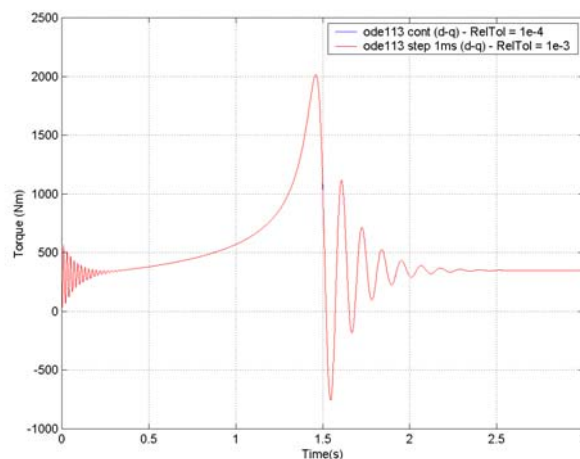
Figure 16-26 ODE Solver test: comparison of step vs. continuous solution with d-q model.

Test results for the d-q model generally produced similar results the abc models. In general larger error tolerance parameters can be used.. Figure 16-26 shows a comparison between the stepped and continuous methods with RelTol = 1e-3 for the stepped solution and RelTol = 1e-4 for the continuous solution.

16.4 Summary of ODE Solver test results.

The Matlab ODE solvers were tested using the same motor model and parameters. Initially it appeared as if the use of the Matlab ODE solvers in a stepped mode caused errors since the solution obtained differed from that obtained by using the ODE solver to integrate over a continuous interval. It was found that the solver was in fact, giving inaccurate results when integrating over a 'long' interval. The accuracy can be improved by changing the relative tolerance parameter of the ODE solver algorithm from its default value of 1e-3 to a smaller value. A value of 1e-5 for RelTol was found to give acceptable results.

Using the solver in stepped mode gave accurate results, even with the default tolerance parameters. According to the Matlab documentation, the ODE solver algorithms will give more accurate results over 'short' intervals and the default tolerance parameters might not result in acceptable accuracy of

solutions over 'long' intervals. Using the solvers over multiple short intervals (1ms) in step mode gives accurate results even with the default tolerance parameters. If the step size approaches 10ms in stepped mode, it was found that RelTol <= 1e-5 needs to be used as for the continuous solution.

The various ODE solvers all produced similar results when used with the correct relative tolerance. The main difference observed was the time taken to compute a solution with ode113, a non-stiff solver, being the most efficient and one of the stiff solvers, ode23s being extremely inefficient. The performance of the stiff equation solvers can possibly be improved if the motor model ODE file is modified to return the Jacobian of the system of equations. This was not investigated further since the speed and efficiency with which solutions are obtained is not a primary objective of the present work. This would be a topic for investigation in future work if the size and complexity of the distribution system and motor models is increased.

In summary:

- If using the ode solver in stepped mode, accurate results are obtained with RelTol <= 1e-3 (default value) and a step length of 1ms or less.

- If the ode solver is used in stepped mode with a step length greater than 1ms, RelTol should preferably be <= 1e-5 to obtain accurate results

- If using the ode solver to integrate continuously over a 'long' interval, a value for RelTol <= 1e-5 must be used. Intermediate results returned by the ode solvers are unaffected by the intermediate time step. (This is confirmed in the Matlab documentation.)

16.5 Matlab Software Listings for additional ODE solver tests.

The source code for the Matlab software used to carry out these additional tests is listed in this section.

16.5.1 Induction motor model (abc)

```
function  dS = induction_motor_01(t, S, flag, v_mot, MP)
% ODE Function to simulate induction motor performance
% abc reference frame model:
% Does not model saturation
% Models friction and windage with a constant torque proportional to speed^2
%
#########################################################################
% Rev | Comment
% ----+------------------------------------------------------------------
% 00  | Corrected error in friction and windage torque calculation
%     | Printed: 26/06/2005 - before adding synchronous machine model
% 01  | Added function to reduce rotor resistance and increase rotor
%     | reactance
%     | as a function of slip to give approximation of a double cage rotor
%
#########################################################################
% Use with ODE solver as follows:
% [T,Y] = odeXX( 'induction_motor_01', tspan, S1_IM1, options, vbus,
% MP(1,:));
%
% tspan = [t0 tfinal]
% S = motor model state variables
% S = [isa; isb; isc; ira; irb; irc; rotor_angle; rotor_speed]
% S(1,1) = isa - stator currents
% S(2,1) = isb
% S(3,1) = isc
% S(4,1) = ira - rotor currents
% etc
% S(7,1) = rotor_angle is in radians
```

```
% S(8,1) = rotor_speed is in rad/sec
%
% flag - used to set ODE solver return values:
% '' = F(t,S) (emply flag)
%
% v_mot = rms line voltage and phase angle on motor connection bus from
loadflow
%
%
% MP = motor model parameters
% All inductance and resistance values are in MKSA units
% MP = [Lsl, Lsm, Lsrm, Lrm, Lrl, Rs, Rr H, LC, LT, P, Tf, tds, tde, dt,
dp1, dp2]
% MP(1) = Lsl = Stator leakage inductance
% MP(2) = Lsm = Stator mutual induxctance
% MP(3) = Lsrm = Stator/rotor mutual inductance - set according to model
%          Vas gives Lsrm = 2/3Lsm = 2/3Lrm
% MP(4) = Lrm = rotor mutual inductance
% MP(5) = Lrl = rotor leakage inductance
% MP(6) = Rs = stator resistance
% MP(7) = Rr = rotor resistance
% MP(8) = H = inertia constant
% MP(9) = L = load constant
% MP(10) = LT = load type: 1=load proportional to speed
%                          2=load proportional to speed^2
% MP(11) = number of pole pairs
% MP(12) = Torque due to friction and windage at rated speed.
% MP(13) = Rotor resistance variation factor
% MP(14) = Rotor reactance variation factor
% MP(15) to MP(21) = not used
%
##############################################################################

global TWOpi3

if isempty(flag)
   %Return dS/dt = F(t,S)
   TWOpi3 = 2*pi/3;
   %Keep rotor angle value between zero and 2*pi
   rotor_angle = S(7,1);
   if rotor_angle > (2*pi)
      rotor_angle = rotor_angle - (2*pi);
   end
   % Make adjustment to rotor resistance and reactance to account for
   % double cage rotor
   sync_spd = 100*pi/MP(11);
   slip = (sync_spd - S(8))/sync_spd;
   % Adjust rotor resistance
   MP(7) = MP(7)*(1 + (MP(13)*slip));
   % Adjust rotor reactance
   MP(5) = MP(5)*(1 - (MP(14)*slip));
   I = S(1:6,1); %Extract rotor and stator currents
   V = calculate_voltage_vector(v_mot,t);
   L = calculate_inductance_matrix(rotor_angle, MP);
   G = calculate_rotational_inductance_matrix(rotor_angle, MP);
   R = create_resistance_matrix(MP);
   Linv = inv(L); %Invert inductance matrix
   %Calculate [V] - [R]*[I]
   dI = V - R*I;
   %Calculate [V]-[R][I]-rotor_speed*[G][I]
   dI = dI - (S(8)*G*I);
```

```matlab
    %Calculate dI = 1/[L]*([V]-[R][I]-rotor_speed*[G][I])
    dI = Linv * dI;
    % rate of change of rotor angle = rotor speed
    % thus d/dt rotor_angle = rotor speed
    % calculate and return d/dt rotor_speed
    rotor_accel = calc_rotor_acceleration(I,G,S(8,1),MP);
    dS = [dI; S(8,1); rotor_accel];
else
    %The flag argument is not used
    error('Motor model requires initial values');
end




%#########################################################################
% END OF MAIN FUNCTION
%#########################################################################

function dw = calc_rotor_acceleration(I,G,rotor_speed,MP)
% Calculate rotor acceleration
% Note to take pole pairs into account - multiply Te by the number
% of pole pairs (MP(11). Since rotor speed in electrical radians, the load
% torque calculations must also take pole pairs into account
% Friction and windage loss torque is assumed to increase with the square of
the
% rotor speed up to the maximum value given by MP(12). To simplify the
calculation
% it is assumed that the maximum speed = synchronous speed, thus the
friction and
% windage torque is not strictly accurate since it would be determined at
motor
% rated speed. The value is an estimate, so slight error does not really
mattter

% Calculate airgap electrical torque = 1/2*P*I'*G*I (Vas)
Te = (MP(11)/2)*I'*G*I;
% Calculate friction and windage torque
Tfw = MP(12)*((rotor_speed)/(100*pi))^2;
%Calculate load torque
switch MP(10)
case 1
    % Load proportional to speed * load constant
    Tl = MP(9)  * (rotor_speed/MP(11));
case 2
    % Load proportional to speed^2
    Tl = MP(9)  * (rotor_speed/MP(11))^2;
end
%Calculate acceleration = (Te - Tl)/(2*H) where H = MP(8) = inertia constant
dw = (Te- Tfw - Tl)/(2*MP(8));


%#########################################################################

function V = calculate_voltage_vector(v,t)
% Calculate instantaneous motor voltages
% It is assumed that the motor is connected in star. v = the rms line
voltage at the
% motor connection bus. The 30degree phase shift between Vline and Vphase is
taken
```

```matlab
% into account here and the phase (l-g) p-p voltage used in the model is
calculated
% The phase voltage lags the line voltage by 30deg(pi/6) This is subtracted
from the
% loadflow voltage angle to get the actual phase voltage angle.
% Vphase = Vline/sqrt(3) and Vpp = Vphase*sqrt(2)

global TWOpi3

V = zeros(6,1);
v_angle = v(2)-(pi/6); %Voltage angle from loadflow - 30degrees
% a = instantaneous bus voltage angle
a = (100 * pi * t)+ v_angle;
vpeak = v(1)*sqrt(2/3);
V(1,1) = vpeak*cos( a );
V(2,1) = vpeak*cos( a - TWOpi3);
V(3,1) = vpeak*cos( a + TWOpi3);


%#########################################################################

function L = calculate_inductance_matrix(rotor_angle, MP)
% L = calculate_inductance_matrix(S(3), MP) - calculate motor inductance
matrix
% MP(1) = Lsl = Stator leakage inductance
% MP(2) = Lsm = Stator mutual inductance
% MP(3) = Lsrm = Stator/rotor mutual inductance - this is set accoring to
model
% MP(4) = Lrm = rotor mutual inductance
% MP(5) = Lrl = rotor leakage inductance

global TWOpi3

L = zeros(6); %Create empty array
temp = MP(1) + MP(2); % Lsm + Lsl - Smith/chen
for i = 1:3
   L(i,i)=temp; %Lss diagonal elements
end
temp = MP(4) + MP(5); %Lrm + Lrl - Smith/Chen
for i = 4:6
   L(i,i) = temp; %Lrr diagonal
end
temp = -MP(2)/2; %Lss off diagonal elements = -Lsm/2
for i = 1:3
   for j = 1:3
      if i ~= j
         L(i,j) = temp;
      end
   end
end
temp = -MP(4)/2; %Lrr off diagonal elements = -Lrm/2
for i = 4:6
   for j = 4:6
      if i ~= j
         L(i,j) = temp;
      end
   end
end
temp = cos(rotor_angle)* MP(3); %cos(@)*Lsrm
for i = 1:3
   L(i,i+3) = temp; %Lsr diagonal
```

```matlab
    L(i+3,i) = temp; %Lrs diagonal
end
% Calc Lsr off diagonal elements
temp = cos(rotor_angle - TWOpi3)*MP(3);
L(2,4) = temp;
L(3,5) = temp;
L(1,6) = temp;
L(4,2) = temp;
L(5,3) = temp;
L(6,1) = temp;
temp = cos(rotor_angle + TWOpi3)*MP(3);
L(1,5) = temp;
L(2,6) = temp;
L(3,4) = temp;
L(4,3) = temp;
L(5,1) = temp;
L(6,2) = temp;


%#########################################################################

function G = calculate_rotational_inductance_matrix(rotor_angle, MP)
% G = calculate_rotational_inductance_matrix(rotor_angle, MP)
% rotor_angle = rotor electrical angle
% MP(1) = Lsl = Stator leakage inductance - not used here
% MP(2) = Lsm = Stator mutual inductance - not used here
% MP(3) = Lsrm = Stator/rotor mutual inductance
% MP(4) = Lrm = rotor mutual inductance - not used here
% MP(5) = Lrl = rotor leakage inductance - not used here

global TWOpi3

G = zeros(6); %Create empty array
temp = -MP(3) * sin(rotor_angle);
for i = 1:3
    G(i,i+3) = temp; %Gsr diagonal
    G(i+3,i) = temp; %Grs diagonal
end
% Calc Gsr and Grs off diagonal elements for rotor angle - 120
temp = -MP(3) * sin(rotor_angle - TWOpi3);
G(1,6) = temp;
G(2,4) = temp;
G(3,5) = temp;
G(4,2) = temp;
G(5,3) = temp;
G(6,1) = temp;
%Calc Gsr & Grs off diagonal elements for theta + 120
temp = -MP(3) * sin(rotor_angle + TWOpi3);
G(1,5) = temp;
G(2,6) = temp;
G(3,4) = temp;
G(4,3) = temp;
G(5,1) = temp;
G(6,2) = temp;


%#########################################################################

function R = create_resistance_matrix(MP)
% Create resistance matrix using Rs and Rr

R = eye(6);
Rs = R(1:3,:)*MP(6); %Enter Rs values into array
```

```
Rr = R(4:6,:)*MP(7); %Enter Rr values into array
R = [Rs;Rr]; %Form complete matrix
```

16.5.2 Induction motor model (d-q)

```
function  dS = induction_motor_03(t, S, flag, v_mot, MP)
% ODE Function to simulate induction motor performance
% Simplified Equivalent Circuit d-q model cf Arrilaga pg. 212
% Does not model saturation
%
#########################################################################
% Rev | Comment
% ----+-------------------------------------------------------------------
--
% 00  | Initial version
%
%
#########################################################################

% Use with ODE solver as follows:
% [T,Y] = solver('induction_motor_01', tspan , Y0,'',busdata, MP)
%
% tspan = [t0 tfinal]
% S = motor model state variables
% S = [ E'r; E'm; S; ]
% S(1,1) = E'r - Thevinin equivalent circuit voltage (real axis component)
% S(2,1) = E'm - Thevinin equivalent circuit voltage (imaginary axis
component)
% S(3,1) = Slip
%
% flag - used to set ODE solver return values:
% '' = F(t,S) (emply flag)
%
% v_mot = [Vbus V_angle] where Vbus = rms l-l Bus voltage(kV)
%
% MP = motor model parameters in MKSA
%
% MP = [X', T'o, Xo, R1, Hm, L, LT, tds, tde, dt, dp1, dp2]
% MP(1) = X': Transient reactance
% MP(2) = T'o: open circuit time constant
% MP(3) = Xo: open circuit reactance
% MP(4) = R1: Stator resistance
% MP(5) = Hm = inertia constant
% MP(6) = L = load constant
% MP(7) = LT = load type: 1=load proportional to speed
%                         2=load proportional to speed^2
% MP(8) = Disturbance start time - not used
% MP(9) = Disturbance end time - not used
% MP(10) = Disturbance type - not used
% MP(11) = Distrubance parameter 1 - not used
% MP(12) = Disturbance parameter 2 - not used
% MP(13) = Motor base MVA
% MP(14) - MP(21) are not used for this model



if isempty(flag)
    %Return dS/dt = F(t,S)
    % Use variables Vr,Vm, wo to simplify code
```

```matlab
    temp = v_mot(1) / sqrt(3); %convert to phase voltage
    Vr = temp*cos(v_mot(2));
    Vm = temp*sin(v_mot(2));
    wo = 100*pi; %omega_o
    % Ir = (R1(Vr-E'r)+X'(Vm-E'm))/(R1^2+X'^2)
    Ir = ((MP(4)*(Vr-S(1,1)))+(MP(1)*(Vm-S(2,1))))/(MP(4)^2+MP(1)^2);
    % Im = (Vm-E'm-X'Ir)/R1
    Im = (Vm-S(2,1)-(MP(1)*Ir))/MP(4);
    %temp = X0-X'
    temp = MP(3)-MP(1);
    %dE'r/dt=2*pi*fo*S*E'm-(E'r+(X0-X')Im)/T'o
    dEr = wo*S(3,1)*S(2,1)-(S(1,1)+(temp*Im))/MP(2);
    %dE'm/dt=-2*pi*fo*E'r-(E'm-(X0-X')Ir)/T'o
    dEm = -wo*S(3,1)*S(1,1)-(S(2,1)-(temp*Ir))/MP(2);
    % Electrical torque Te
    Te = ((S(1,1)*Ir)+(S(2,1)*Im))/wo;
    % Mechanical torque
    if MP(7) == 1
        Tm = MP(6)*wo*(1-S(3,1)); %load proportional to speed (fan)
    else
        Tm = MP(6)*(wo*(1-S(3,1)))^2; %Load prop. to speed^2 (pumps)
    end
    % Slip
    %dSl/dt = (Tm-Te)/2*Hm
    dSl = (Tm-Te)/(2*MP(5));
    dS = [dEr; dEm; dSl;];
else
    % Flag argument not used
    error('Model requires initial values');
end
```

16.5.3 Motor model parameters

```matlab
function [MP, MOTOR_BUS] = set_motor_parameters(motor_count)
%[MP, MOTOR_BUS] = set_motor_parameters()
%Set up induction motor model parameters

% MP = motor model parameters
% All inductance and resistance values are in MKSA units
% MP = [Lsl, Lsm, Lsrm, Lrm, Lrl, Rs, Rr H, LC, LT, P, Tf, tds, tde, dt,
dp1, dp2]
% MP(1) = Lsl = Stator leakage inductance
% MP(2) = Lsm = Stator mutual induxctance
% MP(3) = Lsrm = Stator/rotor mutual inductance - set according to model
%          Vas gives Lsrm = 2/3Lsm = 2/3Lrm
% MP(4) = Lrm = rotor mutual inductance
% MP(5) = Lrl = rotor leakage inductance
% MP(6) = Rs = stator resistance
% MP(7) = Rr = rotor resistance
% MP(8) = H = inertia constant
% MP(9) = L = load constant
% MP(10) = LT = load type: 1=load proportional to speed
%                          2=load proportional to speed^2
% MP(11) = number of pole pairs
% MP(12) = Torque due to friction and windage at rated speed.
% MP(13) = Rotor resistance variation factor Rr at standstill =
Rr*(1+(factor*slip))
% MP(14) = Rotor reactance variation factor Xr at standstill = Xr*(1-
(factor*slip))
% MP(15) = not used
% MP(16) = not used
```

```
% MP(17) = not used
% MP(18) = I0 = base current at which no saturation is assumed
% MP(19) = B0 = flux density corresponding to I0 - calculated from
saturation curve
% MP(20) = Saturation current multiplication factor - scale Im to At/m
% MP(21) = Saturation scaling factor

% MOTOR_BUS = loadflow motor bus

%====================================================================
% Revision History
% 2005/06/26 - Used as basis for adding synchronous generator model
% 2005/08/02 - Added parameters for single-cage induction motor model
%====================================================================

MP = zeros(motor_count*2, 21);
MOTOR_BUS = zeros(motor_count,1);

%====================================================================
% Parameters for abc model
%
% Note: MOTOR_BUS is an array storing the connection bus numbers of the
% motors to be simulated. There is no value stored for the d-q model
% since this simply uses the abc model data

%====================================================================
% MOTOR 01 - 24KC101AM 550kW - bus 49
%====================================================================
MOTOR_BUS(1) = 49; %Motor 1 bus number

MP(1,1) = 0.03592; %Lsl = Stator leakage inductance (=equiv. ckt param)
MP(1,2) = 0.8726; %Lsm = Stator magnetising inductance
MP(1,3) = MP(1,2); %Lsrm = Stator/rotor mutual inductance = 2/3Lsm = 2/3Lrm
MP(1,4) = MP(1,2); %Lrm = rotor magnetising inductance
MP(1,5) = 0.05389; %Lrl = rotor leakage inductance
MP(1,6) = 1.1895; %Rs = stator resistance
MP(1,7) = 0.6479; %Rr = rotor resistance (running resistance)
MP(1,8) = 5.5; %H = inertia constant
MP(1,9) = 0.018; %L = load constant approx 50% of 550kW load
MP(1,10) = 2;%LT = load type: 1= proportional to speed 2= proportional to
speed^2
MP(1,11) = 1; %pole pairs
MP(1,12) = 37.93; %Torque due to friction and Windage at rated speed (Nm)
MP(1,13) = 2; %Rr standstill = 3Rr
MP(1,14) = 0.5; %Xr standstill = 0.5*Xr
%Saturation - not used
MP(1,18) = 0; %I0 - base current
MP(1,19) = 0; %B0 = I0 flux density
MP(1,20) = 0; %current scale factor
MP(1,21) = 0; %saturation scaling factor ( 0 = no saturation)


%====================================================================
% MOTOR 02 - 24PC101AM 300kW - bus 50
%====================================================================
MOTOR_BUS(2) = 50; %Motor 2 bus number

MP(2,1) = 0.0671; %Lsl = Stator leakage inductance (=equiv. ckt param)
MP(2,2) = 1.844; %Lsm = Stator magnetising inductance
MP(2,3) = MP(2,2); %Lsrm = Stator/rotor mutual inductance = 2/3Lsm = 2/3Lrm
MP(2,4) = MP(2,2); %Lrm = rotor magnetising inductance
```

```
MP(2,5) = 0.1005; %Lrl = rotor leakage inductance
MP(2,6) = 1.456; %Rs = stator resistance
MP(2,7) = 2.739; %Rr = rotor resistance
MP(2,8) = 3.3; %H = inertia constant
MP(2,9) = 7e-3; %L = load constant  70% of load
MP(2,10) = 2;%LT = load type: 1= proportional to speed 2= proportional to
speed^2
MP(2,11) = 1; %pole pairs
MP(2,12) = 27; %Torque due to friction and Windage at rated speed
MP(2,13) = 2; %Rr standstill = 2.5Rr
MP(2,14) = 0.5; %Xr standstill = 0.5*Xr
%Saturation - not used
MP(2,18) = 0; %I0 - base current
MP(2,19) = 0; %B0 = I0 flux density
MP(2,20) = 0; %current scale factor
MP(2,21) = 0; %saturation scaling factor ( 0 = no saturation)


%=================================================================
% MOTOR 03 - 24PC104AM 300kW - bus 52
%=================================================================
MOTOR_BUS(3) = 52; %Motor 3 bus number

MP(3,1) = 0.0671; %Lsl = Stator leakage inductance (=equiv. ckt param)
MP(3,2) = 1.844; %Lsm = Stator magnetising inductance
MP(3,3) = MP(2,2); %Lsrm = Stator/rotor mutual inductance = 2/3Lsm = 2/3Lrm
MP(3,4) = MP(2,2); %Lrm = rotor magnetising inductance
MP(3,5) = 0.1005; %Lrl = rotor leakage inductance
MP(3,6) = 1.456; %Rs = stator resistance
MP(3,7) = 2.739; %Rr = rotor resistance
MP(3,8) = 2.6; %6.3 H = inertia constant
MP(3,9) = 8e-3; %L = load constant 80% of load
MP(3,10) = 2;%LT = load type: 1= proportional to speed 2= proportional to
speed^2
MP(3,11) = 1; %pole pairs
MP(3,12) = 27; %Torque due to friction and Windage at rated speed
MP(3,13) = 2; %Rr standstill = 4Rr
MP(3,14) = 0.5; %Xr standstill = 0.5*Xr
%Saturation - not used
MP(3,18) = 0; %I0 - base current
MP(3,19) = 0; %B0 = I0 flux density
MP(3,20) = 0; % current scale factor
MP(3,21) = 0; % saturation scaling factor ( 0 = no saturation)

%=================================================================
% MOTOR 04 - 24PC102AM 850kW - bus 51
%=================================================================
MOTOR_BUS(4) = 51; %Motor 4 bus number

MP(4,1) = 0.023393; %Lsl = Stator leakage inductance (=equiv. ckt param)
MP(4,2) = 0.7080; %Lsm = Stator magnetising inductance
MP(4,3) = MP(4,2); %Lsrm = Stator/rotor mutual inductance = 2/3Lsm = 2/3Lrm
MP(4,4) = MP(4,2); %Lrm = rotor magnetising inductance
MP(4,5) = 0.03509; %Lrl = rotor leakage inductance
MP(4,6) = 1.2555; %Rs = stator resistance
MP(4,7) = 1.133; %Rr = rotor resistance
MP(4,8) = 9; %H = inertia constant
MP(4,9) = 0.02064; %L = load constant 80% of load
MP(4,10) = 2;%LT = load type: 1= proportional to speed 2= proportional to
speed^2
MP(4,11) = 1; %pole pairs
```

```matlab
MP(4,12) = 24; %Torque due to friction and Windage at rated speed (Nm)
MP(4,13) = 2; %Rr standstill = 3Rr
MP(4,14) = 0.5; %Xr standstill = 0.5*Xr
%Saturation
MP(4,18) = 0; %I0 - base current
MP(4,19) = 0; %B0 = I0 flux density
MP(4,20) = 0; % current scale factor
MP(4,21) = 0; % saturation scaling factor ( 0 = no saturation)

%##################################################################
% Parameters for simplified motor models
%##################################################################
% MP = motor model parameters in MKSA
%
% MP = [X', T'o, Xo, R1, Hm, L, LT, tds, tde, dt, dp1, dp2]
% MP(1) = X': Transient reactance
% MP(2) = T'o: open circuit time constant
% MP(3) = Xo: open circuit reactance
% MP(4) = R1: Stator resistance
% MP(5) = Hm = inertia constant
% MP(6) = L = load constant
% MP(7) = LT = load type: 1=load proportional to speed
%                         2=load proportional to speed^2
% MP(8) = bus voltage (kV)
% MP(9) = not used
% MP(10) = not used
% MP(11) = not used
% MP(12) = not used
% MP(13) = Motor base MVA
% MP(14) - MP(21) are not used for this model


%==================================================================
% MOTOR 01 - 24KC101AM 550kW - bus 49
%==================================================================
R1 = 1.189;
X1 = 6.7716;
Xm = 274;
X2 = 10.1574;
R2 = 0.647;

MP(5,1) = X1 + ((X2*Xm)/(X2+Xm));    %Transient reactance
MP(5,2) = (X2+Xm)/(100*pi*R2);    %open circuit time constant
MP(5,3) = X1+Xm;                  %open circuit reactance
MP(5,4) = R1;                     %Stator resistance
MP(5,5) = 125;           %H, inertia constant
MP(5,6) = 1.1825e-3;       %load constant 50% load
MP(5,7) = 2;           %Load type
MP(5,8) = 6.6;        %bus voltage (kv)
MP(5,13) = 0.55; %Sb(MVA) for motor


%==================================================================
% MOTOR 02 - 24PC101AM 300kW - bus 50
%==================================================================
R1 = 1.456;
X1 = 12.64;
Xm = 579;
X2 = 18.96;
R2 = 0.913;

MP(6,1) = X1 + ((X2*Xm)/(X2+Xm));    %Transient reactance
MP(6,2) = (X2+Xm)/(100*pi*R2);    %open circuit time constant
```

```
MP(6,3) = X1+Xm;                 %open circuit reactance
MP(6,4) = R1;                    %Stator resistance
MP(6,5) = 70;        %H, inertia constant
MP(6,6) = 2.162e-3;  %load constant 80% load
MP(6,7) = 2;            %Load type
MP(6,8) = 6.6;        %bus voltage (kv)
MP(6,13) = 0.3; %Sb(MVA) for motor


%=====================================================================
% MOTOR 03 - 24PC104AM 300kW - bus 52
%=====================================================================

R1 = 3.464;
X1 = 14.09;
Xm = 420.6;
X2 = 21.14;
R2 = 1.259;

MP(7,1) = X1 + ((X2*Xm)/(X2+Xm));    %Transient reactance
MP(7,2) = (X2+Xm)/(100*pi*R2);    %open circuit time constant
MP(7,3) = X1+Xm;                 %open circuit reactance
MP(7,4) = R1;                    %Stator resistance
MP(7,5) = 70;        %H, inertia constant
MP(7,6) = 2.162e-3;        %load constant 80% load
MP(7,7) = 2;            %Load type
MP(7,8) = 6.6;        %bus voltage (kv)
MP(7,13) = 0.3; %Sb(MVA) for motor


%=====================================================================
% MOTOR 04 - 24PC102AM 800kW - bus 51
%=====================================================================


R1 = 1.255;
X1 = 4.409;
Xm = 222.4;
X2 = 6.614;
R2 = 0.377;

MP(8,1) = X1 + ((X2*Xm)/(X2+Xm));    %Transient reactance
MP(8,2) = (X2+Xm)/(100*pi*R2);    %open circuit time constant
MP(8,3) = X1+Xm;                 %open circuit reactance
MP(8,4) = R1;                    %Stator resistance
MP(8,5) = 200;        %H, inertia constant
MP(8,6) = 6.485e-3;  %load constant 80% load
MP(8,7) = 2;            %Load type
MP(8,8) = 6.6;        %bus voltage (kv)
MP(8,13) = 0.8; %Sb(MVA) for motor
```

16.5.4 Motor model Test Subroutine

```
function [T,Y,Z] = test_motor_model(tstart, tstep, tstop, motor_num, mode)
%[t_final,Y,s_final] = test_motor_model(tstart, tstep, tstop, motor_num,
mode)
%Test motor model independently of loadflow
%tstart = start time
%tstep = step size
%tstop = end time
%motor_num = motor number
%mode = discrete step (=0) or continuous(=1) solution
```

```matlab
% discrete step = ode solver is stopped and started in same manner as
% used in conjunction with loadflow
% continuous = ode solver calculates solution over entire interval in one
step
%
########################################################################
% Rev | Comment
% ----+-----------------------------------------------------------------
% 00  | Initial version - only tested abc models with various parameters
% 01  | Added d-q model and functions to run ode solver in stepped mode
%     | or continuous mode. Removed plotting functions and moved to GUI
%     | subroutines (19/05/07)
%
########################################################################

global IM1 T Y



v1 = [6600 0]; %Motor rms line voltage
if motor_num < 5
   %abc model
   S0 = zeros(8,1); % Set state vector length to 8
else
   %d-q model
   S0 = zeros(3,1); % Set state vector length to 3
   S0(3,1) = 1; %Set initial slip = 1 ie standstill
end %if
[MP, temp] = set_motor_parameters(4); %Set up motor parametere
% temp = motor bus - not used here

switch motor_num
case 1
   IM1 = MP(1,:);
   ode_model = 'induction_motor_01';
case 2
   IM1 = MP(2,:);
   ode_model = 'induction_motor_01';
case 3
   IM1 = MP(3,:);
   ode_model = 'induction_motor_01';
case 4
   IM1 = MP(4,:);
   ode_model = 'induction_motor_01';
case 5 %d-q models
   IM1 = MP(5,:);
   ode_model = 'induction_motor_03';
case 6
   IM1 = MP(6,:);
   ode_model = 'induction_motor_03';
case 7
   IM1 = MP(7,:);
   ode_model = 'induction_motor_03';
case 8
   IM1 = MP(8,:);
   ode_model = 'induction_motor_03';
end


%Set ODE options
options = odeset('AbsTol', 1e-6, 'RelTol', 1e-4);
```

```matlab
fprintf(1,DATESTR(NOW)); %Print start of ODE solution
switch mode
    case 1 %continuous solution
        tspan = [tstart:tstep:tstop];
        [T,Y] = ode113( ode_model, tspan, S0, options, v1, IM1);
    case 0 %stepped solution
        end_sim = 0;
        data_points = ceil((tstop - tstart)/tstep);
        T = zeros(data_points,1);
        if motor_num < 5
            Y = zeros(data_points,8); %abc model state vector
        else
            Y = zeros(data_points,3); %d-q model state vector
        end %if
        r = 1;
        t1 = tstart;
        while end_sim ~= 1
            t2 = t1 + tstep;
            tspan = [t1 t2];
            [t,y] = ode113( ode_model, tspan, S0, options, v1, IM1);
            S0 = y(end,:)'; %save final state to use as initital state for next
step
            Y(r,:) = y(end,:);
            T(r) = t(end);
            r=r+1;
            t1 = t2;
            if t1 >= tstop
                end_sim = 1;
            end
        end %while
    end %switch

fprintf(1,'\n');
fprintf(1,DATESTR(NOW)); %End of ODE solution
fprintf(1,'\n');
if motor_num < 5
    %calculate data for abc model
    %Calculate torque
    TRQ = calc_torque;
    tp3 = (2*pi)/3;
    A = (T*100*pi) - (pi/6) + v1(2);
    %Calculate motor stator voltages
    vpk = v1(1)*sqrt(2/3);
    VA = vpk*cos(A);
    VB = vpk*cos(A-tp3);
    VC = vpk*cos(A+tp3);
    %Input Power
    PWR = ((VA.*Y(:,1))+(VB.*Y(:,2))+(VC.*Y(:,3)))/1e3; %kW
    VAR = -(VA.*(Y(:,2)-Y(:,3))+VB.*(Y(:,3)-Y(:,1))+VC.*(Y(:,1)-
Y(:,2)))/(1e3*sqrt(3));
    ISTAT = sqrt((1/3)*(Y(:,1).^2+Y(:,2).^2+Y(:,3).^2)); %Stator rms current
else
    %calculate data for d-q model
    points = size(T,1);
    %Since bus voltage angle is assumed = 0 for these tests,
    %Vm = Vbus/sqrt3 * sin (bus angle) = 0
    Vr = v1(1)/sqrt(3); % Vr = Vbus/sqrt3 *cos(bus angle)
    % Voltage Vm = 0 and  has been omitted from the
    % calculations which follow
    %Ir = (R1(Vr-E'r)+X'(Vm-E'm))/(R1^2+X'^2)
    Ir = ((IM1(4).*(Vr-Y(:,1)))+(IM1(1).*(-Y(:,2))))/(IM1(4)^2+IM1(1)^2);
```

```matlab
    %Im = (Vm-E'm-X'Ir)/R1
    Im = (-Y(:,2)-(IM1(1)*Ir))/IM1(4);
    TRQ = 3*((Y(:,1).*Ir)+(Y(:,2).*Im))/(100*pi);
    It = complex(Ir,Im); %Stator current - rms
    Vt = complex(Vr,0);
    Sm = Vt*conj(It);
    PWR = real(Sm)*0.003;%w
    VAR = imag(Sm)*0.003;%VAr
    ISTAT = abs(It);
end %if
Z = [TRQ PWR VAR ISTAT];


%#######################################################################

function TRQ = calc_torque()
%Calculate motor inst. torque

global IM1 T Y

points = size(T,1);
TRQ = zeros(points,1);
for index = 1:points
   MC = Y(index,1:6); %get currents
   r_angle = Y(index,7);
   G = calculate_G(r_angle, IM1);
   TRQ(index) = (IM1(11)/2)*MC*G*MC';
end




%#######################################################################
% This function is only needed in the induction motor ODE solver program
when calculating
% system transient response - used in the test program to calculate
instantaneous motor
% torque for plotting

function G = calculate_G(rotor_angle, MP)
% G = calculate_rotational_inductance_matrix(rotor_angle, MP)
% rotor_angle = rotor electrical angle
% MP(1) = Lsl = Stator leakage inductance - not used here
% MP(2) = Lsm = Stator mutual inductance - not used here
% MP(3) = Lsrm = Stator/rotor mutual inductance
% MP(4) = Lrm = rotor mutual inductance - not used here
% MP(5) = Lrl = rotor leakage inductance - not used here

TWOpi3 = (2*pi)/3;

G = zeros(6); %Create empty array
temp = -MP(3) * sin(rotor_angle);
for i = 1:3
   G(i,i+3) = temp; %Gsr diagonal
   G(i+3,i) = temp; %Grs diagonal
end
% Calc Gsr and Grs off diagonal elements for rotor angle - 120
temp = -MP(3) * sin(rotor_angle - TWOpi3);
G(1,6) = temp;
G(2,4) = temp;
G(3,5) = temp;
G(4,2) = temp;
```

```
G(5,3) = temp;
G(6,1) = temp;
%Calc Gsr & Grs off diagonal elements for theta + 120
temp = -MP(3) * sin(rotor_angle + TWOpi3);
G(1,5) = temp;
G(2,6) = temp;
G(3,4) = temp;
G(4,3) = temp;
G(5,1) = temp;
G(6,2) = temp;
```